AD

USAAMRDL TECHNICAL REPORT 71-19

AN EXPERIMENTAL INVESTIGATION OF COMPOUND HELICOPTER AERODYNAMICS IN LEVEL AND DESCENDING FORWARD FLIGHT AND IN GROUND PROXIMITY

By

William F. Putman

Joseph J. Traybar

July 1971

EUSTIS DIRECTORATE
U. S. ARMY AIR MOBILITY RESEARCH AND DEVELOPMENT LABORATORY
FORT EUSTIS, VIRGINIA

CONTRACT DAAJ02-67-C-0025
DEPARTMENT OF AEROSPACE AND MECHANICAL SCIENCES
PRINCETON UNIVERSITY
PRINCETON, NEW JERSEY

U S ARMY MATERIEL COMMAND

Approved for public release; distribution unlimited.

DISCLAIMERS

The findings in this report are not to be construed as an official Department of the Army position unless so designated by other authorized documents.

When Government drawings, specifications, or other data are used for any purpose other than in connection with a definitely related Government procurement operation, the United States Government thereby incurs no responsibility nor any obligation whatsoever; and the fact that the Government may have formulated, furnished, or in any way supplied the said drawings, specifications, or other data is not to be regarded by implication or otherwise as in any manner licensing the holder or any other person or corporation, or conveying any rights or permission, to manufacture, use, or sell any patented invention that may in any way be related thereto.

DISPOSITION INSTRUCTIONS

Destroy this report when no longer needed. Do not return it to the originator.

DEPARTMENT OF THE ARMY
U. S. ARMY AIR MOBILITY RESEARCH & DEVELOPMENT LABORATORY
EUSTIS DIRECTORATE
FORT EUSTIS, VIRGINIA 23604

This report has been reviewed by the Eustis Directorate of the U. S. Army Air Mobility Research and Development Laboratory and is considered to be technically sound. The report is published for the exchange of information and the stimulation of ideas. The program was conducted under the technical management of Mr. Robert P. Smith of the Aeromechanics Division of this Directorate.

Unclassified
Security Classification

DOCUMENT CONTROL DATA - R & D

(Security classification of title, body of abstract and indexing annotation must be entered when the overall report is classified)

1. ORIGINATING ACTIVITY (Corporate author)	2a. REPORT SECURITY CLASSIFICATION
Department of Aerospace and Mechanical Sciences Princeton University Princeton, New Jersey	Unclassified 2b. GROUP

3. REPORT TITLE

AN EXPERIMENTAL INVESTIGATION OF COMPOUND HELICOPTER AERODYNAMICS IN LEVEL AND DESCENDING FORWARD FLIGHT AND IN GROUND PROXIMITY

4. DESCRIPTIVE NOTES (Type of report and inclusive dates)

Final Data Report

5. AUTHOR(S) (First name, middle initial, last name)

William F. Putman
Joseph J. Traybar

6. REPORT DATE	7a. TOTAL NO. OF PAGES	7b. NO. OF REFS
July 1971	313	5

8a. CONTRACT OR GRANT NO.	9a. ORIGINATOR'S REPORT NUMBER(S)
DAAJ02-67-C-0025 b. PROJECT NO. Task 1F162204A14233 c. d.	USAAMRDL Technical Report 71-19 9b. OTHER REPORT NO(S) (Any other numbers that may be assigned this report) Aerospace Sciences Report 971

10. DISTRIBUTION STATEMENT

Approved for public release; distribution unlimited.

11. SUPPLEMENTARY NOTES	12. SPONSORING MILITARY ACTIVITY
	Eustis Directorate U.S. Army Air Mobility Research and Development Laboratory, Fort Eustis, Va.

13. ABSTRACT

A series of experiments was performed on the Princeton Dynamic Model Track on a compound helicopter model with an 8-foot-diameter hingeless rotor. Rotor, wing and fuselage forces and moments were measured as functions of advance ratio, rotor angle of attack, and collective pitch at various combinations of wing size and position, including wing off and wing and fuselage off. Test conditions included forward level flight, partial-power steep descent, and slow longitudinal and lateral flight in ground proximity.

The results of these experiments are presented as functions of advance ratio in non-dimensional coefficient form based on rotor tip speed and an appropriate characteristic area, such as rotor area or wing area.

DD FORM 1 NOV 65 1473 REPLACES DD FORM 1473, 1 JAN 64, WHICH IS OBSOLETE FOR ARMY USE.

Unclassified
Security Classification

Unclassified
Security Classification

14. KEY WORDS	LINK A		LINK B		LINK C	
	ROLE	WT	ROLE	WT	ROLE	WT
Helicopter Compound Helicopter Aerodynamic Experimental Data Ground Effect Descending Flight Level Flight						

Unclassified
Security Classification

Task 1F162204A14233
Contract DAAJ02-67-C-0025
USAAMRDL Technical Report 71-19
July 1971

AN EXPERIMENTAL INVESTIGATION OF COMPOUND HELICOPTER AERODYNAMICS IN LEVEL AND DESCENDING FORWARD FLIGHT AND IN GROUND PROXIMITY

Aerospace Sciences Report 971

By
William F. Putman
Joseph J. Traybar

Prepared By

Department of Aerospace and Mechanical Sciences
Princeton University
Princeton, New Jersey

for

EUSTIS DIRECTORATE
U. S. ARMY AIR MOBILITY RESEARCH AND DEVELOPMENT LABORATORY
FORT EUSTIS, VIRGINIA

SUMMARY

A series of experiments was performed on the Princeton Dynamic Model Track on a compound helicopter model with an 8-foot-diameter hingeless rotor. Rotor, wing and fuselage forces and moments were measured as functions of advance ratio, rotor angle of attack, and collective pitch at various combinations of wing size and position, including wing off and wing and fuselage off. Test conditions included forward level flight, partial-power steep descent, and slow longitudinal and lateral flight in ground proximity.

The results of these experiments are presented as functions of advance ratio in nondimensional coefficient form based on rotor tip speed and an appropriate characteristic area, such as rotor area or wing area.

FOREWORD

This research was performed by the Department of Aerospace and Mechanical Sciences, Princeton University, under the sponsorship of the Eustis Directorate, U. S. Army Air Mobility Research and Development Laboratory, Contract DAAJ02-67-C-0025. The research was monitored by Mr. Robert P. Smith of USAAMRDL.

TABLE OF CONTENTS

LIST OF ILLUSTRATIONS

Figure		Page

Figure		Page

Figure		Page
42	Rotor Force and Moment Coefficients as Functions of Advance Ratio, $\theta_{.75R} = 0$, Large Wing on High.	88
43	Fuselage Vertical Force and Pitching Moment Coefficients as Functions of Advance Ratio, $\theta_{.75R} = 0$, Large Wing on High . .	92
44	Wing Normal Force and Rolling Moment Coefficients as Functions of Advance Ratio, $\theta_{.75R} = 0$, Large Wing on High . .	94
45	Rotor Force and Moment Coefficients as Functions of Advance Ratio, $\theta_{.75R} = 2^\circ$, Large Wing on High.	95
46	Fuselage Vertical Force and Pitching Moment Coefficients as Functions of Advance Ratio, $\theta_{.75R} = 2^\circ$, Large Wing on High .	99
47	Wing Normal Force and Rolling Moment Coefficients as Functions of Advance Ratio, $\theta_{.75R} = 2^\circ$, Large Wing on High .	101
48	Rotor Force and Moment Coefficients as Functions of Advance Ratio, $\theta_{.75R} = 4^\circ$, Large Wing on High	102
49	Fuselage Vertical Force and Pitching Moment Coefficients as Functions of Advance Ratio, $\theta_{.75R} = 4^\circ$, Large Wing on High .	106
50	Wing Normal Force and Rolling Moment Coefficients as Functions of Advance Ratio, $\theta_{.75R} = 4^\circ$, Large Wing on High .	108
51	Fuselage Vertical Force and Pitching Moment Coefficients as Functions of Advance Ratio, $\theta_{.75R} = 4^\circ$, Large Wing on Low. .	109
52	Wing Normal Force and Rolling Moment Coefficients as Functions of Advance Ratio, $\theta_{.75R} = 4^\circ$, Large Wing on Low. .	111
53	Fuselage Vertical Force and Pitching Moment Coefficients as Functions of Advance Ratio, $\theta_{.75R} = 4^\circ$, Small Wing on High .	112
54	Wing Normal Force and Rolling Moment Coefficients as Functions of Advance Ratio, $\theta_{.75R} = 4^\circ$, Small Wing on High .	114
55	Fuselage Vertical Force and Pitching Moment Coefficients as Functions of Advance Ratio, $\theta_{.75R} = 4^\circ$, Small Wing on Low. .	115

Figure		Page

Figure		Page

Figure		Page

Figure		Page

Figure **Page**

Figure		Page

LIST OF SYMBOLS

Dimensional

A — rotor area, square inches or square feet, $A = \pi R^2$

A_W — total wing area, square inches or square feet

A_{1_s} — first harmonic lateral cyclic pitch angle with respect to the shaft, degrees

B_{1_s} — first harmonic longitudinal cyclic pitch angle with respect to the shaft, degrees

b_W — wing span, inches or feet

c — rotor blade chord, inches or feet

$c_W/4$ — wing quarter chord, inches or feet

D — rotor diameter, inches or feet

g — acceleration due to gravity, feet per second squared

h — reference height above ground, inches

$\frac{h}{D}$ — height - diameter ratio

i_P — port wing incidence, degrees

i_S — starboard wing incidence, degrees

i_W — average wing incidence, degrees; $i_W = \dfrac{i_P + i_S}{2}$

ℓ — rotor rolling moment, foot-pounds

ℓ'_P — port wing rolling moment in wing axis system, foot-pounds

ℓ'_S — starboard wing rolling moment in wing axis system, foot-pounds

ℓ'_W — wing rolling moment, foot-pounds, where $\ell'_W = \ell'_P + \ell'_S$

M — rotor pitching moment, foot-pounds

M_F — fuselage pitching moment, foot-pounds

N	rotor yawing moment, foot-pounds
n_p	port wing normal force, pounds
n_s	starboard normal force, pounds
n_w	wing normal force, pounds, where $n_w = n_p + n_s$
q	dynamic pressure factor, pounds per square foot, $q = \rho (\Omega R)^2$
R	rotor radius, inches or feet
rpm	revolutions per minute
T	rotor thrust, pounds
V	model velocity, feet/second
X,Y,Z	rotor axis system
X_F, Y_F, Z_F	fuselage axis system
X	rotor axial force, pounds
X'	wing-fixed chordwise axis
Y	rotor side force, pounds
Z	rotor vertical force, pounds
Z_F	fuselage vertical force, pounds
Z'	wing-fixed axis perpendicular to chordal plane
α_s	rotor shaft angle of attack, degrees
γ	phasing angle for B_{1s} input, degrees
$\theta_{.75R}$	rotor collective pitch measured at 0.75R, degrees
θ_{TV}	tail vane pitch angle, degrees
ρ	air density, slugs per cubic foot
ψ_{TV}	tail vane yaw angle, degrees
Ω	rotor angle velocity, revolutions per minute or radians/second

Nondimensional

b number of blades, $b = 4$

C_ℓ rotor rolling moment coefficient,

$$C_\ell = \frac{\ell}{q A \sigma R}$$

C_ℓ' individual wing rolling moment coefficient,

$$C_\ell' = C_\ell'_p \text{ or } C_\ell'_s$$

$C_\ell'_p$ port wing rolling moment coefficient

$$C_\ell'_p = \frac{\ell'_p}{q A_W b_W}$$

$C_\ell'_s$ starboard wing rolling moment coefficient,

$$C_\ell'_s = \frac{\ell'_s}{q A_W b_W}$$

C_M rotor pitching moment coefficient,

$$C_M = \frac{M}{q A \sigma R}$$

C_{M_F} fuselage pitching moment coefficient,

$$C_{M_F} = \frac{M_F}{q A \sigma R}$$

C_N rotor yawing moment coefficient,

$$C_N = \frac{N}{q A \sigma R}$$

C_n individual wing normal force coefficient,

$$C_n = C_{n_p} \text{ or } C_{n_s}$$

C_{n_p} — port wing normal force coefficient,

$$C_{n_p} = \frac{n_s}{q\,A_W}$$

C_{n_s} — starboard wing normal force coefficient,

$$C_{n_s} = \frac{n_s}{q\,A_W}$$

C_x — rotor axial force coefficient,

$$C_x = \frac{X}{q\,A\,\sigma}$$

C_y — rotor side force coefficient,

$$C_y = \frac{Y}{q\,A\,\sigma}$$

C_z — rotor vertical force coefficient,

$$C_z = \frac{Z}{q\,A\,\sigma}$$

C_{z_F} — fuselage vertical force coefficient,

$$C_{z_F} = \frac{Z_F}{q\,A\,\sigma}$$

μ — advance ratio, $\mu = \frac{V}{\Omega R}$

σ — solidity ratio, $\sigma = \frac{bc}{\Pi R}$

INTRODUCTION

It is generally recognized that some of the high-speed performance capabilities of a fixed-wing aircraft and the hovering capabilities of a helicopter can be obtained by adding wings and auxiliary propulsion to a pure helicopter. The compound helicopter resulting could be expected to exhibit higher speed capability than a pure helicopter and yet maintain most of the helicopter's hover capabilities.

Significant contributions to the determination of the high-speed characteristics of compound helicopter configurations have been made in References 1, 2 and 3. However, qualitative references to the low-speed characteristics of these aircraft made in References 2 and 3 indicate that in such areas as gust sensitivity and other stability, control and handling quality items,certain deficiencies are likely to be encountered. In particular, the flight regimes near autorotative flight and in ground proximity are suspect from the point of view that significant changes in wing and fuselage air-loads can be expected due to large local angle-of-attack changes.

It was therefore proposed to undertake a series of experiments in the Princeton Dynamic Model Track to measure the low-speed aero-dynamic characteristics of a compound helicopter model. In the interest of continuity of information,it was determined that the model employed for these experiments should be similar to the model used in the experiments of Reference 1,and a scale factor of 8/9 of the Reference 1 model scale was selected for the Dynamic Model Track Model.

Further, it was proposed that the experimental test program encompass test conditions simulating steady level flight and partial power descent at low advance ratios as well as slow-speed flight in ground proximity. This report presents the experimental rotor, fuselage and wing aerodynamic data obtained in these experiments.

DESCRIPTION OF TEST APPARATUS

The Princeton Dynamic Model Track is a unique facility which, although designed primarily for dynamic testing, possesses the capability of performing static testing under carefully controlled conditions. In particular, it is possible to perform tests in a 30-foot by 30-foot test section at flight speeds down to zero and backward velocities with accurate and continuous velocity control. This is accomplished by means of a servo-controlled hydraulically-driven carriage that rides on a track in a 750-foot-long enclosed building. A model is attached to this carriage through suitable force measuring instrumentation, and the aerodynamic forces acting on the model can be measured as it is driven through still air by the powered carriage. For a more comprehensive discussion of this apparatus and its capabilities, the reader is referred to Reference 4.

STATIC CARRIAGE

A special shock and acceleration-attenuating static testing carriage is used to support the model and the force measuring instrumentation. This static carriage is unpowered and is pushed by the main dynamic carriage; a photograph of the main carriage - static carriage-model system is shown in Figure 1. A special feature of this carriage is a rolling degree-of-freedom of the model support boom which allows it to pivot about an axis located parallel to and just above the track. The model-boom system is nearly mass balanced about this point, and an on-off servo positions a counterweight which balances out aerodynamic model forces during a run. The resulting system is very insensitive to the principal source of vibrational noise which comes from carriage-track roll excitation.

MODEL AND INSTRUMENTATION

A photograph of the compound helicopter model mounted in the Dynamic Model Track for the simulated descent tests is shown in Figure 2, and the mounting arrangement for ground proximity tests is shown in Figure 3. A drawing of the model general arrangment is shown in Figure 4.

In general, the model is geometrically similar to the model used in Reference 1, with the exception of solidity ratio. The rotor diameter is 8/9 the rotor diameter of the Reference 1 model, the fuselage is an exact 8/9 scale of the Reference 1 model, and the wings are 8/9 scale models of the large and medium wings of the Reference 1 model.

Rotor System

The compound helicopter model rotor is a four-bladed nonarticulated rotor with provisions for adjustable collective pitch and two

adjustable-phase mutually-perpendicular cyclic pitch actuation mechanism. A detail photograph of the mechanical components is shown in Figure 5, in which can be seen the blades, hub, swash plate, slip ring and transmission assembly.

The rotor is powered by a 5-hp, 400-cycle, air-cooled electric motor, driven by the Dynamic Model Track's variable-frequency model drive system.

The rotor blades are constructed of an epoxy-resin-impregnated glass fiber cloth skin and a urethane foam core bonded to a tubular stainless steel spar. Estimated blade dynamic characteristics are as presented in Figure 6.

The rotor transmission system was attached to the model support sting by a six-component internal strain gage balance, which was used to measure rotor forces and moments independent of all other model component loads, except in the ground proximity test arrangement, where both fuselage and wing loads appear in the rotor balance.

Fuselage

The model fuselage was constructed of glass fiber cloth laminated in a female mold by the vacuum-bag technique. Fuselage geometric characteristics are as shown in Figure 7.

Fuselage instrumentation consisted of a two-component strain gage balance which measured fuselage vertical force and pitching moment and supported the fuselage independent of all other components. Flexural pivots and links were used in the fuselage balance system to isolate the measured quantities; this arrangement and the bulkhead to which the fuselage shell was attached can be seen in Figure 8.

Wings

The wings were made of epoxy-resin impregnated with glass fiber laminated in female molds by the vacuum-bag technique. Both large and small wings were attached to the model support sting by means of an instrumented spar for each side, port and starboard of the model. The instrumented spar measured bending moment at two spanwise locations; bending moment, in turn, was converted to wing normal force and rolling moment. In addition, the spars incorporated wing incidence drive motors and position potentiometers, and the entire mechanism could be located at any of three vertical positions on the model. The starboard wing spar mounted in the lowest position can be seen in Figure 8.

Downwash Vanes

A downwash vane was provided in the vicinity of a typical tail location to measure the pitch and sideslip component of the airflow in that vicinity. In addition, angle-of-attack vanes were available for mounting in any of the wing locations and were used for wing-off tests.

Cyclic Pitch Control

The longitudinal cyclic pitch control on the model was phased so as to produce nearly pure pitching moment at the nominal advance ratio, $\mu = 0.10$. The phase angle required to satisfy this criterion was found to be $\gamma = 54^\circ$ as shown in Figure 9; this corresponds to a phase lag between feathering and flapping of 36° less than that for a fully articulated rotor, for which $\gamma = 90^\circ$ would be expected.

Ground Proximity Model Support

For ground proximity operations, the model transmission is inverted so that the rotor hub is below the transmission swash plate strain gage balance system. The fuselage and wing support system is then suspended from a nonrotating inner spindle concentric to the rotor shaft, and the instrumentation wires pass up through this spindle. This arrangement can be seen in Figure 3, and the ground proximity reference locations are defined in Figure 10.

EXPERIMENTAL DATA

The experimental data are presented in nondimensional form about axis systems as defined in Figure 9; reference locations for various model components are shown in Figure 10. In particular, it should be noted that wing normal force and rolling moment coefficients are resolved about an axis located in the vertical plane which includes the rotor shaft axis.

All force and moment coefficients are based on rotor tip speed; rotor and fuselage coefficients are based on rotor radius and disk area times solidity ratio (i.e., blade area), and wing coefficients are based on the proper (large or small) wing span and planform area.

The data from these experiments are presented in Figures 13 through 127 as plots of the force or moment coefficients as functions of advance ratio. A summary of test conditions and data plots is presented in the summary of test conditions.

TEST PROCEDURE

All data presented in Figures 13 through 127 were obtained from quasi-steady tests wherein the rotor rpm was held constant and the velocity was programmed to vary during the course of the run. A continuous history was thereby obtained of the various forces and moments as functions of the advance ratio. Rate of variation of the variable was kept low so as to allow interpretation of the data as steady state. Specifically, model velocity was varied at a rate of approximately 0.7 ft/sec/sec ($\approx$ .02g). This technique of testing produced not only a large quantity of information in a given run, but also presented a clear indication of the slightest variation of the dependent forces and moments with the independent variable.

DATA ACQUISITION AND REDUCTION

Each data channel was sampled 20 times per second, and the data was telemetered from the moving carriage and recorded on magnetic tape at the telemetering ground station. This magnetic tape was subsequently processed through an analog to digital converter and digital computer system to provide the corrected coefficients presented. The data plots were drawn by the computer and represent linear interpolations between discrete data points, which were, in turn, 68 data samples averaged over 1.692 seconds. Therefore, in Figures 13 through 127, a data point was computed approximately every 1 ft/sec of velocity (i.e., an increment in μ = 0.004), and a straight line between these points was fitted by the computer.

MODEL TEST CONDITIONS

The nature of testing operations in the Dynamic Model Track requires that the model rotor be increased to testing rpm before the model is accelerated to test velocities. As a consequence, during a run the model encounters flight conditions ranging from hover to the maximum test velocity. For a helicopter rotor, this produces large magnitudes of blade flapping and, particularly for a hingeless rotor, very large blade and hub bending loads. To maintain blade stresses below allowable limits through the velocity range encountered, it was necessary to attenuate blade flapping by means of cyclic pitch control. This control was applied in proportion to carriage velocity during the accelerating nondata portion of a run and then held fixed at a predetermined level during the data portion of the run. Thus, even though velocity was varied during the runs for which the data are presented in Figures 13 through 127, the cyclic pitch was maintained constant during the data portion of the run at the value indicated in the summary of test conditions

LATERAL TEST CONDITIONS

In the lateral ground proximity tests, the fuselage-wing support system was yawed through 90° with respect to the longitudinal axis of the Dynamic Model Track and the six-component rotor balance. The data from these tests are presented in Figures 108 through 127 about the same axis system as used for the remainder of the data. Thus, for the lateral tests only, the fuselage pitching moment acts about an axis that is parallel to the rotor pitch axis. The velocity is still varied along the rotor-strain gage balance longitudinal axis; rotor shaft angle of attack produces a wing/fuselage roll angle of equal but opposite magnitude.

HOVER TESTS OUT OF GROUND EFFECT

Previous experiments were performed on the subject compound helicopter model on the Dynamic Model Track at flight conditions near hovering flight out of ground proximity. Data from these experiments are reported in Reference 5.

SUMMARY OF TEST CONDITIONS						
Ω = 550 rpm, A_{1s} = 0° , i_W = 0°						
Collective Pitch $\theta_{.75R}$ (deg)	Wing Size	Wing Position	Rotor Shaft Angle α_s (deg)	Run Numbers	Figure Numbers	Long. Cyclic B_{1s} (deg)
12	-	OFF	-12, -8, -4, 0, +4	94, 93, 90, 91, 92	35, 36	6.5
	LARGE	HIGH	-12, -8, -4, 0, +4	95, 96, 100, 98, 99	37,38,39	
		LOW	-4, +4	103, 104	40, 41	
10	-	OFF	-12, -8, -4, 0, +4	25, 24, 19, 21, 23	24, 25	
	LARGE	HIGH	-12, -8, -4, 0, +4	42, 40, 35, 33, 34	26,27,28	
		LOW	-12, -8, -4, 0, +4	43, 44, 45, 49, 48	29, 30	
	SMALL	HIGH	-12, -8, -4, 0	27, 28, 29, 32	31, 32	
		LOW	-8, -4, 0	52, 54, 51	33, 34	
8	-	OFF	-12, -8, -4 0, +4	82, 81, 87, 86, 83	13, 14	
	LARGE	HIGH	-12, -8, -4 0, +4	74, 73, 72, 76, 75	15,16,17	
		LOW	-12, -8, -4, 0, +4	66, 63, 67, 61, 62	18, 19	
	SMALL	HIGH	-8, -4, 0	80, 78, 77	20, 21	
		LOW	-8, -4, 0	59, 58, 60	22, 23	
6	LARGE	HIGH	40, 44, 48, 52, 56	276, 275, 274, 273, 271	57,58,59	1.8
		LOW	40, 48, 56	258, 259, 261	60, 61	
	SMALL	HIGH	40, 48, 56	266, 267, 268	62, 63	
		LOW	40, 48, 56	264, 263, 262	64, 65	
4	LARGE	HIGH	40, 44, 48, 52, 56	243, 244, 235, 245, 246	48,49,50	
		LOW	40, 48, 56	255, 254, 253	51, 52	
	SMALL	HIGH	40, 48, 56	249, 248, 247	53, 54	
		LOW	40, 48, 56	250, 251, 252	55, 56	
2	LARGE	HIGH	40, 44, 48, 52, 56	225, 226, 227, 228, 229	45,46,47	
0	LARGE	HIGH	36, 48, 60, 72, 80, 90	242, 241, 240, 238, 239, 288	42,43,44	

SUMMARY OF TEST CONDITIONS (CONTINUED)

GROUND PROXIMITY TESTS

$\Omega = 550$ rpm, $A_{1_s} = 0^\circ$, $i_W = 0^\circ$ $\qquad \frac{h}{D} = 0.75$

Collective Pitch $\theta_{.75R}$ (deg)	Wing Size	Wing Position	Rotor Shaft Angle α_s (deg)	Run Numbers	Figure Numbers	Long. Cyclic B_{1_s} (deg)
12	FUSELAGE OFF		-4, 0, +4	121, 122, 120	68	0
	-	OFF	0	124	73, 74	
10	FUSELAGE OFF		-8, -4, 0, +4, +8	113, 115, 107, 109, 111	67	0
	-	OFF	-4, 0, +4	129, 126, 128	71, 72	
	LARGE	HIGH	-4, 0, +4	140, 138, 139	78,79,80	
	LARGE	LOW	-4, 0, +4	157, 155, 156	83, 84	
	SMALL	HIGH	-4, 0, +4	130, 132, 131	85, 86	
8	FUSELAGE OFF		-4, 0, +4	117, 118, 119	66	0
	-	OFF	0	125	69, 70	
	LARGE	HIGH	0	141	75,76,77	
	LARGE	LOW	0	151	81, 82	
$\frac{h}{D} = 0.30$						
12	FUSELAGE OFF		-4, 0, +4	202, 203, 201	89	0
	-	OFF	0	190	94, 95	
10	FUSELAGE OFF		-8, -4, 0, +4, +8	197, 196, 193, 194, 195	88	0
	-	OFF	-4, 0, +4	185, 183, 187	92, 93	
	LARGE	HIGH	-4, 0, +4	179, 177, 176	99, 100, 101	
	LARGE	LOW	-4, 0, +4	161, 162	104,105	
	SMALL	HIGH	-4, 0, +4	180, 182, 181	106,107	

SUMMARY OF TEST CONDITIONS (CONCLUDED)

GROUND PROXIMITY TESTS

Ω = 550 rpm, $A_{1_s} = 0^\circ$, $i_w = 0^\circ$

Collective Pitch $\theta_{.75R}$ (deg)	Wing Size	Wing Position	Rotor Shaft Angle α_s (deg)	Run Numbers	Figure Numbers	Long. Cyclic B_{1_s} (deg)
LONGITUDINAL $\frac{h}{D} = 0.30$						
8	FUSELAGE OFF		-4, 0, +4	198, 199, 200	87	0
	-	OFF	0	189	90, 91	
	LARGE	HIGH	0	169	96, 97, 98	
		LOW	0	167	102,103	
LATERAL $\frac{h}{D} = 0.75$						
10	LARGE	HIGH	0, +4, +8	143, 144, 145	111,112, 113	0
		LOW	0, 4, 8	149, 148, 147	116,117	
8	LARGE	HIGH	0	142	108,109, 110	0
		LOW	0	150	114,115	
LATERAL $\frac{h}{D} = 0.30$						
10	LARGE	HIGH	0, +4	173, 174	121,122, 123	0
		LOW	0, +4	165, 164	126,127	
8	LARGE	HIGH	0	171	118,119, 120	0
		LOW	0	166	124,125	

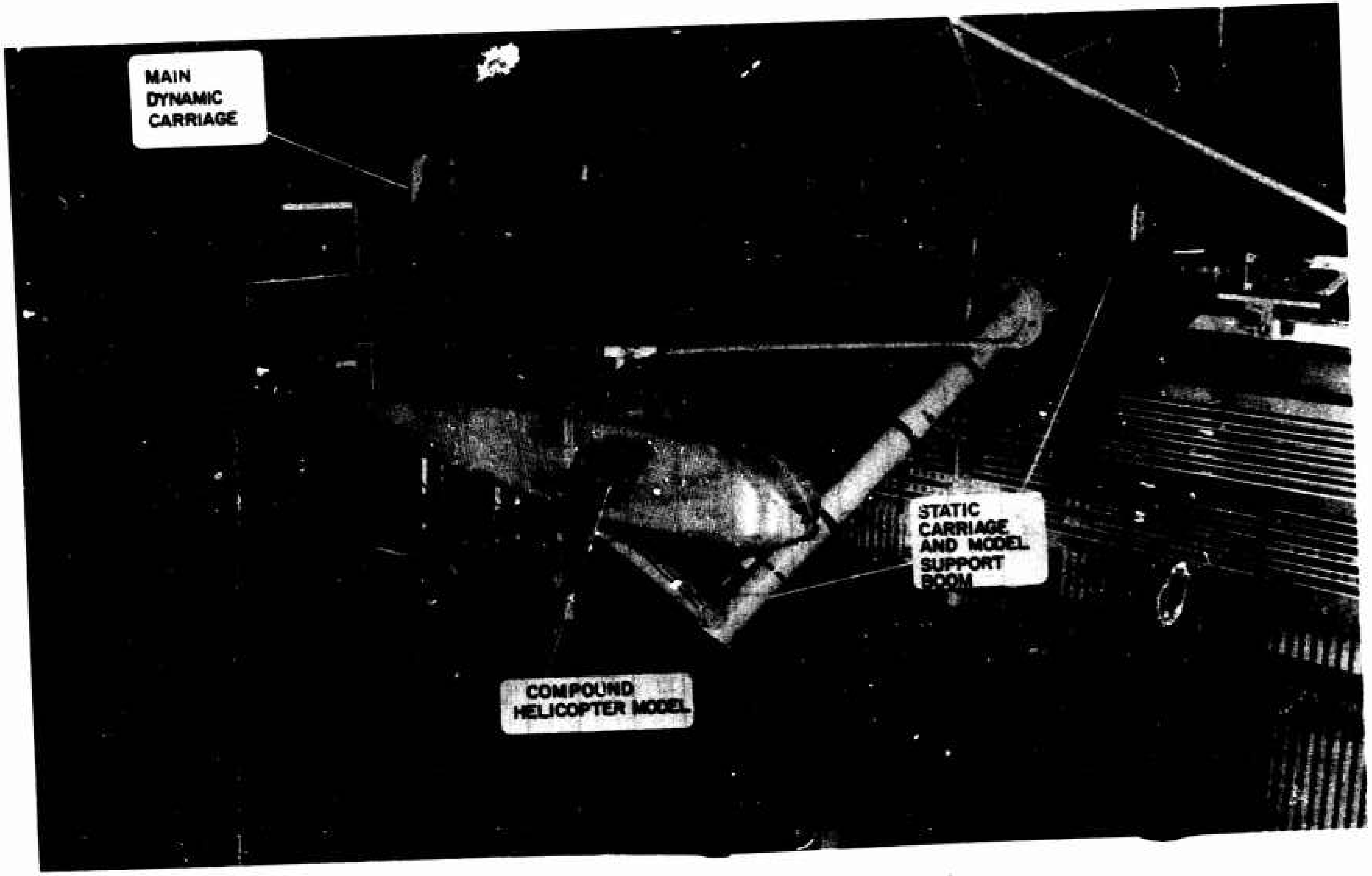

Figure 1. Carriage Model System Arrangement.

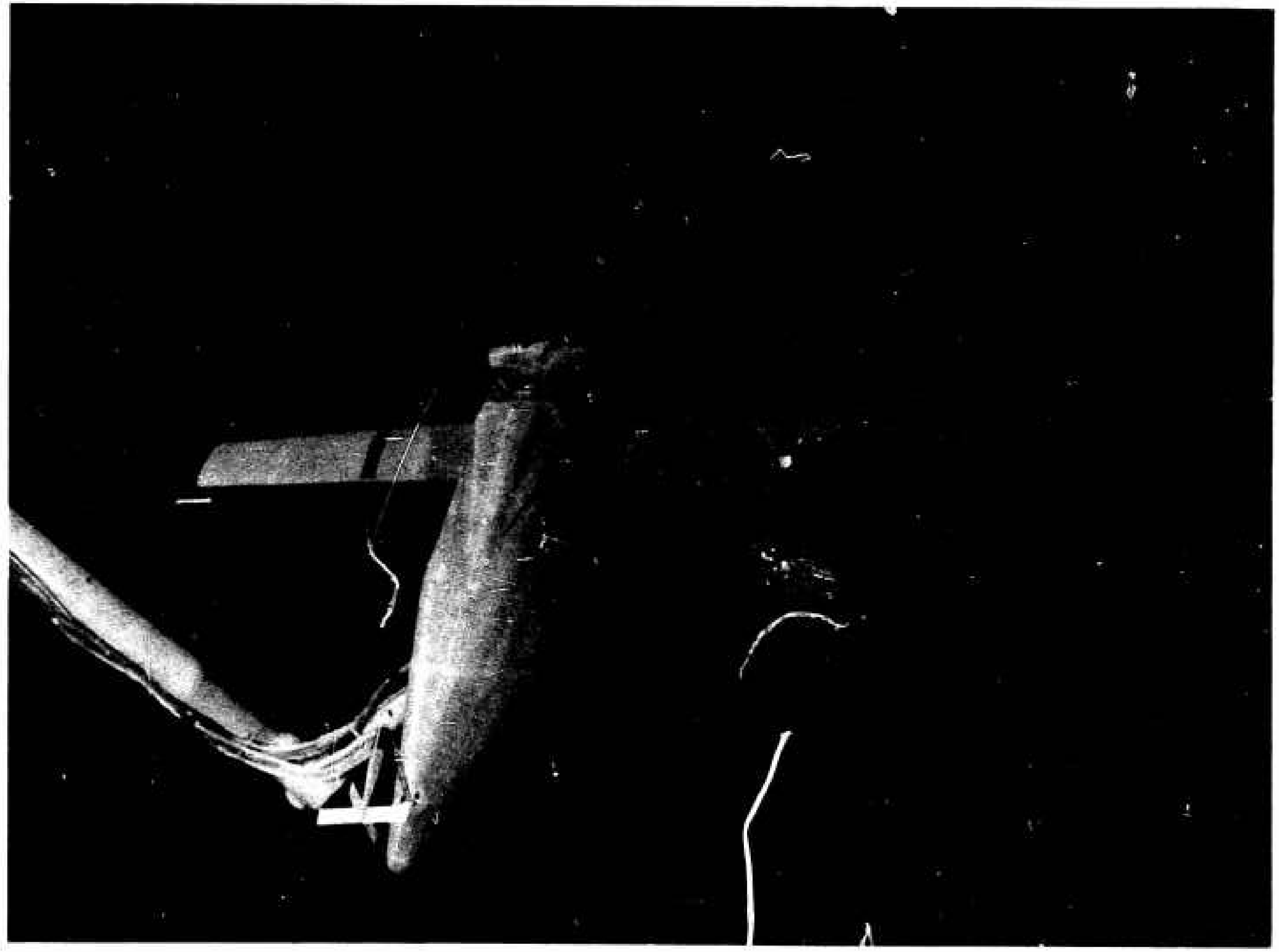

Figure 2. Compound Helicopter Model Mounted in Dynamic Model Track.

Figure 3. Compound Helicopter Model Mounted for Ground Proximity Tests.

GEOMETRIC CHARACTERISTICS

ROTOR		
NO. OF BLADES	4	
DIAMETER	96"	
BLADE CORD	2.5"	
AIRFOIL SECTION	NACA 0015	
SOLIDITY	0.0662	
DISC AREA	7238 in^2	
LINEAR TWIST	8°	
WINGS		
AIRFOIL SECTION	NACA 63_2 A415	
ASPECT RATIO	6	
TAPER RATIO	3:2	
SWEEP $C_{w/4}$ LINE	0	
TWIST	0	
DIHEDRAL	0	
	LARGE	SMALL
SPAN	72"	48"
AREA	868 in.^{2}	399 in.^{2}
C_{root}	14.4"	9.6"
C_{tip}	9.6"	6.4"
$\frac{\text{WING AREA}}{\text{ROTOR AREA}}$	12%	5.5%

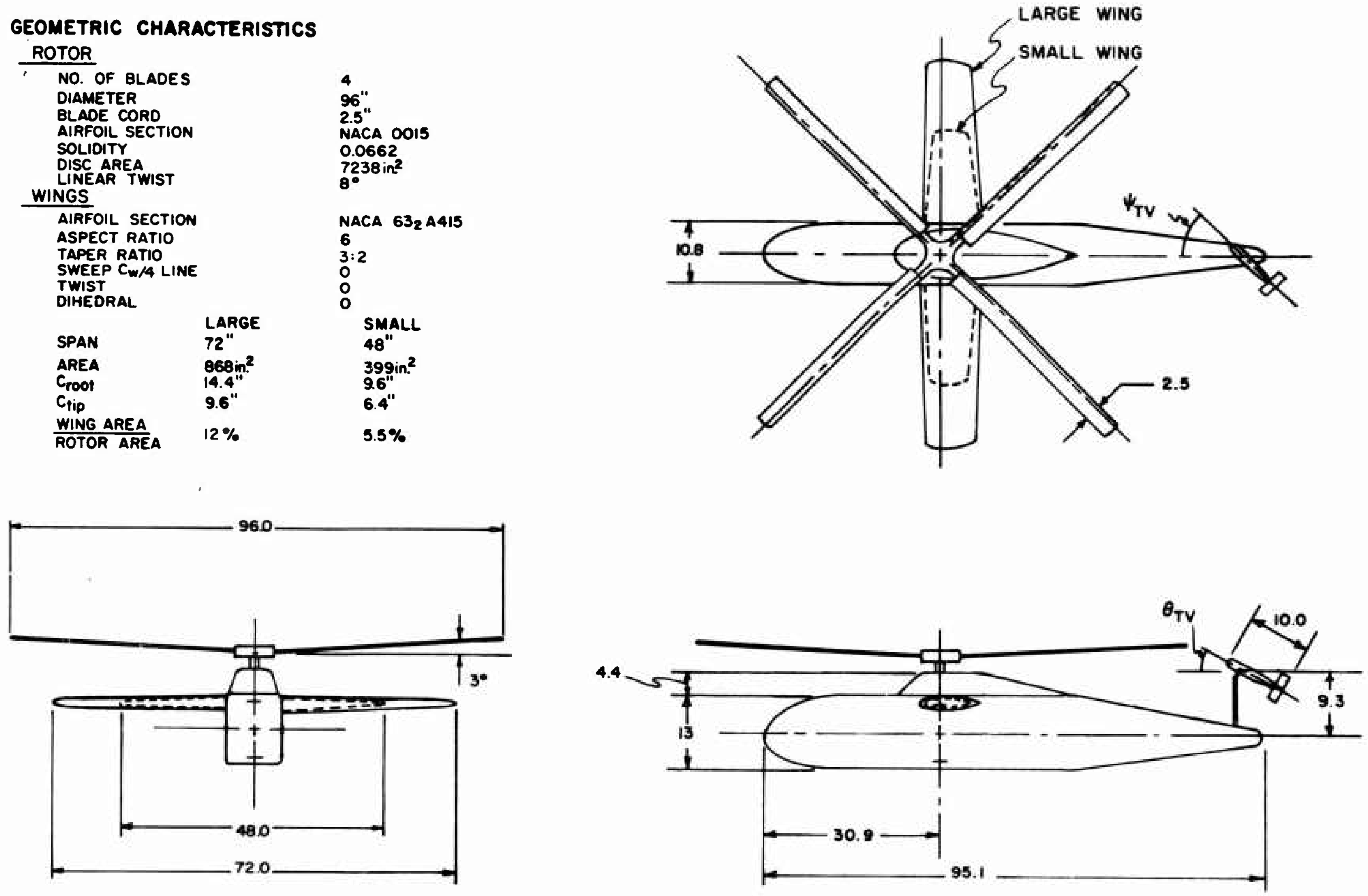

Figure 4. Compound Helicopter Model, General Arrangement.

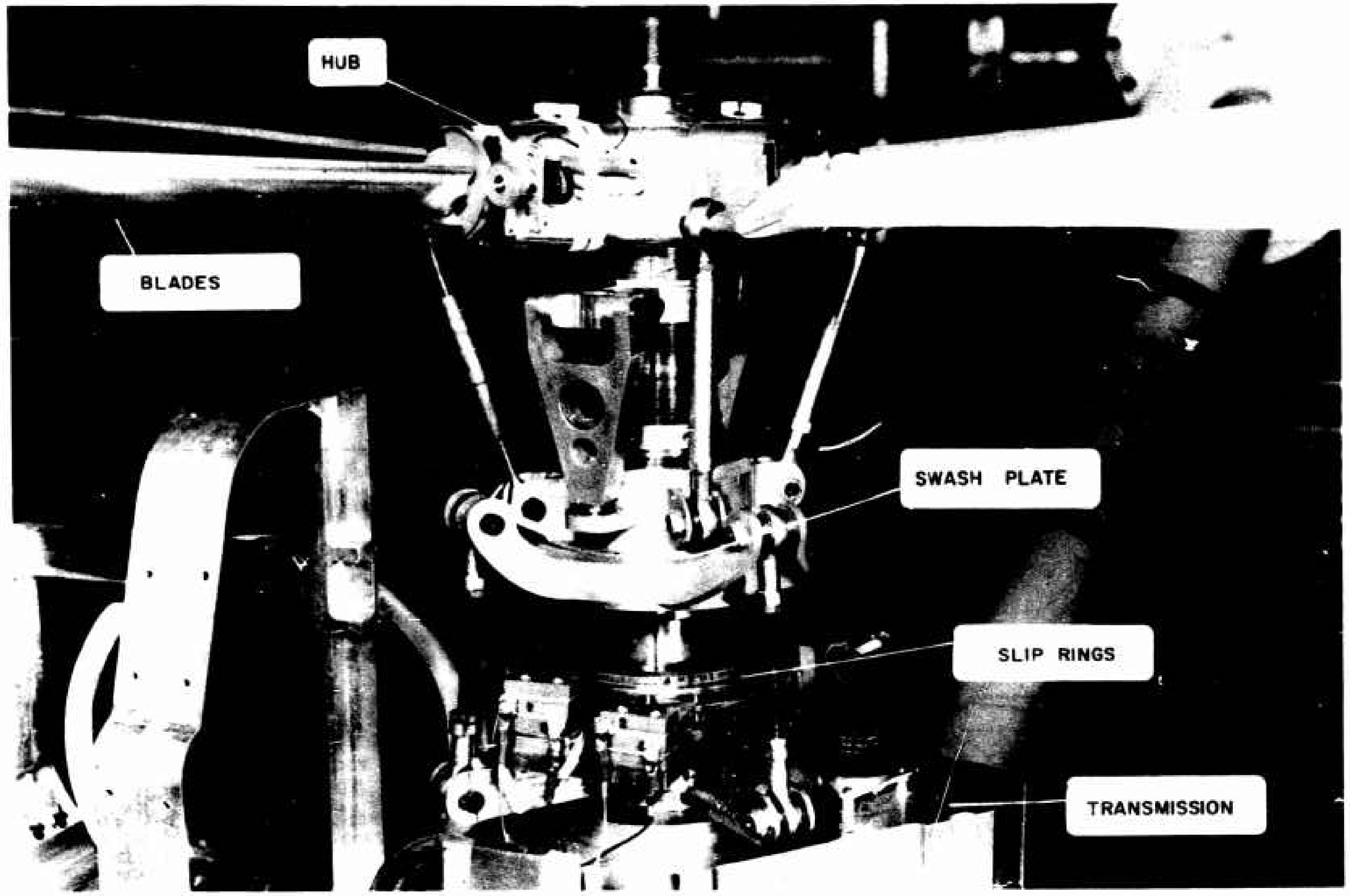

Figure 5. Detail of Rotor Mechanical System.

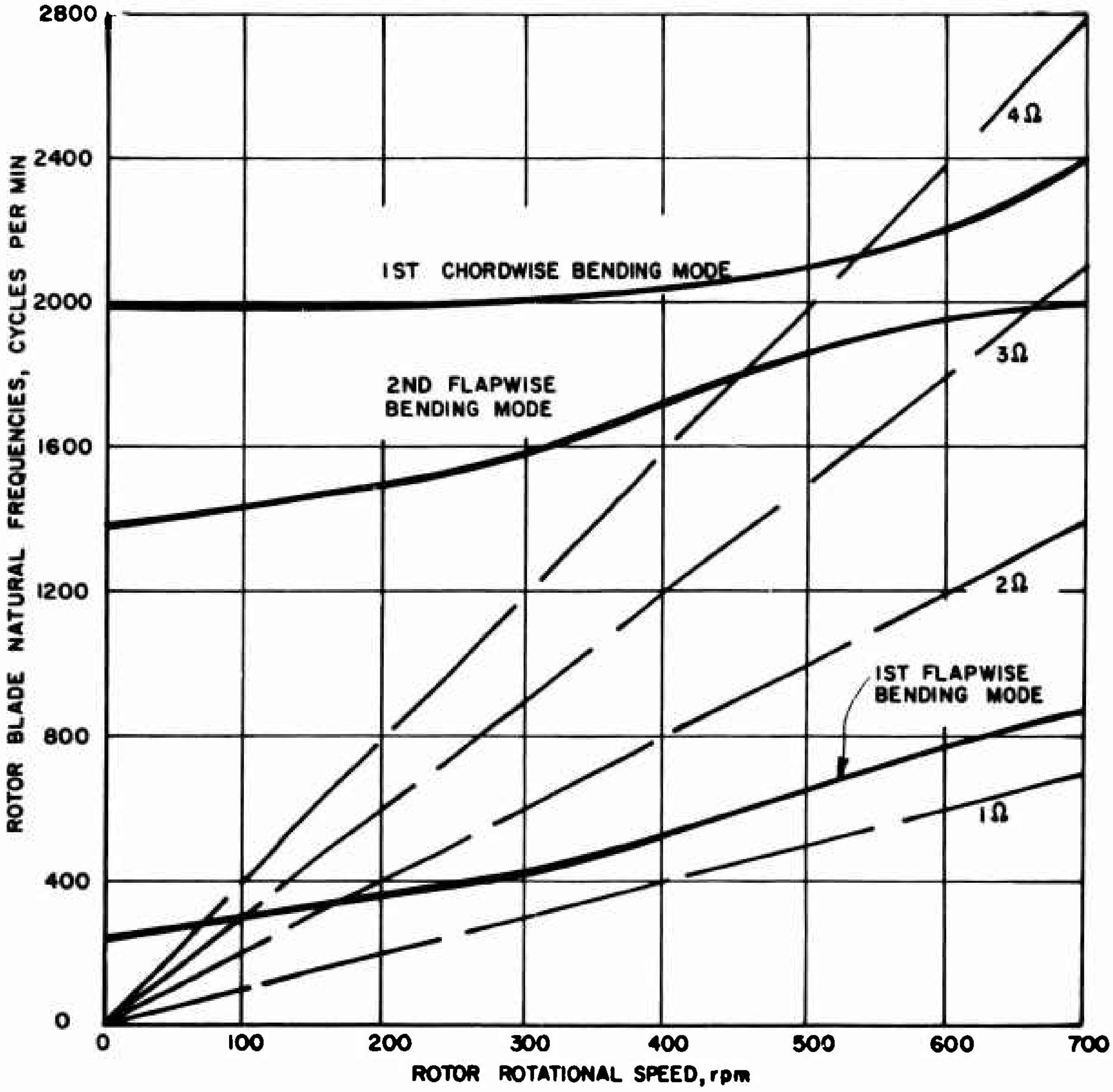

Figure 6. Blade Natural Frequencies.

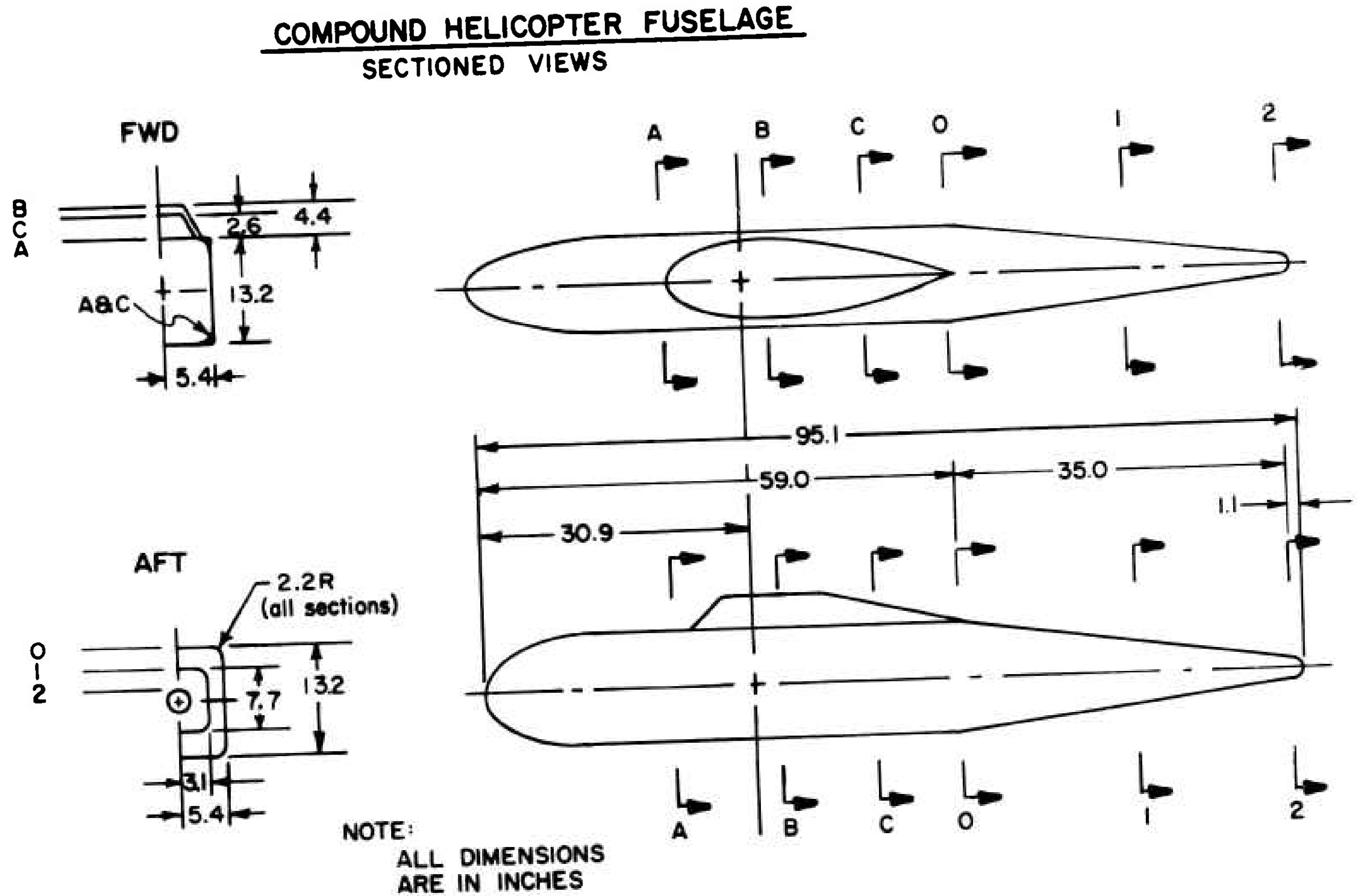

Figure 7. Fuselage Geometric Characteristics.

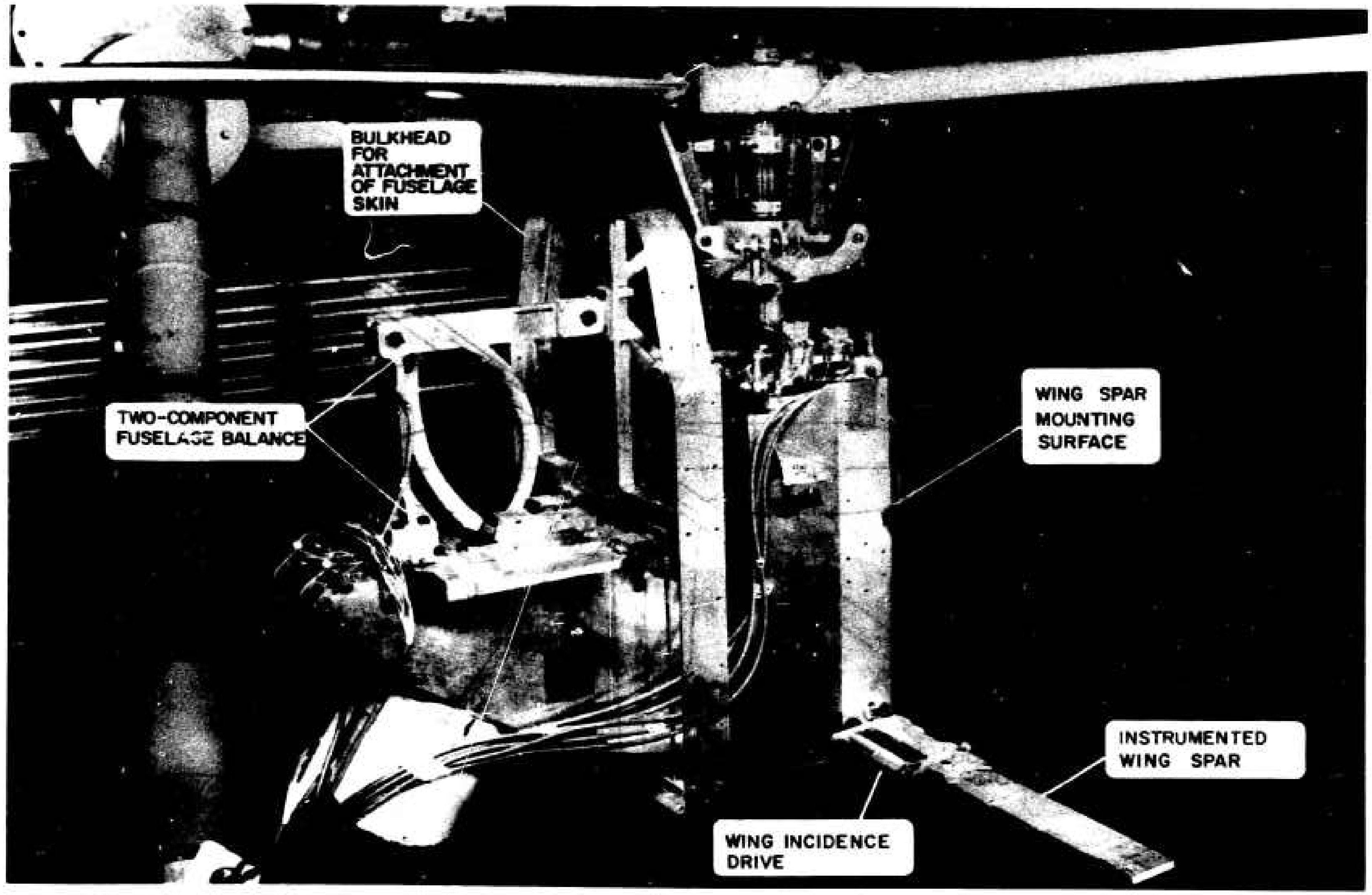

Figure 8. Photograph of Model Mechanical System Showing Fuselage and Wing Attachments.

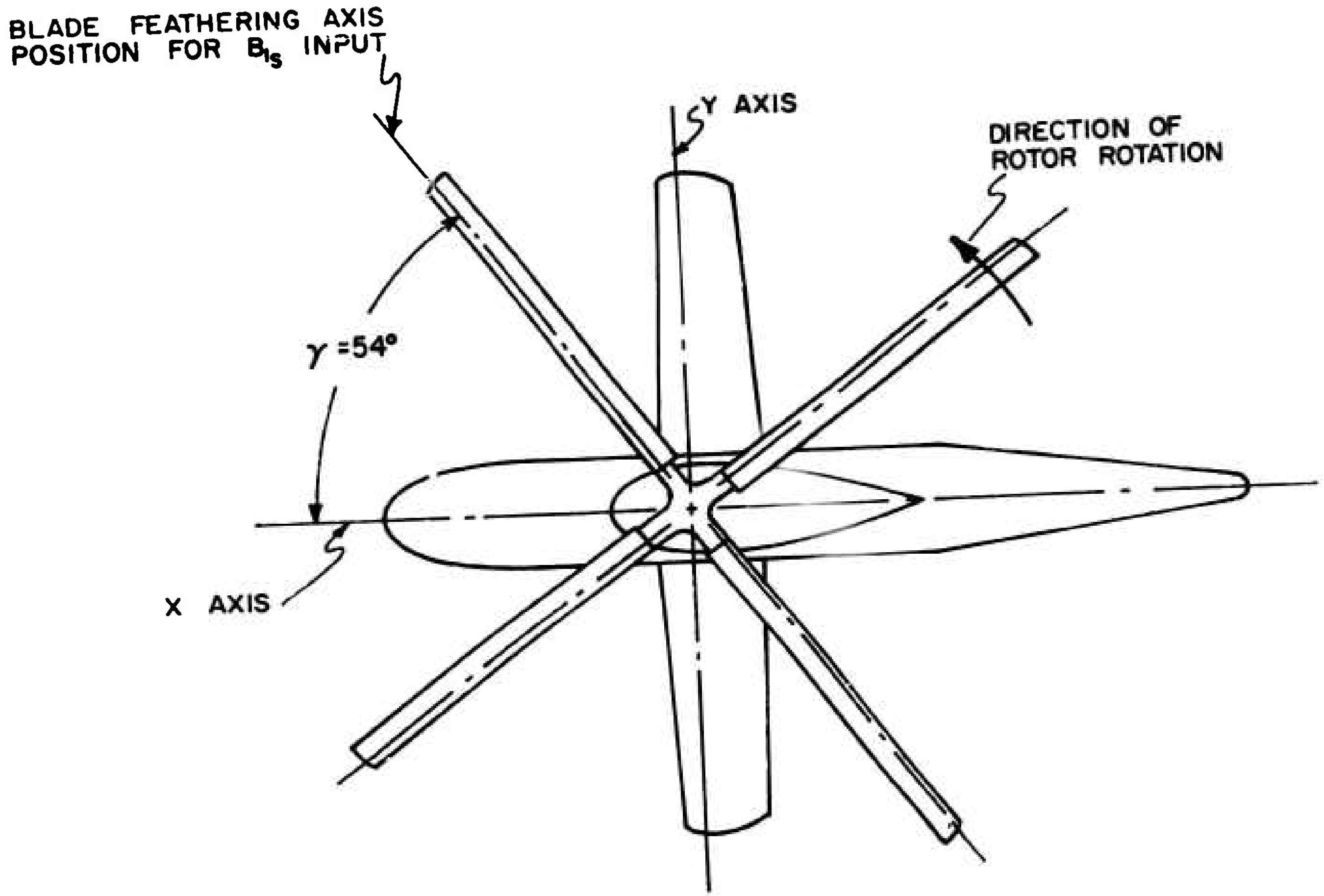

Figure 9. Swash Plate Phasing for Cyclic Pitch Program.

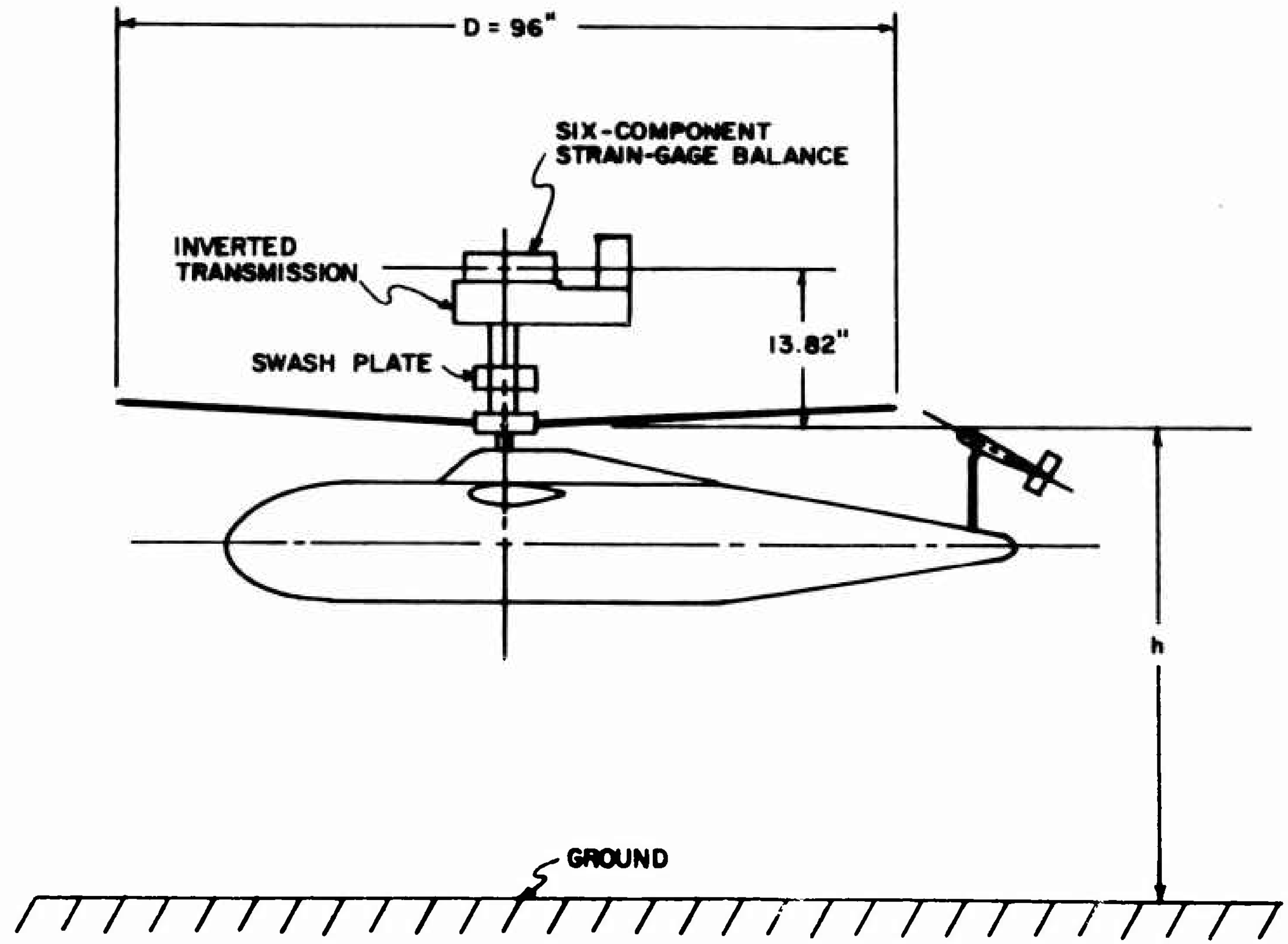

Figure 10. Model Reference Locations for Ground Proximity Tests.

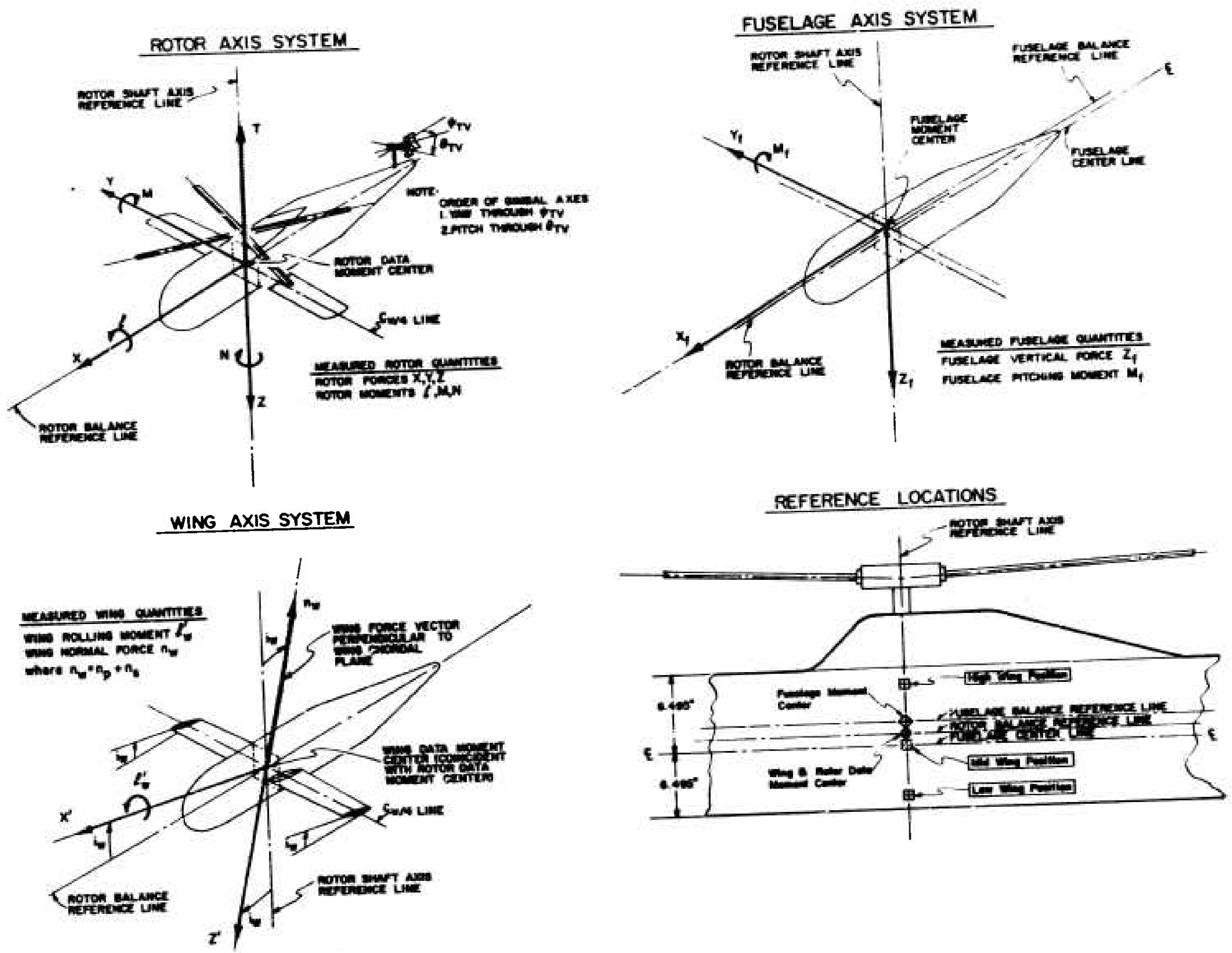

Figure 11. Axis System for Data Presentation.

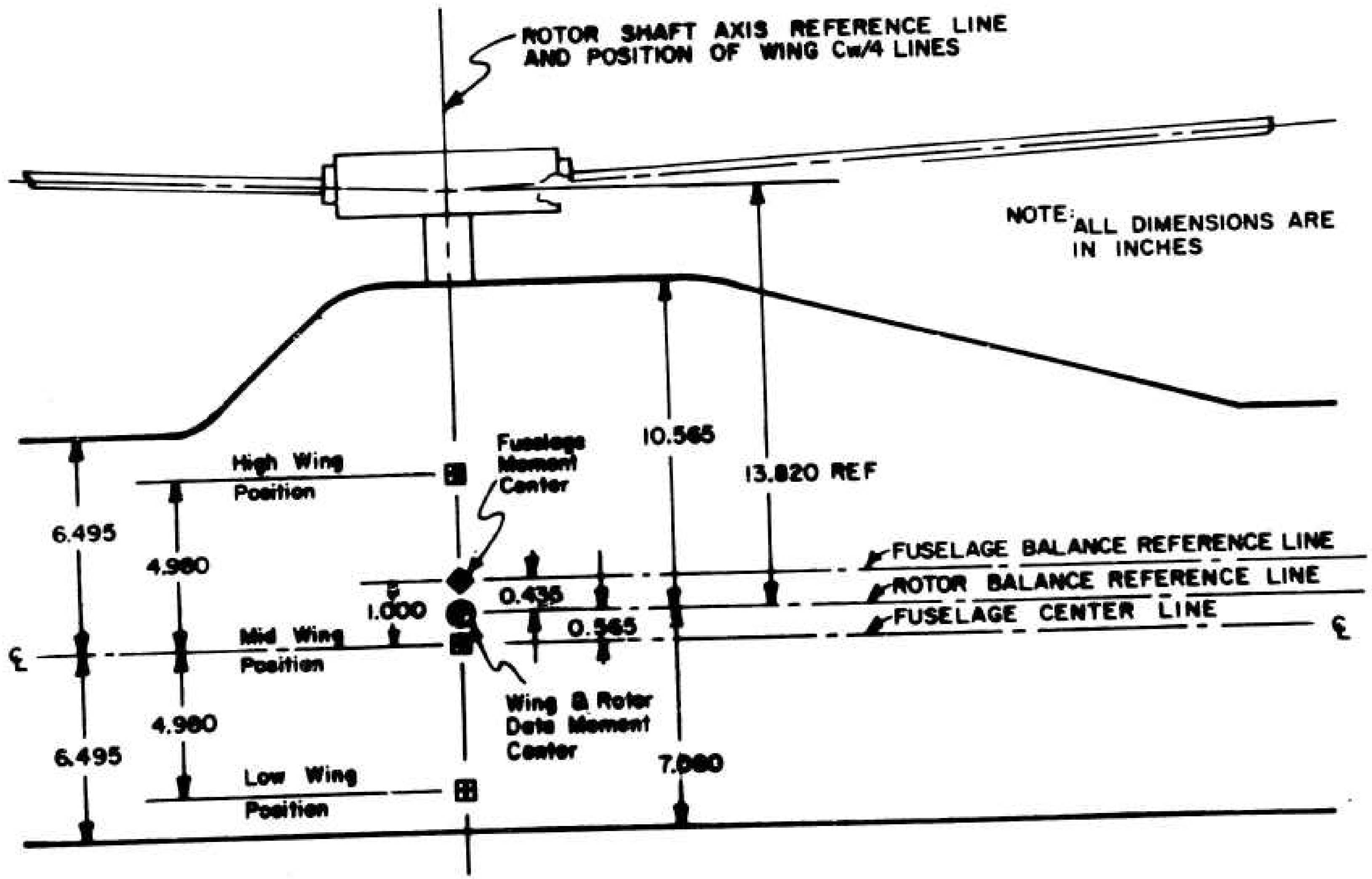

Figure 12. Model Component Reference Locations.

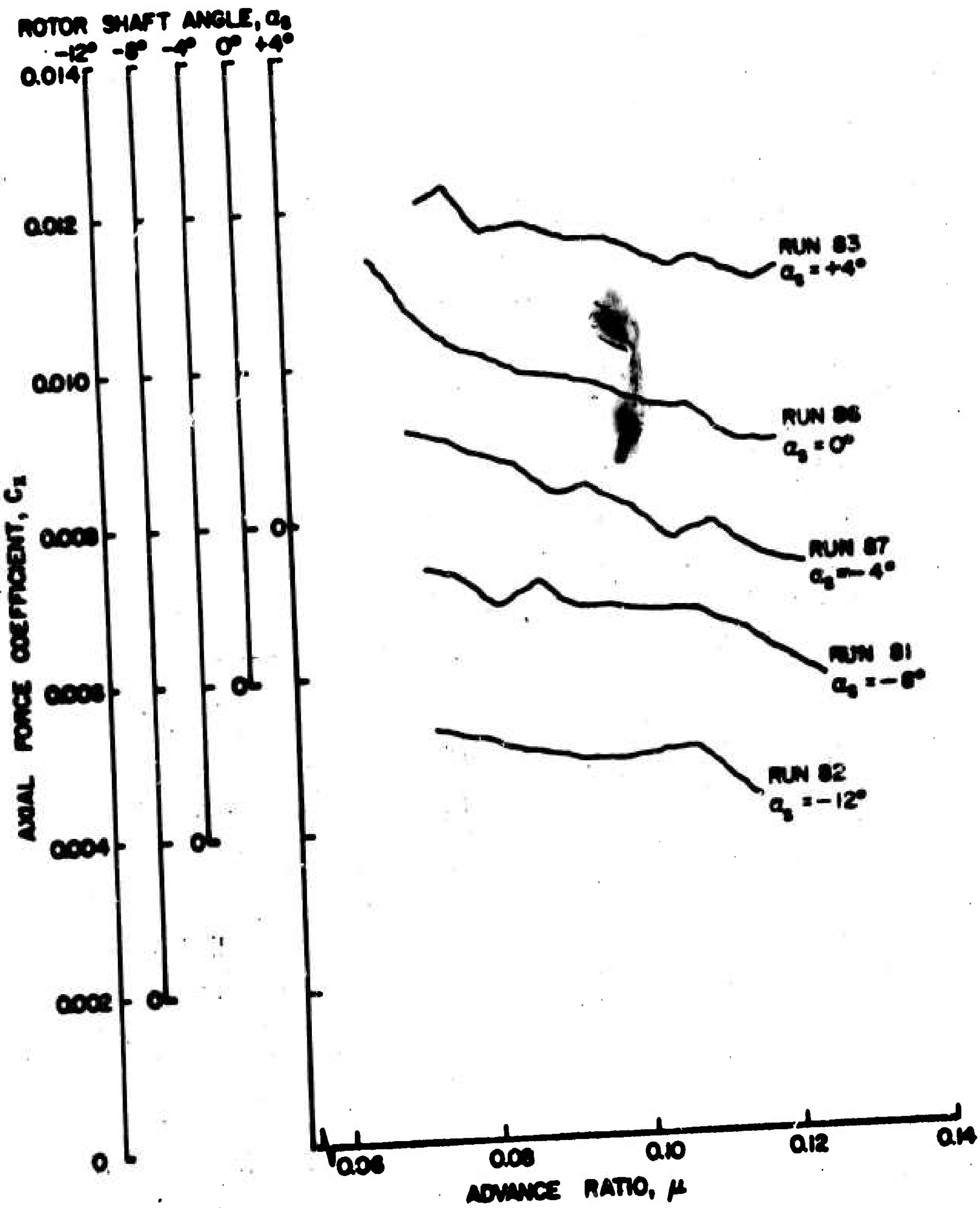

Figure 13a. Rotor Force and Moment Coefficients as Functions of Advance Ratio, $\theta_{.75R} = 8^\circ$, Wing Off.

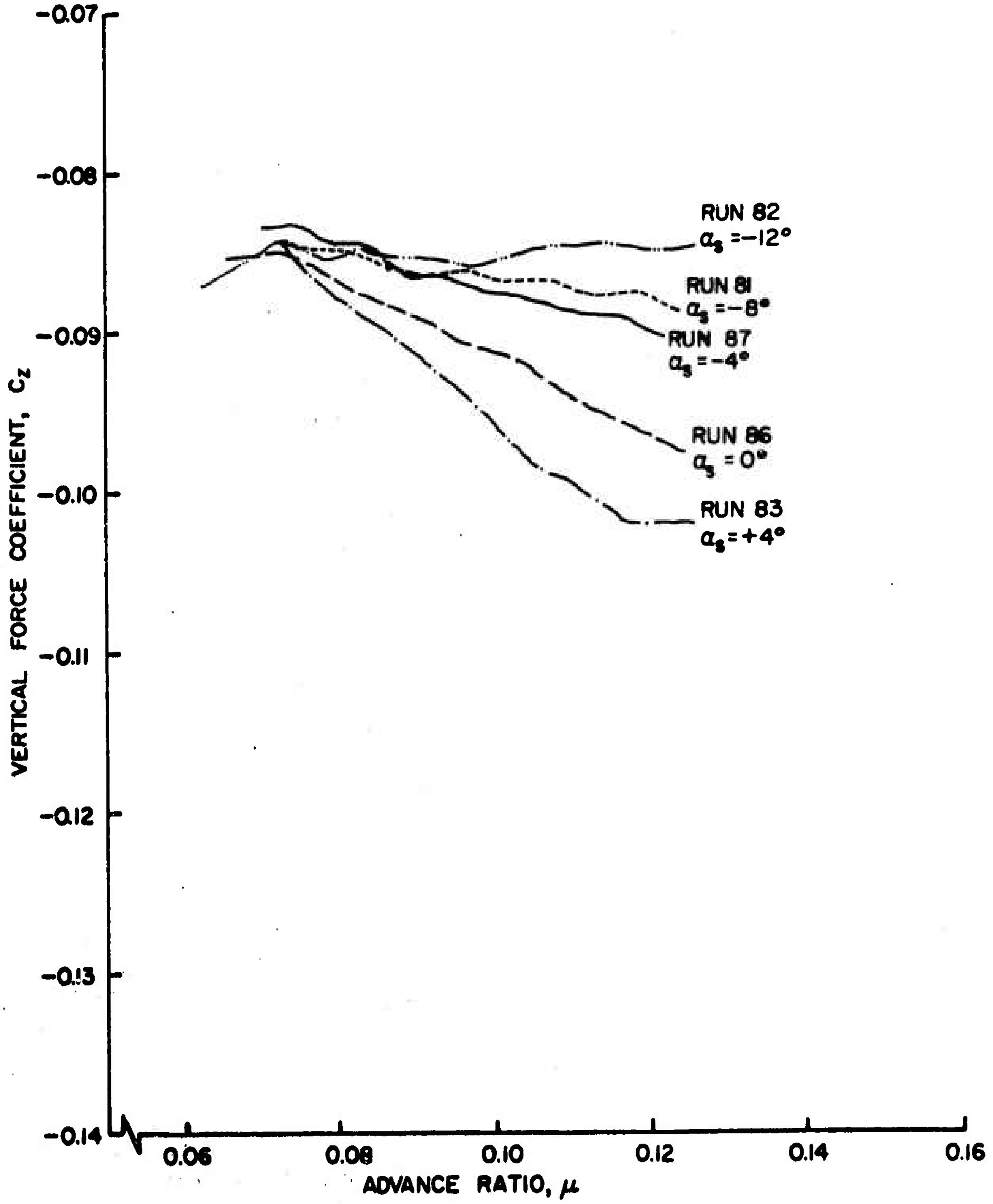

Figure 13b. Rotor Force and Moment Coefficients as Functions of Advance Ratio, $\theta_{.75R} = 8^{\circ}$, Wing Off.

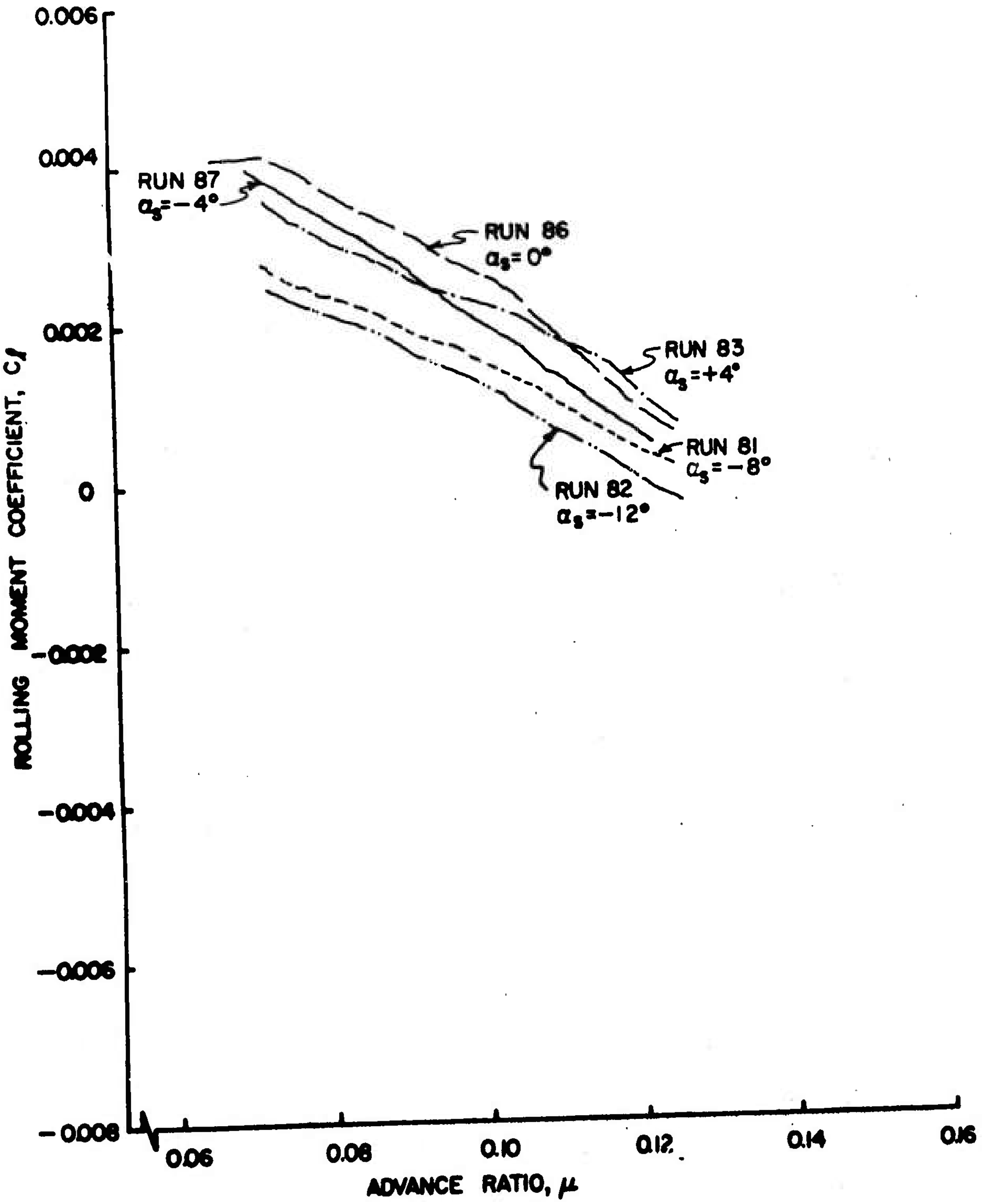

Figure 13c. Rotor Force and Moment Coefficients as Functions of Advance Ratio, $\theta_{.75R} = 8^\circ$, Wing Off.

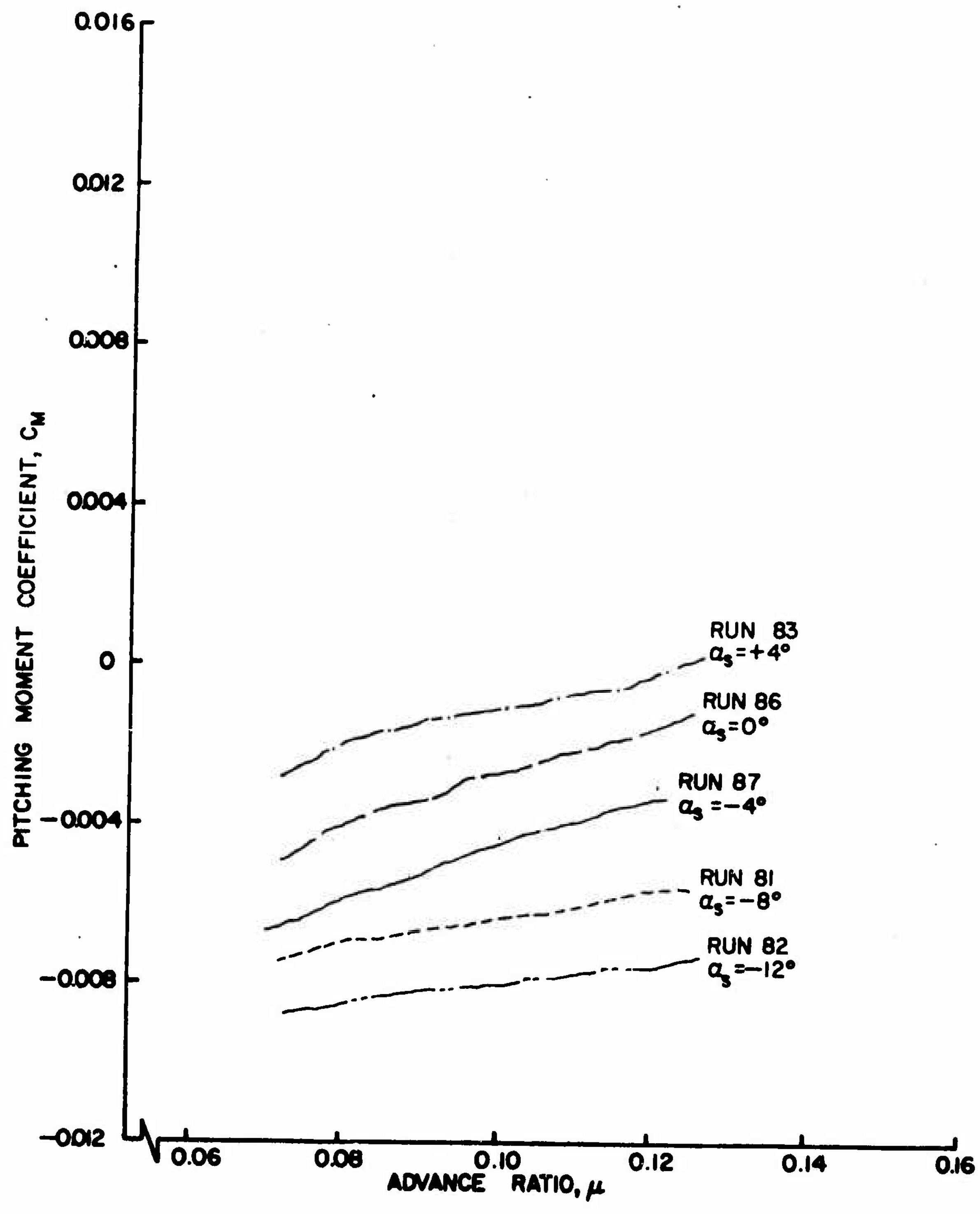

Figure 13d. Rotor Force and Moment Coefficients as Functions of Advance Ratio, $\theta_{.75R} = 8^\circ$, Wing Off.

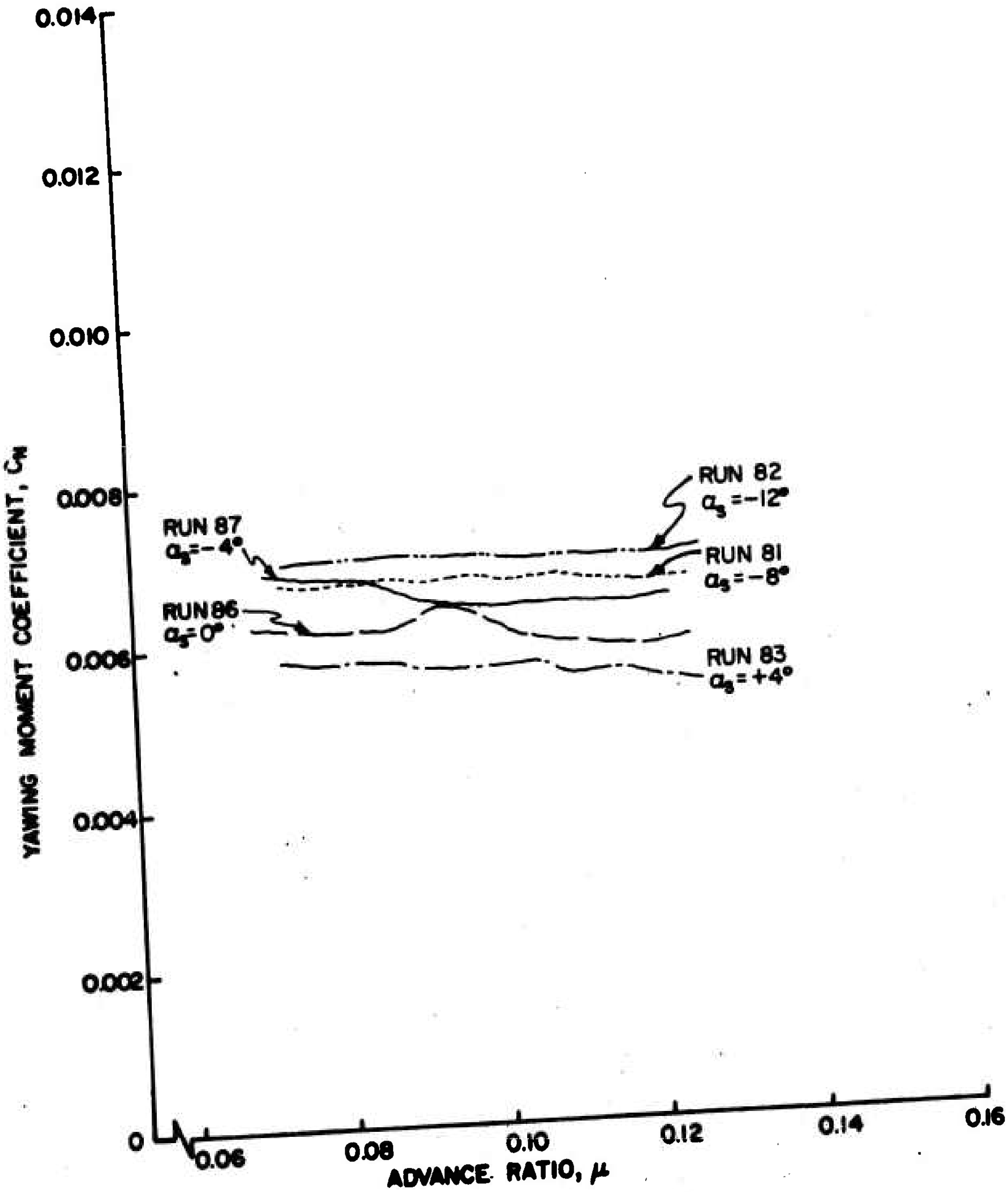

Figure 13e. Rotor Force and Moment Coefficients as Functions of Advance Ratio, $\theta_{.75R} = 8^{\circ}$, Wing Off.

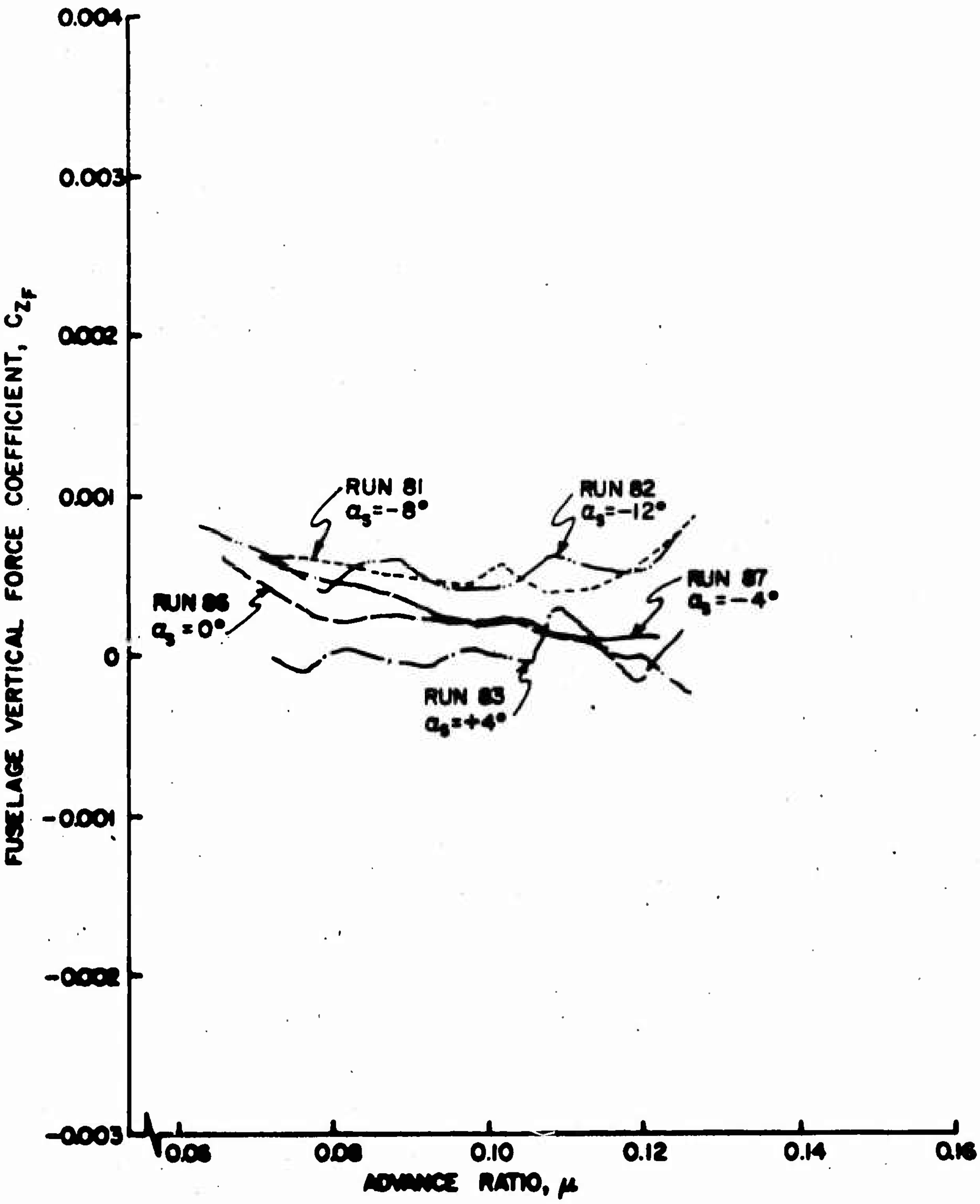

Figure 14a. Fuselage Vertical Force and Pitching Moment Coefficients as Functions of Advance Ratio, $\theta_{.75R} = 8°$, Wing Off.

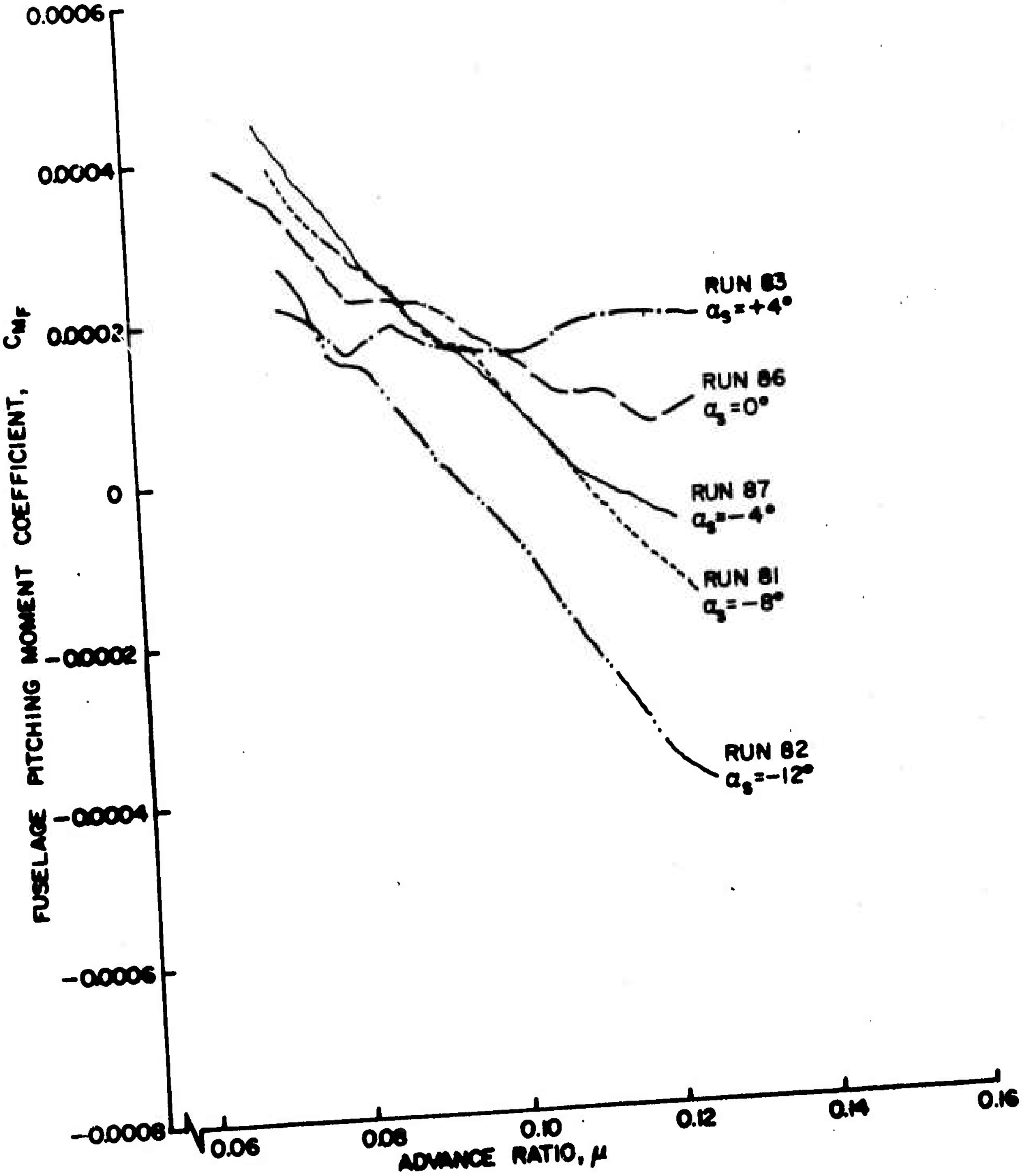

Figure 14b. Fuselage Vertical Force and Pitching Moment Coefficieients as Functions of Advance Ratio, $\theta_{.75R} = 8°$, Wing Off.

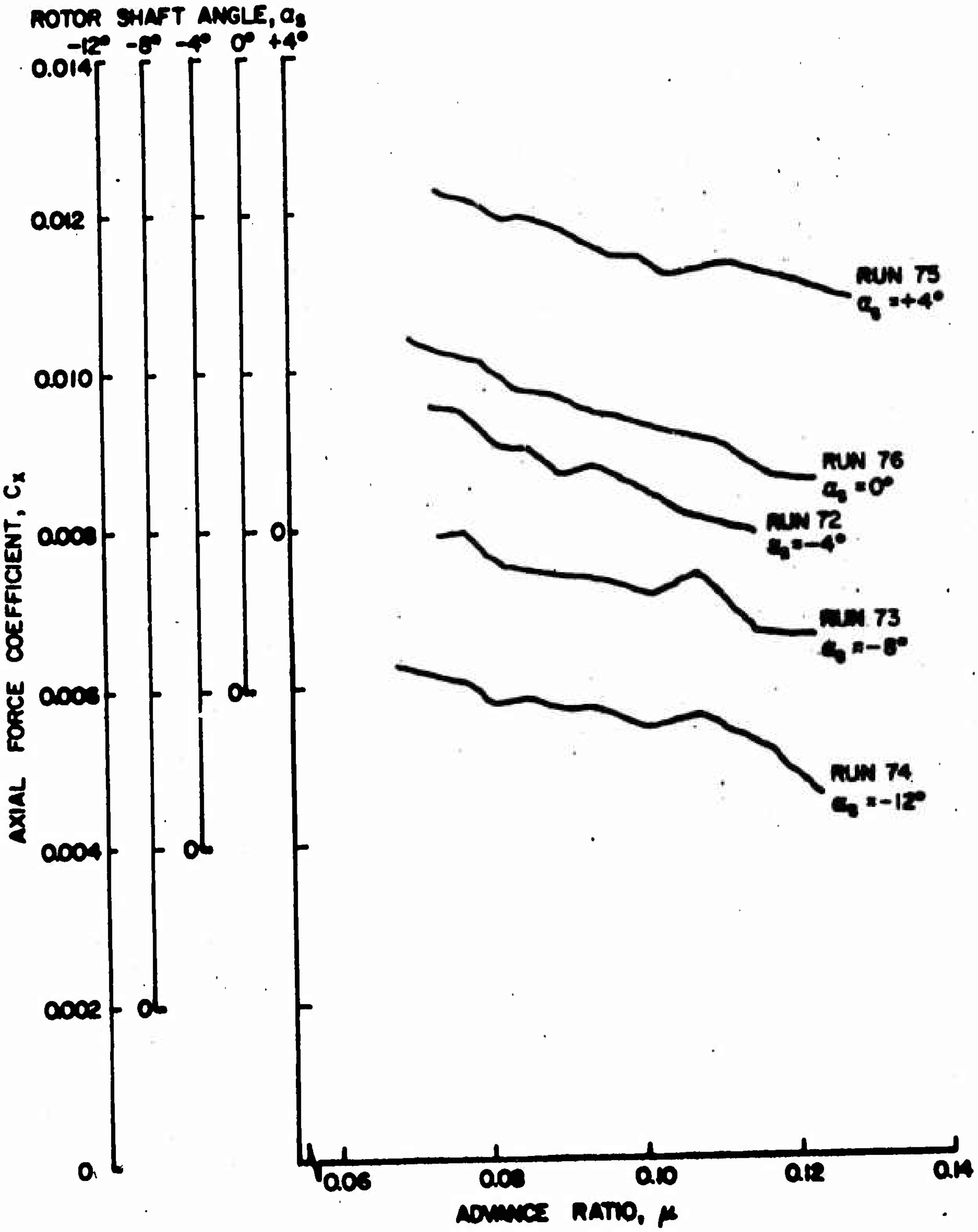

Figure 15a. Rotor Force and Moment Coefficients as Functions of Advance Ratio, $\theta_{.75R} = 8°$, Large Wing on High.

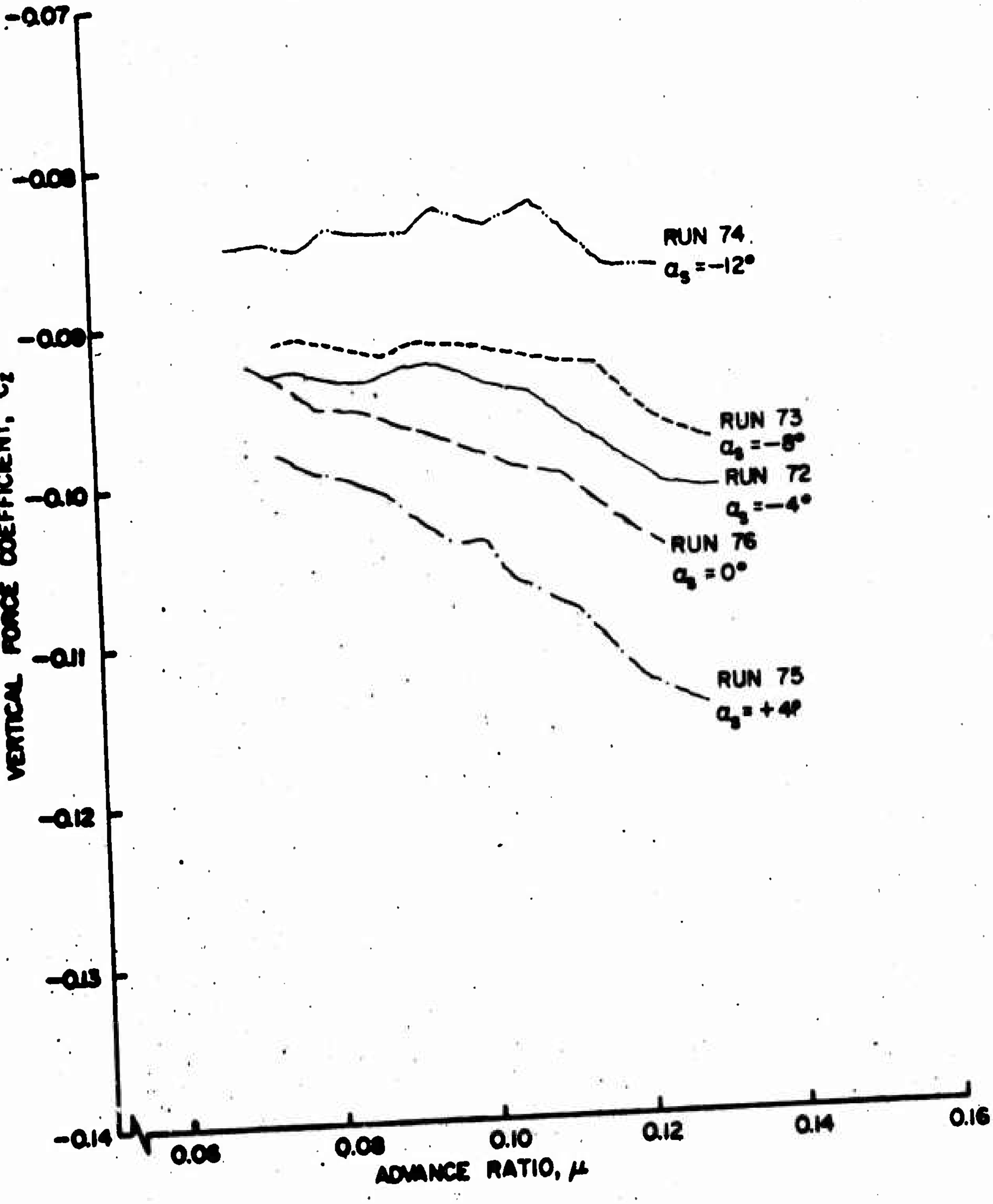

Figure 15b. Rotor Force and Moment Coefficients as Functions of Advance Ratio, $\theta_{.75R} = 8°$, Large Wing on High.

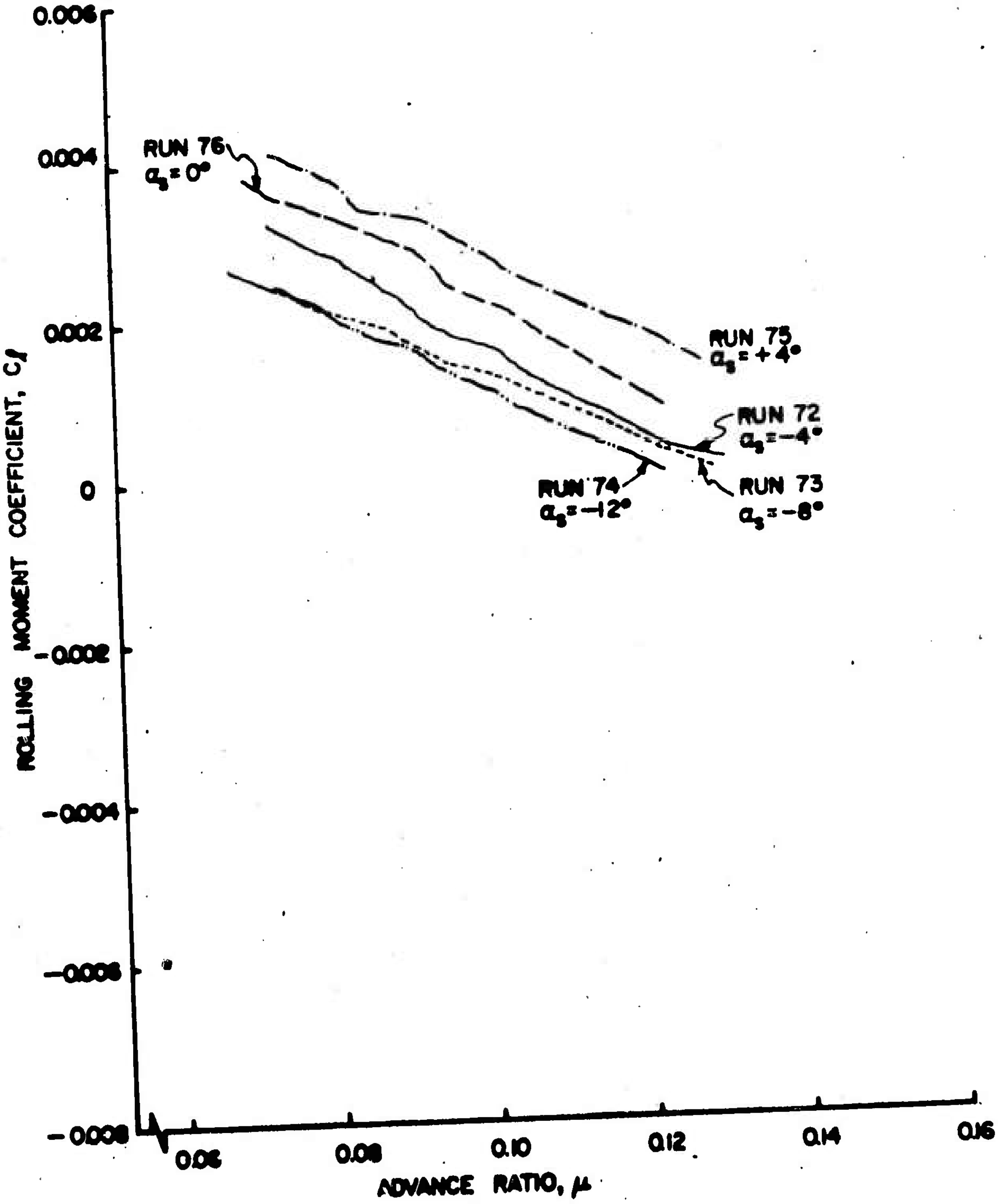

Figure 15c. Rotor Force and Moment Coefficients as Functions of Advance Ratio, $\theta_{.75R} = 8°$, Large Wing on High.

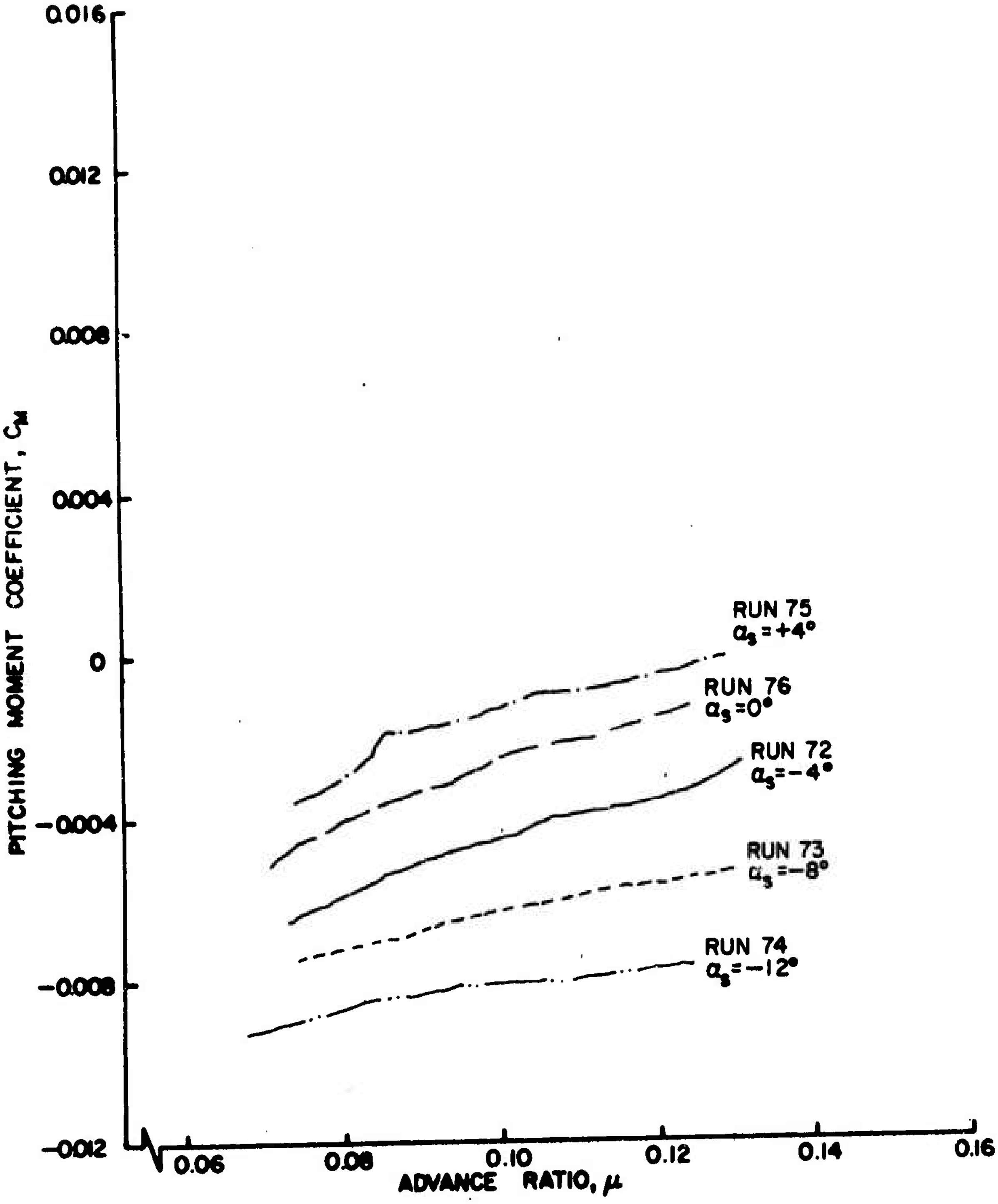

Figure 15d. Rotor Force and Moment Coefficients as Functions of Advance Ratio, $\theta_{.75R} = 8°$, Large Wing on High.

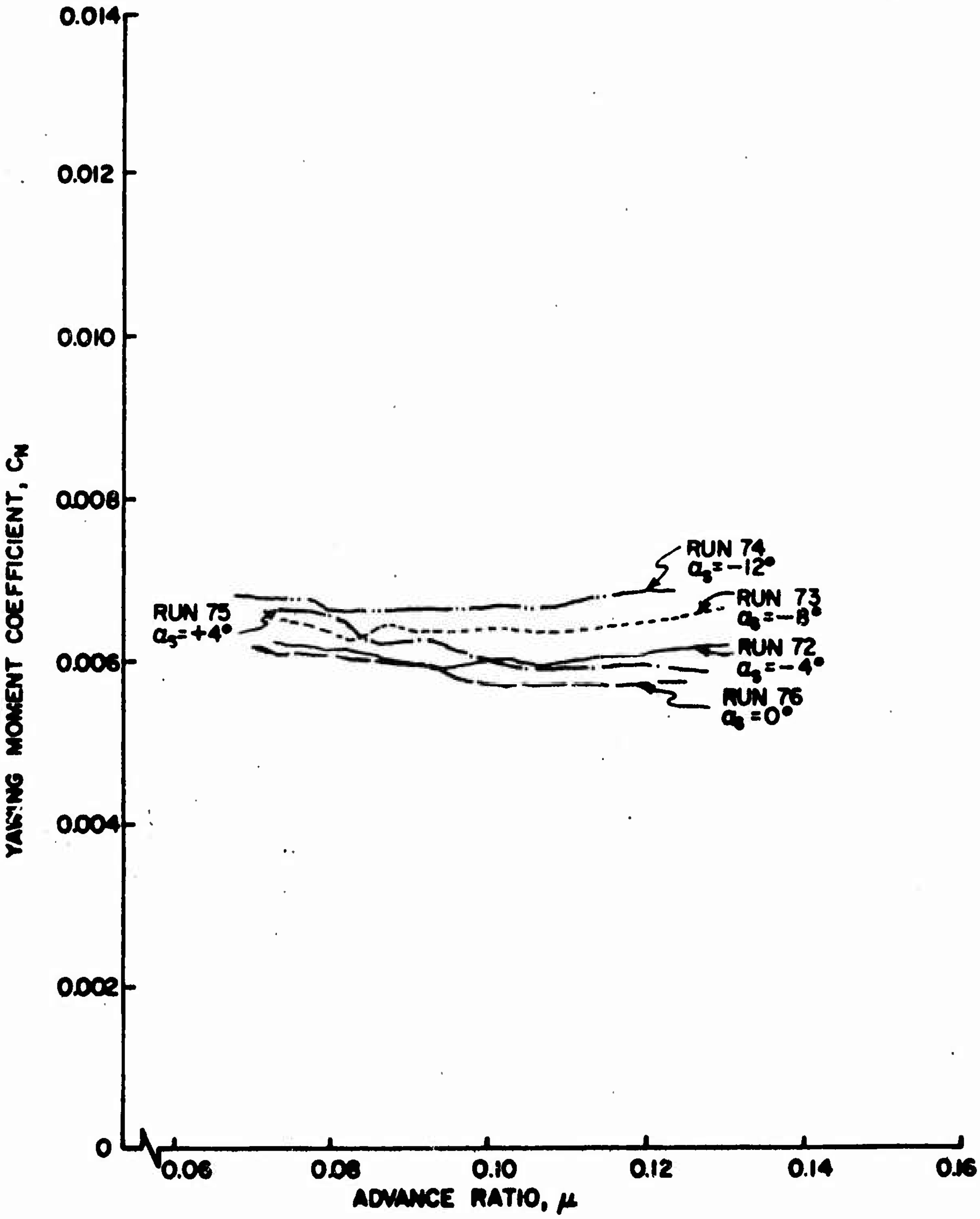

Figure 15e. Rotor Force and Moment Coefficients as Functions of Advance Ratio, $\theta_{.75R} = 8°$, Large Wing on High.

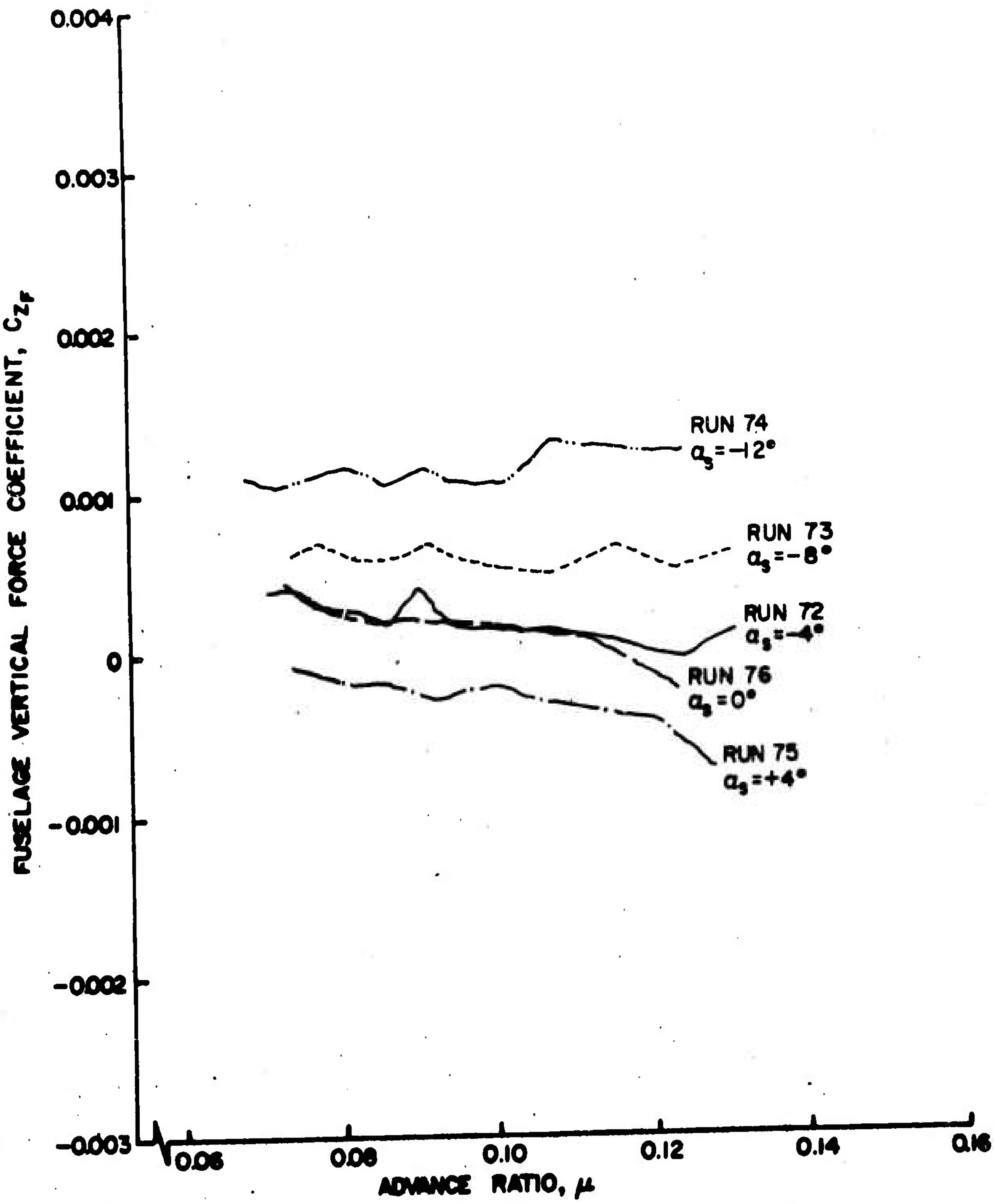

Figure 16a. Fuselage Vertical Force and Pitching Moment Coefficients as Functions of Advance Ratio, $\theta_{.75R} = 8°$, Large Wing on High.

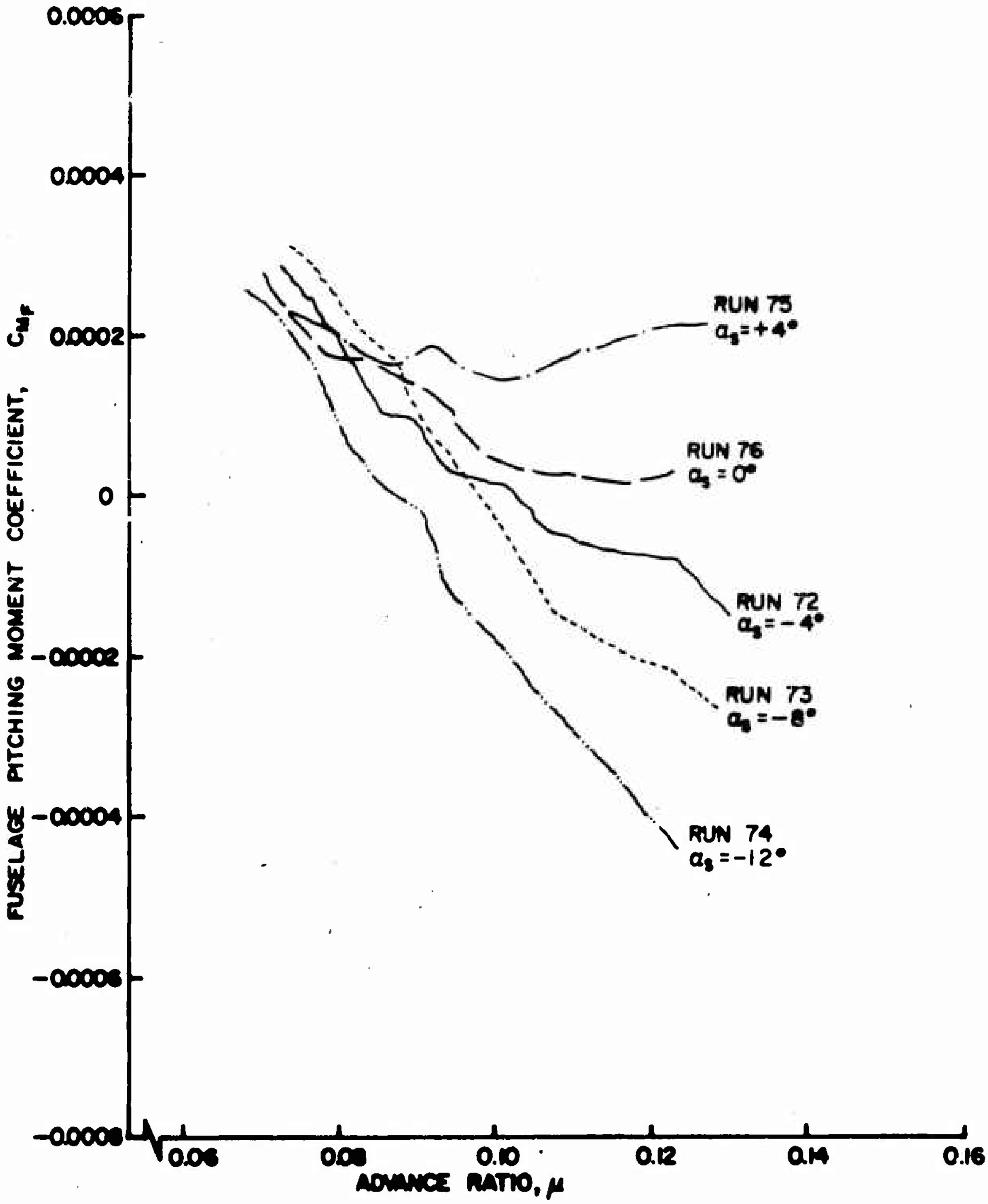

Figure 16b. Fuselage Vertical Force and Pitching Moment Coefficients as Functions of Advance Ratio, $\theta_{.75R} = 8^{\circ}$, Large Wing on High.

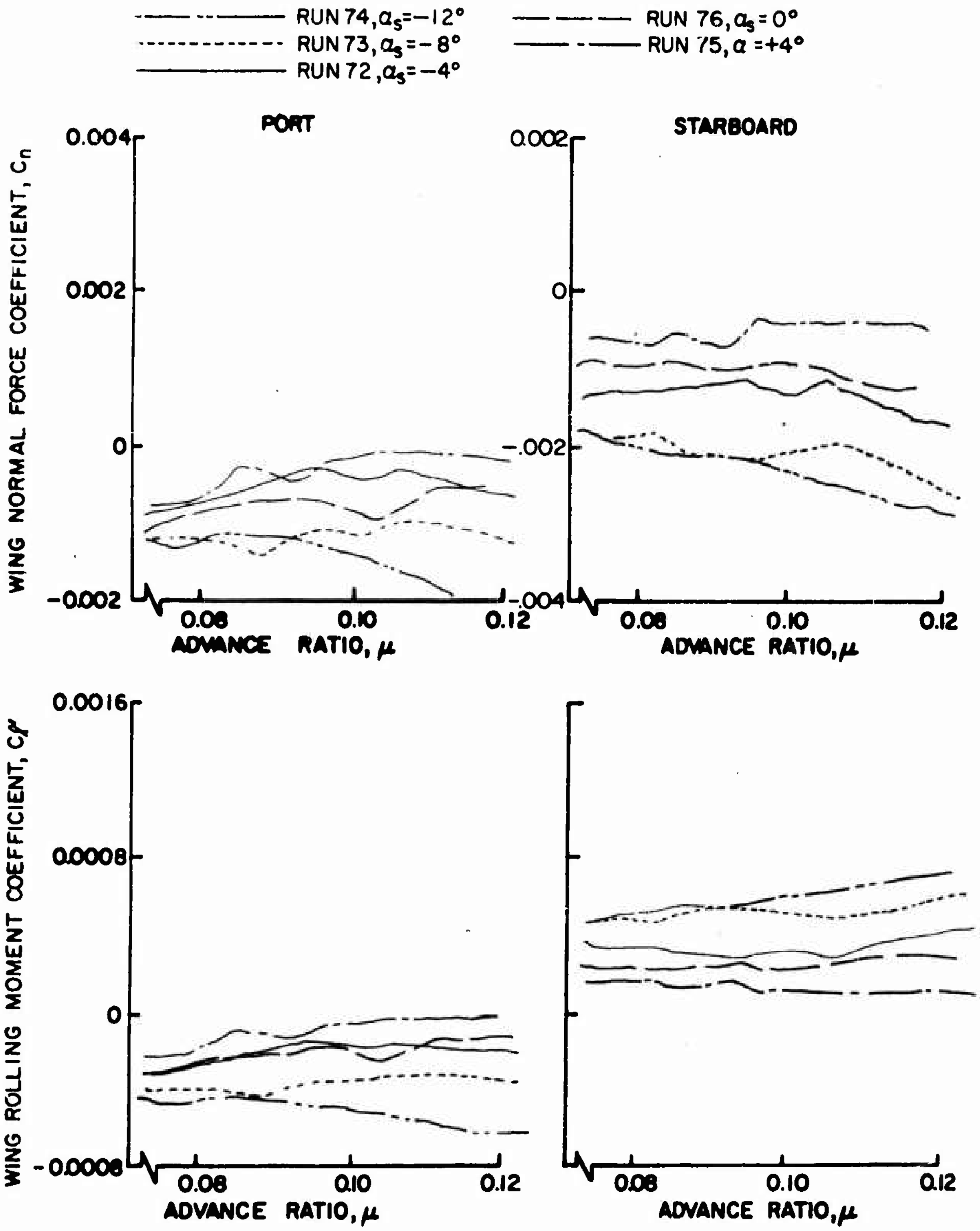

Figure 17. Wing Normal Force and Rolling Moment Coefficients as Functions of Advance Ratio, $\theta_{.75R} = 8^\circ$, Large Wing on High.

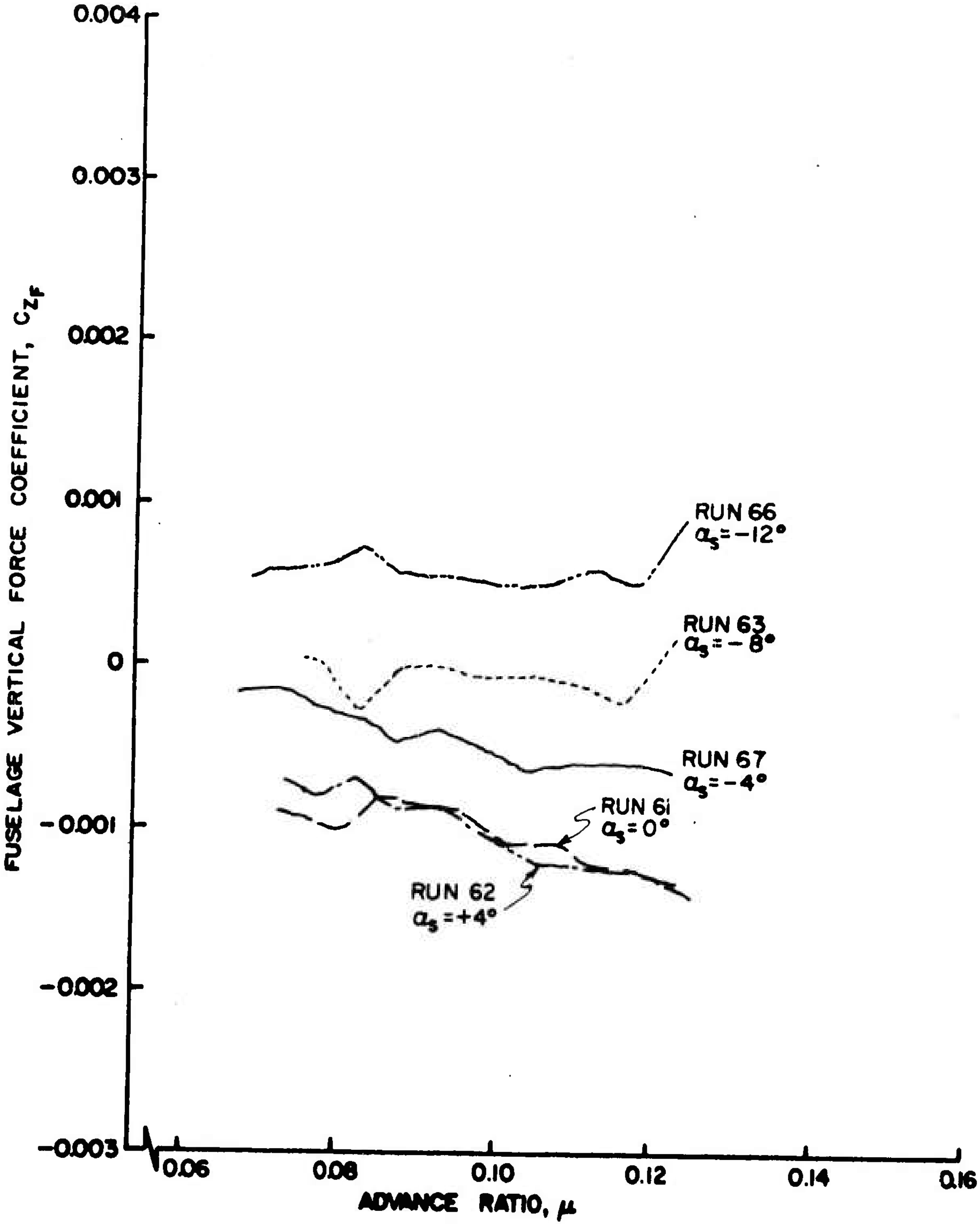

Figure 18a. Fuselage Vertical Force and Pitching Moment Coefficients as Functions of Advance Ratio, $\alpha_{.75R} = 8°$, Large Wing on Low.

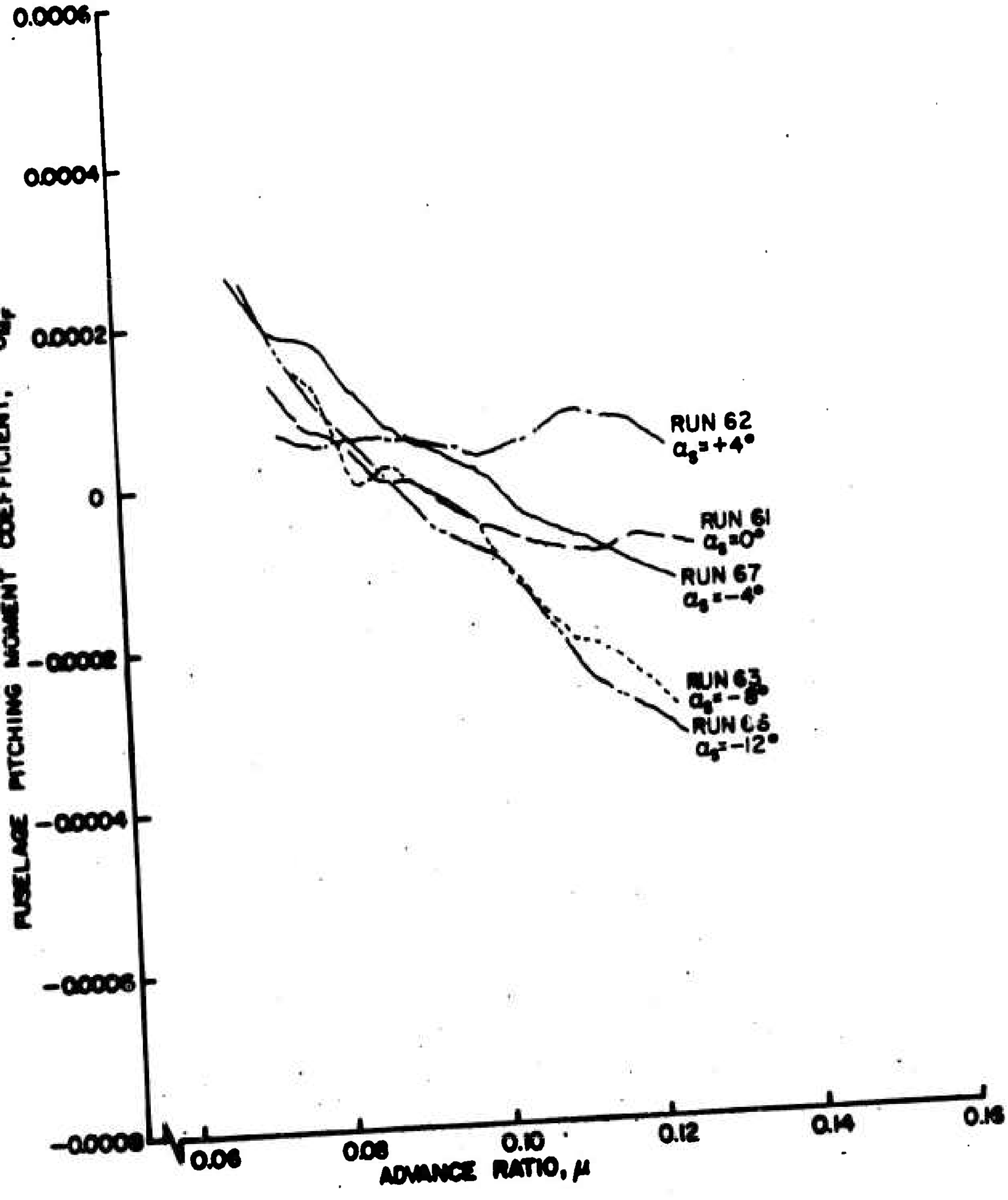

Figure 18b. Fuselage Vertical Force and Pitching Moment Coefficients as Functions of Advance Ratio, $\theta_{.75R} = 8°$, Large Wing on Low.

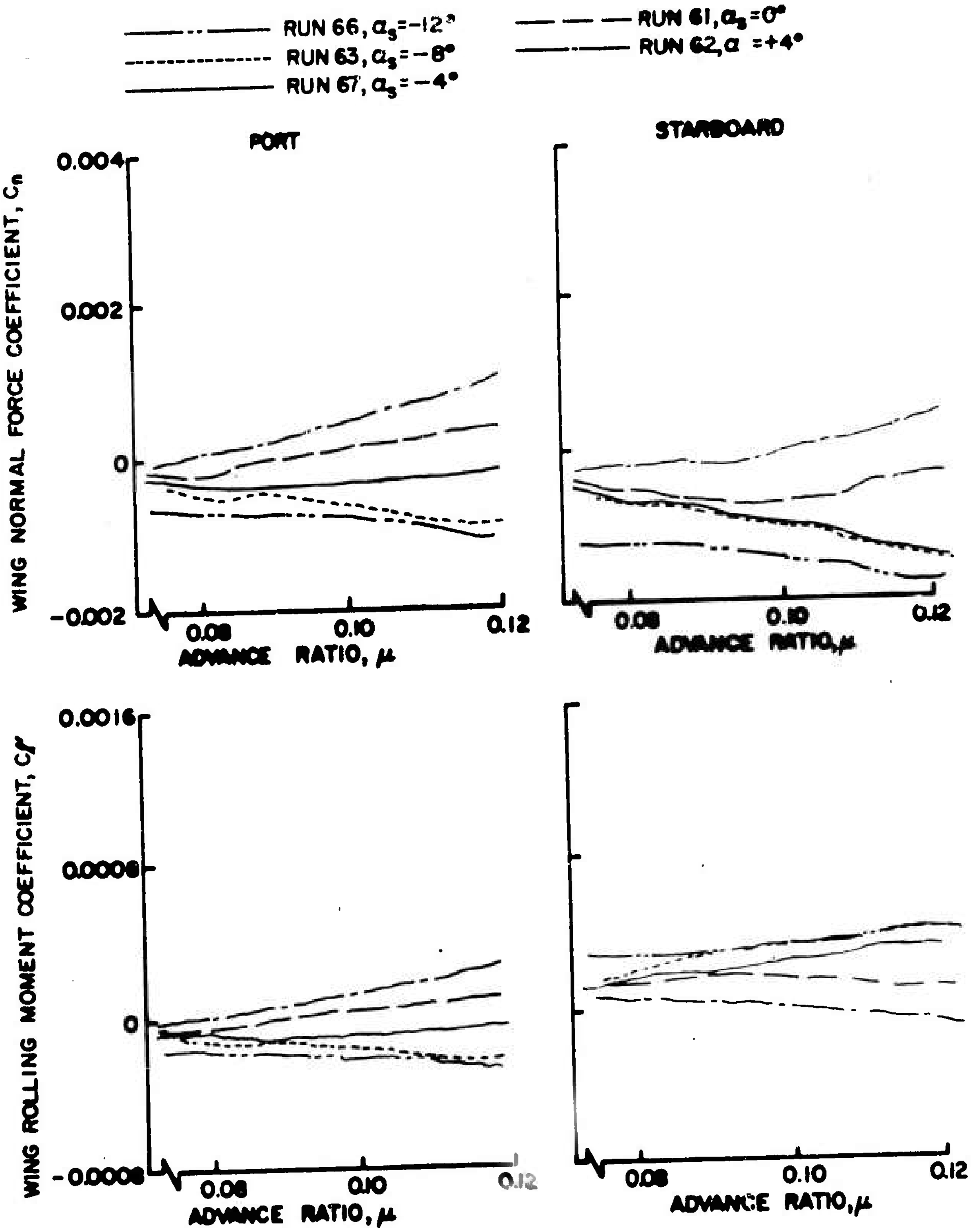

Figure 19. Wing Normal Force and Rolling Moment Coefficients as Functions of Advance Ratio, $\theta_{.75R} = 8°$, Large Wing on Low.

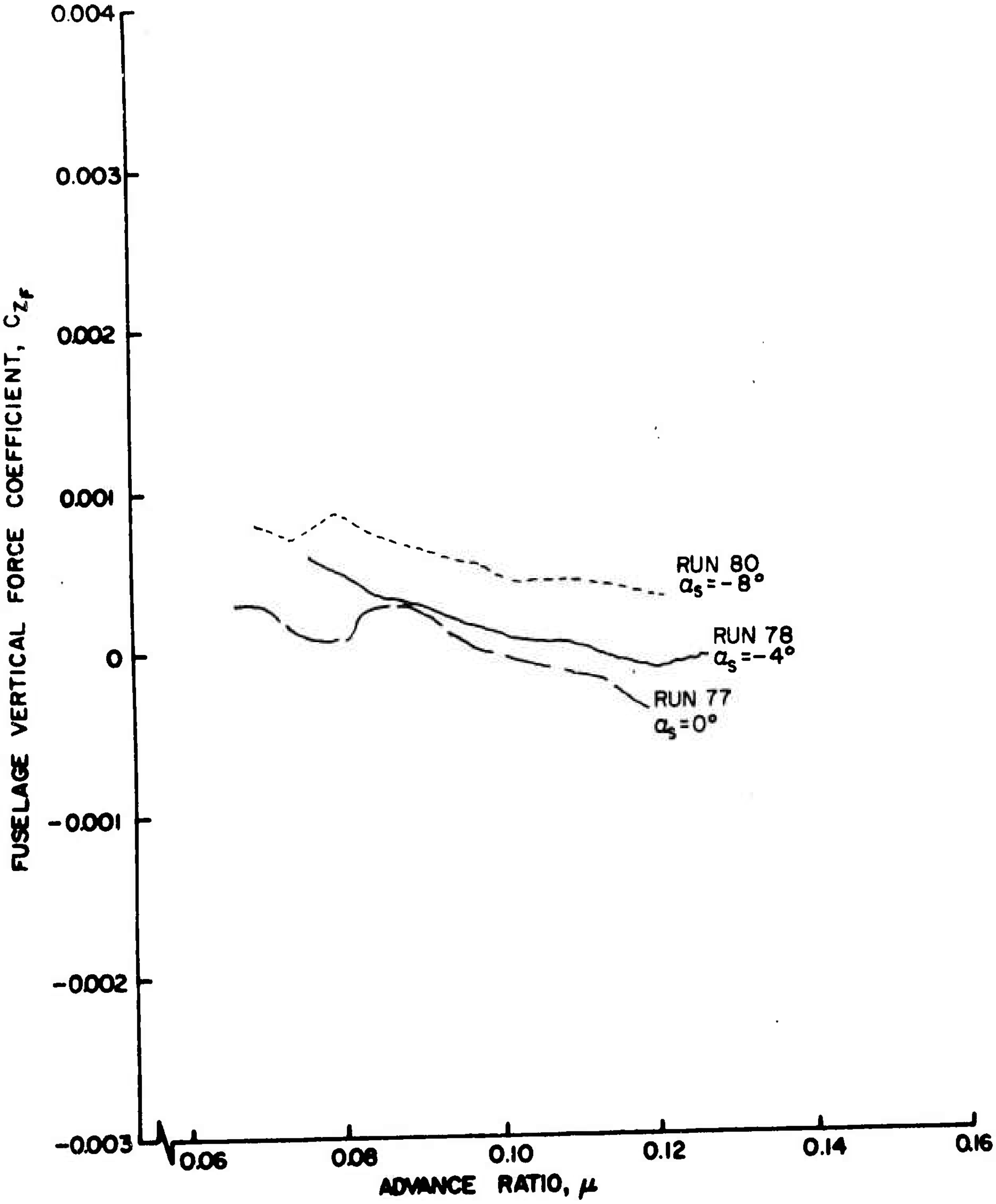

Figure 20a. Fuselage Vertical Force and Pitching Moment Coefficients as Functions of Advance Ratio, $\theta_{.75R} = 8°$, Small Wing on High.

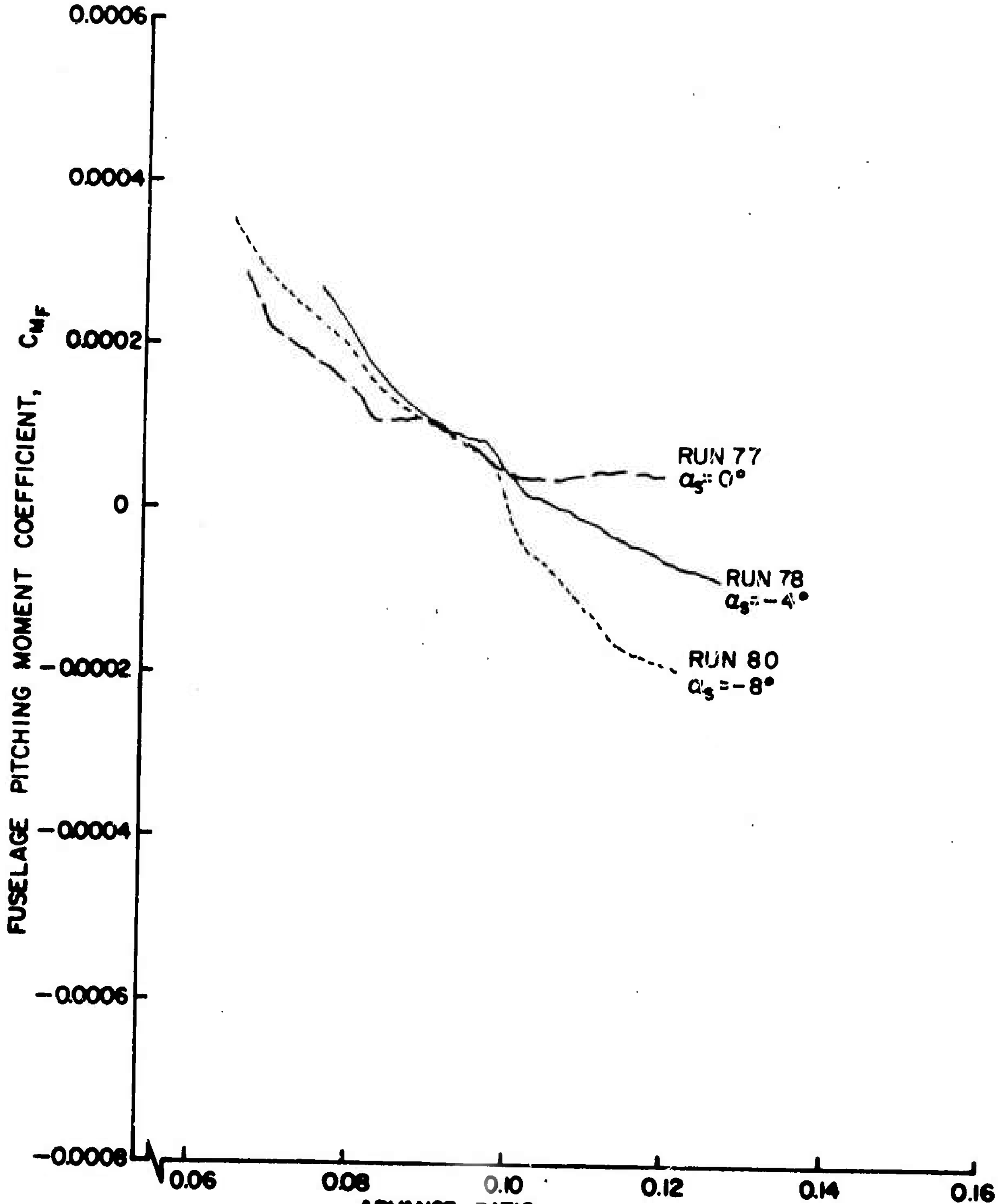

Figure 20b. Fuselage Vertical Force and Pitching Moment Coefficients as Functions of Advance Ratio, $\theta_{.75R} = 8°$, Small Wing on High.

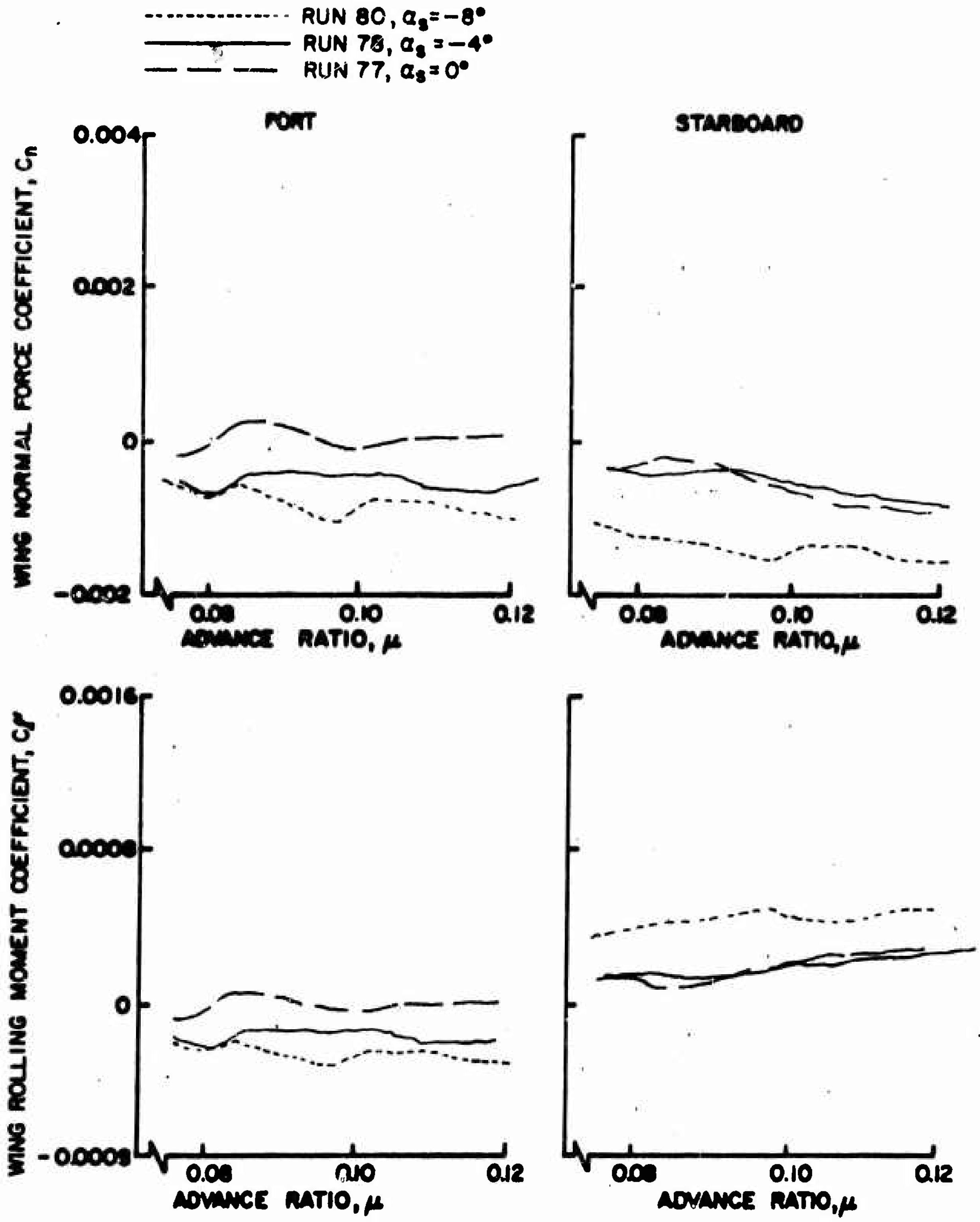

Figure 21. Wing Normal Force and Rolling Moment Coefficients as Functions of Advance Ratio, $\theta_{.75R} = 8°$, Small Wing on High.

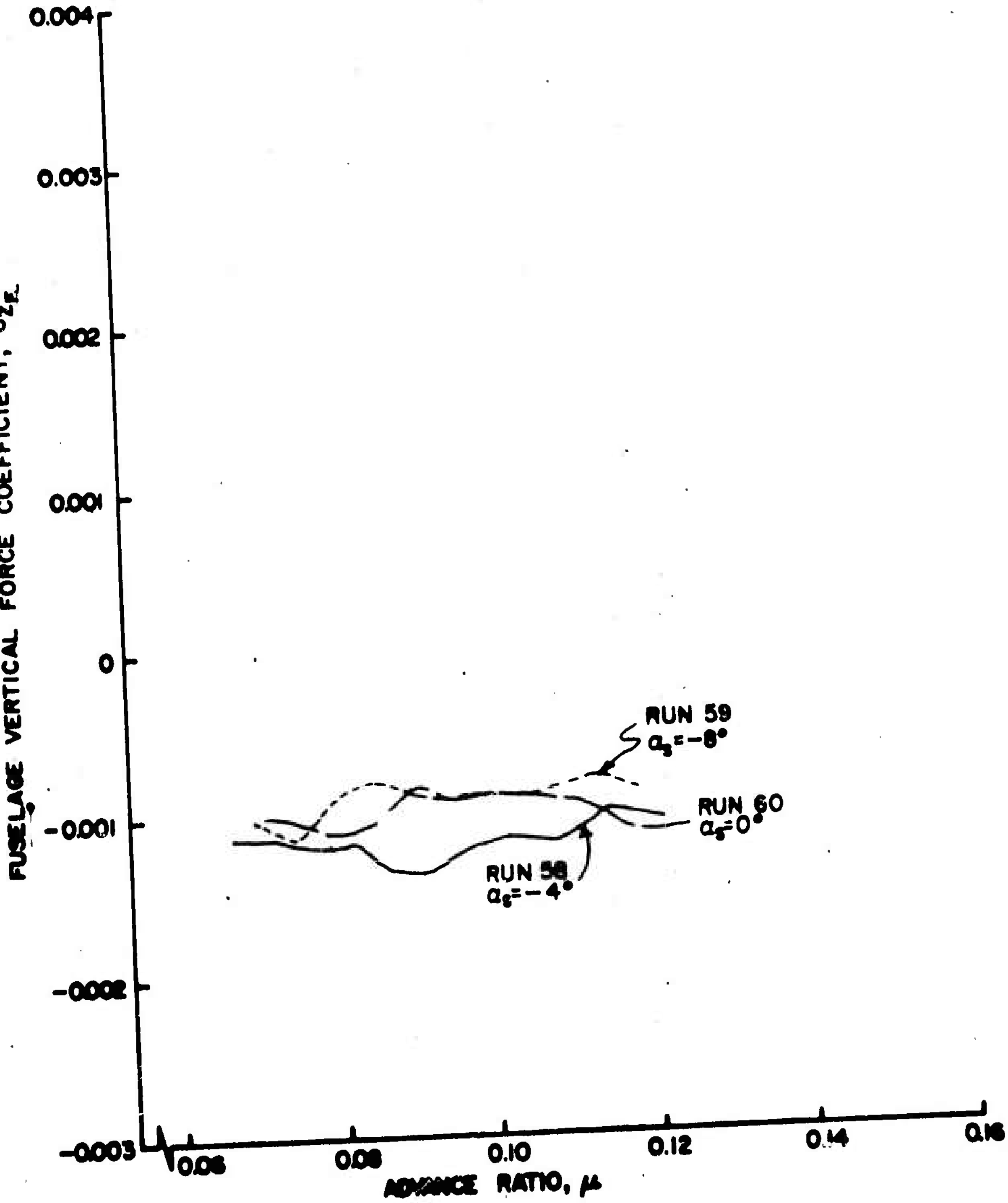

Figure 22a. Fuselage Vertical Force and Pitching Moment Coefficients as Functions of Advance Ratio, $\theta_{.75R} = 8°$, Small Wing on Low.

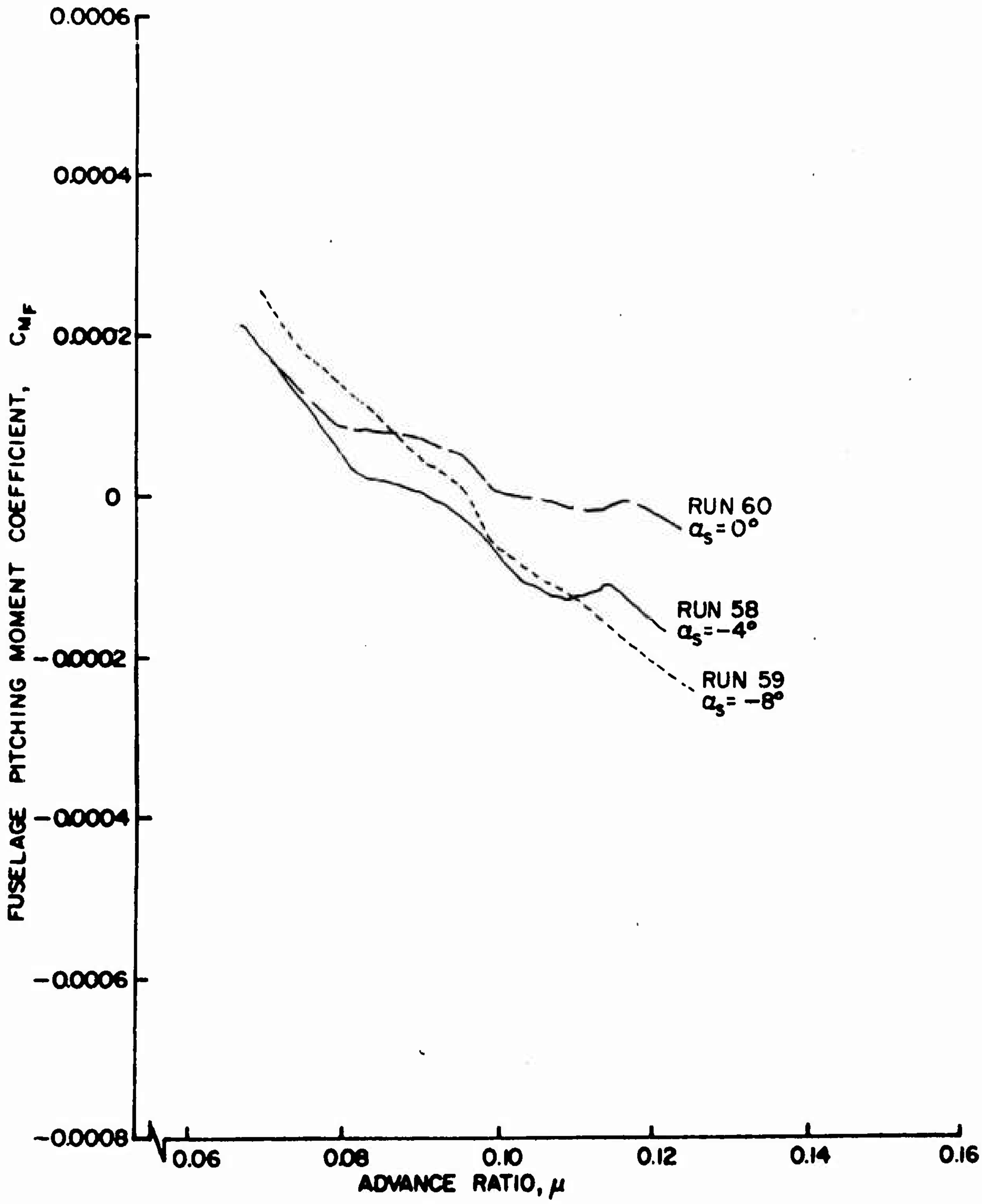

Figure 22b. Fuselage Vertical Force and Pitching Moment Coefficients as Functions of Advance Ratio, $\theta_{.75R} = 8°$, Small Wing on Low.

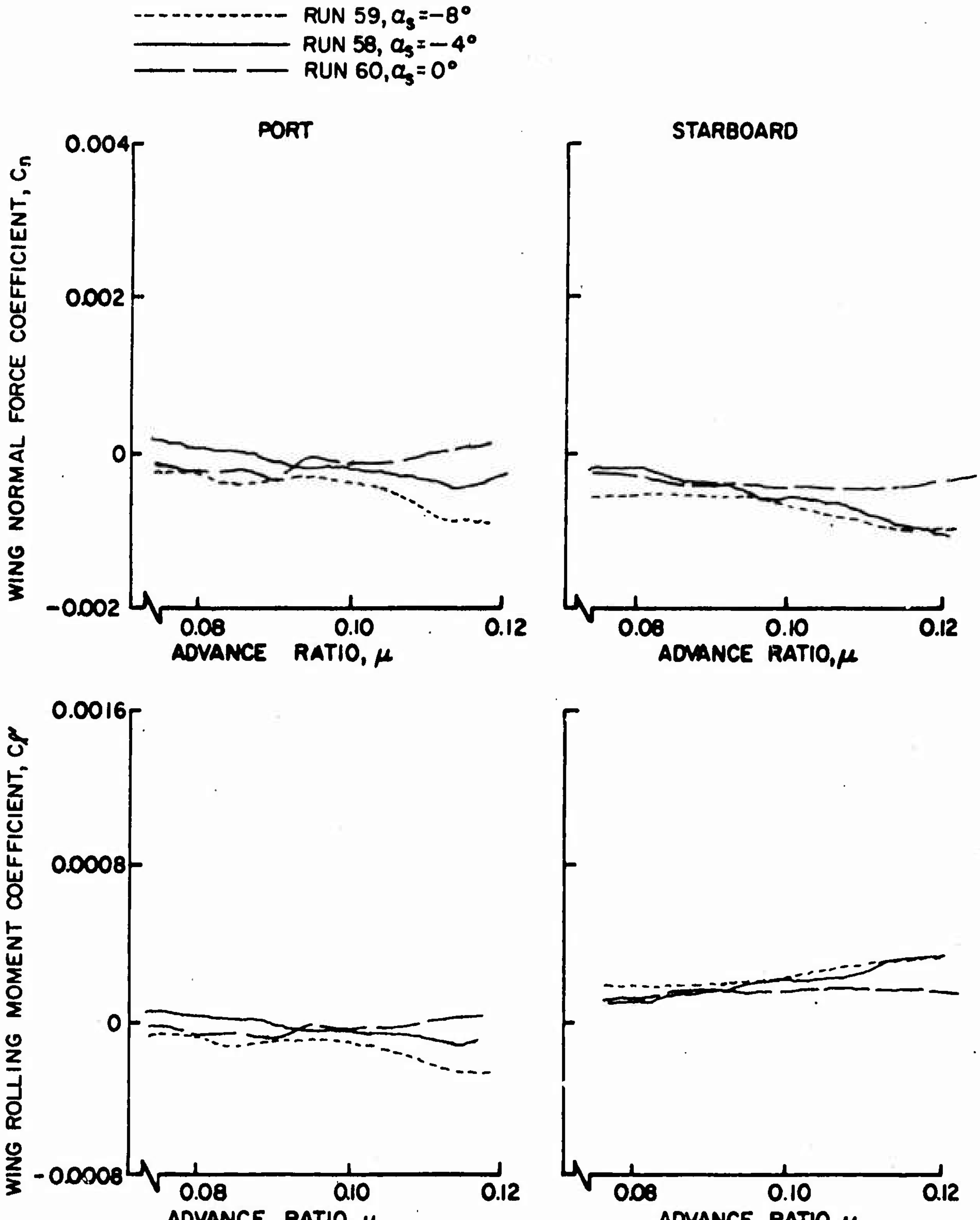

Figure 23. Wing Normal Force and Rolling Moment Coefficients as Functions of Advance Ratio, $\theta_{.75R} = 8^{\circ}$, Small Wing on Low.

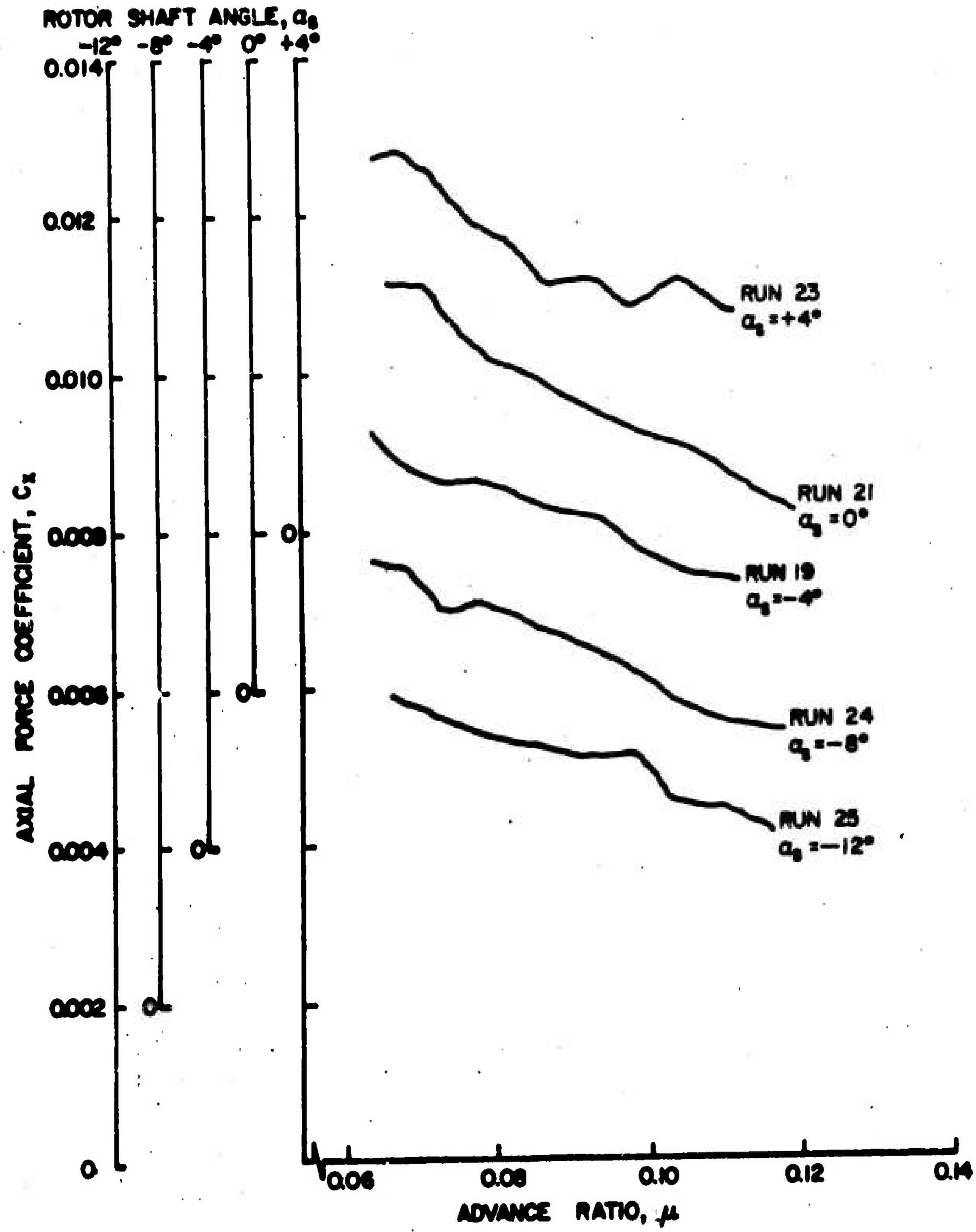

Figure 24a. Rotor Force and Moment Coefficients as Functions of Advance Ratio, $\theta_{.75R} = 10^\circ$, Wing Off.

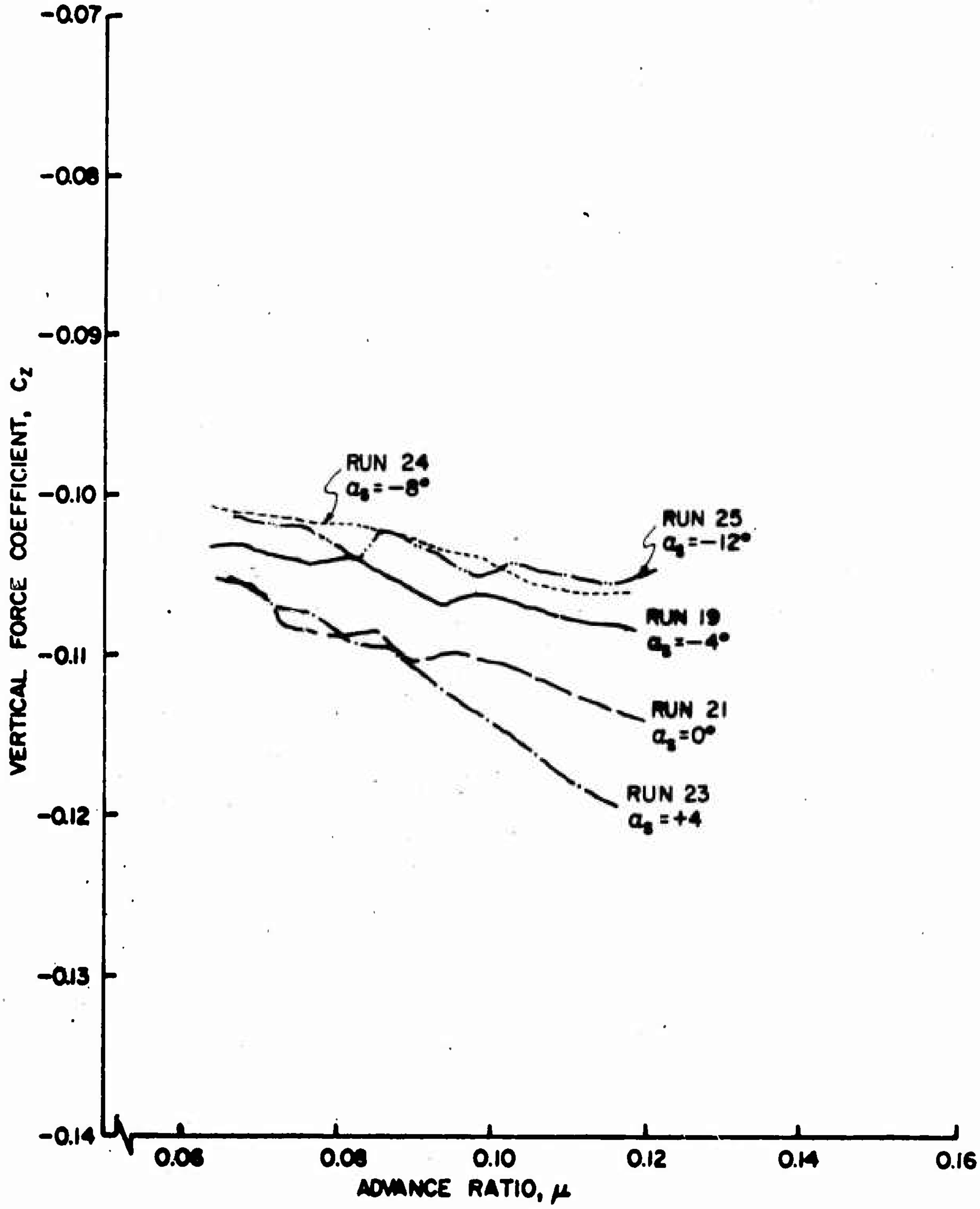

Figure 24b. Rotor Force and Moment Coefficients as Functions of Advance Ratio, $\theta_{.75R} = 10°$, Wing Off.

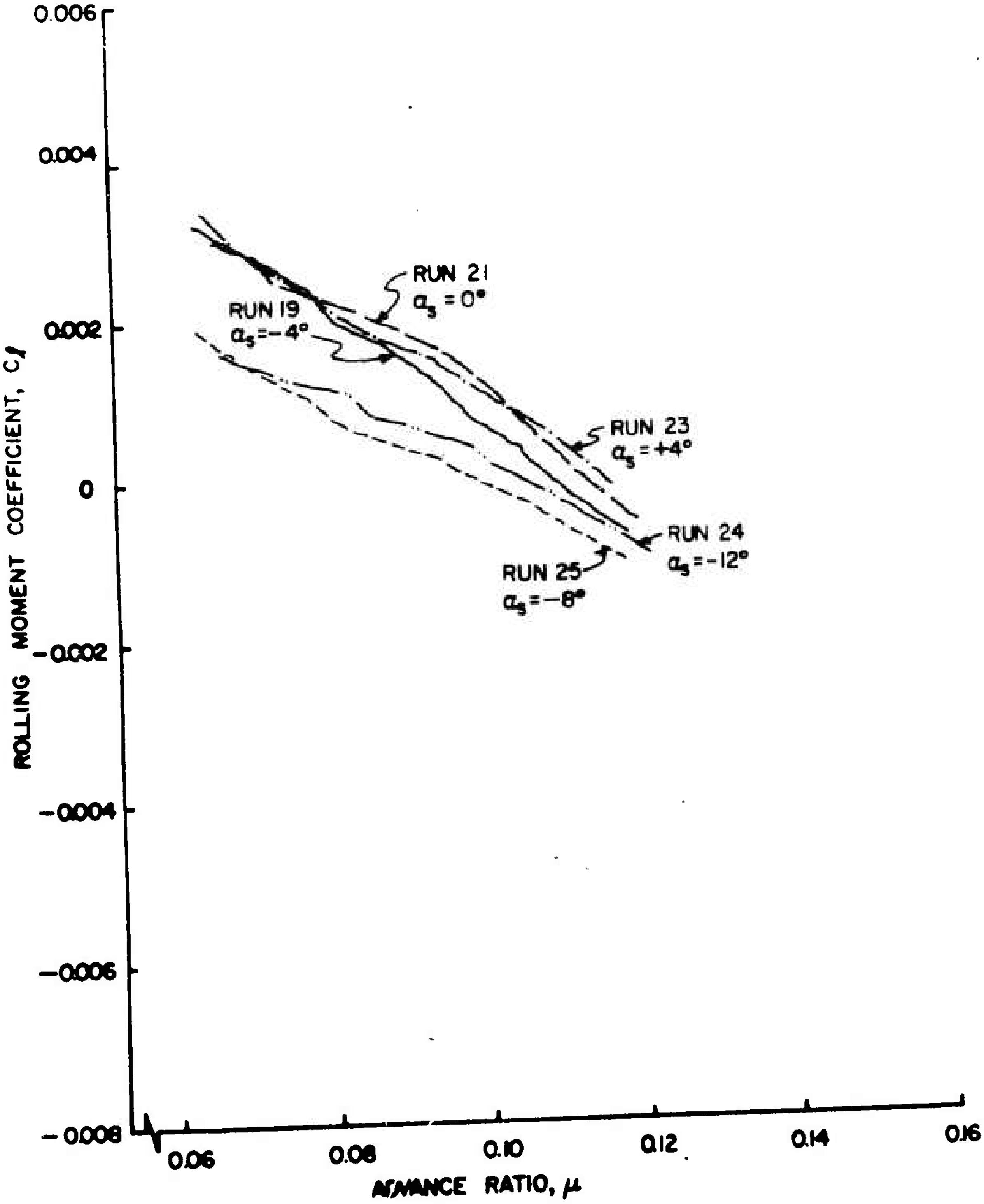

Figure 24c. Rotor Force and Moment Coefficients as Functions of Advance Ratio, $\theta_{.75R} = 10°$, Wing Off.

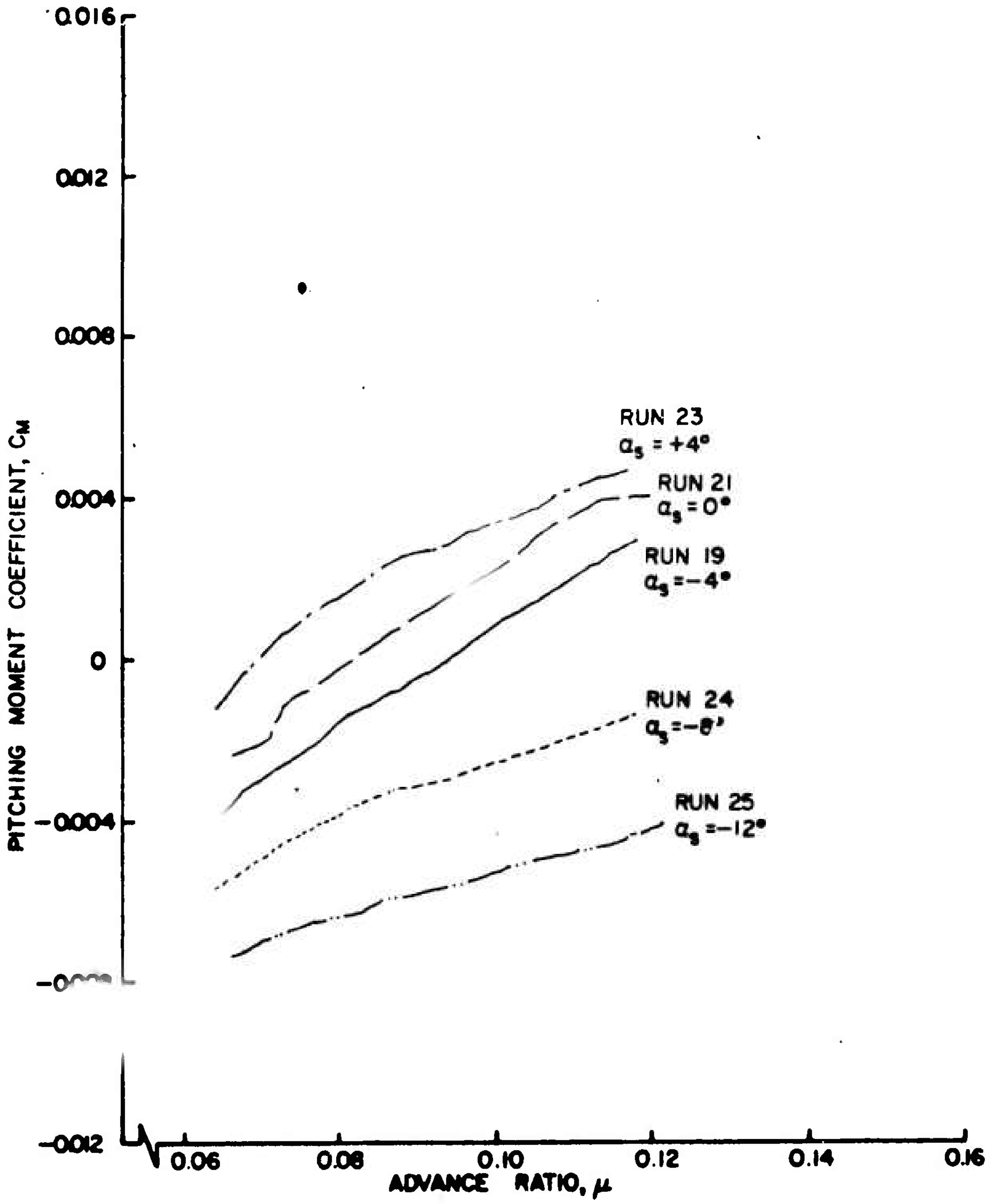

Figure 24d. Rotor Force and Moment Coefficients as Functions of Advance Ratio, $\theta_{.75R} = 10^\circ$, Wing Off.

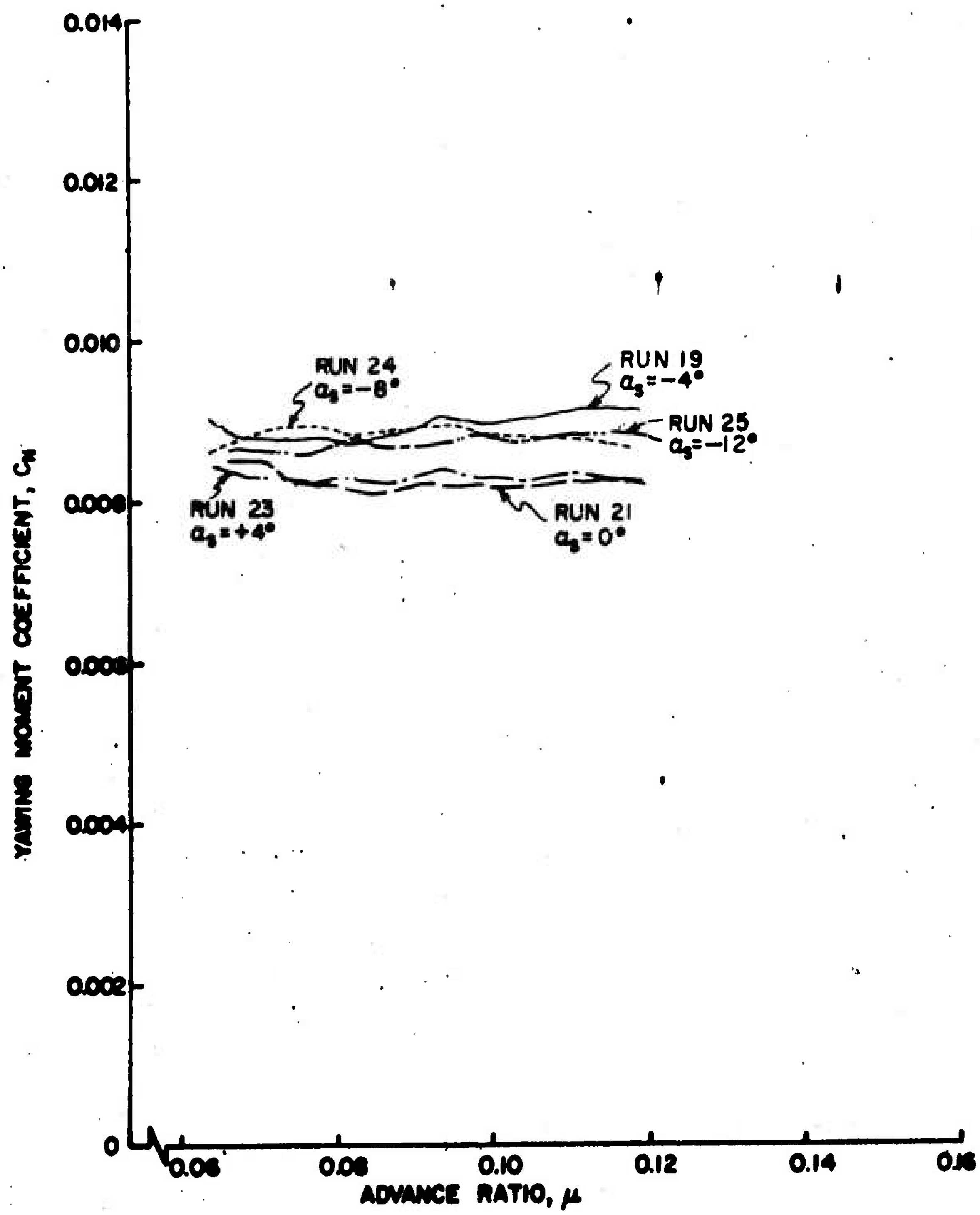

Figure 24e. Rotor Force and Moment Coefficients as Functions of Advance Ratio, $\theta_{.75R} = 10°$, Wing Off.

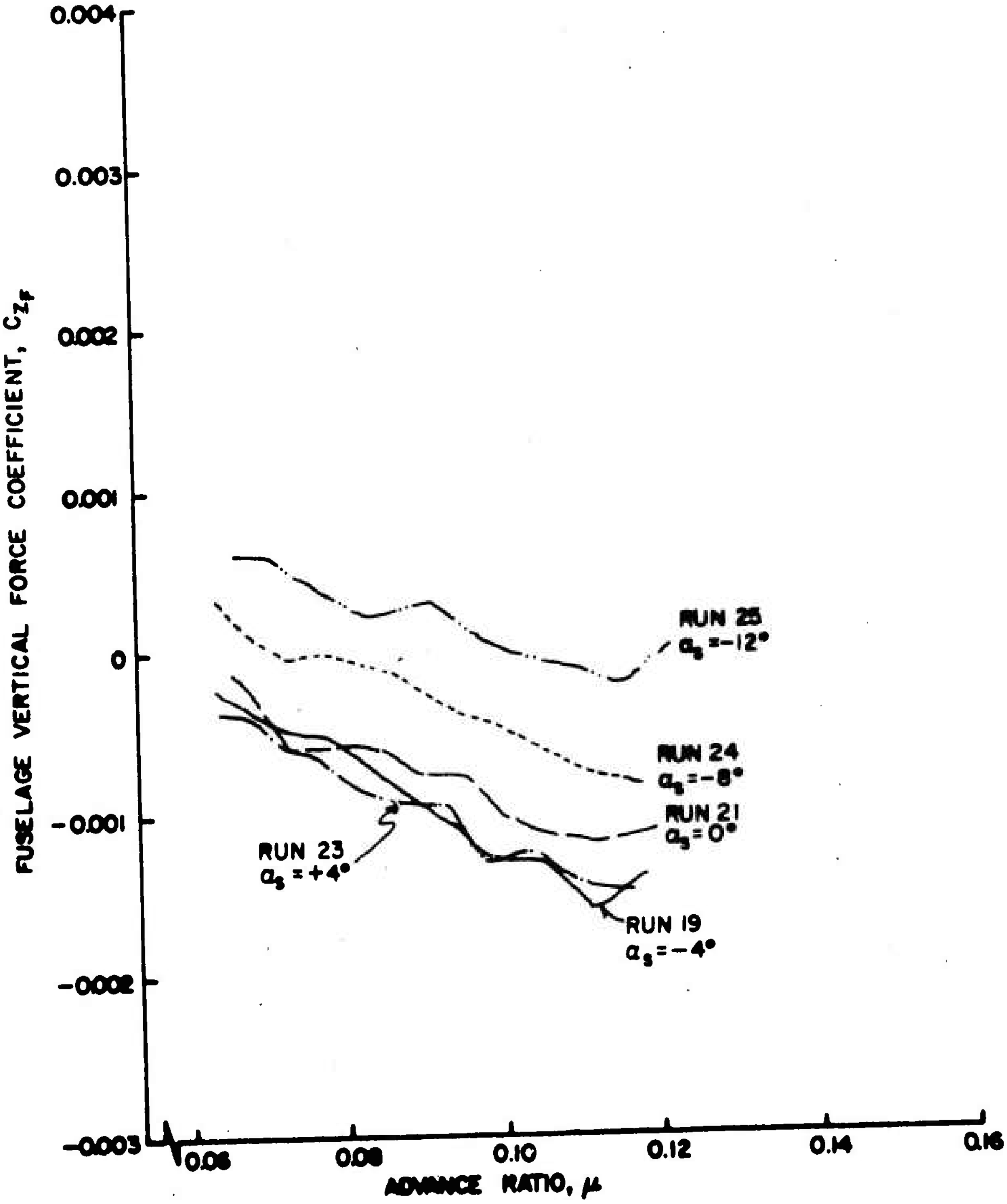

Figure 25a. Fuselage Vertical Force and Pitching Moment Coefficients as Functions of Advance Ratio, $\theta_{.75R} = 10^{\circ}$, Wing Off.

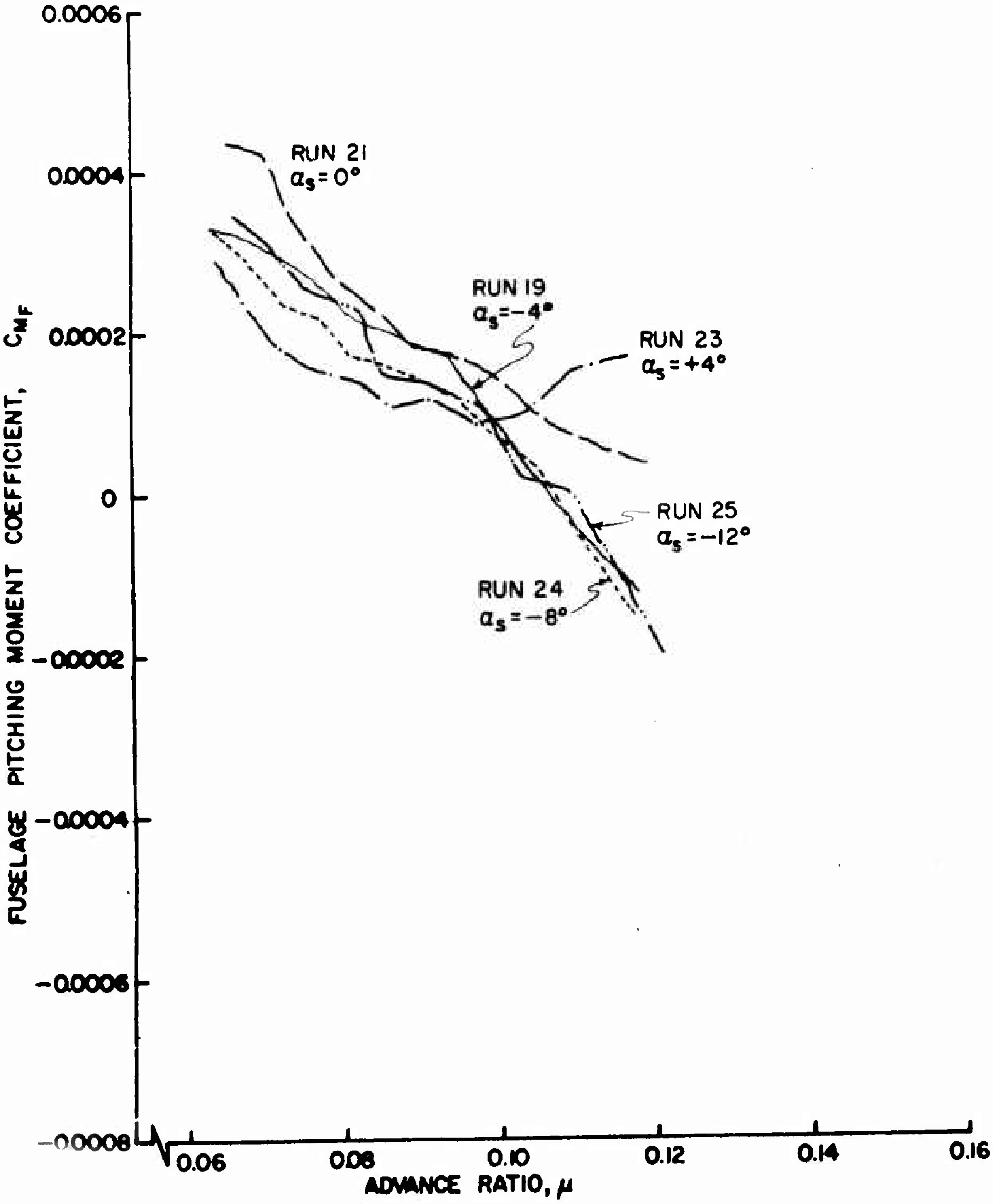

Figure 25b. Fuselage Vertical Force and Pitching Moment Coefficients as Functions of Advance Ratio, $\theta_{.75R} = 10°$, Wing Off.

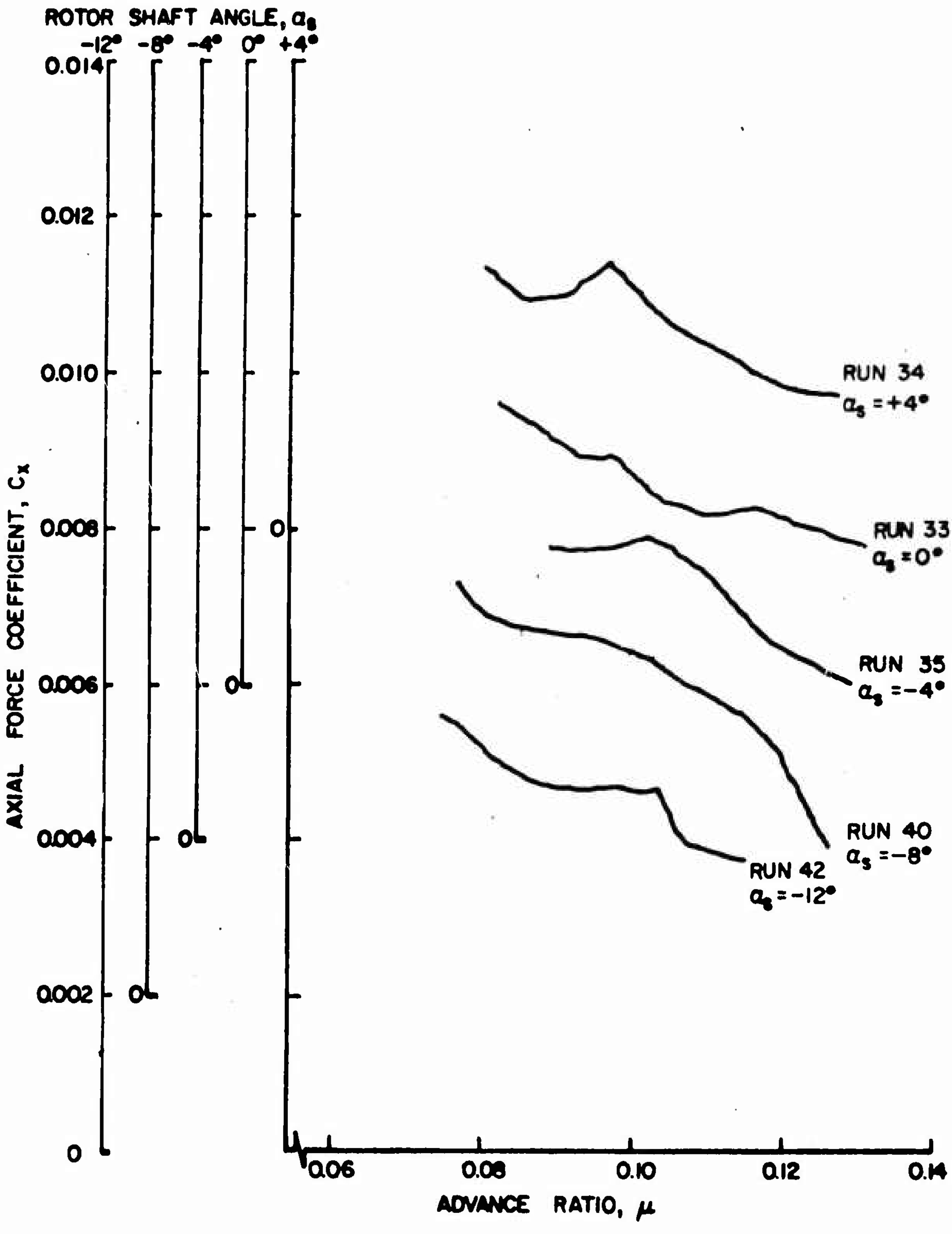

Figure 26a. Rotor Force and Moment Coefficients as Functions of Advance Ratio, $\theta_{.75R} = 10^\circ$, Large Wing on High.

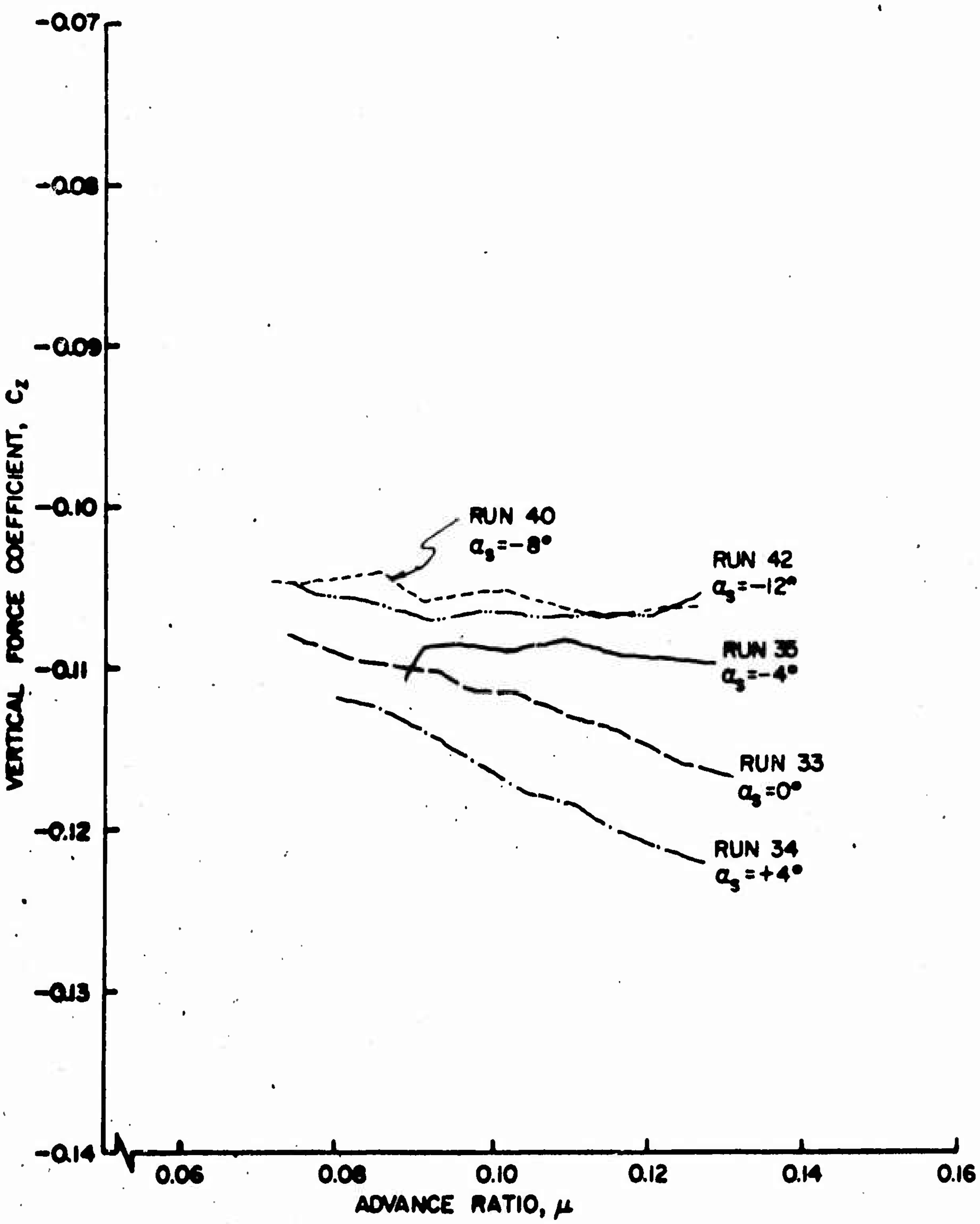

Figure 26b. Rotor Force and Moment Coefficients as Functions of Advance Ratio, $\theta_{.75R} = 10°$, Large Wing on High.

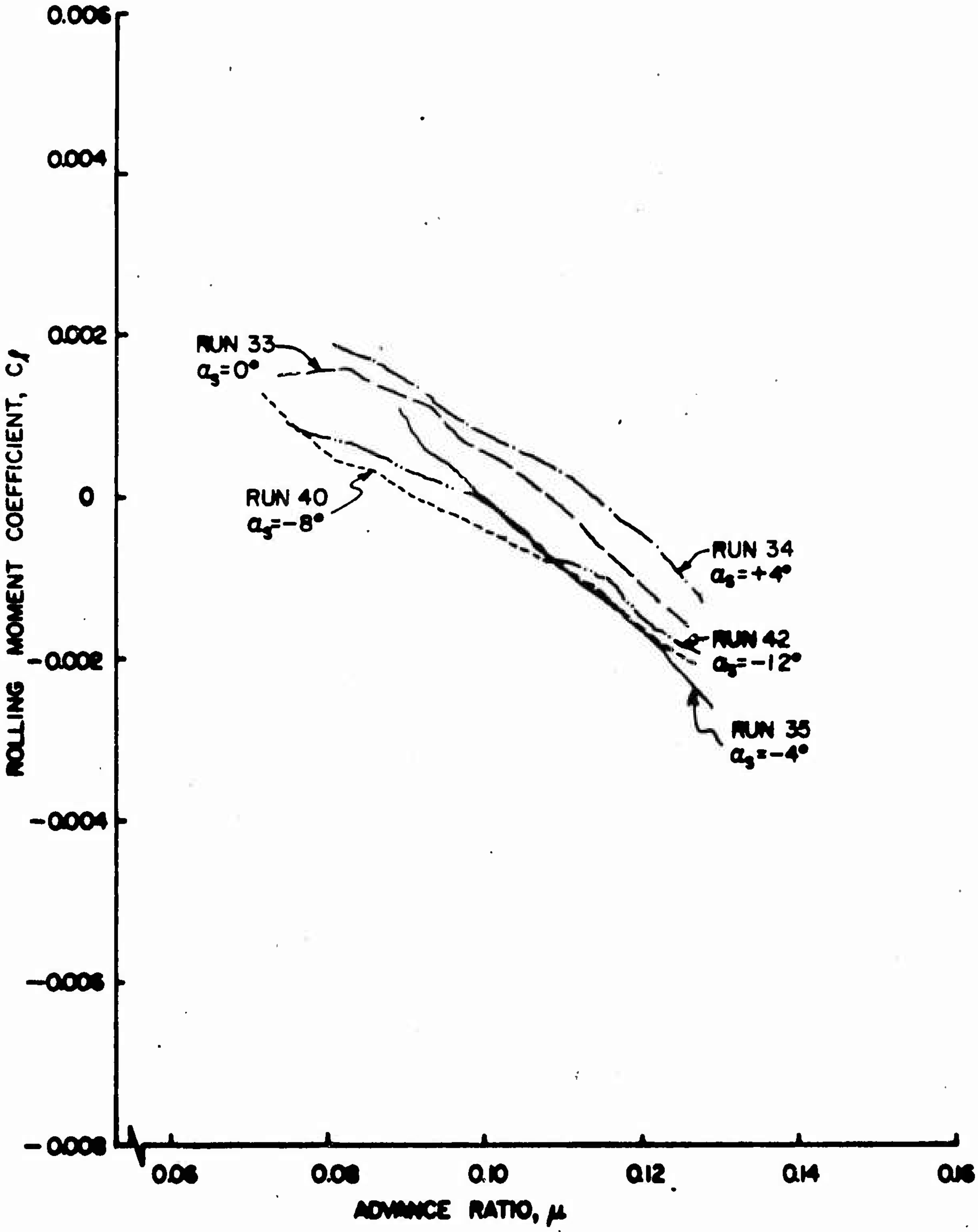

Figure 26c. Rotor Force and Moment Coefficients as Functions of Advance Ratio, $\theta_{.75R} = 10^\circ$, Large Wing on High.

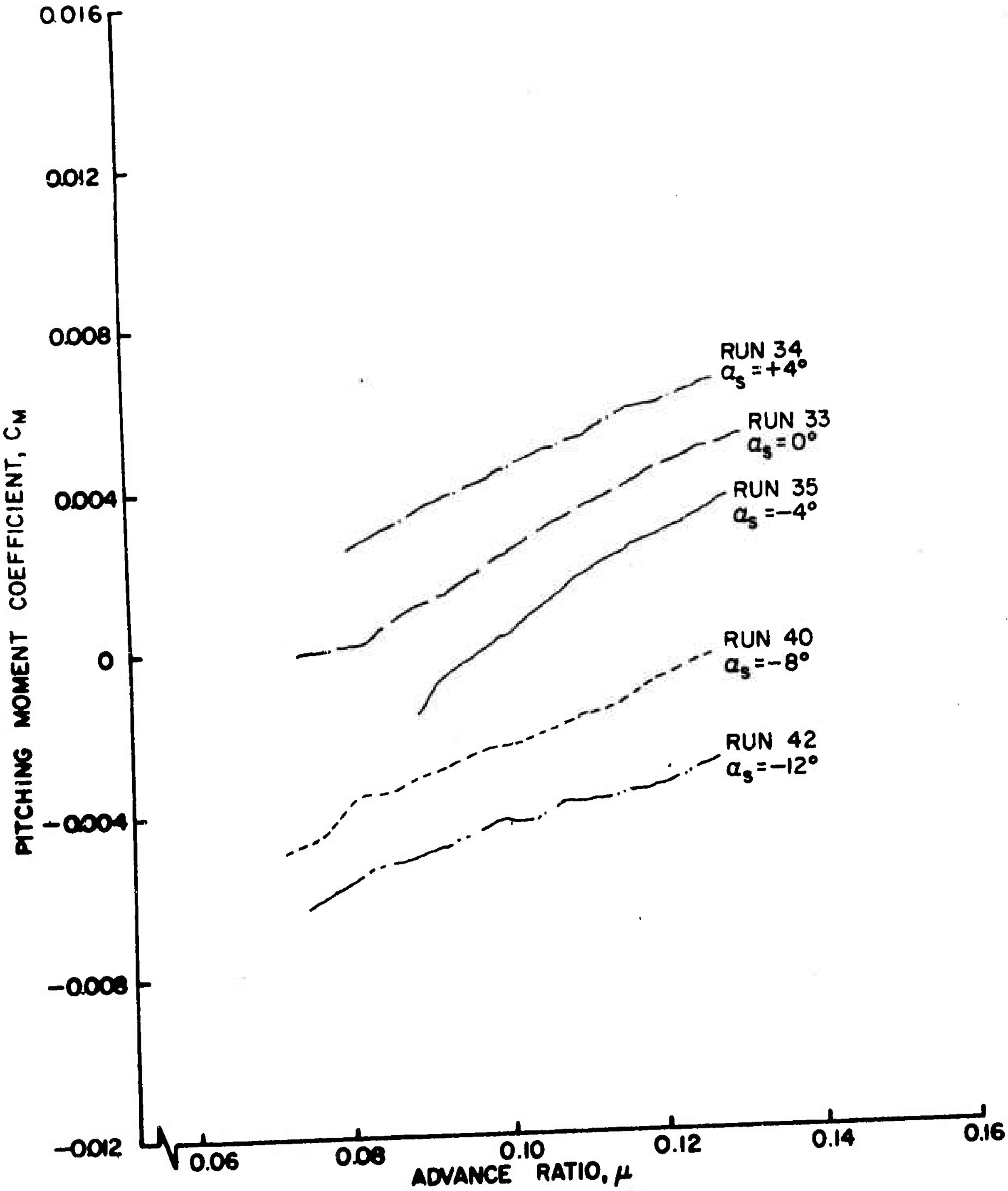

Figure 26d. Rotor Force and Moment Coefficients as Functions of Advance Ratio, $\theta_{.75R} = 10°$, Large Wing on High.

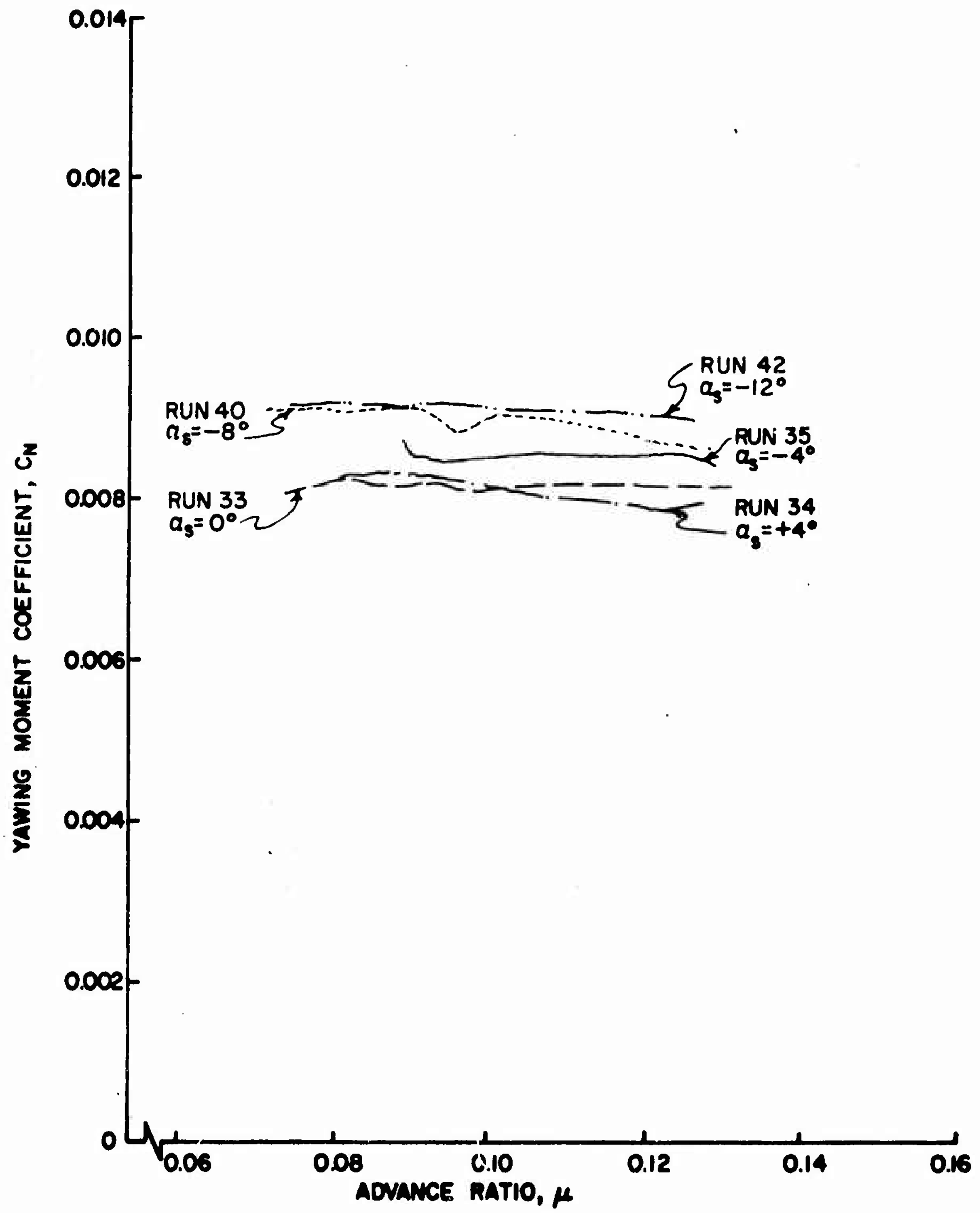

Figure 26e. Rotor Force and Moment Coefficients as Functions of Advance Ratio, $\theta_{.75R} = 10°$, Large Wing on High.

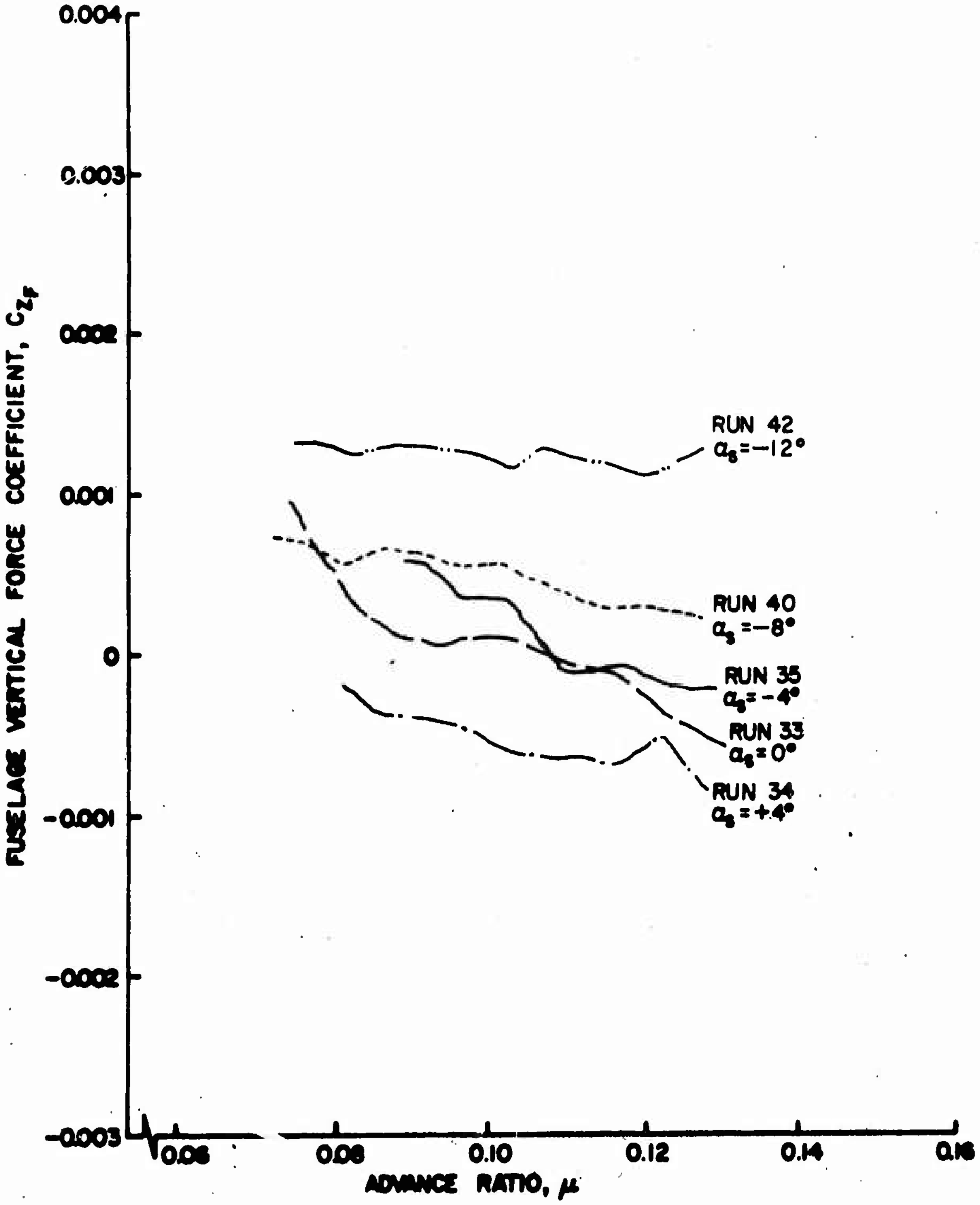

Figure 27a. Fuselage Vertical Force and Pitching Moment Coefficients as Functions of Advance Ratio, $\theta_{.75R} = 10°$, Large Wing on High.

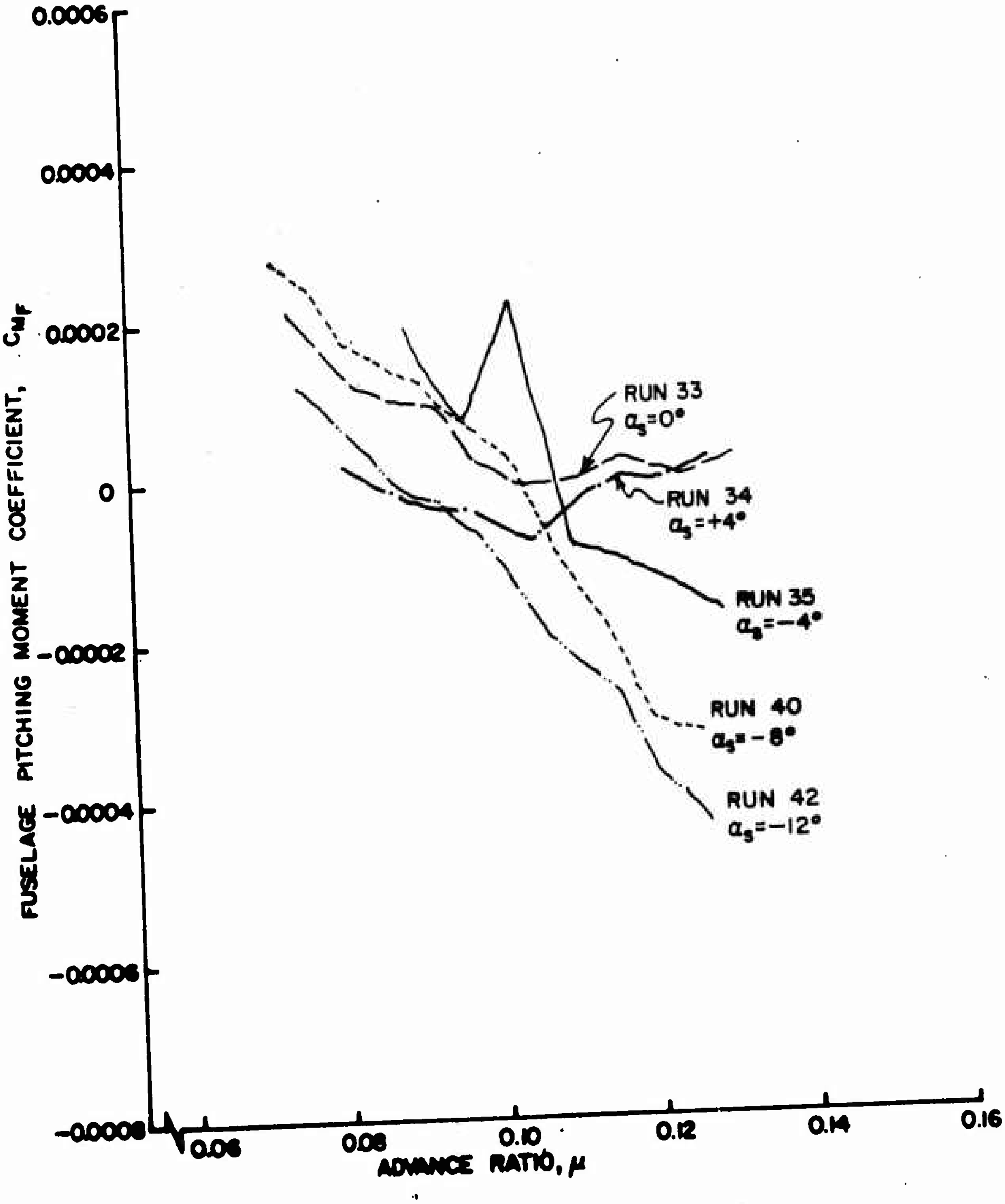

Figure 27b. Fuselage Vertical Force and Pitching Moment Coefficients as Functions of Advance Ratio, $\theta_{.75R} = 10^{\circ}$, Large Wing on High.

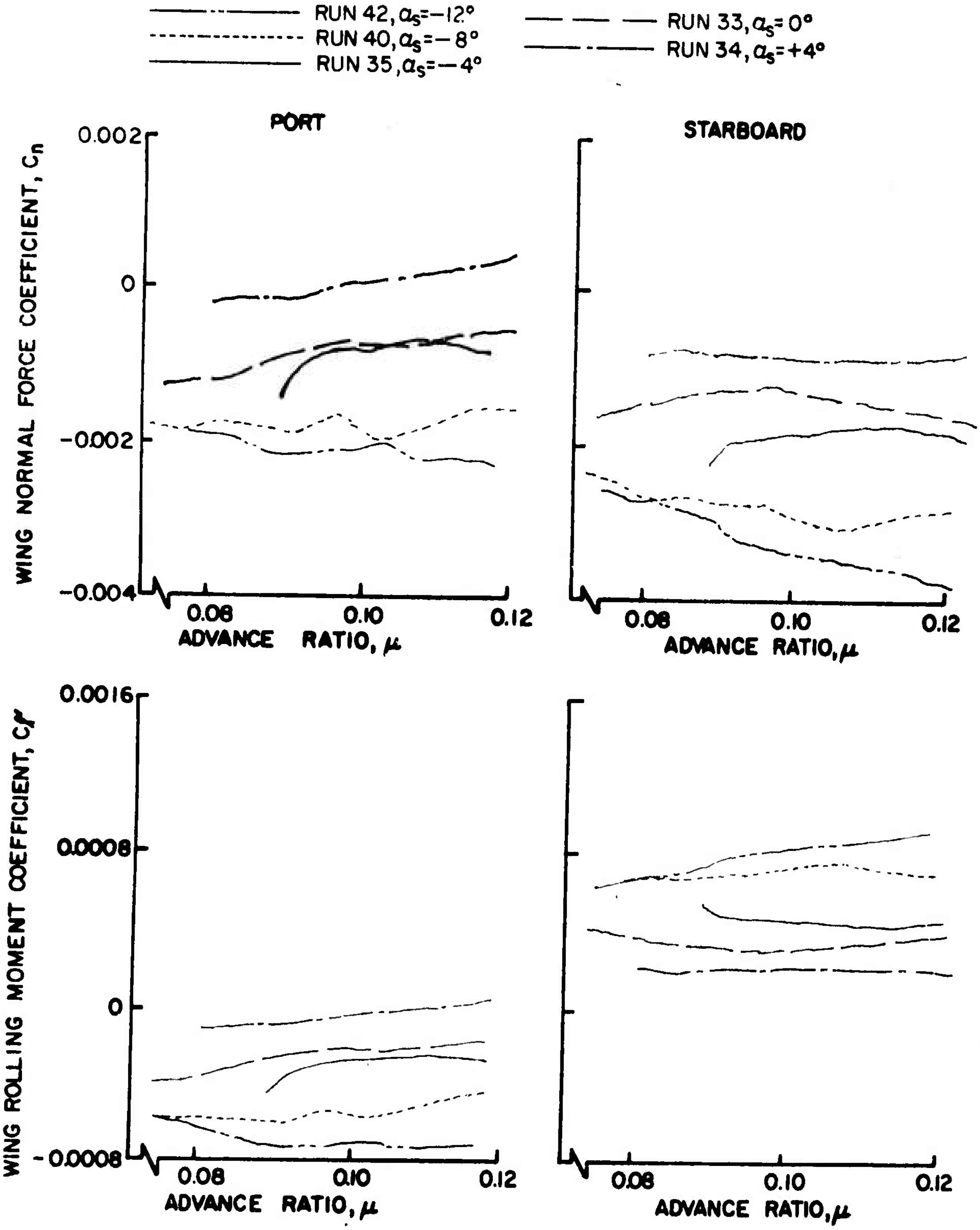

Figure 28. Wing Normal Force and Rolling Moment Coefficients as Functions of Advance Ratio, $\theta_{.75R} = 10°$, Large Wing on High.

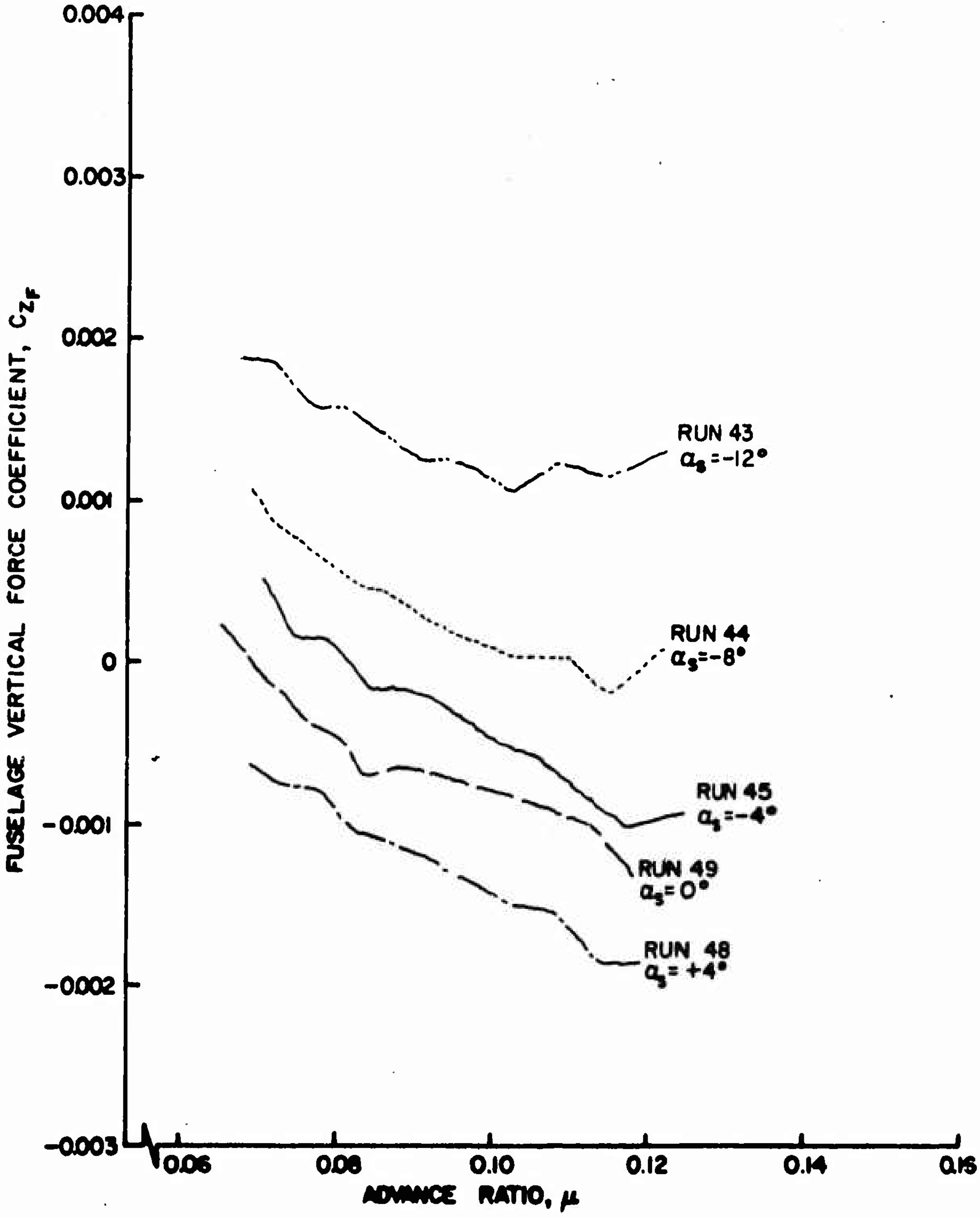

Figure 29a. Fuselage Vertical Force and Pitching Moment Coefficients as Functions of Advance Ratio, $\theta_{.75R} = 10^{\circ}$, Large Wing on Low.

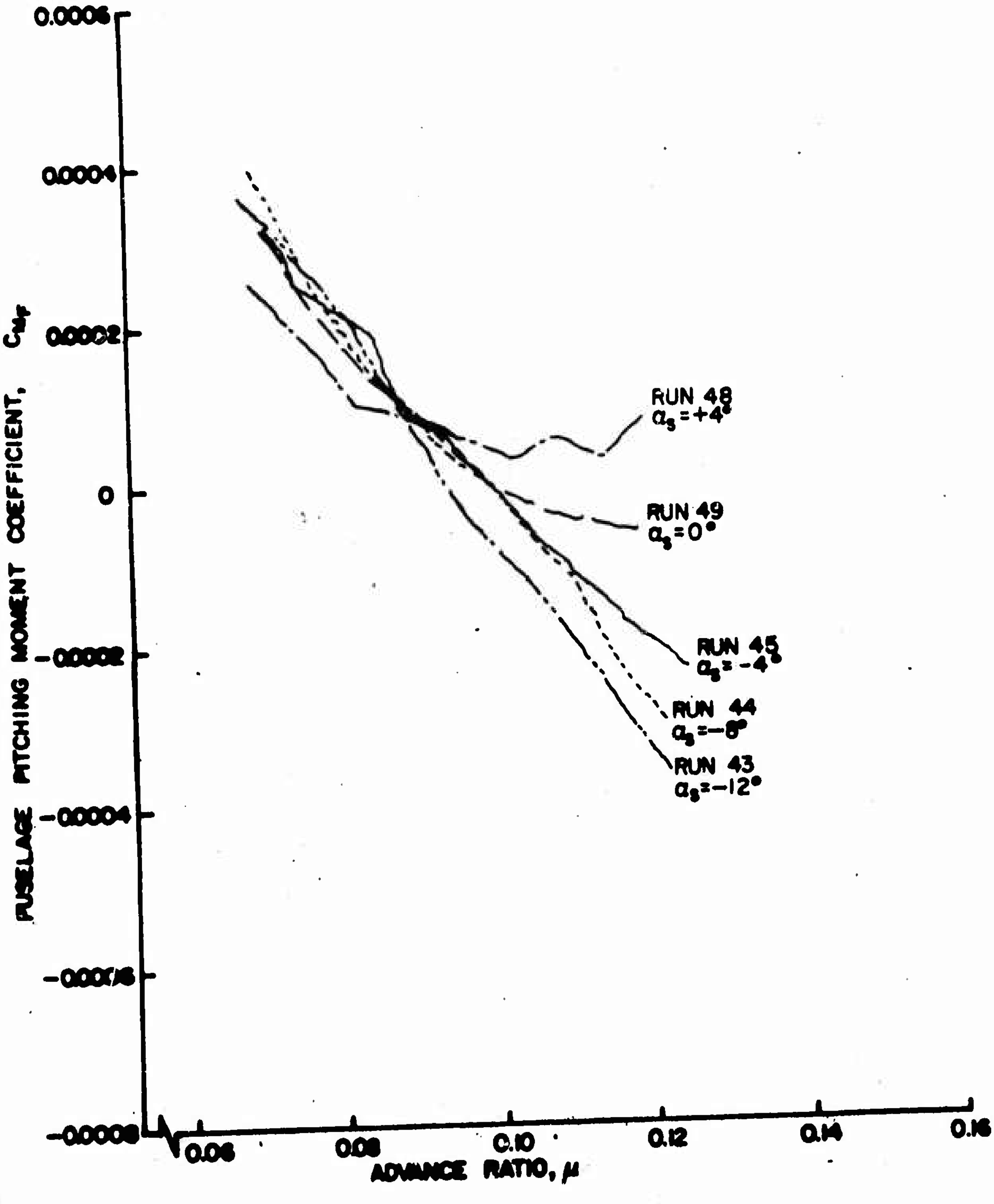

Figure 29b. Fuselage Vertical Force and Pitching Moment Coefficients as Functions of Advance Ratio, $\theta_{.75R} = 10°$, Large Wing on Low.

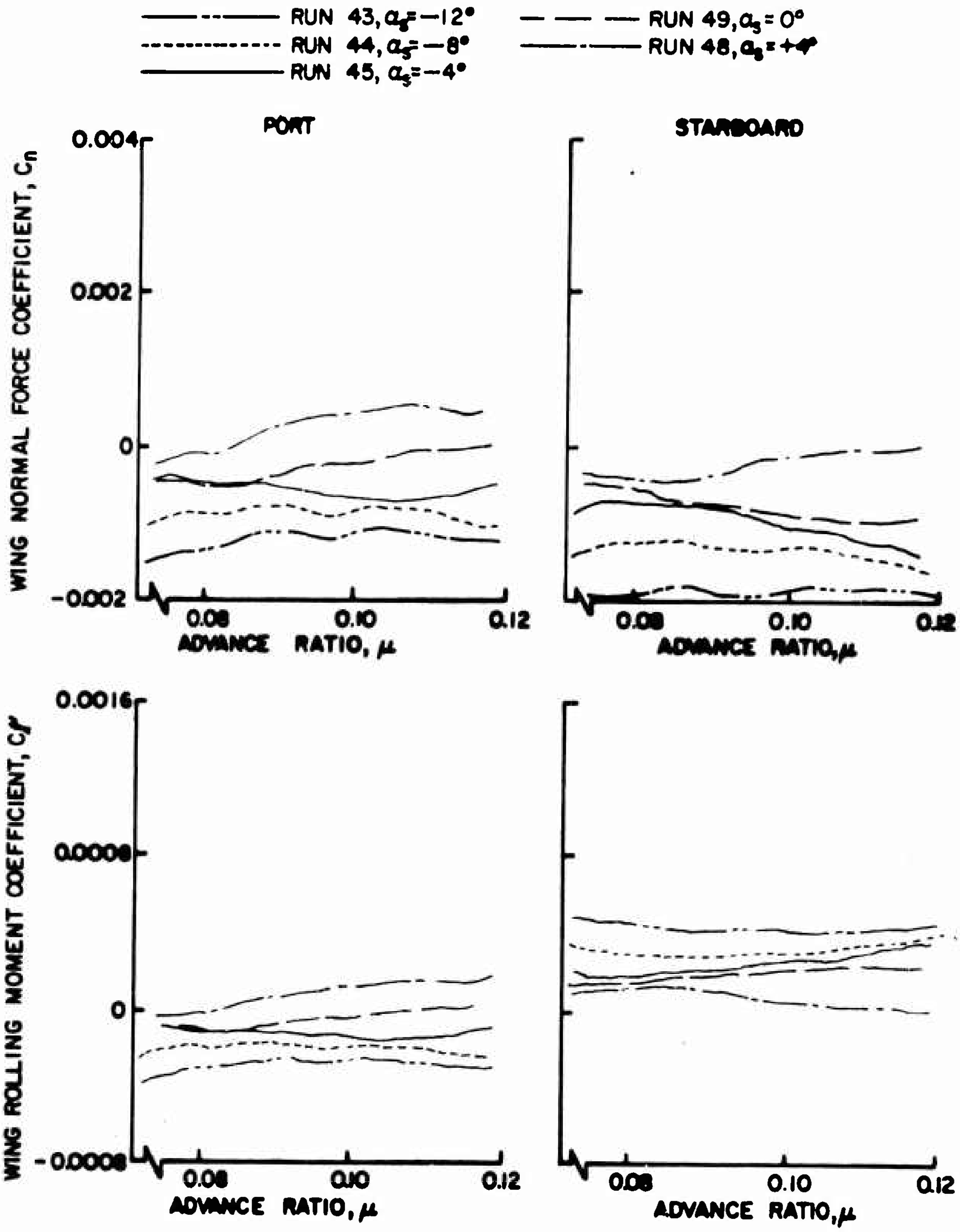

Figure 30. Wing Normal Force and Rolling Moment Coefficients as Functions of Advance Ratio, $\theta_{.75R} = 10^\circ$, Large Wing on Low.

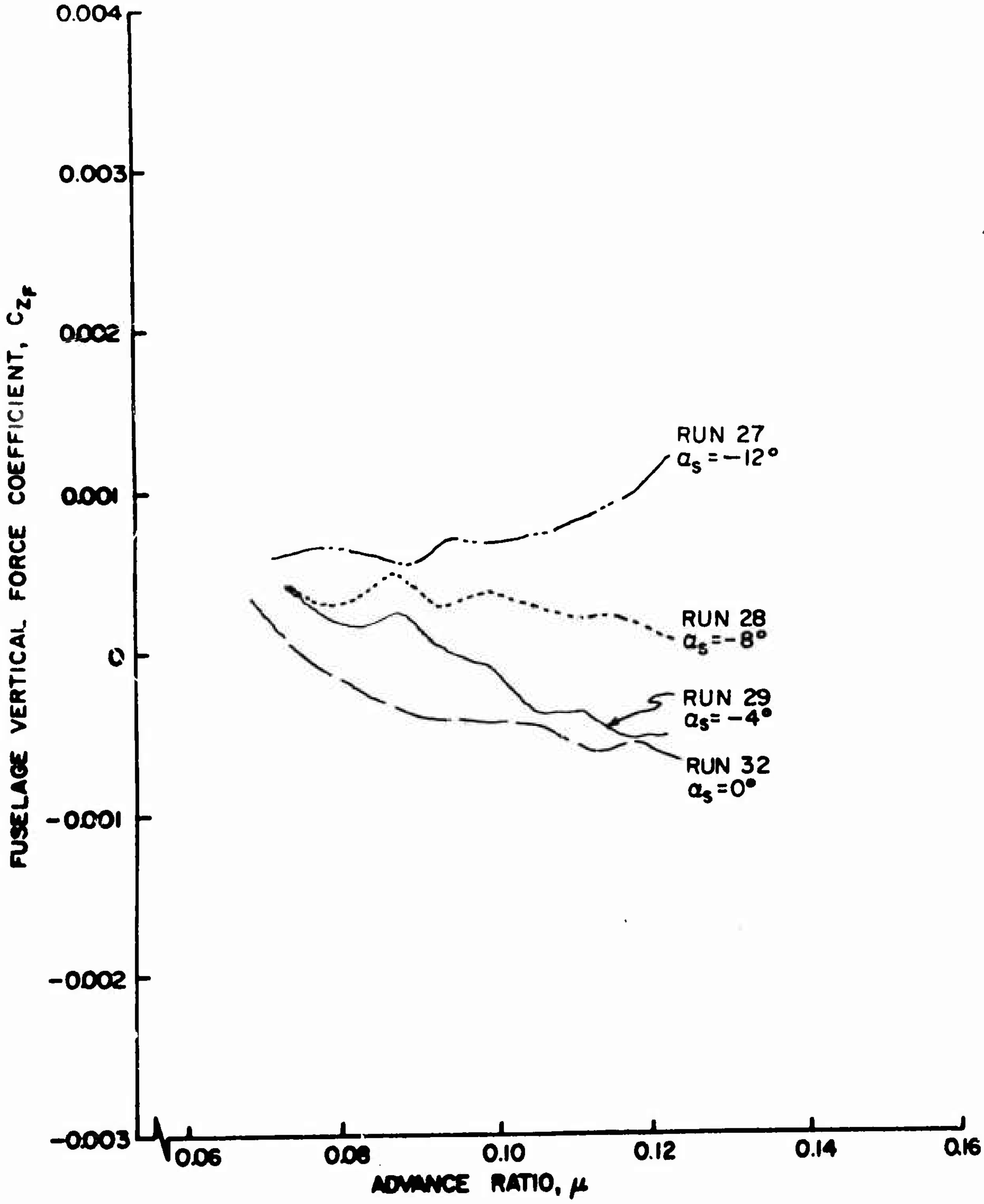

Figure 31a. Fuselage Vertical Force and Pitching Moment Coefficients as Functions of Advance Ratio, $\theta_{.75R} = 10°$, Small Wing on High.

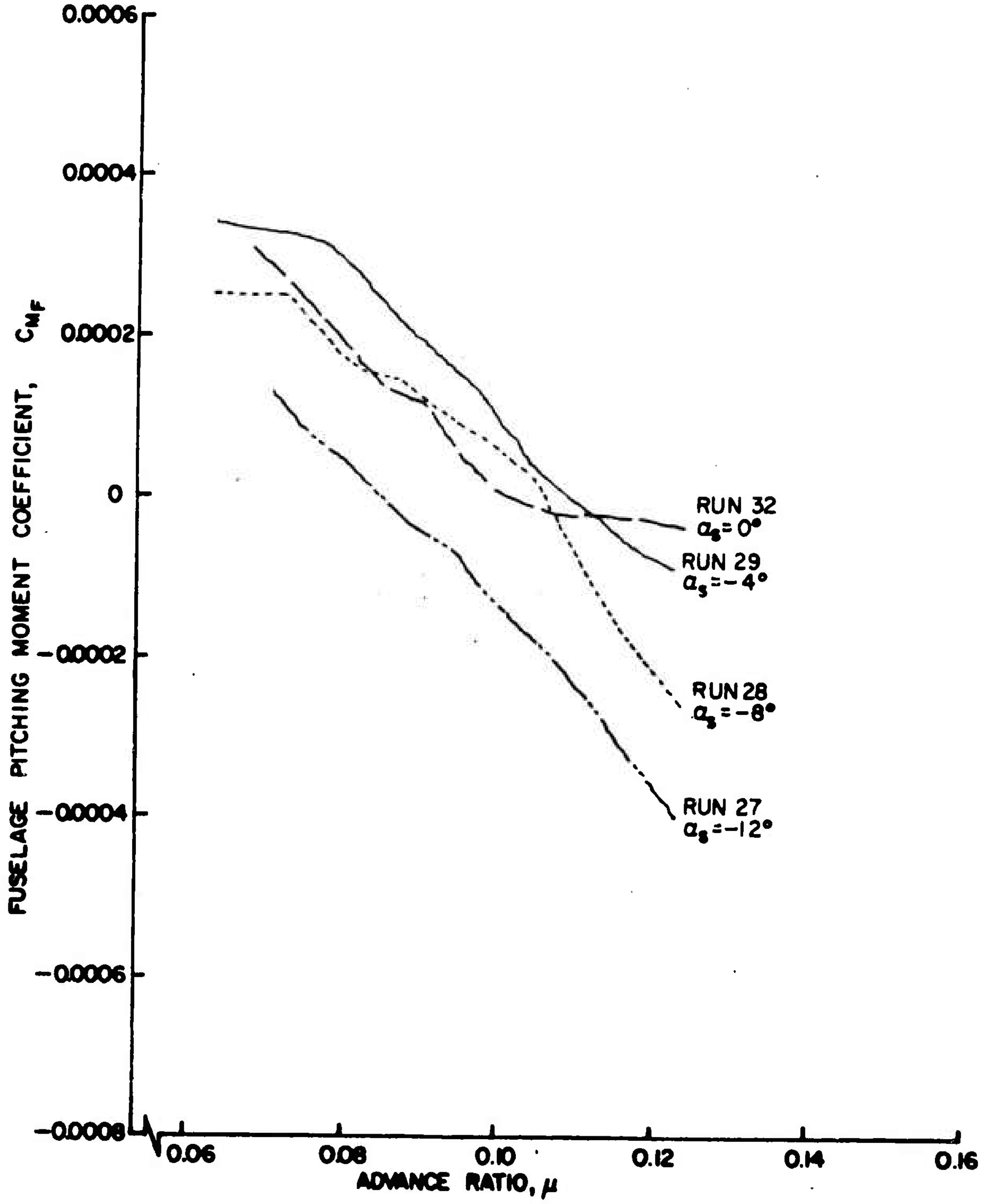

Figure 31b. Fuselage Vertical Force and Pitching Moment Coefficients as Functions of Advance Ratio, $\theta_{.75R} = 10°$, Small Wing on High.

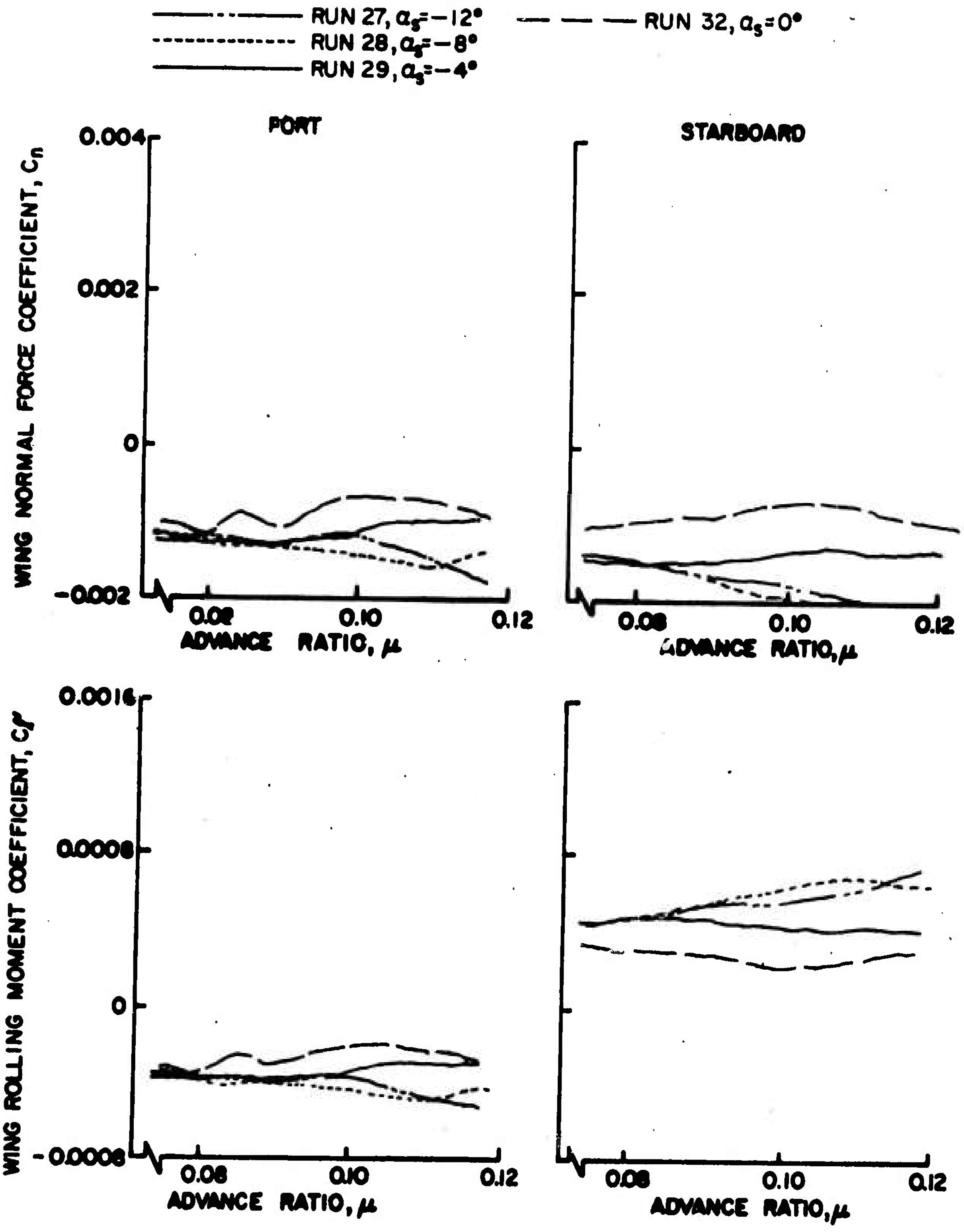

Figure 32. Wing Normal Force and Rolling Moment Coefficients as Functions of Advance Ratio, $\theta_{.75R} = 10°$, Small Wing on High.

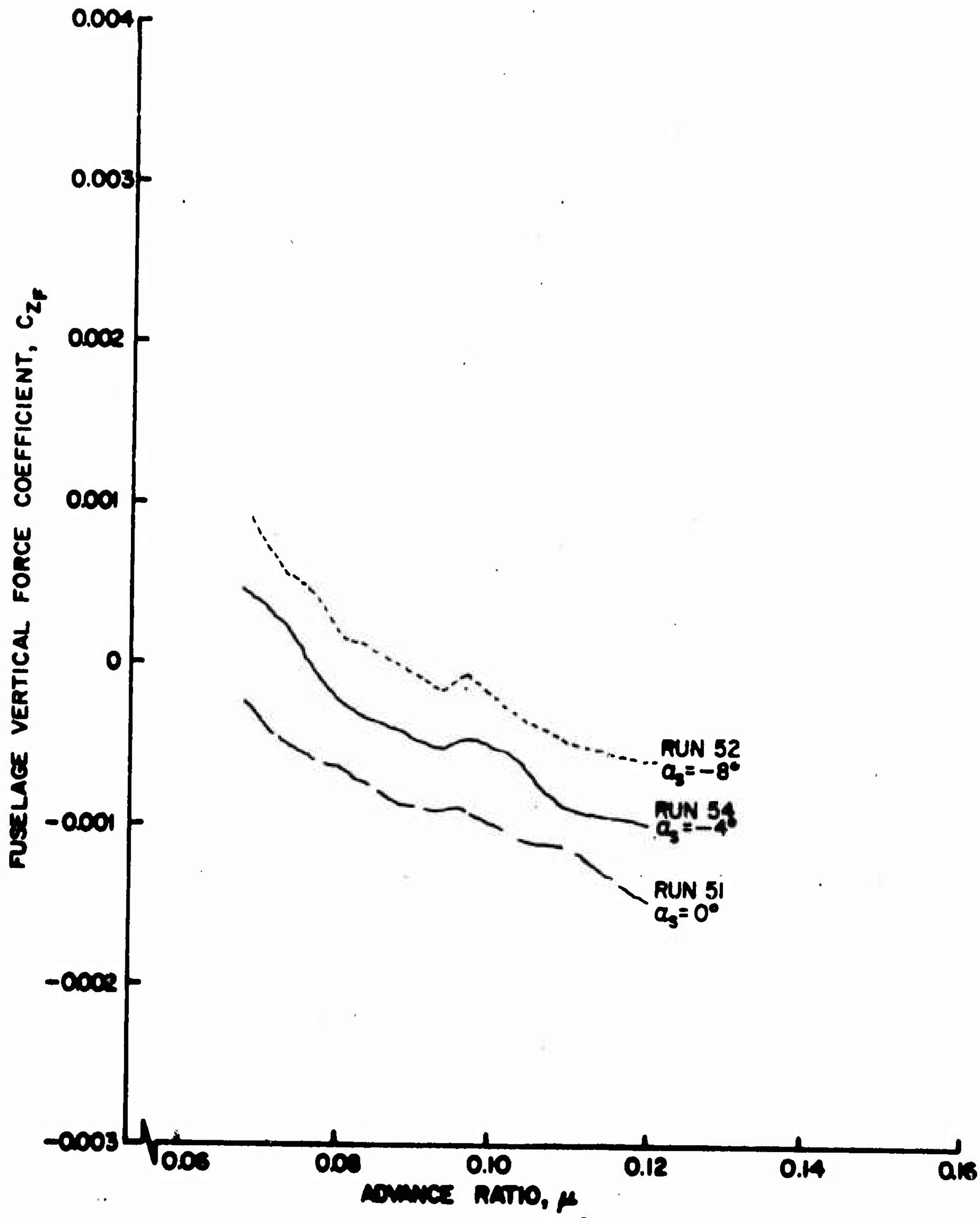

Figure 33a. Fuselage Vertical Force and Pitching Moment Coefficients as Functions of Advance Ratio, $\theta_{.75R} = 10°$, Small Wing on Low.

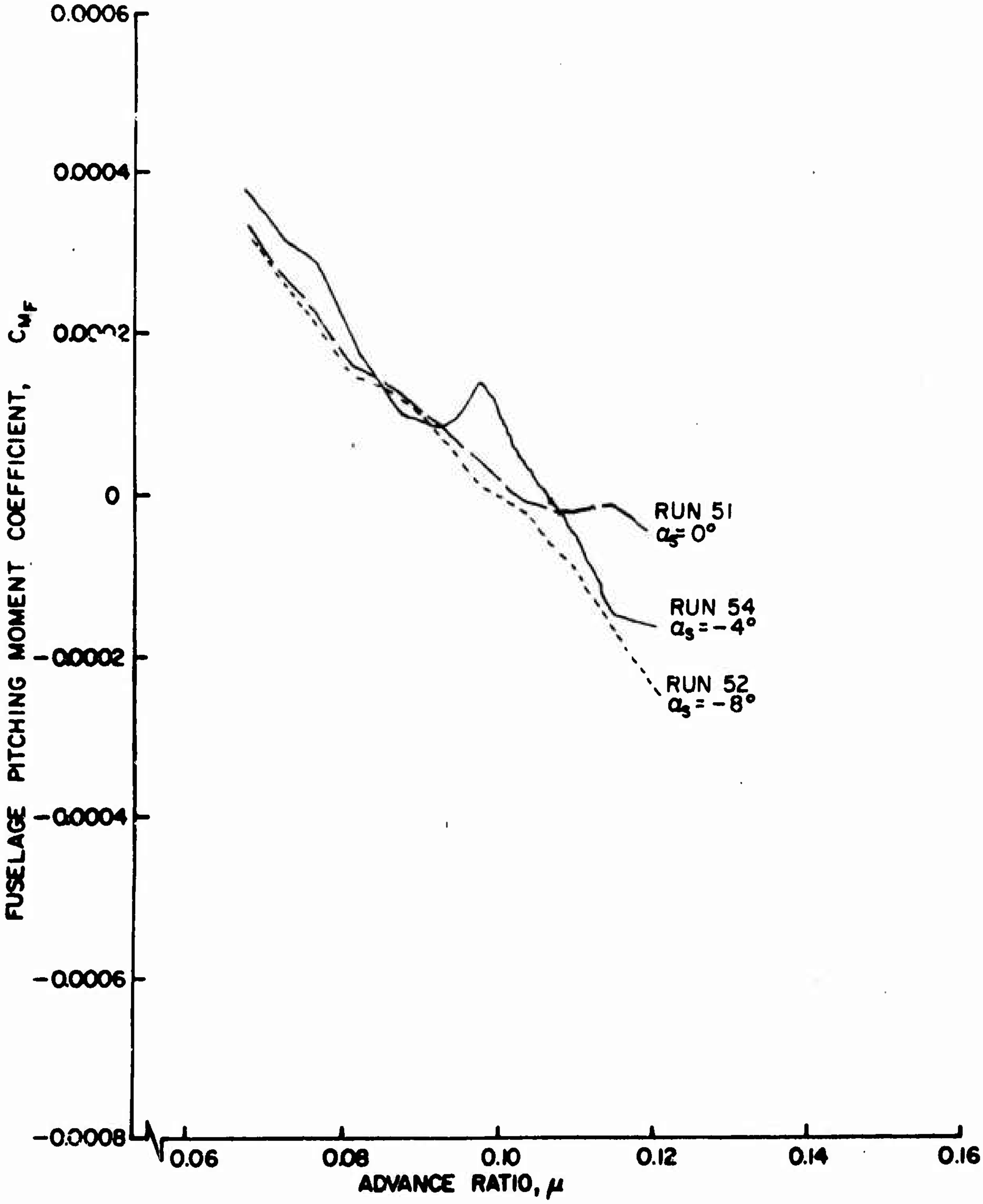

Figure 33b. Fuselage Vertical Force and Pitching Moment Coefficients as Functions of Advance Ratio, $\theta_{.75R} = 10°$, Small Wing on Low.

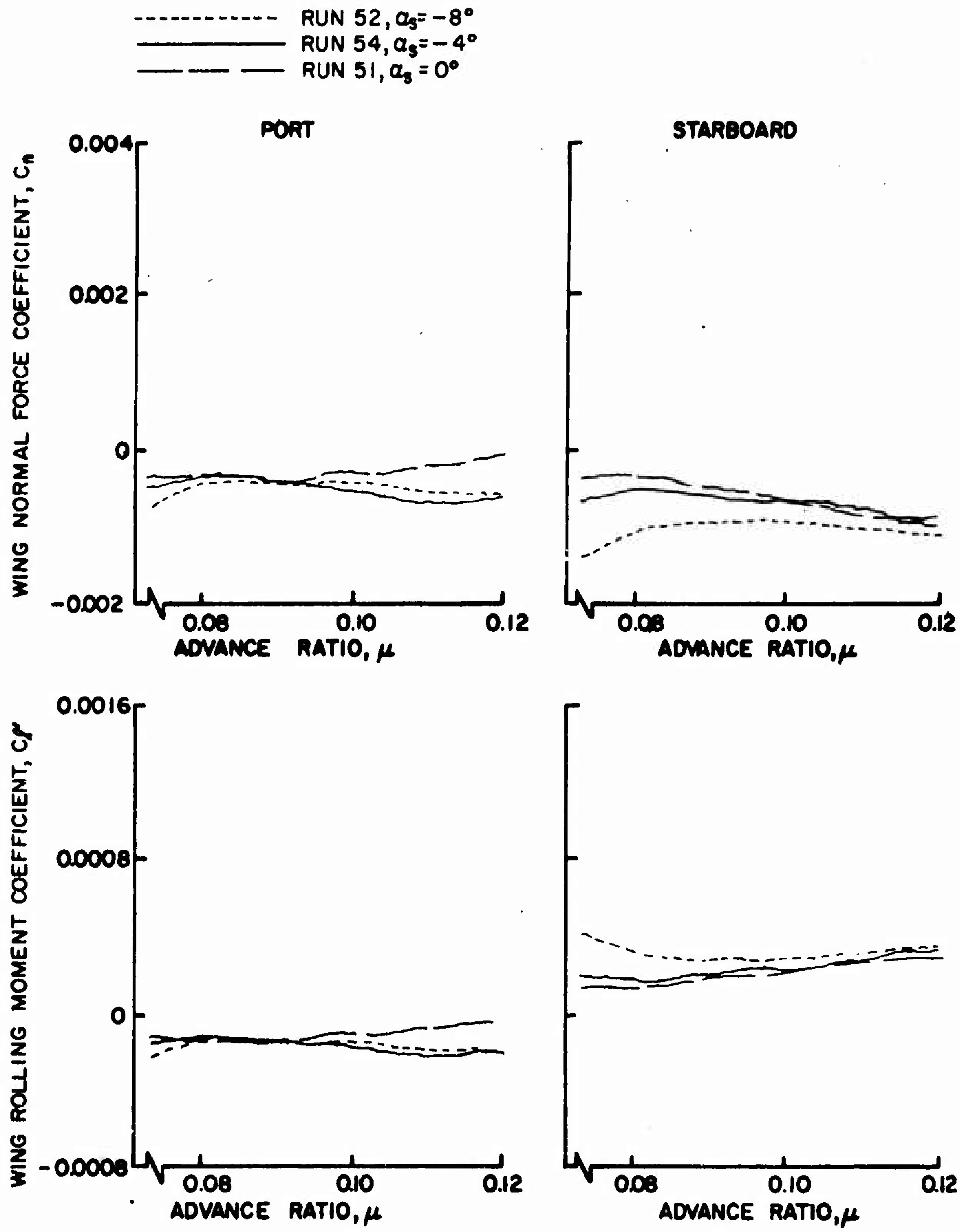

Figure 34. Wing Normal Force and Rolling Moment Coefficients as Functions of Advance Ratio, $\theta_{.75R}$ = 10°, Small Wing on Low.

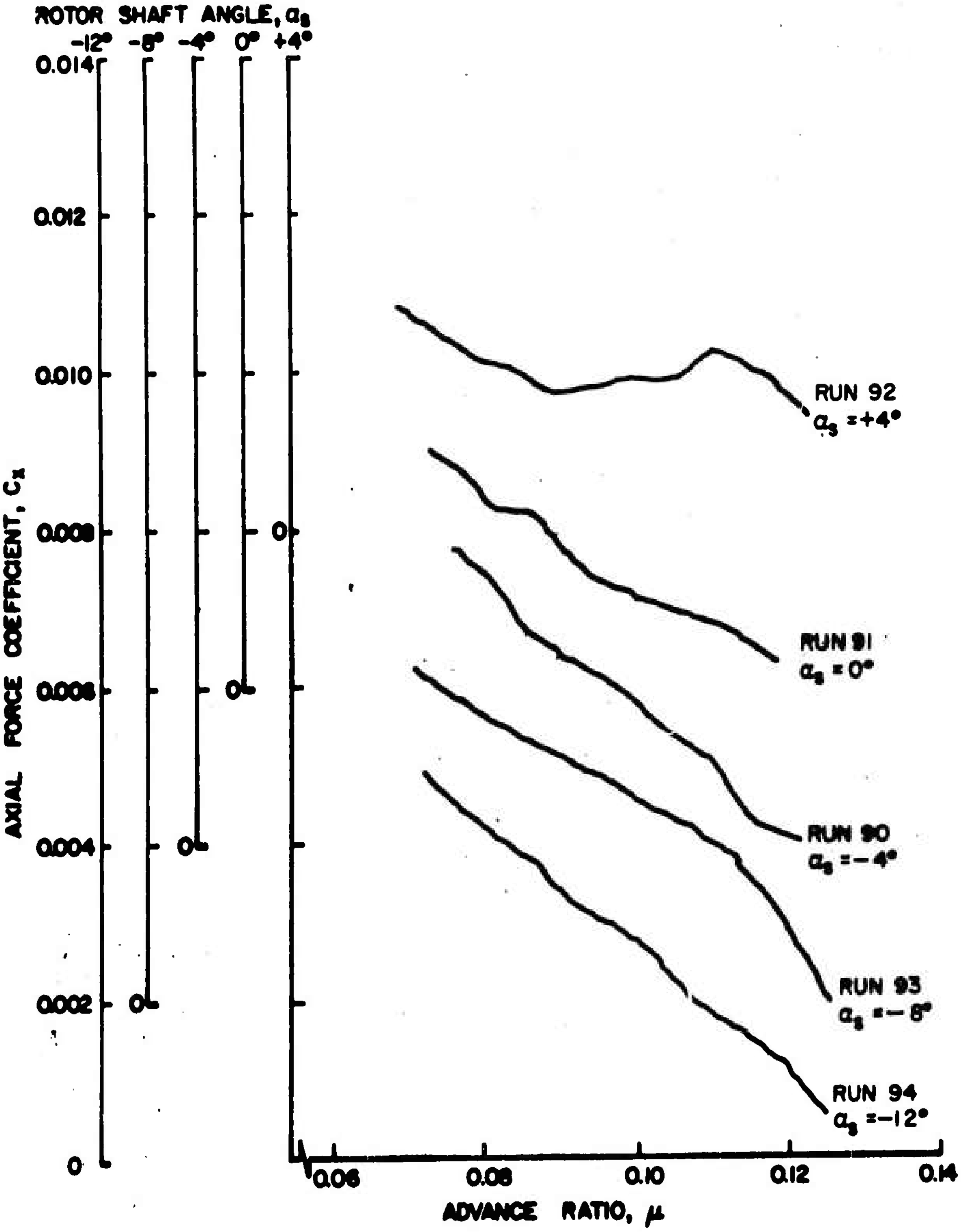

Figure 35a. Rotor Force and Moment Coefficients as Functions of Advance Ratio, $\theta_{.75R} = 12°$, Wing Off.

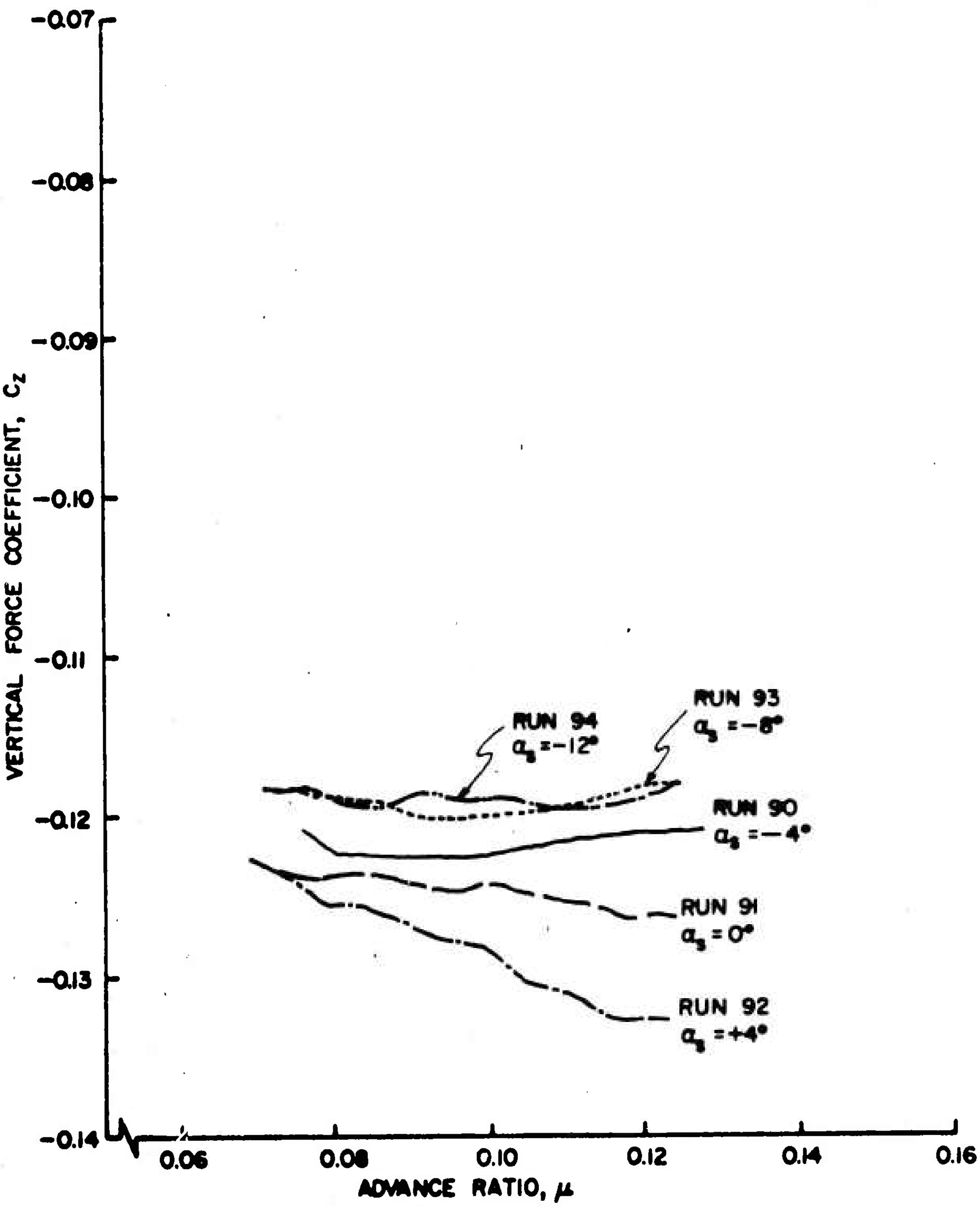

Figure 35b. Rotor Force and Moment Coefficients as Functions of Advance Ratio, $\theta_{.75R} = 12°$, Wing Off.

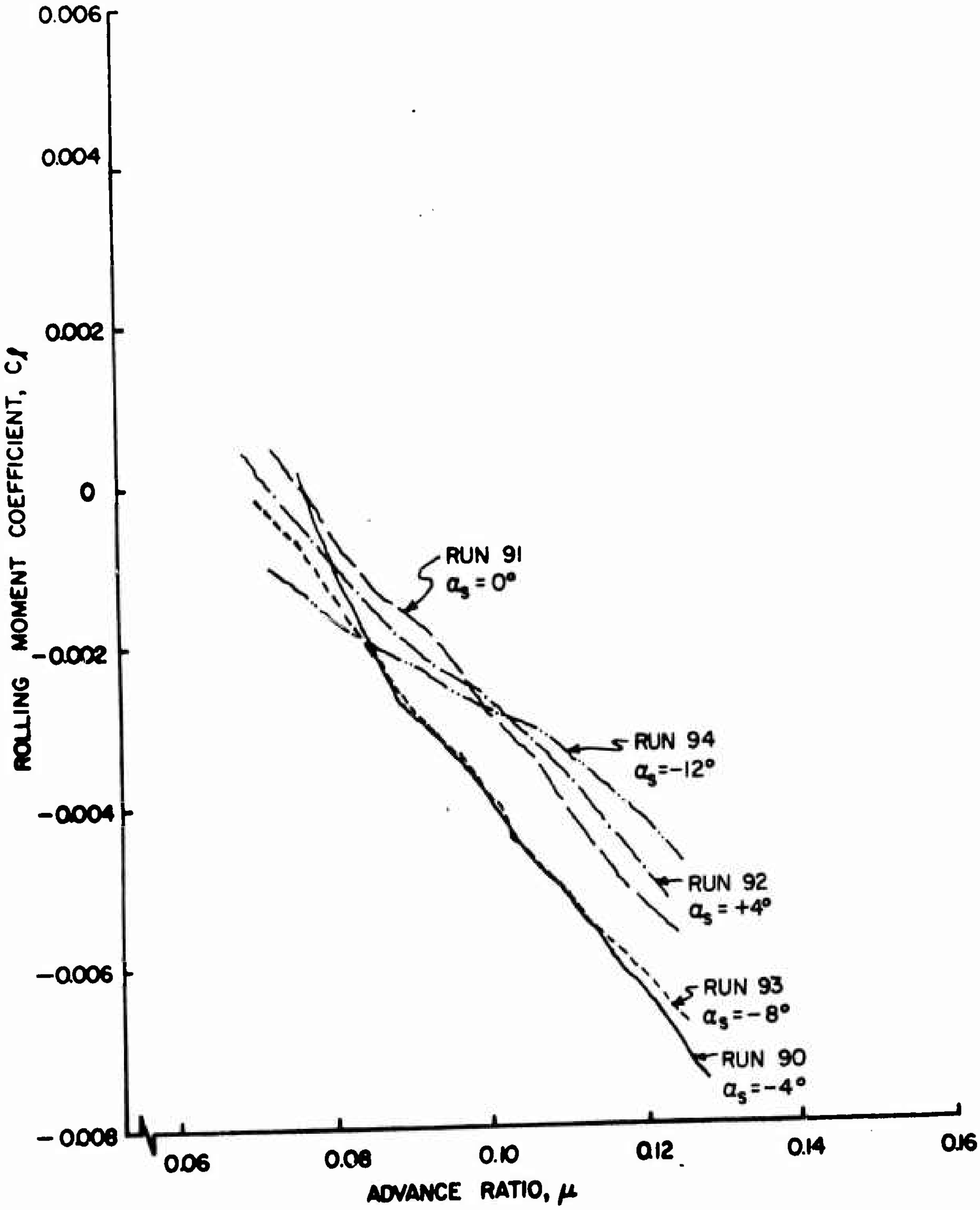

Figure 35c. Rotor Force and Moment Coefficients as Functions of Advance Ratio, $\theta_{.75R} = 12°$, Wing Off.

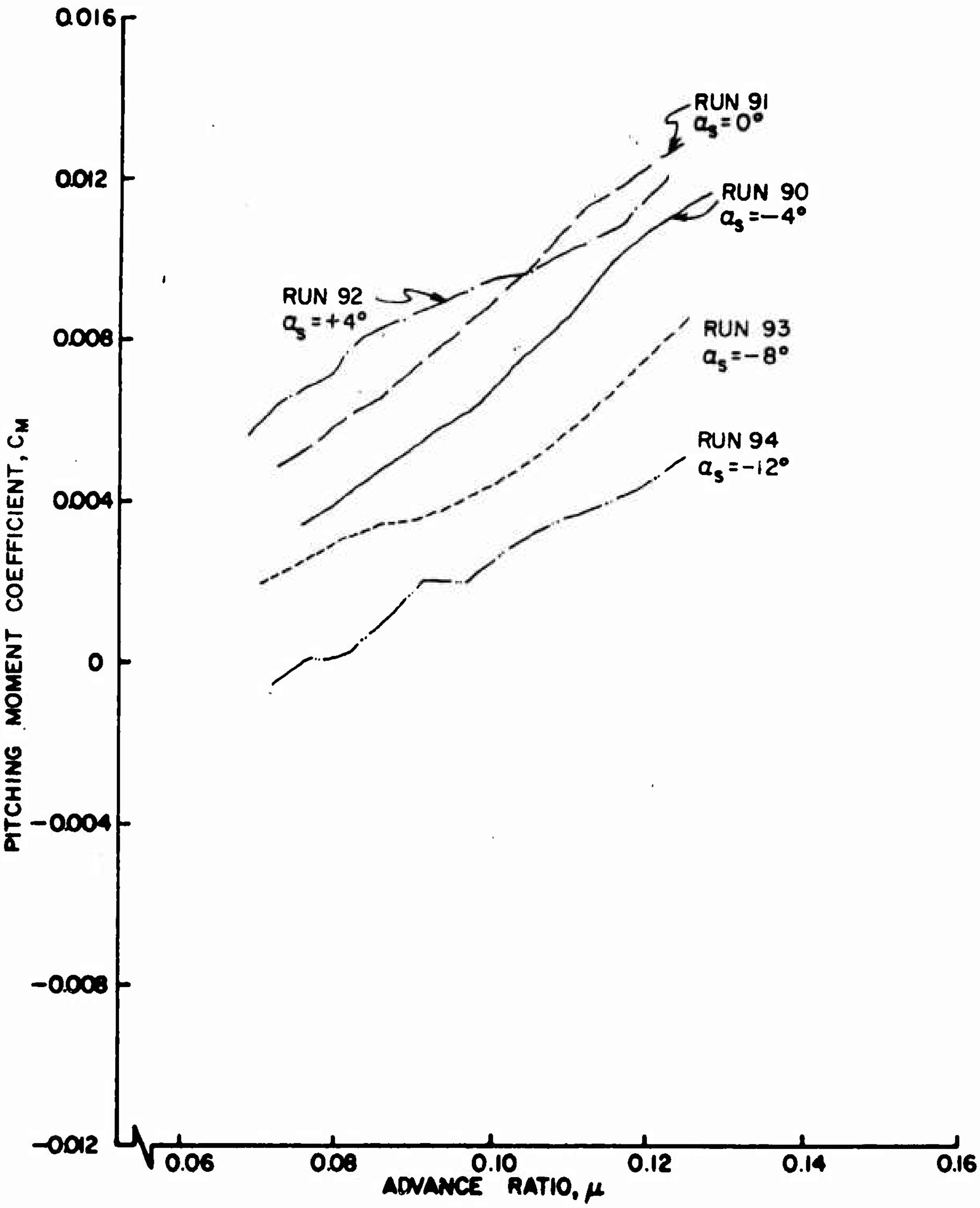

Figure 35d. Rotor Force and Moment Coefficients as Functions of Advance Ratio, $\theta_{.75R} = 12^{\circ}$, Wing Off.

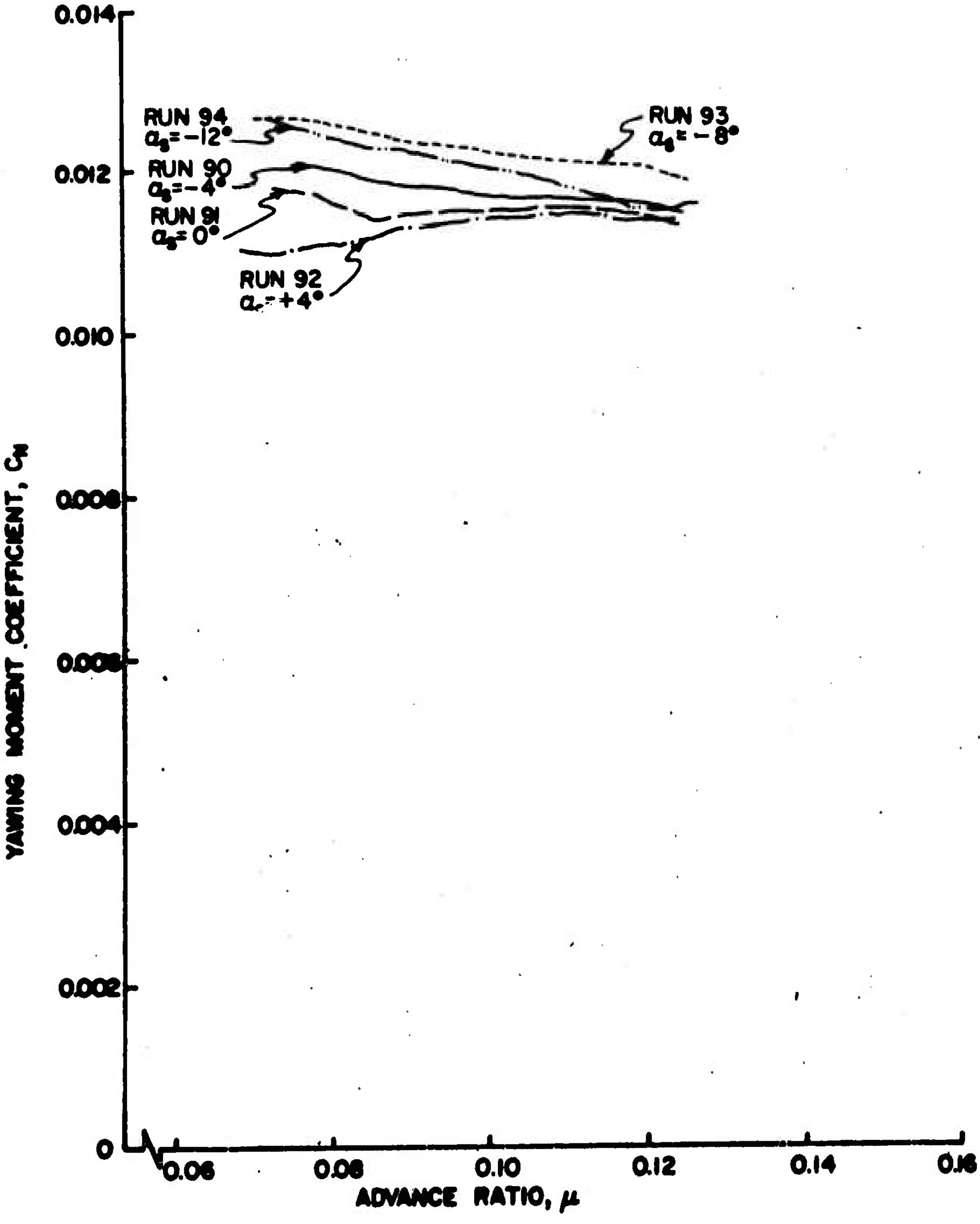

Figure 35e. Rotor Force and Moment Coefficients as Functions of Advance Ratio, $\theta_{.75R} = 12°$, Wing Off.

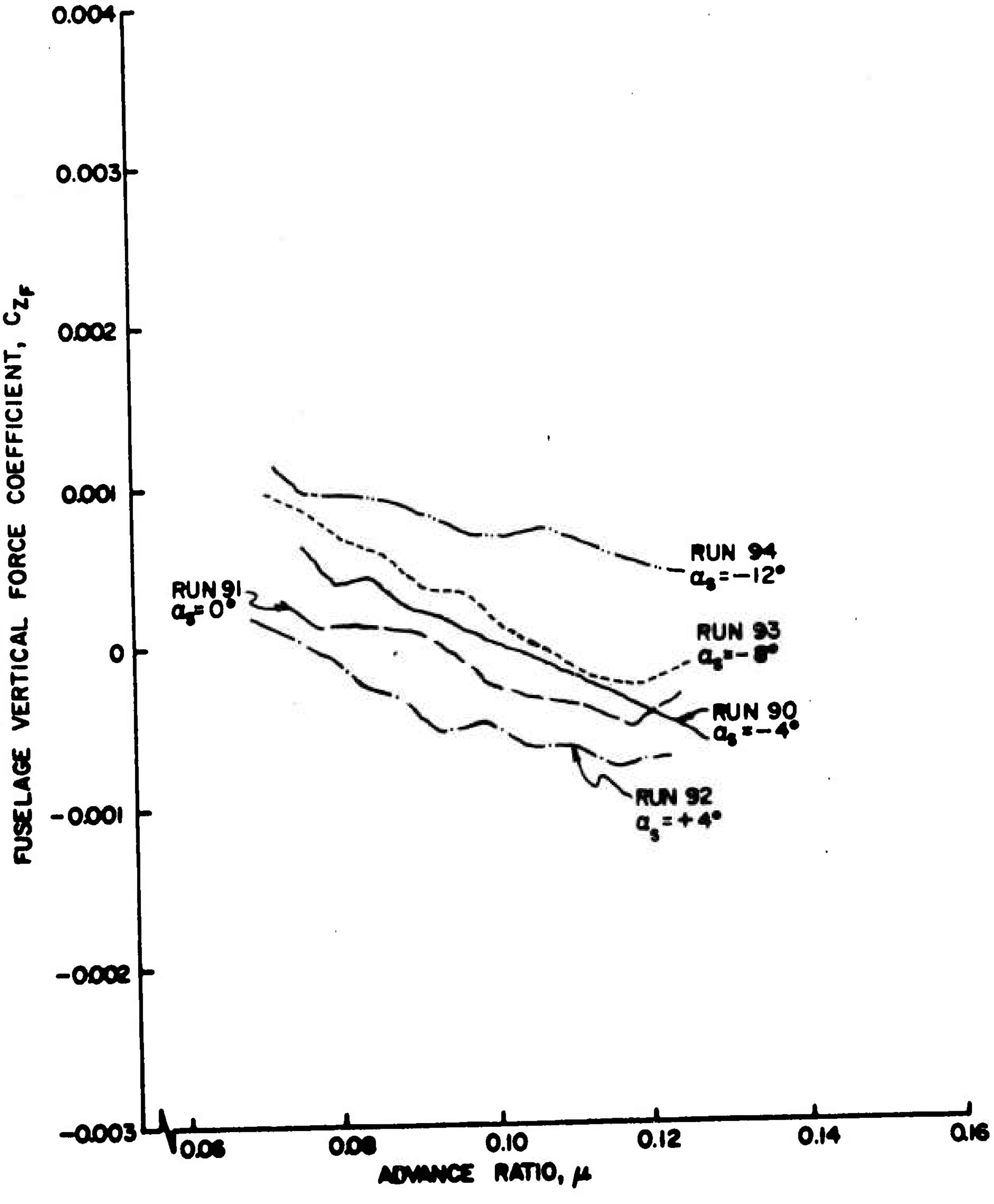

Figure 36a. Fuselage Vertical Force and Pitching Moment Coefficients as Functions of Advance Ratio, $\theta_{.75R} = 12°$, Wing Off.

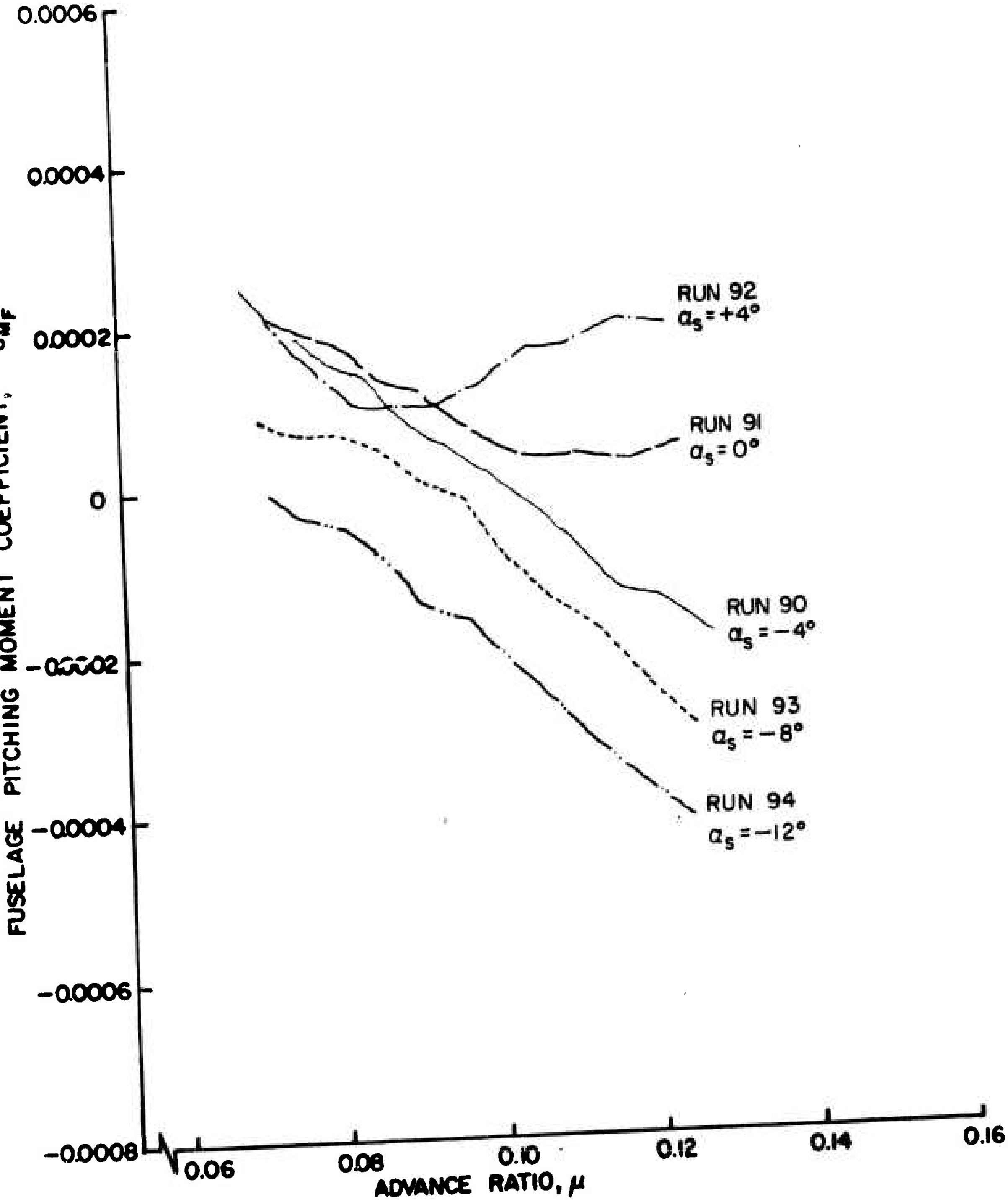

Figure 36b. Fuselage Vertical Force and Pitching Moment Coefficients as Functions of Advance Ratio, $\theta_{.75R} = 12°$, Wing Off.

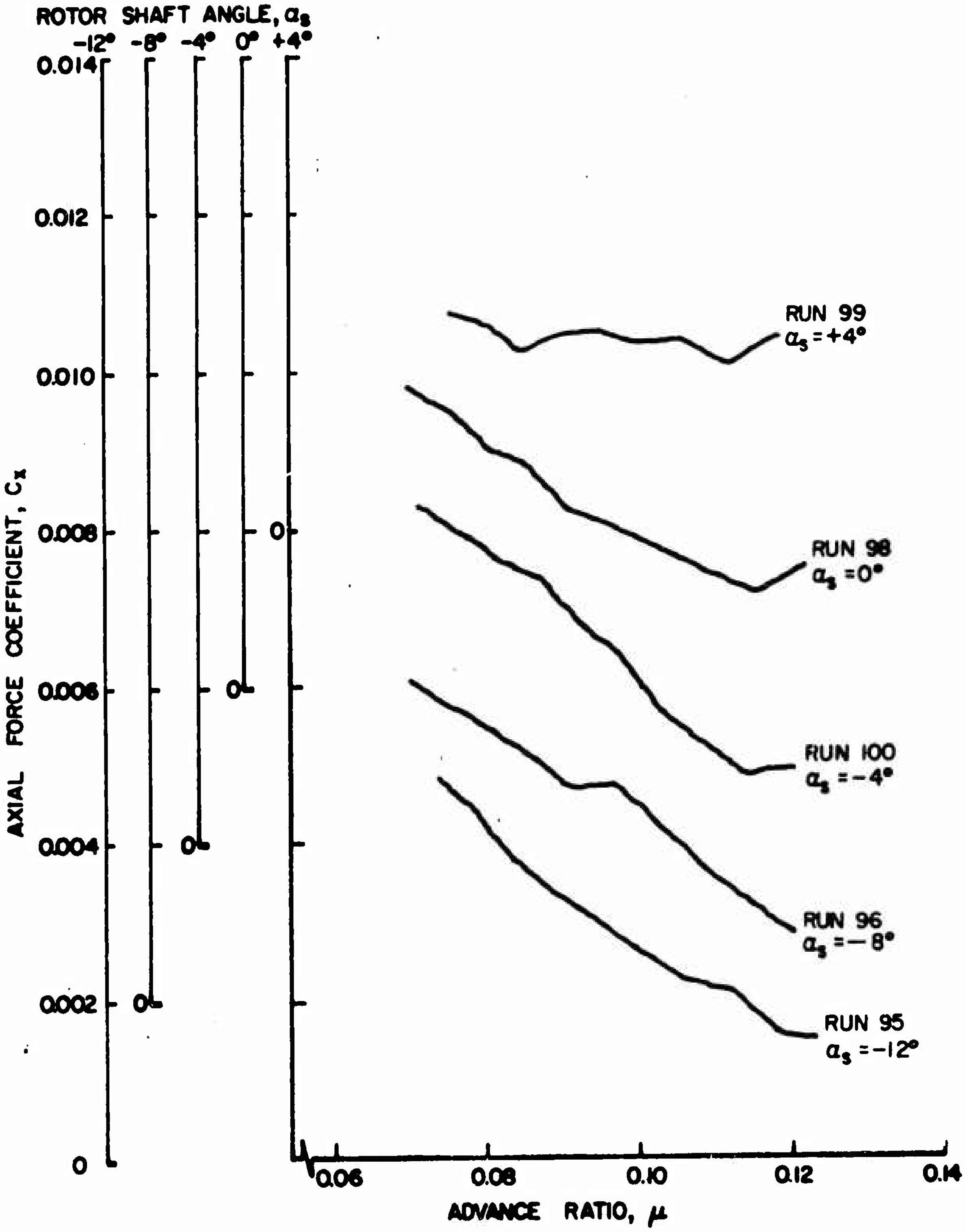

Figure 37a. Rotor Force and Moment Coefficients as Functions of Advance Ratio, $\theta_{.75R} = 12^\circ$, Large Wing on High.

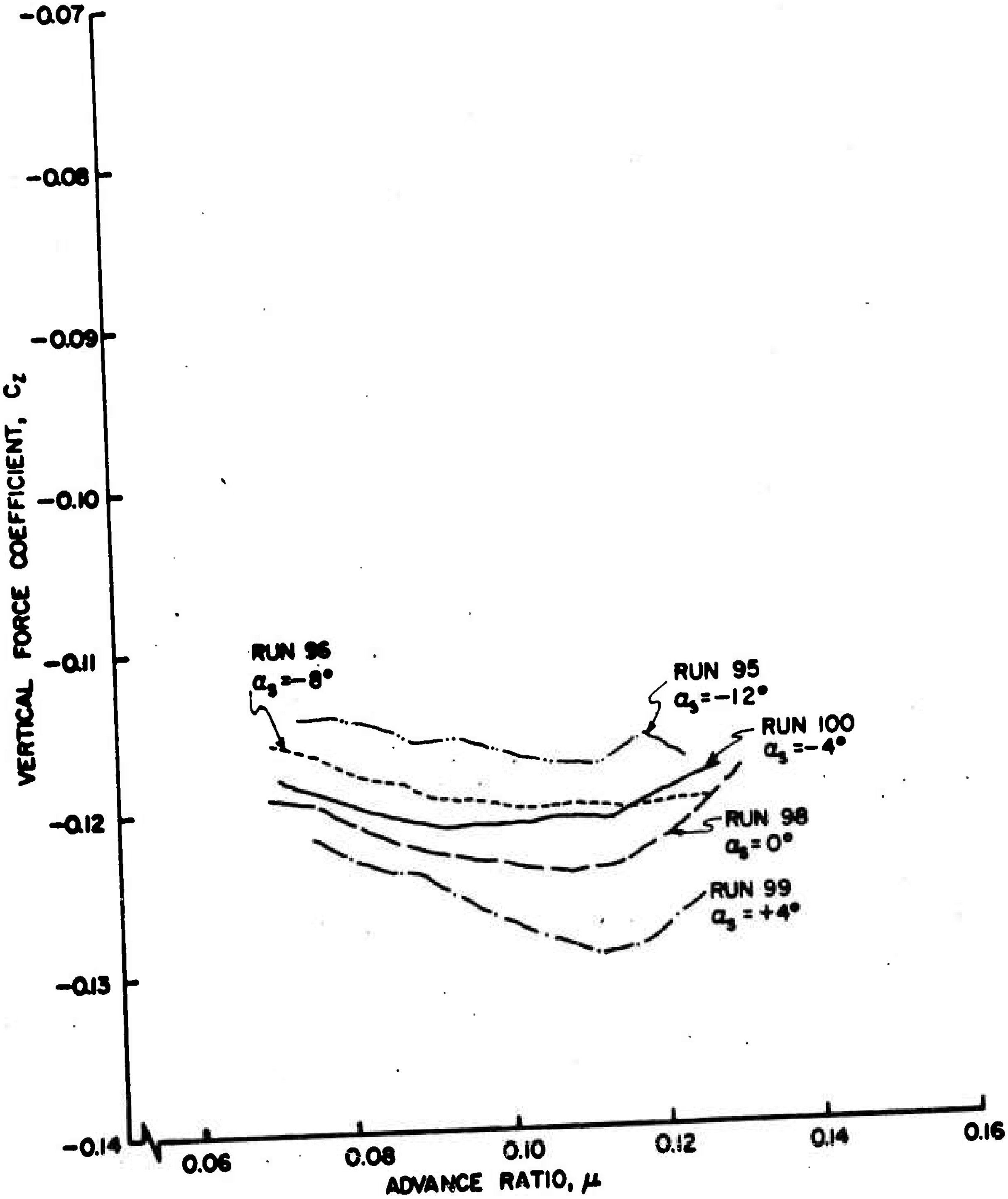

Figure 37b. Rotor Force and Moment Coefficients as Functions of Advance Ratio, $\theta_{.75R} = 12^{\circ}$, Large Wing on High.

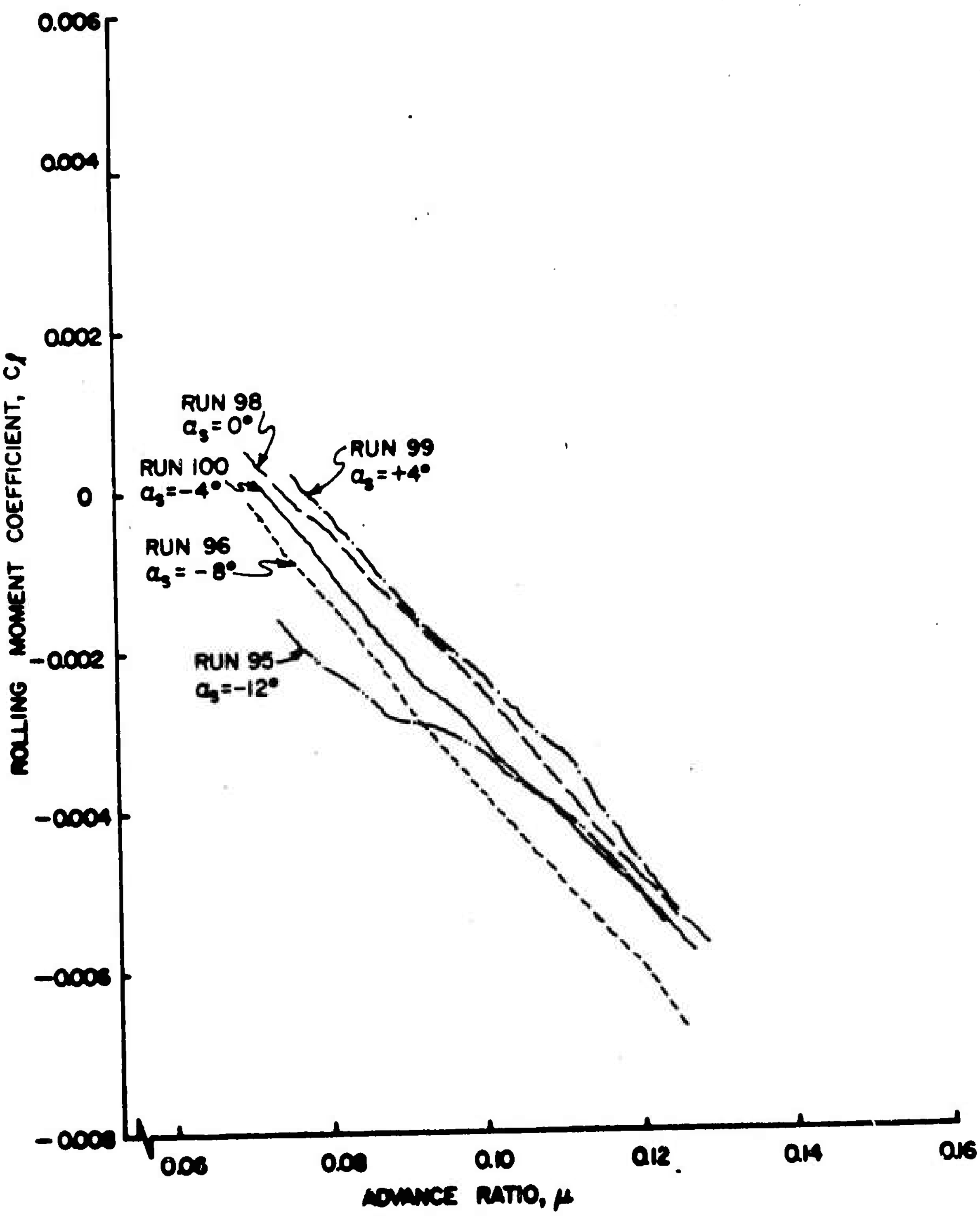

Figure 37c. Rotor Force and Moment Coefficients as Functions of Advance Ratio, $\theta_{.75R} = 12^\circ$, Large Wing on High.

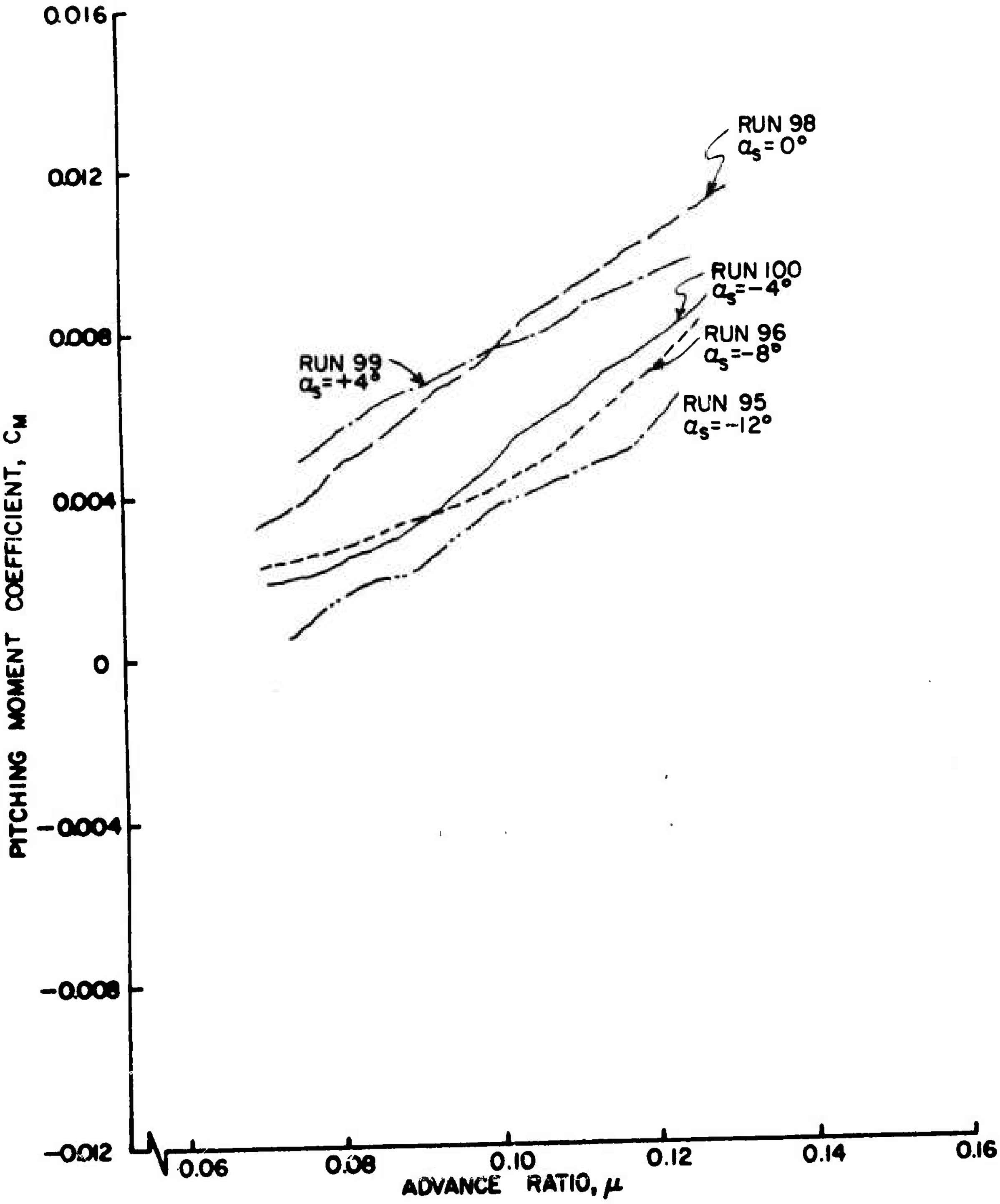

Figure 37d. Rotor Force and Moment Coefficients as Functions of Advance Ratio, $\theta_{.75R} = 12^{\circ}$, Large Wing on High.

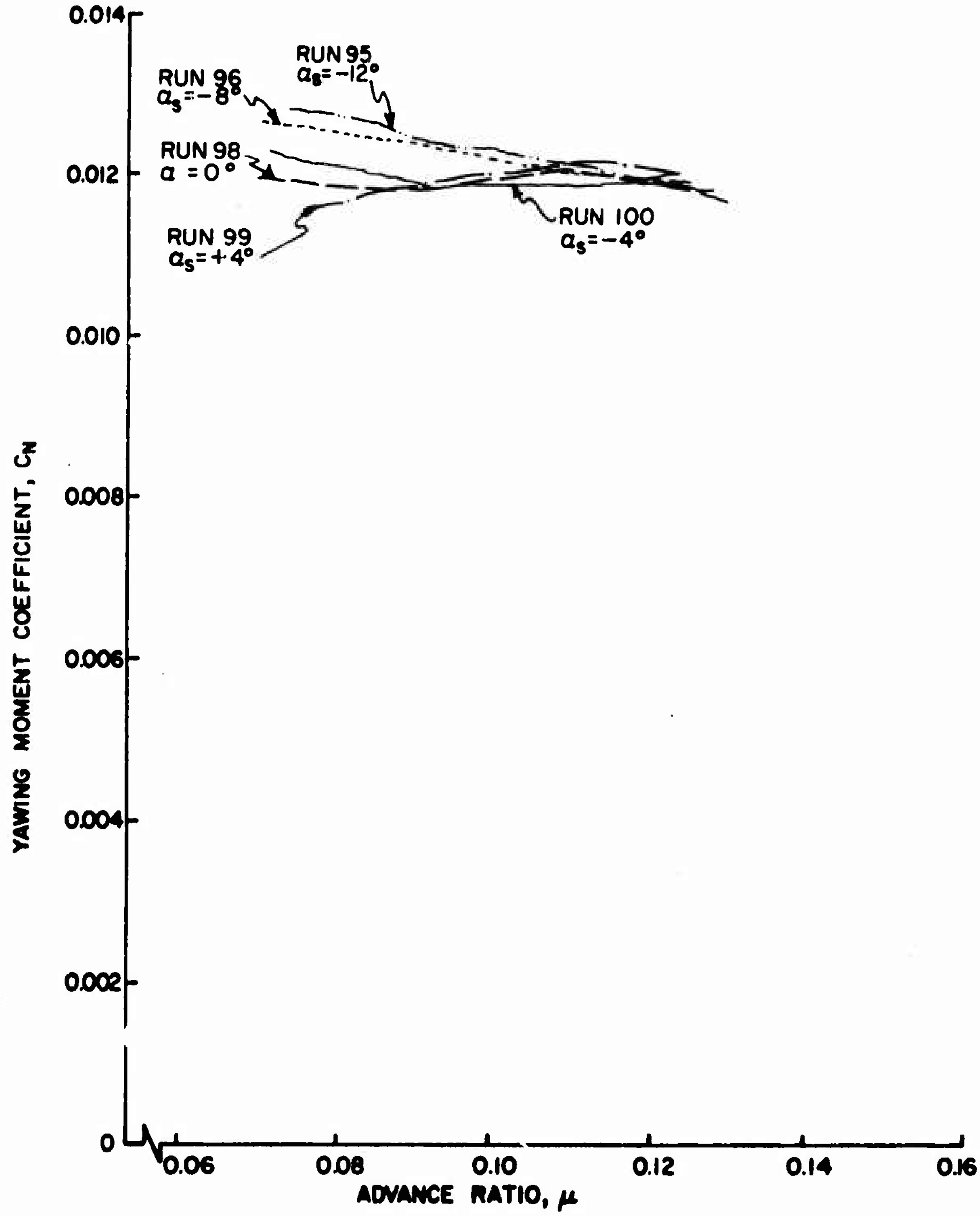

Figure 37e. Rotor Force and Moment Coefficients as Functions of Advance Ratio, $\theta_{.75R} = 12°$, Large Wing on High.

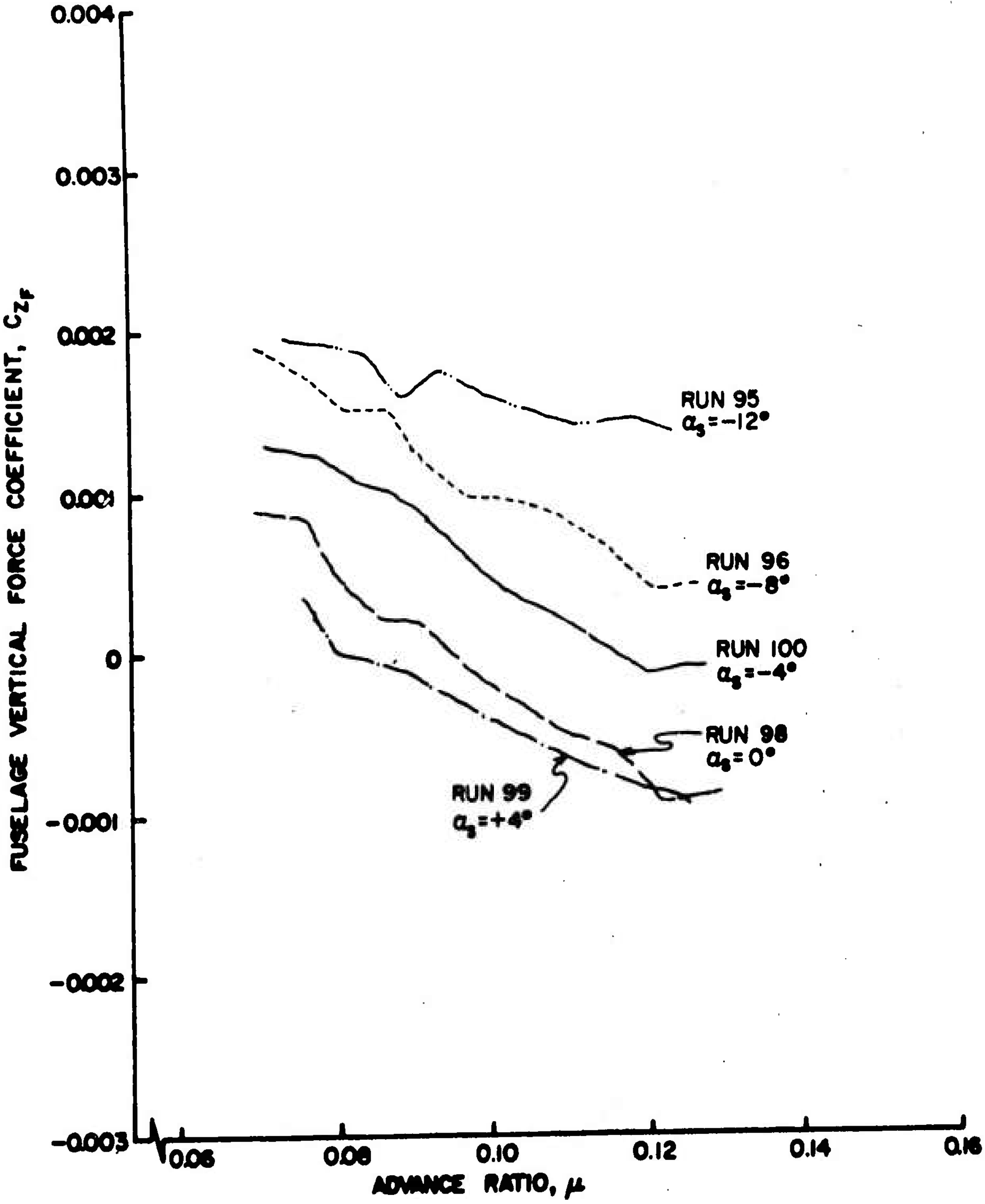

Figure 38a. Fuselage Vertical Force and Pitching Moment Coefficients as Functions of Advance Ratio, $\theta_{.75R} = 12°$, Large Wing on High.

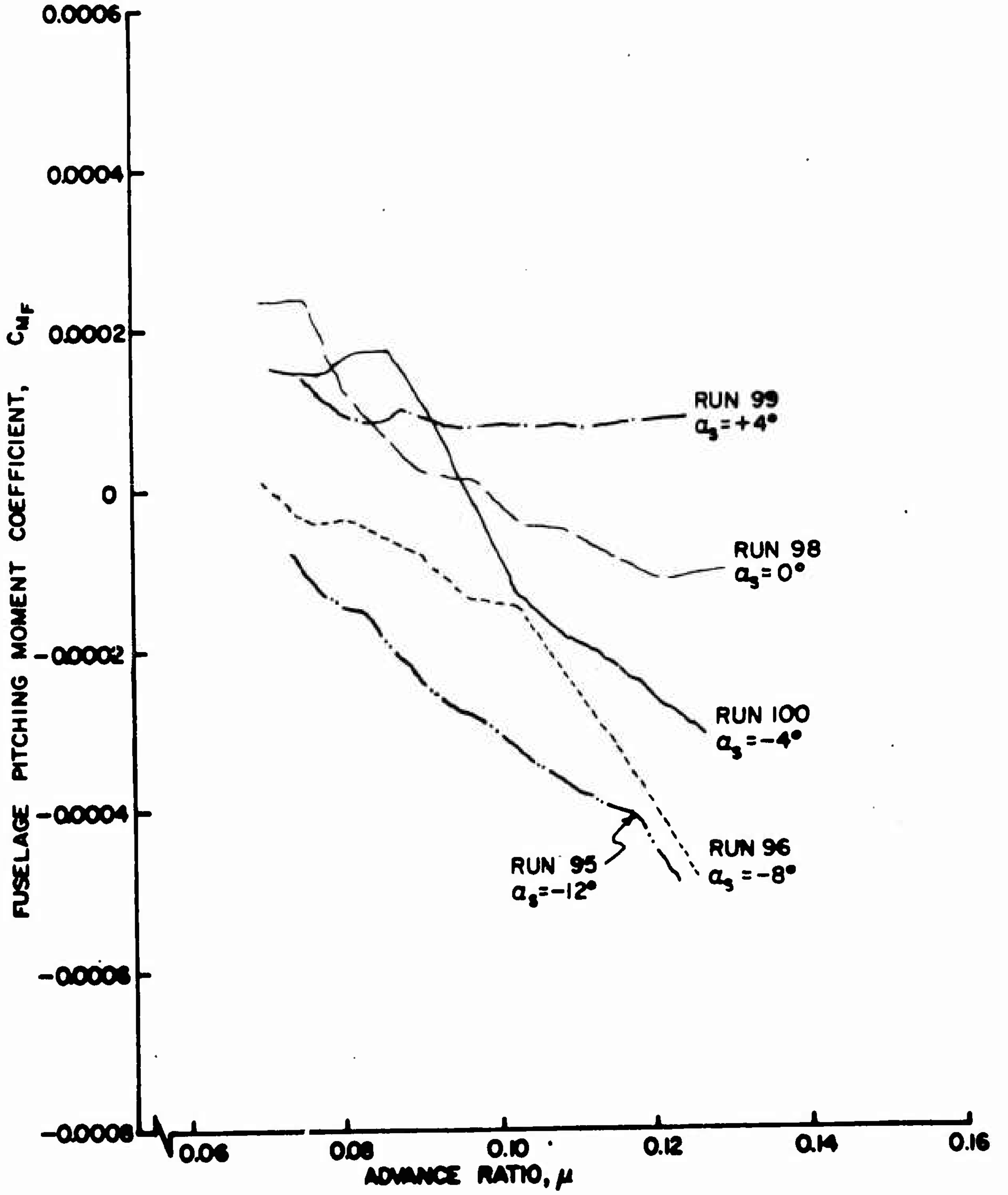

Figure 38b. Fuselage Vertical Force and Pitching Moment Coefficients as Functions of Advance Ratio, $\theta_{.75R} = 12°$, Large Wing on High.

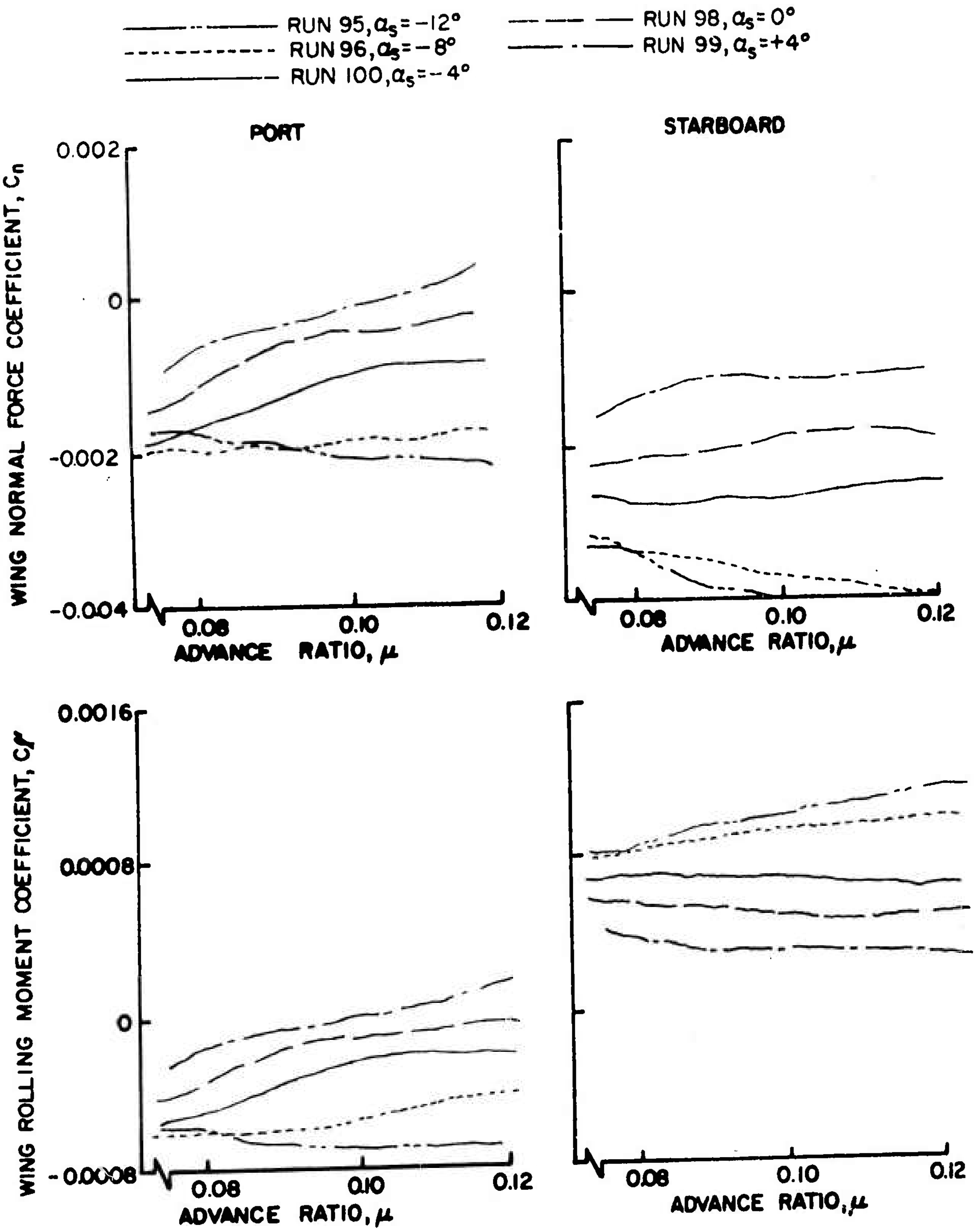

Figure 39. Wing Normal Force and Rolling Moment Coefficients as Functions of Advance Ratio, $\theta_{.75R} = 12°$, Large Wing on High.

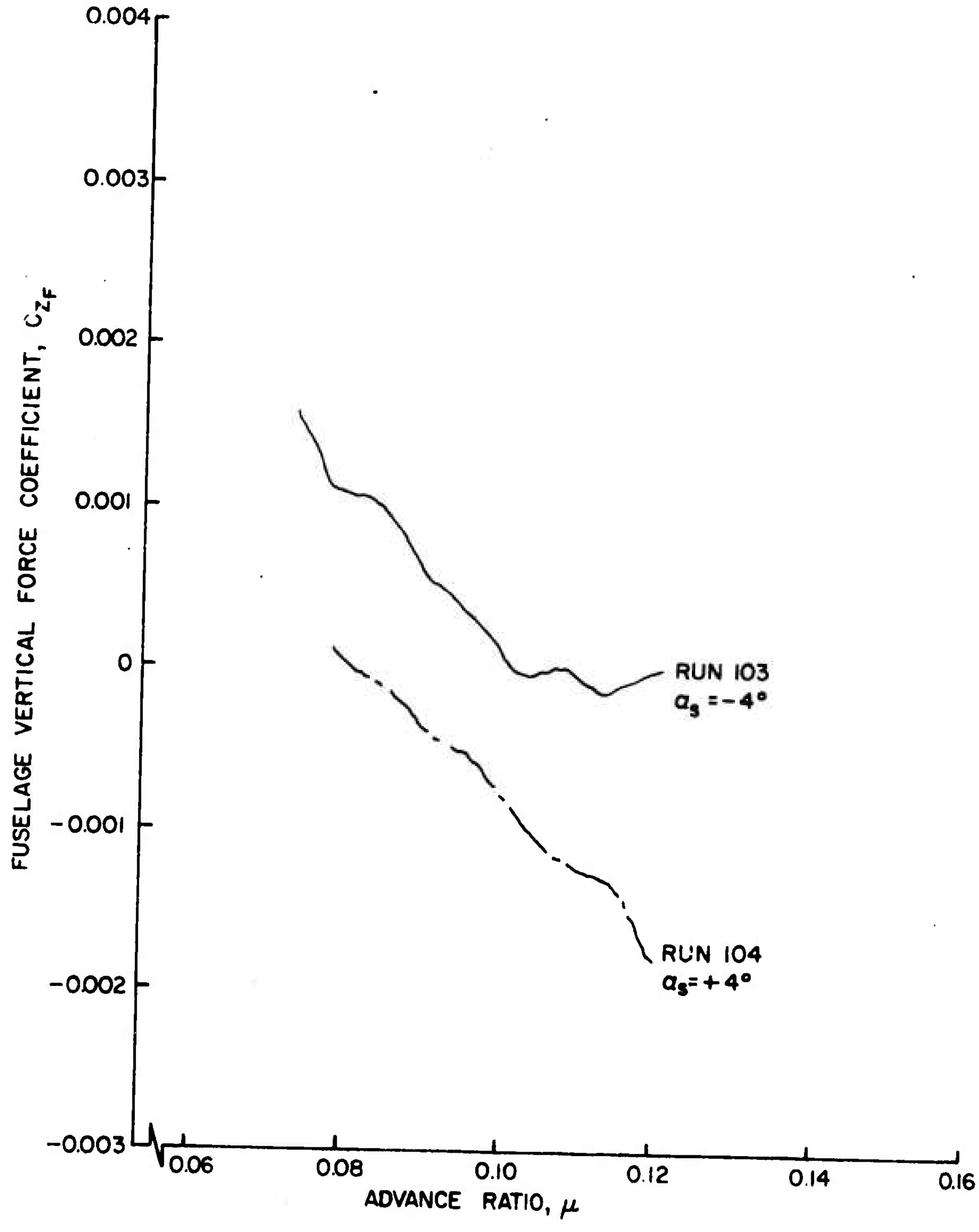

Figure 40a. Fuselage Vertical Force and Pitching Moment Coefficients as Functions of Advance Ratio, $\theta_{.75R} = 12°$, Large Wing on Low.

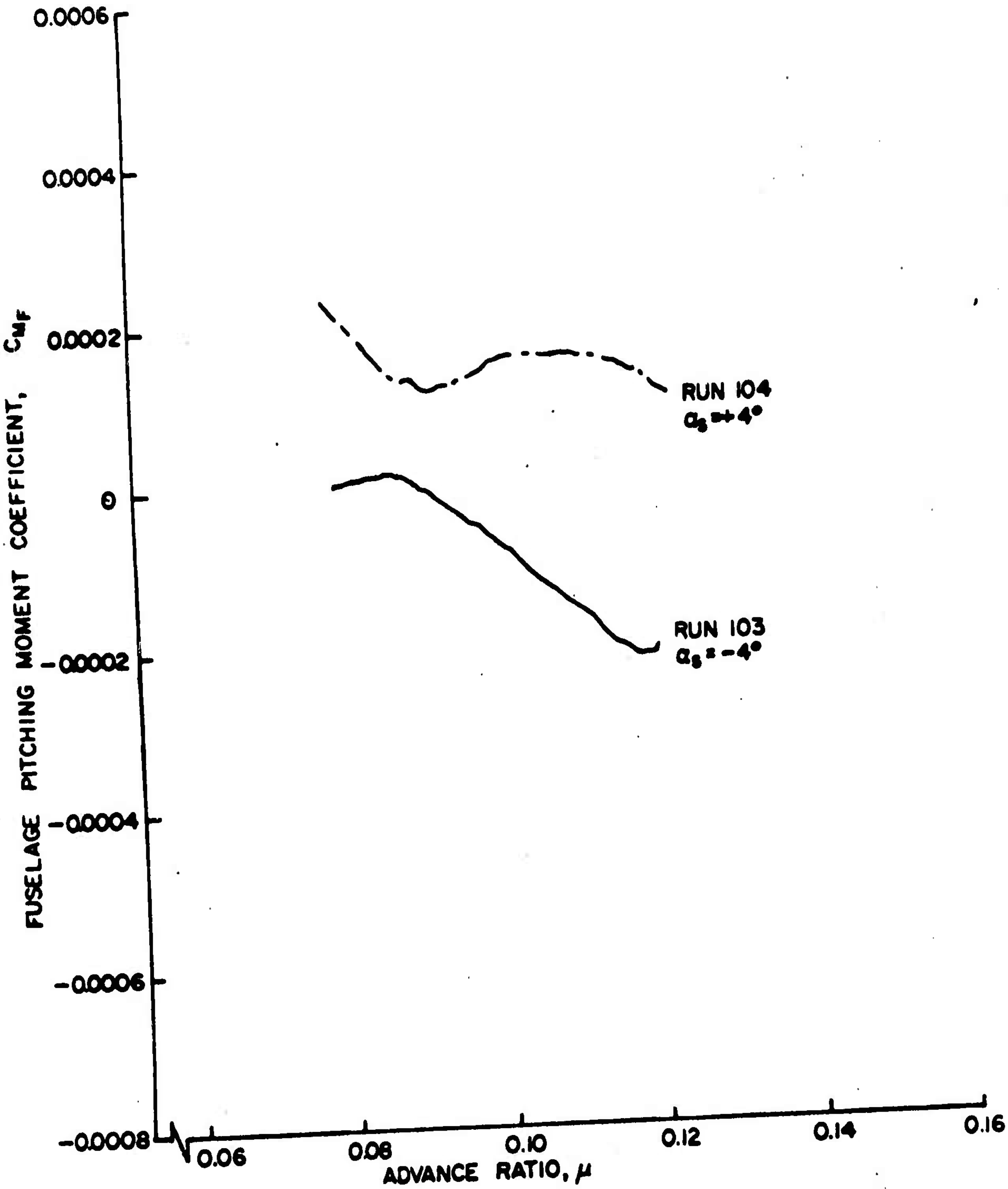

Figure 40b. Fuselage Vertical Force and Pitching Moment Coefficients as Functions of Advance Ratio, $\theta_{.75R} = 12°$, Large Wing on Low.

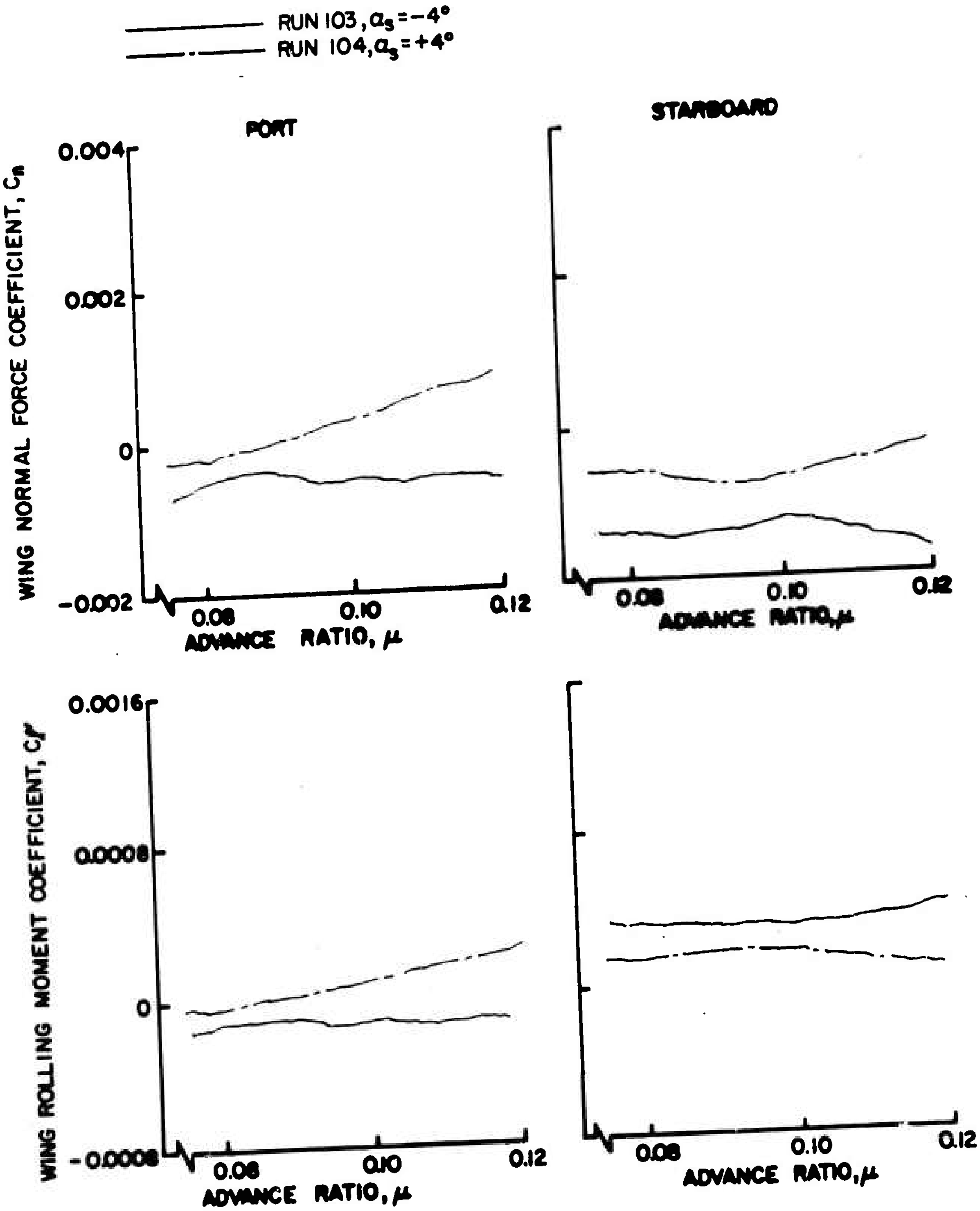

Figure 41. Wing Normal Force and Rolling Moment Coefficients as Functions of Advance Ratio, $\theta_{.75R} = 12^\circ$, Large Wing on Low.

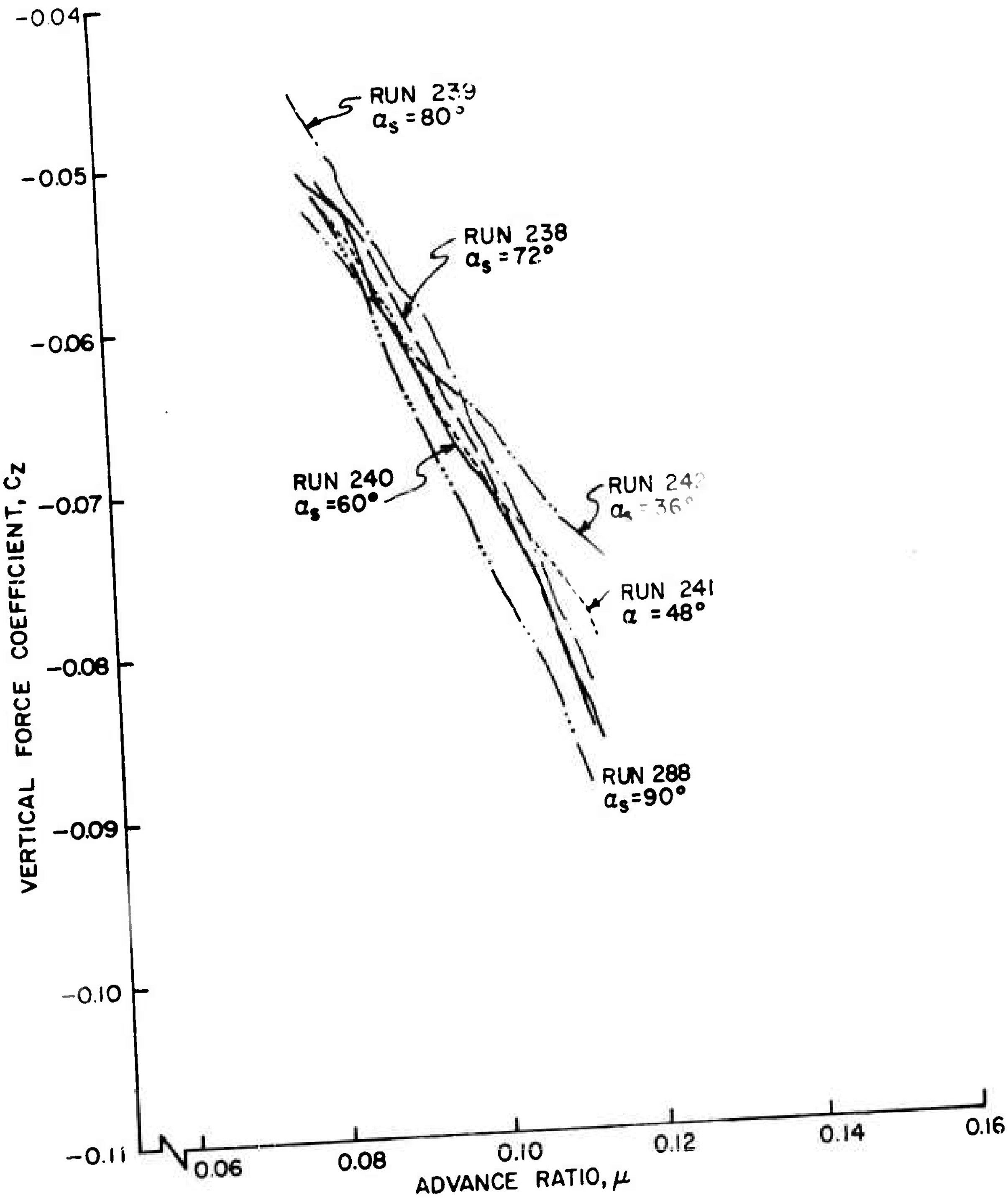

Figure 42a. Rotor Force and Moment Coefficients as Functions of Advance Ratio, $\theta_{.75R}$ = 0, Large Wing on High.

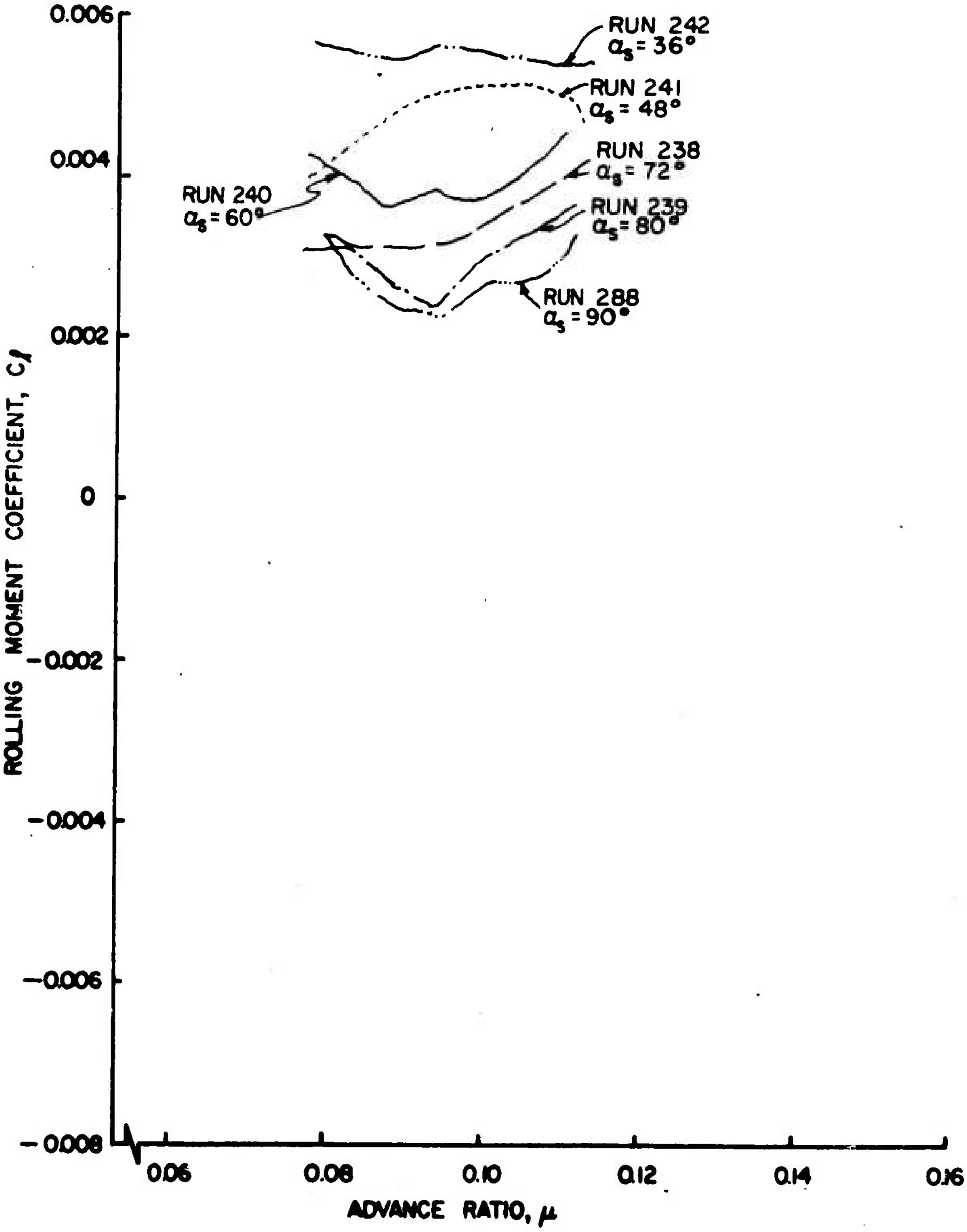

Figure 42b. Rotor Force and Moment Coefficients as Functions of Advance Ratio, $\theta_{.75R} = 0$, Large Wing on High.

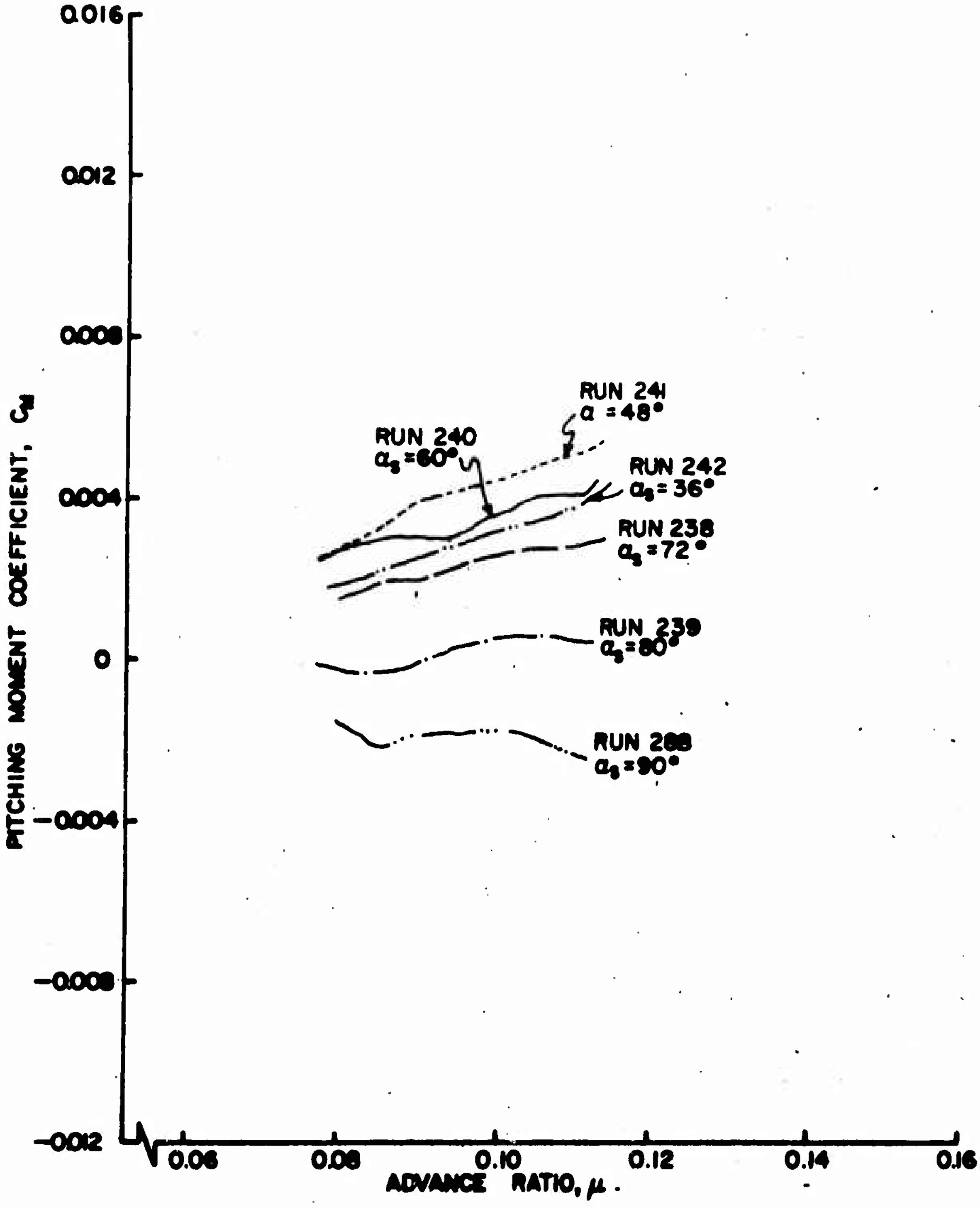

Figure 42c. Rotor Force and Moment Coefficients as Functions of Advance Ratio, $\theta_{.75R} = 0$, Large Wing on High.

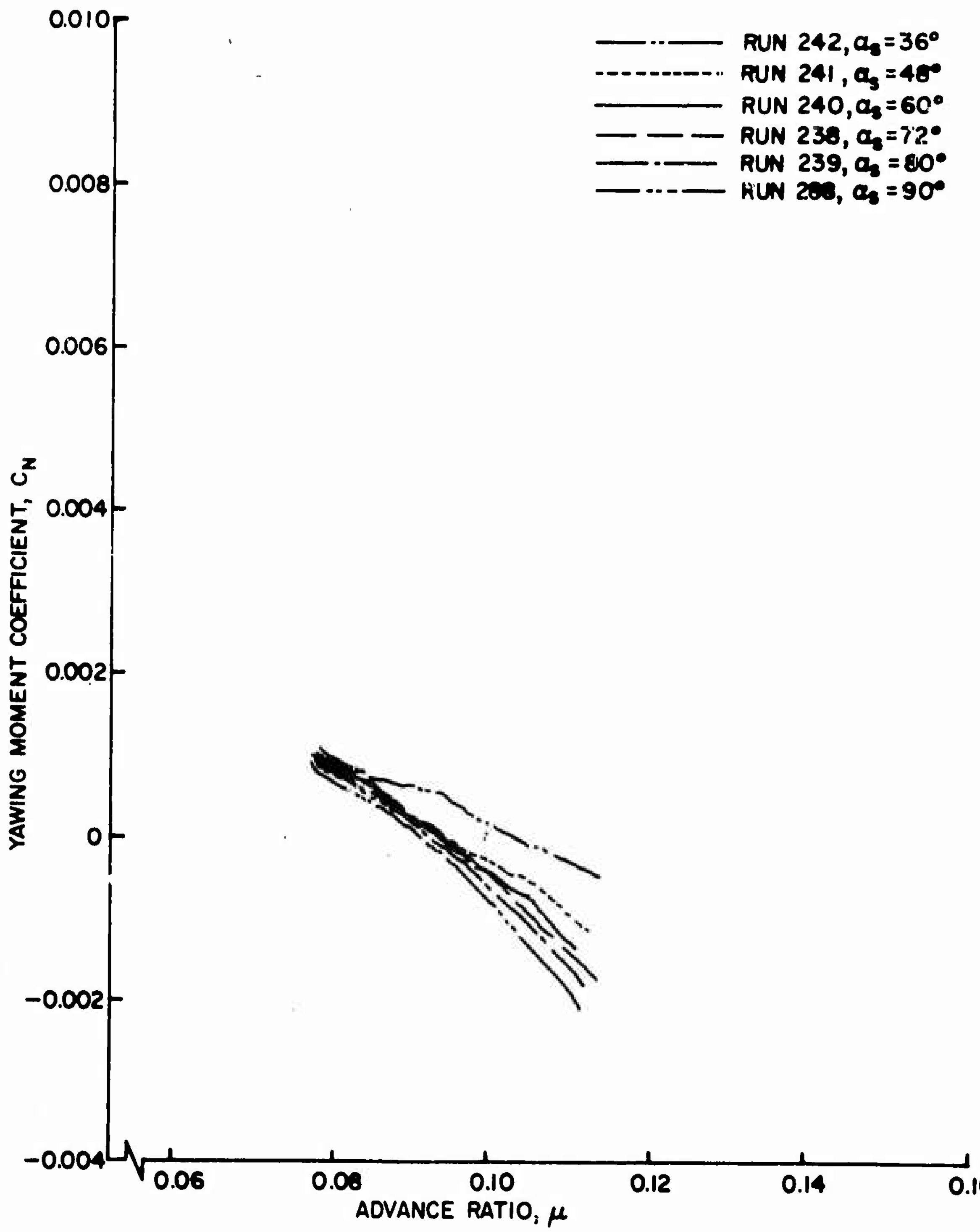

Figure 42d. Rotor Force and Moment Coefficients as Functions of Advance Ratio, $\theta_{.75R}$ = 0, Large Wing on High.

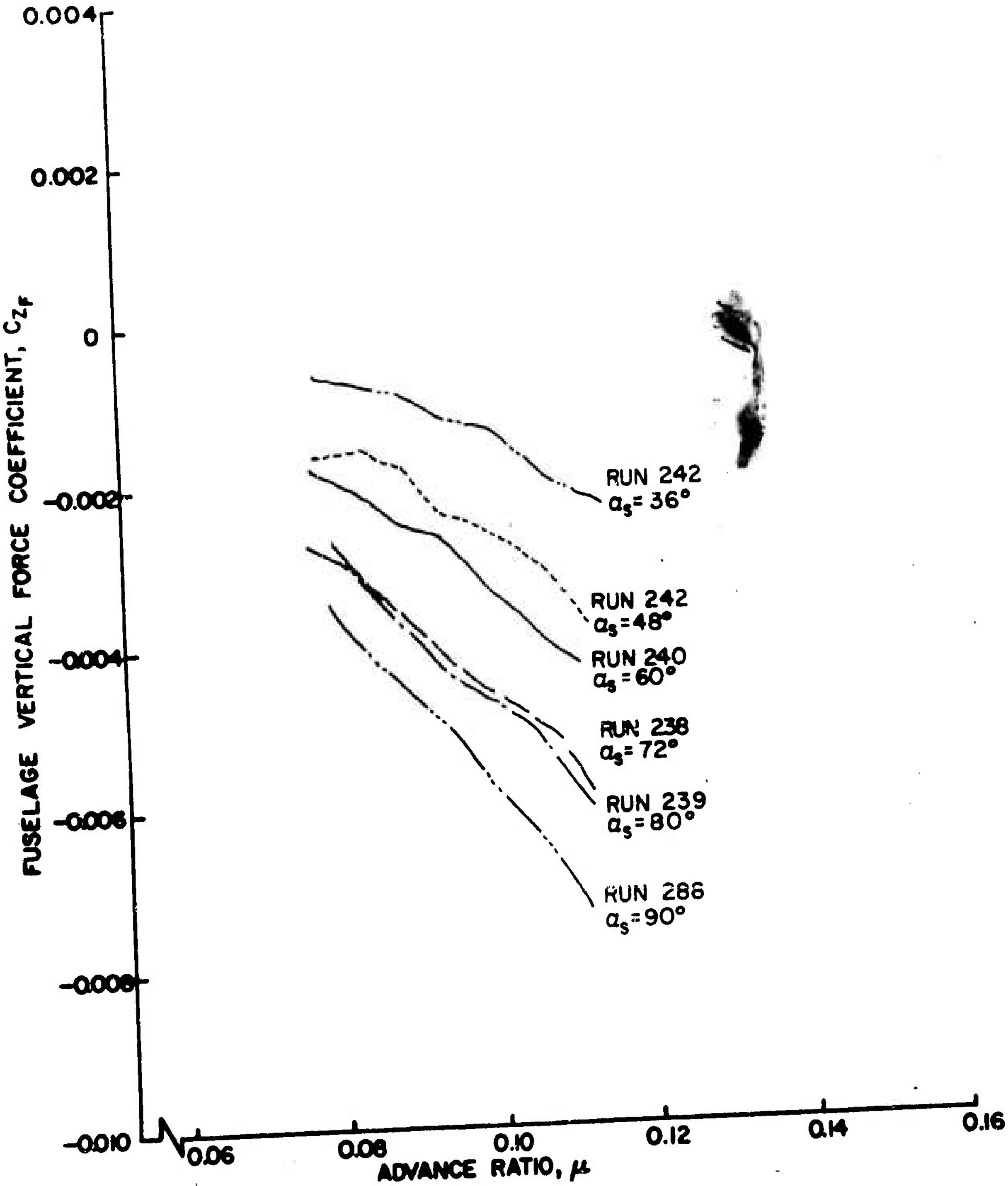

Figure 43a. Fuselage Vertical Force and Pitching Moment Coefficients as Functions of Advance Ratio, $\theta_{.75R}$ = 0, Large Wing on High.

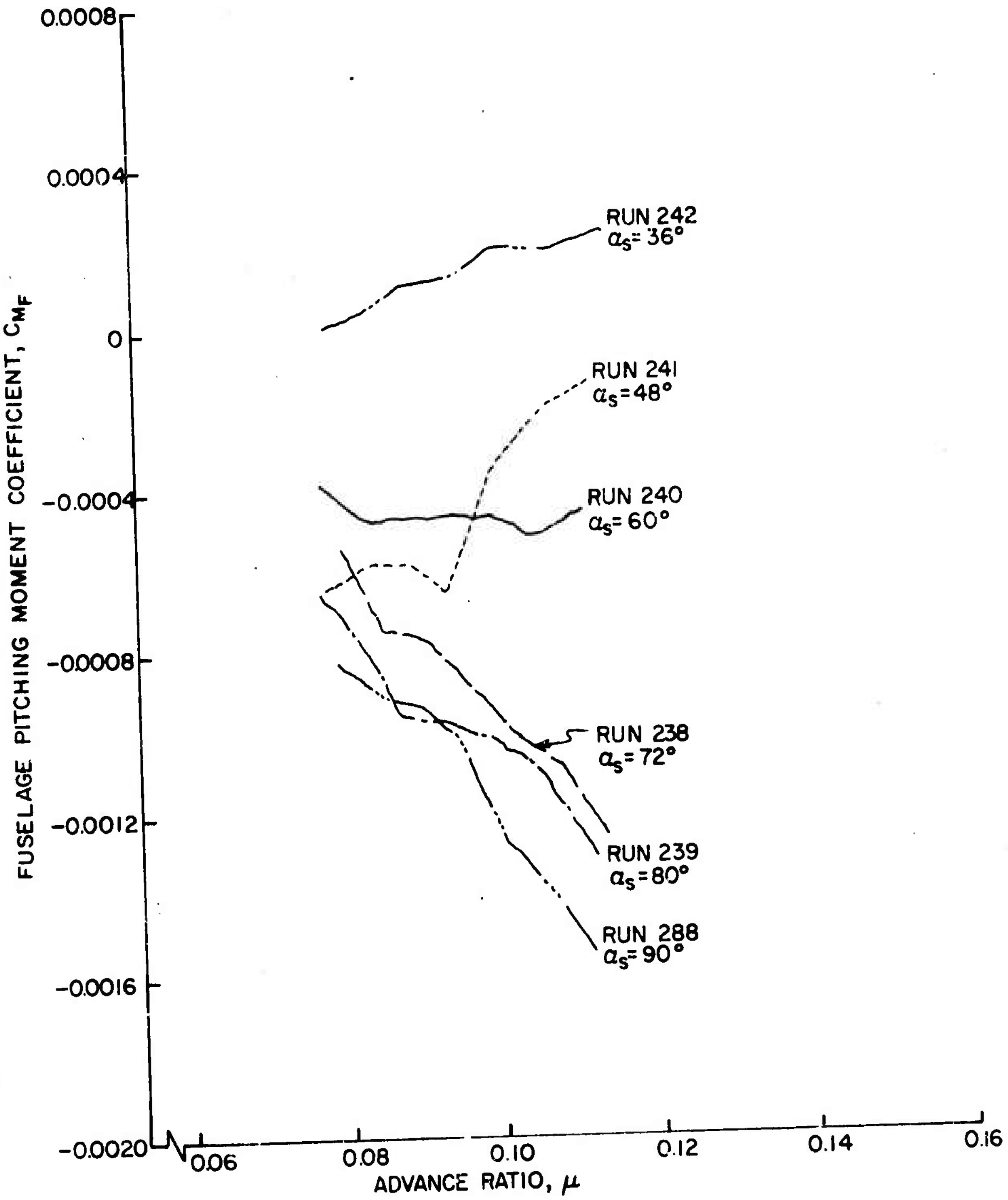

Figure 43b. Fuselage Vertical Force and Pitching Moment Coefficients as Functions of Advance Ratio, $\theta_{.75R} = 0$, Large Wing on High.

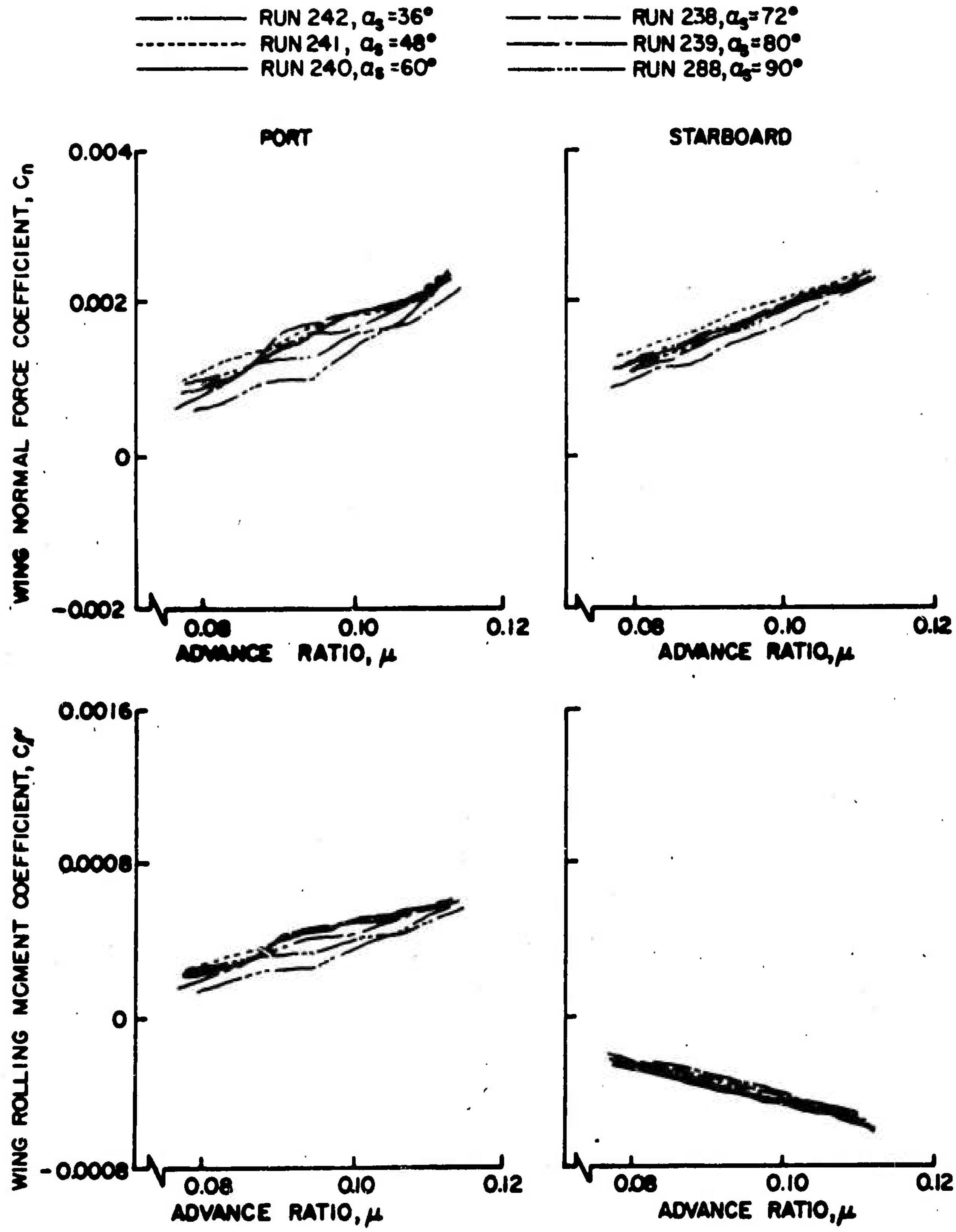

Figure 44. Wing Normal Force and Rolling Moment Coefficients as Functions of Advance Ratio, $\theta_{.75R} = 0$, Large Wing on High.

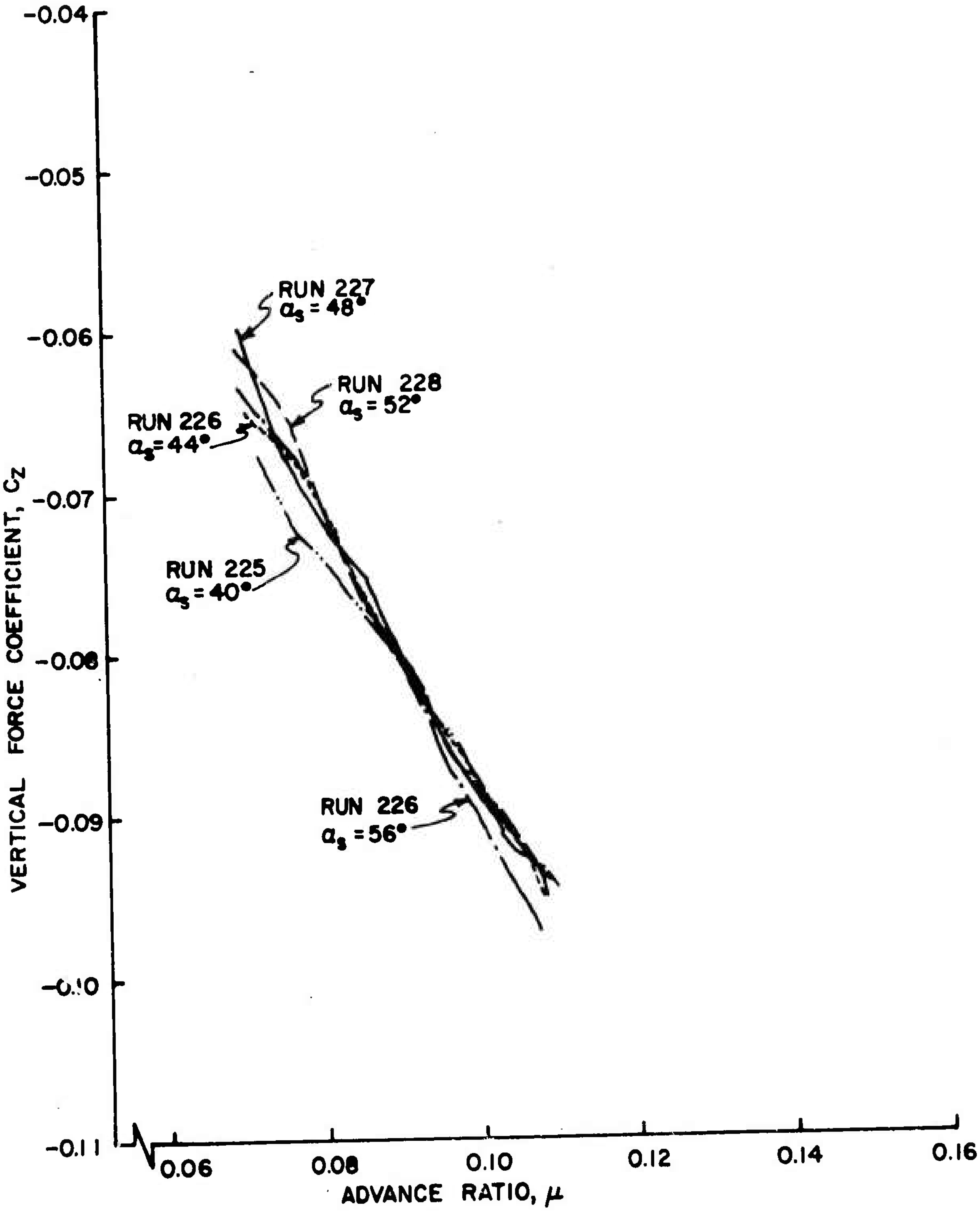

Figure 45a. Rotor Force and Moment Coefficients as Functions of Advance Ratio, $\theta_{.75R} = 2^{\circ}$, Large Wing on High.

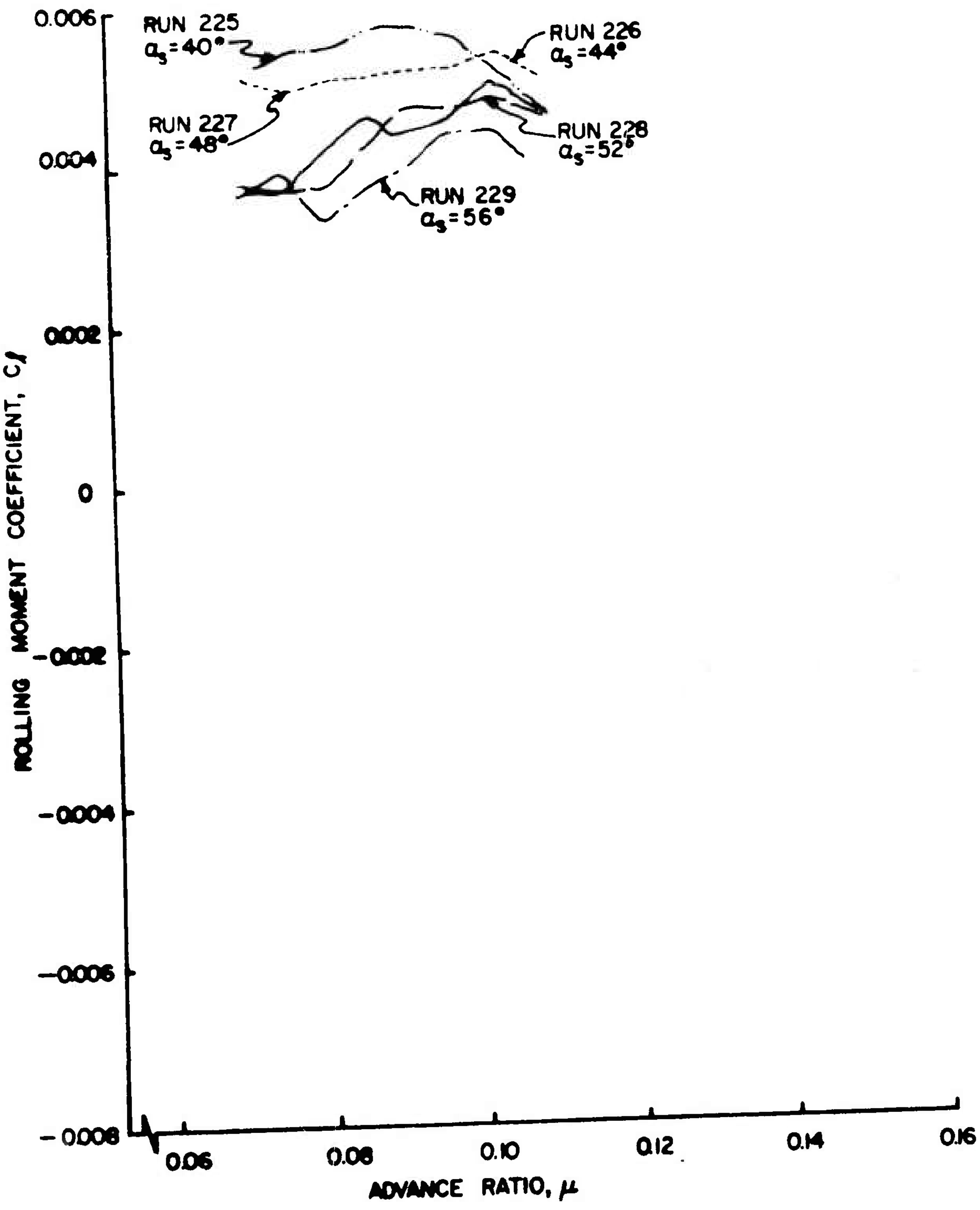

Figure 45b. Rotor Force and Moment Coefficients as Functions of Advance Ratio, $\theta_{.75R} = 2^{\circ}$, Large Wing on High.

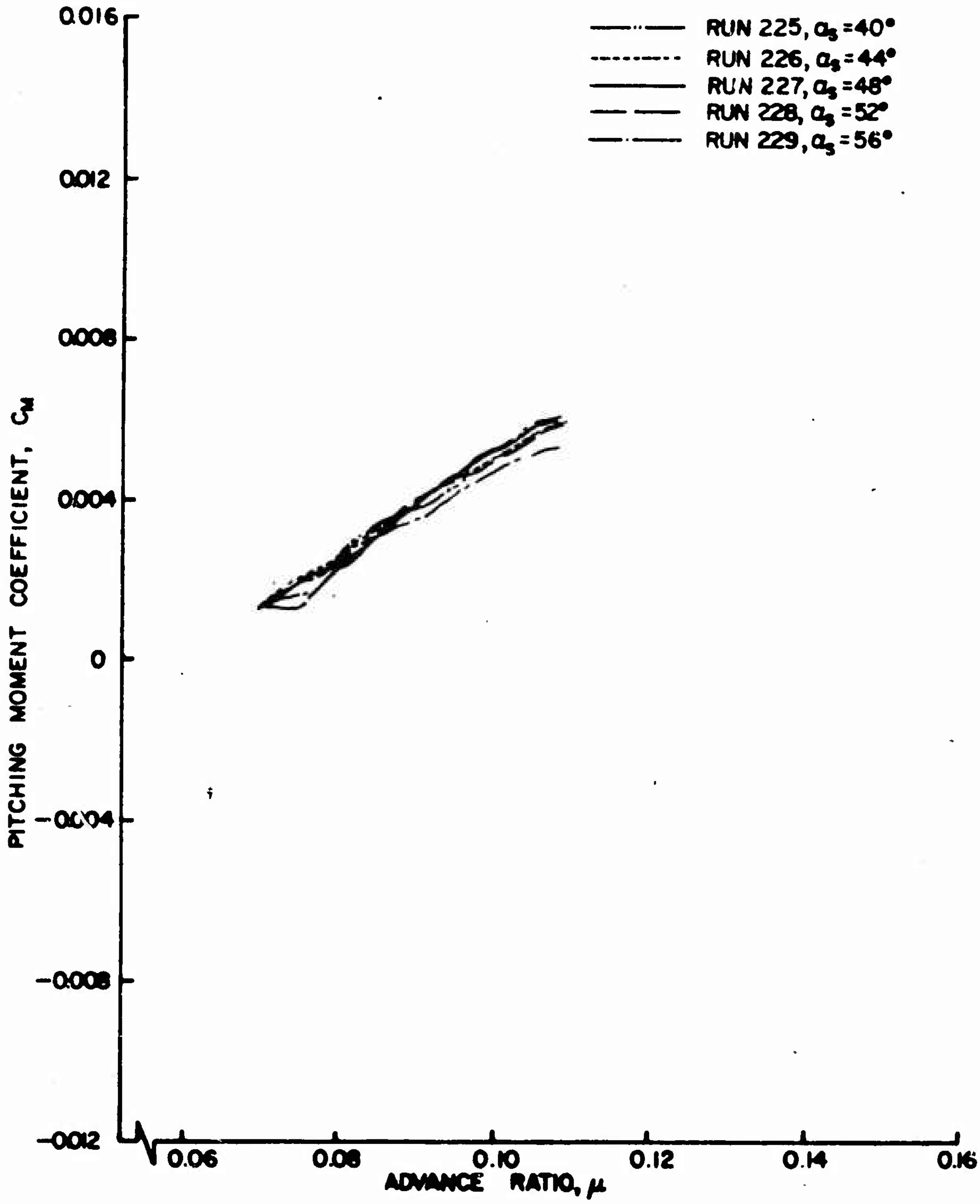

Figure 45c. Rotor Force and Moment Coefficients as Functions of Advance Ratio, $\theta_{.75R} = 2^\circ$, Large Wing on High.

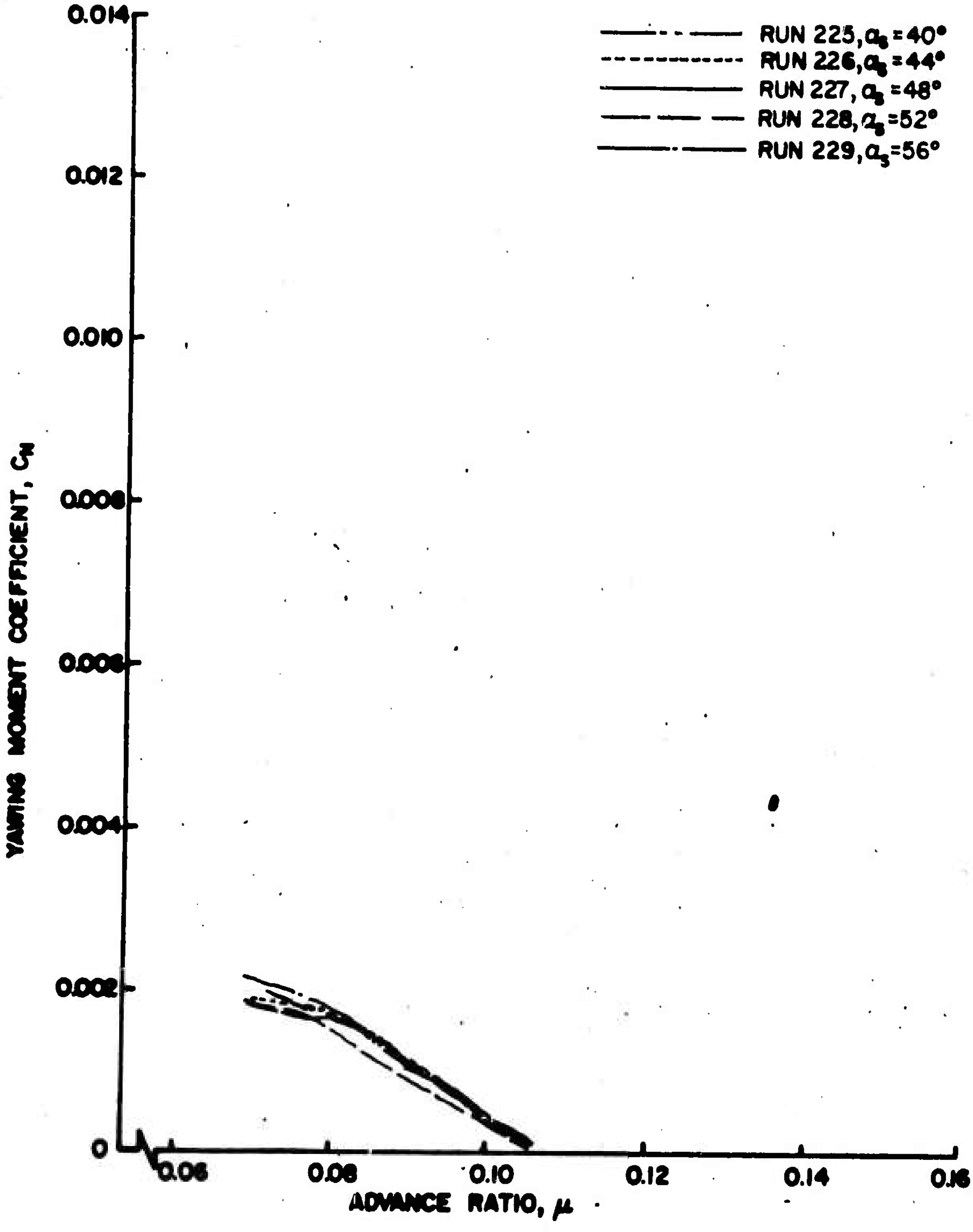

Figure 45d. Rotor Force and Moment Coefficients as Functions of Advance Ratio, $\theta_{.75R} = 2^\circ$, Large Wing on High.

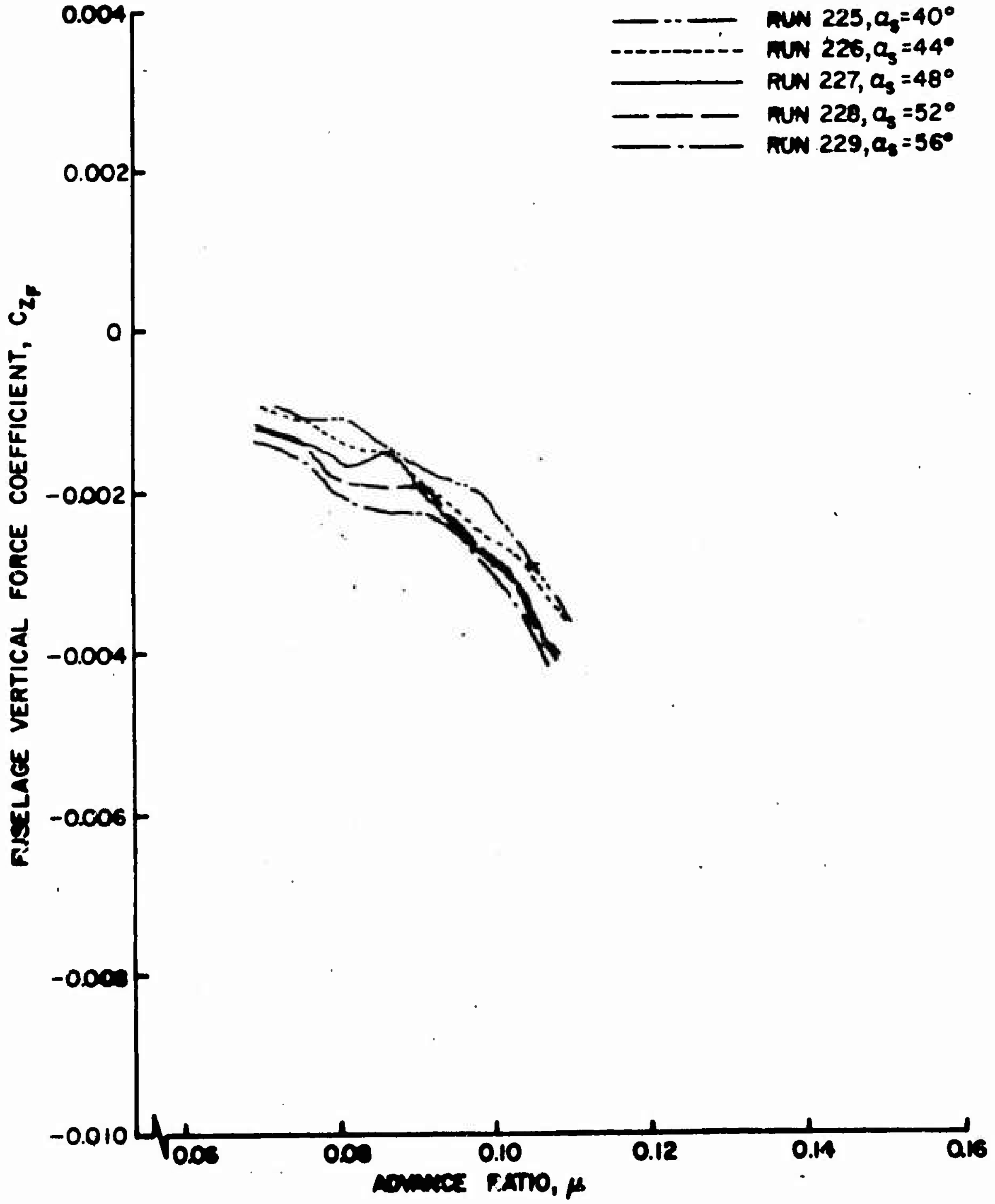

Figure 46a. Fuselage Vertical Force and Pitching Moment Coefficients as Functions of Advance Ratio, $\theta_{.75R} = 2^\circ$, Large Wing on High.

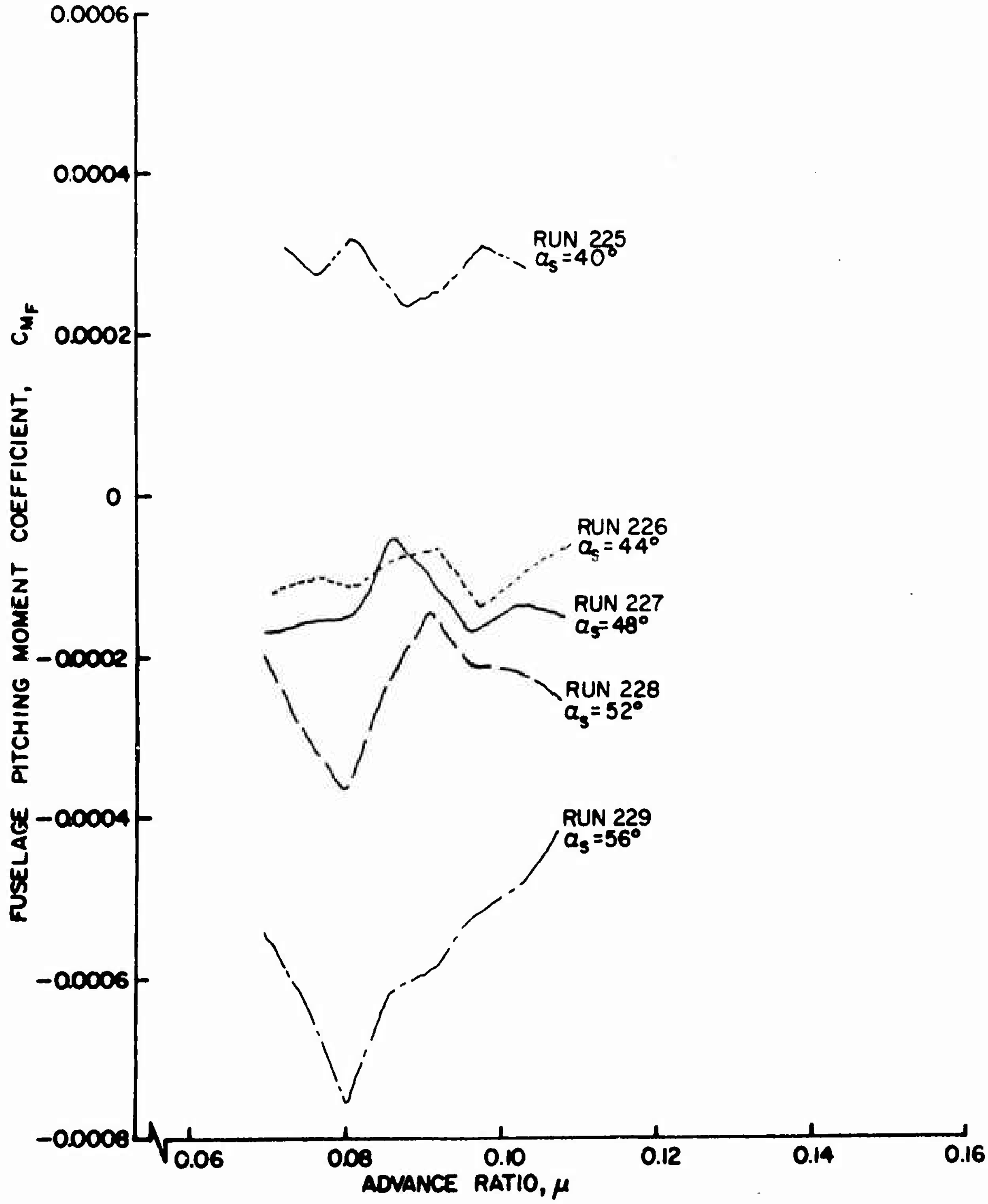

Figure 46b. Fuselage Vertical Force and Pitching Moment Coefficients as Functions of Advance Ratio, $\theta_{.75R} = 2^\circ$, Large Wing on High.

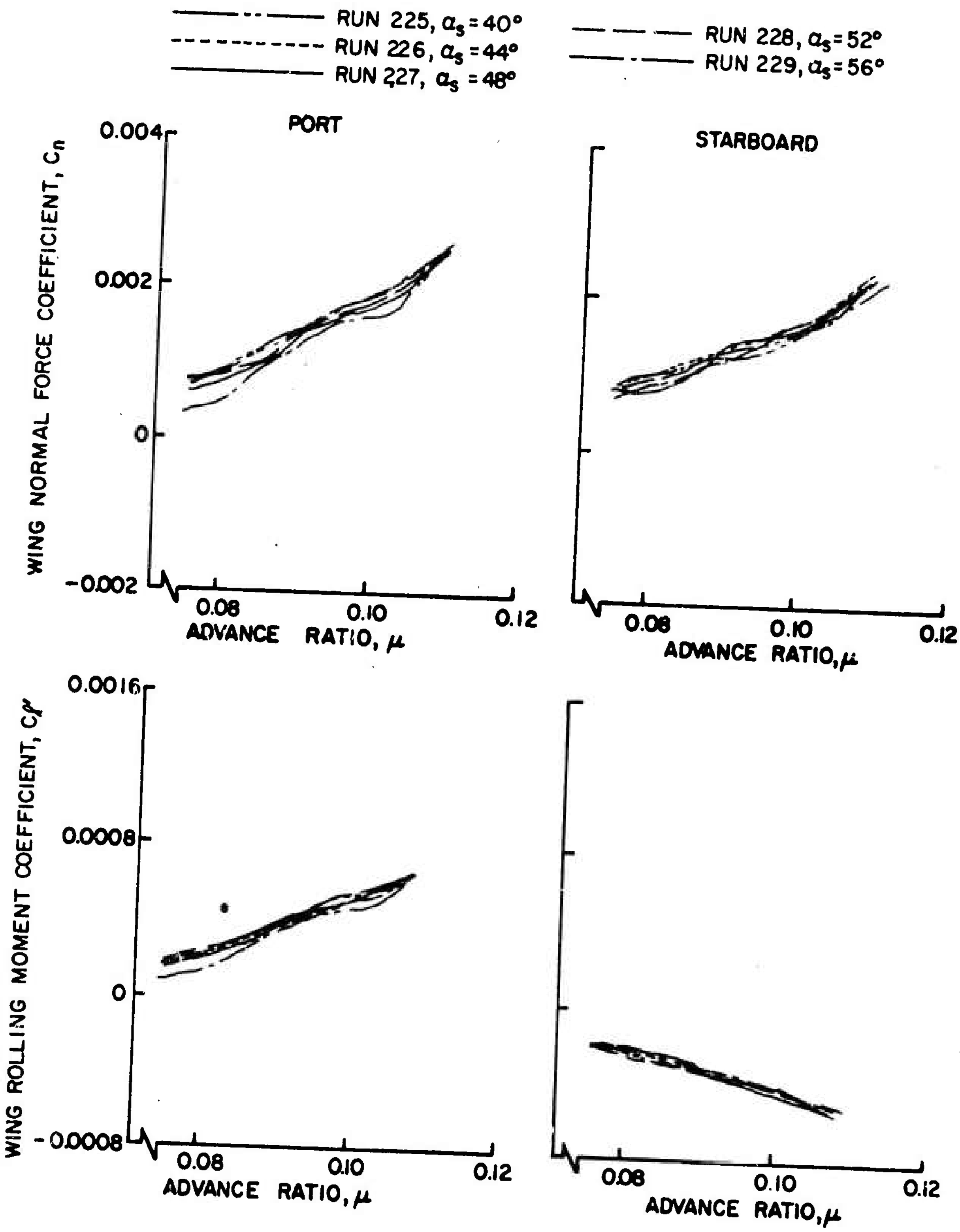

Figure 47. Wing Normal Force and Rolling Moment Coefficients as Functions of Advance Ratio, $\theta_{.75R} = 2^{\circ}$, Large Wing on High.

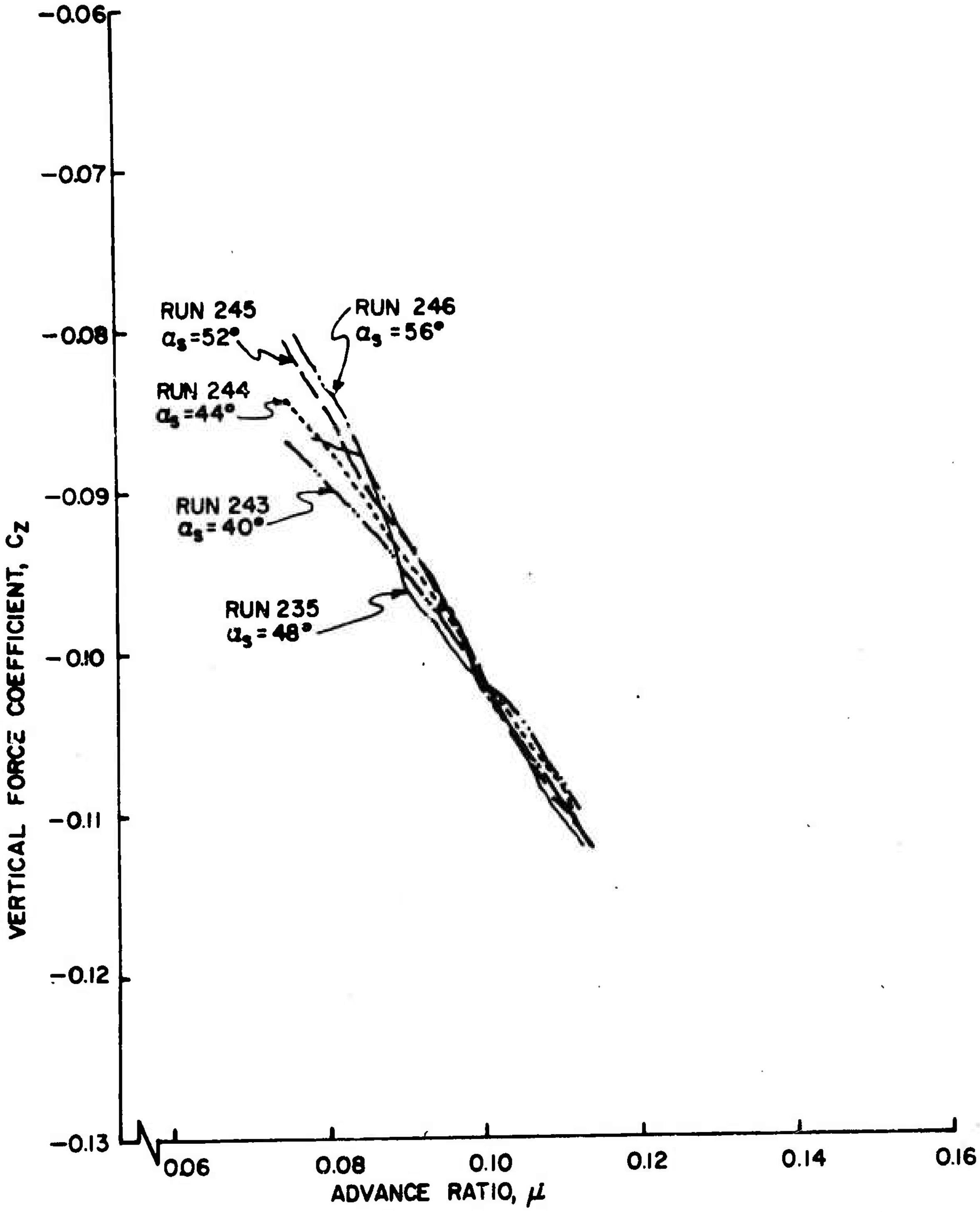

Figure 48a. Rotor Force and Moment Coefficients as Functions of Advance Ratio, $\theta_{.75R} = 4°$, Large Wing on High.

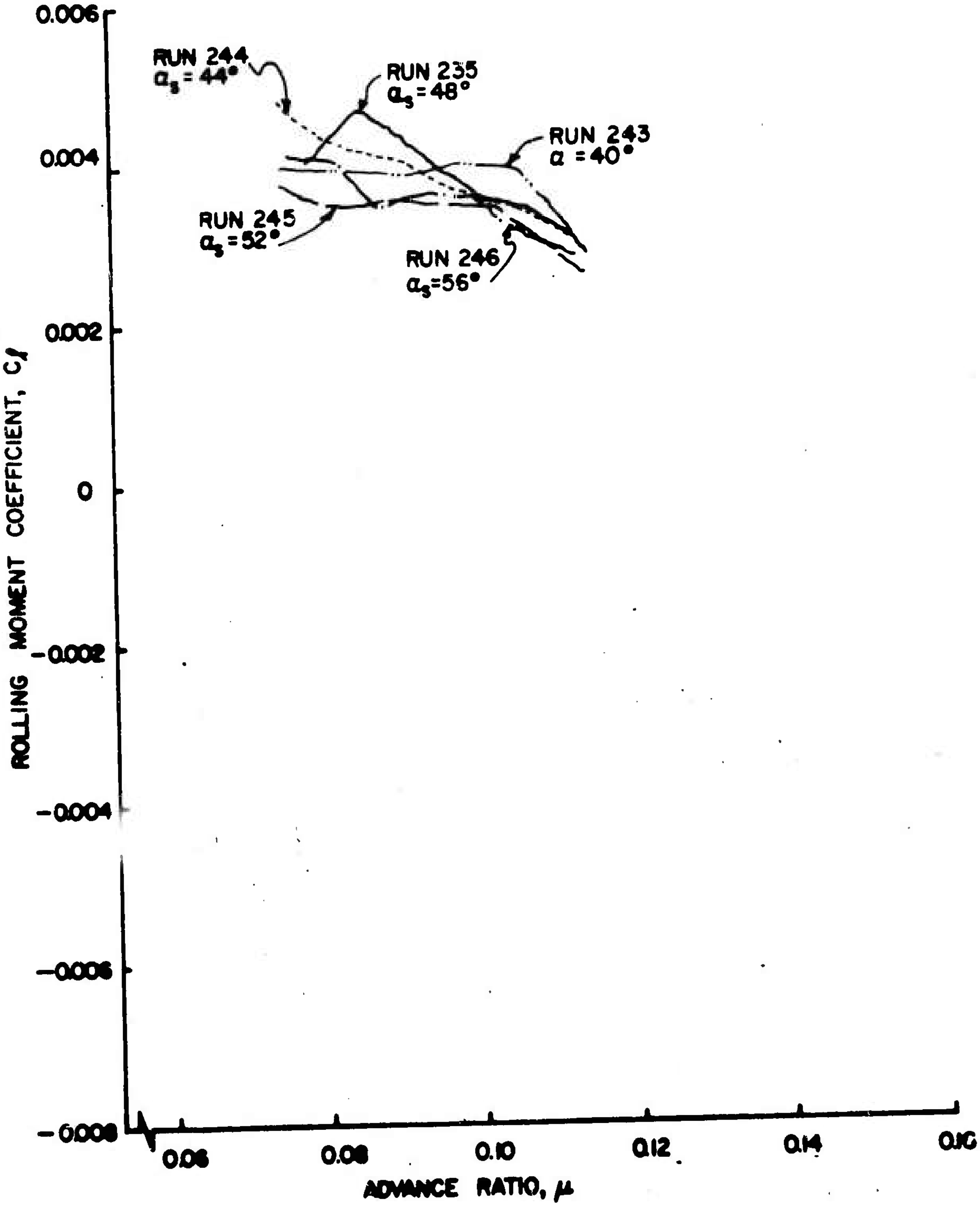

Figure 48b. Rotor Force and Moment Coefficients as Functions of Advance Ratio, $\theta_{.75R} = 4^\circ$, Large Wing on High.

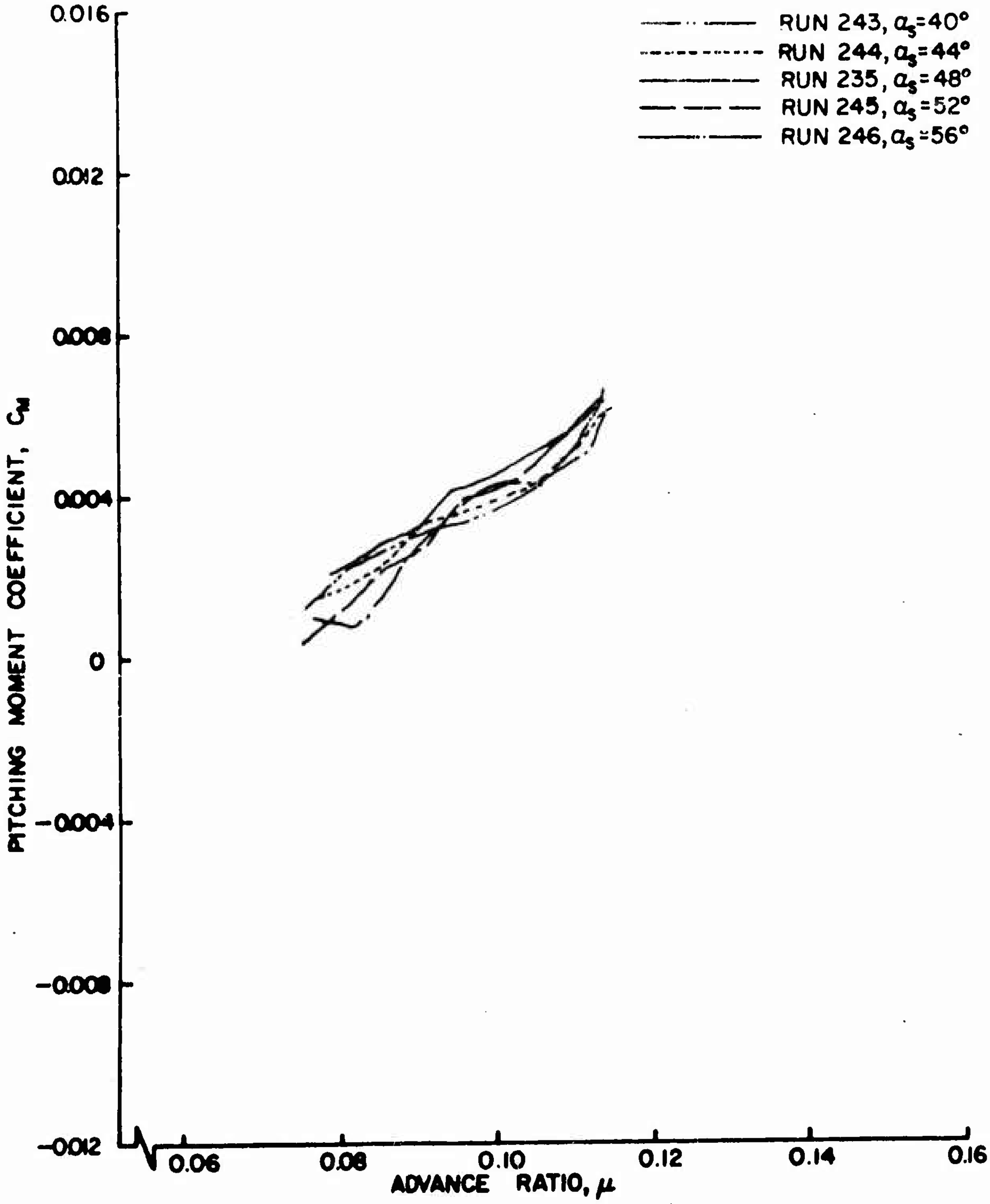

Figure 48c. Rotor Force and Moment Coefficients as Functions of Advance Ratio, $\theta_{.75R} = 4°$, Large Wing on High.

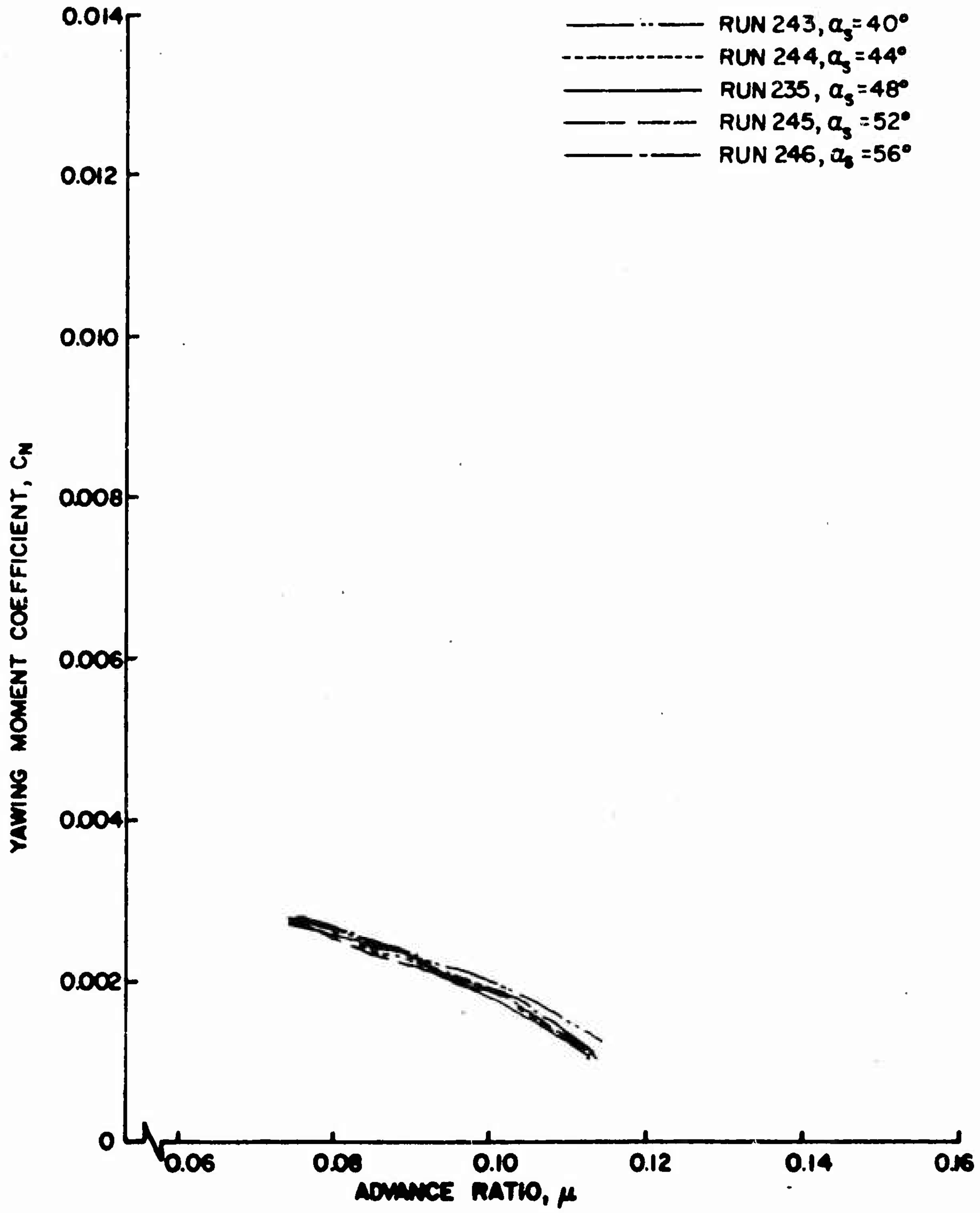

Figure 48d. Rotor Force and Moment Coefficients as Functions of Advance Ratio, $\theta_{.75R} = 4^\circ$, Large Wing on High.

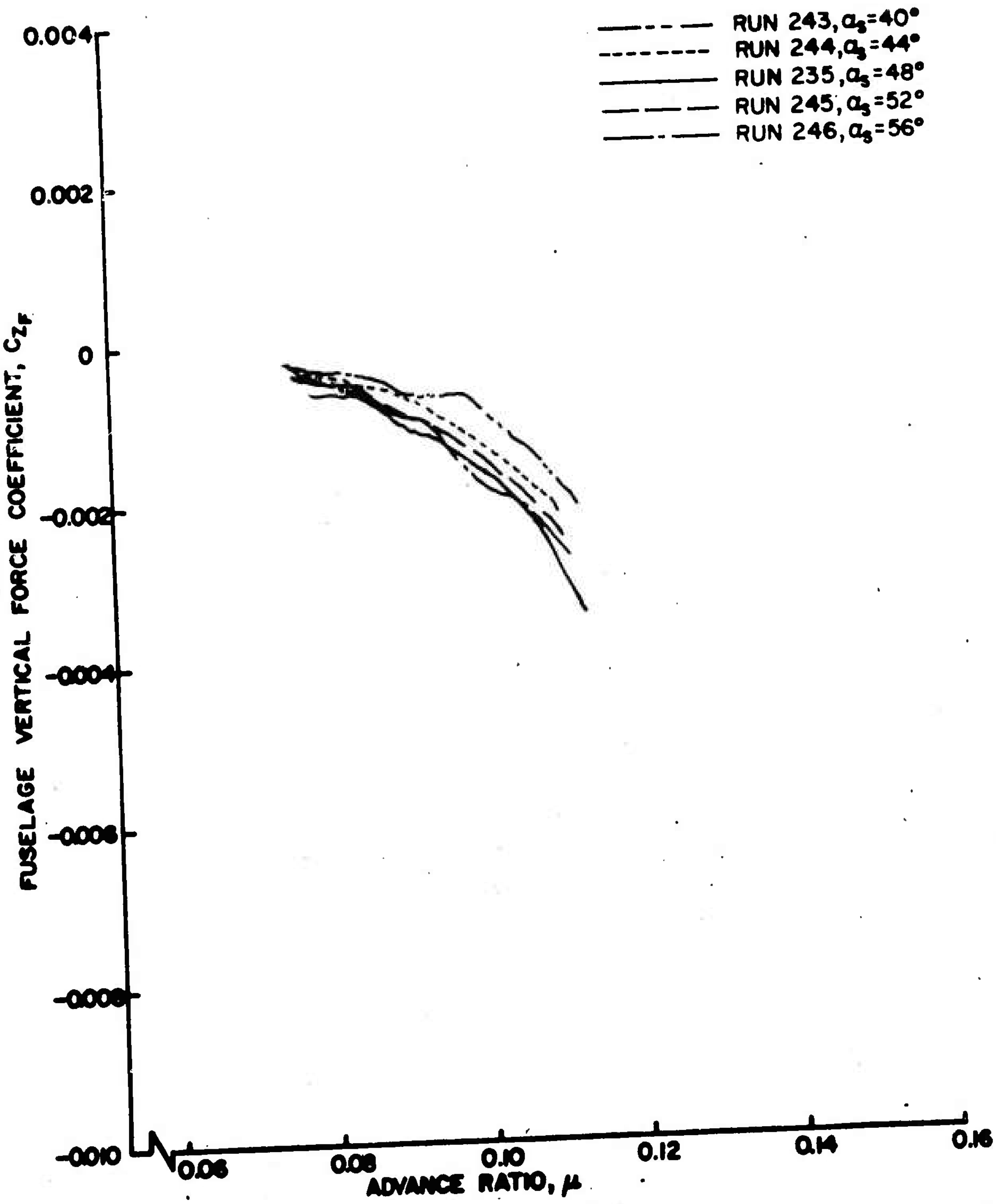

Figure 49a. Fuselage Vertical Force and Pitching Moment Coefficients as Functions of Advance Ratio, $\theta_{.75R} = 4^\circ$, Large Wing on High.

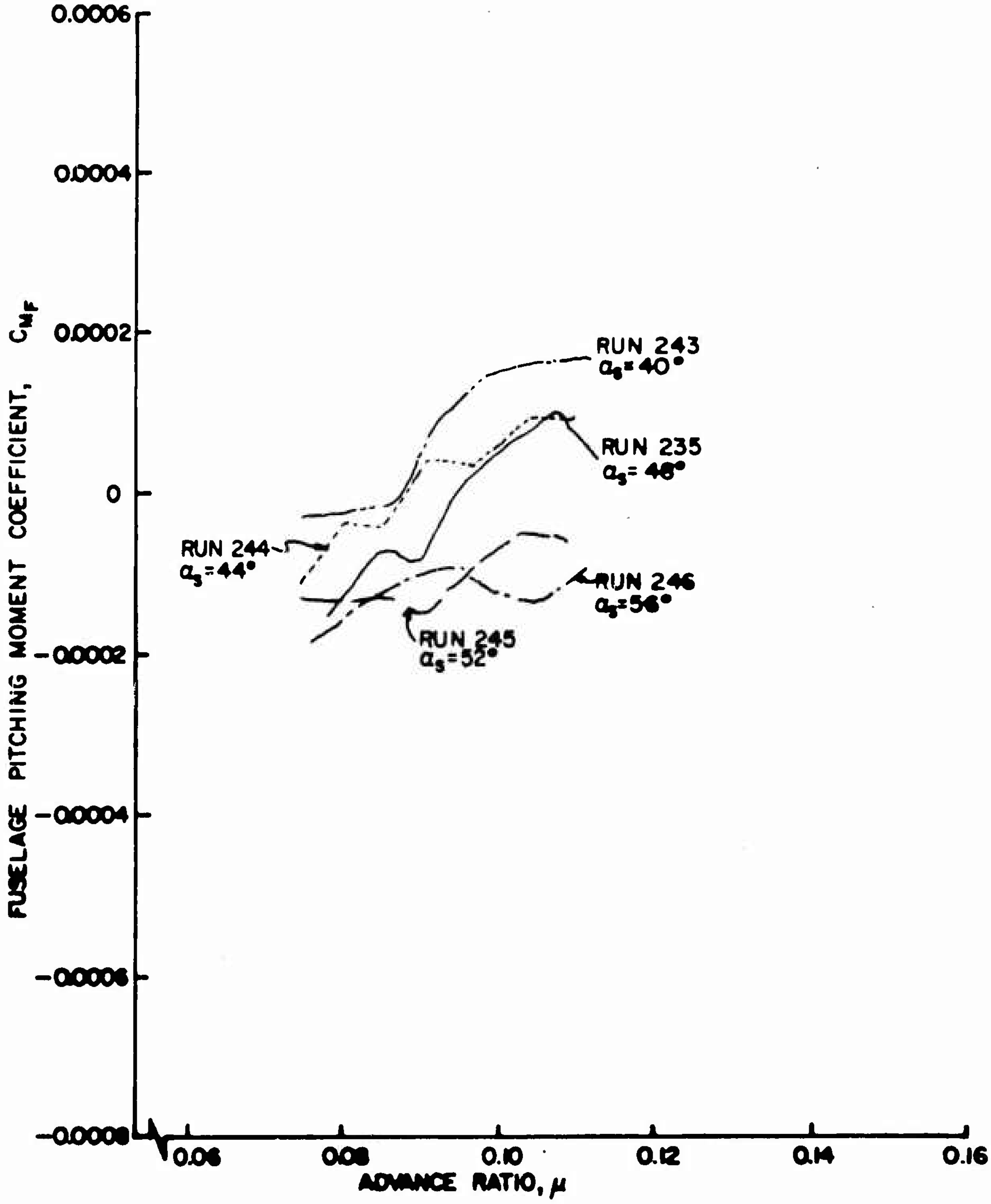

Figure 49b. Fuselage Vertical Force and Pitching Moment Coefficients as Functions of Advance Ratio, $\theta_{.75R} = 4°$, Large Wing on High.

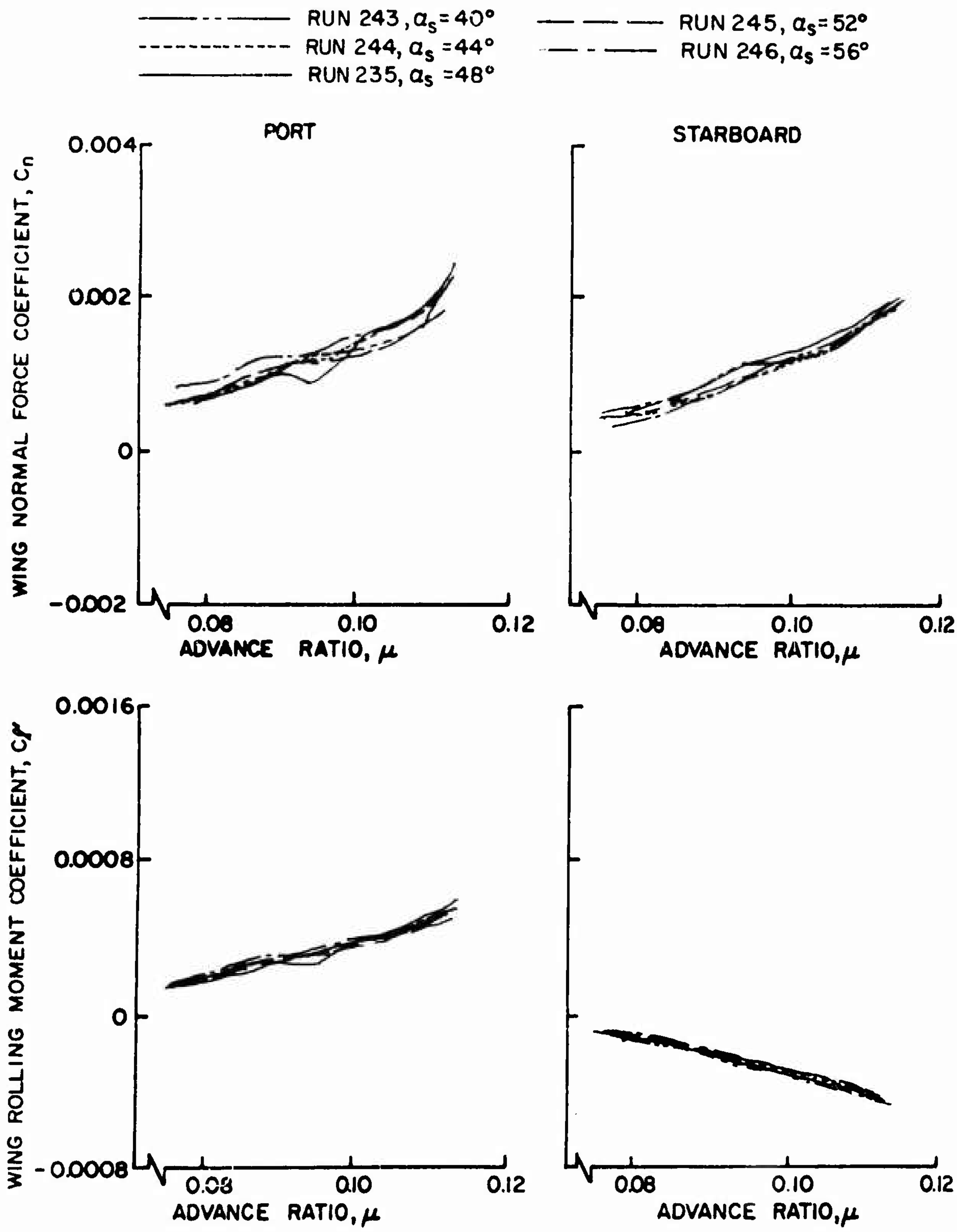

Figure 50. Wing Normal Force and Rolling Moment Coefficients as Functions of Advance Ratio, $\theta_{.75R} = 4^\circ$, Large Wing on High.

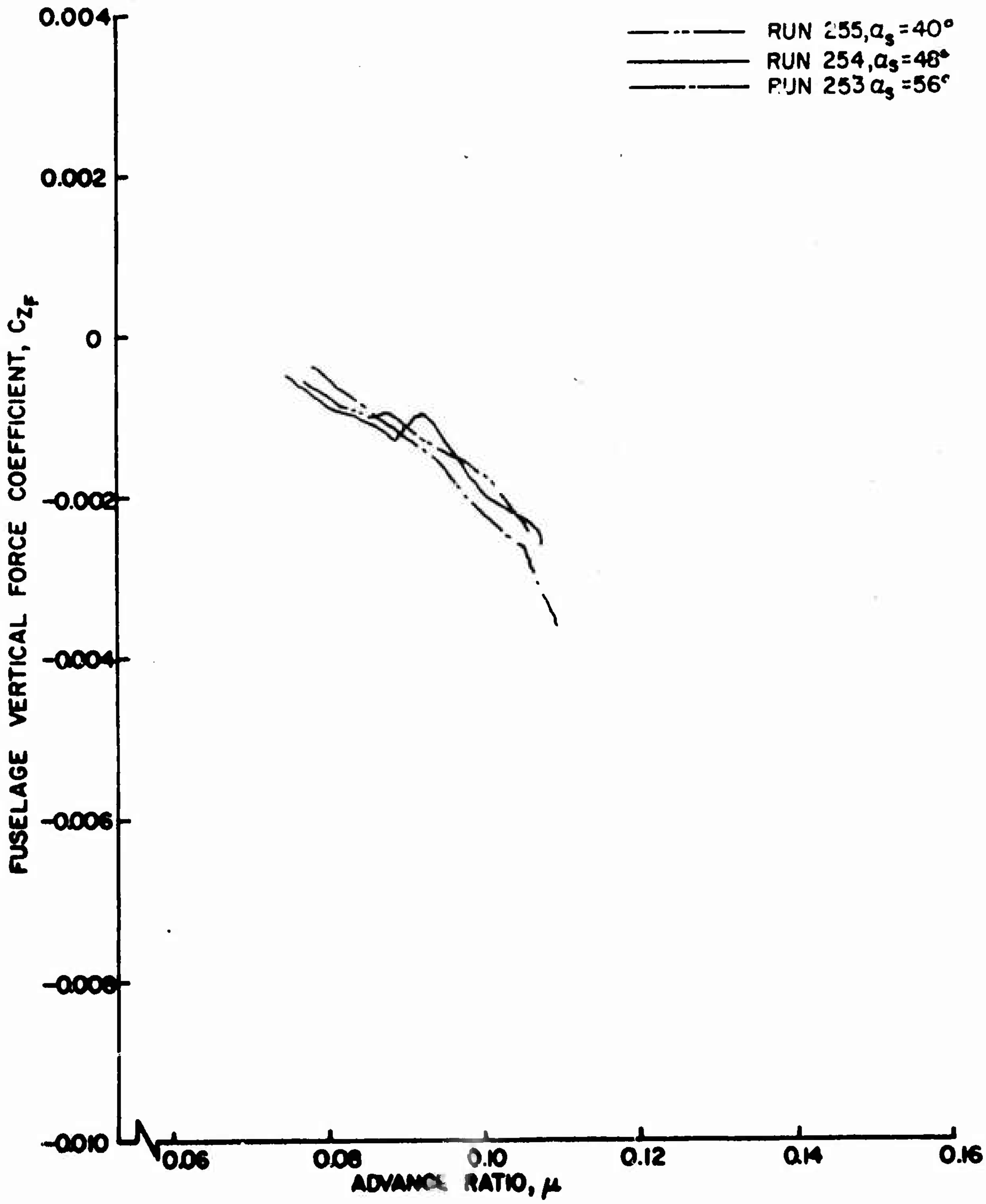

Figure 51a. Fuselage Vertical Force and Pitching Moment Coefficients as Functions of Advance Ratio, $\theta_{.75R} = 4°$, Large Wing on Low.

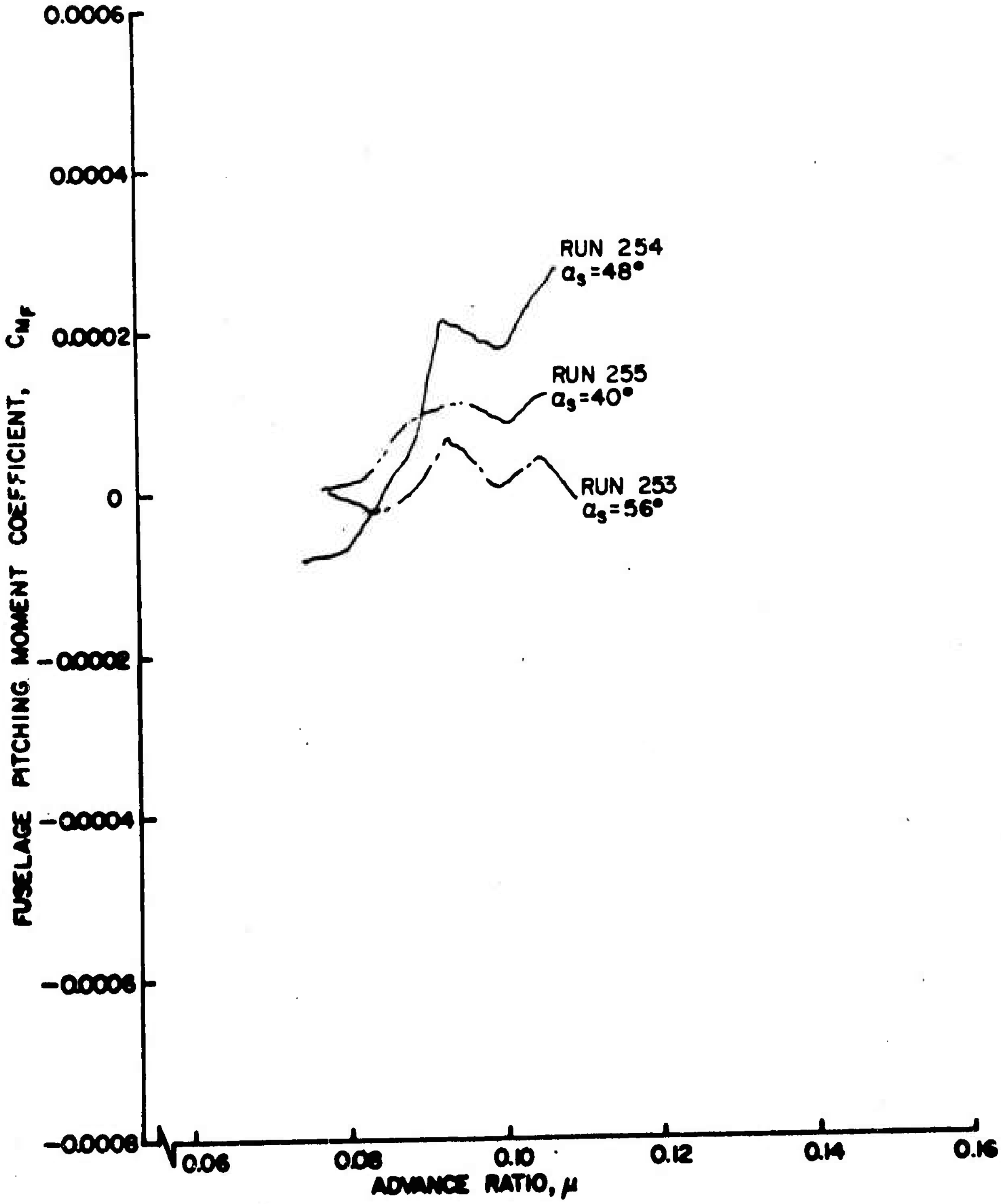

Figure 51b. Fuselage Vertical Force and Pitching Moment Coefficients as Functions of Advance Ratio, $\theta_{.75R} = 4^\circ$, Large Wing on Low.

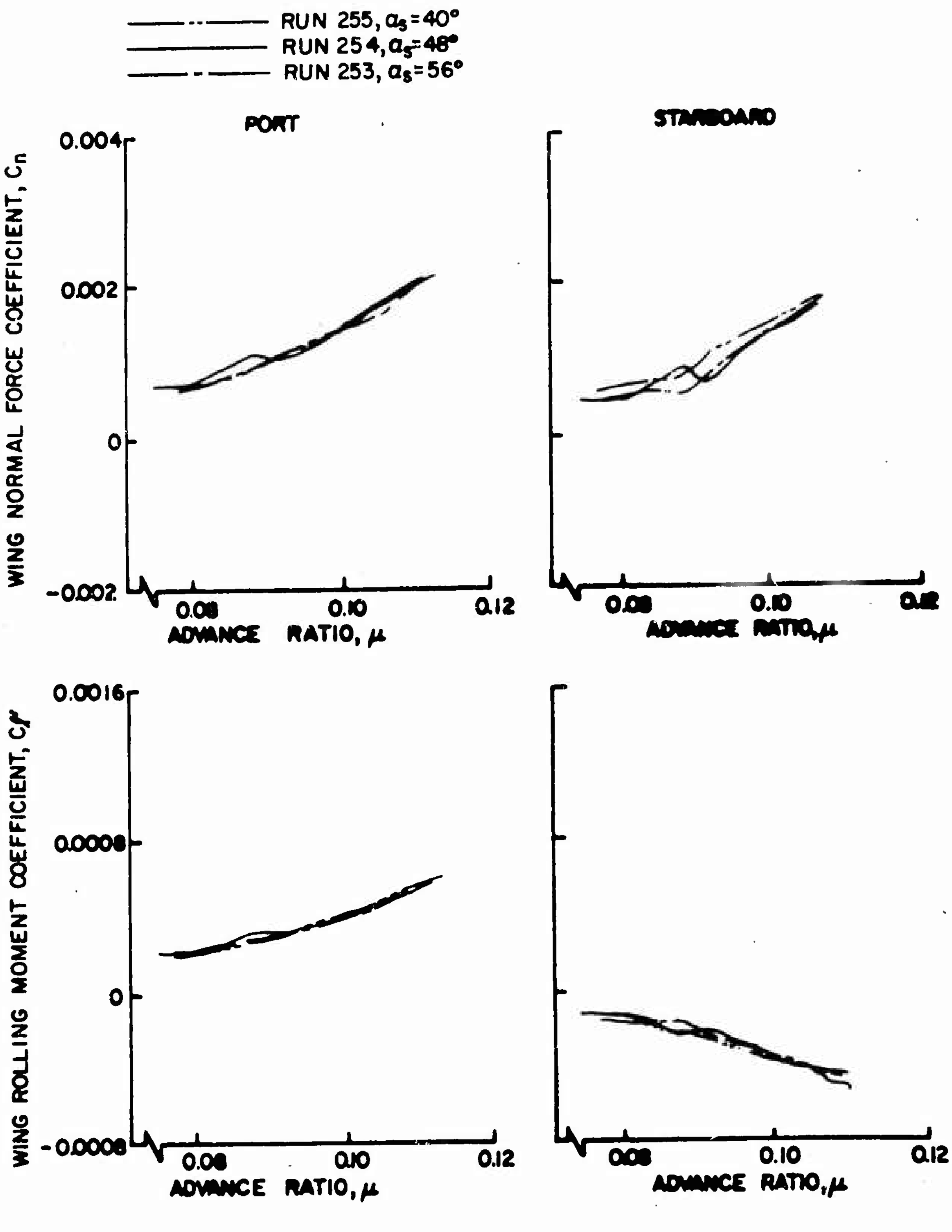

Figure 52. Wing Normal Force and Rolling Moment Coefficients as Functions of Advance Ratio, $\theta_{.75R} = 4°$, Large Wing on Low.

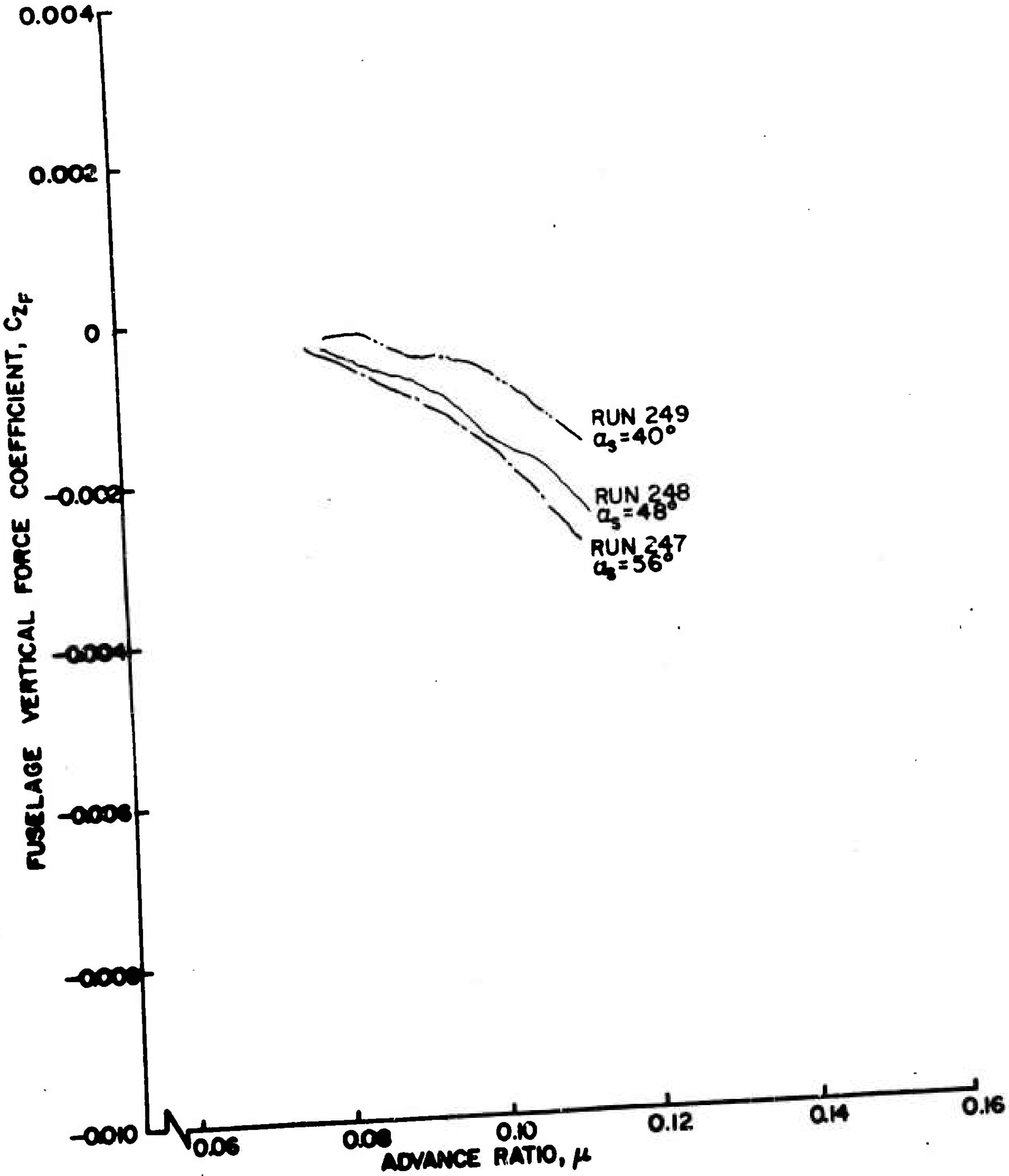

Figure 53a. Fuselage Vertical Force and Pitching Moment Coefficients as Functions of Advance Ratio, $\theta_{.75R} = 4°$, Small Wing on High.

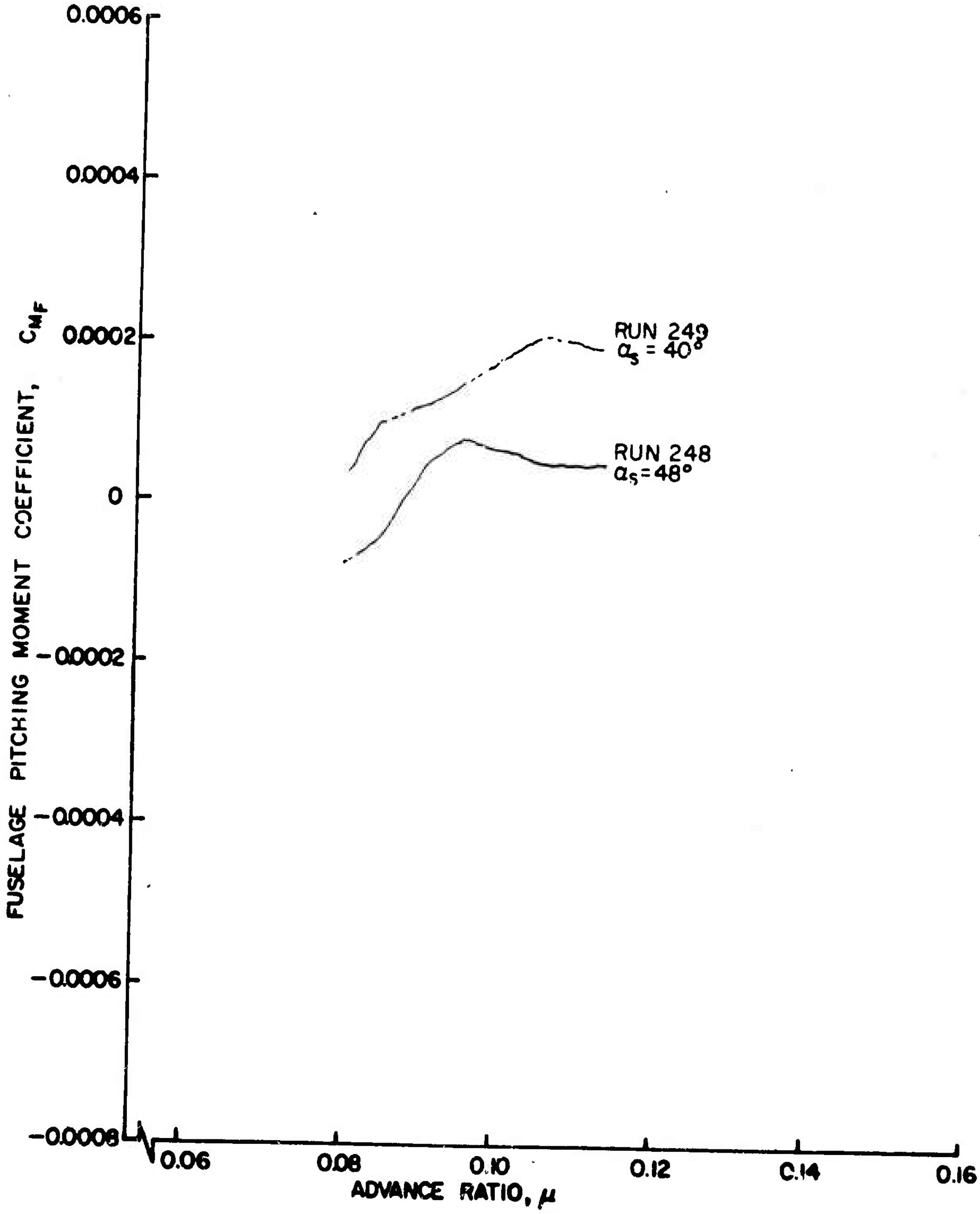

Figure 53b. Fuselage Vertical Force and Pitching Moment Coefficients as Functions of Advance Ratio, $\theta_{.75R} = 4°$, Small Wing on High.

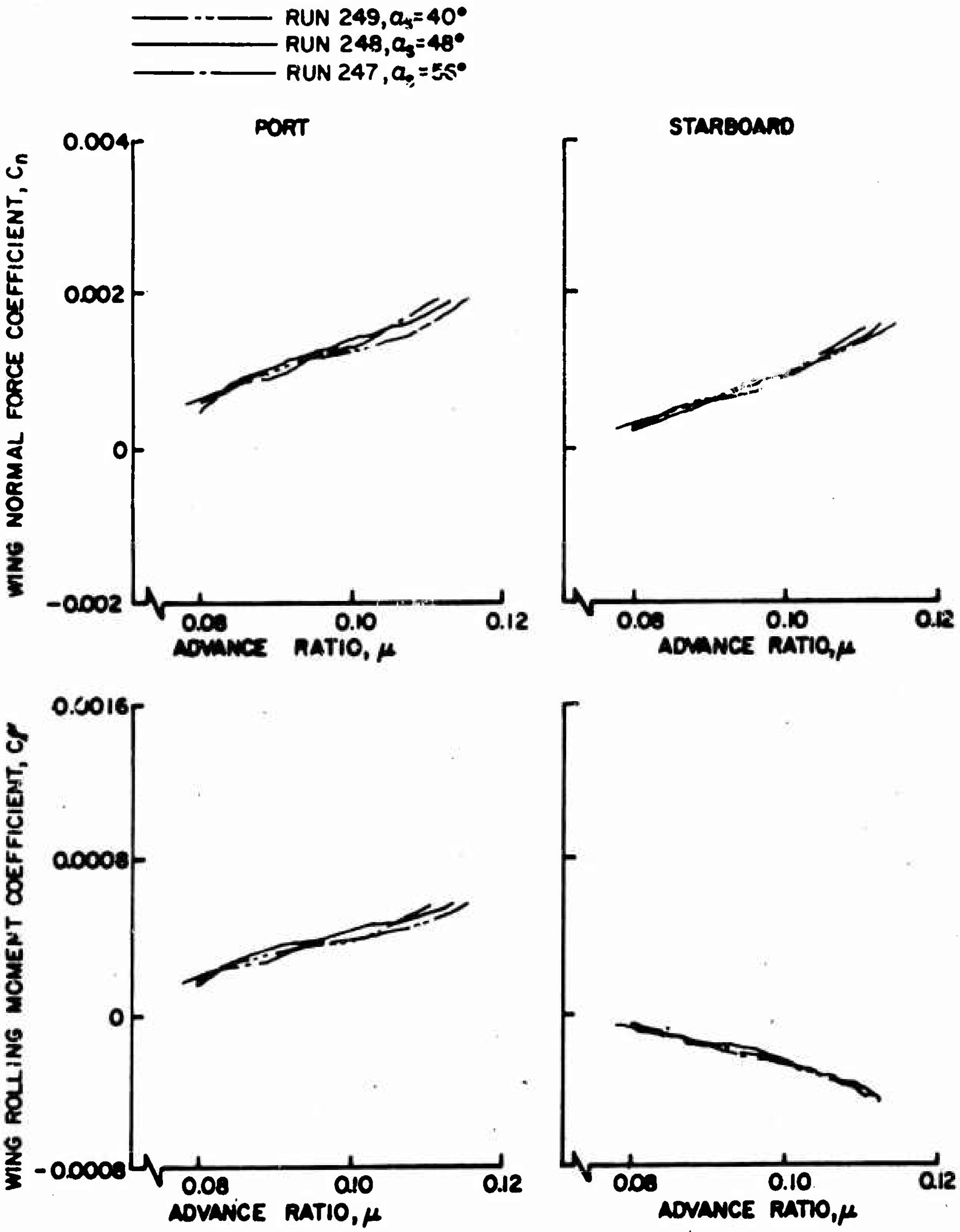

Figure 54. Wing Normal Force and Rolling Moment Coefficients as Functions of Advance Ratio, $\theta_{.75R} = 4°$, Small Wing on High.

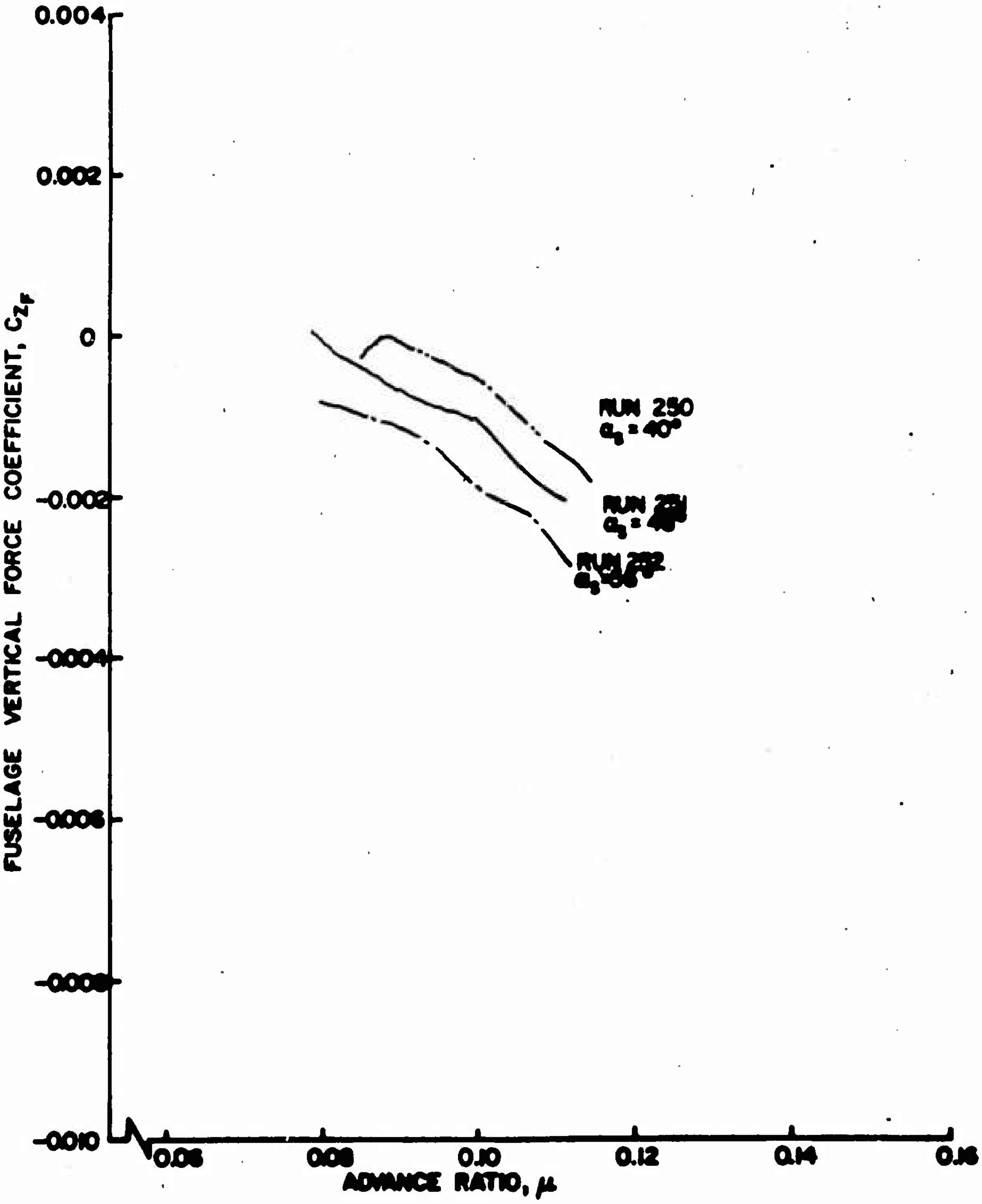

Figure 55a. Fuselage Vertical Force and Pitching Moment Coefficients as Functions of Advance Ratio, $\theta_{.75R} = 4°$, Small Wing on Low.

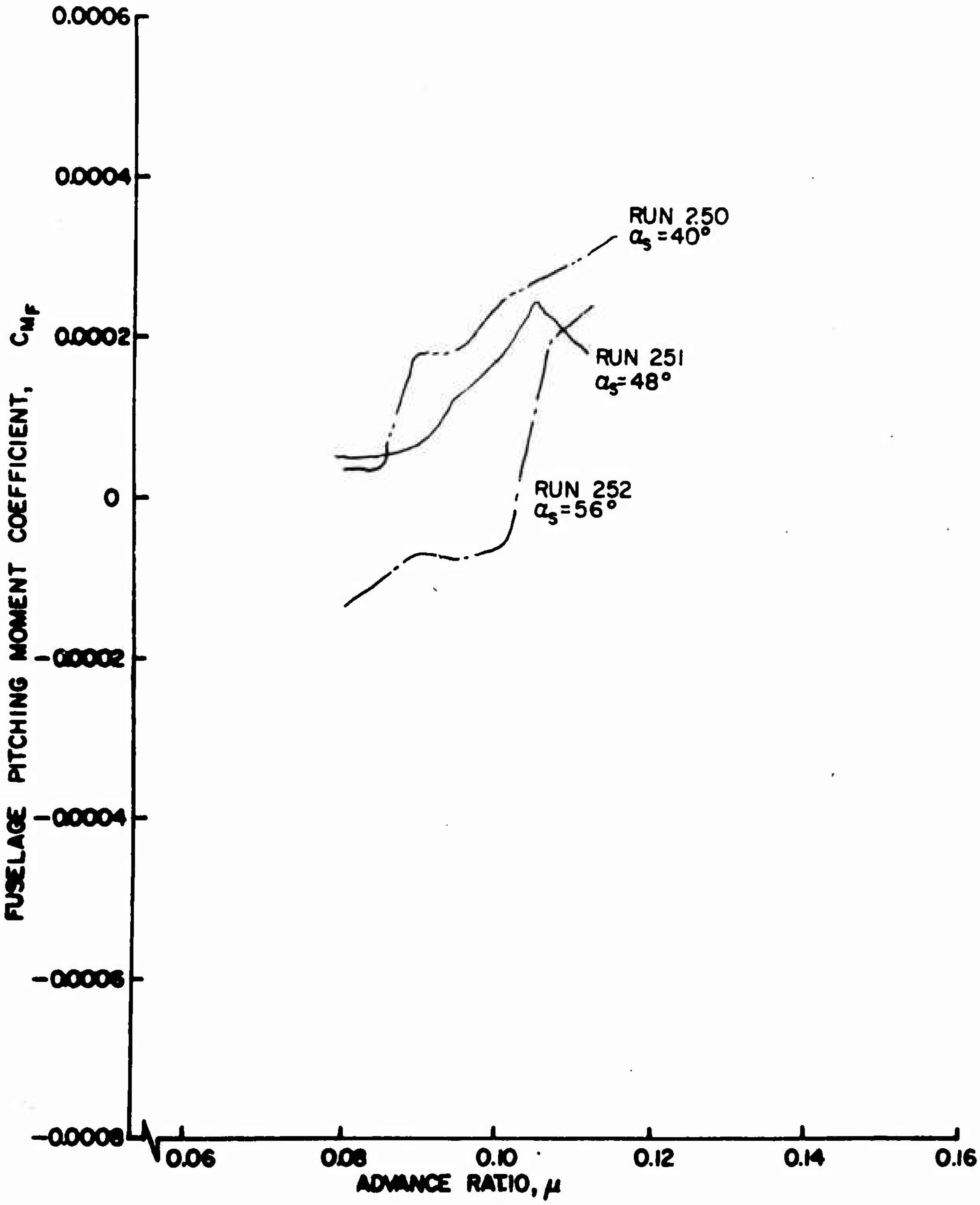

Figure 55b. Fuselage Vertical Force and Pitching Moment Coefficients as Functions of Advance Ratio, $\theta_{.75R} = 4°$, Small Wing on Low.

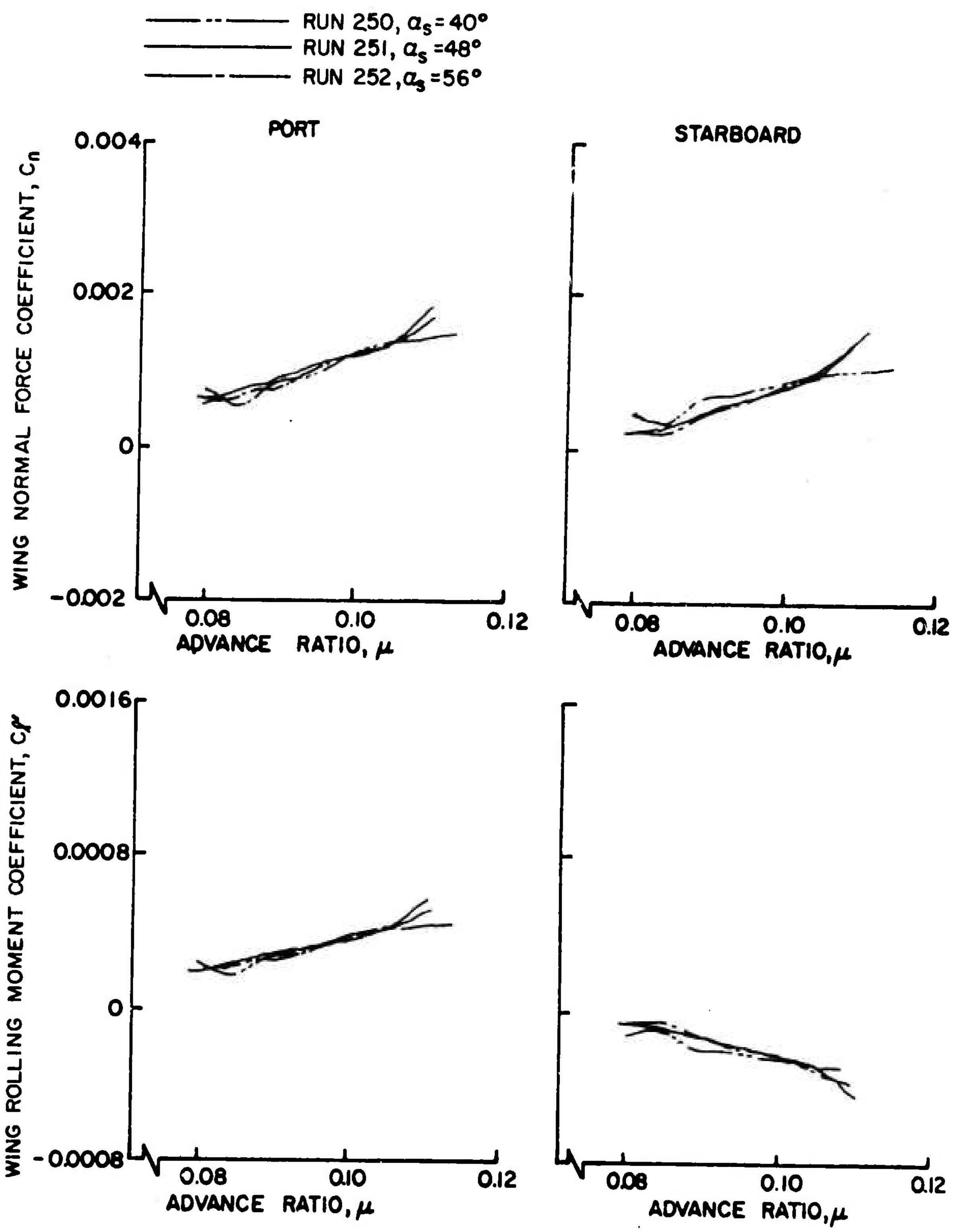

Figure 56. Wing Normal Force and Rolling Moment Coefficients as Functions of Advance Ratio, $\theta_{.75R} = 4°$, Small Wing on Low.

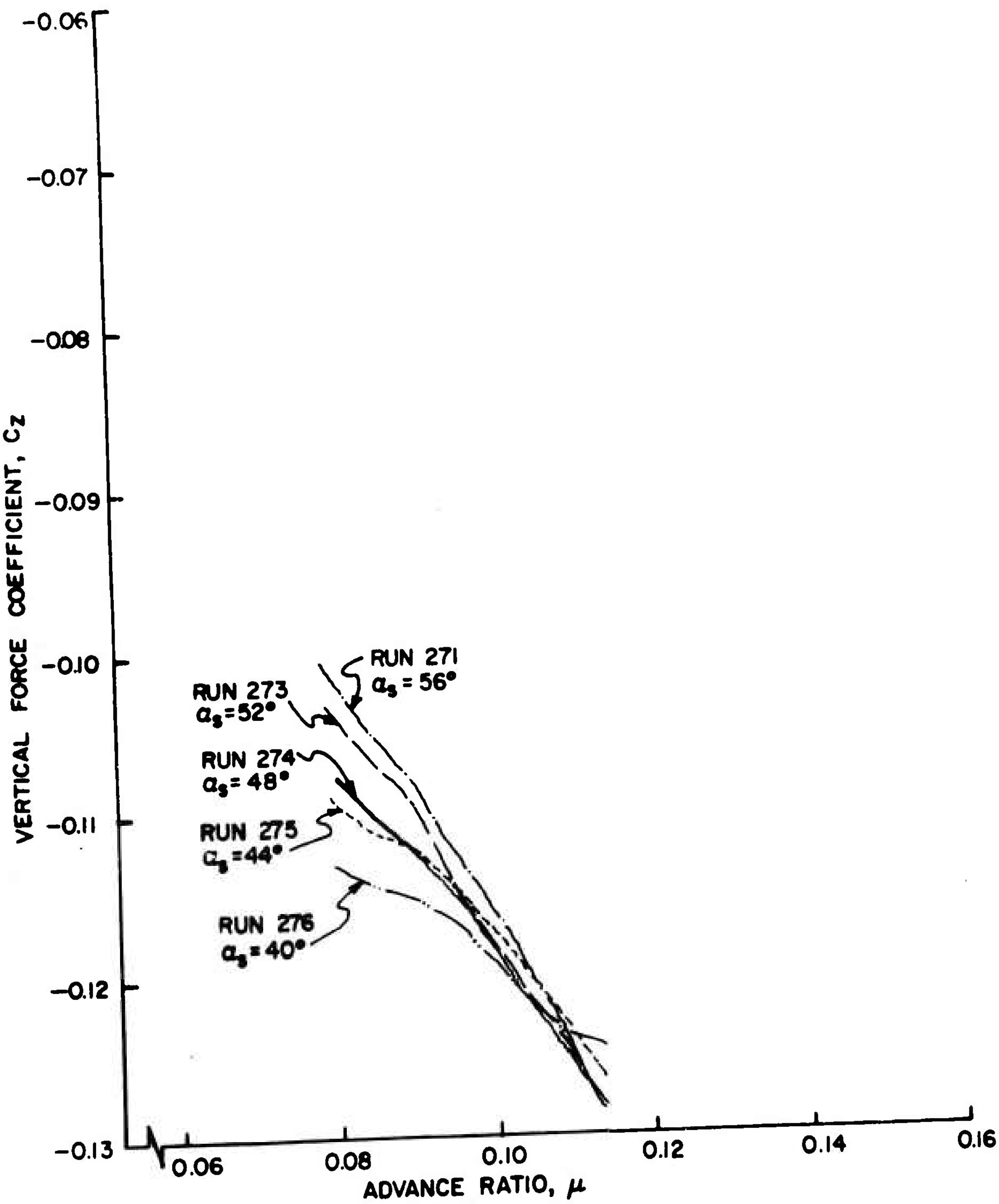

Figure 57a. Rotor Force and Moment Coefficients as Functions of Advance Ratio, $\theta_{.75R} = 6°$, Large Wing on High.

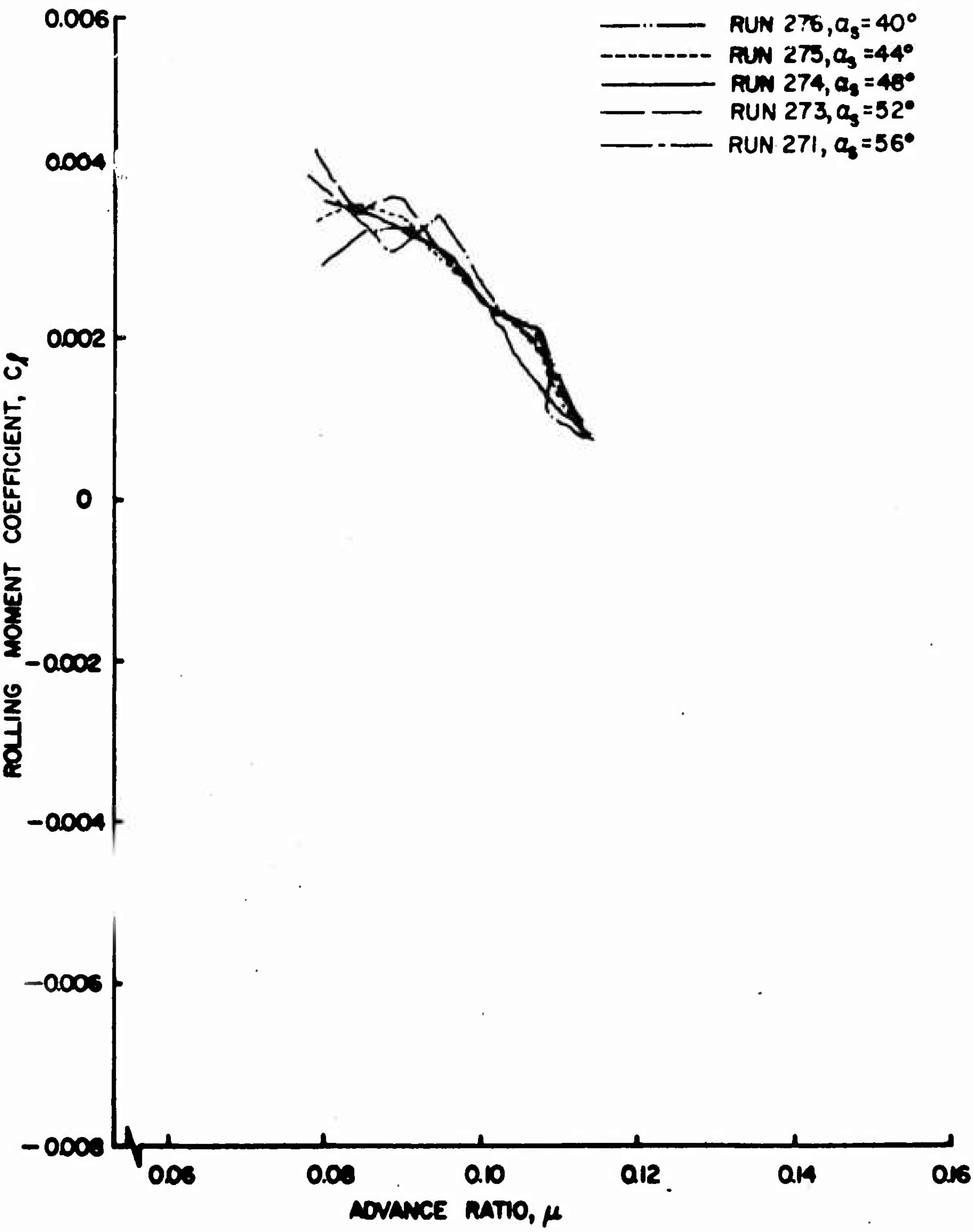

Figure 57b. Rotor Force and Moment Coefficients as Functions of Advance Ratio, $\theta_{.75R} = 6^\circ$, Large Wing on High.

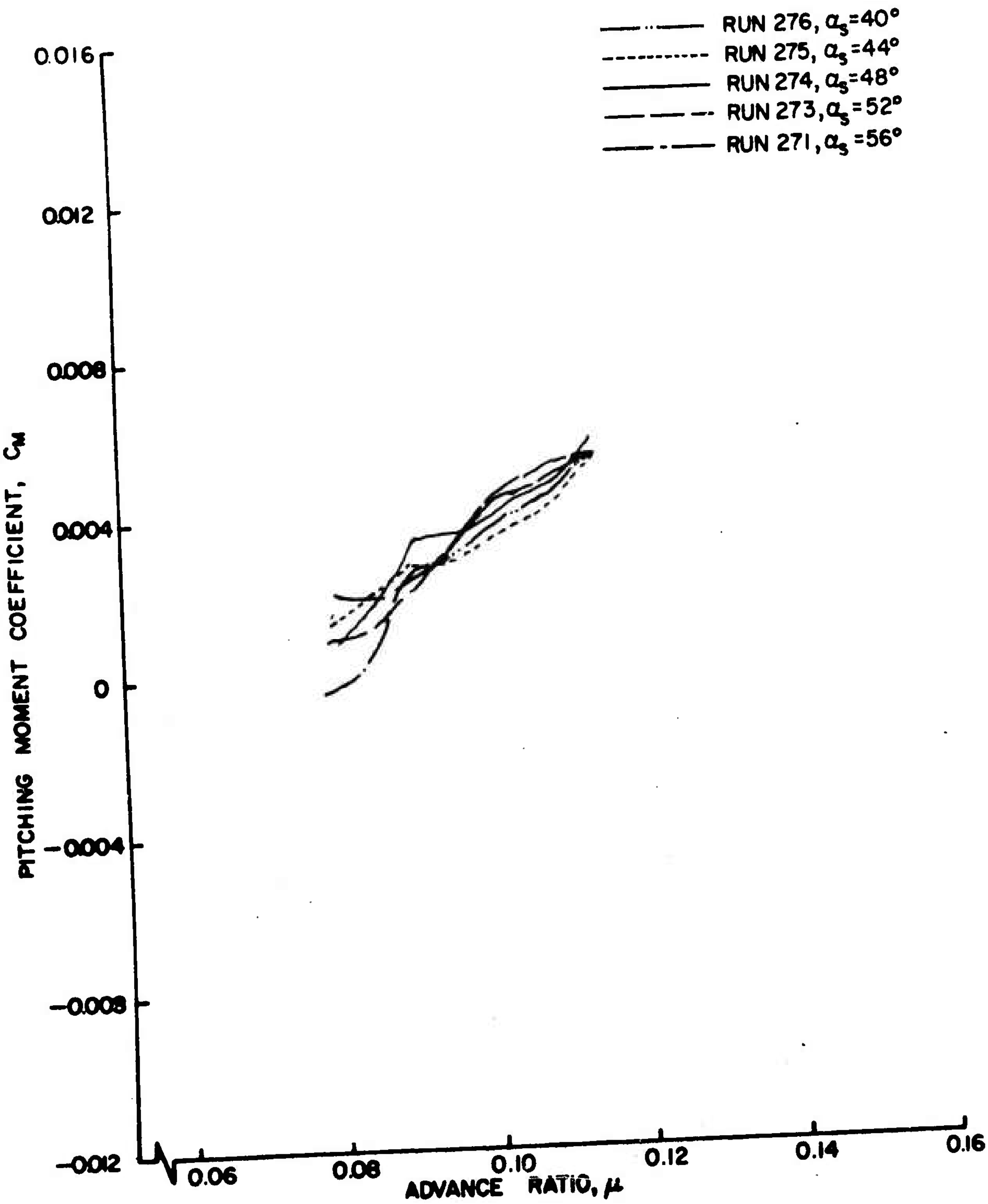

Figure 57c. Rotor Force and Moment Coefficients as Functions of Advance Ratio, $\theta_{.75R} = 6°$, Large Wing on High.

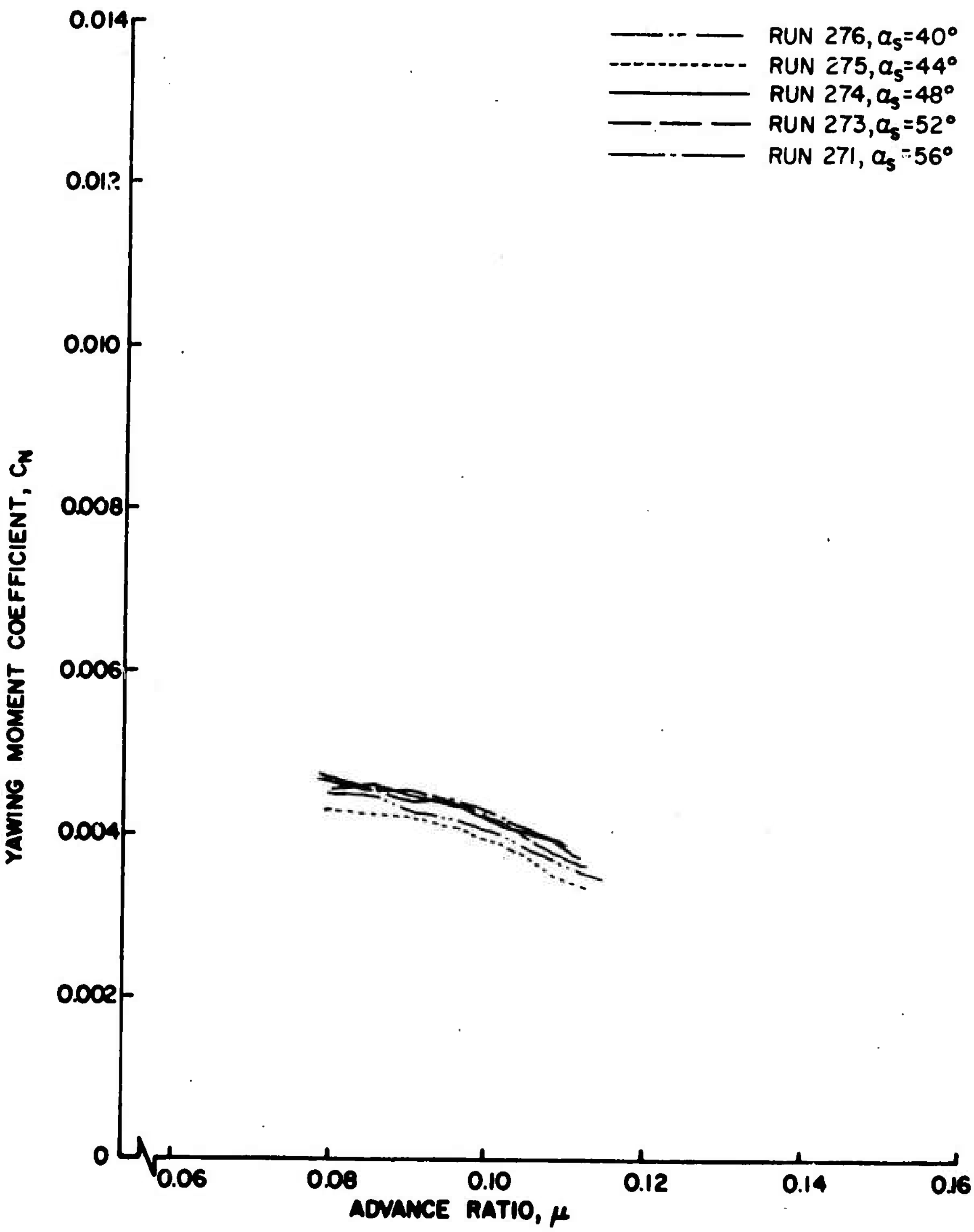

Figure 57d. Rotor Force and Moment Coefficients as Functions of Advance Ratio, $\theta_{.75R} = 6°$, Large Wing on High.

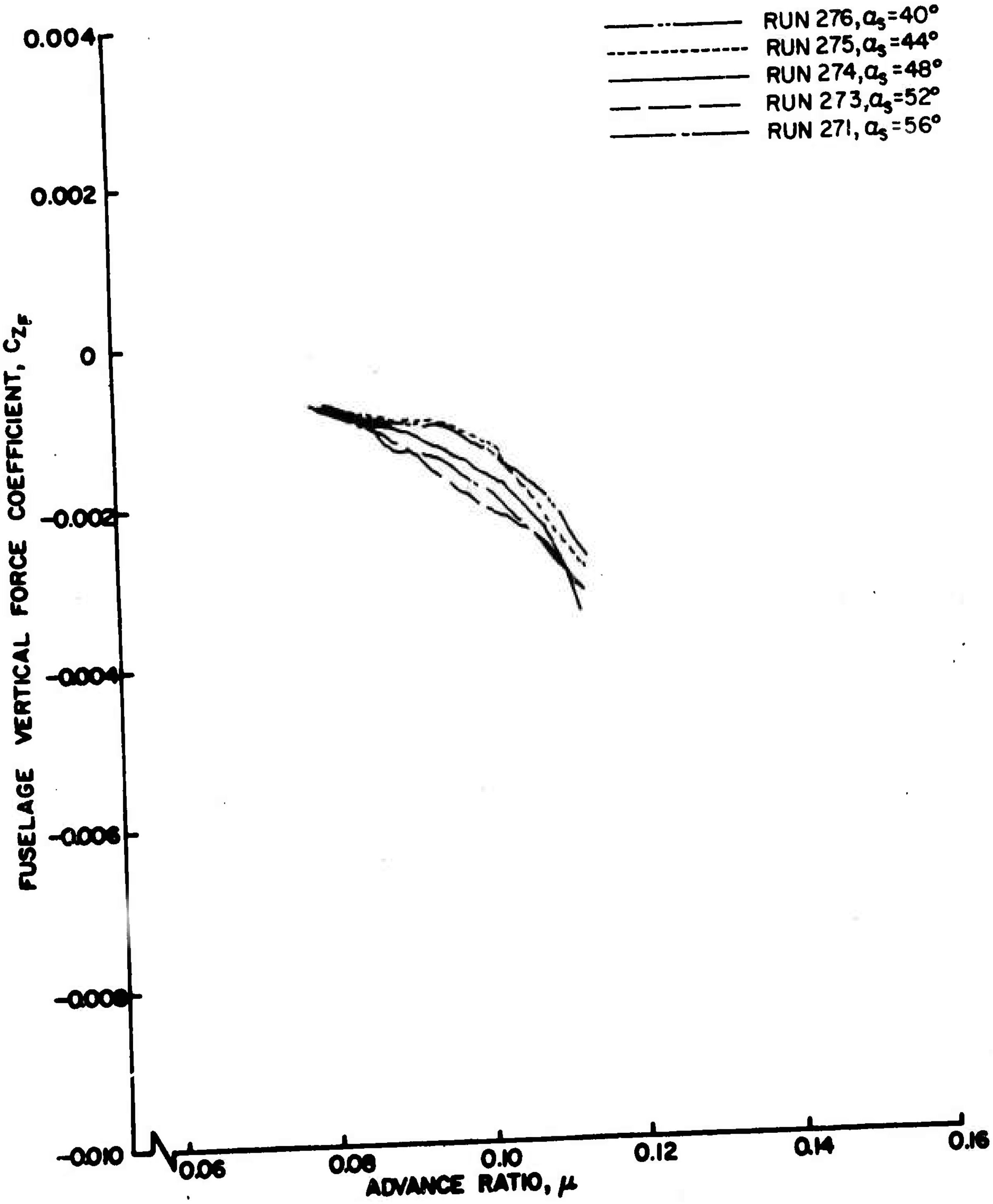

Figure 58a. Fuselage Vertical Force and Pitching Moment Coefficients as Functions of Advance Ratio, $\theta_{.75R} = 6^{\circ}$, Large Wing on High.

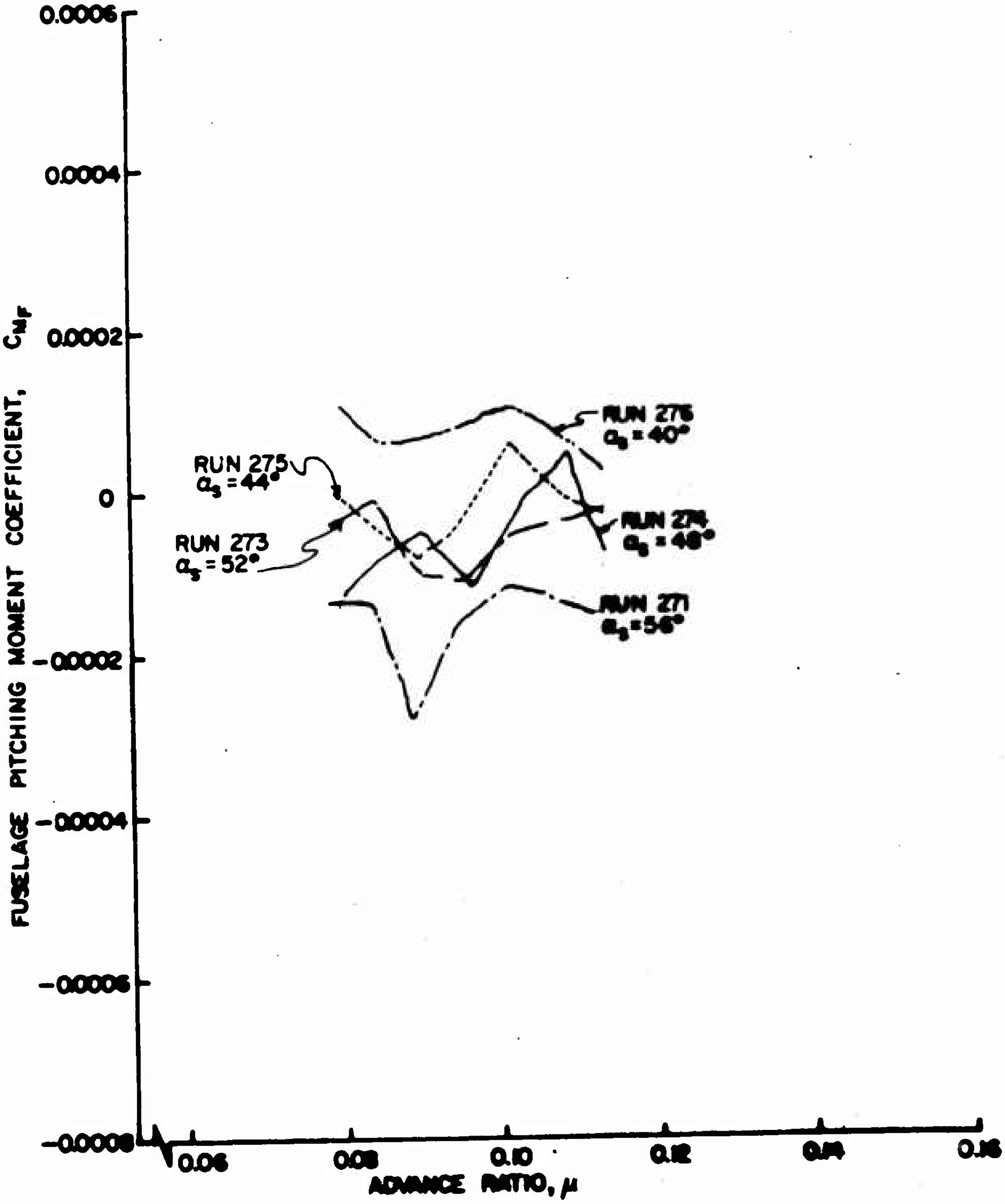

Figure 58b. Fuselage Vertical Force and Pitching Moment Coefficients as Functions of Advance Ratio, $\theta_{.75R} = 6°$, Large Wing on High.

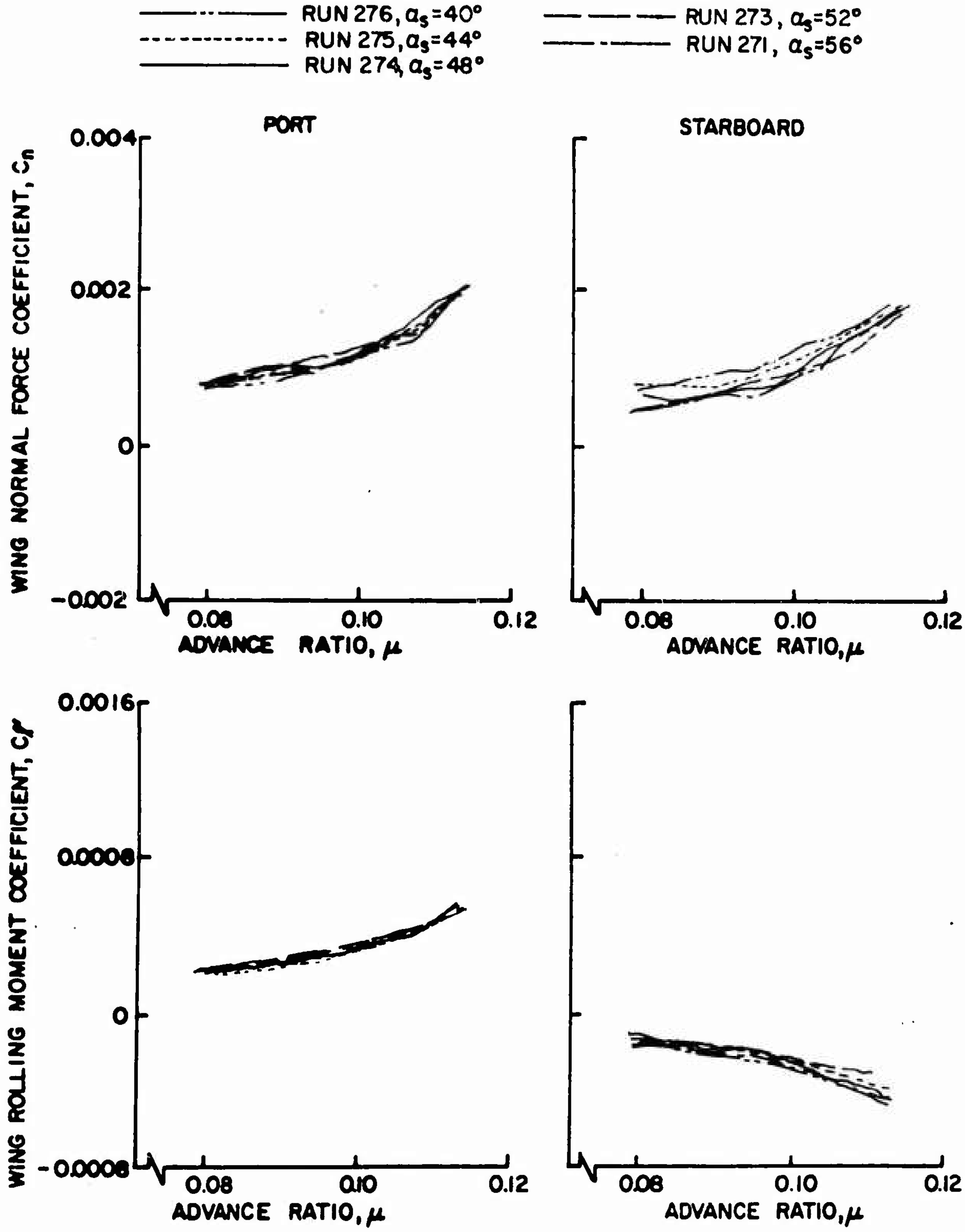

Figure 59. Wing Normal Force and Rolling Moment Coefficients as Functions of Advance Ratio, $\theta_{.75R} = 6^\circ$, Large Wing on High.

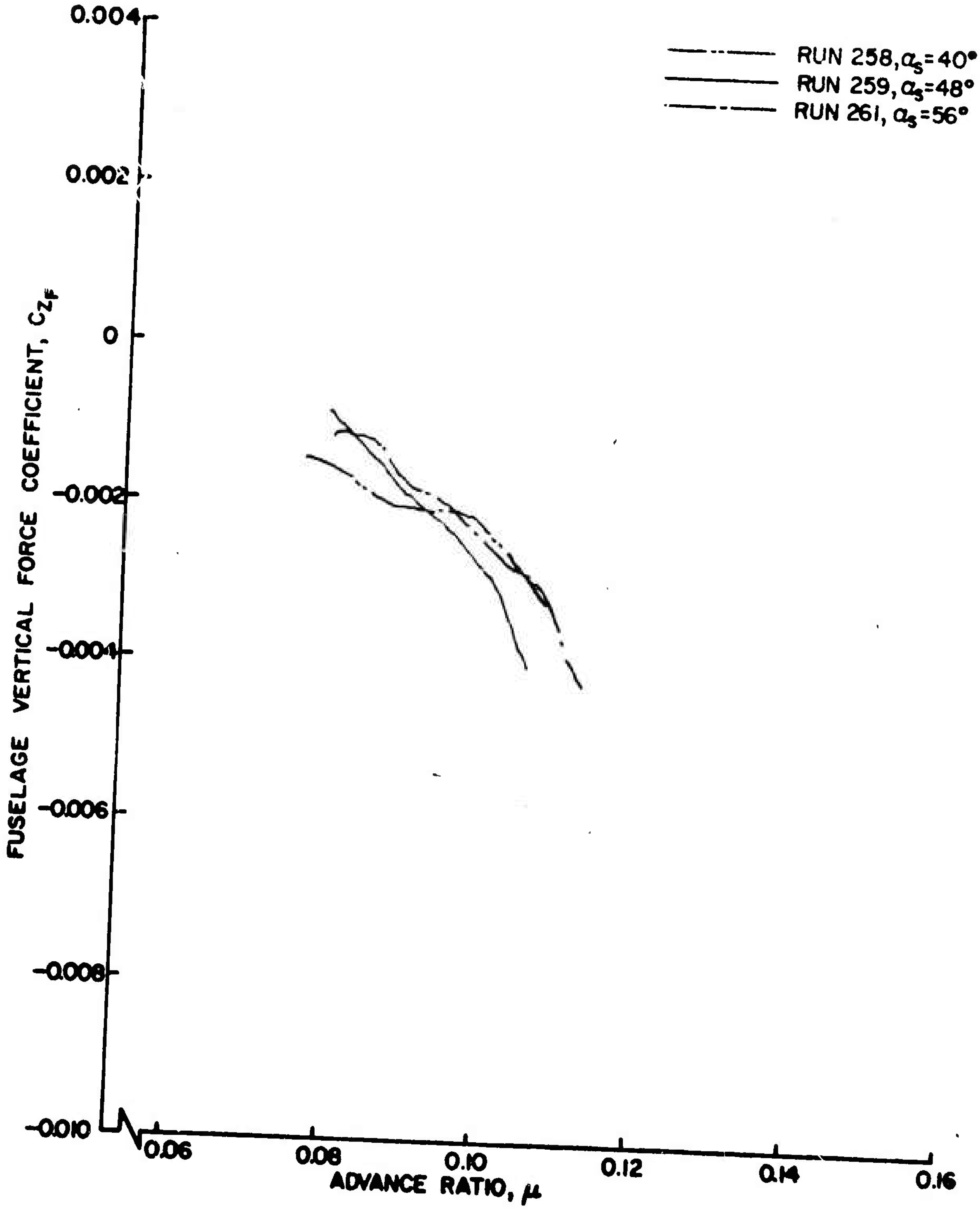

Figure 60a. Fuselage Vertical Force and Pitching Moment Coefficients as Functions of Advance Ratio, $\theta_{.75R} = 6°$, Small Wing on High.

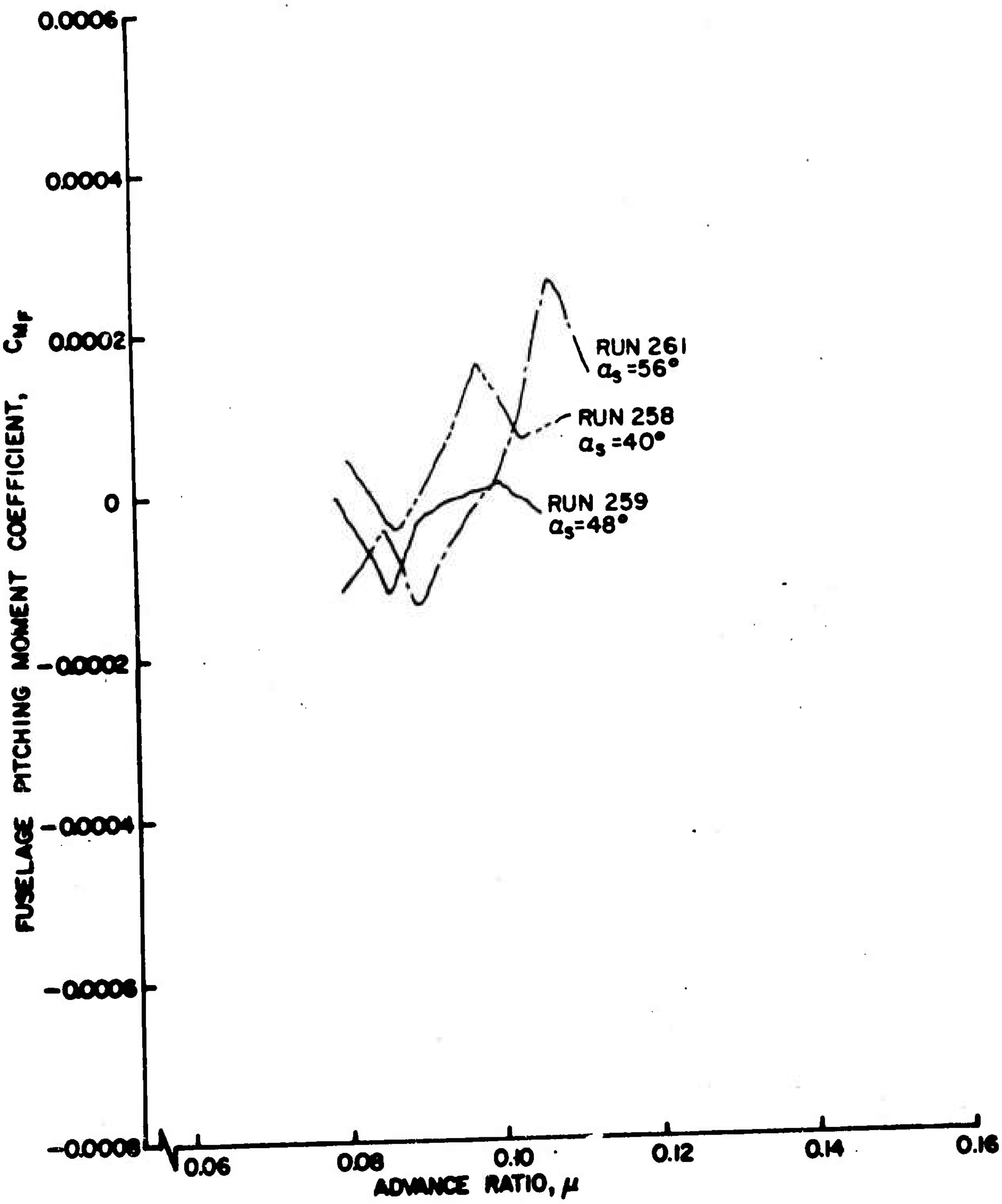

Figure 60b. Fuselage Vertical Force and Pitching Moment Coefficients as Functions of Advance Ratio, $\theta_{.75R} = 6°$, Small Wing on High.

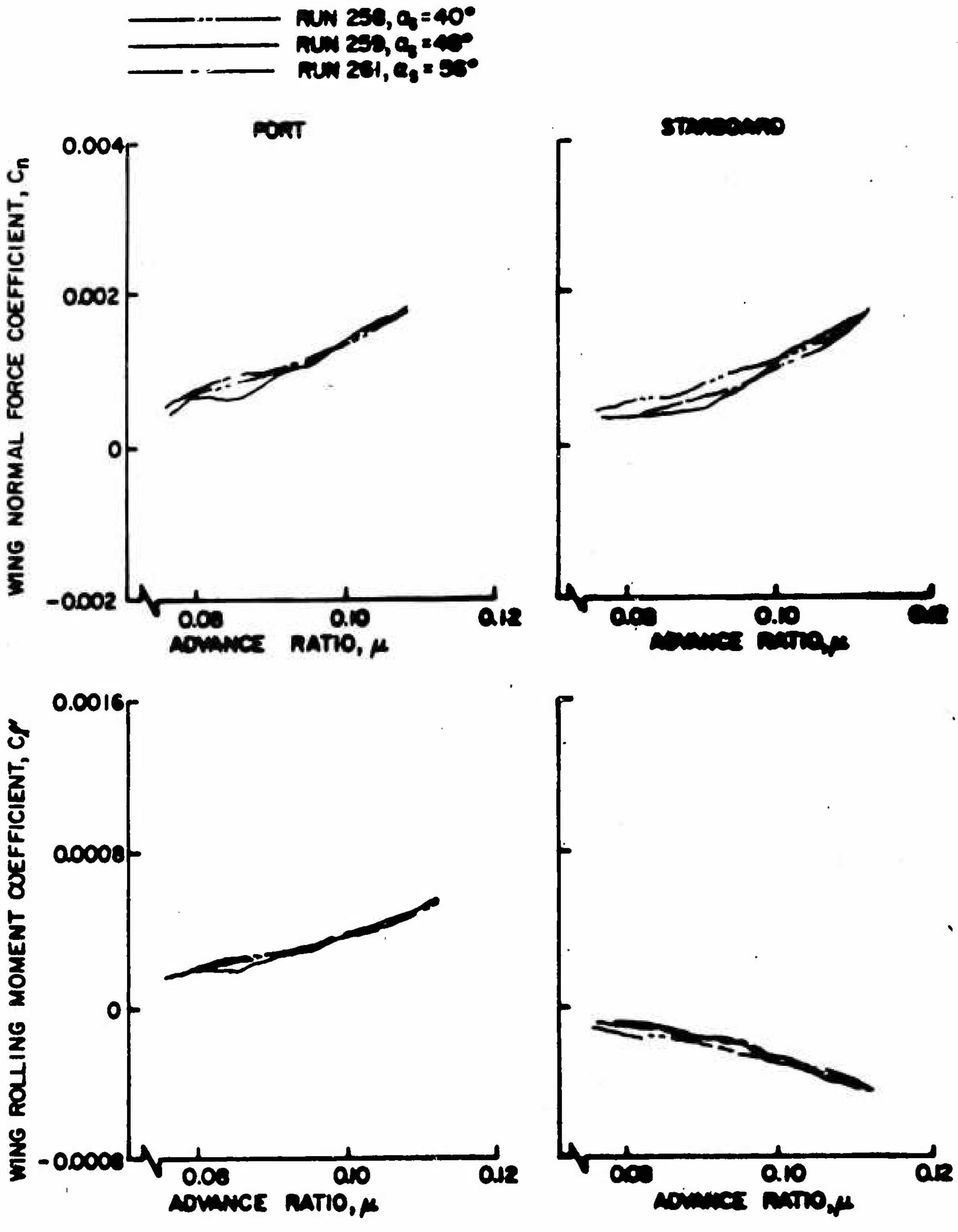

Figure 61. Wing Normal Force and Rolling Moment Coefficients as Functions of Advance Ratio, $\theta_{.75R} = 6^\circ$, Large Wing on Low.

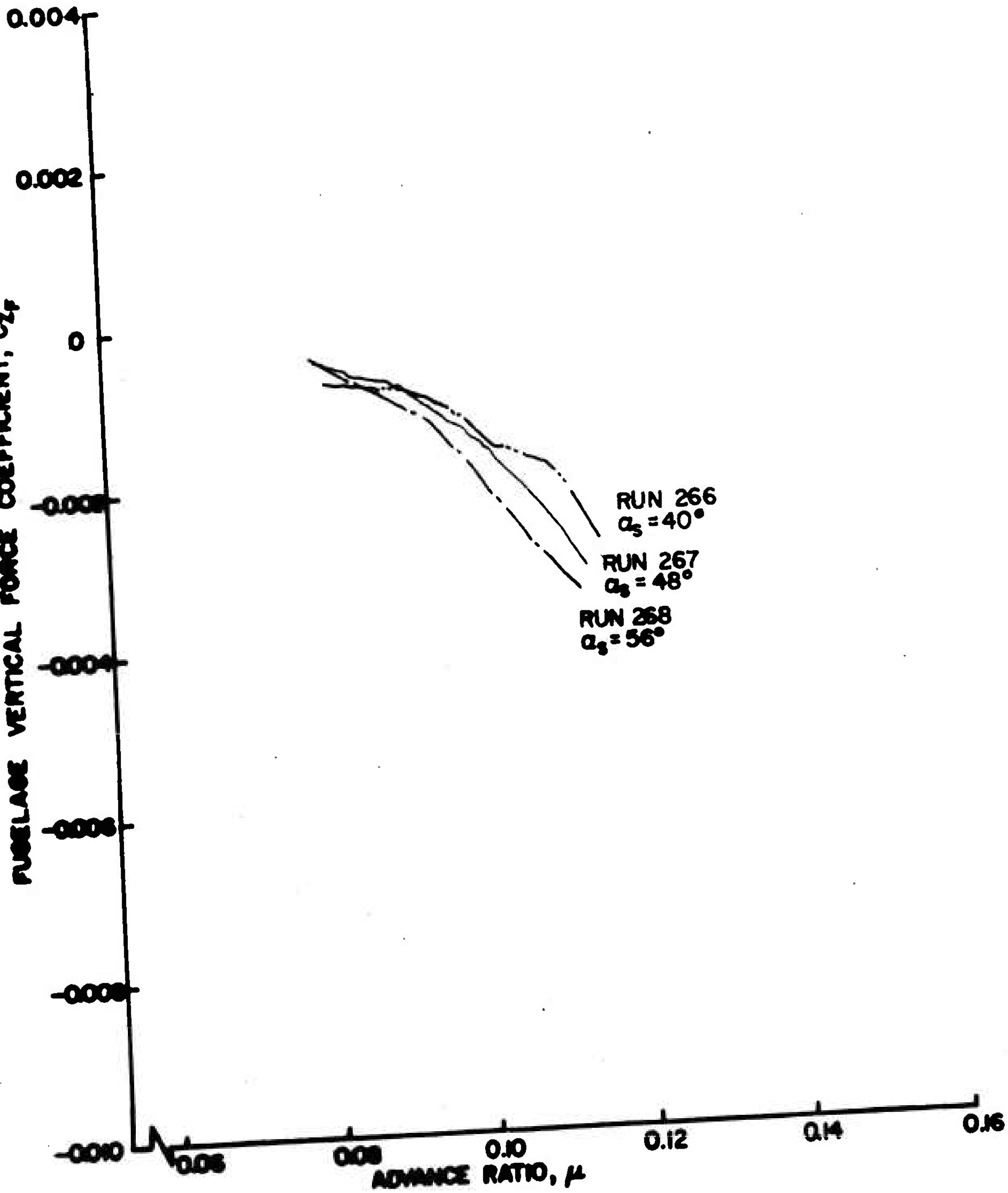

Figure 62a. Fuselage Vertical Force and Pitching Moment Coefficients as Functions of Advance Ratio, $\theta_{.75R} = 6°$, Small Wing on High.

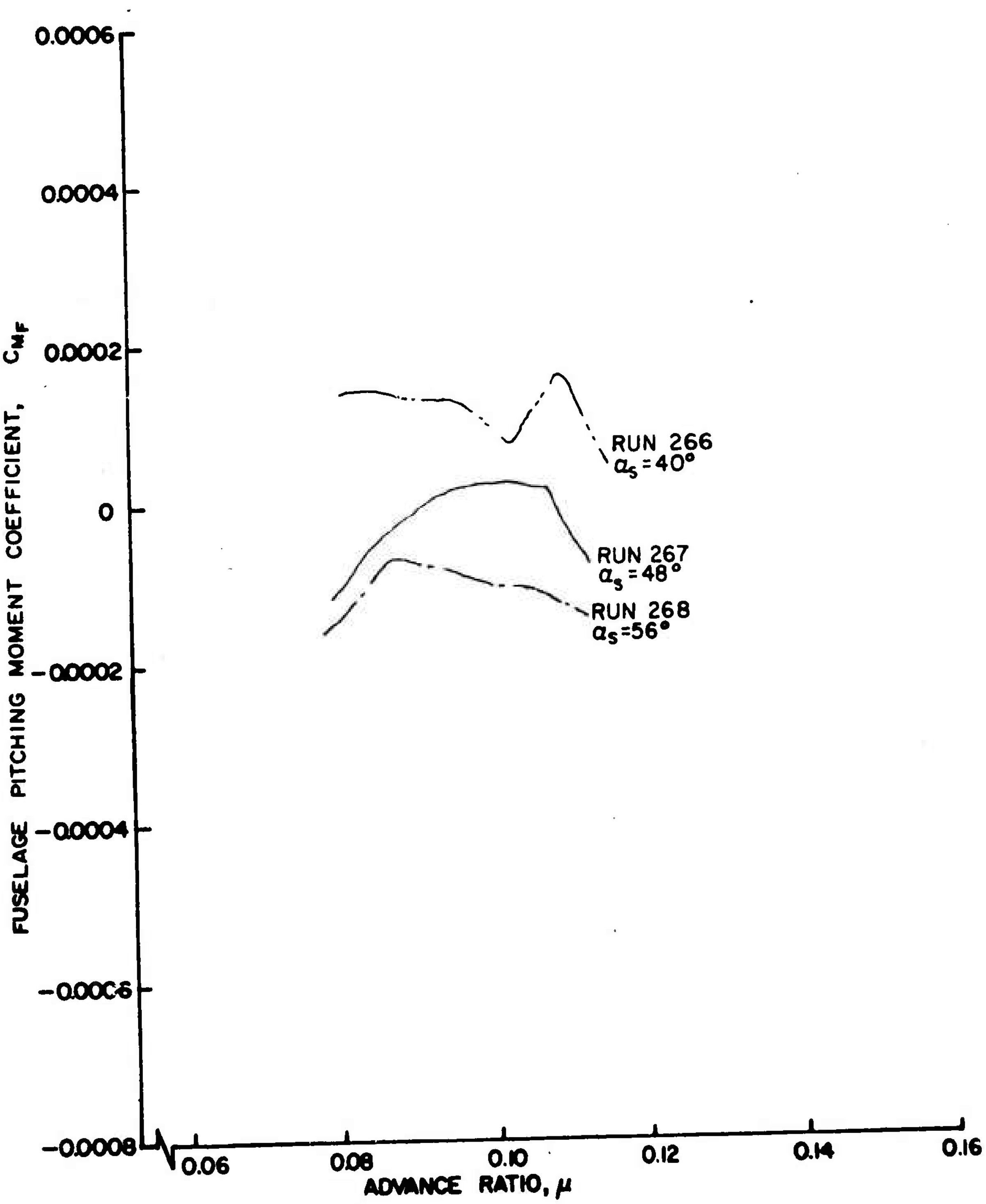

Figure 62b. Fuselage Vertical Force and Pitching Moment Coefficients as Functions of Advance Ratio, $\theta_{.75R} = 6°$, Small Wing on High.

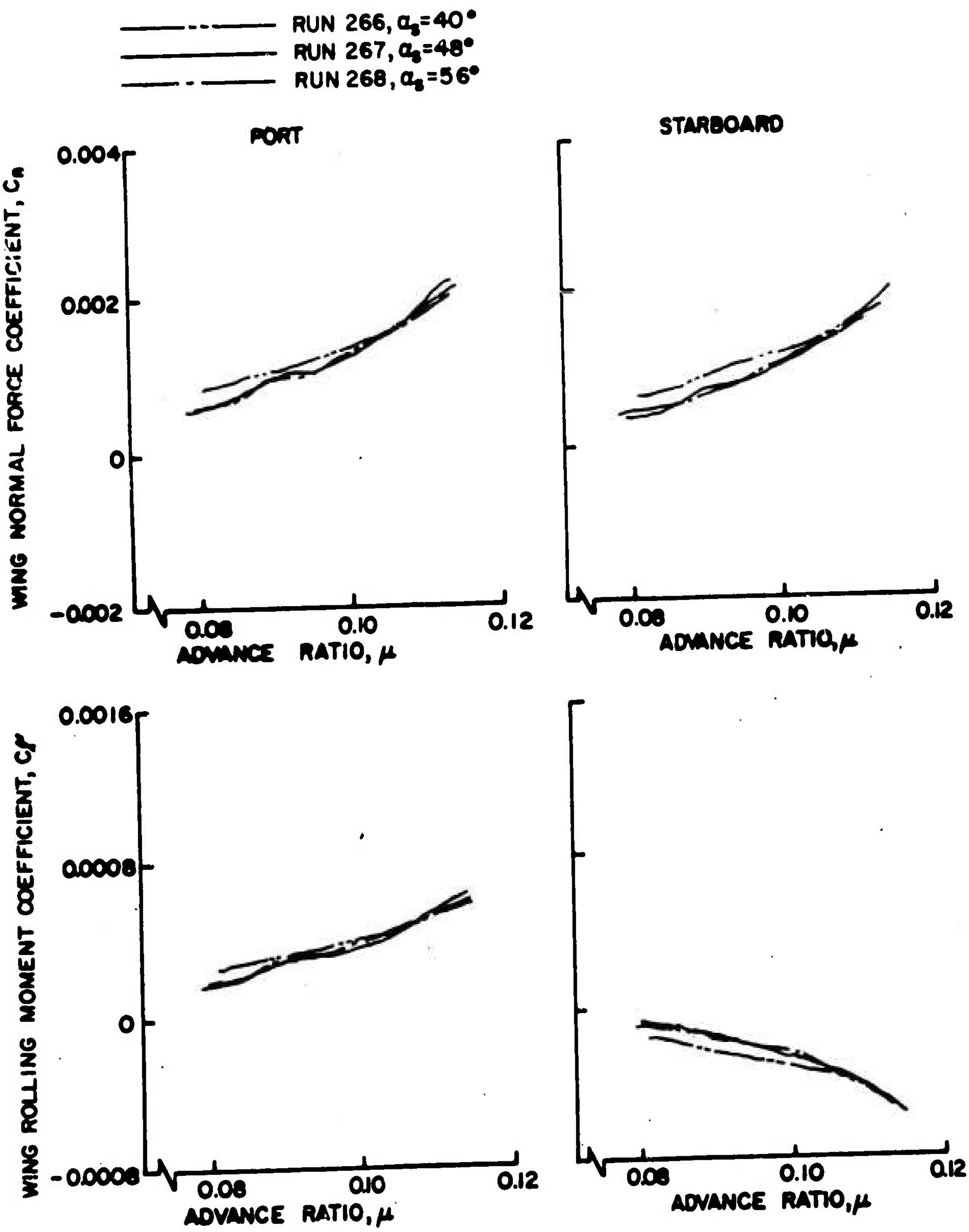

Figure 63. Wing Normal Force and Rolling Moment Coefficients as Functions of Advance Ratio, $\theta_{.75R} = 6°$, Small Wing on High.

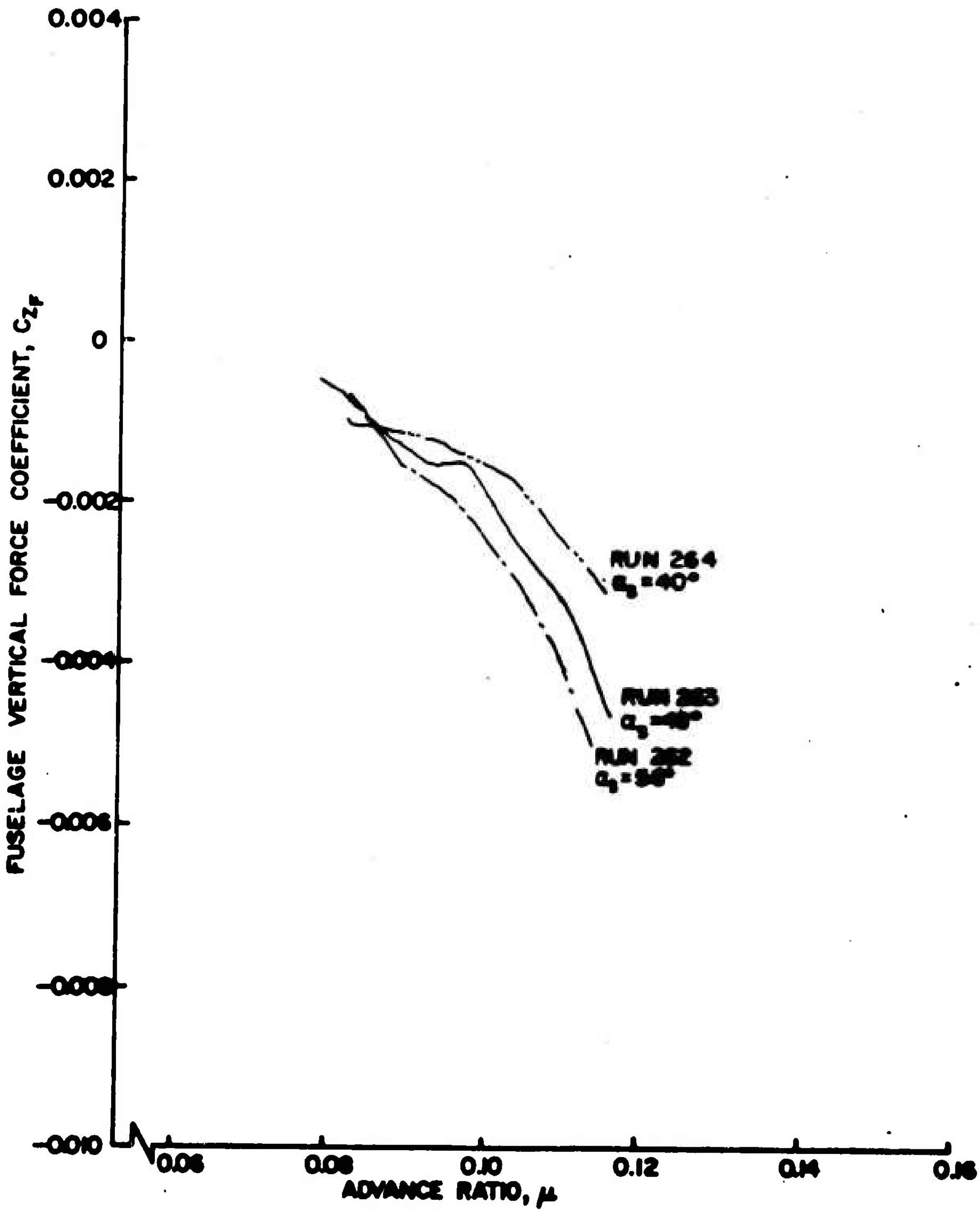

Figure 64a. Fuselage Vertical Force and Pitching Moment Coefficients as Functions of Advance Ratio, $\theta_{.75R} = 6°$, Small Wing on Low.

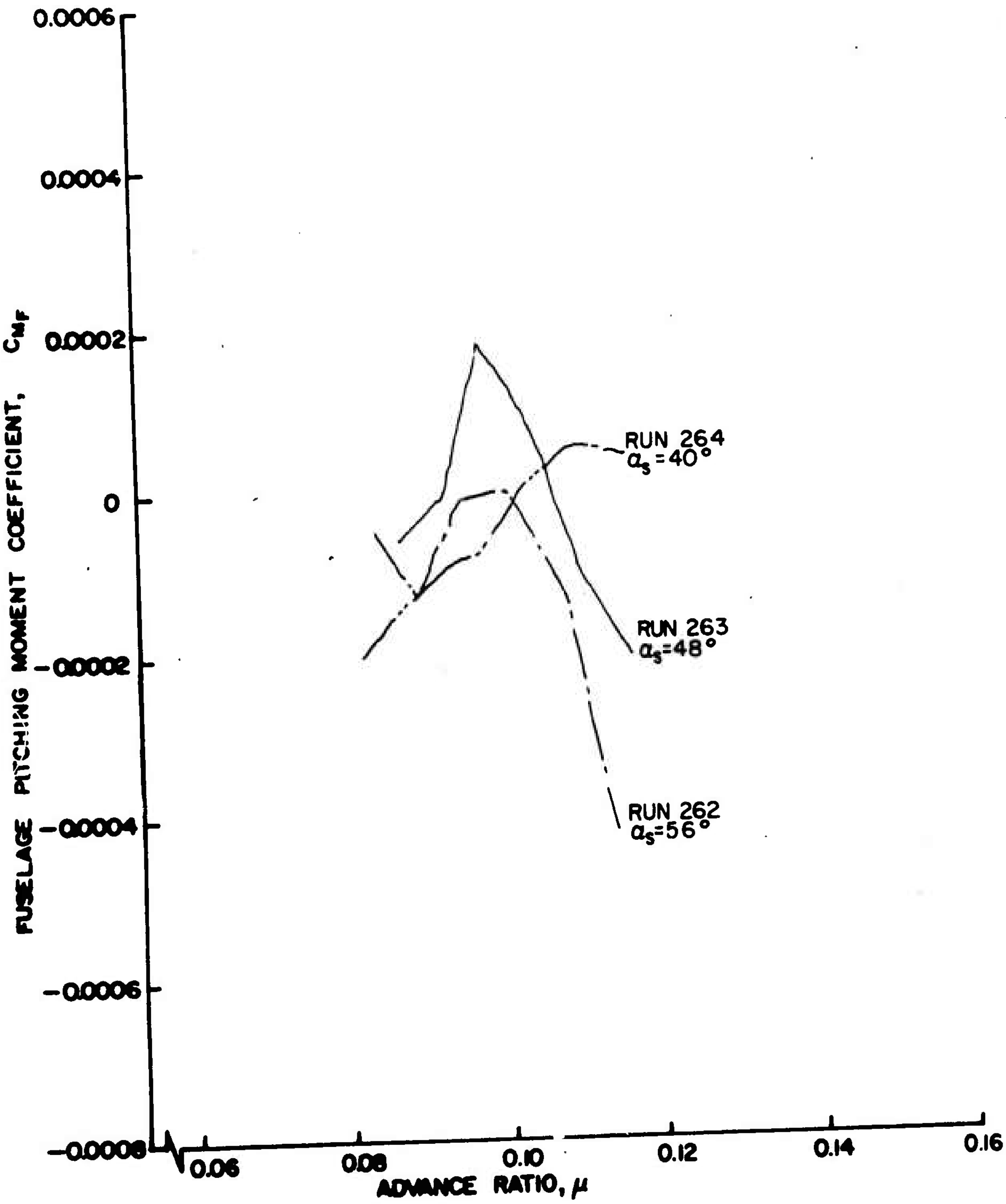

Figure 64b. Fuselage Vertical Force and Pitching Moment Coefficients as Functions of Advance Ratio, $\theta_{.75R} = 6^\circ$, Small Wing on Low.

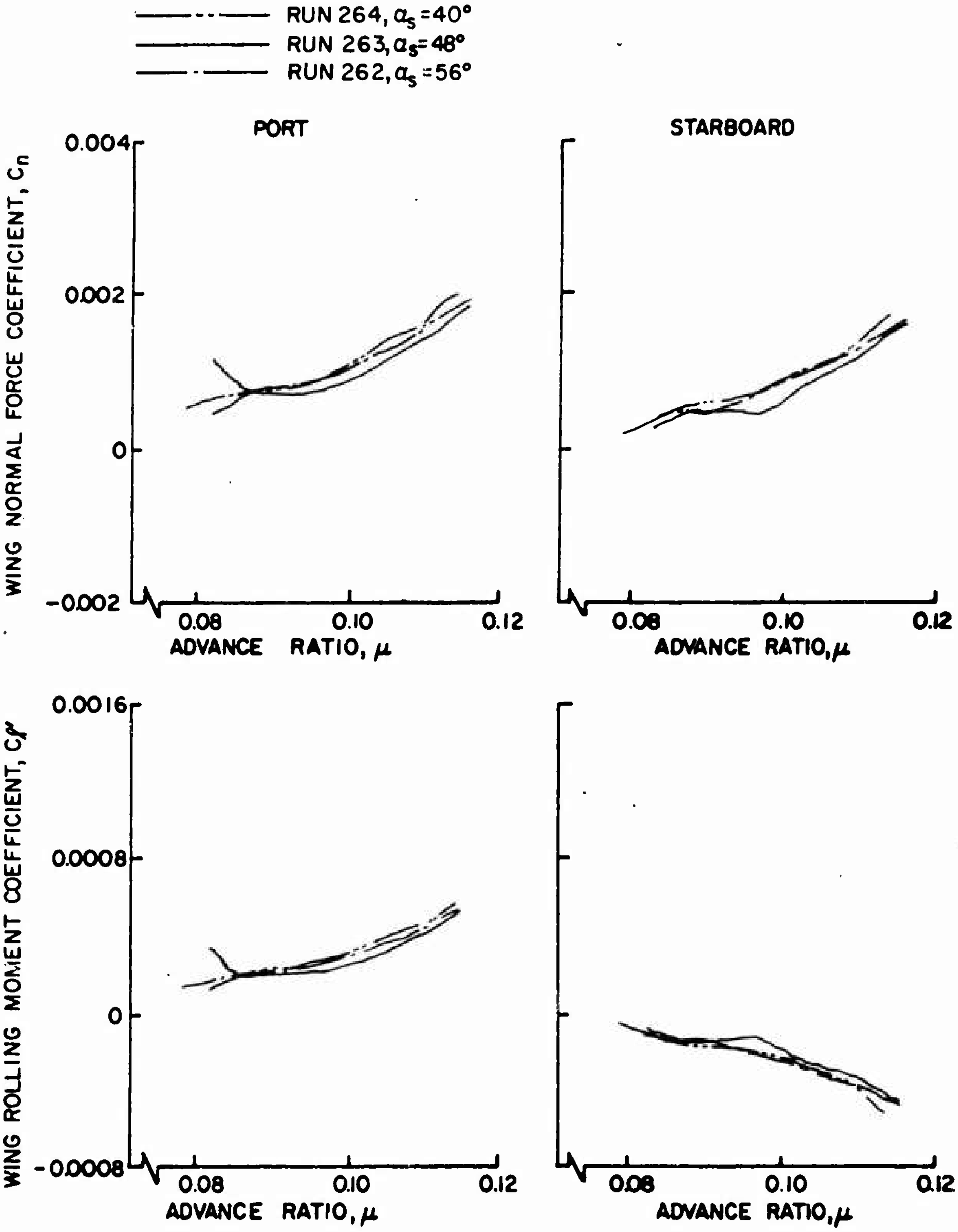

Figure 65. Wing Normal Force and Rolling Moment Coefficients as Functions of Advance Ratio, $\theta_{.75R} = 6°$, Small Wing on Low.

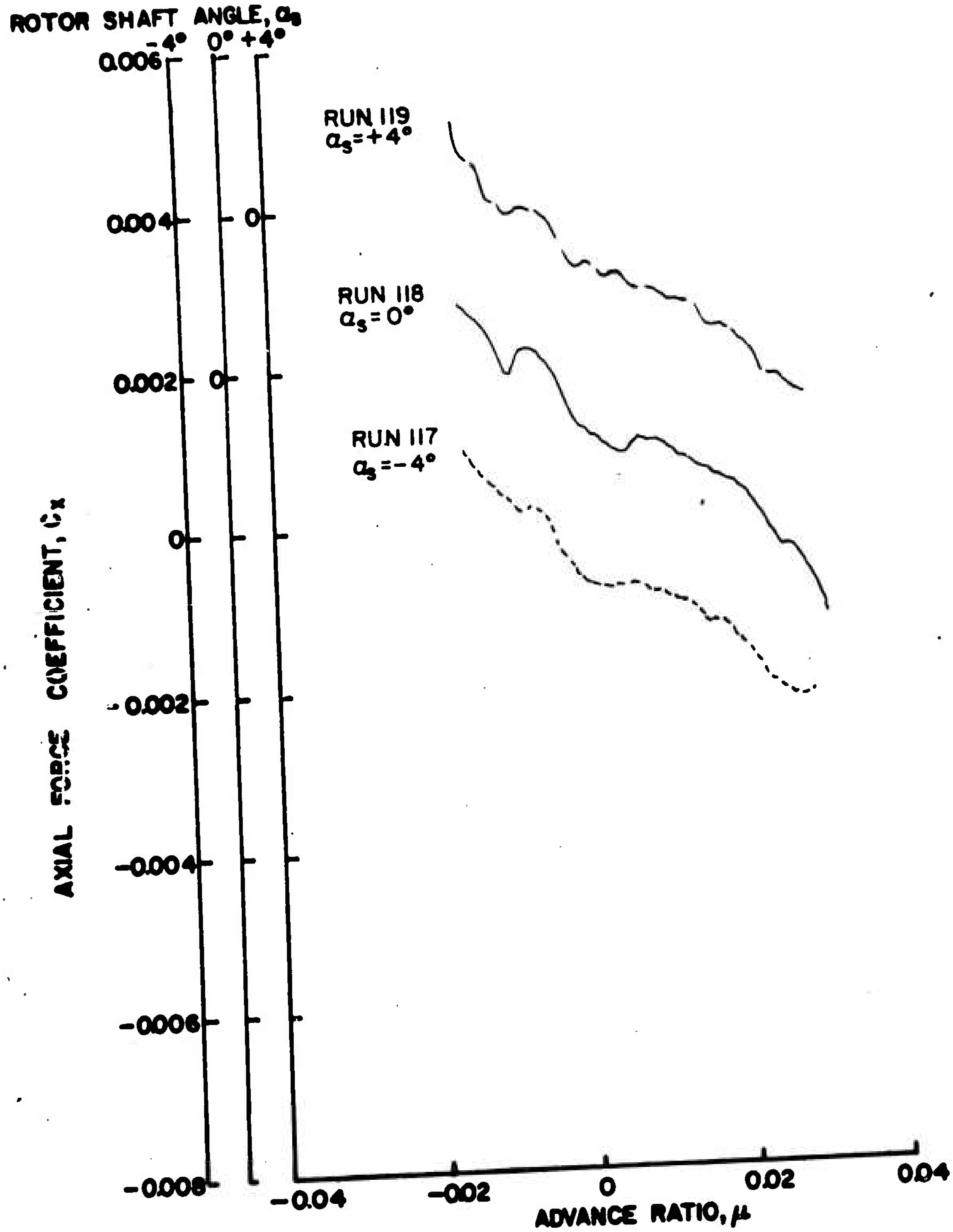

Figure 66a. Rotor Force and Moment Coefficients as Functions of Advance Ratio, $\theta_{.75R} = 8°$, Wing Off, Fuselage Off, $\frac{h}{D} = 0.75$.

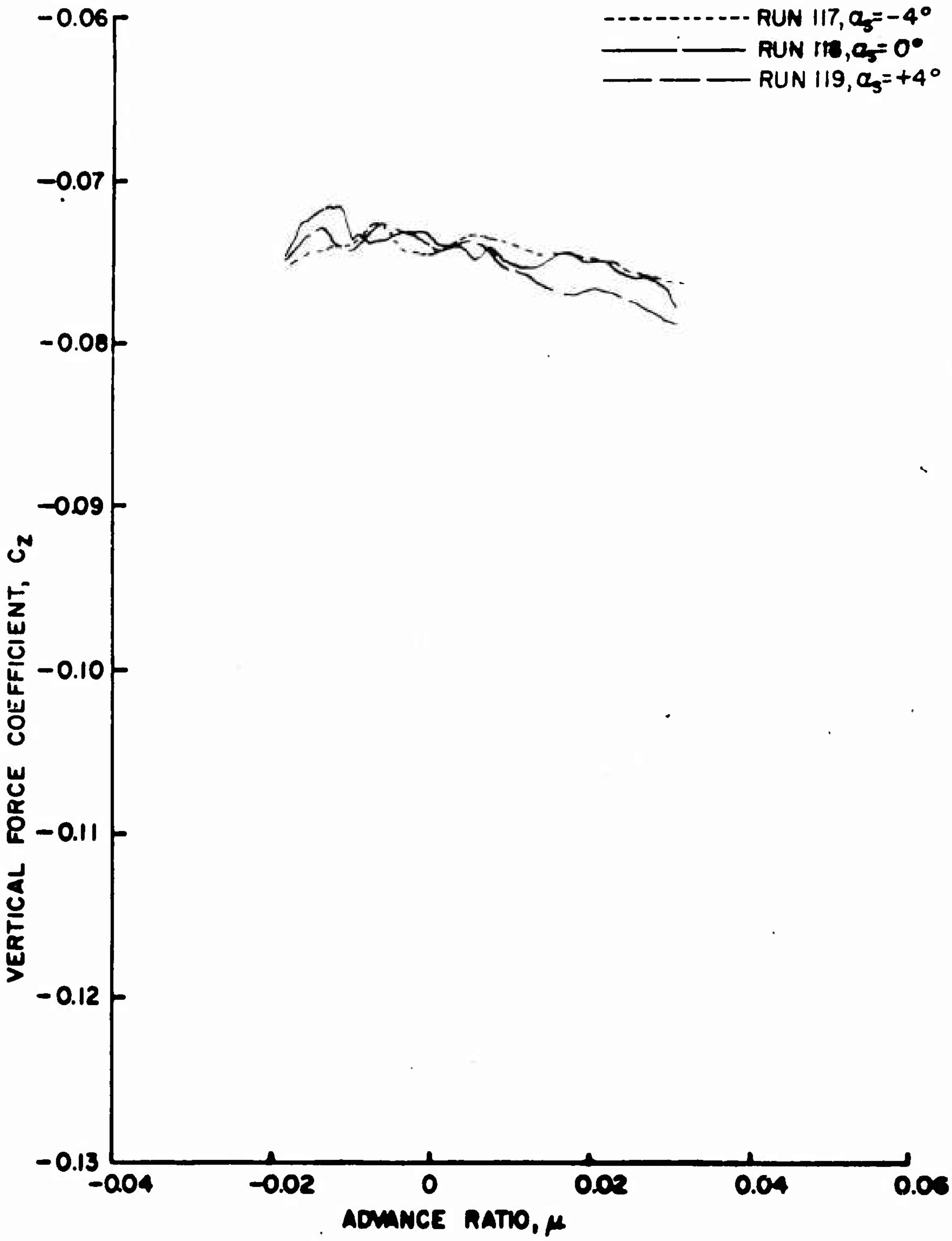

Figure 66b. Rotor Force and Moment Coefficients as Functions of Advance Ratio, $\theta_{.75R} = 8°$, Wing Off, Fuselage Off, $\frac{h}{D} = 0.75$.

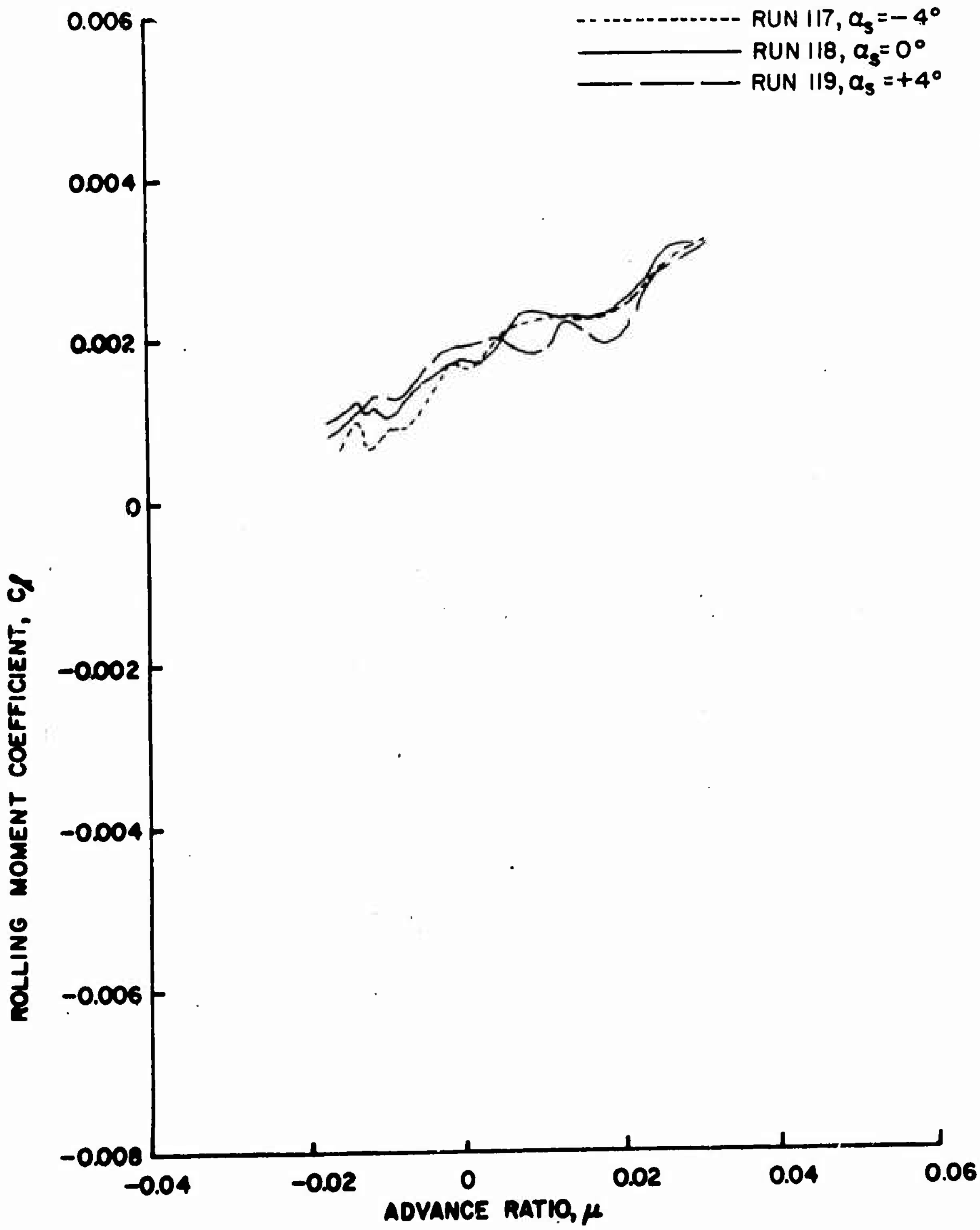

Figure 66c. Rotor Force and Moment Coefficients as Functions of Advance Ratio, $\theta_{.75R} = 8^\circ$, Wing Off, Fuselage Off, $\frac{h}{D} = 0.75$.

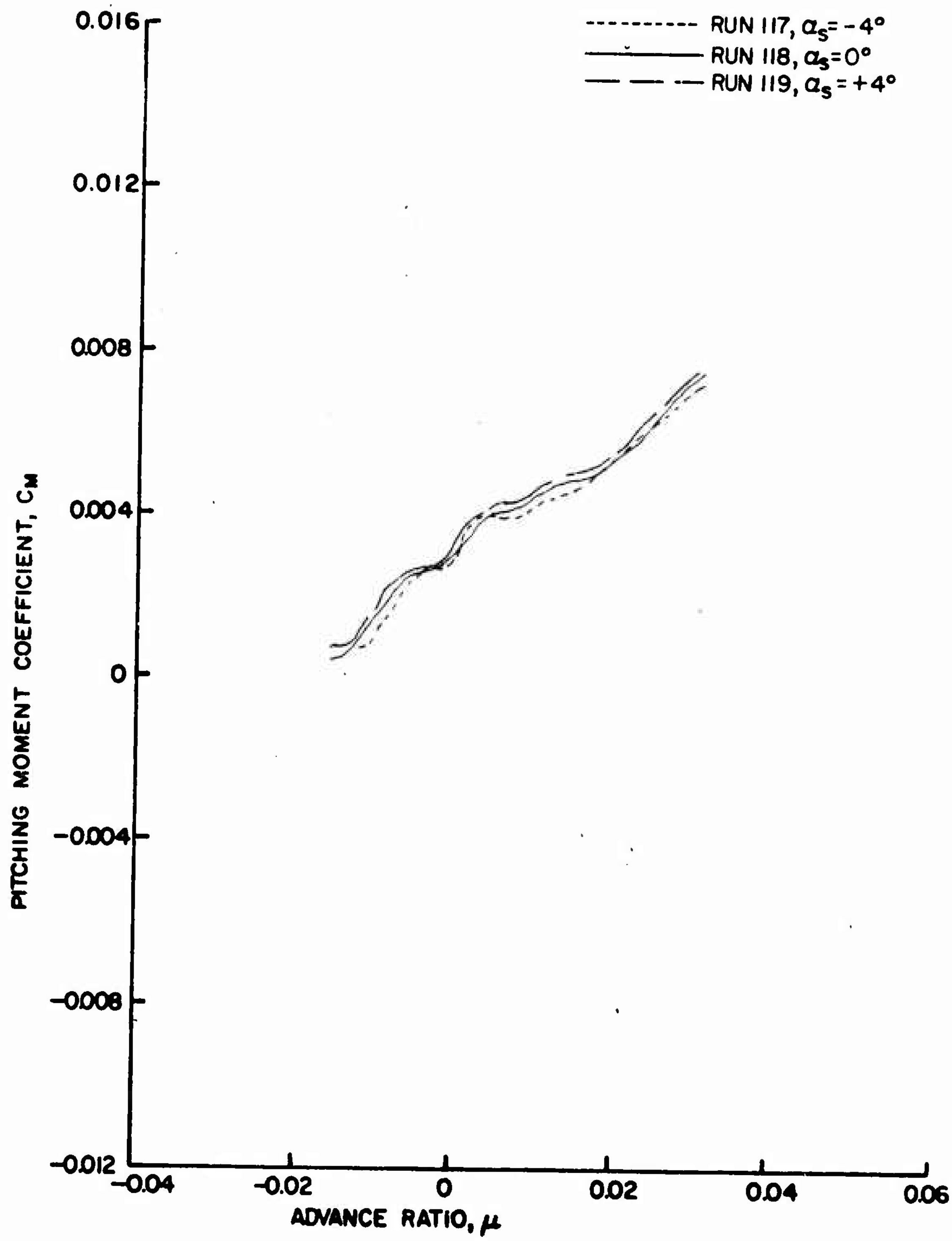

Figure 66d. Rotor Force and Moment Coefficients as Functions of Advance Ratio, $\theta_{.75R} = 8^\circ$, Wing Off, Fuselage Off, $\frac{h}{D} = 0.75$.

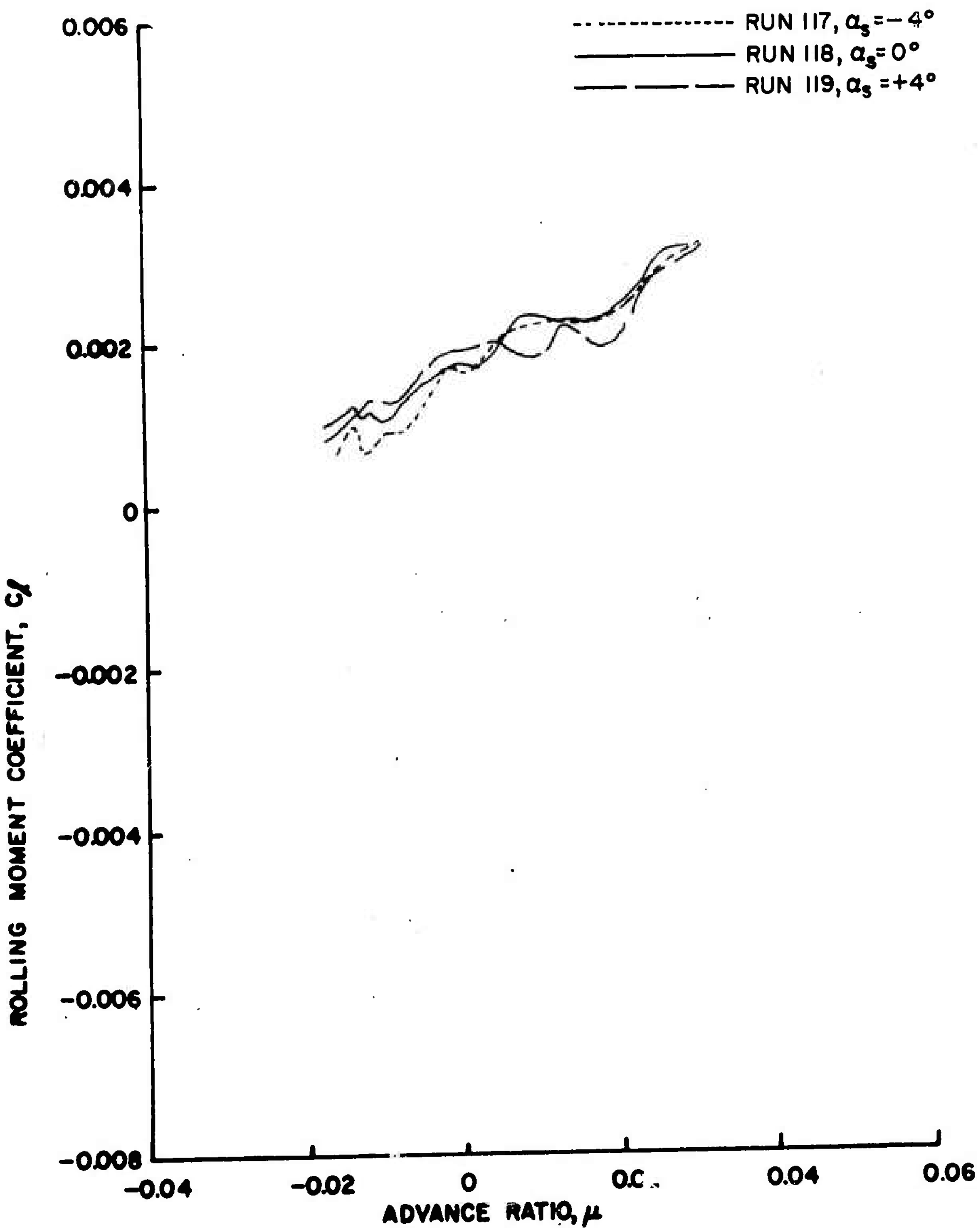

Figure 66c. Rotor Force and Moment Coefficients as Functions of Advance Ratio, $\theta_{.75R} = 8°$, Wing Off, Fuselage Off, $\frac{h}{D} = 0.75$.

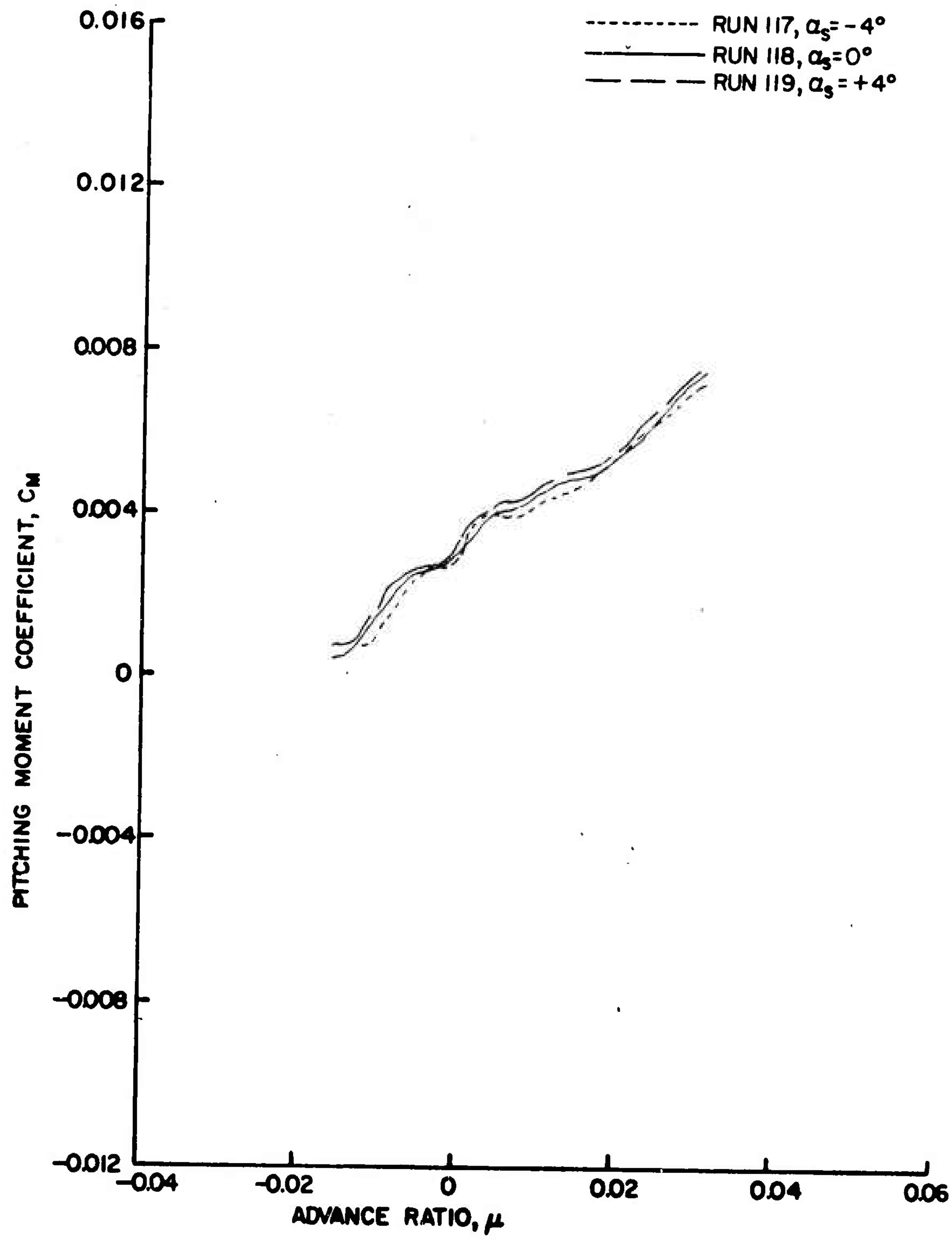

Figure 66d. Rotor Force and Moment Coefficients as Functions of Advance Ratio, $\theta_{.75R} = 8°$, Wing Off, Fuselage Off, $\frac{h}{D} = 0.75$.

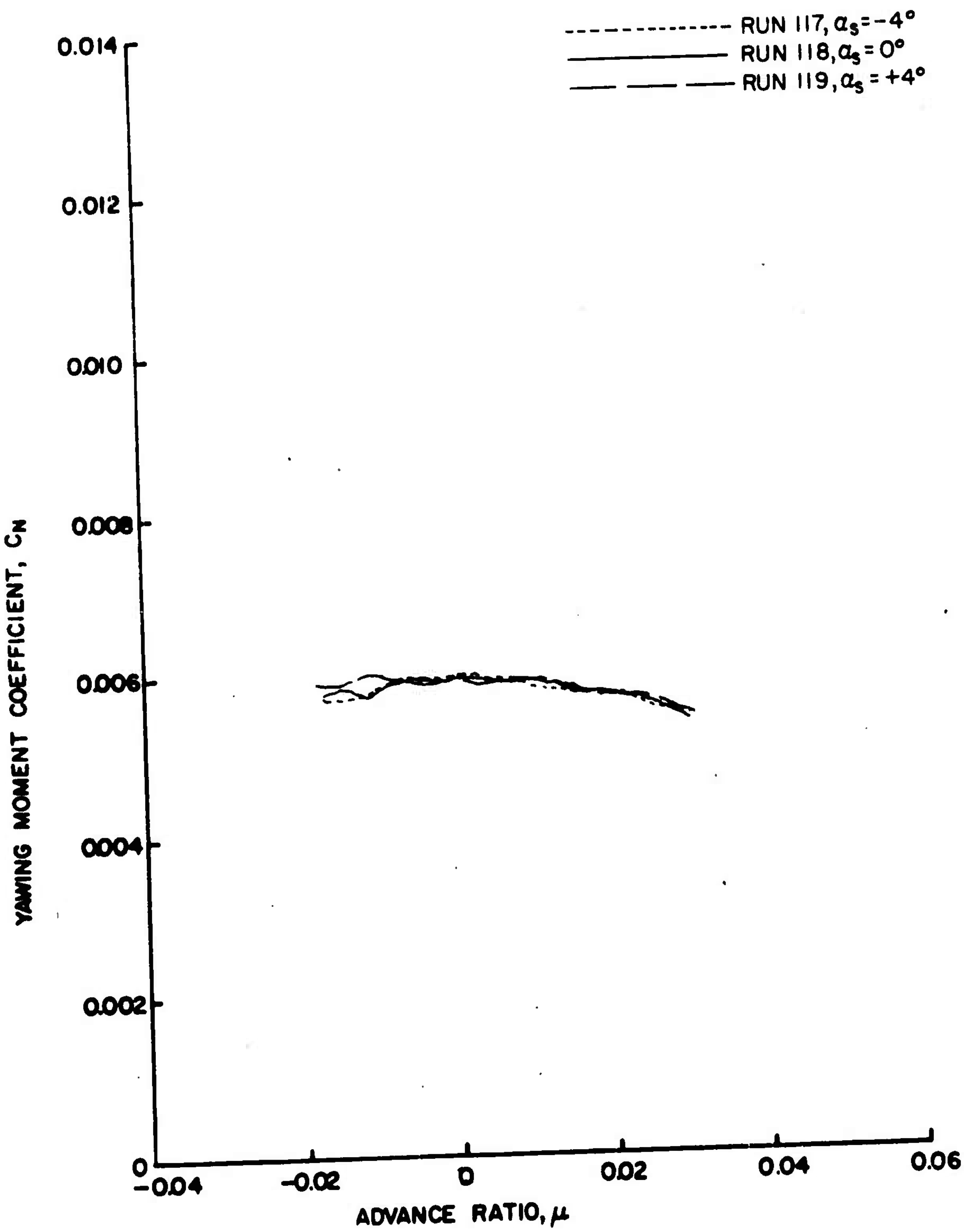

Figure 66e. Rotor Force and Moment Coefficients as Functions of Advance Ratio, $\theta_{.75R} = 8°$, Wing Off, Fuselage Off, $\frac{h}{D}$ = 0.75.

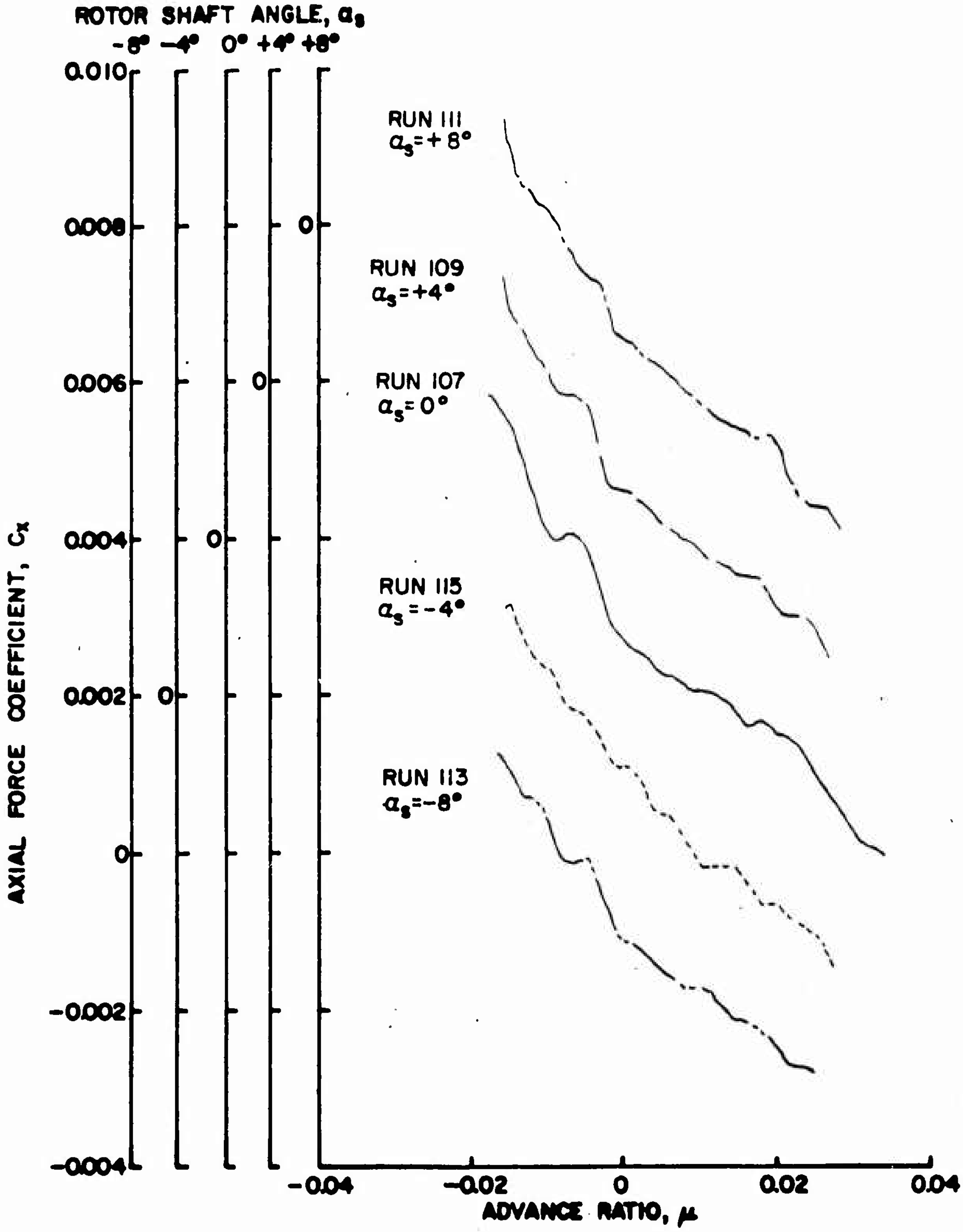

Figure 67a. Rotor Force and Moment Coefficients as Functions of Advance Ratio, $\theta_{.75R} = 10^\circ$, Wing Off, Fuselage Off, $\frac{h}{D} = 0.75$.

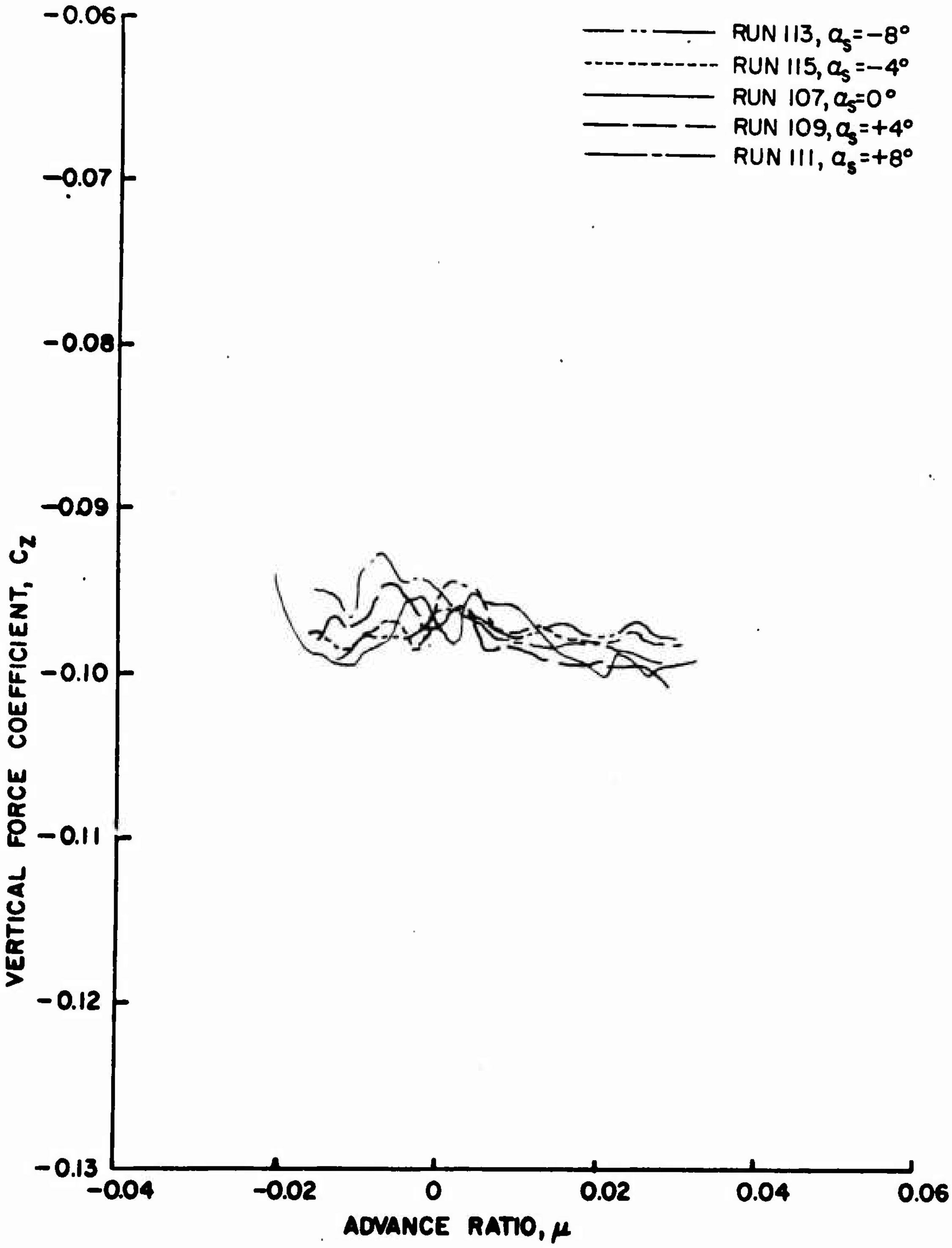

Figure 67b. Rotor Force and Moment Coefficients as Functions of Advance Ratio, $\theta_{.75R} = 10^\circ$, Wing Off, Fuselage Off, $\frac{h}{D} = 0.75$.

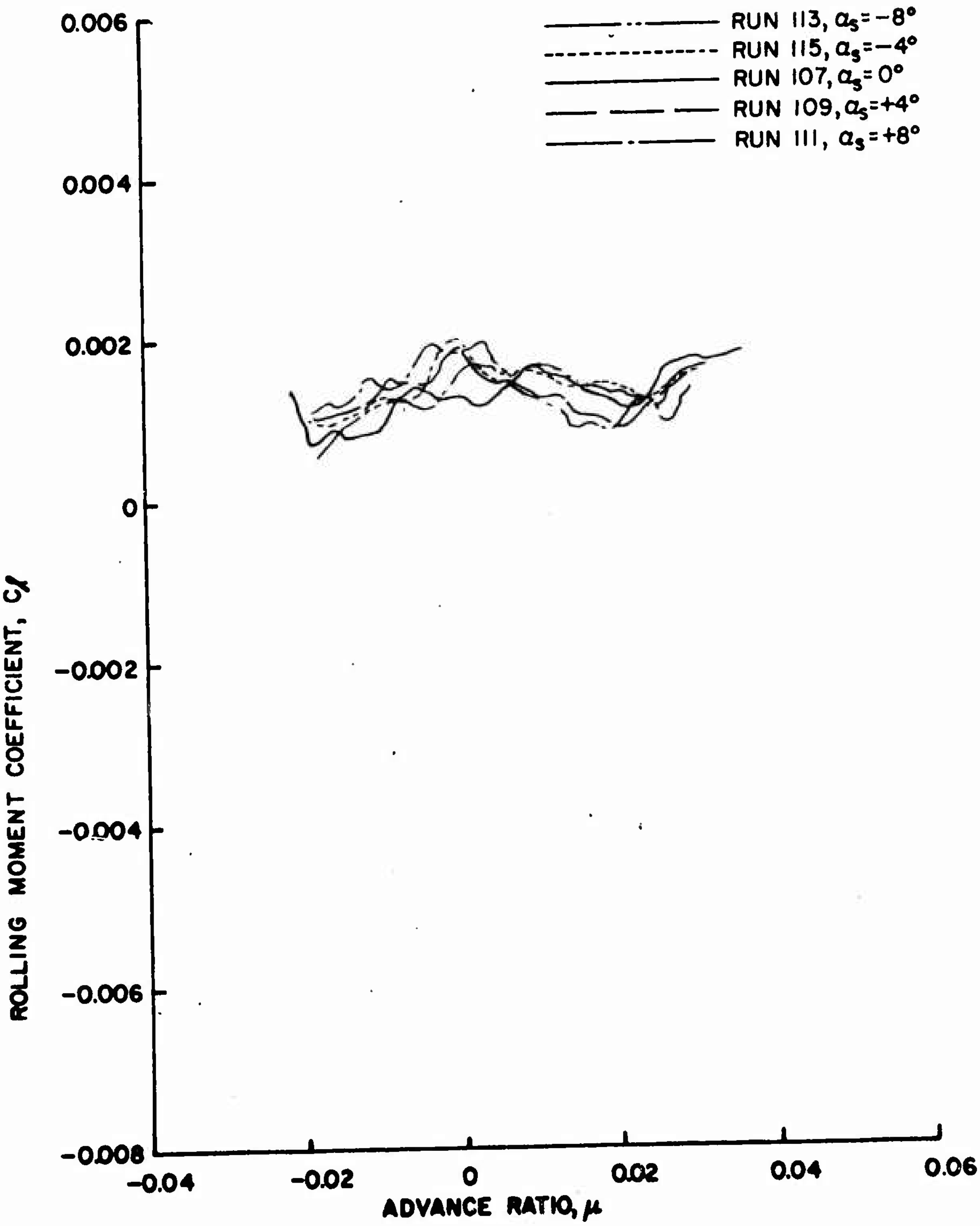

Figure 67c. Rotor Force and Moment Coefficients as Functions of Advance Ratio, $\theta_{.75R} = 10^\circ$, Wing Off, Fuselage Off, $\frac{h}{D} = 0.75$.

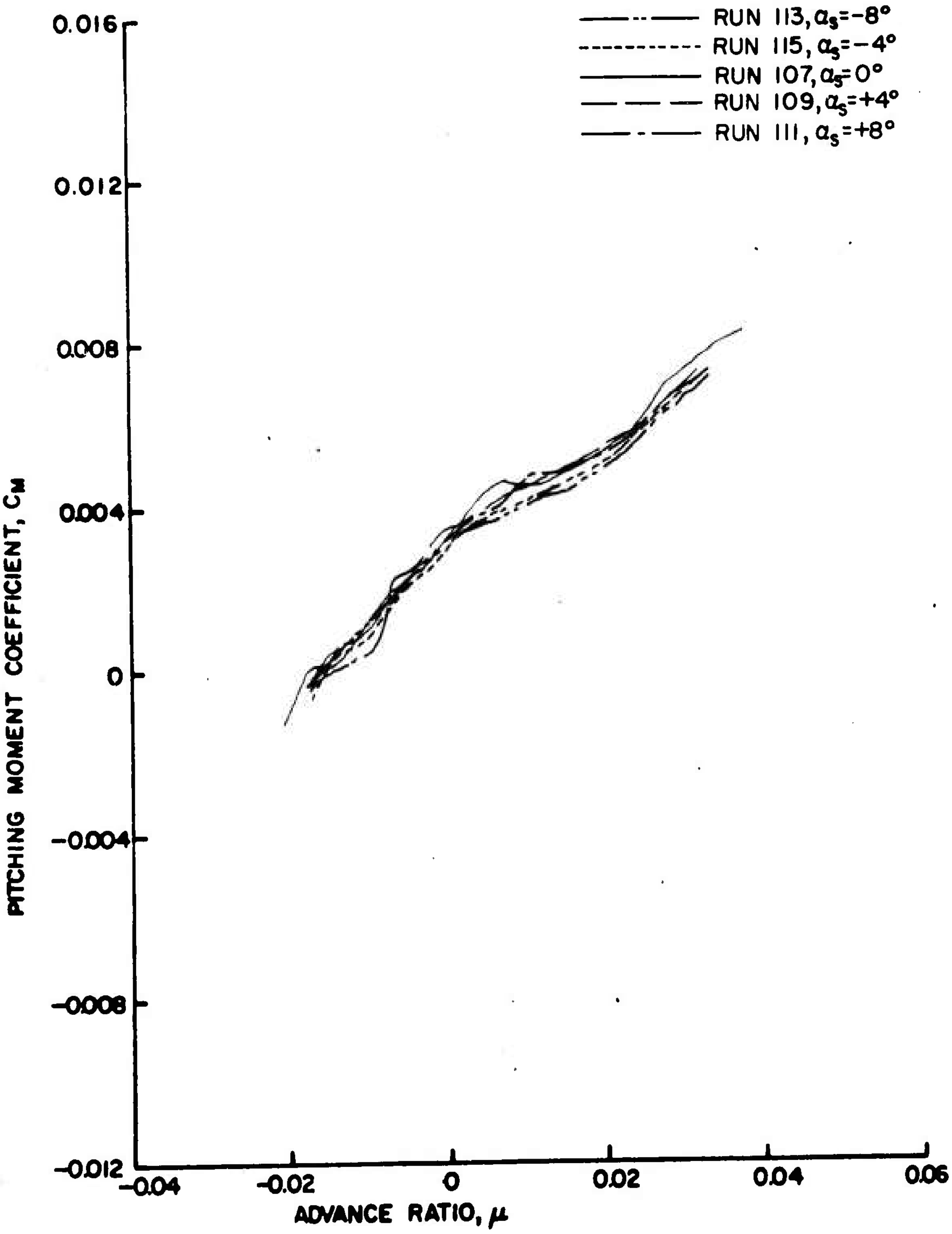

Figure 67d. Rotor Force and Moment Coefficients as Functions of Advance Ratio, $\theta_{.75R} = 10°$, Wing Off, Fuselage Off, $\frac{h}{D} = 0.75$.

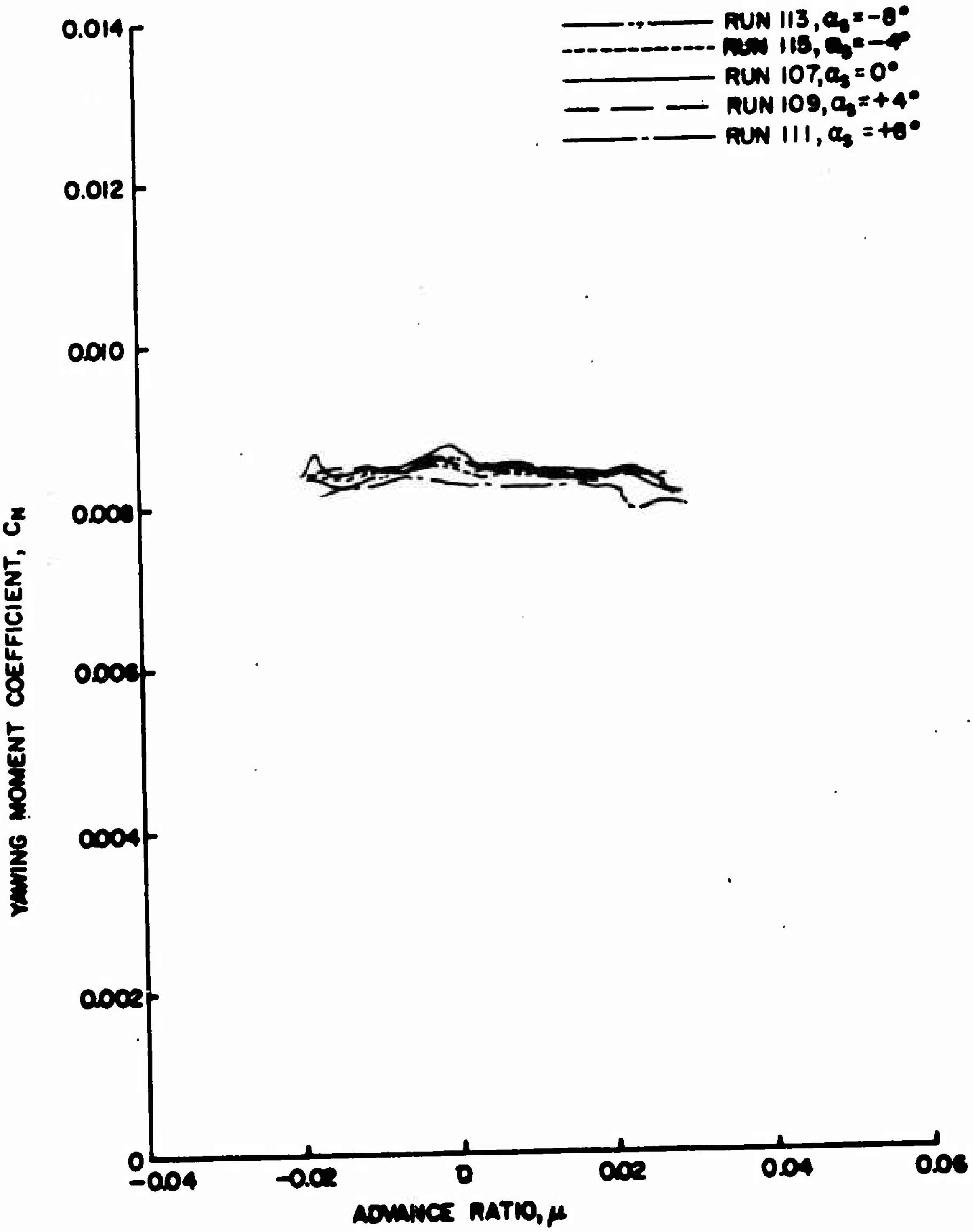

Figure 67e. Rotor Force and Moment Coefficients as Functions of Advance Ratio, $\theta_{.75R} = 10°$, Wing Off, Fuselage Off, $\frac{h}{D} = 0.75$.

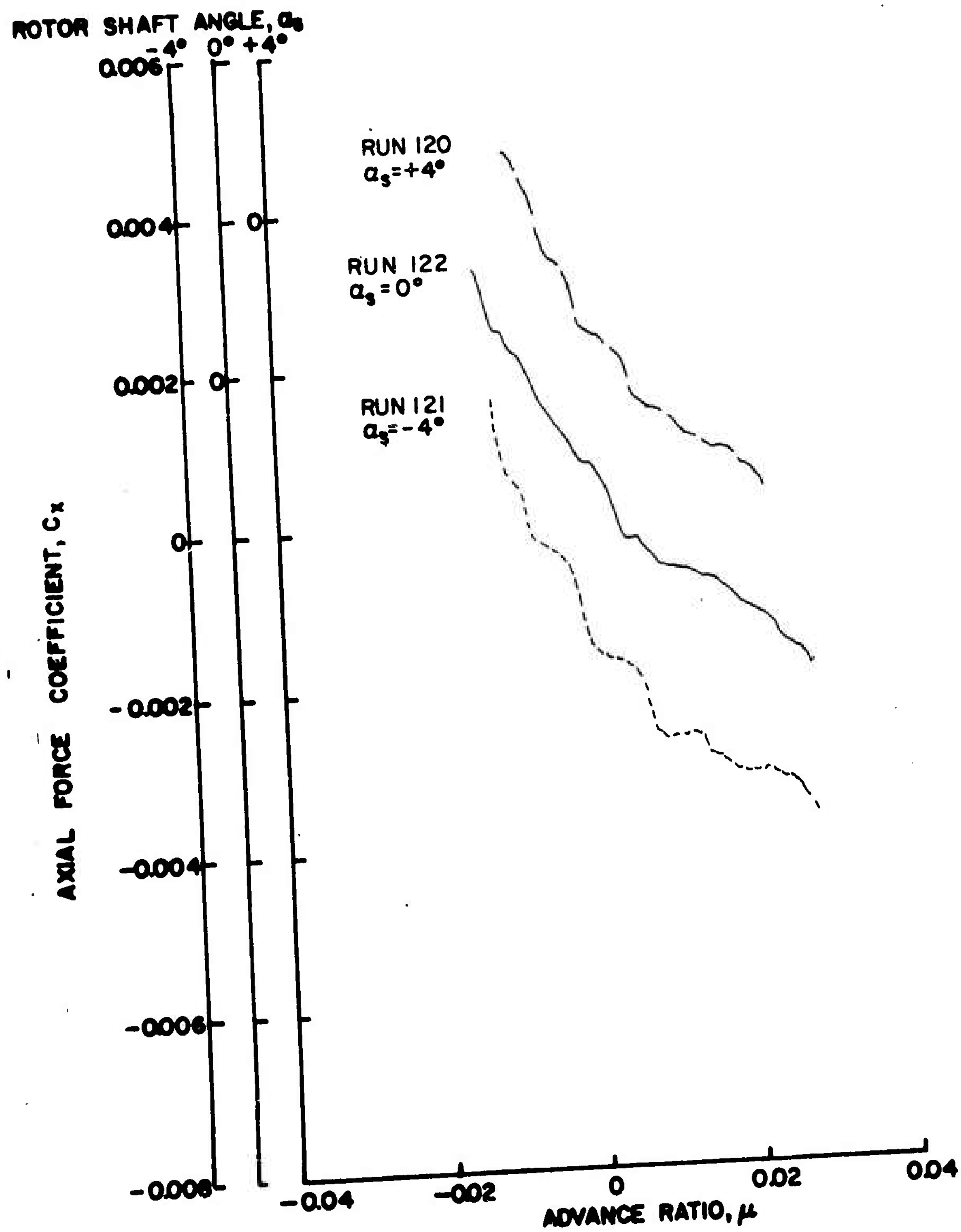

Figure 68a. Rotor Force and Moment Coefficients as Functions of Advance Ratio, $\theta_{.75R} = 12°$, Wing Off, Fuselage Off, $\frac{h}{D} = 0.75$.

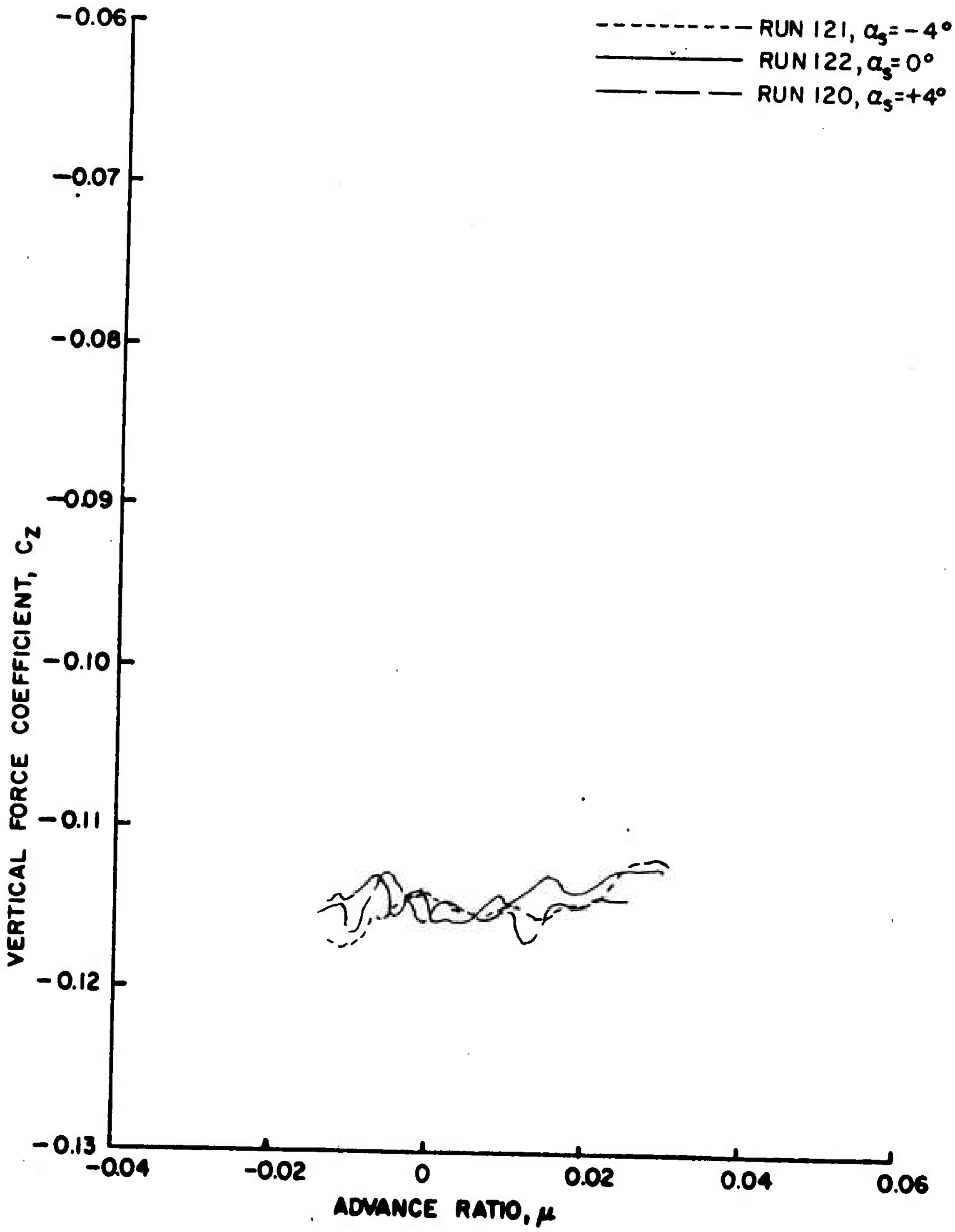

Figure 68b. Rotor Force and Moment Coefficients as Functions of Advance Ratio, $\theta_{.75R} = 12°$, Wing Off, Fuselage Off, $\frac{h}{D} = 0.75$.

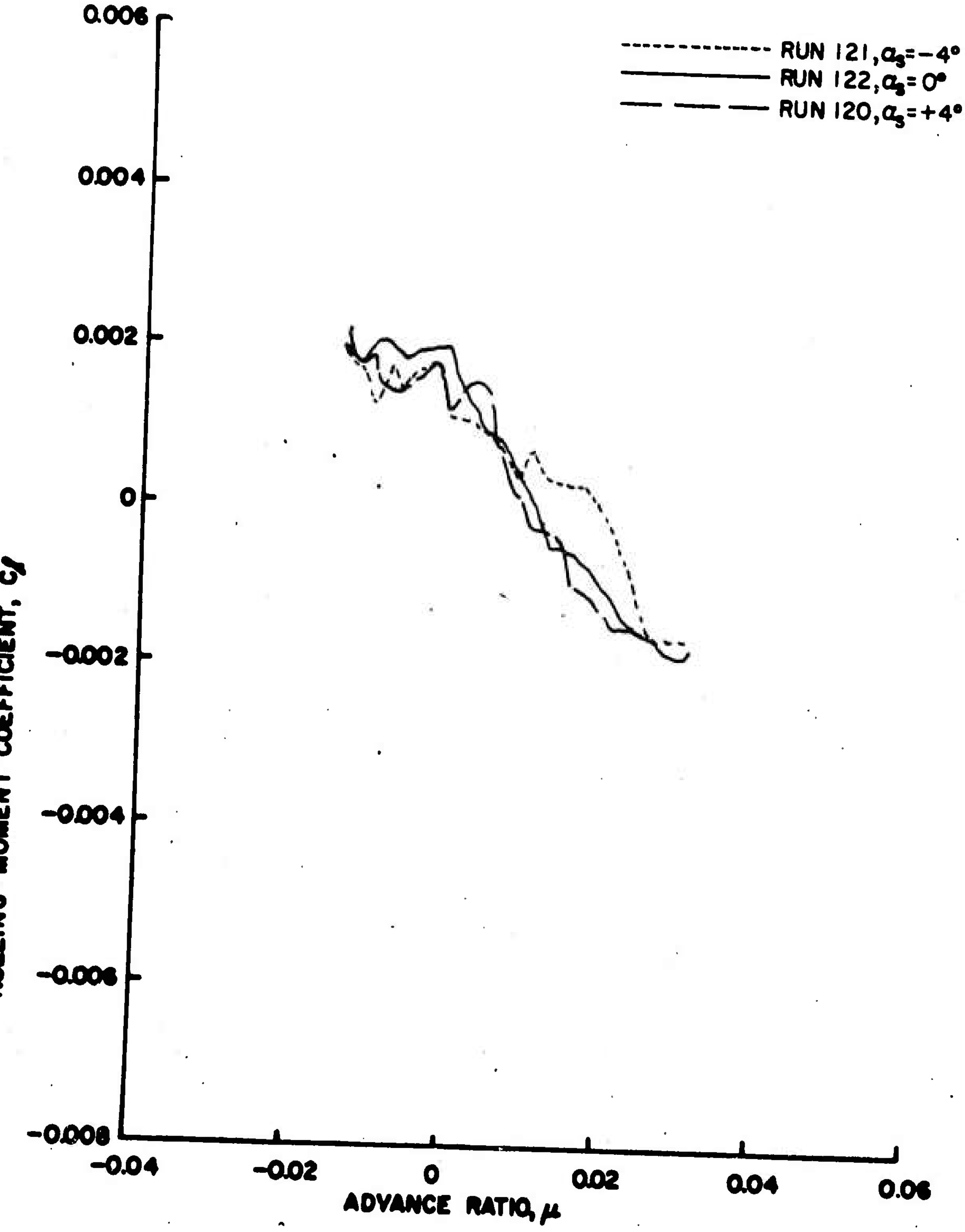

Figure 68c. Rotor Force and Moment Coefficients as Functions of Advance Ratio, $\theta_{.75R} = 12^\circ$, Wing Off, Fuselage Off, $\frac{h}{D} = 0.75$.

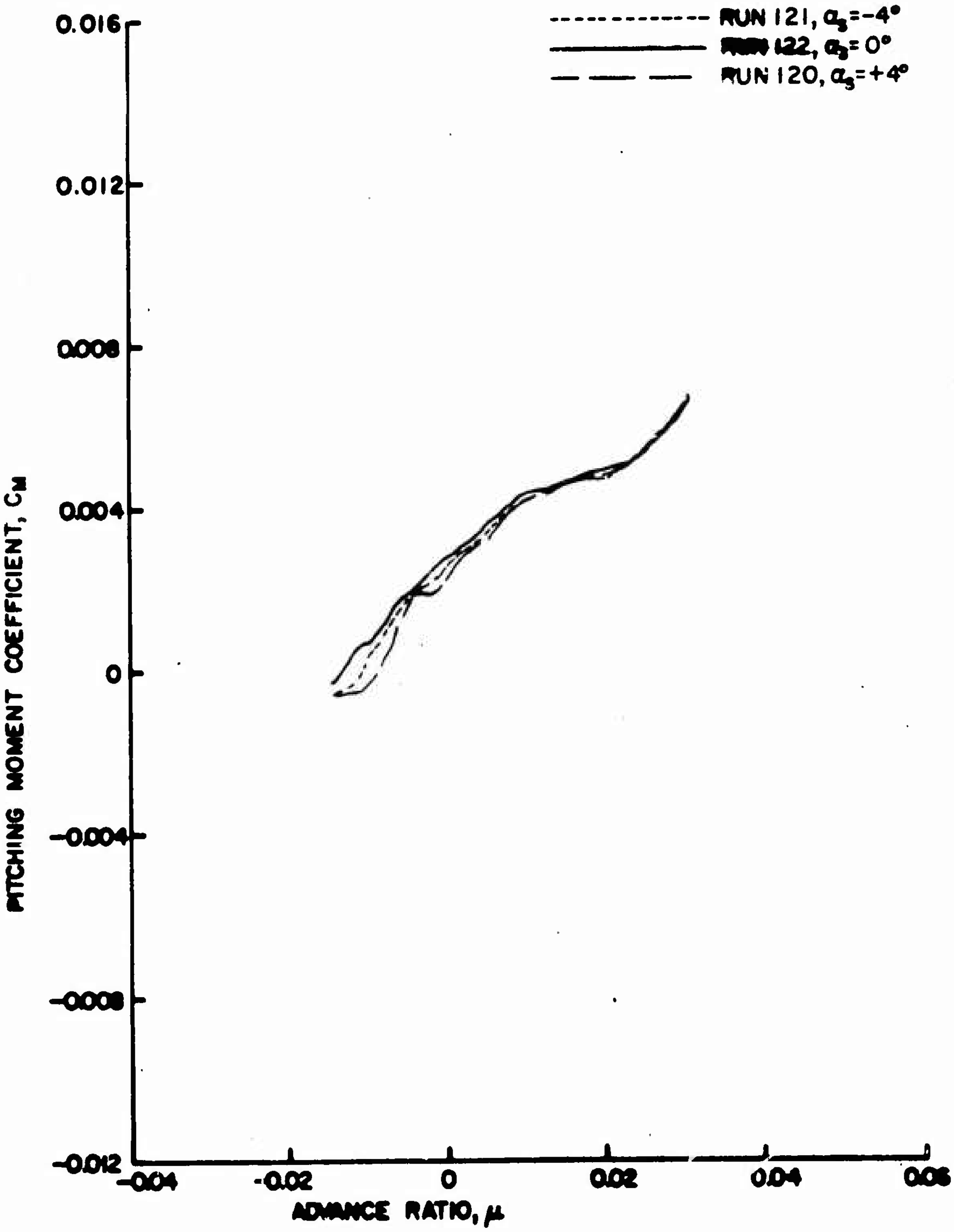

Figure 68d. Rotor Force and Moment Coefficients as Functions of Advance Ratio, $\theta_{.75R} = 12^\circ$, Wing Off, Fuselage Off, $\frac{h}{D} = 0.75$.

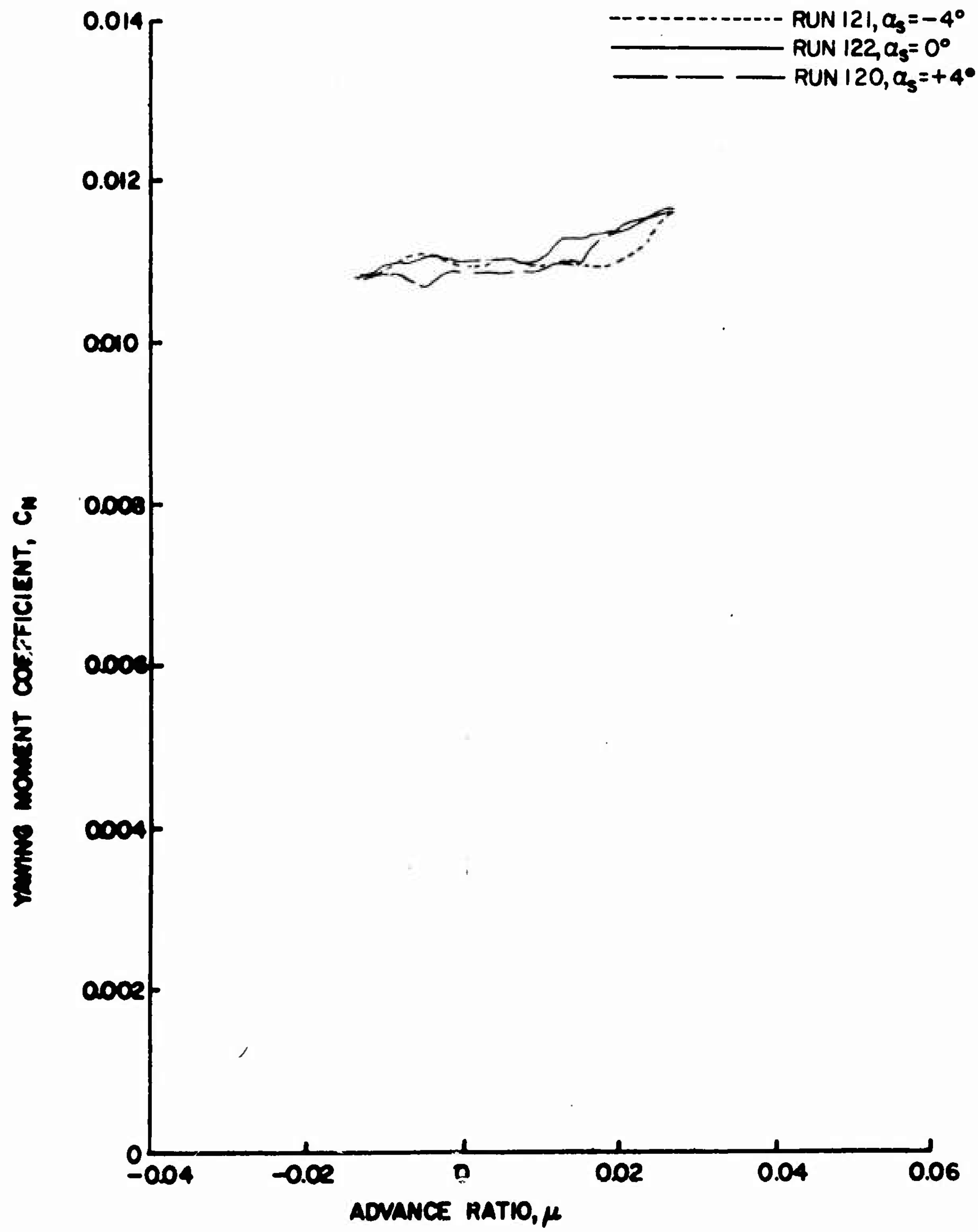

Figure 68e. Rotor Force and Moment Coefficients as Functions of Advance Ratio, $\theta_{.75R} = 12°$, Wing Off, Fuselage Off, $\frac{h}{D} = 0.75$.

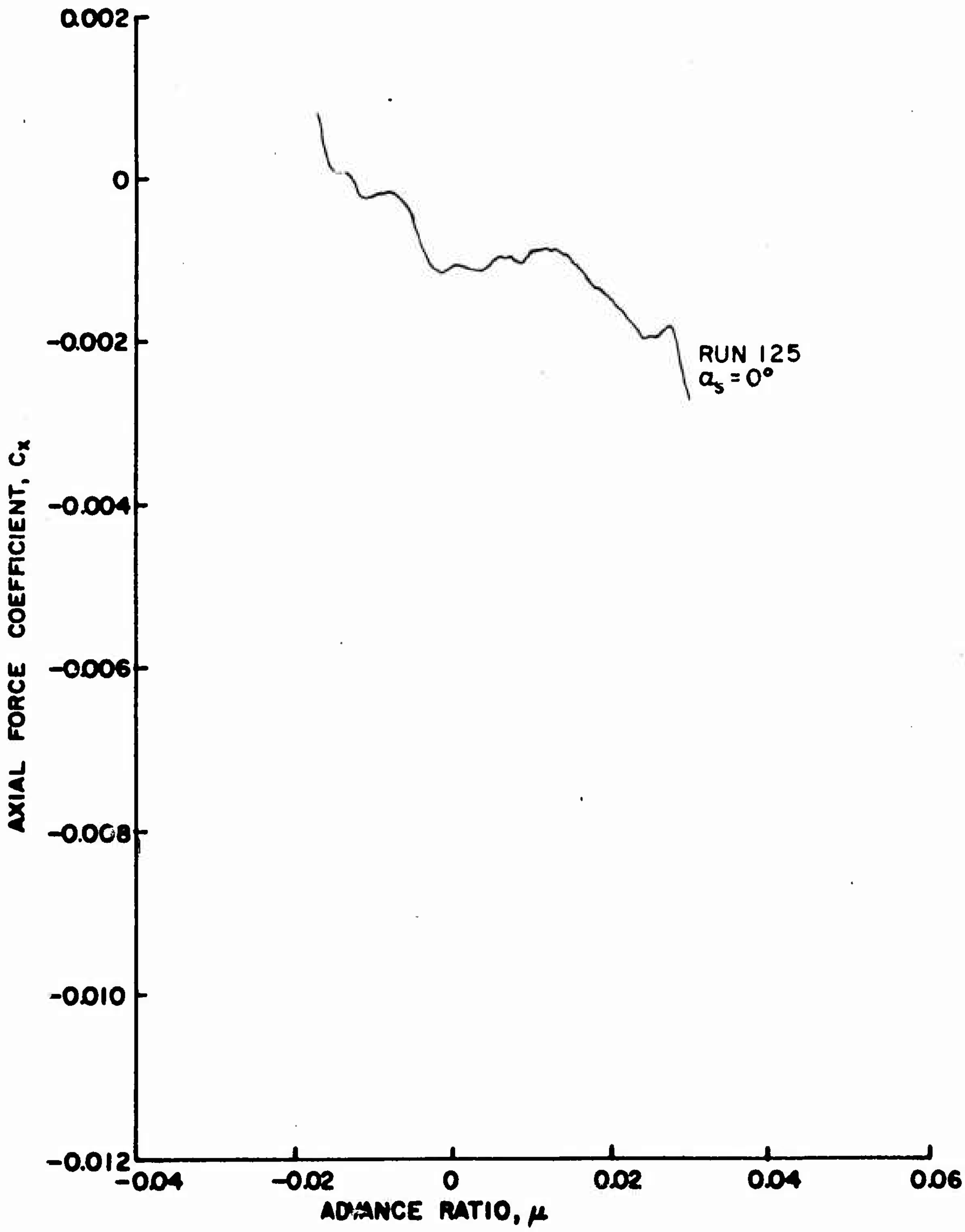

Figure 69a. Rotor Force and Moment Coefficients as Functions of Advance Ratio, $\theta_{.75R} = 8^{\circ}$, Wing Off, Fuselage On, $\frac{h}{D} = 0.75$.

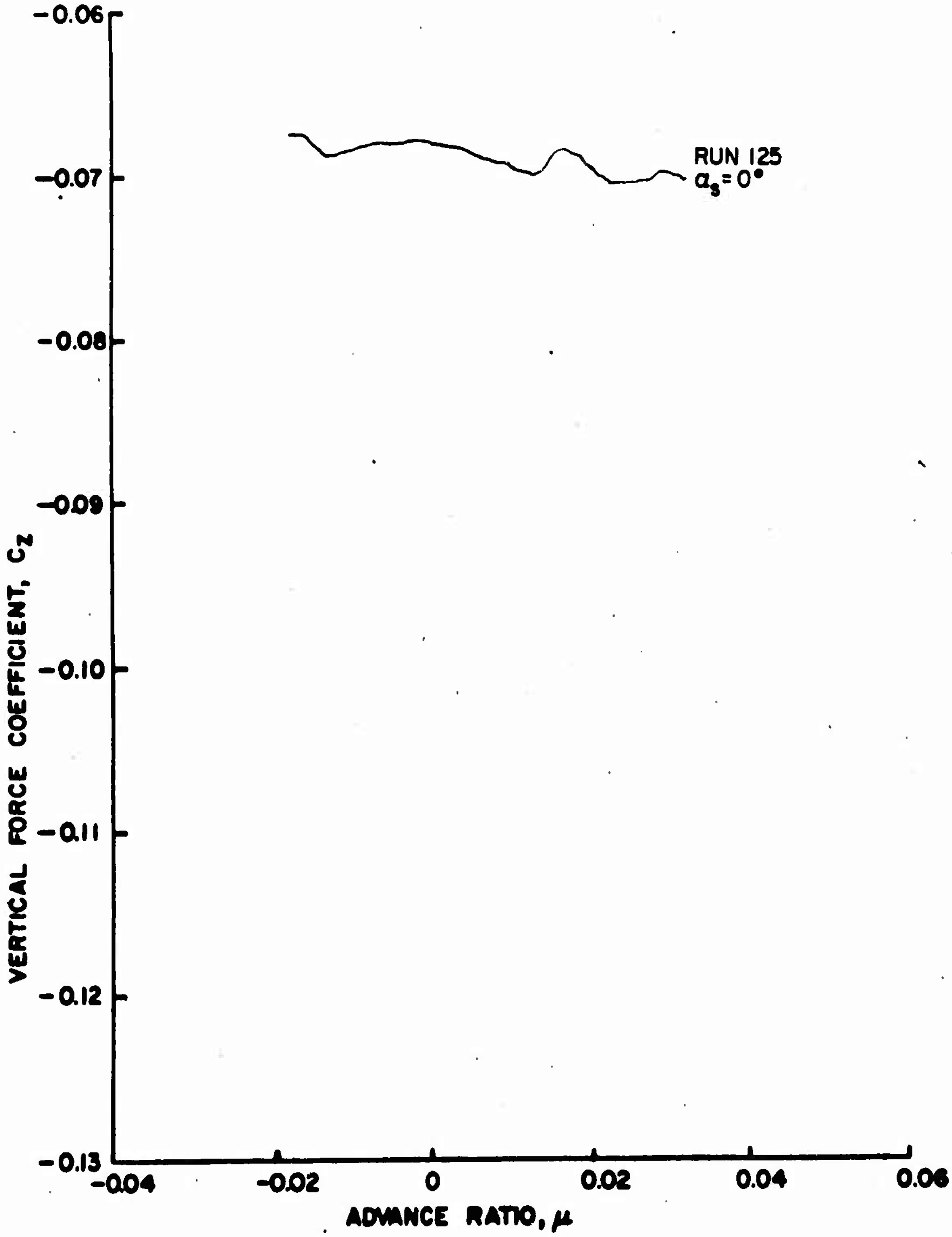

Figure 69b. Rotor Force and Moment Coefficients as Functions of Advance Ratio, $\theta_{.75R} = 8°$, Wing Off, Fuselage On, $\frac{h}{D} = 0.75$.

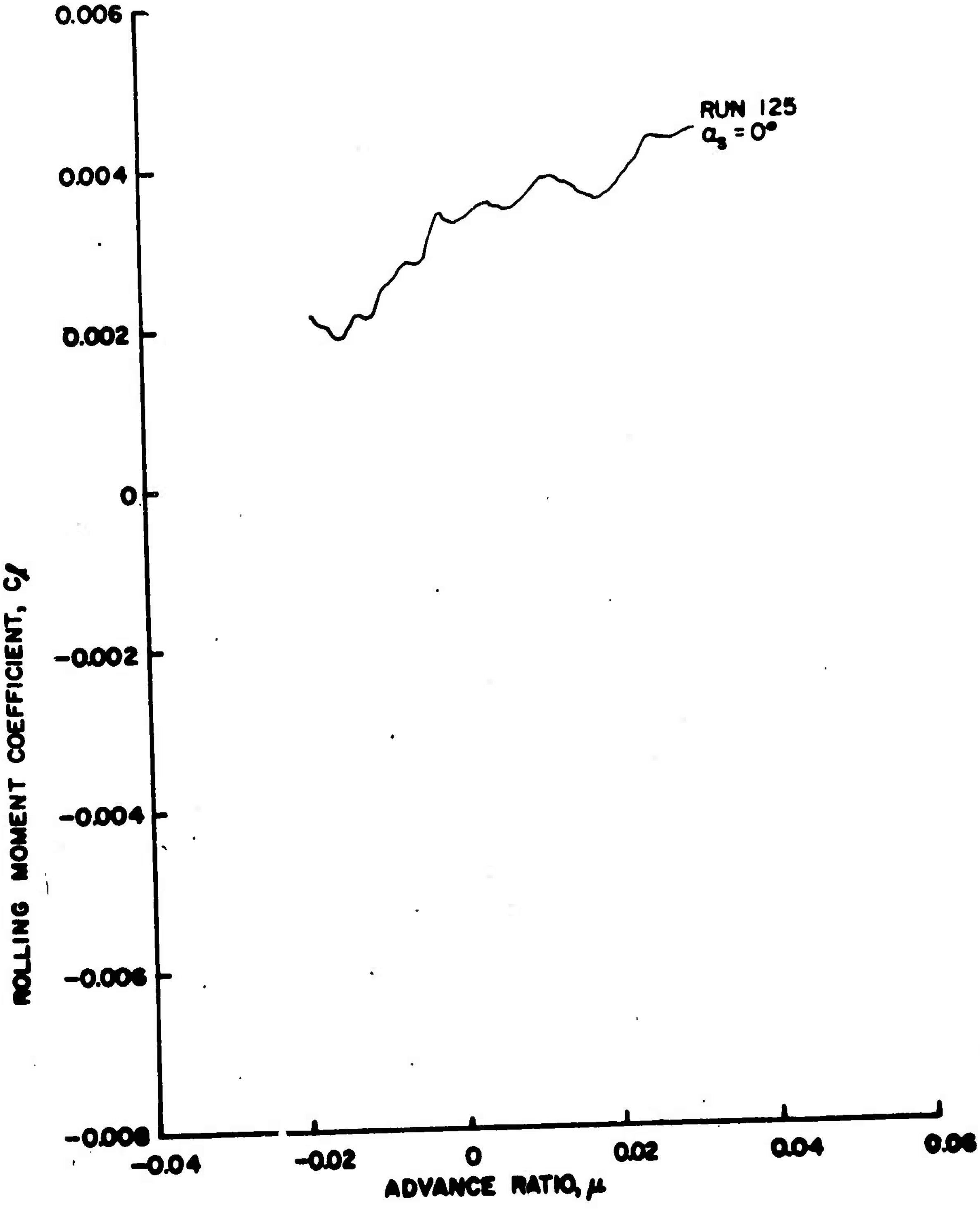

Figure 69c. Rotor Force and Moment Coefficients as Functions of Advance Ratio, $\theta_{.75R} = 8°$, Wing Off, Fuselage On, $\frac{h}{D} = 0.75$.

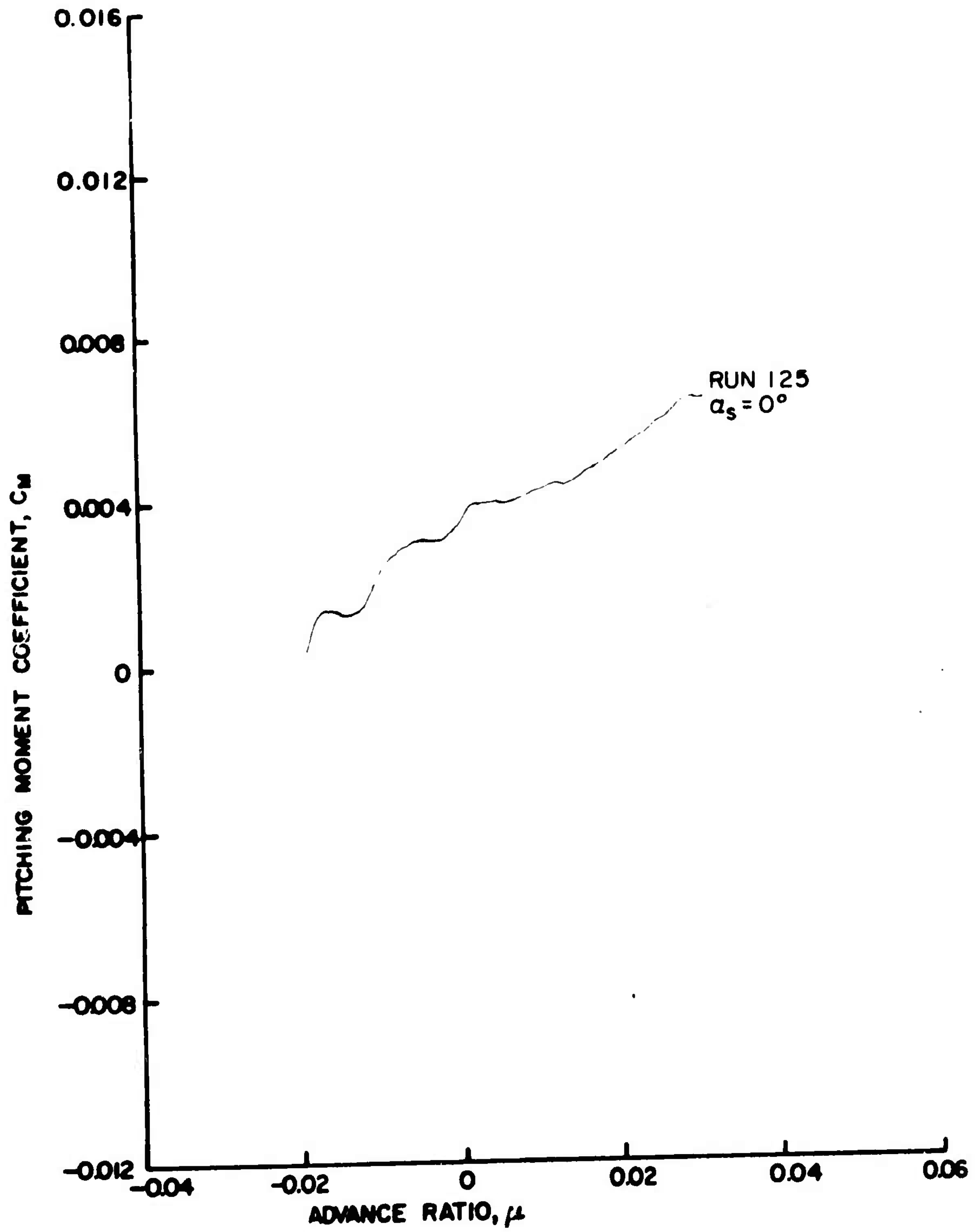

Figure 69d. Rotor Force and Moment Coefficients as Functions of Advance Ratio, $\theta_{.75R} = 8°$, Wing Off, Fuselage On, $\frac{h}{D} = 0.75$.

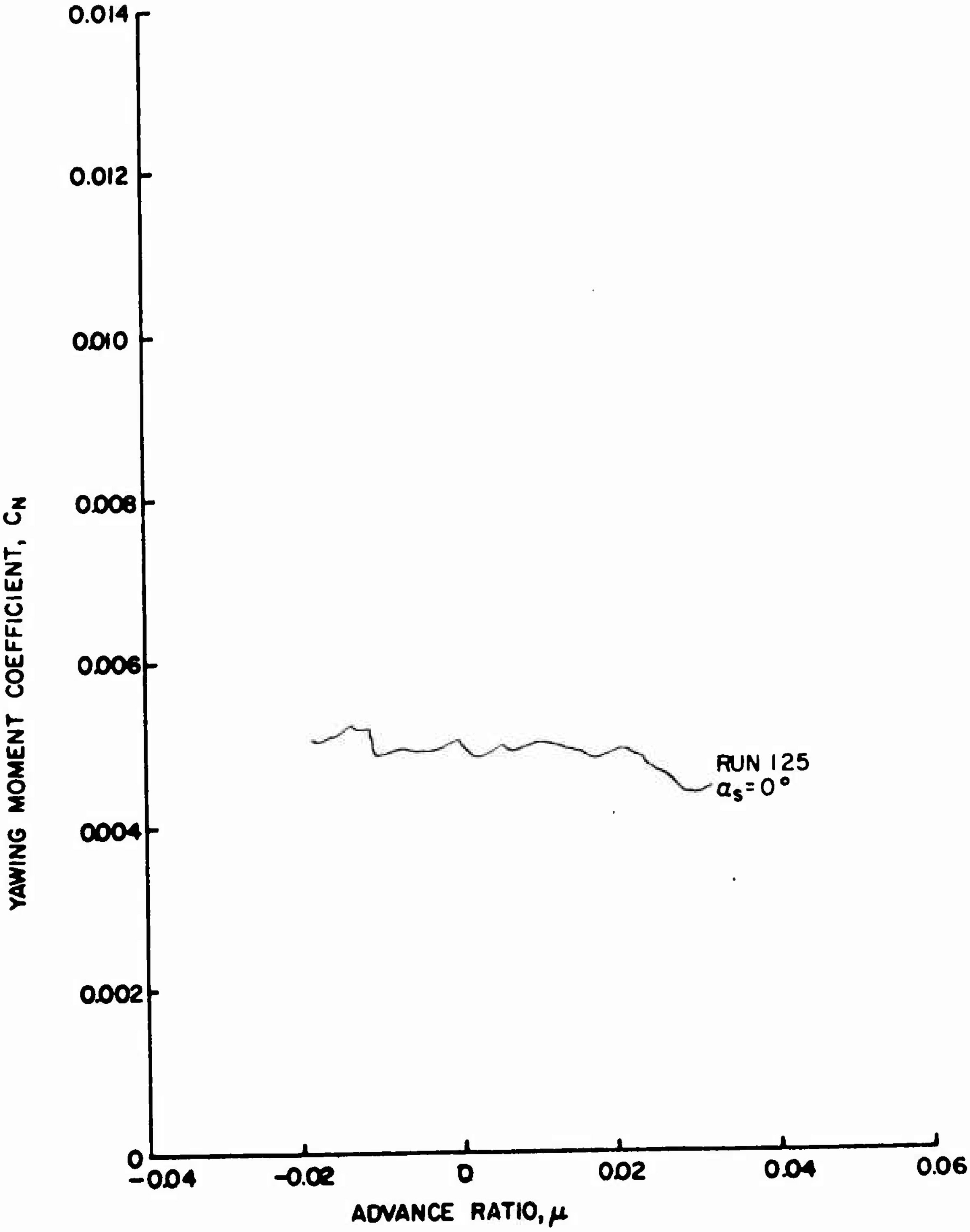

Figure 69e. Rotor Force and Moment Coefficients as Functions of Advance Ratio, $\theta_{.75R} = 8°$, Wing Off, Fuselage On, $\frac{h}{D} = 0.75$.

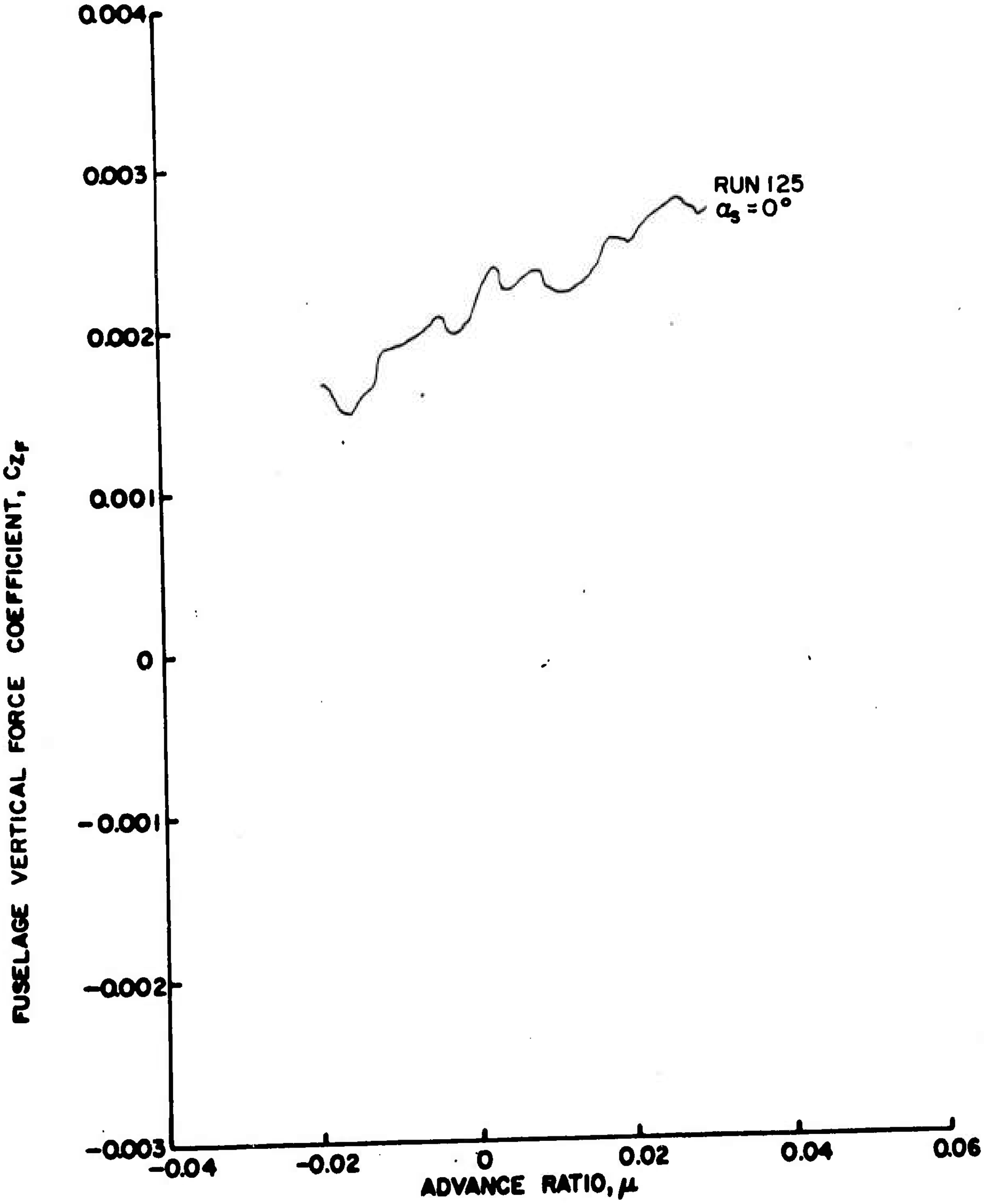

Figure 70a. Fuselage Vertical Force and Pitching Moment Coefficients as Functions of Advance Ratio, $\theta_{.75R} = 8°$, Wing Off, Fuselage On, $\frac{h}{D} = 0.75$.

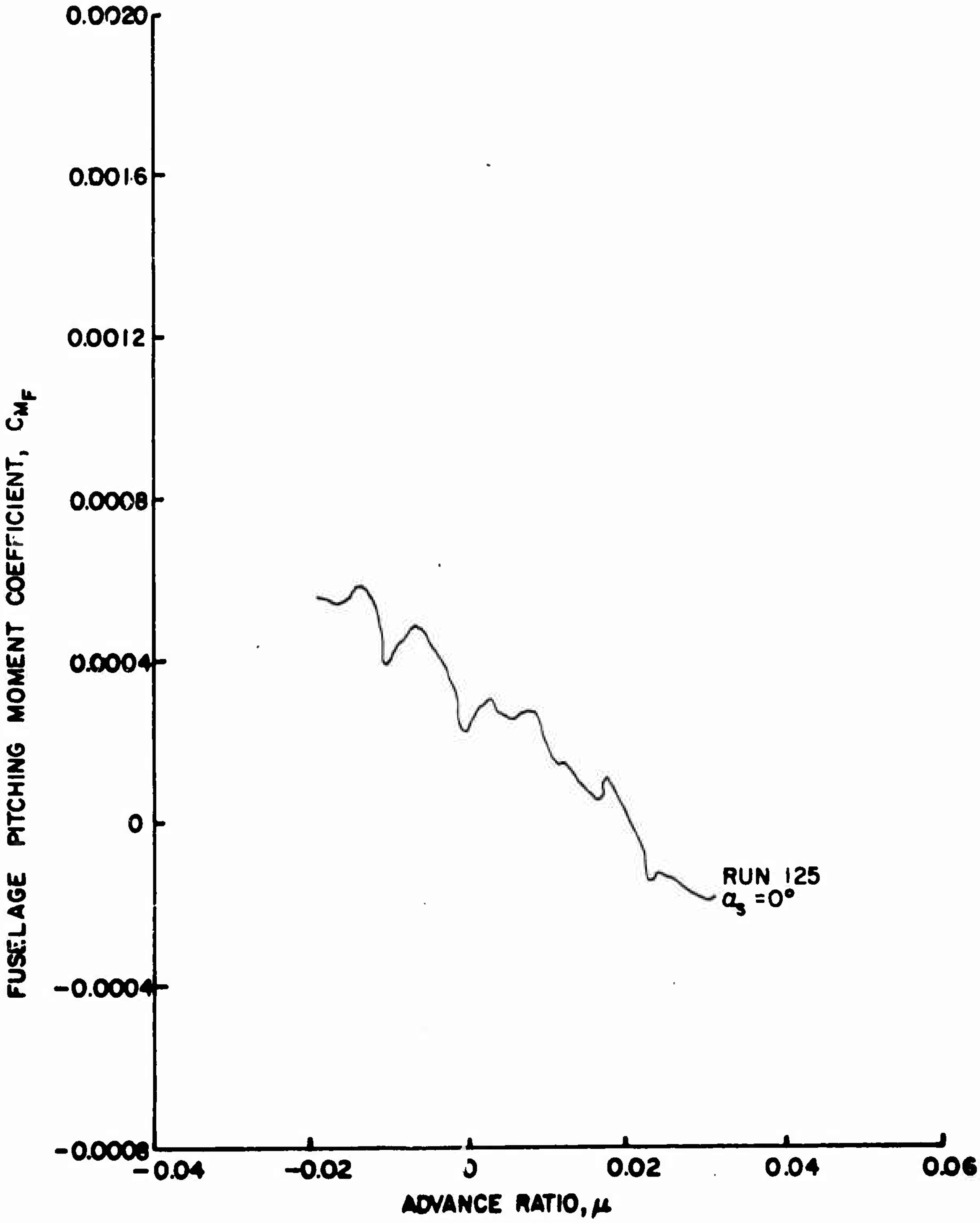

Figure 70b. Fuselage Vertical Force and Pitching Moment Coefficients as Functions of Advance Ratio, $\theta_{.75R} = 8°$, Wing Off, Fuselage On, $\frac{h}{D} = 0.75$.

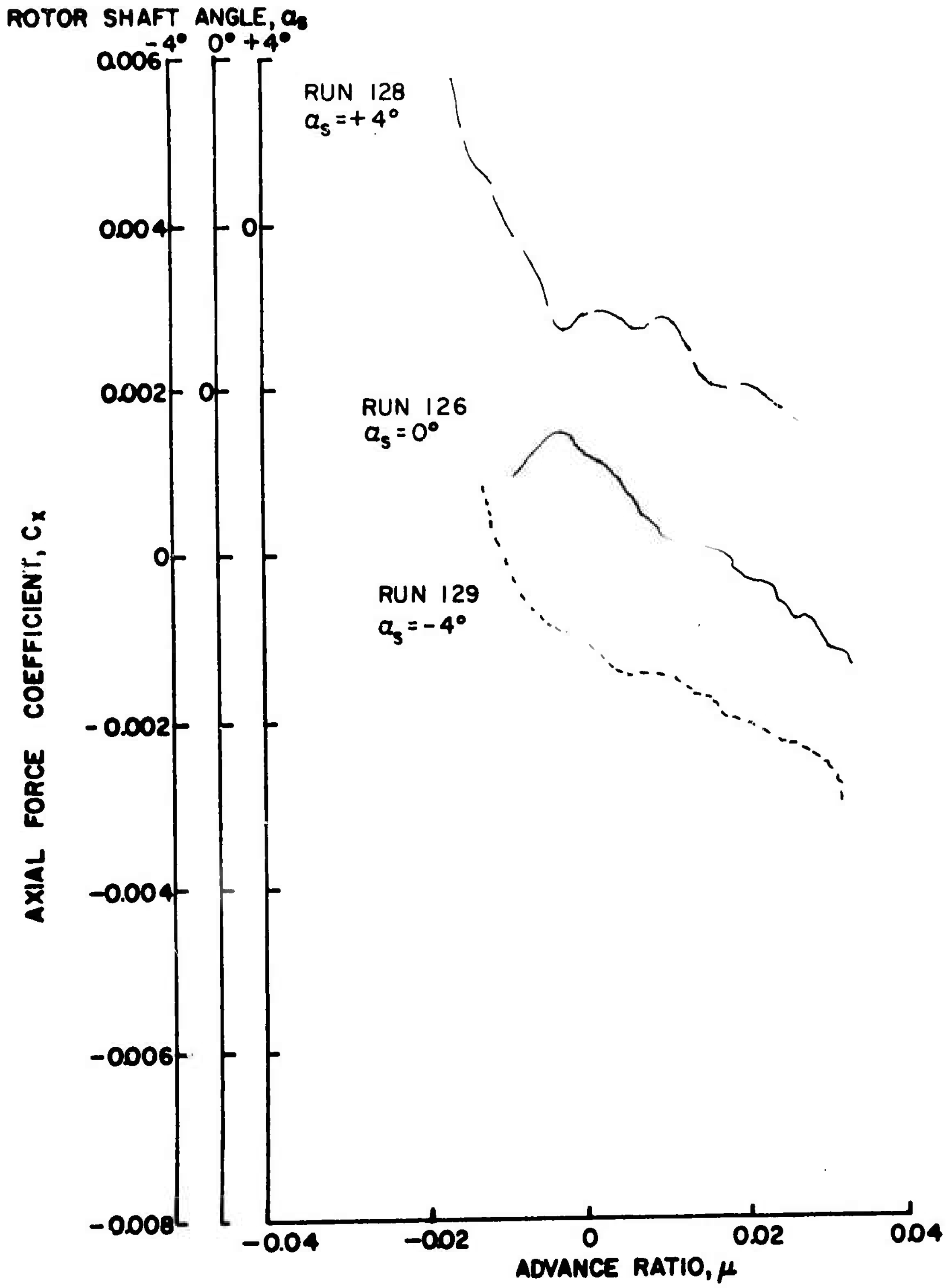

Figure 71a. Rotor Force and Moment Coefficients as Functions of Advance Ratio, $\theta_{.75R} = 10^{\circ}$, Wing Off, Fuselage On, $\frac{h}{D} = 0.75$.

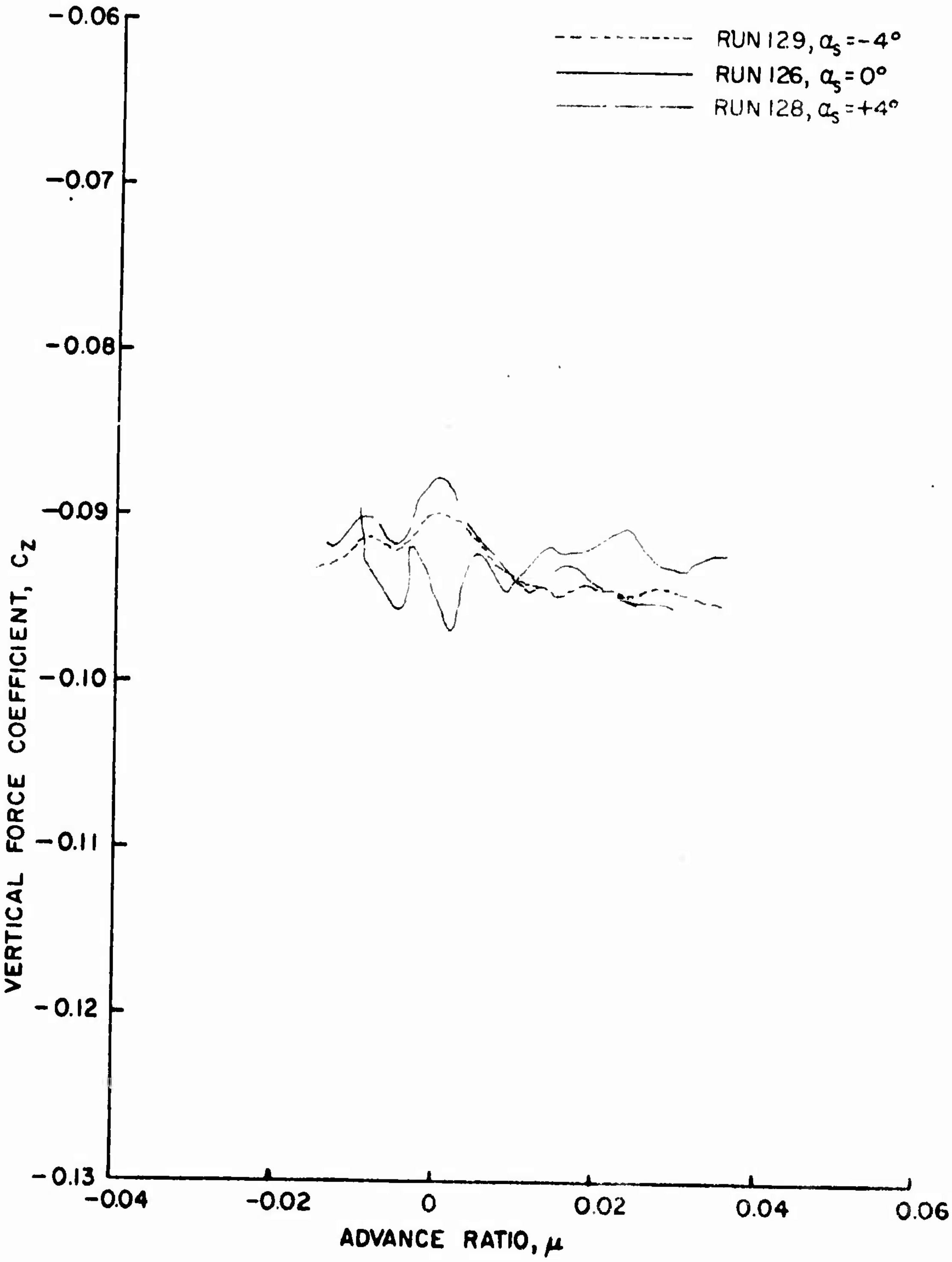

Figure 71b. Rotor Force and Moment Coefficients as Functions of Advance Ratio, $\theta_{.75R} = 10°$. Wing Off, Fuselage On, $\frac{h}{D} = 0.75$.

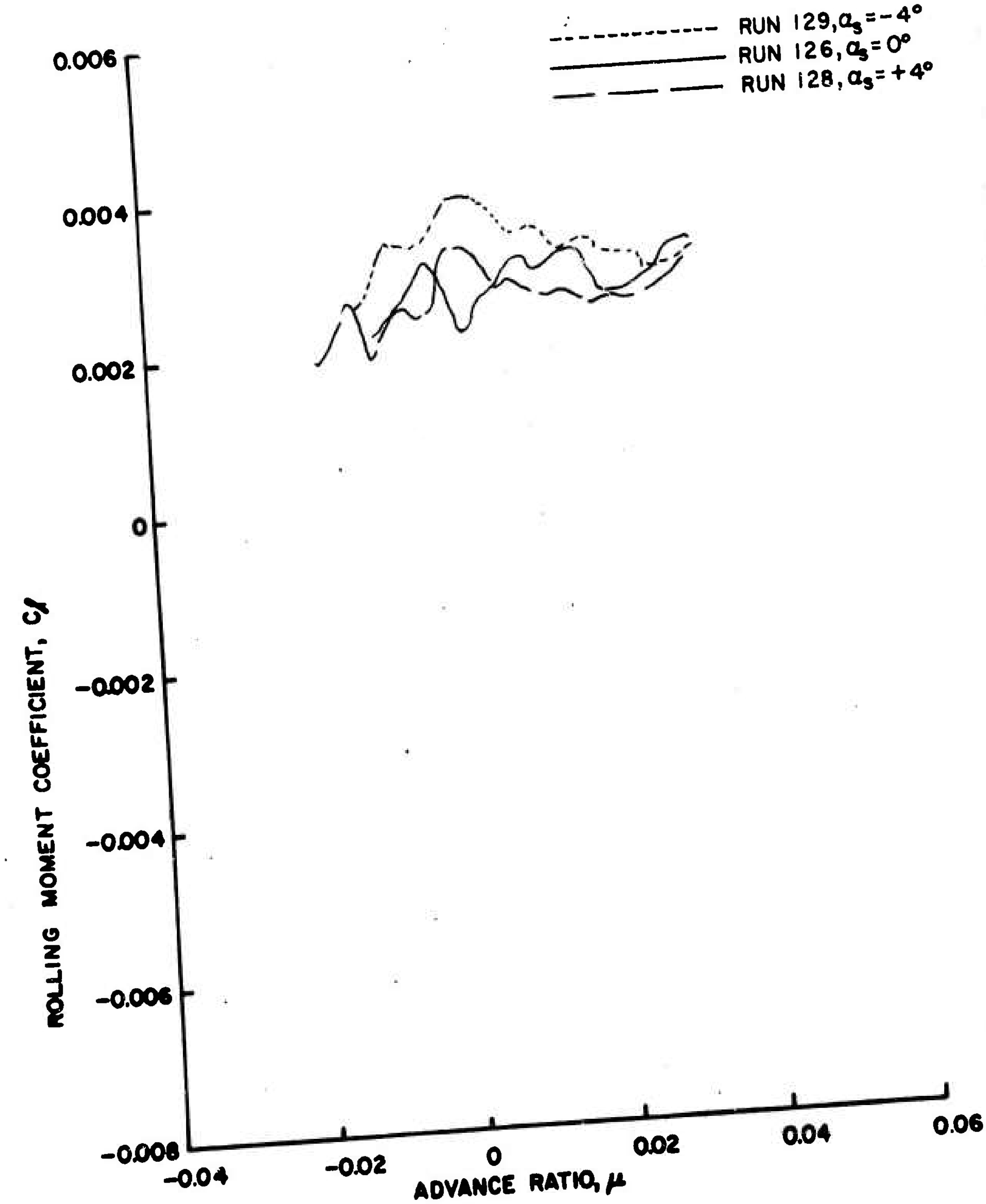

Figure 71c. Rotor Force and Moment Coefficients as Functions of Advance Ratio, $\theta_{.75R} \doteq 10^\circ$, Wing Off, Fuselage On, $\frac{h}{D} = 0.75$.

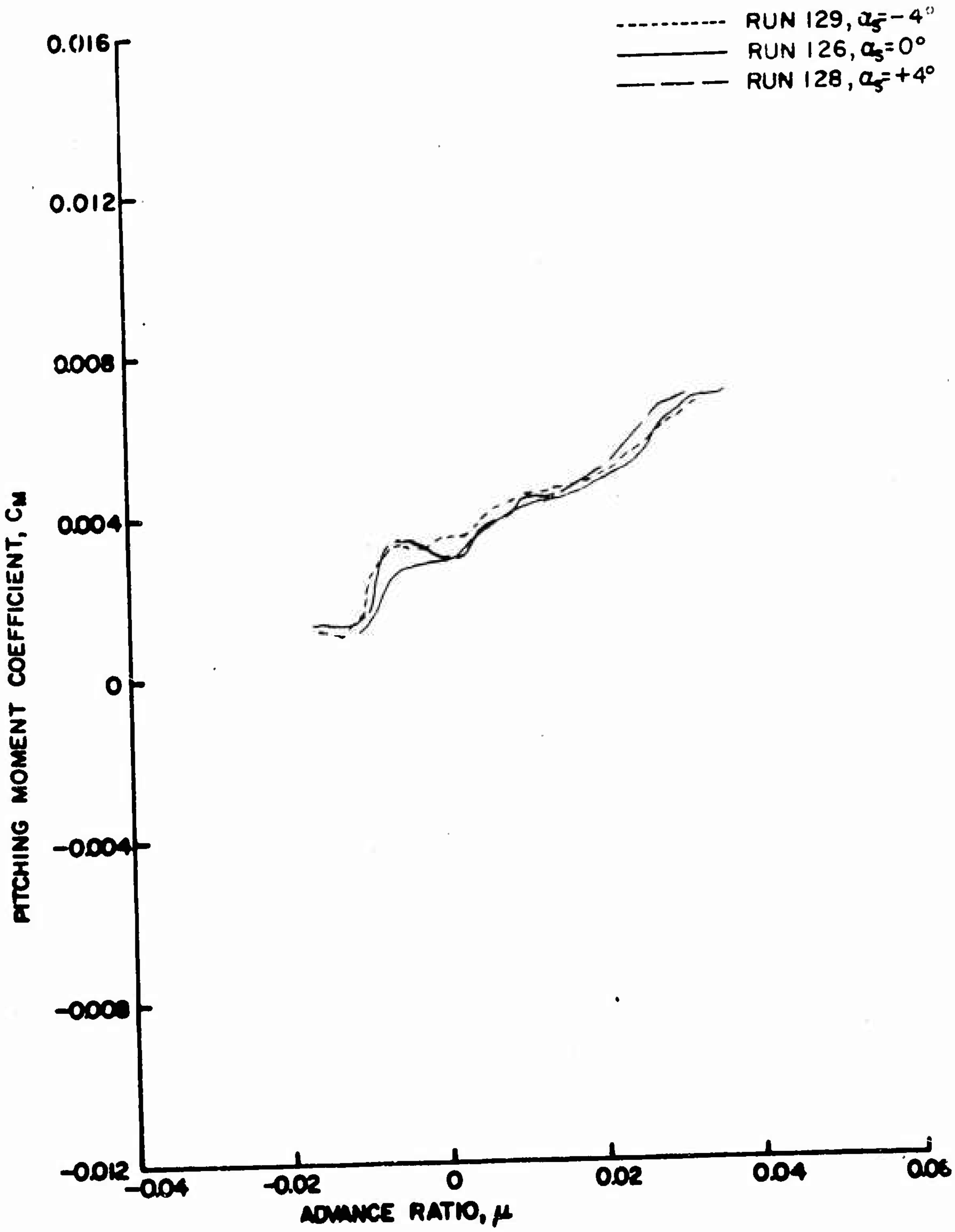

Figure 71d. Rotor Force and Moment Coefficients as Functions of Advance Ratio, $\theta_{.75R} = 10°$, Wing Off, Fuselage On, $\frac{h}{D} = 0.75$.

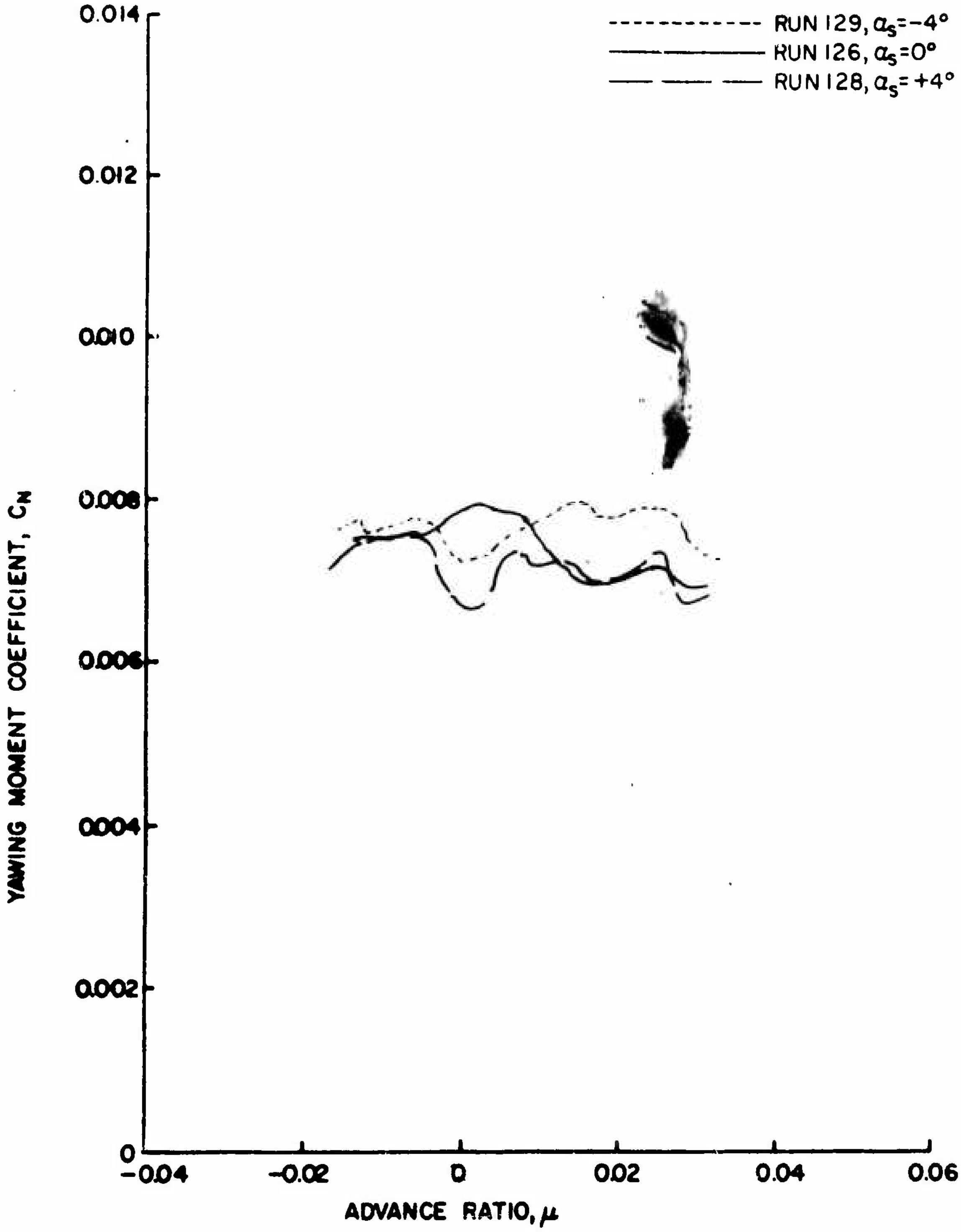

Figure 71e. Rotor Force and Moment Coefficients as Functions of Advance Ratio, $\theta_{.75R} = 10^{\circ}$, Wing Off, Fuselage On, $\frac{h}{D} = 0.75$.

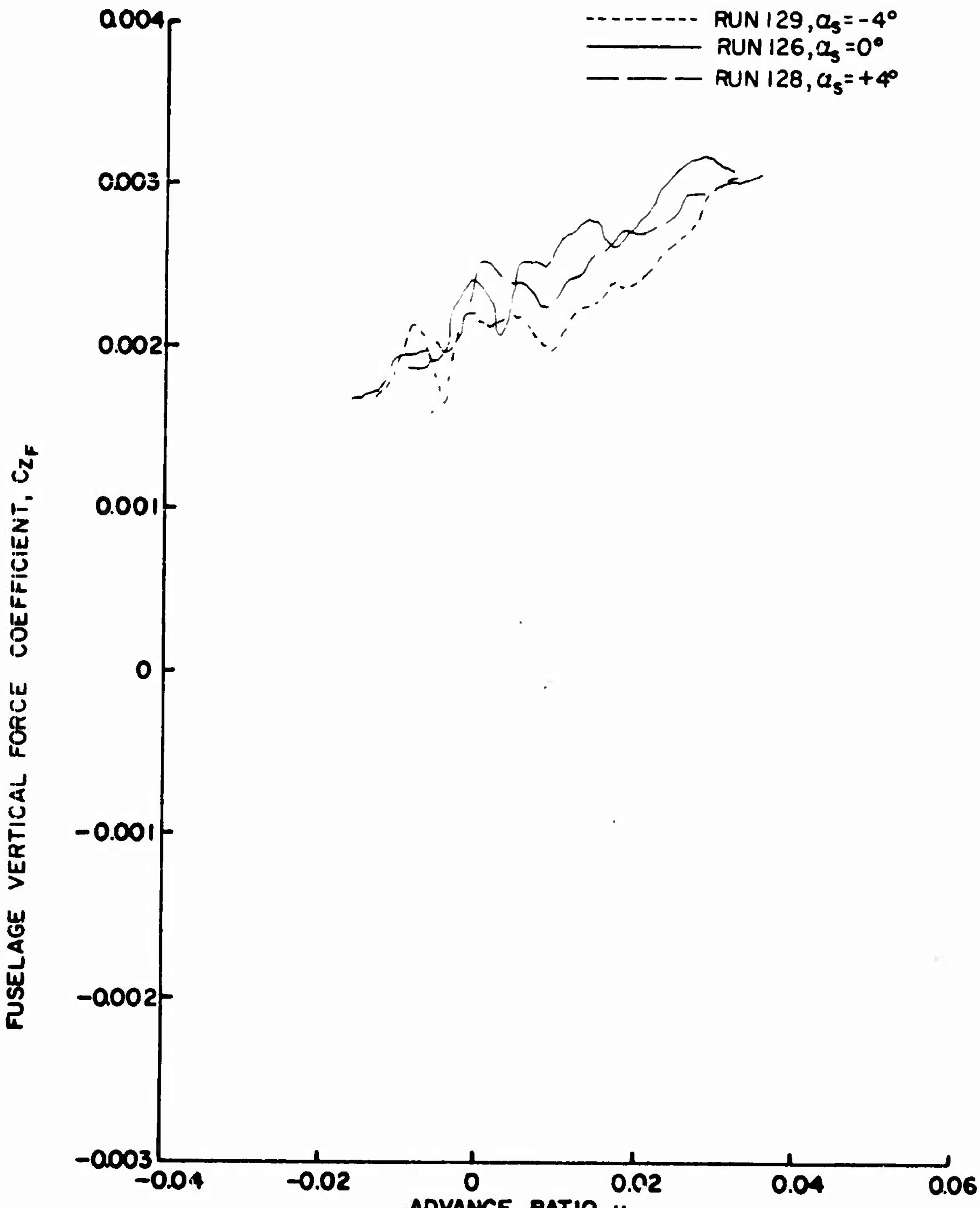

Figure 72a. Fuselage Vertical Force and Pitching Moment Coefficients as Functions of Advance Ratio, $\theta_{.75R} = 10°$, Wing Off, Fuselage On, $\frac{x}{R}$ = 0. .

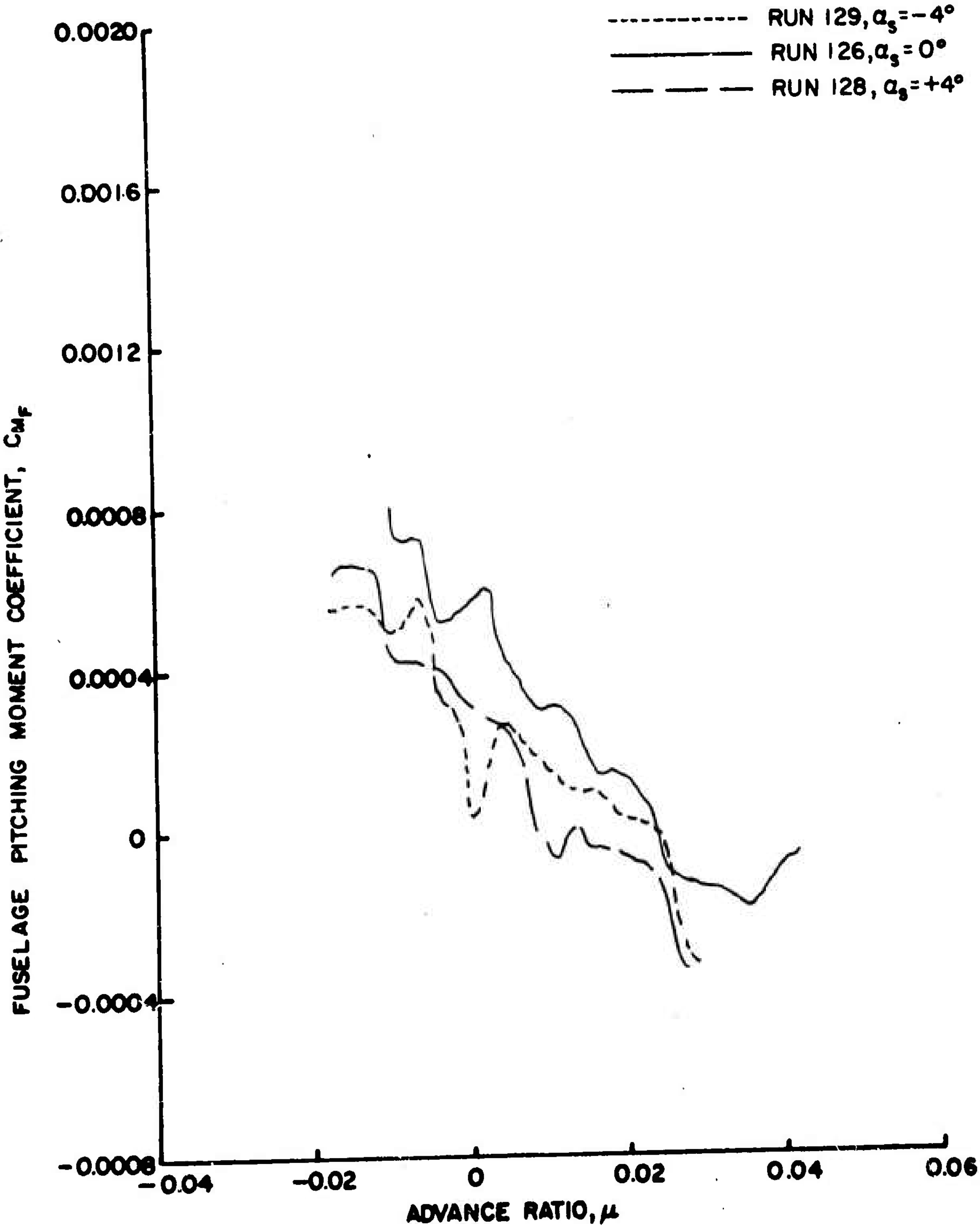

Figure 72b. Fuselage Vertical Force and Pitching Moment Coefficients as Functions of Advance Ratio, $\theta_{.75R} = 10°$, Wing Off, Fuselage On, $\frac{h}{D} = 0.75$.

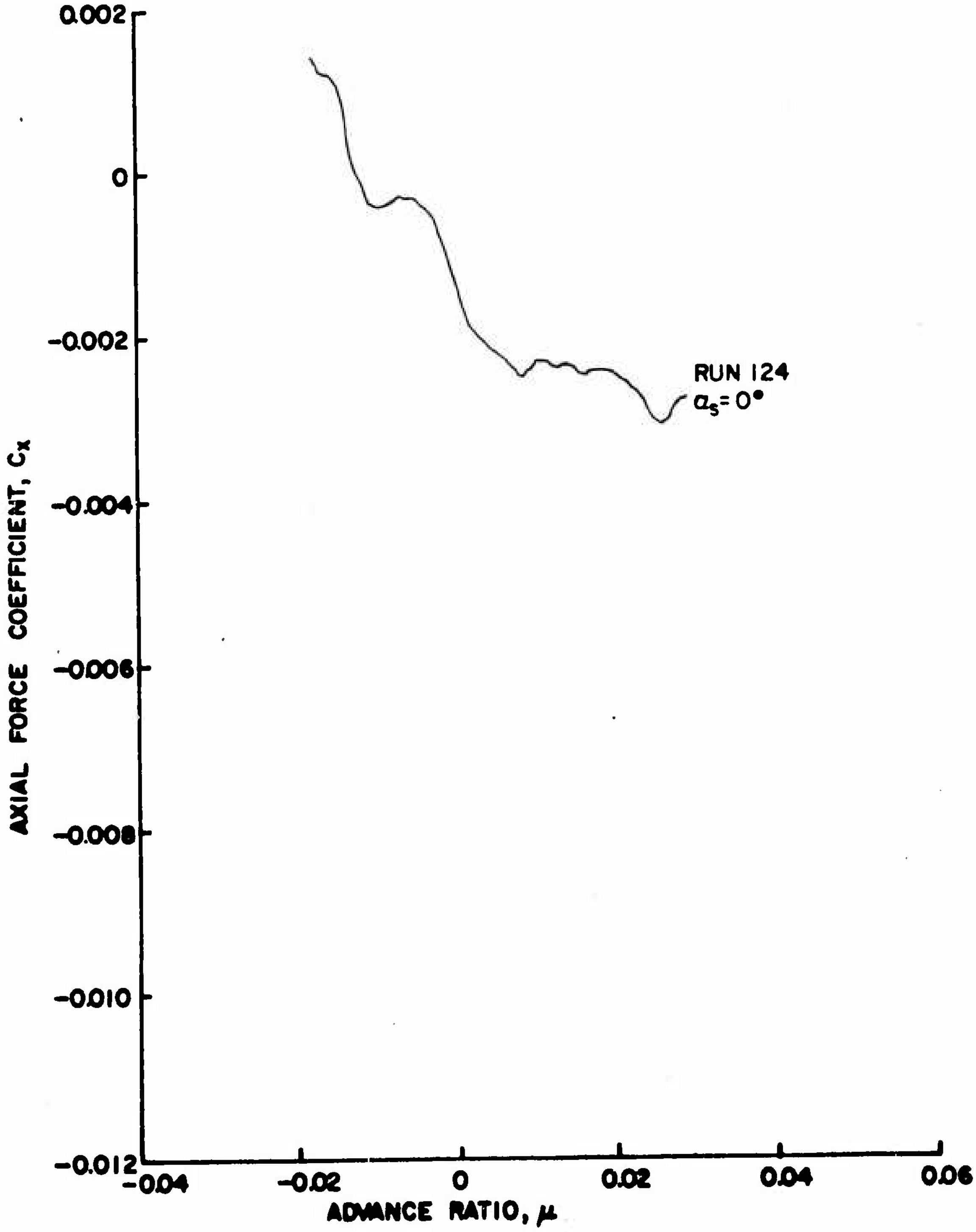

Figure 73a. Rotor Force and Moment Coefficients as Functions of Advance Ratio, $\theta_{.75R} = 12^\circ$, Wing Off, Fuselage On, $\frac{h}{D} = 0.75$.

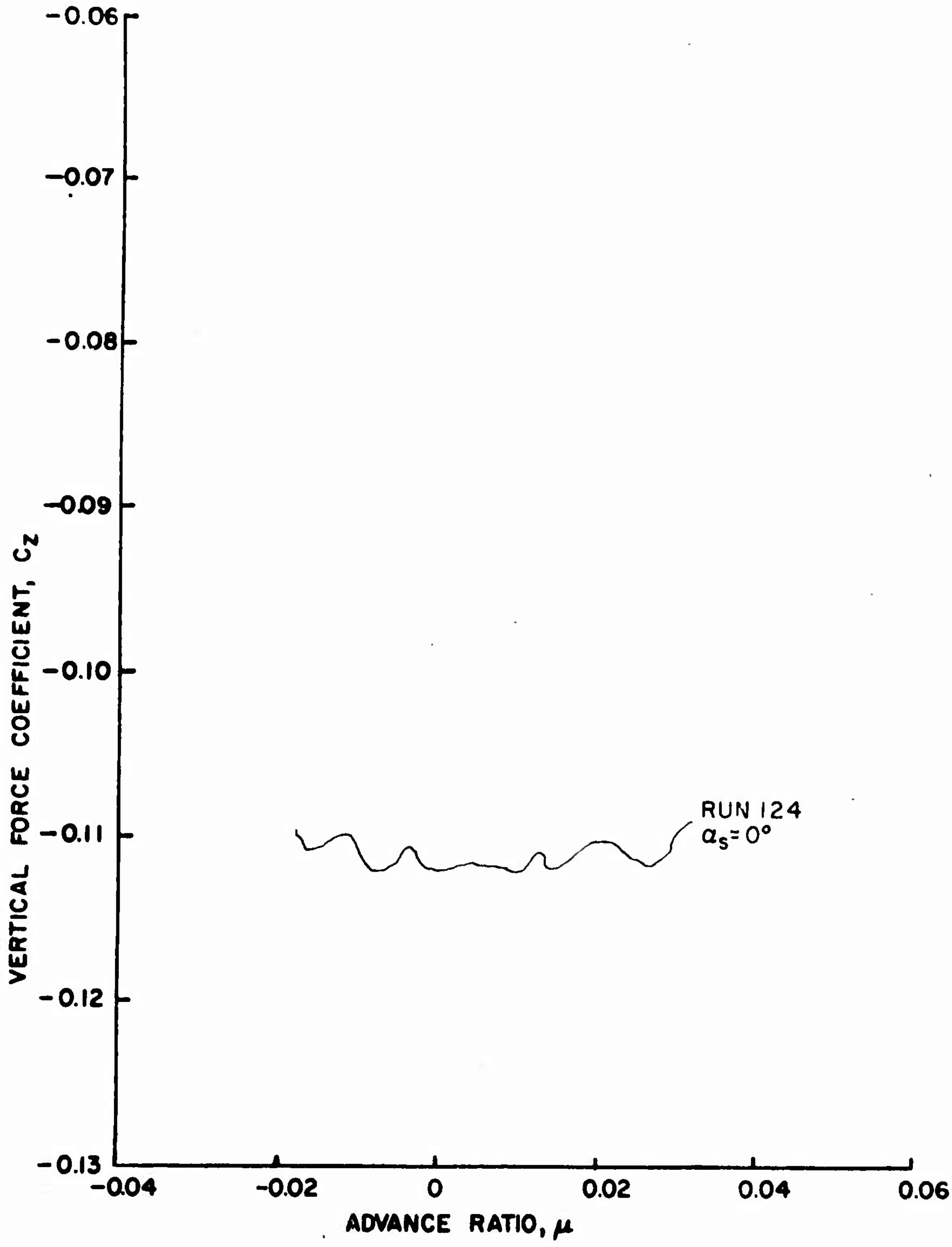

Figure 73b. Rotor Force and Moment Coefficients as Functions of Advance Ratio, $\theta_{.75R} = 12°$, Wing Off, Fuselage On, $\frac{h}{D} = 0.75$.

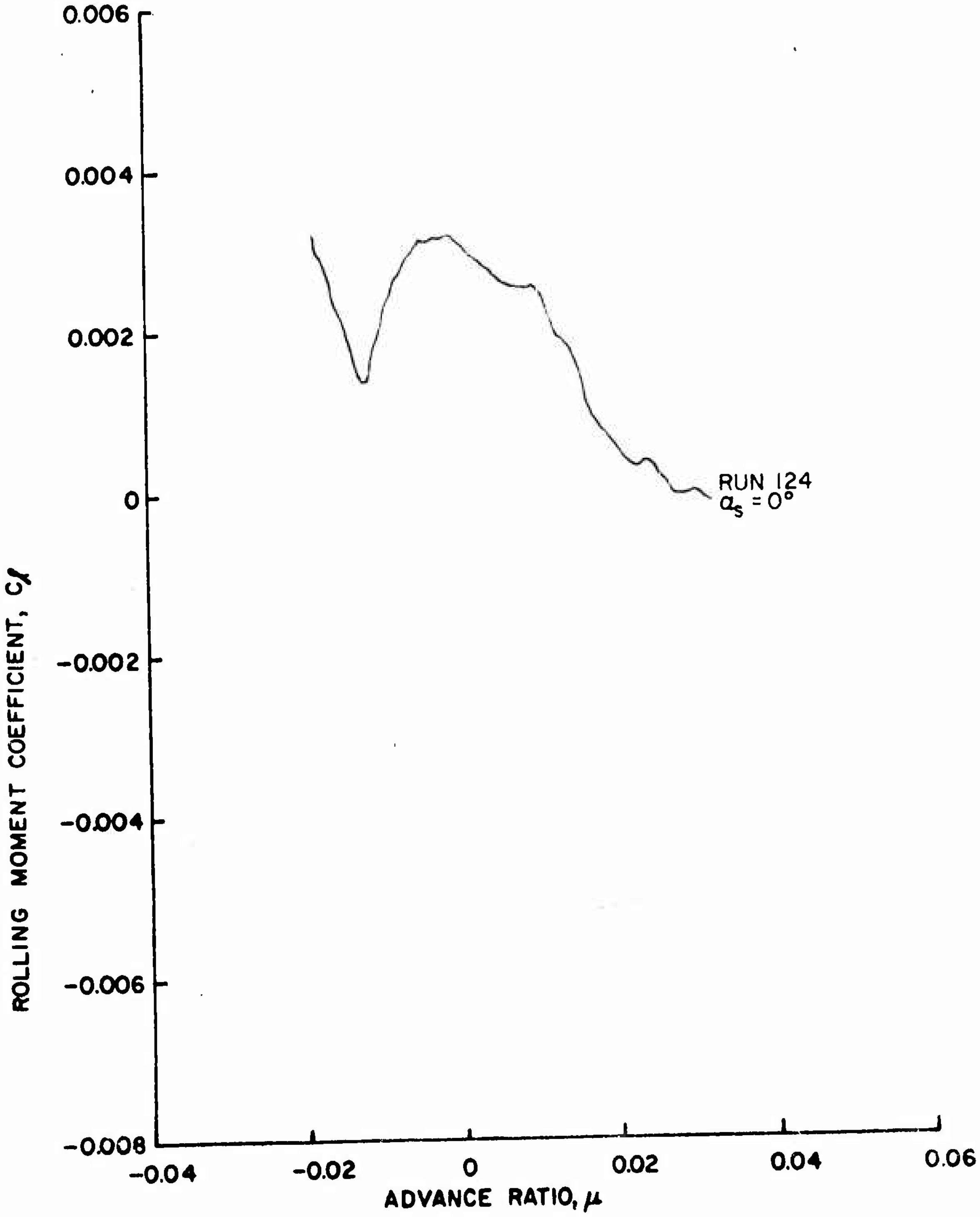

Figure 73c. Rotor Force and Moment Coefficients as Functions of Advance Ratio, $\theta_{.75R} = 12°$, Wing Off, Fuselage On, $\frac{h}{D} = 0.75$.

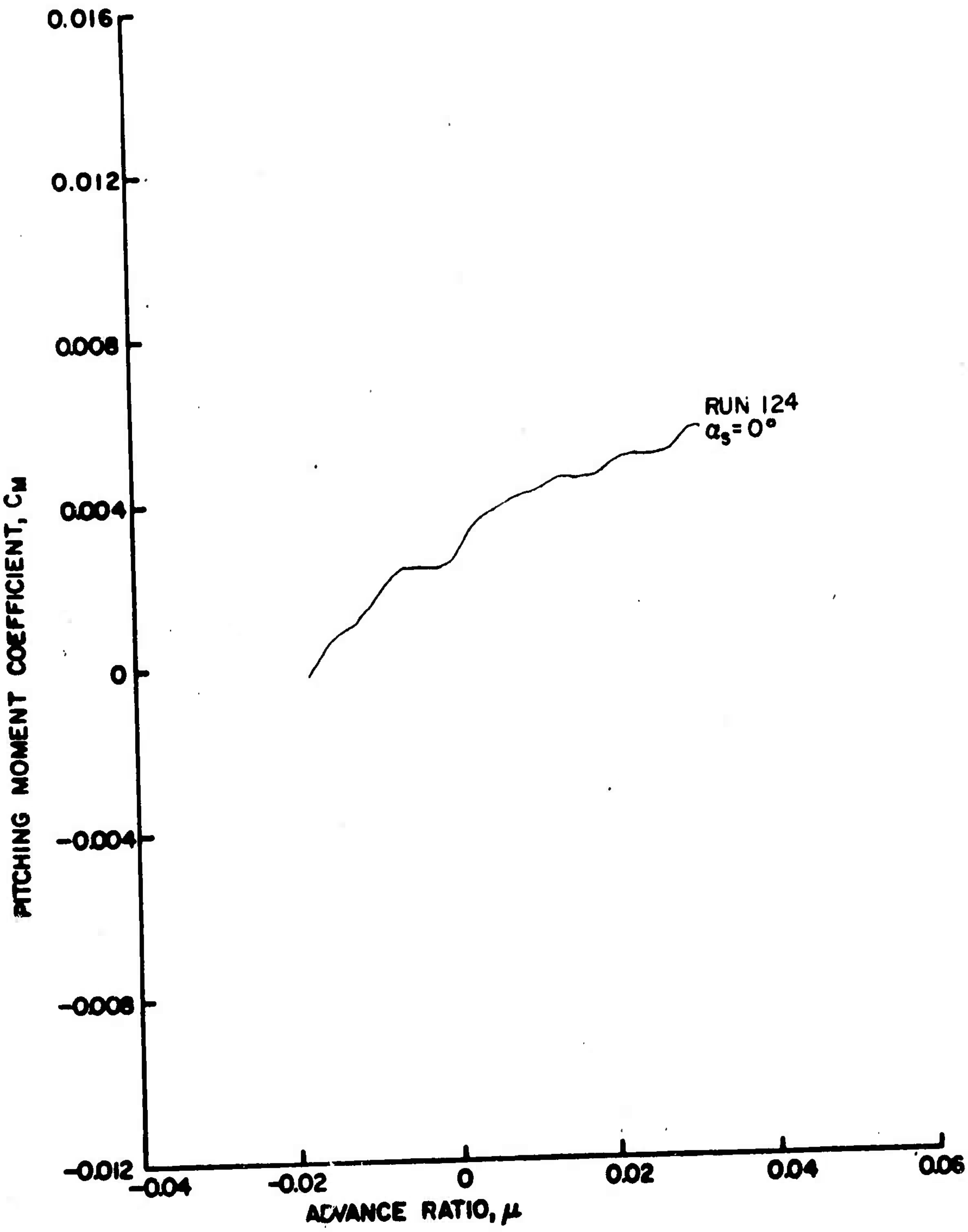

Figure 73d. Rotor Force and Moment Coefficients as Functions of Advance Ratio, $\theta_{.75R} = 12°$, Wing Off, Fuselage On, $\frac{h}{D} = 0.75$.

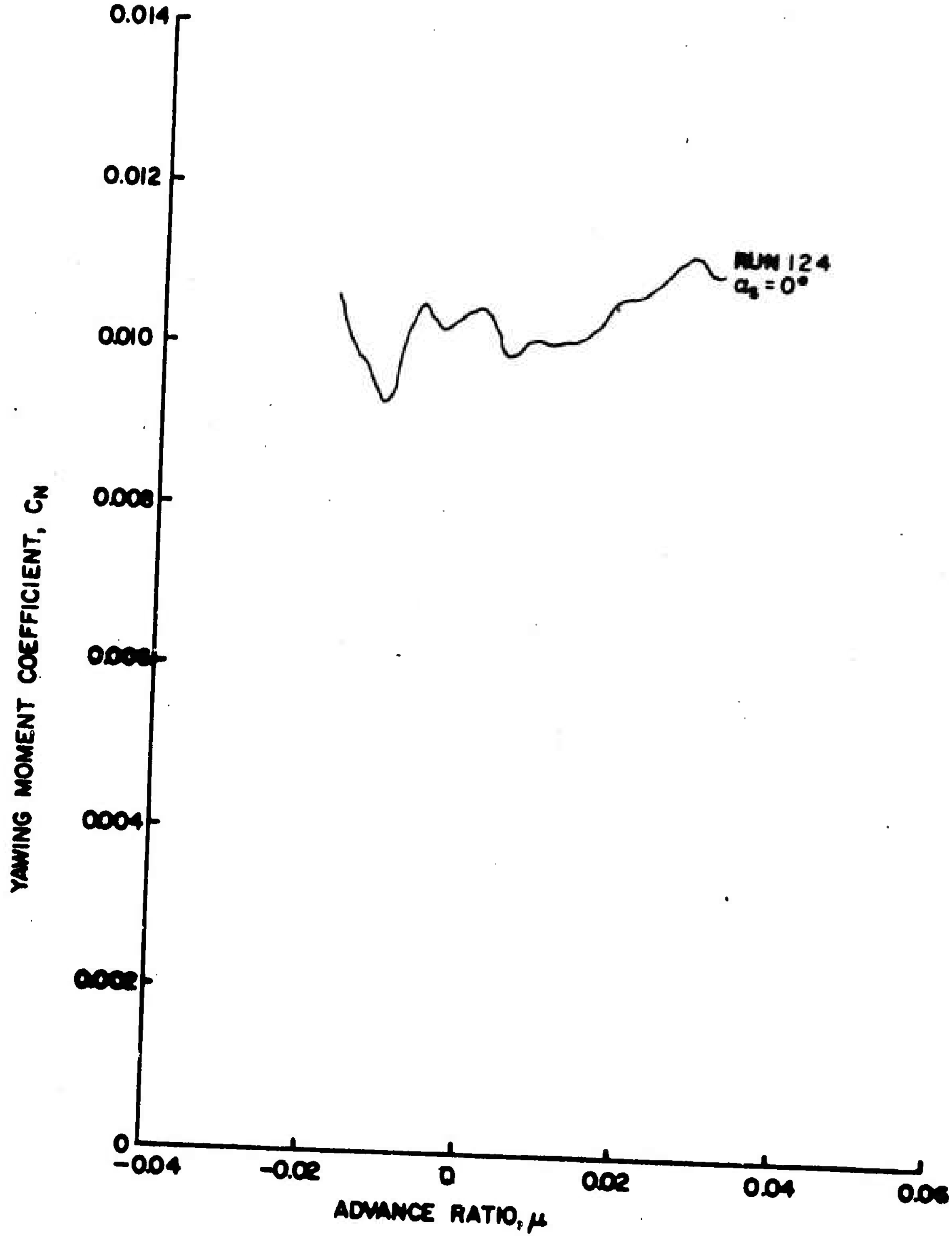

Figure 73e. Rotor Force and Moment Coefficients as Functions of Advance Ratio, $\theta_{.75R} = 12^\circ$, Wing Off, Fuselage On, $\frac{h}{D} = 0.75$.

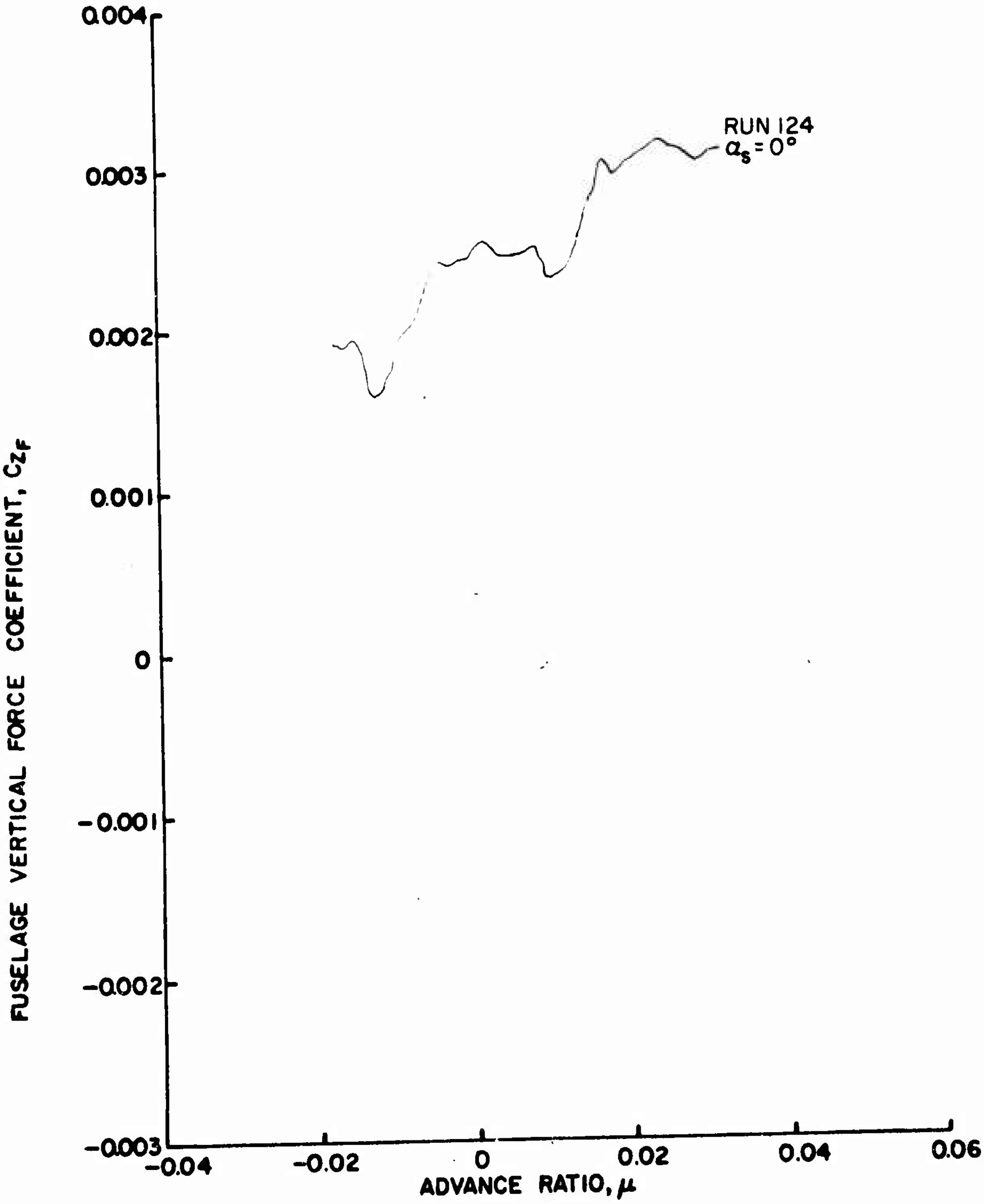

Figure 74a. Fuselage Vertical Force and Pitching Moment Coefficients as Functions of Advance Ratio, $\theta_{.75R} = 12°$, Wing Off, Fuselage On, $\frac{h}{D} = 0.75$.

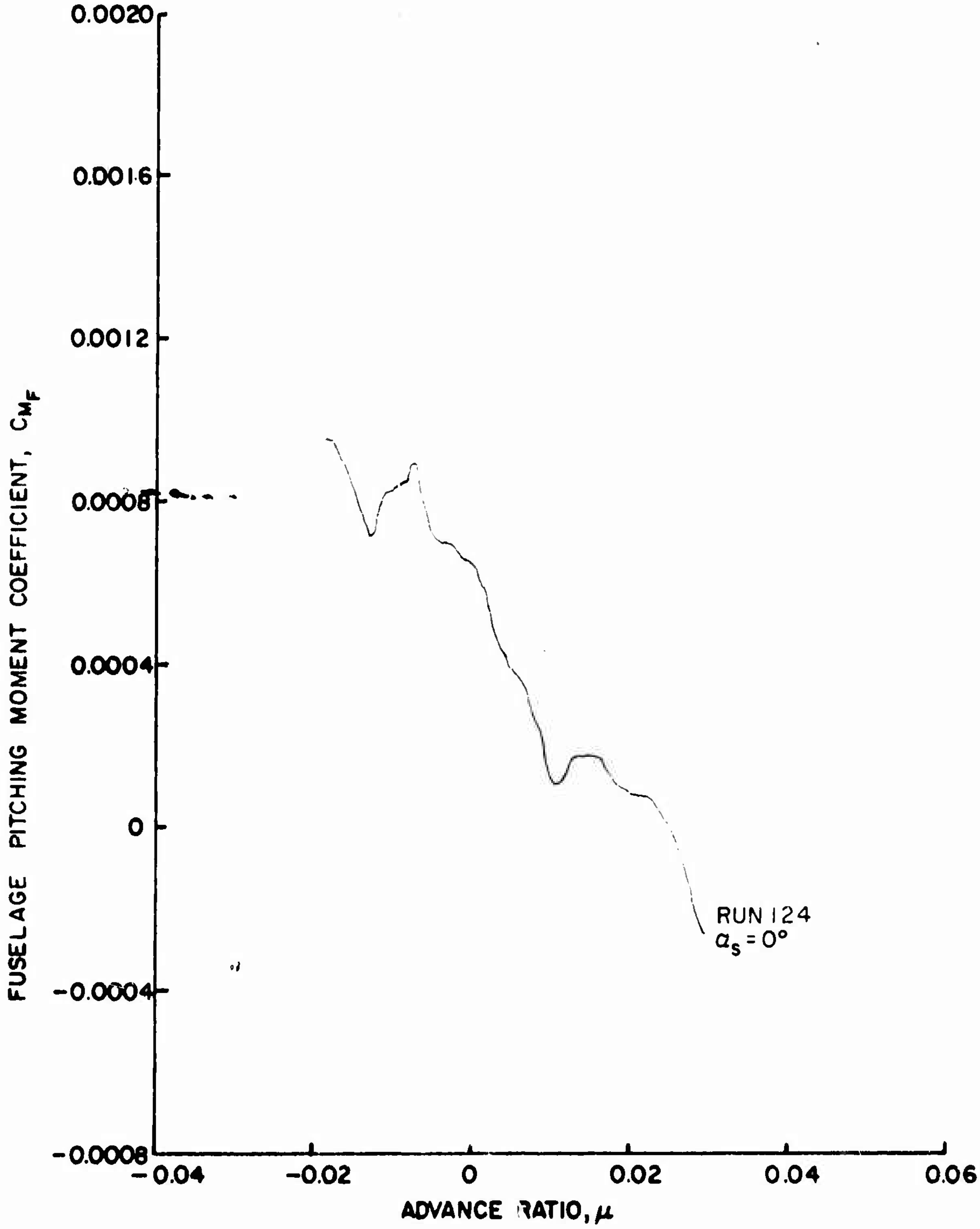

Figure 74b. Fuselage Vertical Force and Pitching Moment Coefficients as Functions of Advance Ratio, $\theta_{.75R} = 12^{\circ}$, Wing Off, Fuselage On, $\frac{h}{D} = 0.75$.

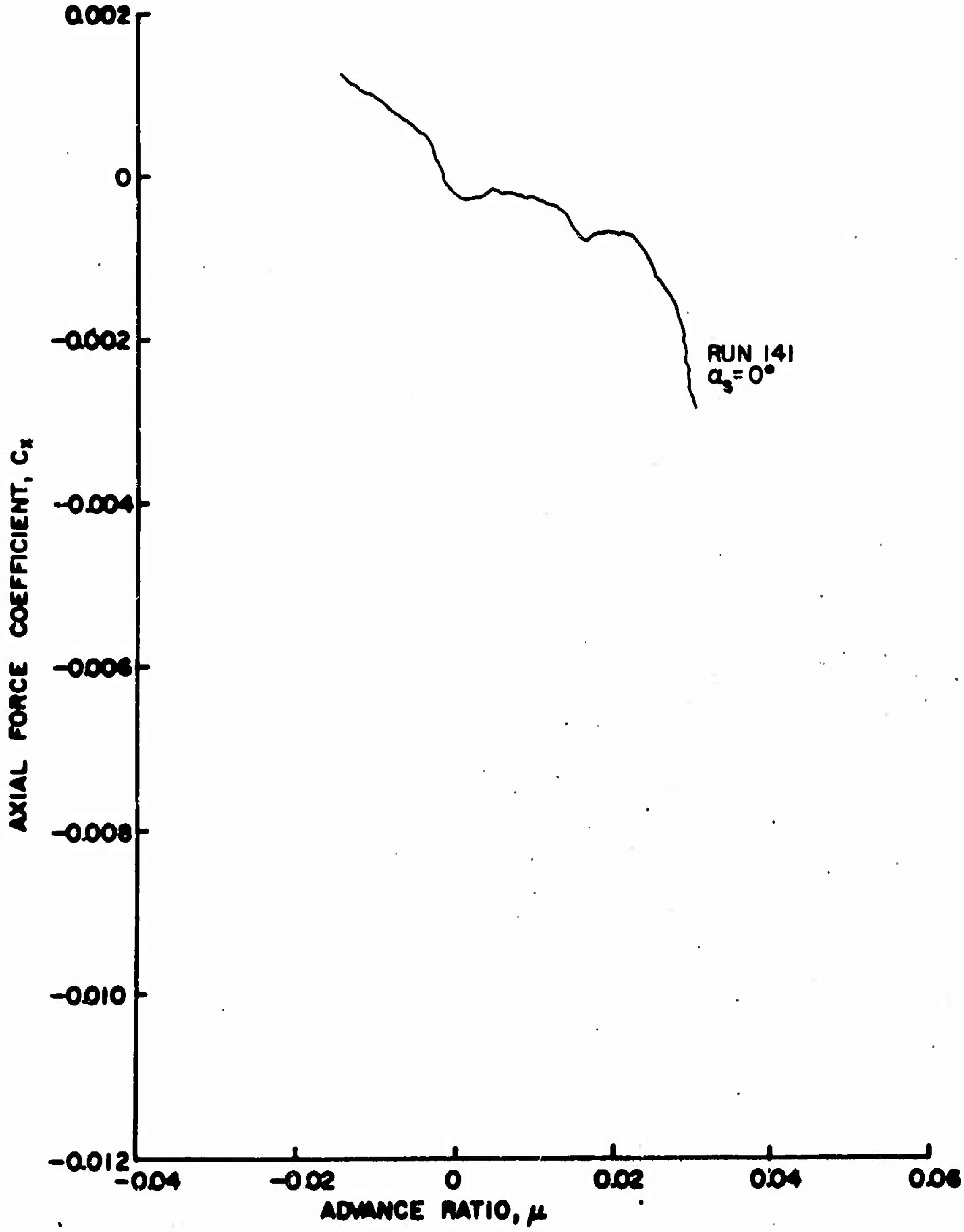

Figure 75a. Rotor Force and Moment Coefficients as Functions of Advance Ratio, $\theta_{.75R} = 8°$, Large Wing on High, $\frac{h}{D} = 0.75$.

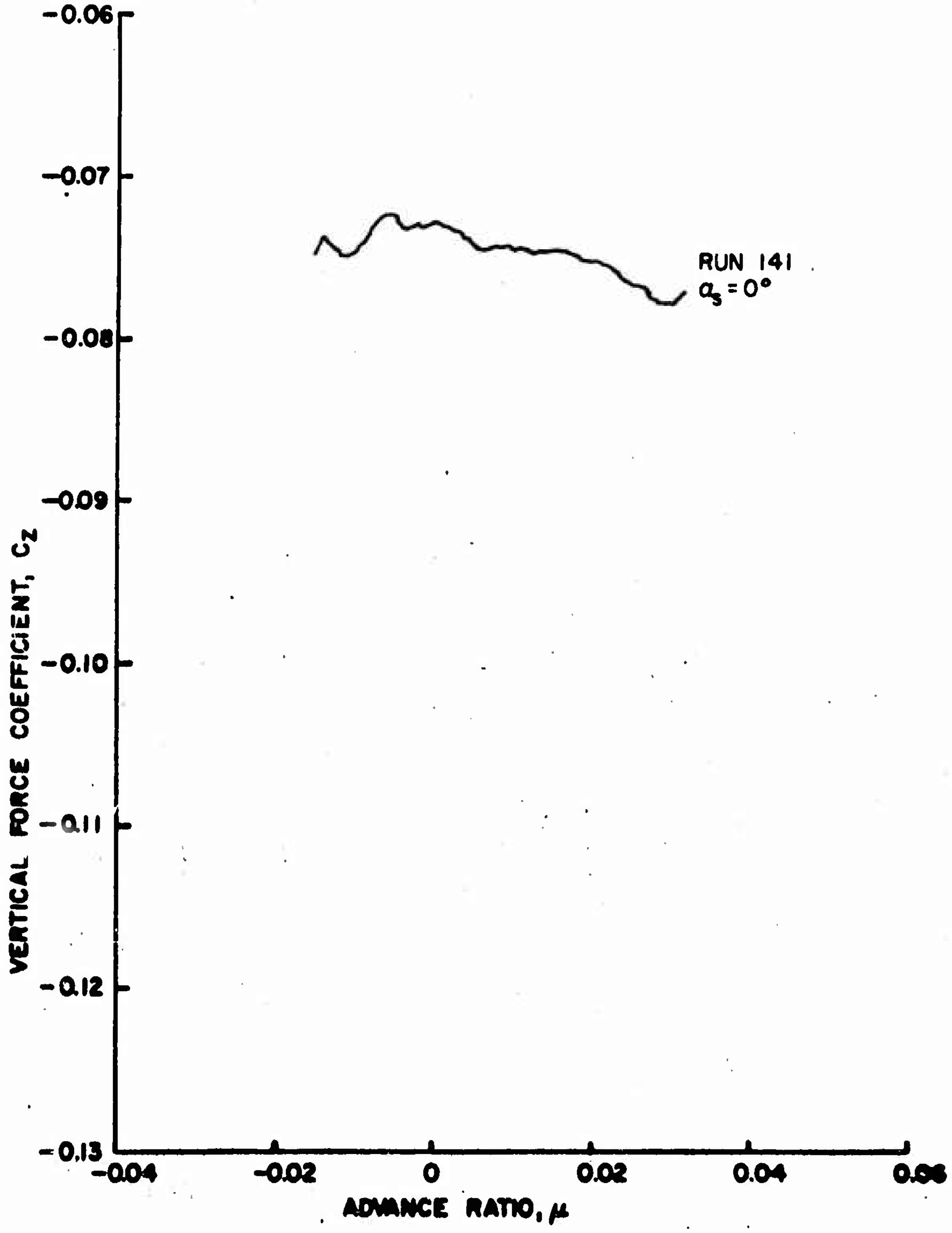

Figure 75b. Rotor Force and Moment Coefficients as Functions of Advance Ratio, $\theta_{.75R} = 8°$, Large Wing on High, $\frac{h}{D} = 0.75$.

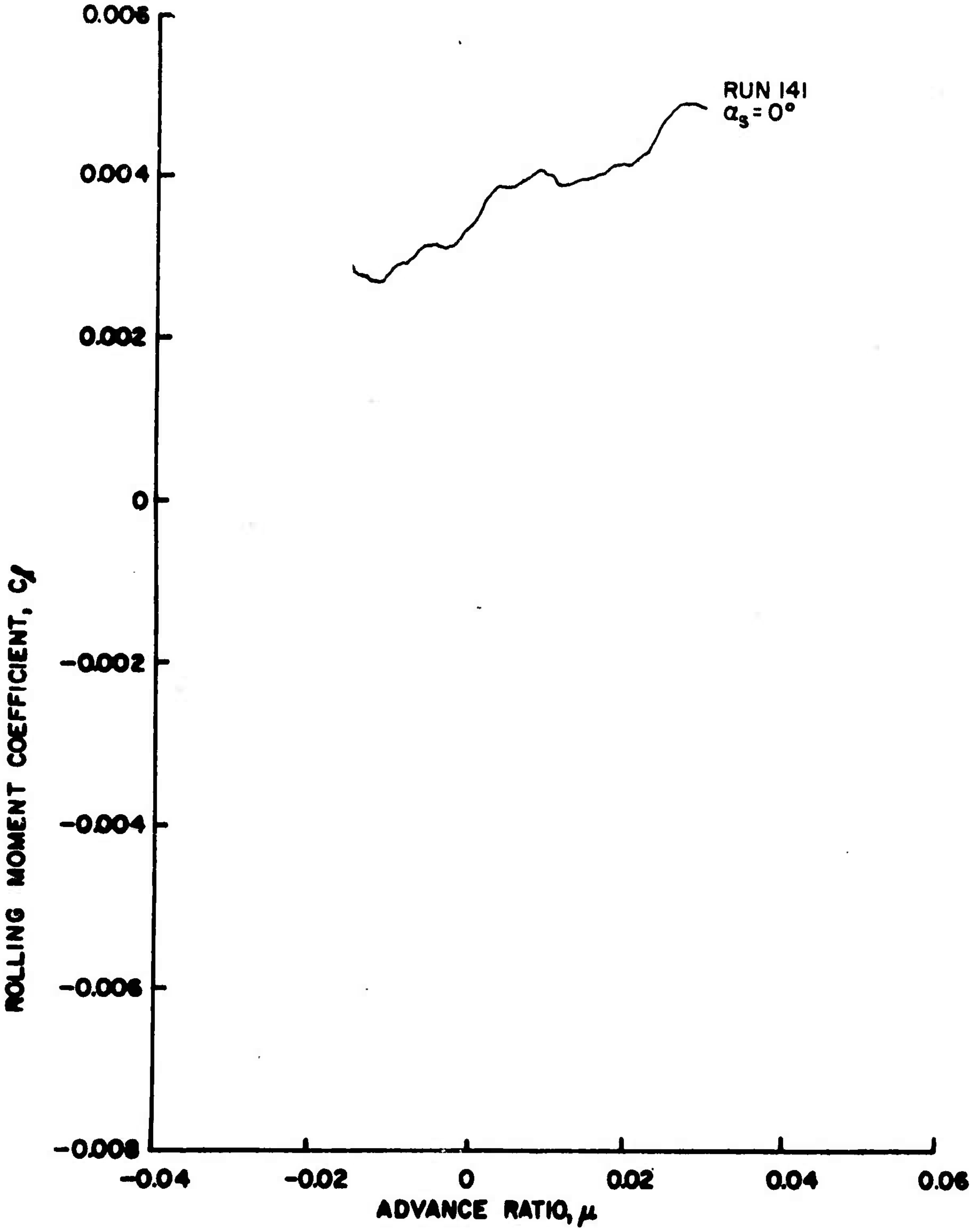

Figure 75c. Rotor Force and Moment Coefficients as Functions of Advance Ratio, $\theta_{.75R} = 8°$, Large Wing on High, $\frac{h}{D} = 0.75$.

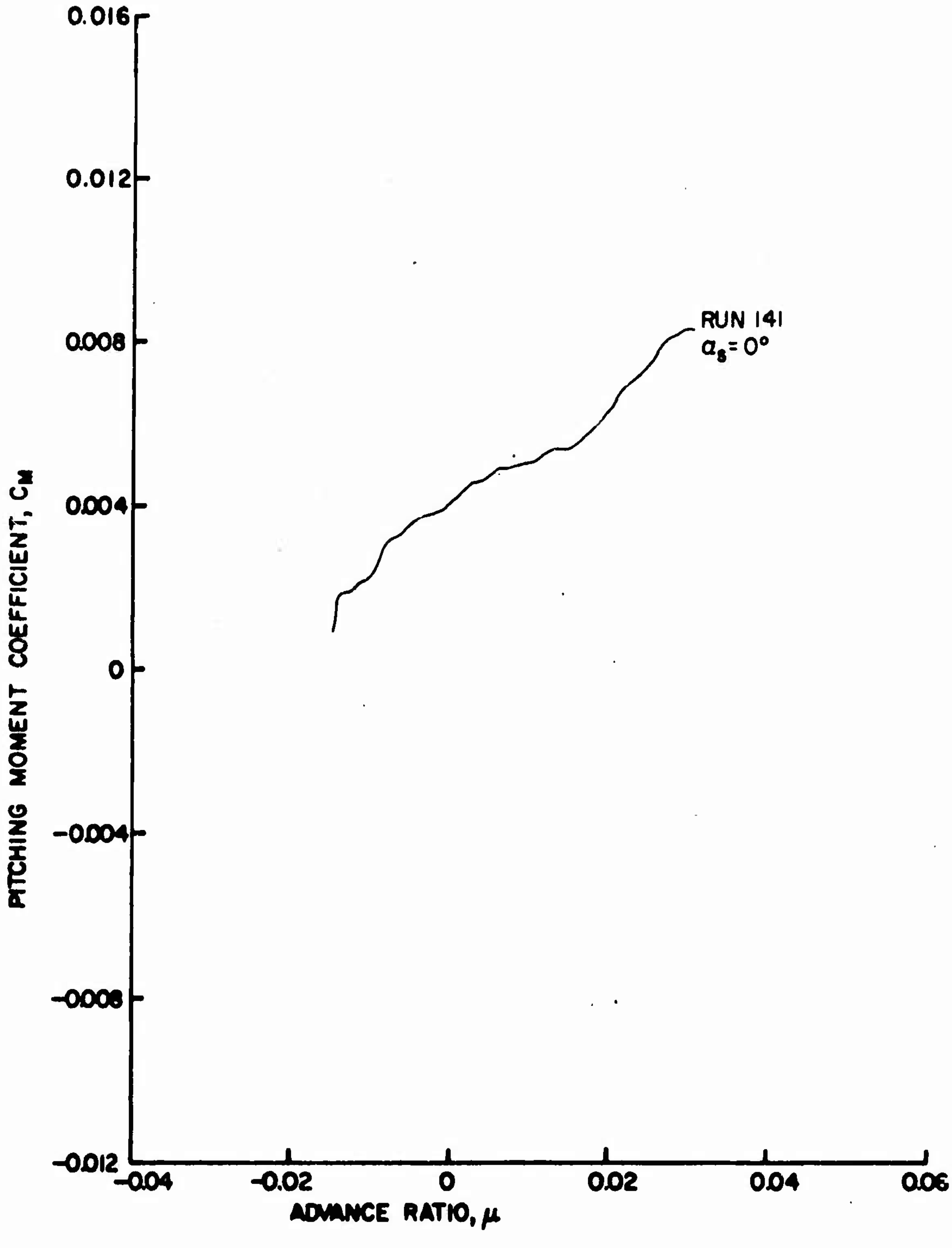

Figure 75d. Rotor Force and Moment Coefficients as Functions of Advance Ratio, $\theta_{.75R} = 8°$, Large Wing on High, $\frac{h}{D} = 0.75$.

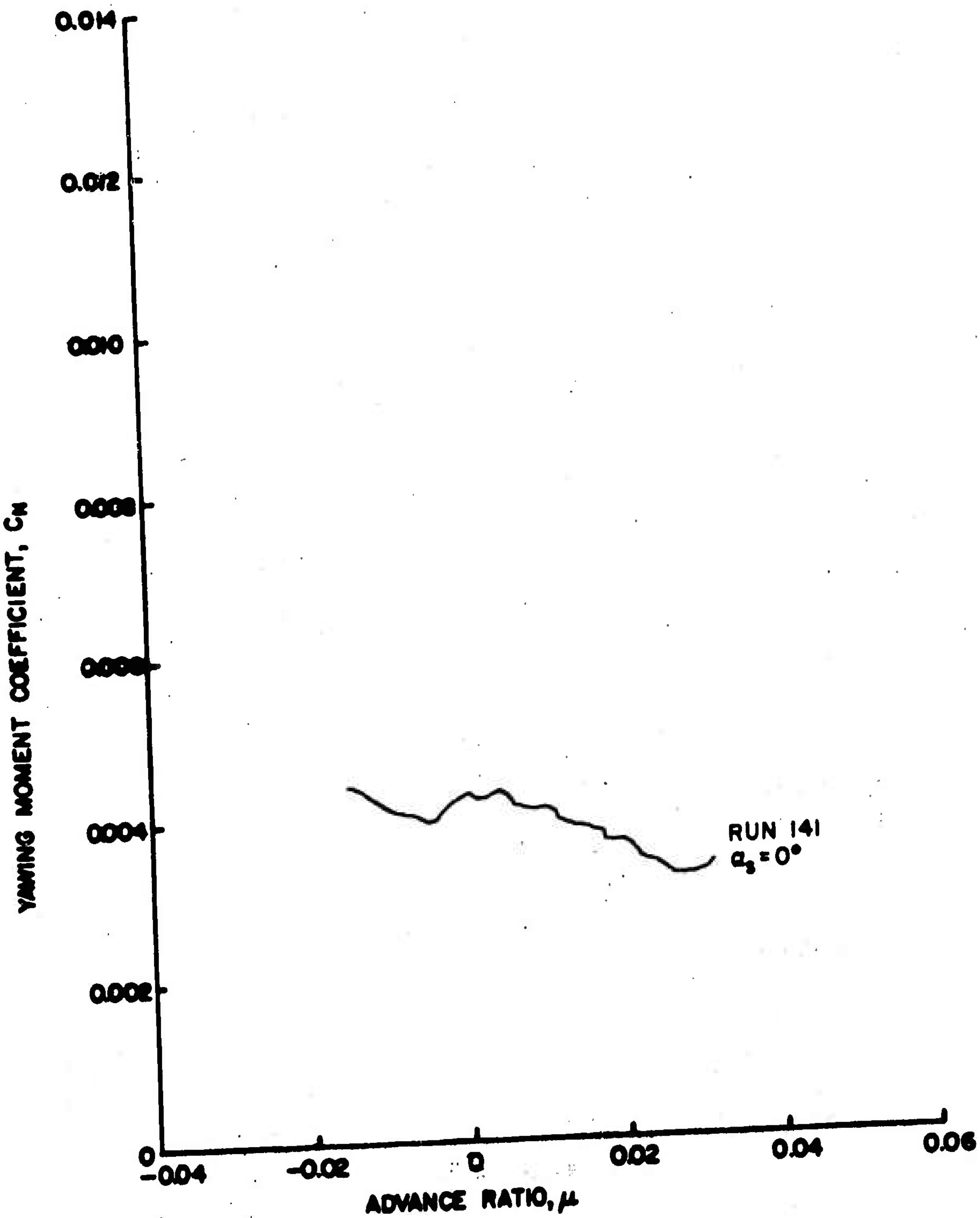

Figure 75e. Rotor Force and Moment Coefficients as Functions of Advance Ratio, $\theta_{.75R} = 8°$, Large Wing on High, $\frac{h}{D} = 0.75$.

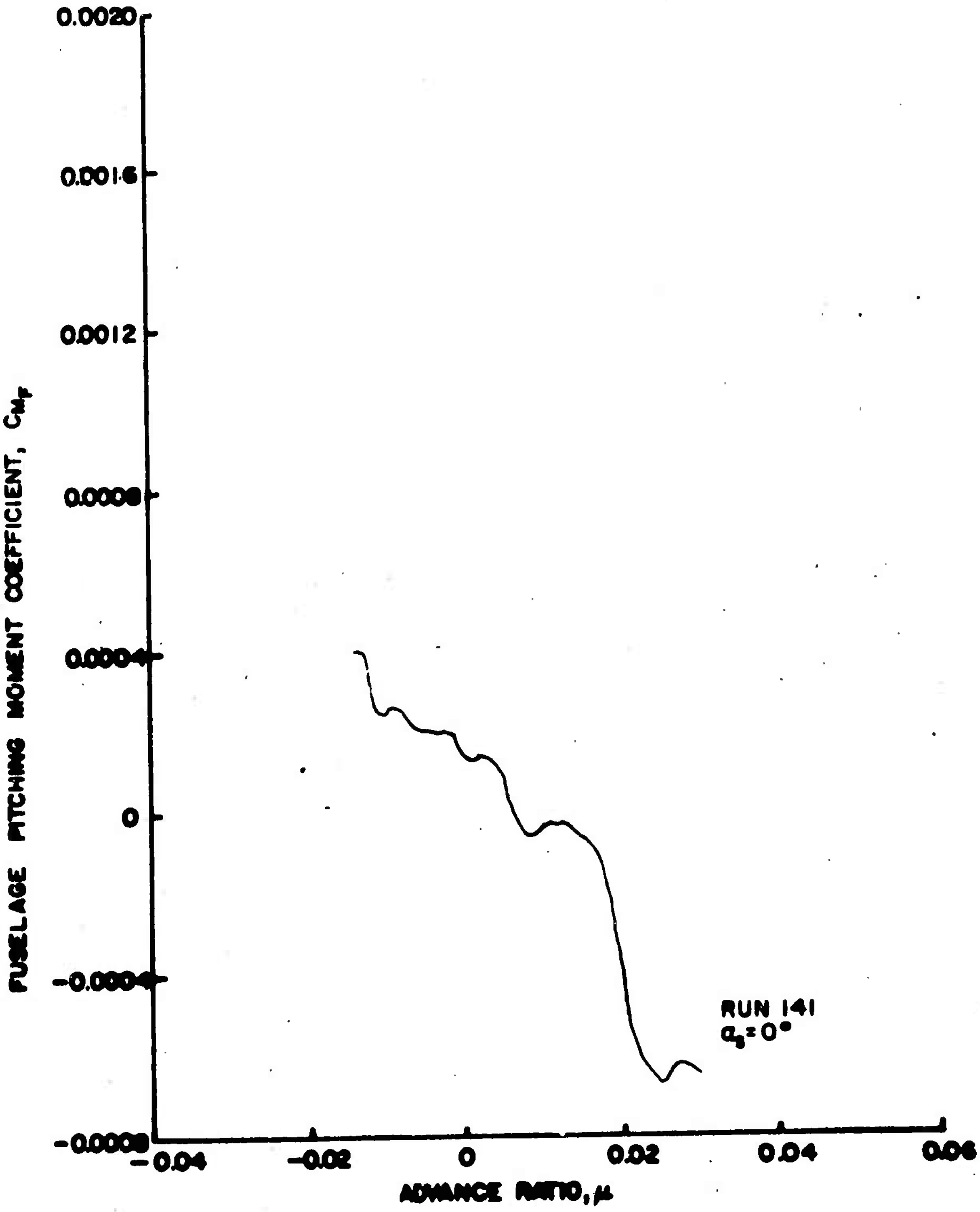

Figure 76. Fuselage Vertical Force and Pitching Moment Coefficients as Functions of Advance Ratio, $\theta_{.75R} = 8°$, Large Wing on High, $\frac{h}{D} = 0.75$.

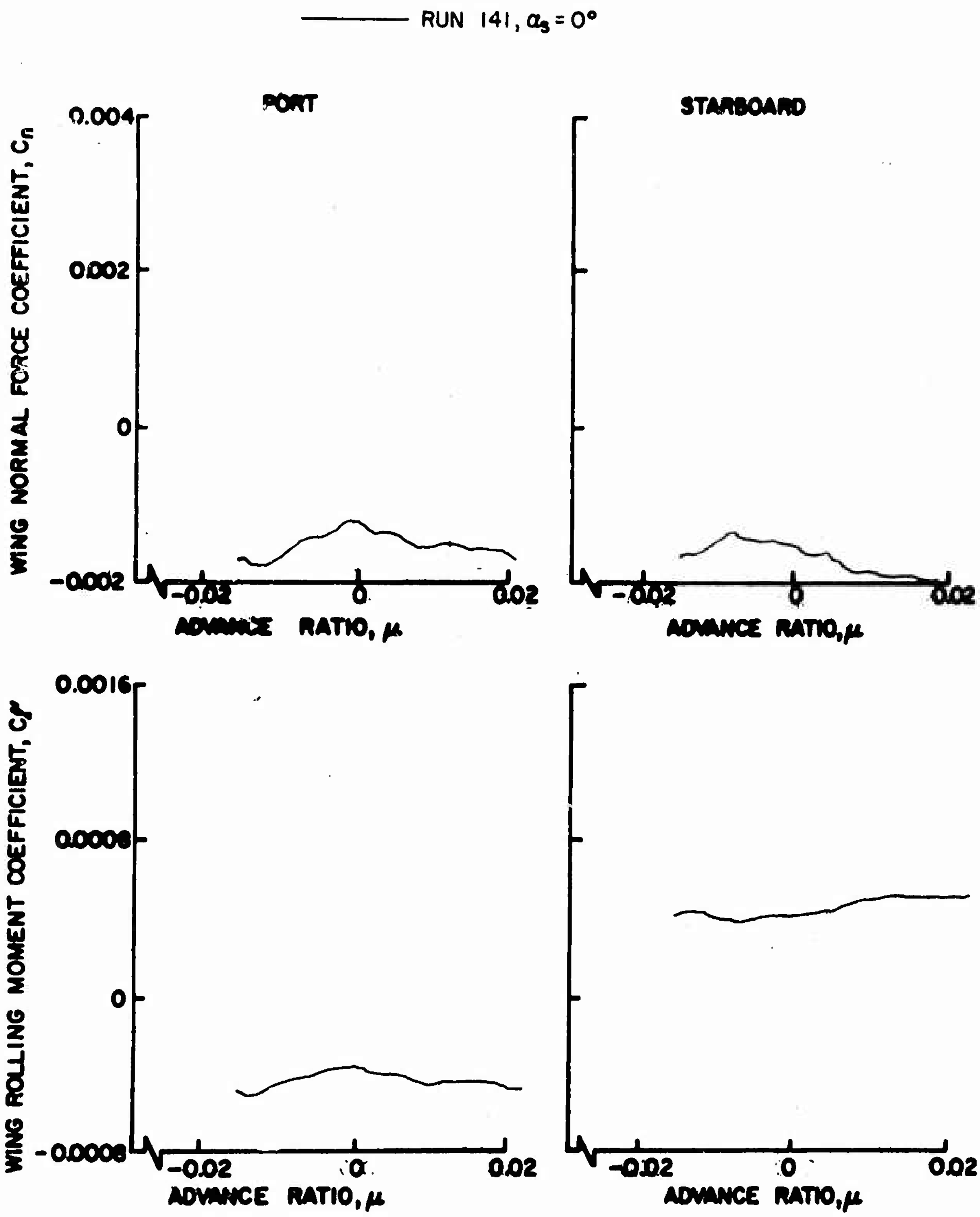

Figure 77. Wing Normal Force and Rolling Moment Coefficients as Functions of Advance Ratio, $\theta_{.75R} = 8^{\circ}$, Large Wing on High, $\frac{h}{D} = 0.75$.

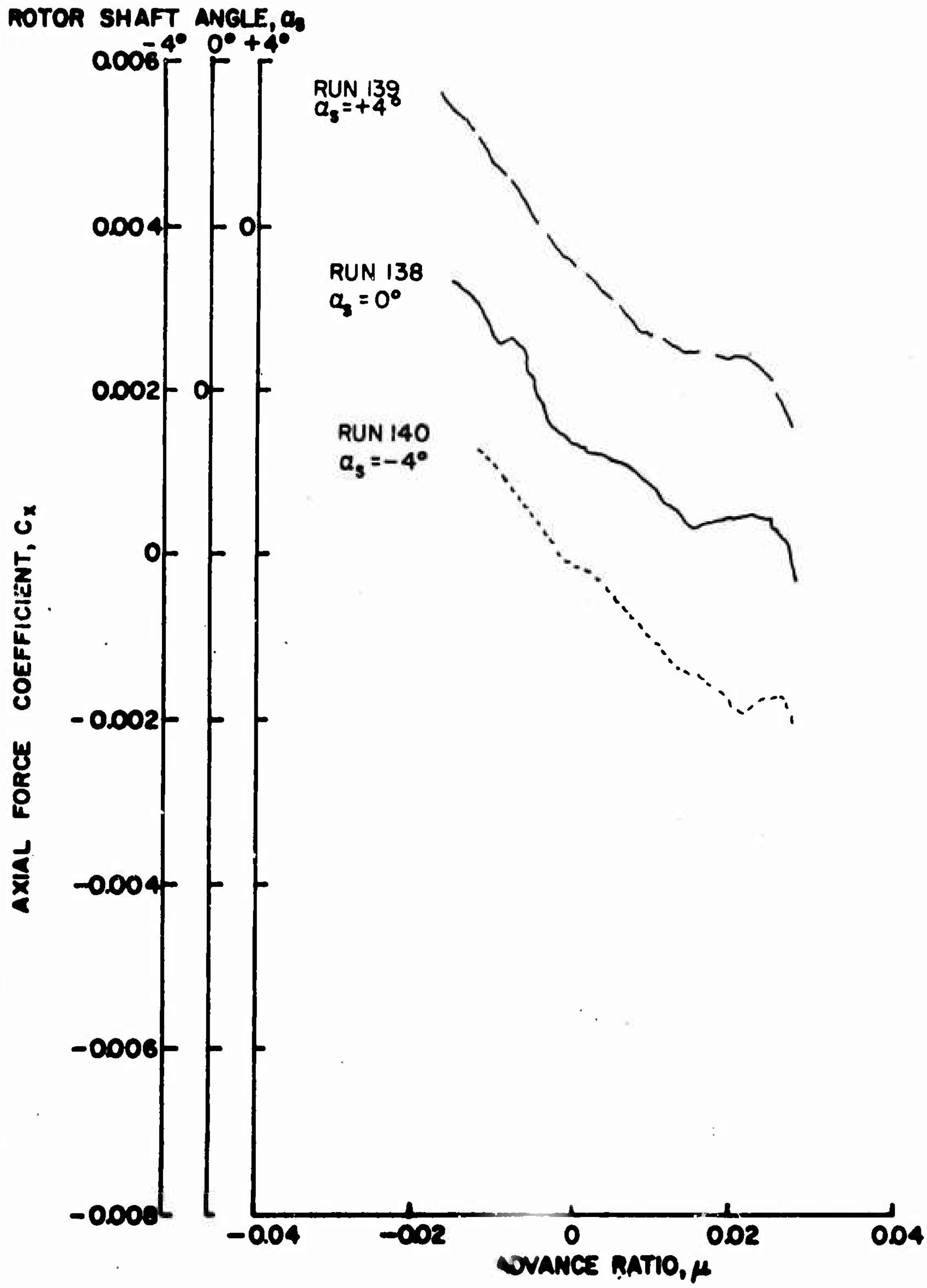

Figure 78a. Rotor Force and Moment Coefficients as Functions of Advance Ratio, $\theta_{.75R} = 10°$, Large Wing on High, $\frac{h}{D} = 0.75$.

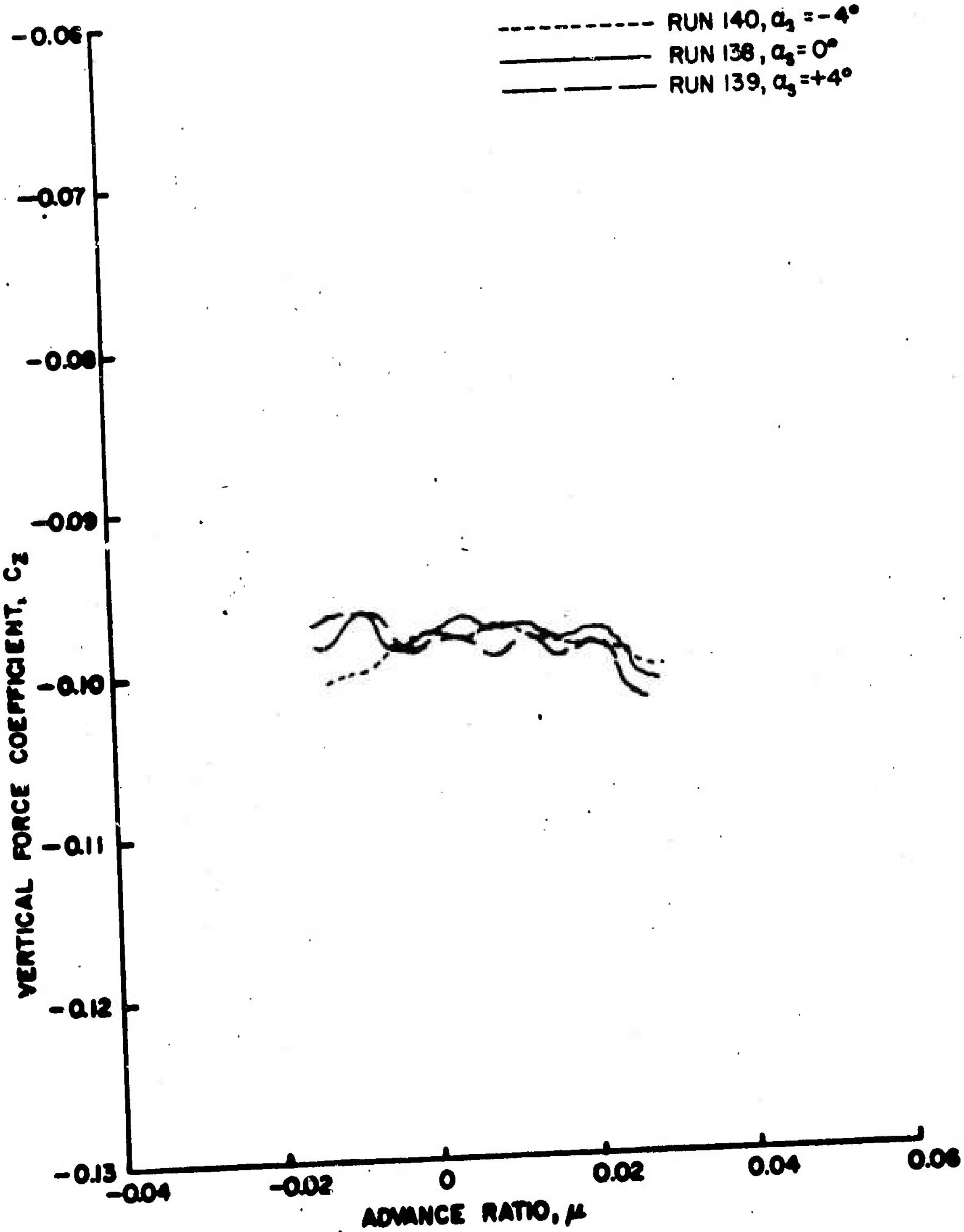

Figure 73b. Rotor Force and Moment Coefficients as Functions of Advance Ratio, $\theta_{.75R} = 10^\circ$, Large Wing on High, $\frac{h}{D} = 0.75$.

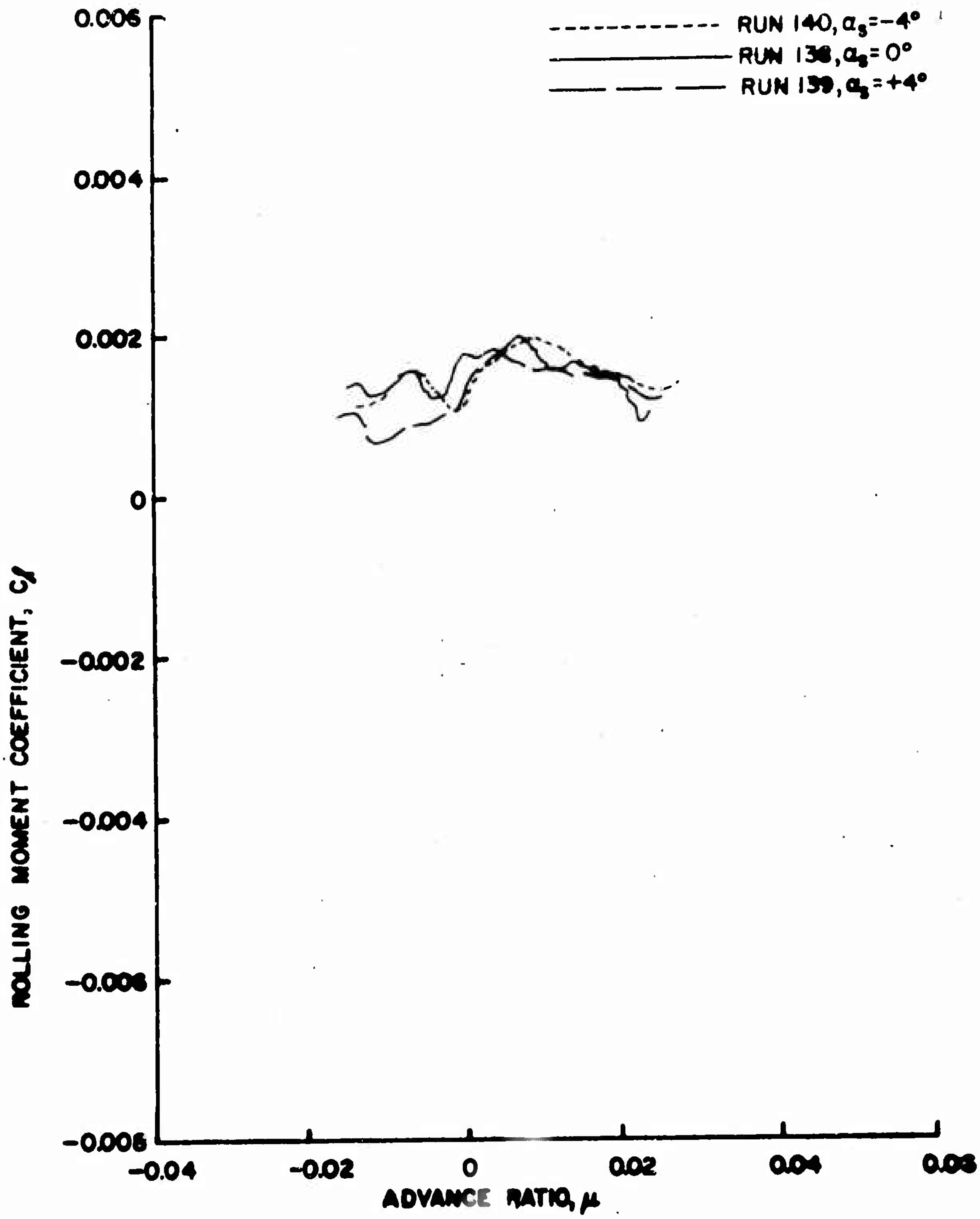

Figure 78w. Rotor Force and Moment Coefficients as Functions of Advance Ratio, $\theta_{.75R} = 10^\circ$, Large Wing on High, $\frac{h}{D} = 0.75$.

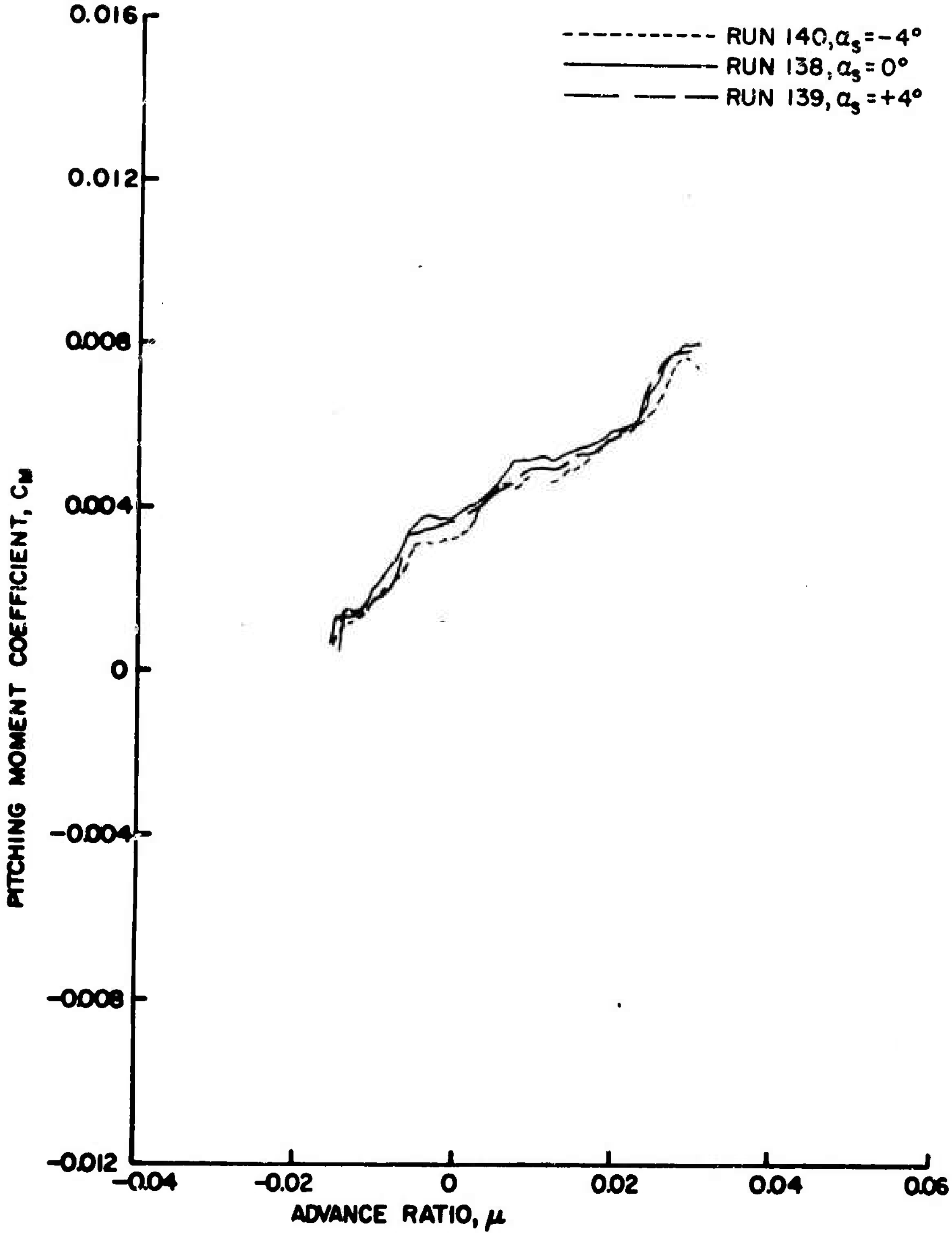

Figure 78d, Rotor Force and Moment Coefficients as Functions of Advance Ratio, $\theta_{.75R} = 10^\circ$, Large Wing on High, $\frac{h}{D} = 0.75$.

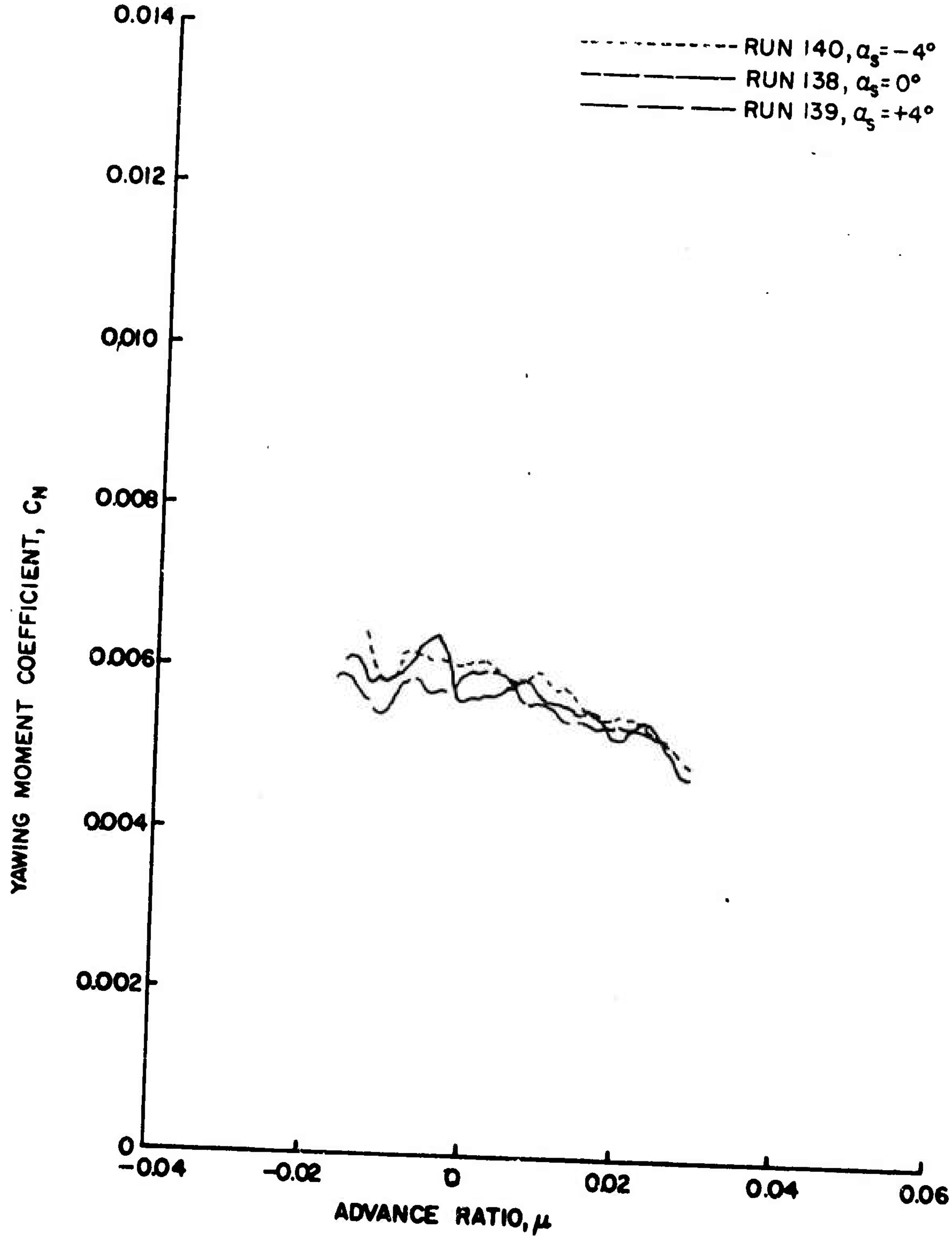

Figure 78e. Rotor Force and Moment Coefficients as Functions of Advance Ratio, $\theta_{.75R} = 10°$, Large Wing on High, $\frac{h}{D} = 0.75$.

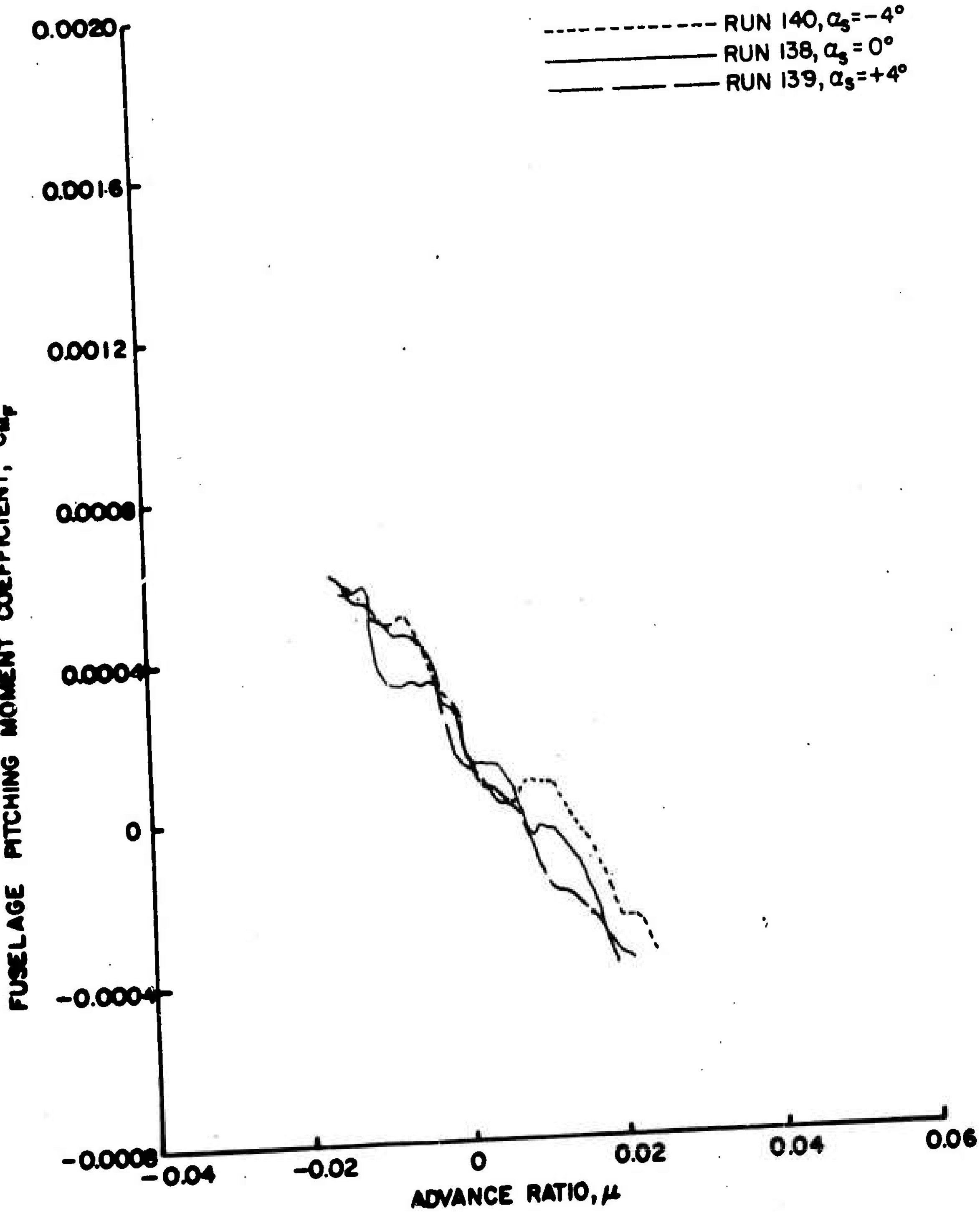

Figure 79. Fuselage Vertical Force and Pitching Moment Coefficients as Functions of Advance Ratio, $\theta_{.75R} = 10^\circ$, Large Wing on High, $\frac{h}{D} = 0.75$.

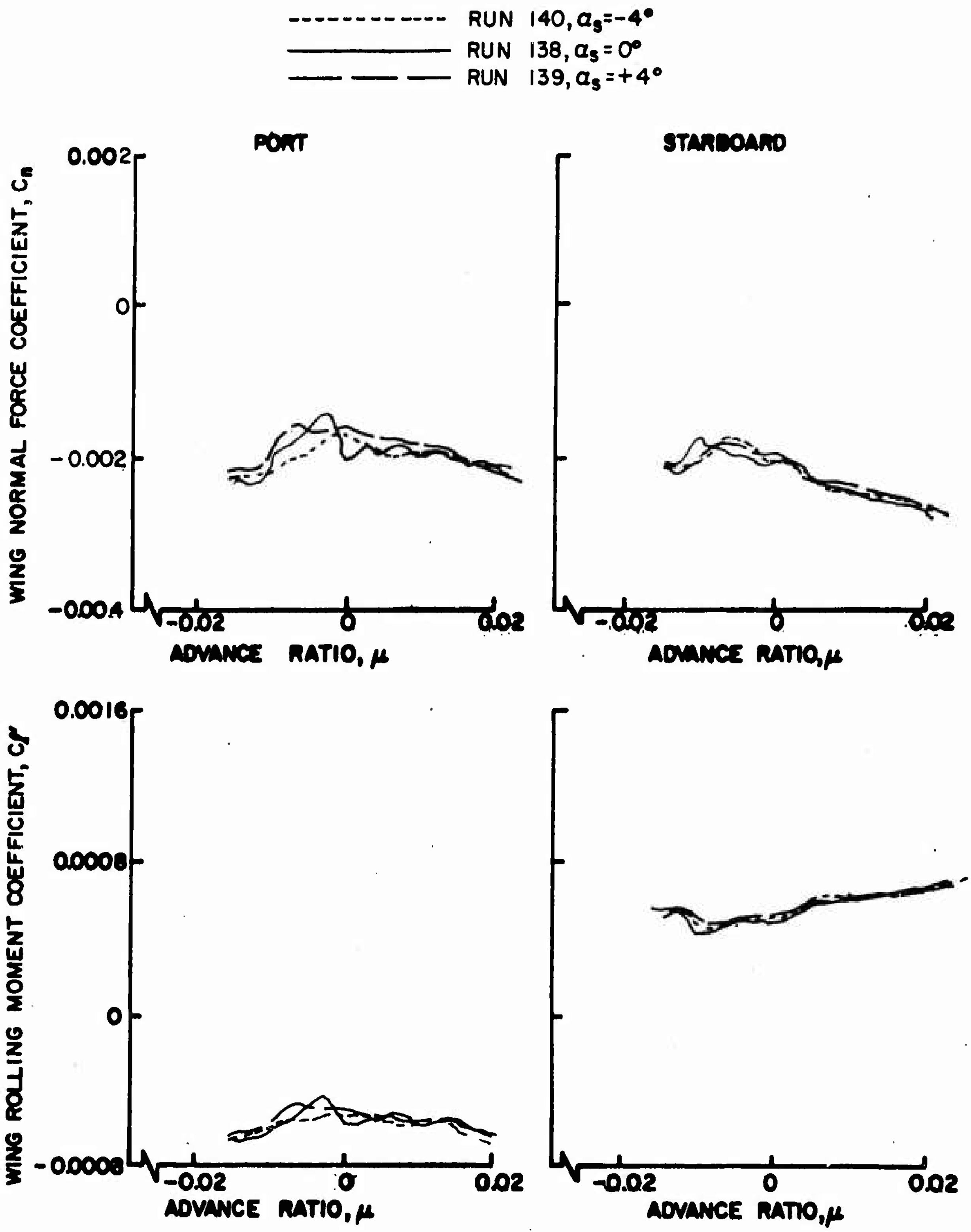

Figure 80. Wing Normal Force and Rolling Moment Coefficients as Functions of Advance Ratio, $\theta_{.75R} = 10°$, Large Wing on High, $\frac{h}{D} = 0.75$.

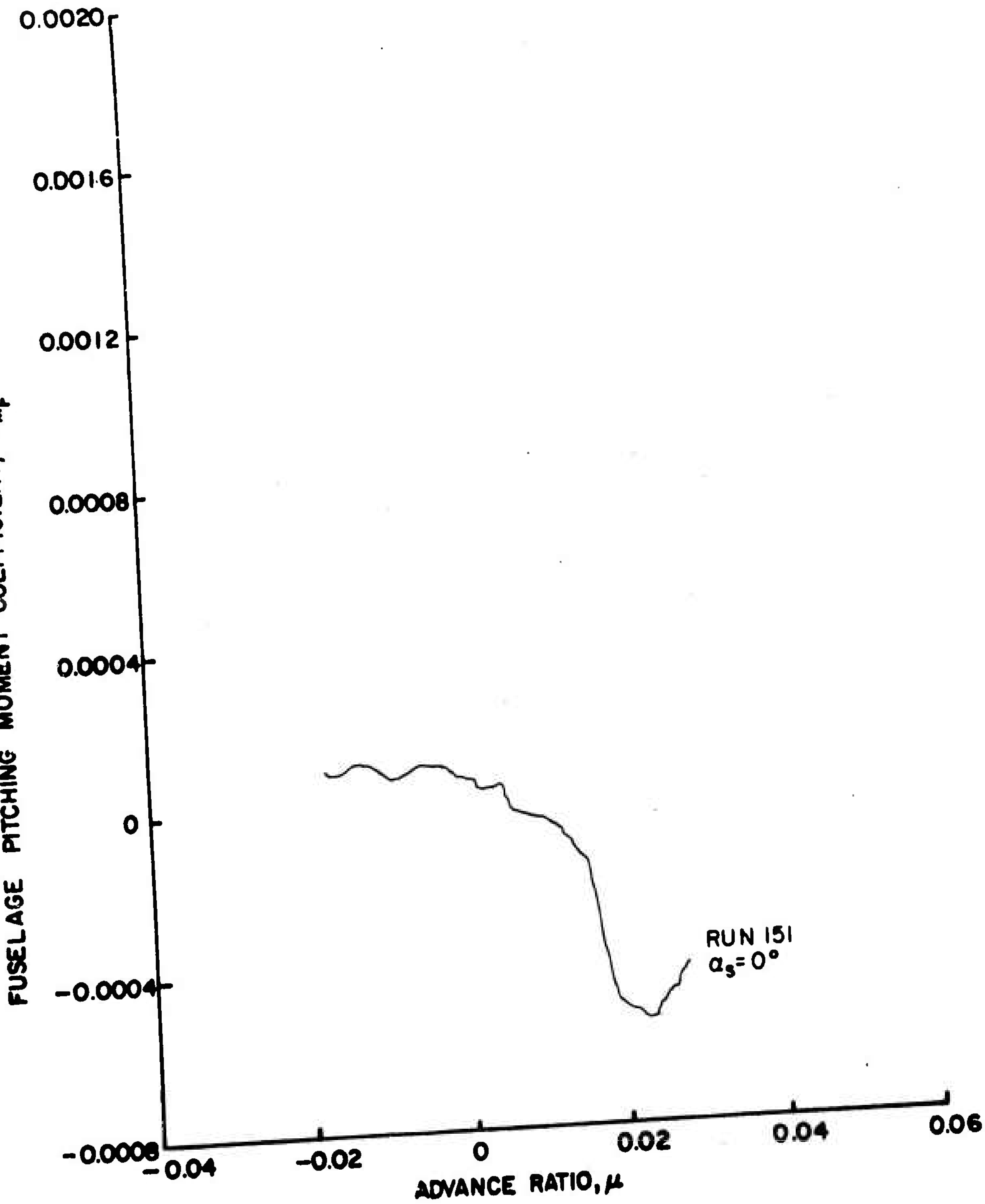

Figure 81. Fuselage Vertical Force and Pitching Moment Coefficients as Functions of Advance Ratio, $\theta_{.75R} = 8°$, Large Wing on Low, $\frac{h}{D} = 0.75$.

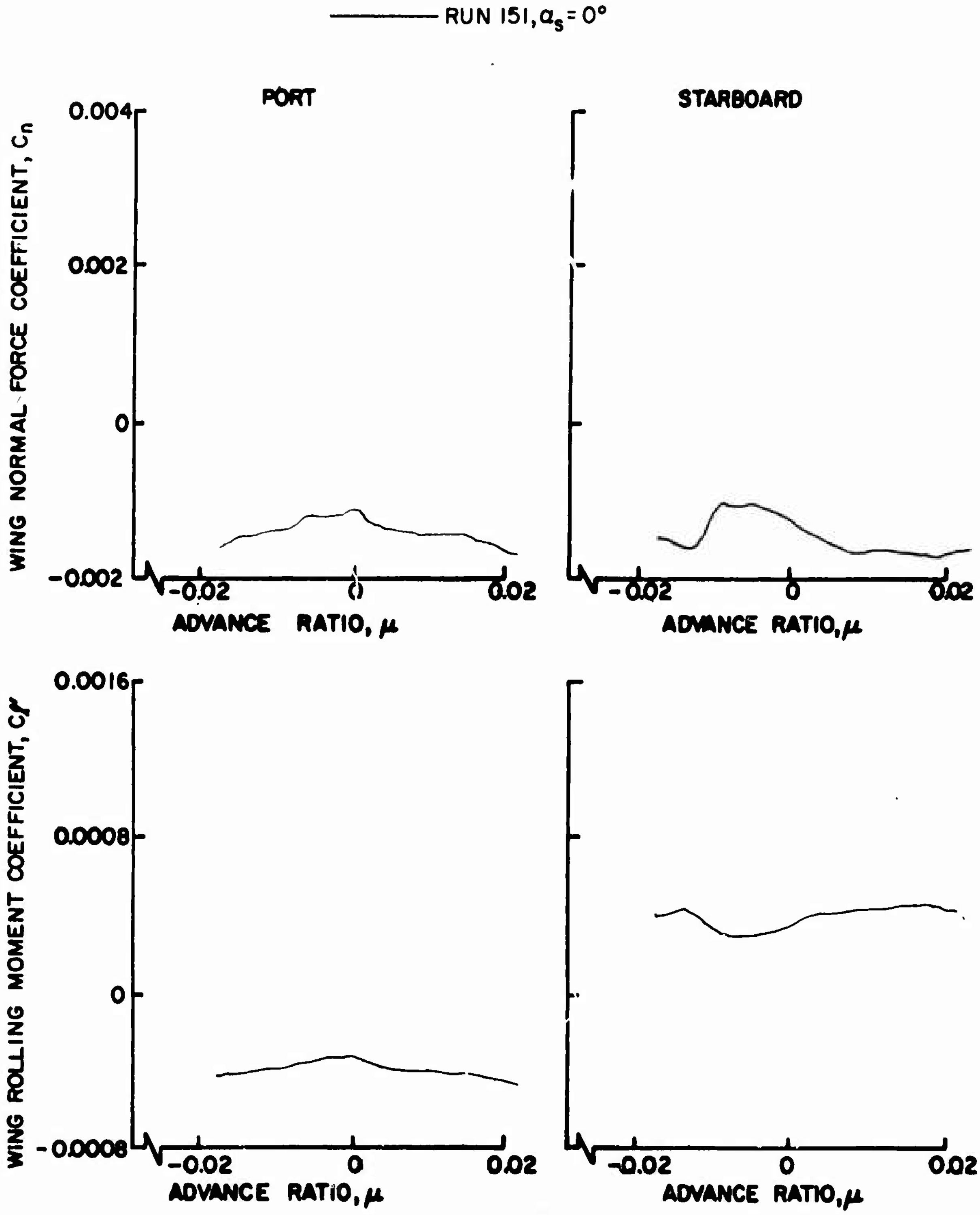

Figure 82. Wing Normal Force and Rolling Moment Coefficients as Functions of Advance Ratio, $\theta_{.75R} = 8^\circ$, Large Wing on Low, $\frac{h}{D} = 0.75$.

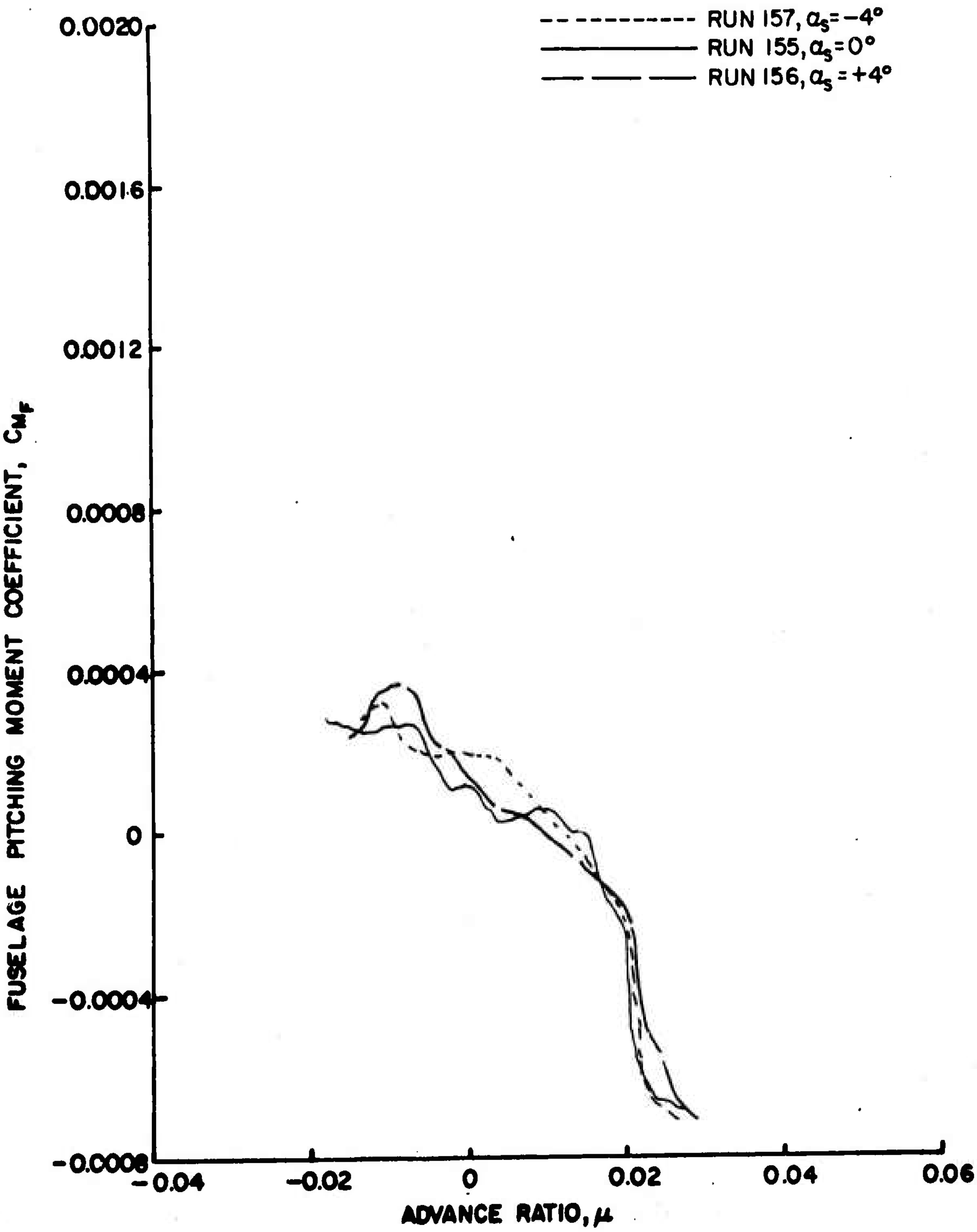

Figure 83. Fuselage Vertical Force and Pitching Moment Coefficients as Functions of Advance Ratio, $\theta_{.75R} = 10°$, Large Wing on Low, $\frac{h}{D} = 0.75$.

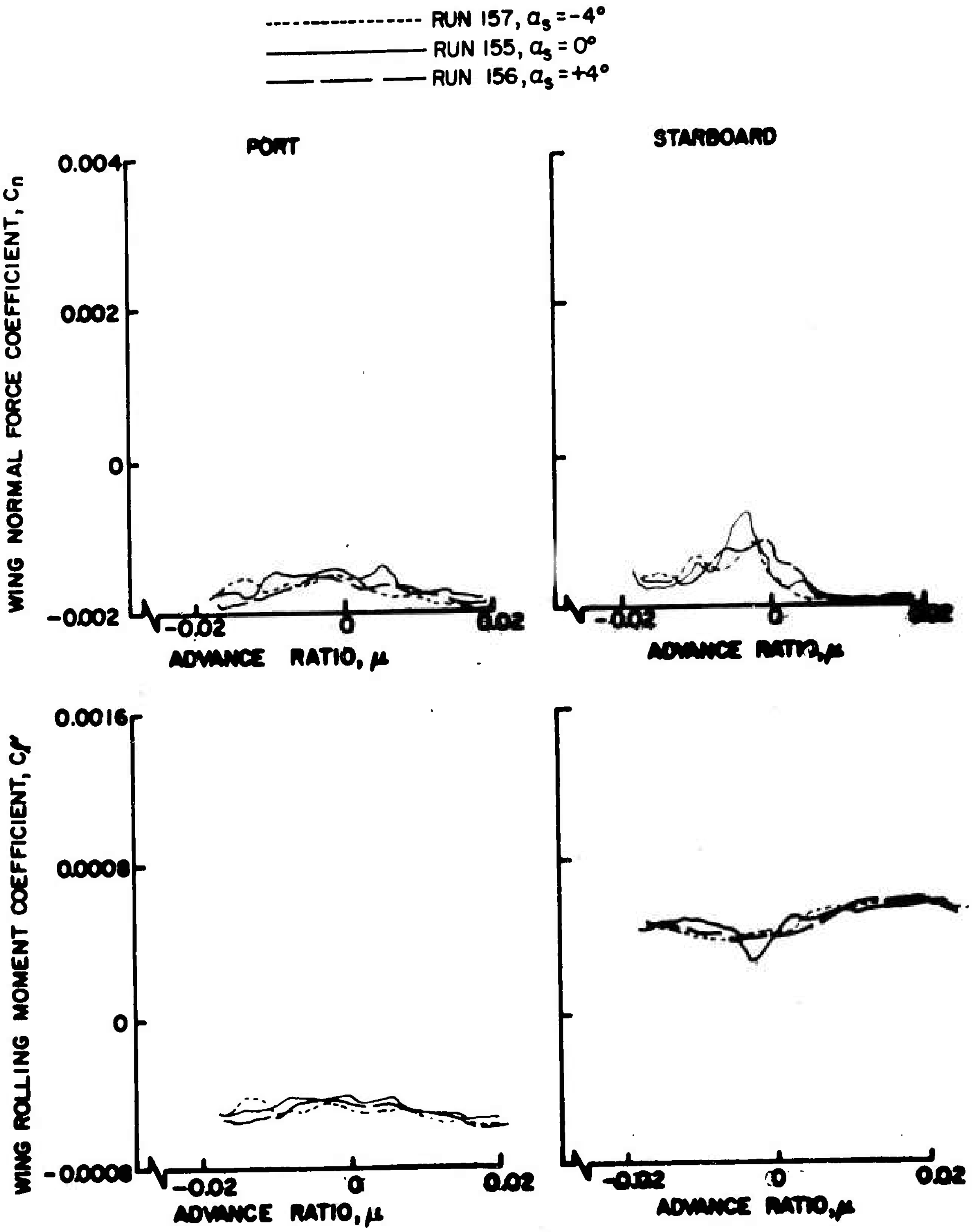

Figure 84. Wing Normal Force and Rolling Moment Coefficients as Functions of Advance Ratio, $\theta_{.75R} = 10°$, Large Wing on Low, $\frac{h}{D} = 0.75$.

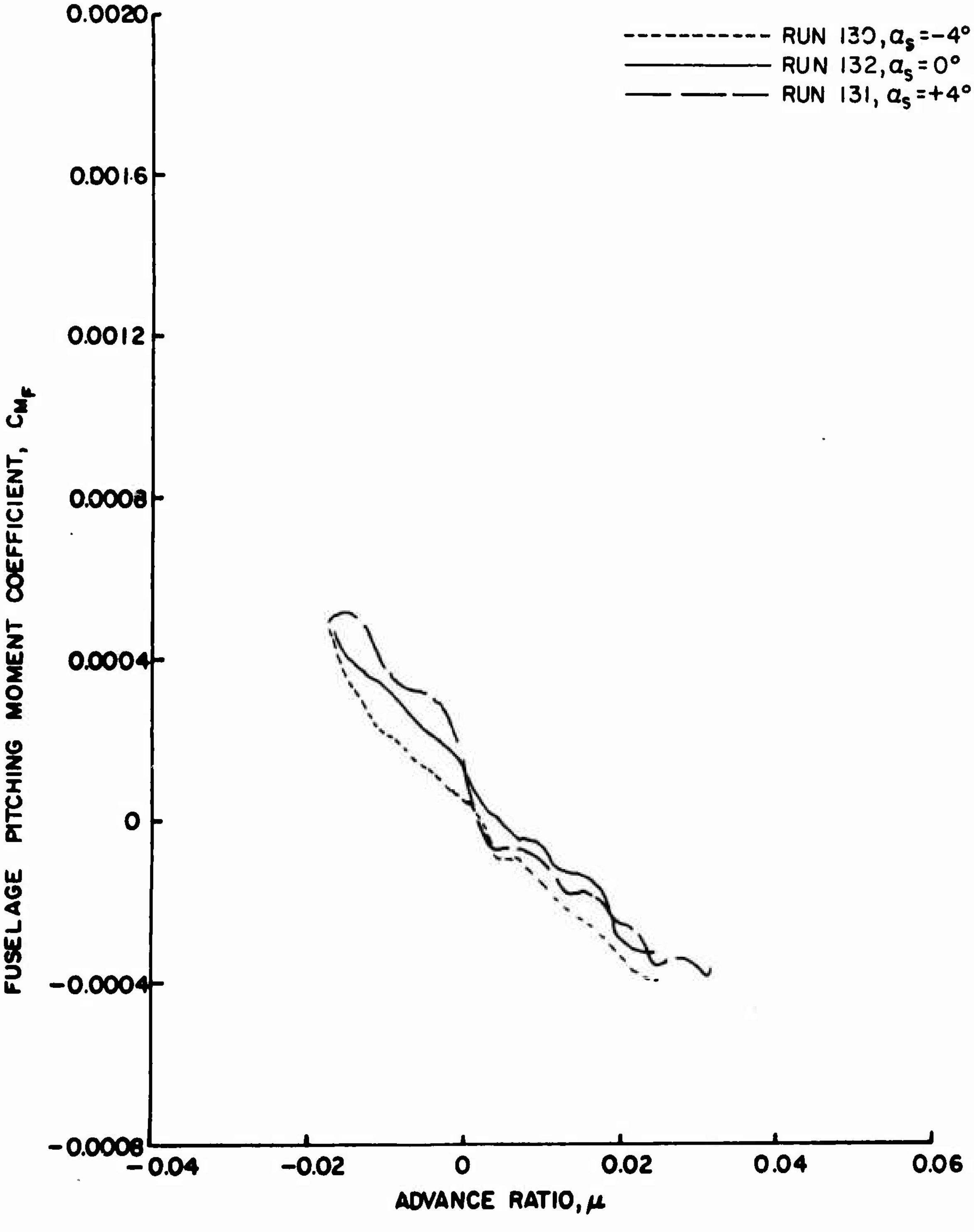

Figure 85. Fuselage Vertical Force and Pitching Moment Coefficients as Functions of Advance Ratio, $\theta_{.75R} = 10^\circ$, Small Wing on High, $\frac{h}{D} = 0.75$.

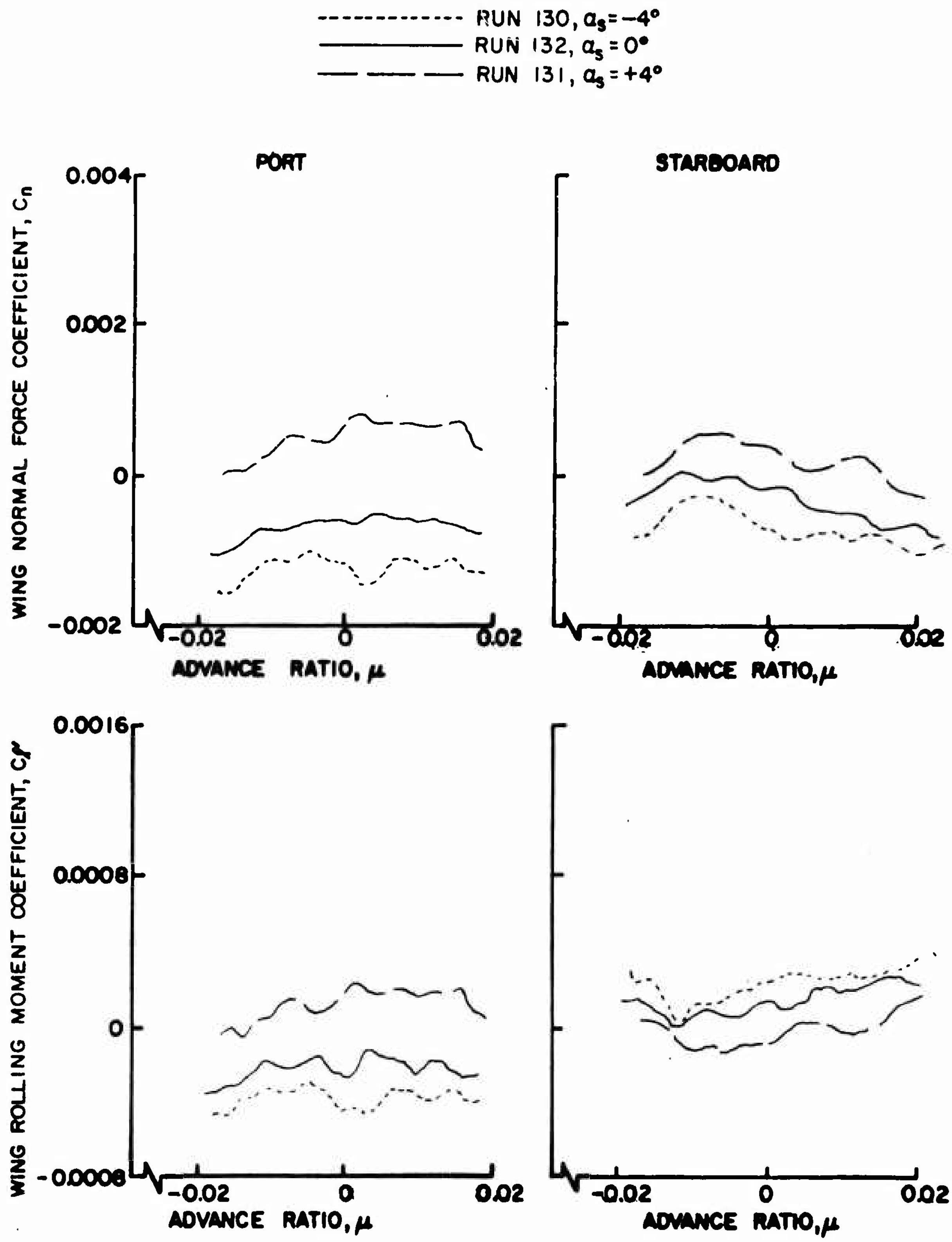

Figure 86. Wing Normal Force and Rolling Moment Coefficients as Functions of Advance Ratio, $\theta_{.75R} = 10°$, Small Wing on High, $\frac{h}{D} = 0.75$.

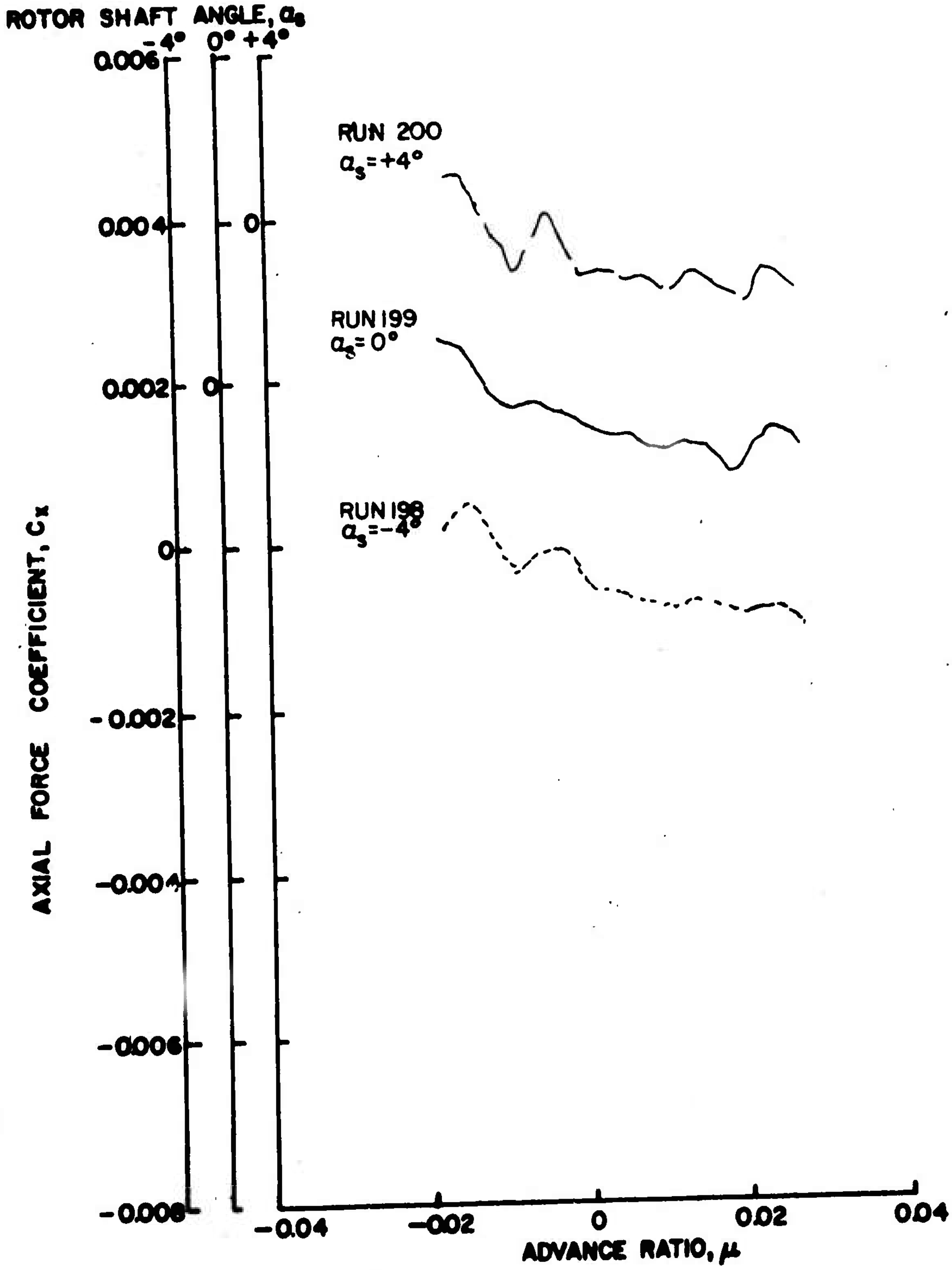

Figure 87a. Rotor Force and Moment Coefficients as Functions of Advance Ratio, $\theta_{.75R} = 8°$, Wing Off, Fuselage Off, $\frac{h}{D} = 0.30$.

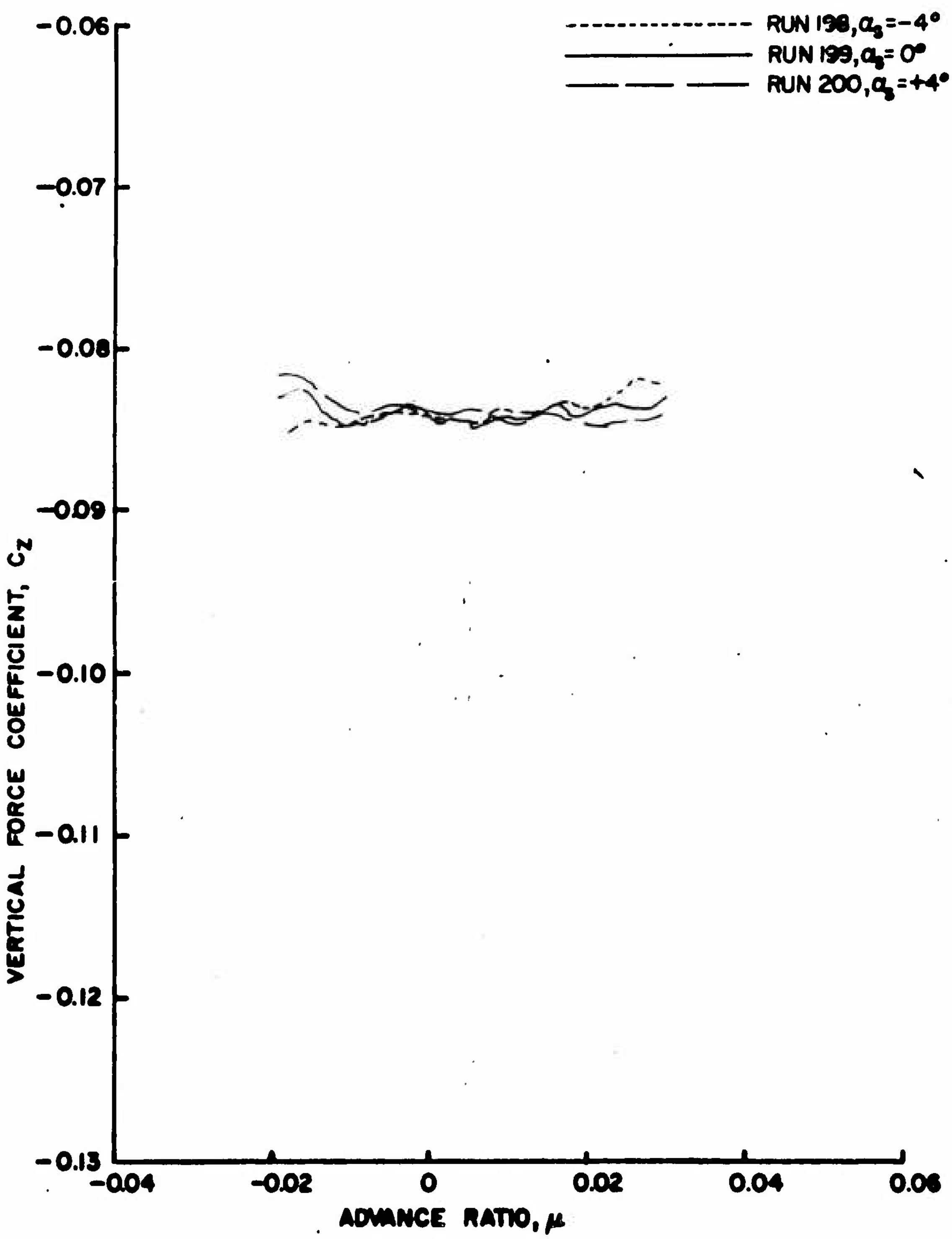

Figure 87b. Rotor Force and Moment Coefficients as Functions of Advance Ratio, $\theta_{.75R} = 8^\circ$, Wing Off, Fuselage Off, $\frac{h}{D} = 0.30$.

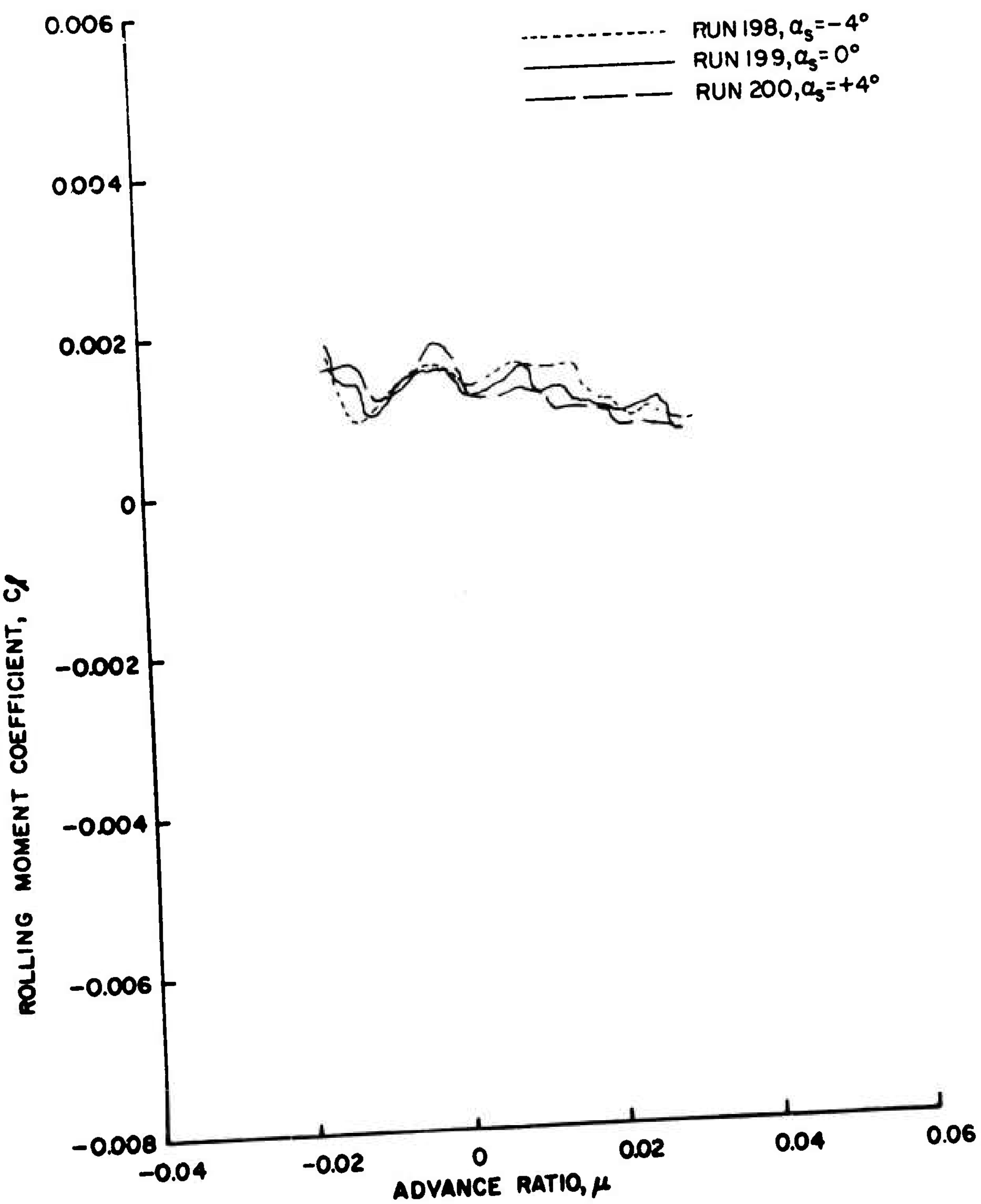

Figure 87c. Rotor Force and Moment Coefficients as Functions of Advance Ratio, $\theta_{.75R} = 8°$, Wing Off, Fuselage Off, $\frac{h}{D} = 0.30$.

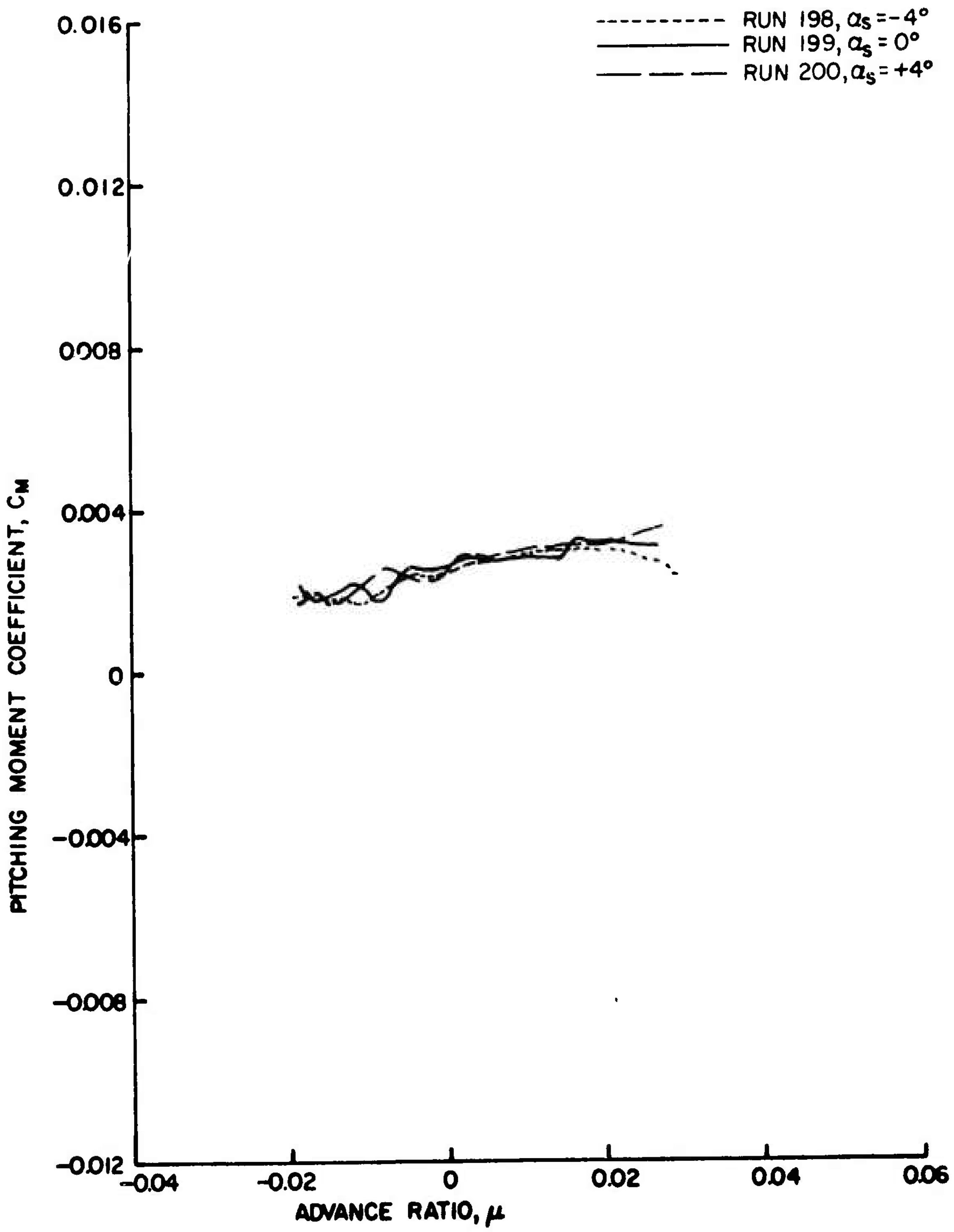

Figure 87d. Rotor Force and Moment Coefficients as Functions of Advance Ratio, $\theta_{.75R} = 8°$, Wing Off, Fuselage Off, $\frac{h}{D} = 0.30$.

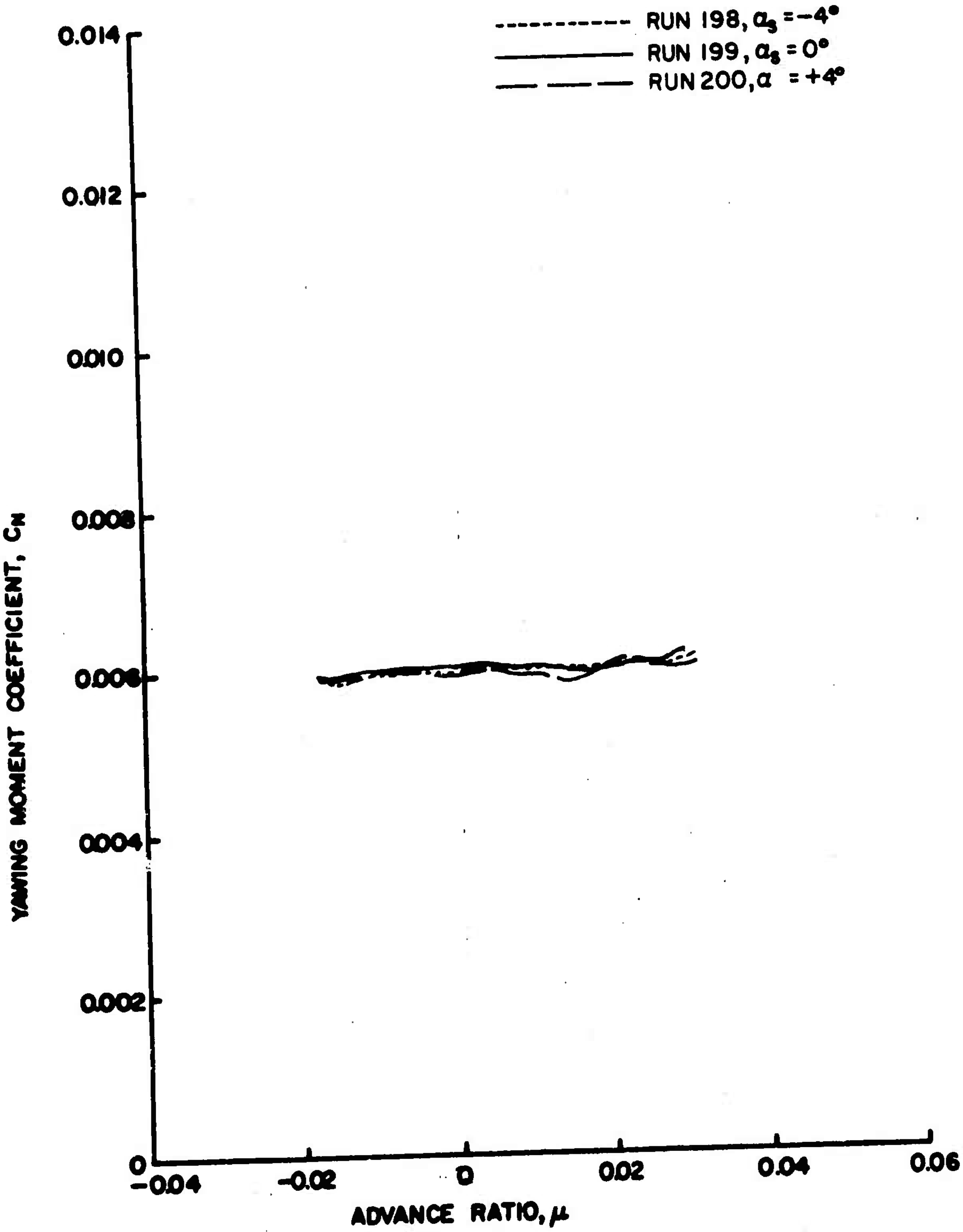

Figure 87e. Rotor Force and Moment Coefficients as Functions of Advance Ratio, $\theta_{.75R} = 8^\circ$, Wing Off, Fuselage Off, $\frac{h}{D} = 0.30$.

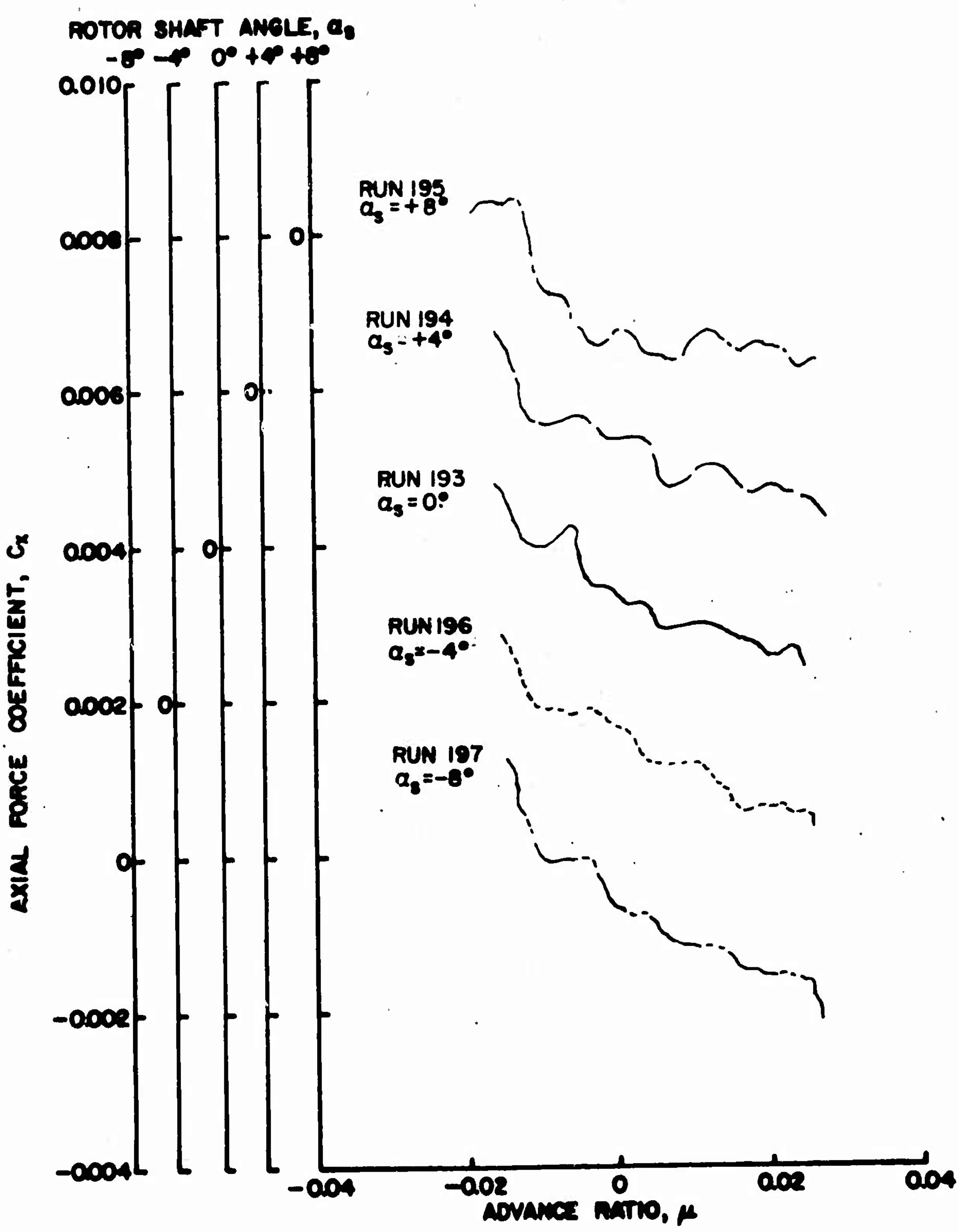

Figure 88a. Rotor Force and Moment Coefficients as Functions of Advance Ratio, $\theta_{.75R} = 10^{\circ}$, Wing Off, Fuselage Off, $\frac{h}{D} = 0.30$.

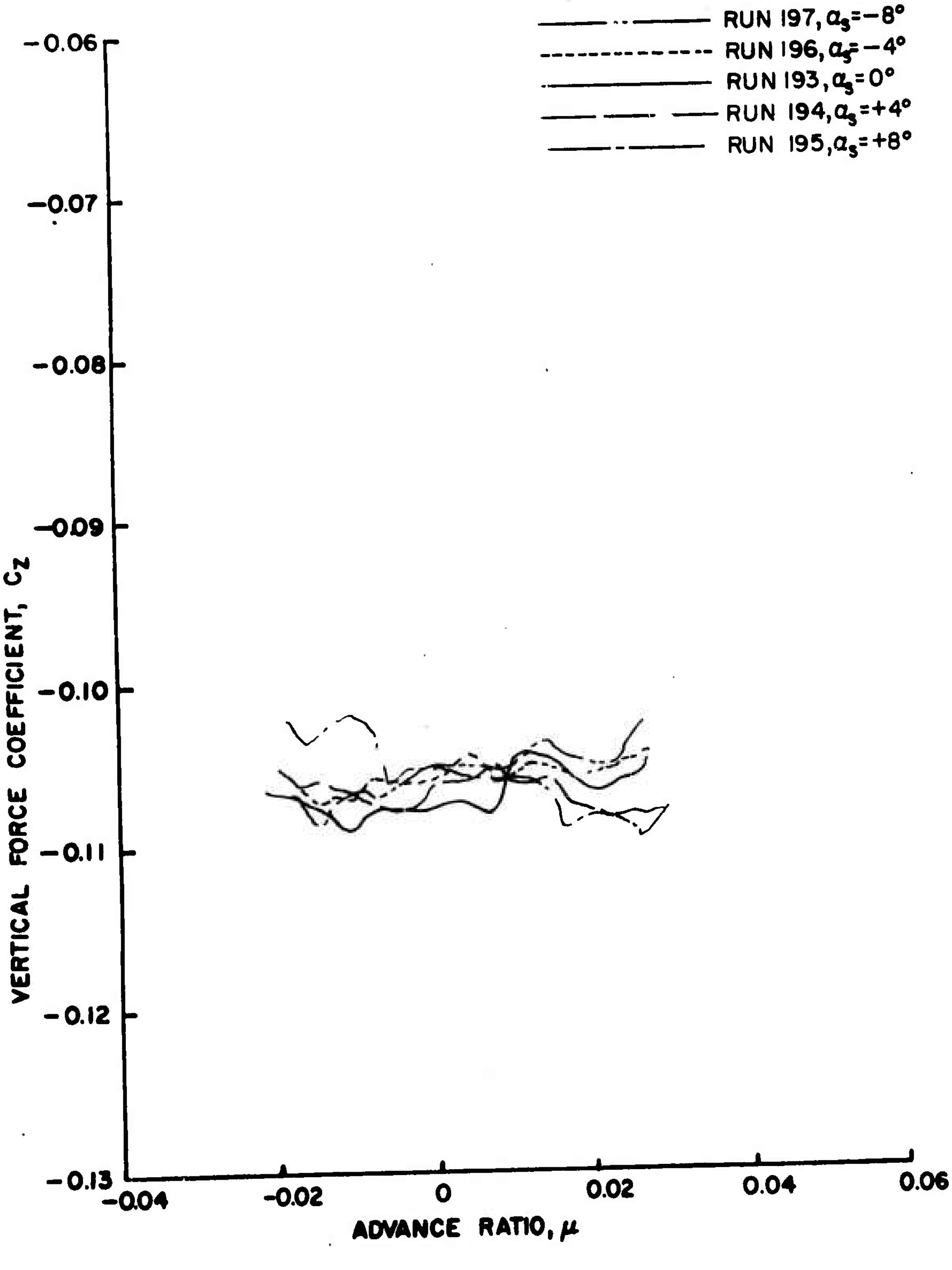

Figure 88b. Rotor Force and Moment Coefficients as Functions of Advance Ratio, $\theta_{.75R} = 10^\circ$, Wing Off, Fuselage Off, $\frac{h}{D}$ = 0.30.

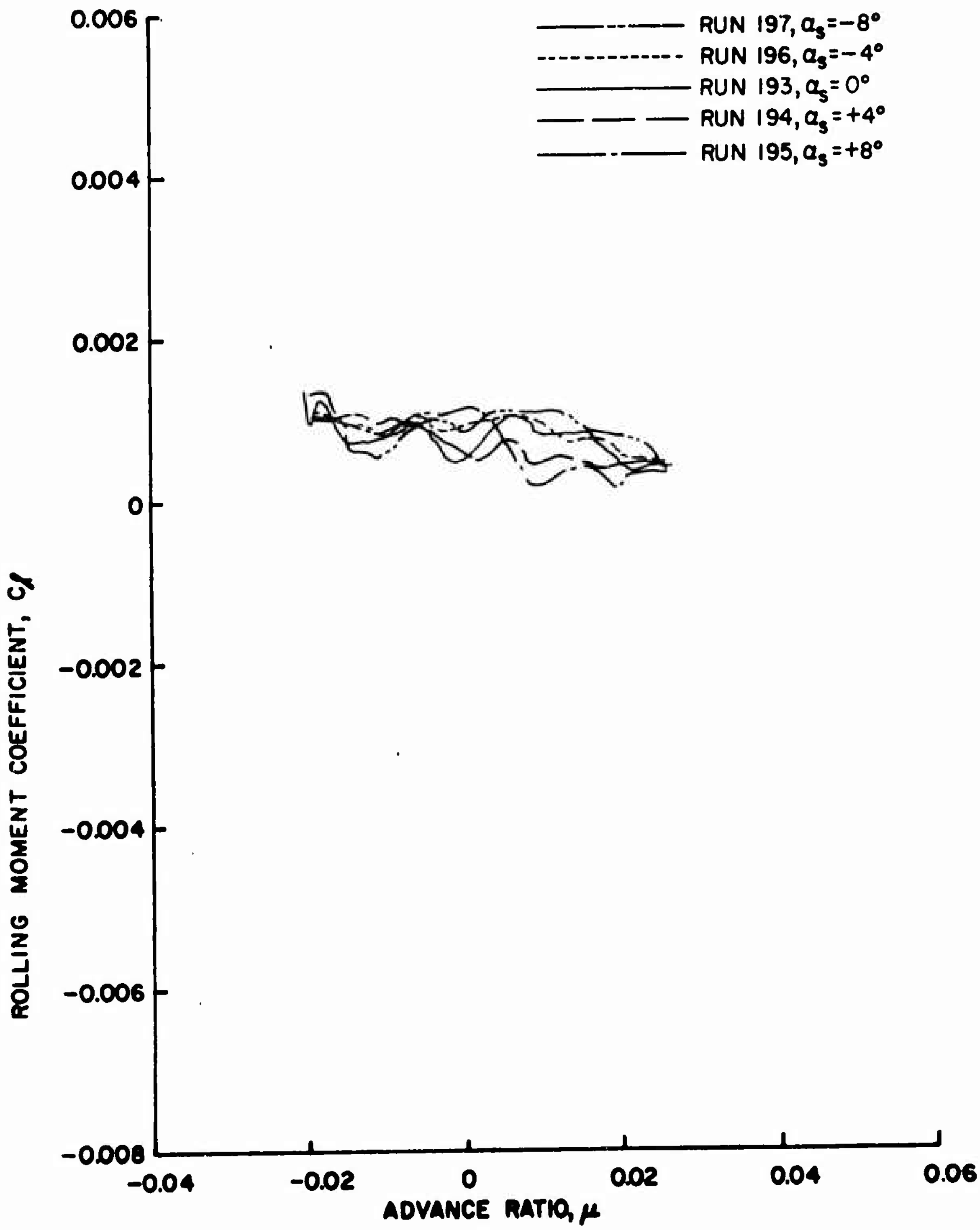

Figure 88c. Rotor Force and Moment Coefficients as Functions of Advance Ratio, $\theta_{.75R} = 10^\circ$, Wing Off, Fuselage Off, $\frac{h}{D} = 0.30$.

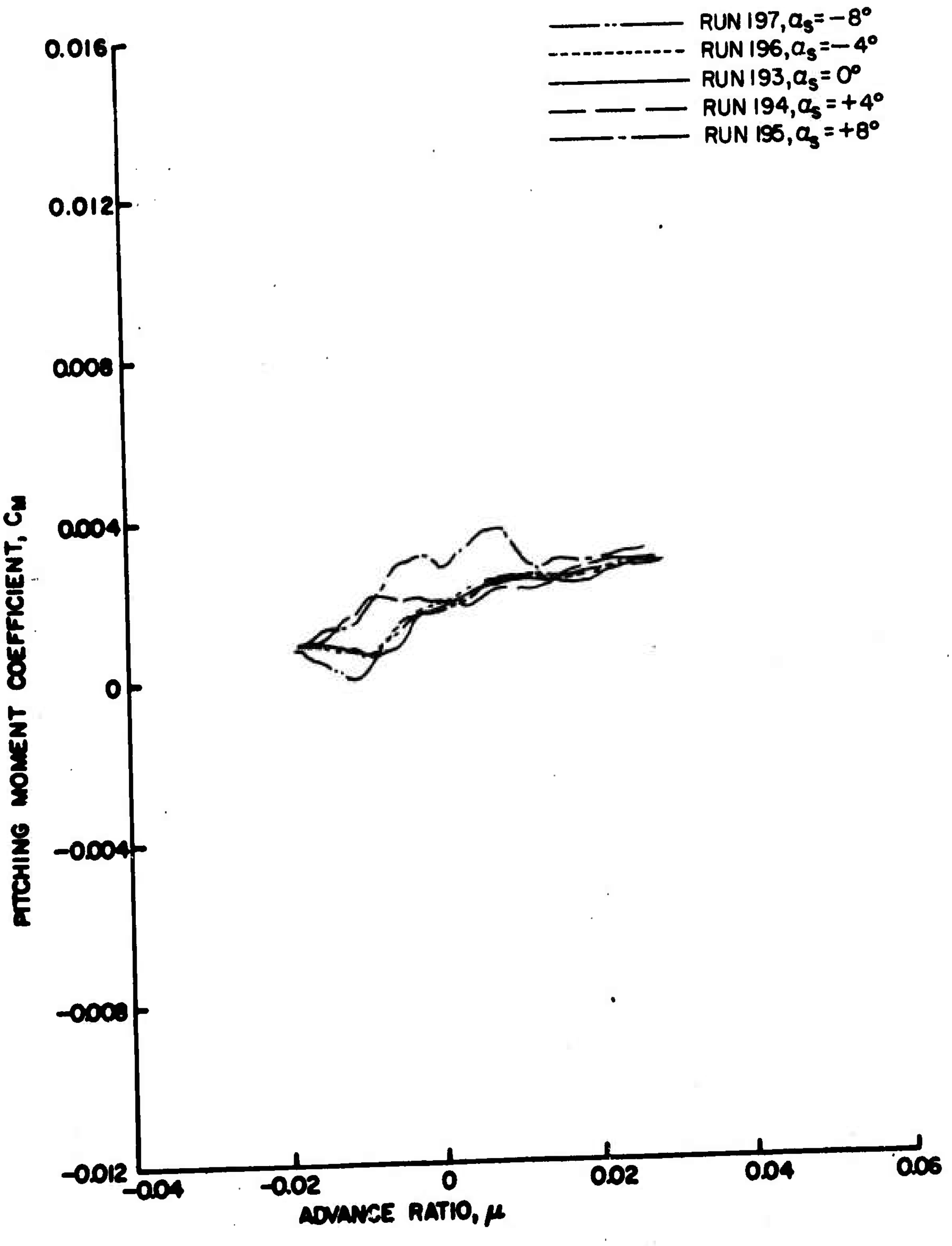

Figure 88d. Rotor Force and Moment Coefficients as Functions of Advance Ratio, $\theta_{.75R} = 10°$, Wing Off, Fuselage Off, $\frac{h}{D} = 0.30$.

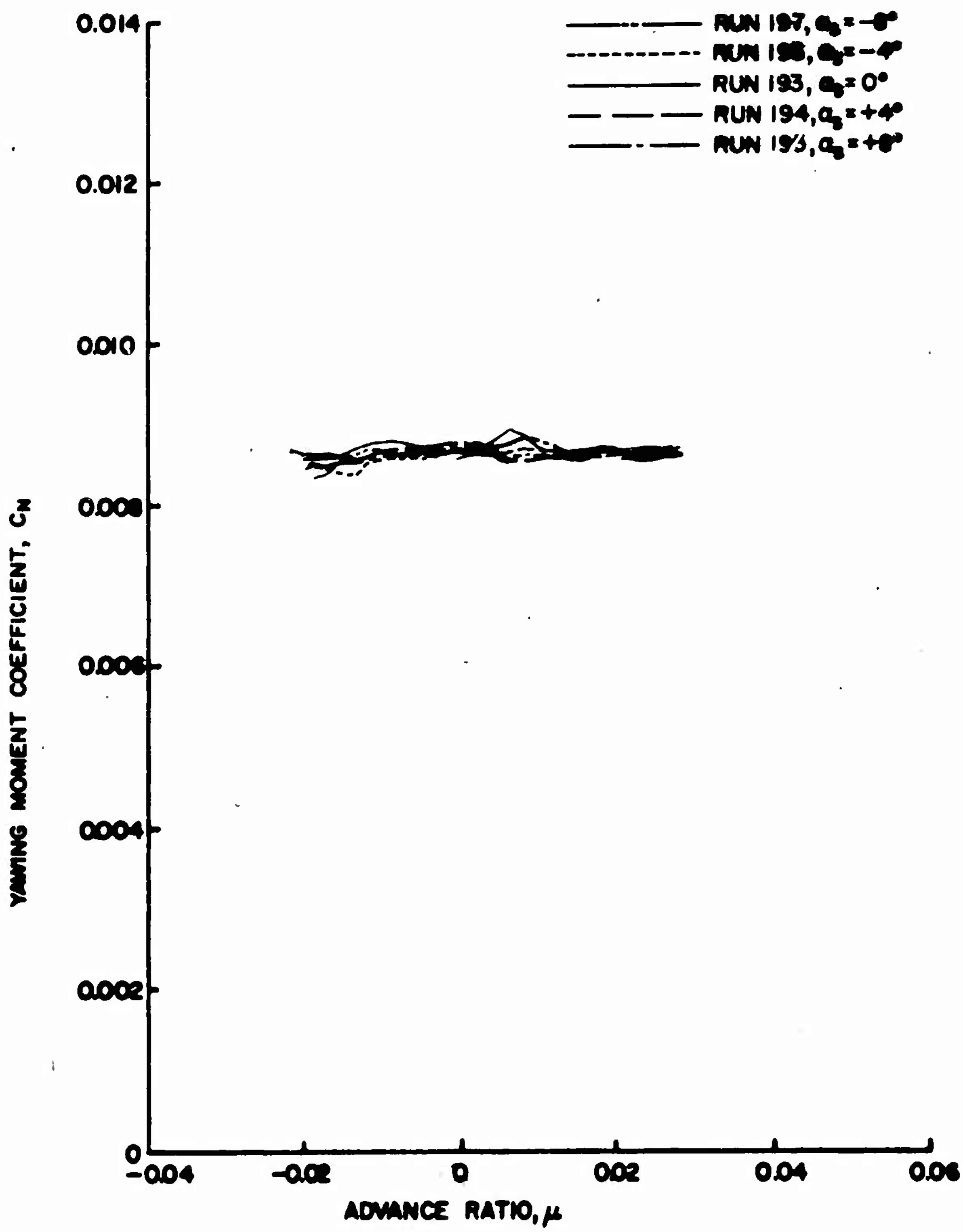

Figure 88e. Rotor Force and Moment Coefficients as Functions of Advance Ratio, $\theta_{.75R} = 10^\circ$, Wing Off, Fuselage Off, $\frac{h}{D} = 0.30$.

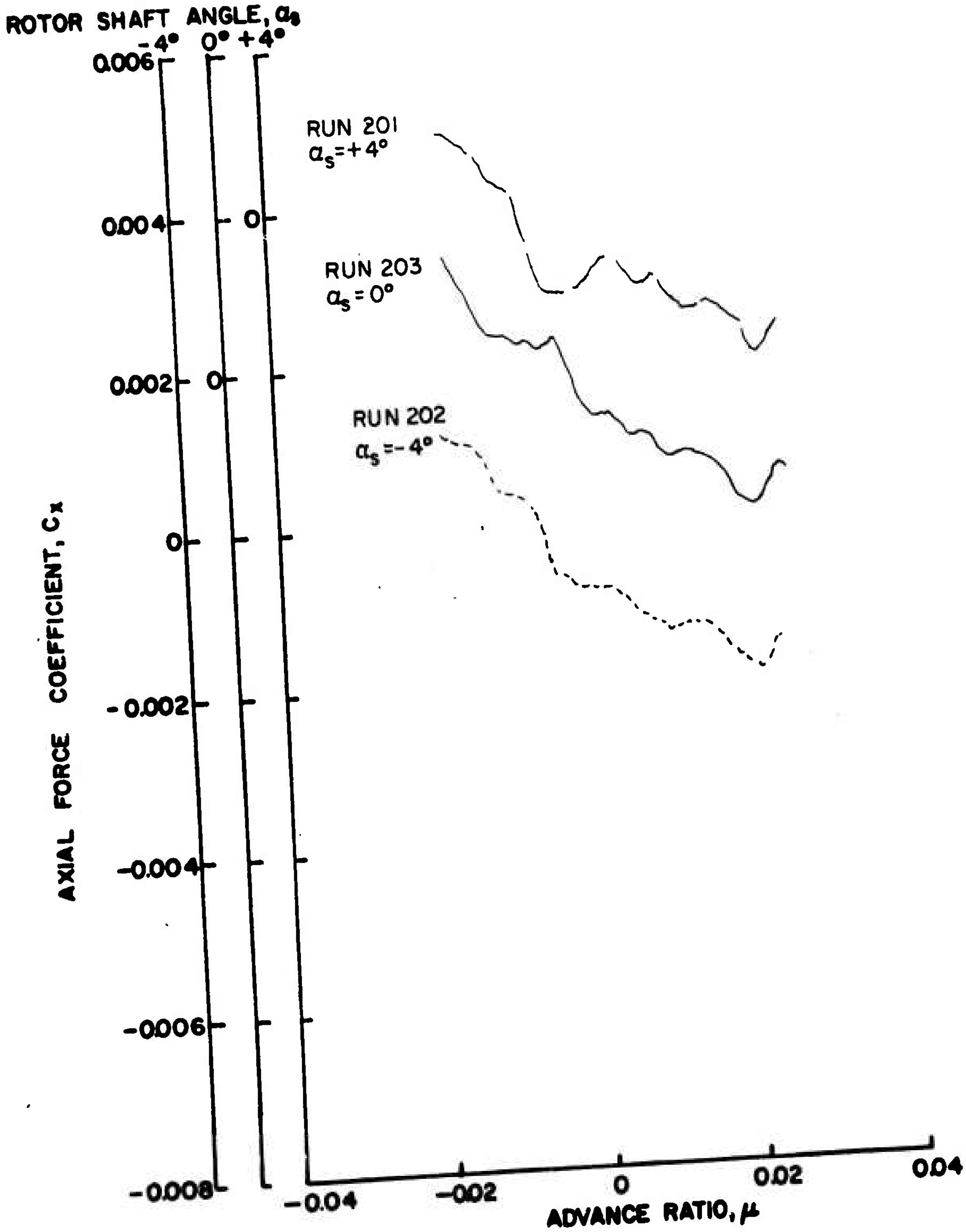

Figure 89a. Rotor Force and Moment Coefficients as Functions of Advance Ratio, $\theta_{.75R} = 12^\circ$, Wing Off, Fuselage Off, $\frac{h}{D} = 0.30$.

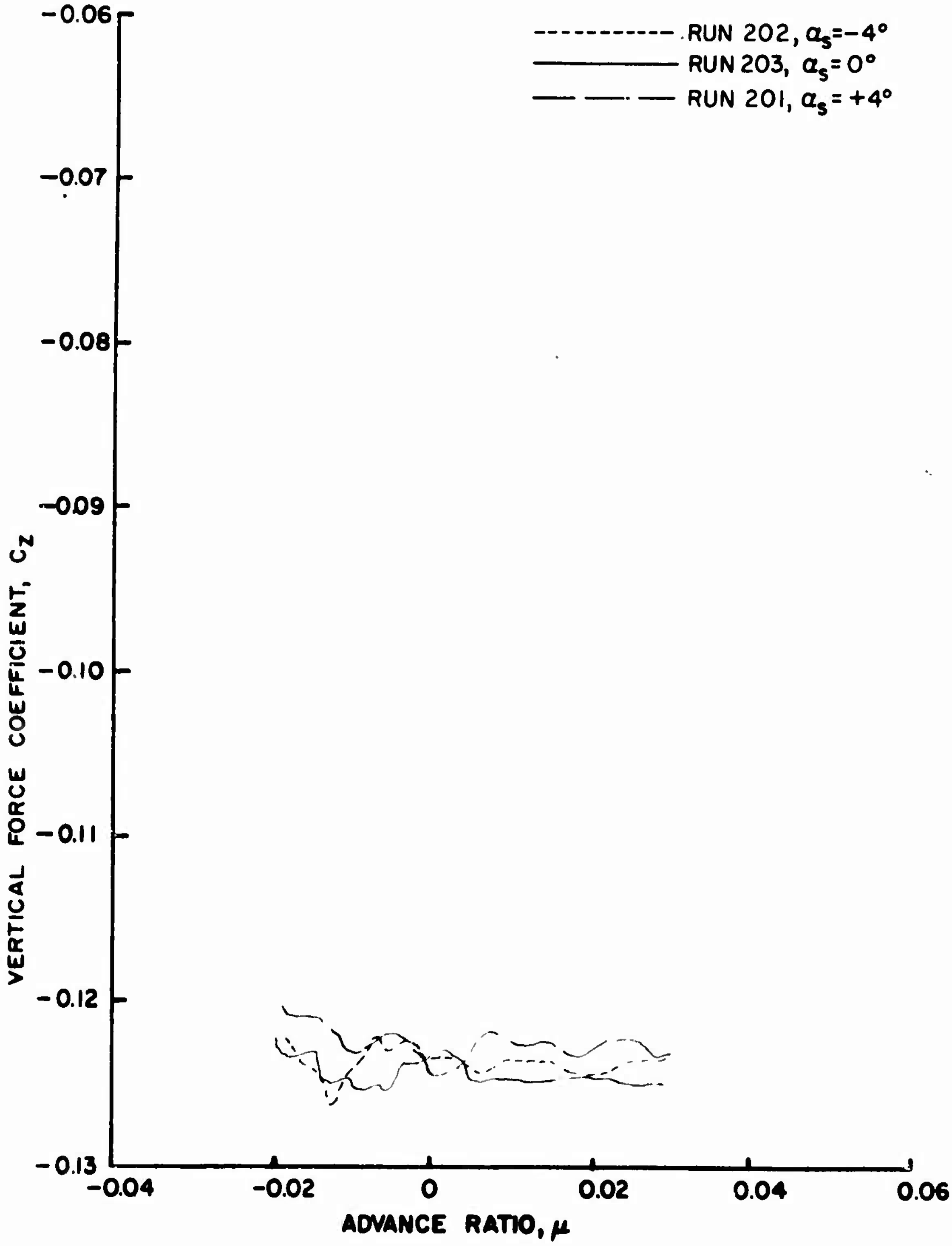

Figure 89b. Rotor Force and Moment Coefficients as Functions of Advance Ratio, $\theta_{.75R} = 12^\circ$, Wing Off, Fuselage Off, $\frac{h}{D} = 0.30$.

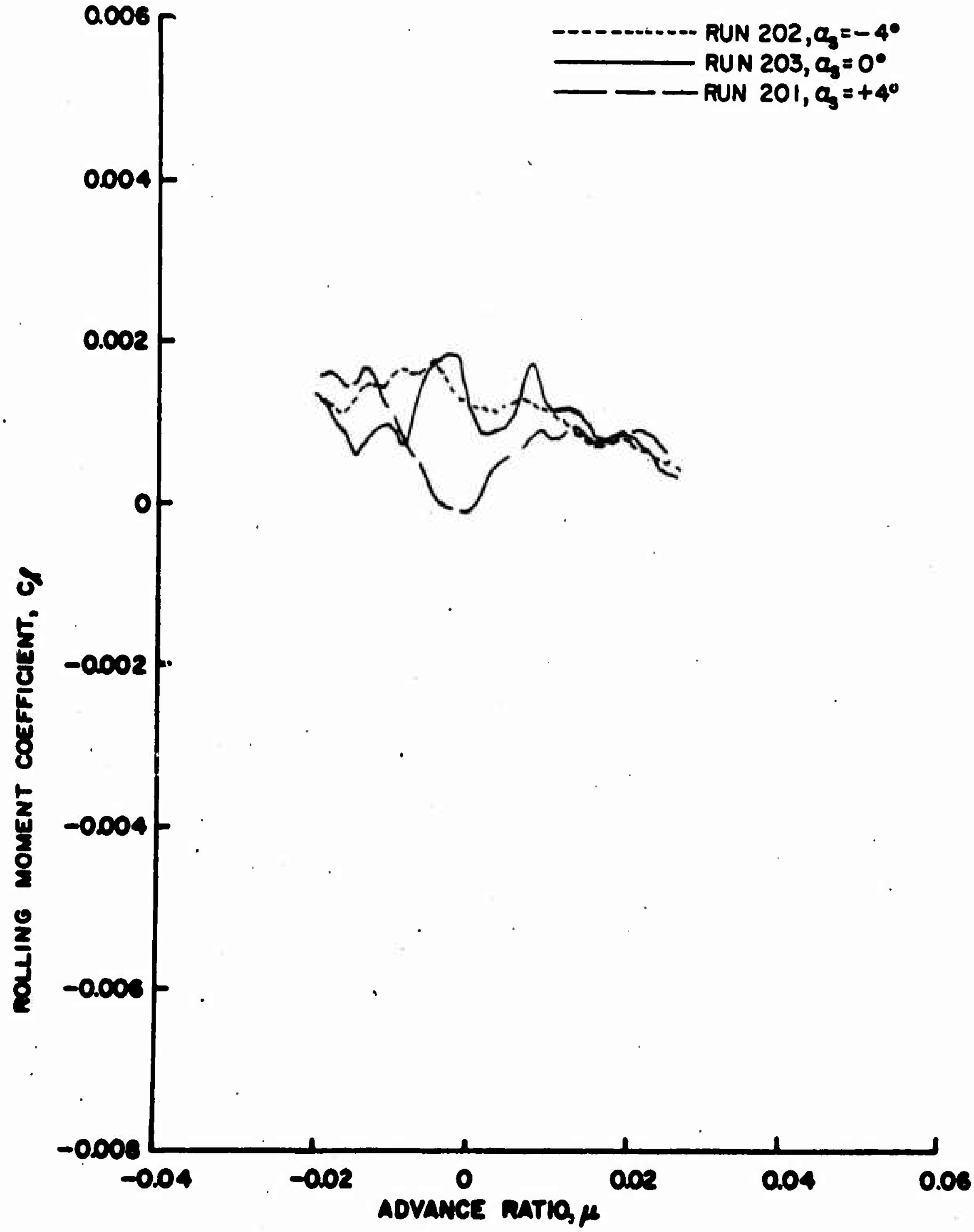

Figure 89c. Rotor Force and Moment Coefficients as Functions of Advance Ratio, $\theta_{.75R} = 12°$, Wing Off, Fuselage Off, $\frac{h}{D} = 0.30$.

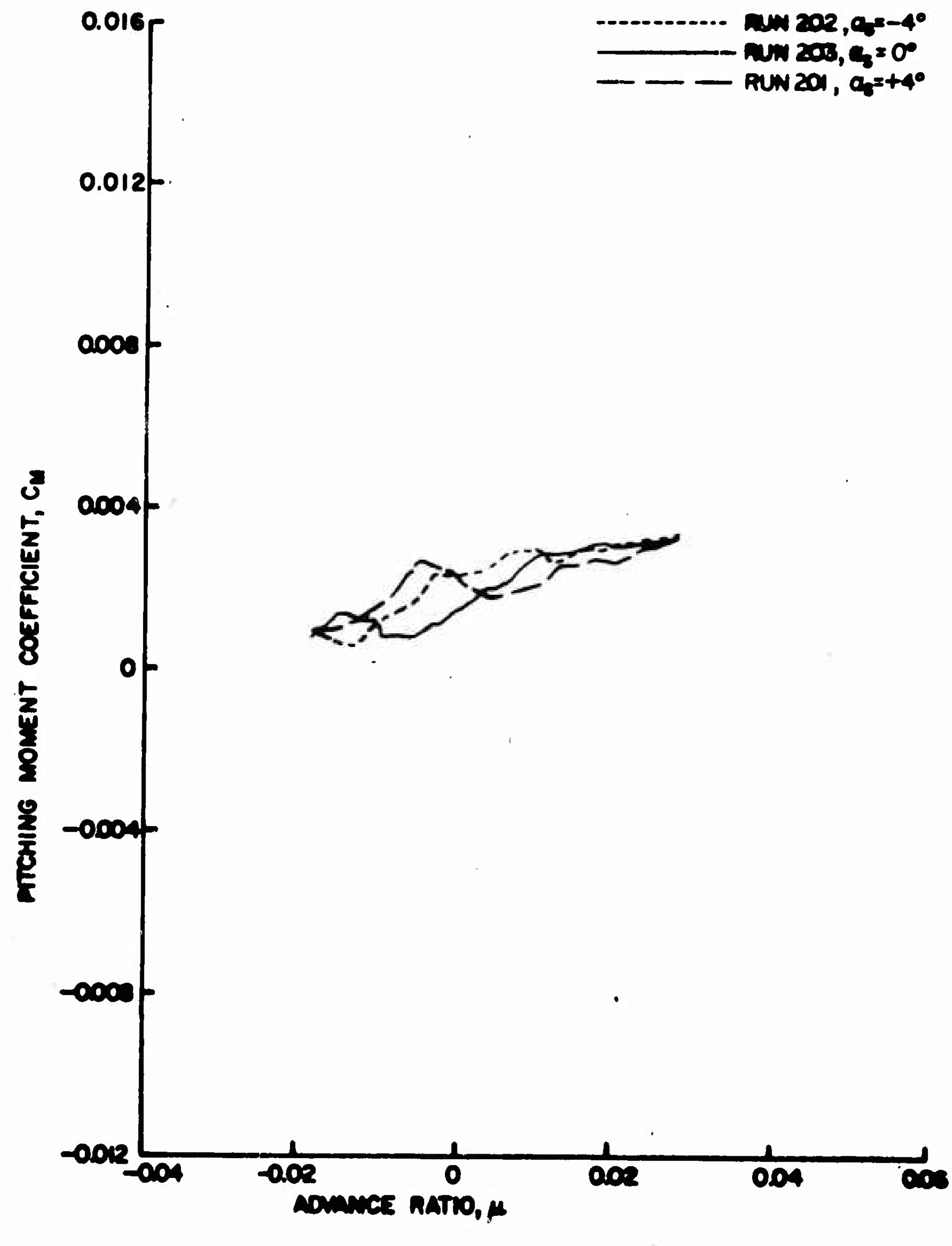

Figure 89d. Rotor Force and Moment Coefficients as Functions of Advance Ratio, $\theta_{.75R} = 12°$, Wing Off, Fuselage Off, $\frac{h}{D} = 0.30$.

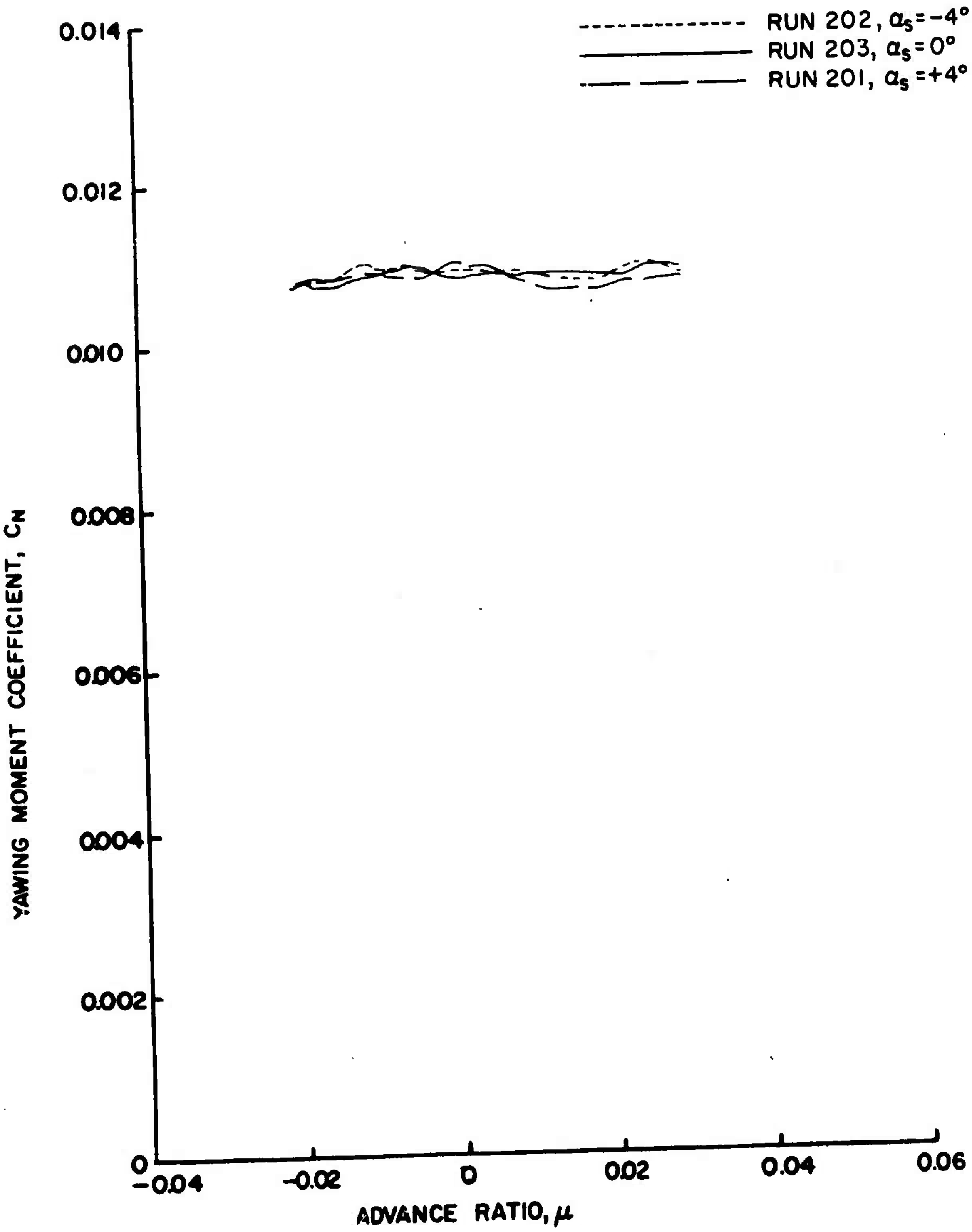

Figure 89e. Rotor Force and Moment Coefficients as Functions of Advance Ratio, $\theta_{.75R} = 12°$, Wing Off, Fuselage Off, $\frac{h}{D} = 0.30$.

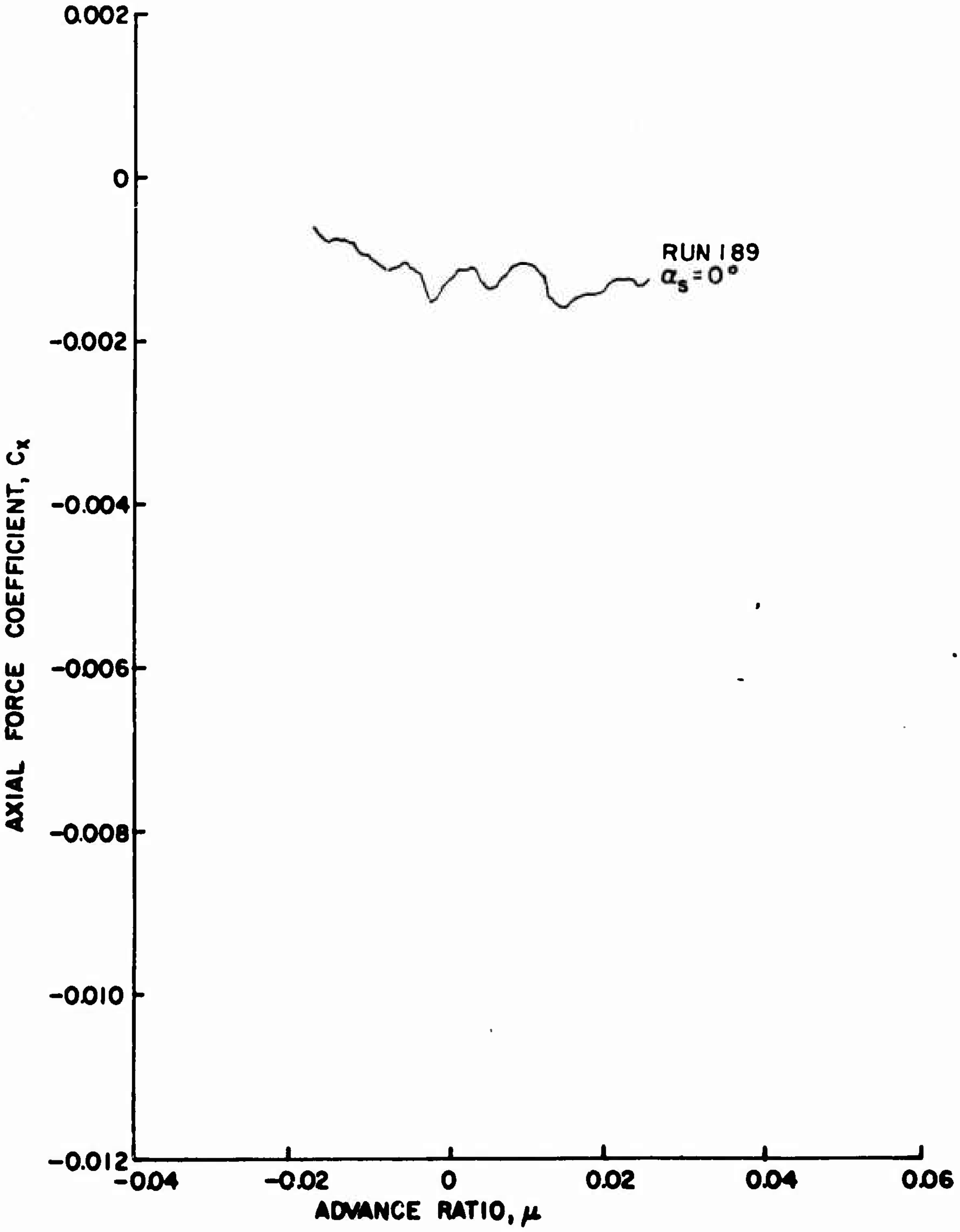

Figure 90a. Rotor Force and Moment Coefficients as Functions of Advance Ratio, $\theta_{.75R} = 8°$, Wing Off, Fuselage On, $\frac{h}{D} = 0.30$.

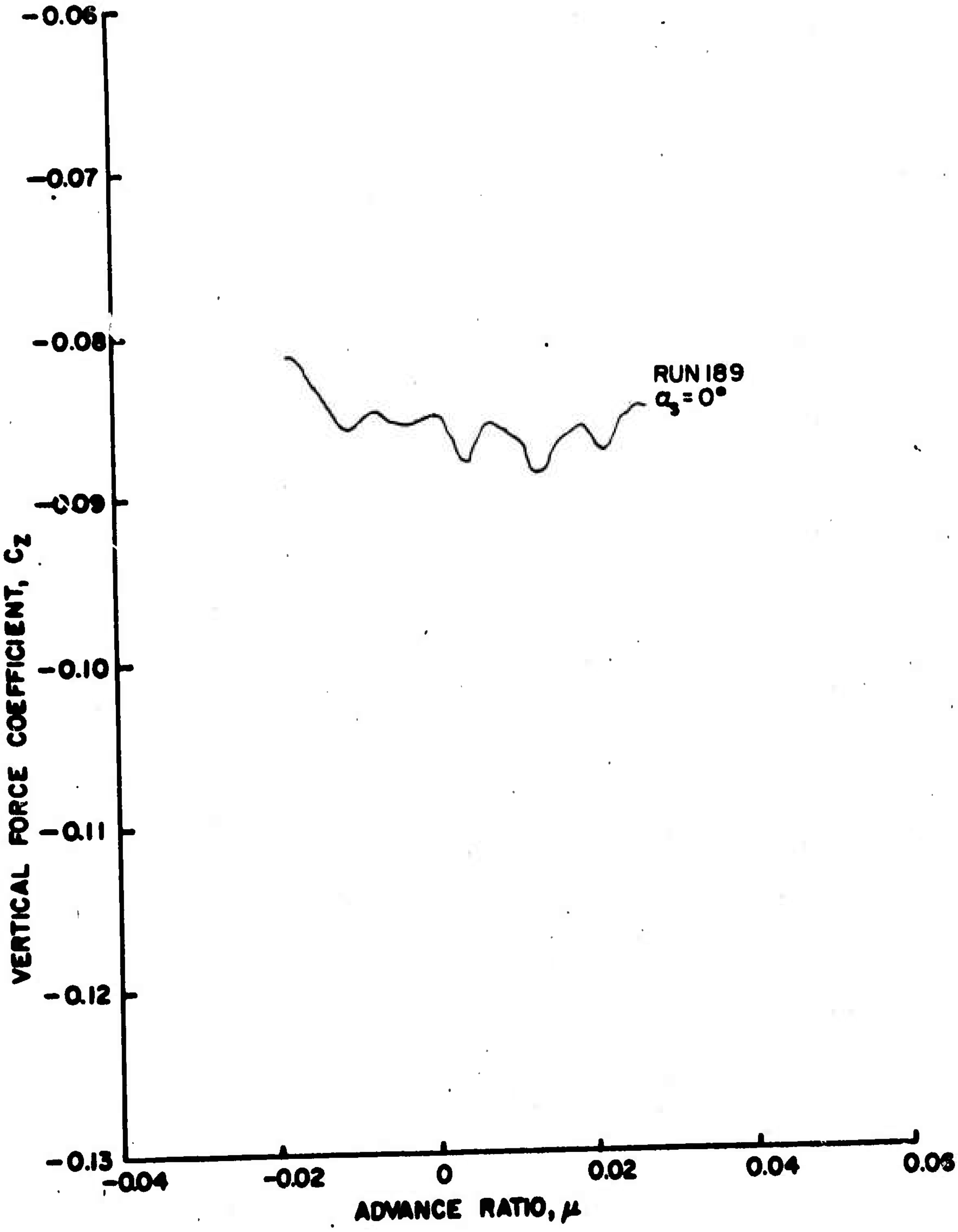

Figure 90b. Rotor Force and Moment Coefficients as Functions of Advance Ratio, $\theta_{.75R} = 8°$, Wing Off, Fuselage On, $\frac{h}{D} = 0.30$.

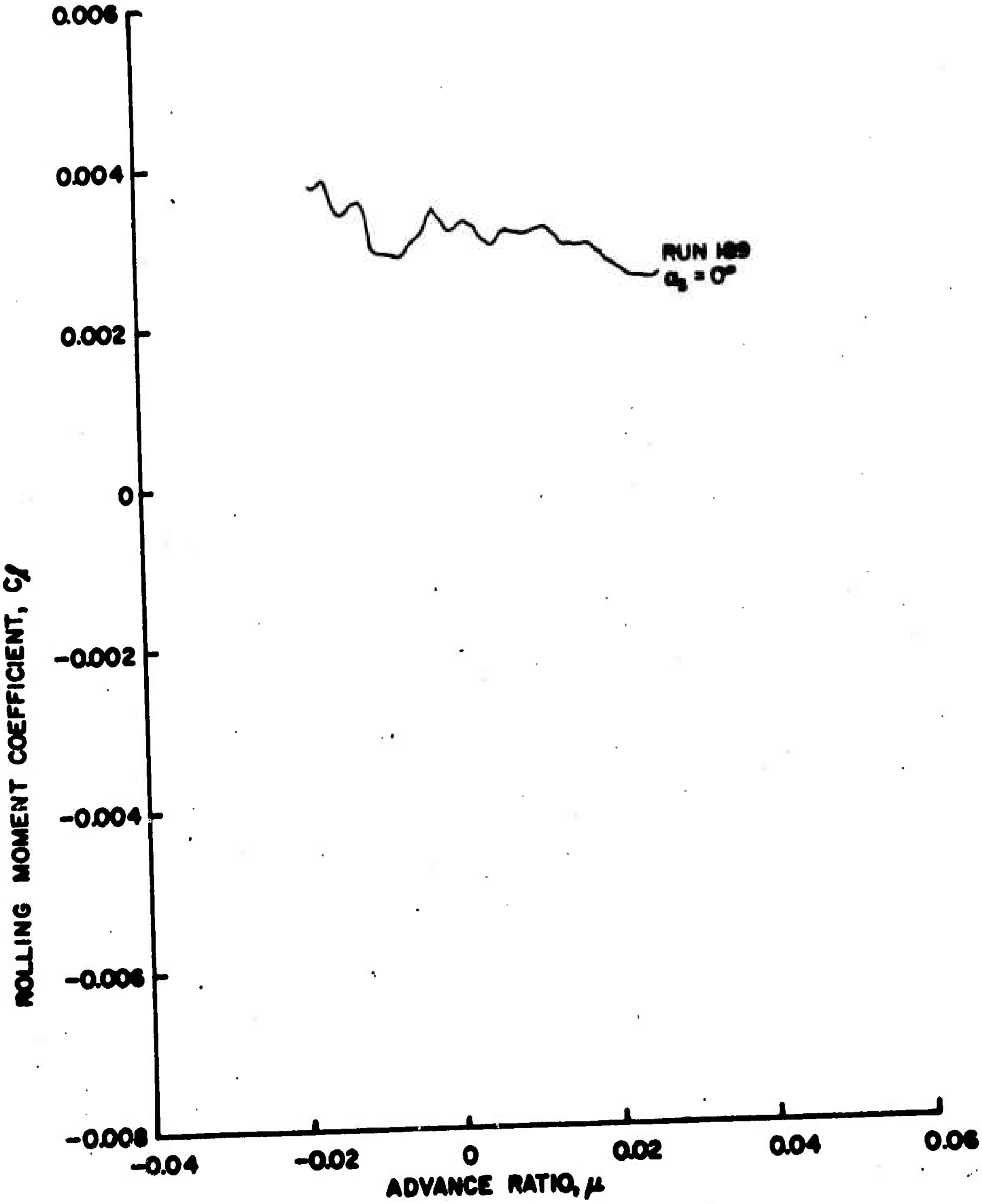

Figure 90c. Rotor Force and Moment Coefficients as Functions of Advance Ratio, $\theta_{.75R} = 8°$, Wing Off, Fuselage On, $\frac{h}{D} = 0.30$.

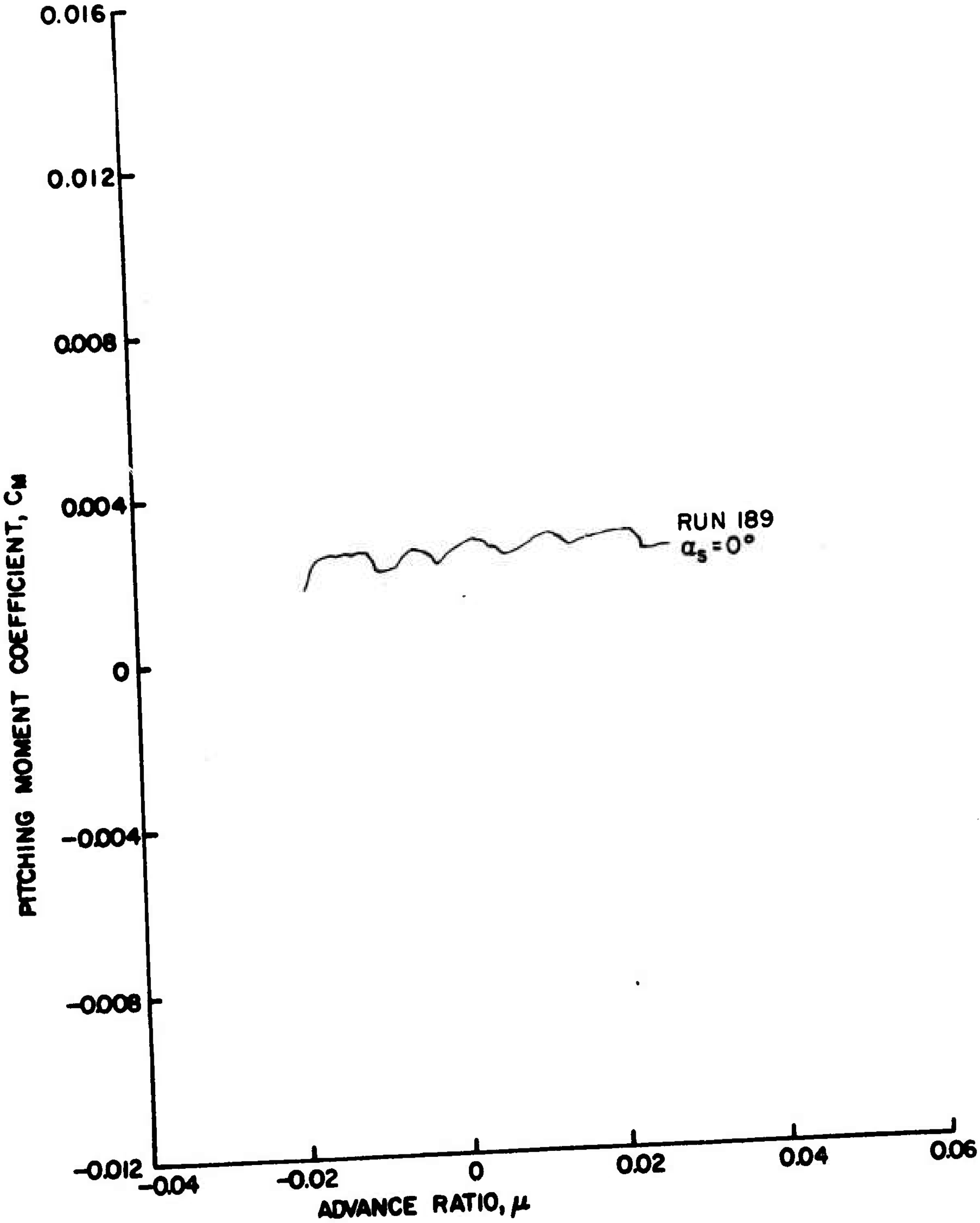

Figure 90d. Rotor Force and Moment Coefficients as Functions of Advance Ratio, $\theta_{.75R} = 8°$, Wing Off, Fuselage On, $\frac{h}{D} = 0.30$.

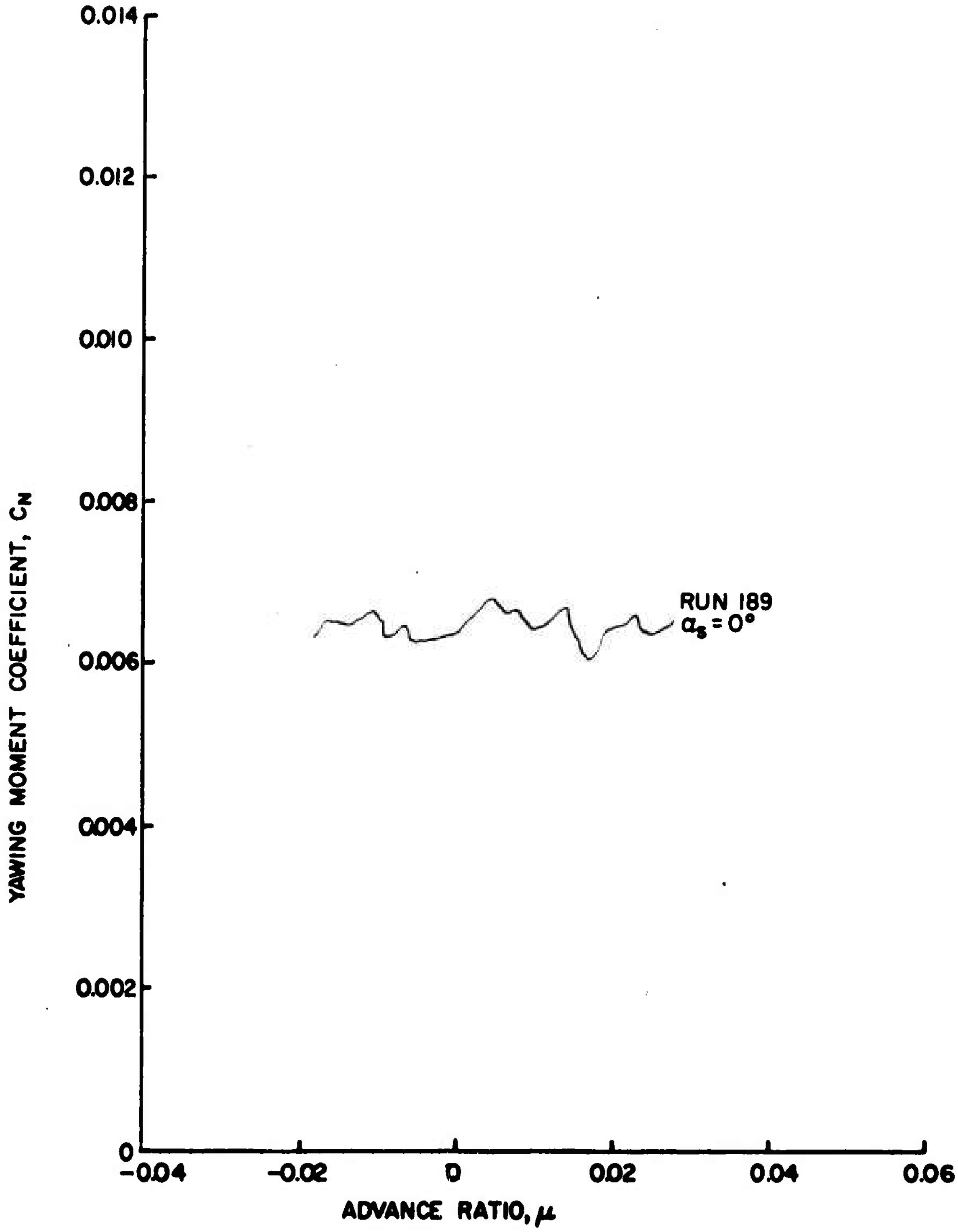

Figure 90e. Rotor Force and Moment Coefficients as Functions of Advance Ratio, $\theta_{.75R} = 8°$, Wing Off, Fuselage On, $\frac{h}{D} = 0.30$.

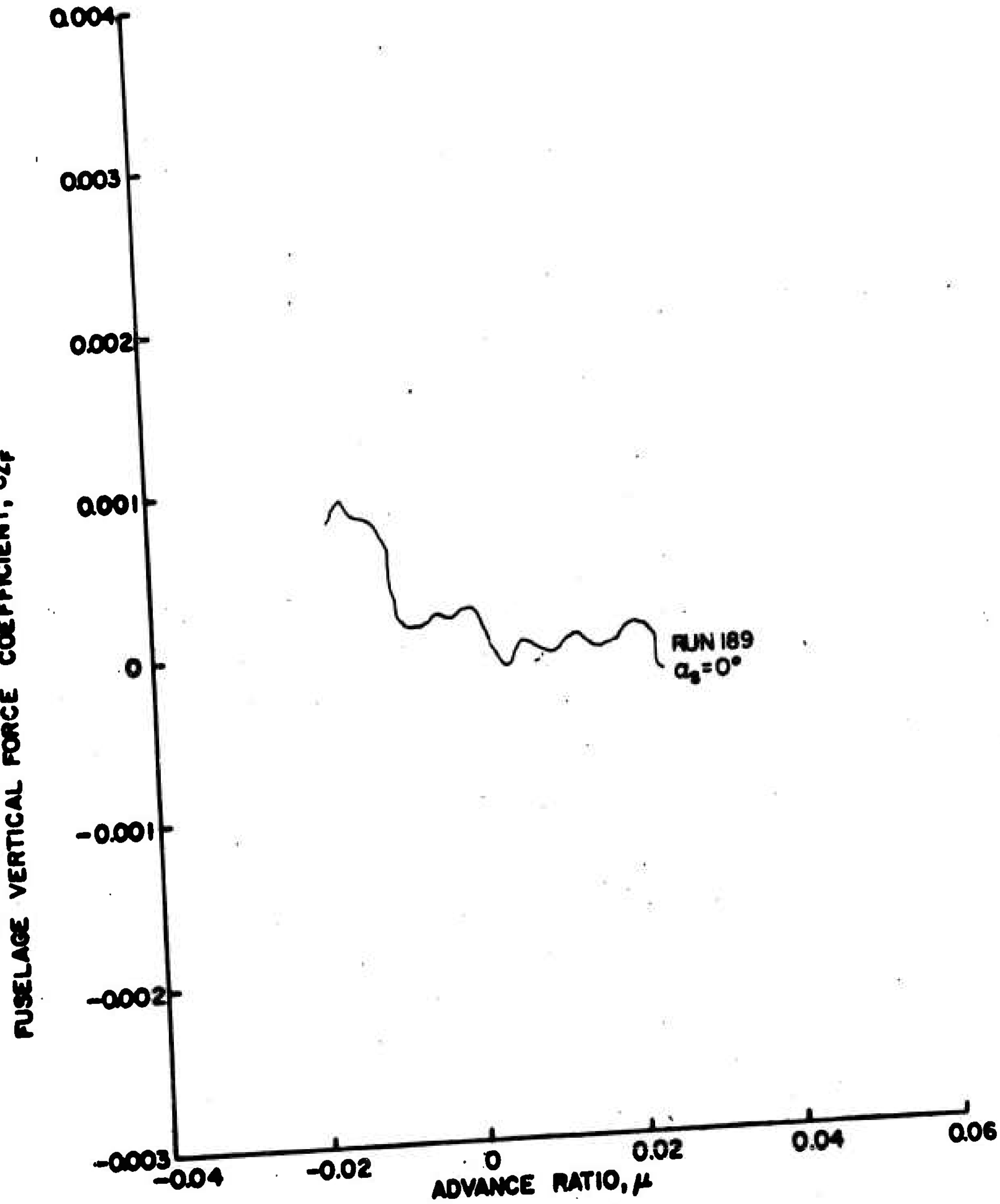

Figure 91a. Fuselage Vertical Force and Pitching Moment Coefficients as Functions of Advance Ratio, $\theta_{.75R} = 8°$, Wing Off, Fuselage On, $\frac{h}{D} = 0.30$.

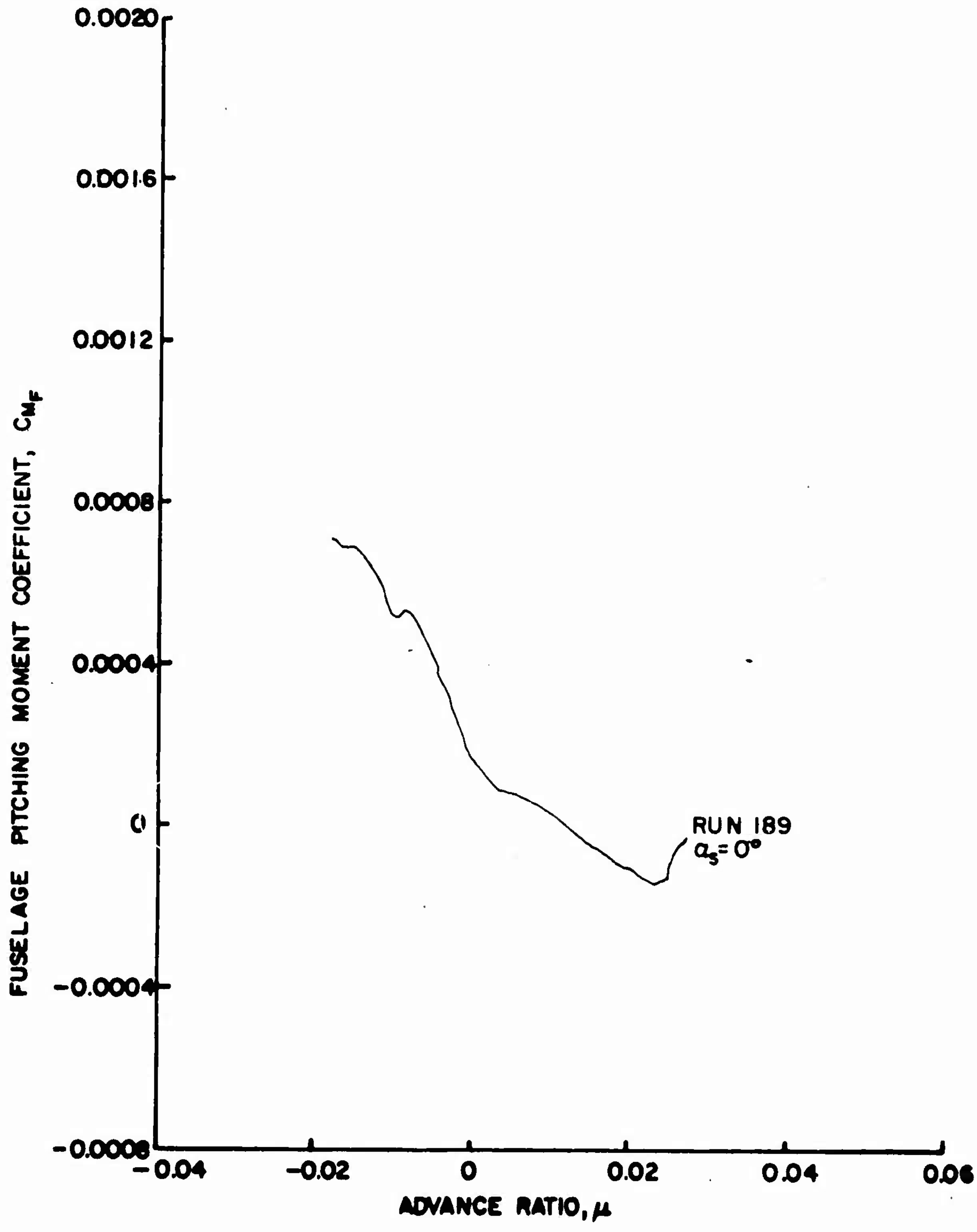

Figure 91b. Fuselage Vertical Force and Pitching Moment Coefficients as Functions of Advance Ratio, $\theta_{.75R} = 8°$, Wing Off, Fuselage On, $\frac{h}{D} = 0.30$.

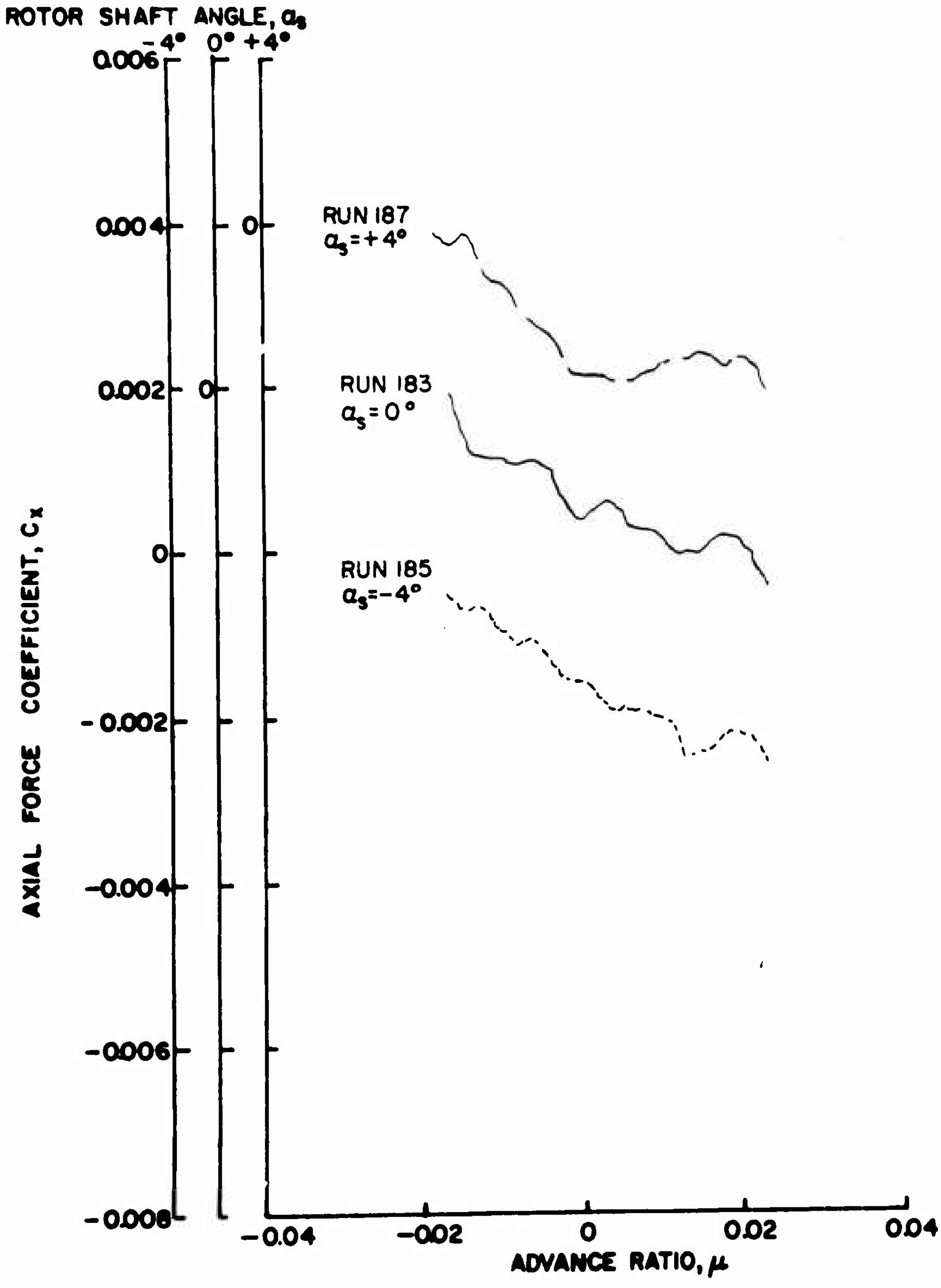

Figure 92a. Rotor Force and Moment Coefficients as Functions of Advance Ratio, $\theta_{.75}$ = 10°, Wing Off, Fuselage On, $\frac{h}{D}$ = 0.30.

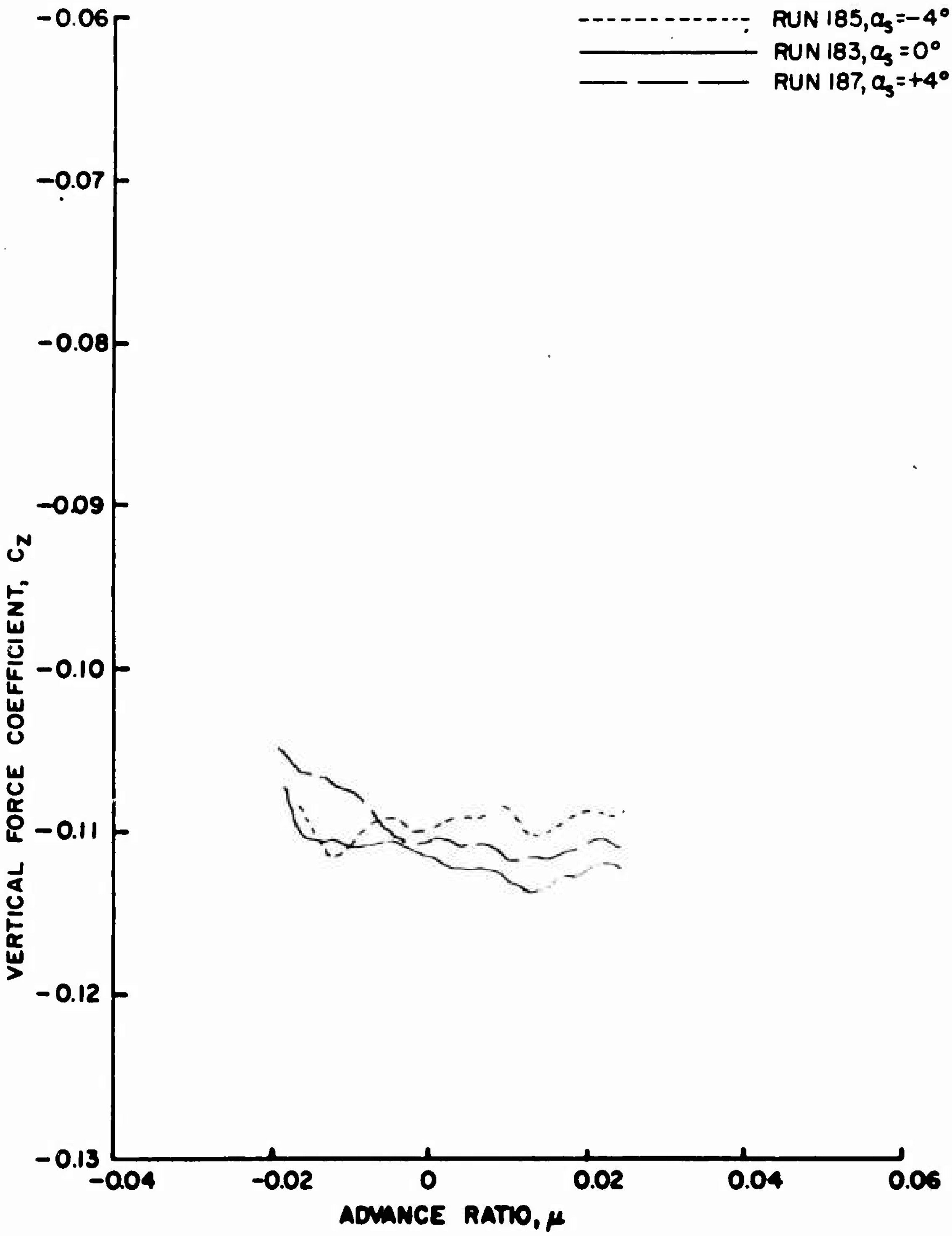

Figure 92b. Rotor Force and Moment Coefficients as Functions of Advance Ratio, $\theta_{.75R} = 10^\circ$, Wing Off, Fuselage On, $\frac{h}{D} = 0.30$.

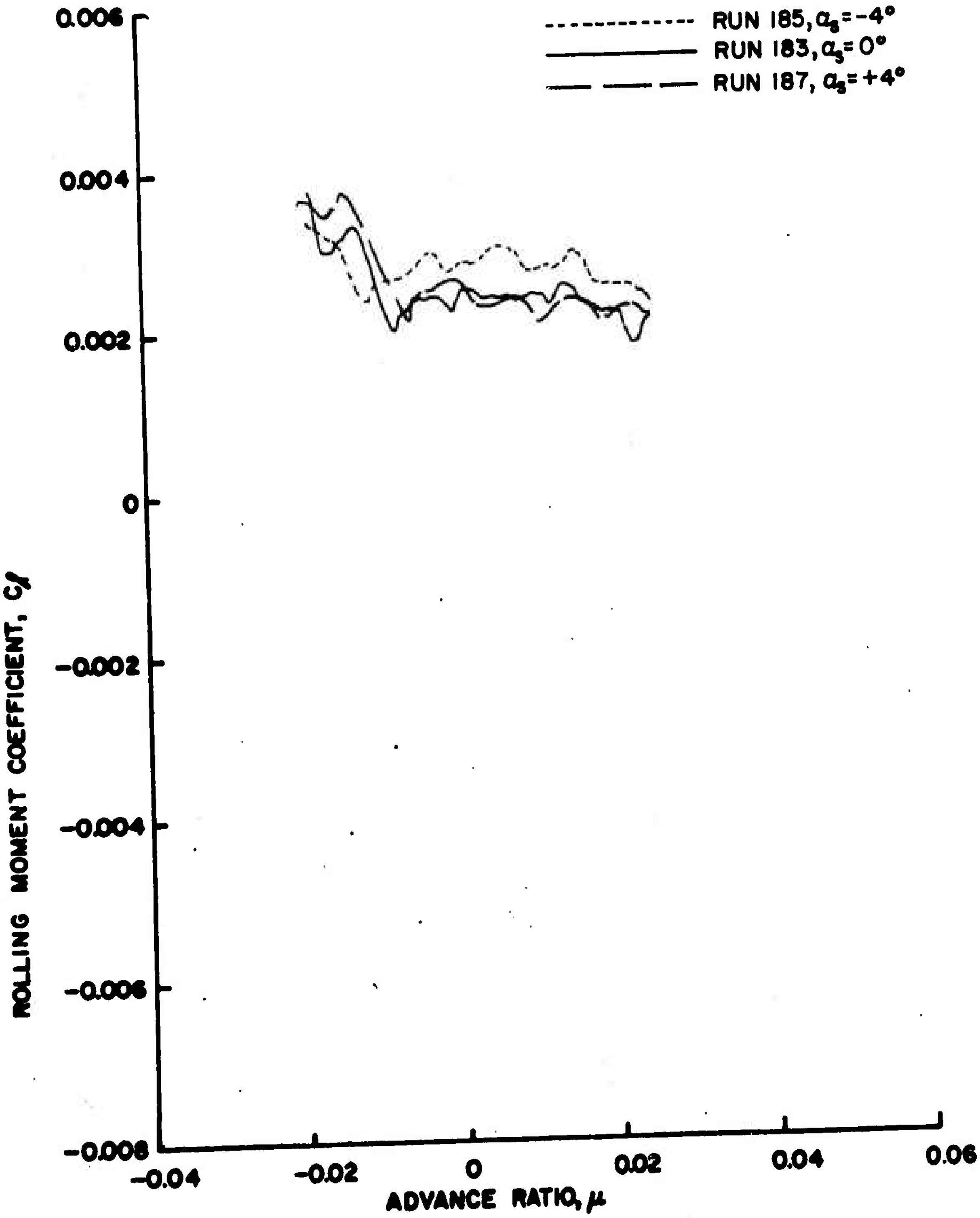

Figure 92c. Rotor Force and Moment Coefficients as Functions of Advance Ratio, $\theta_{.75R}$ = 10° , Wing Off, Fuselage On, $\frac{h}{D}$ = 0.30.

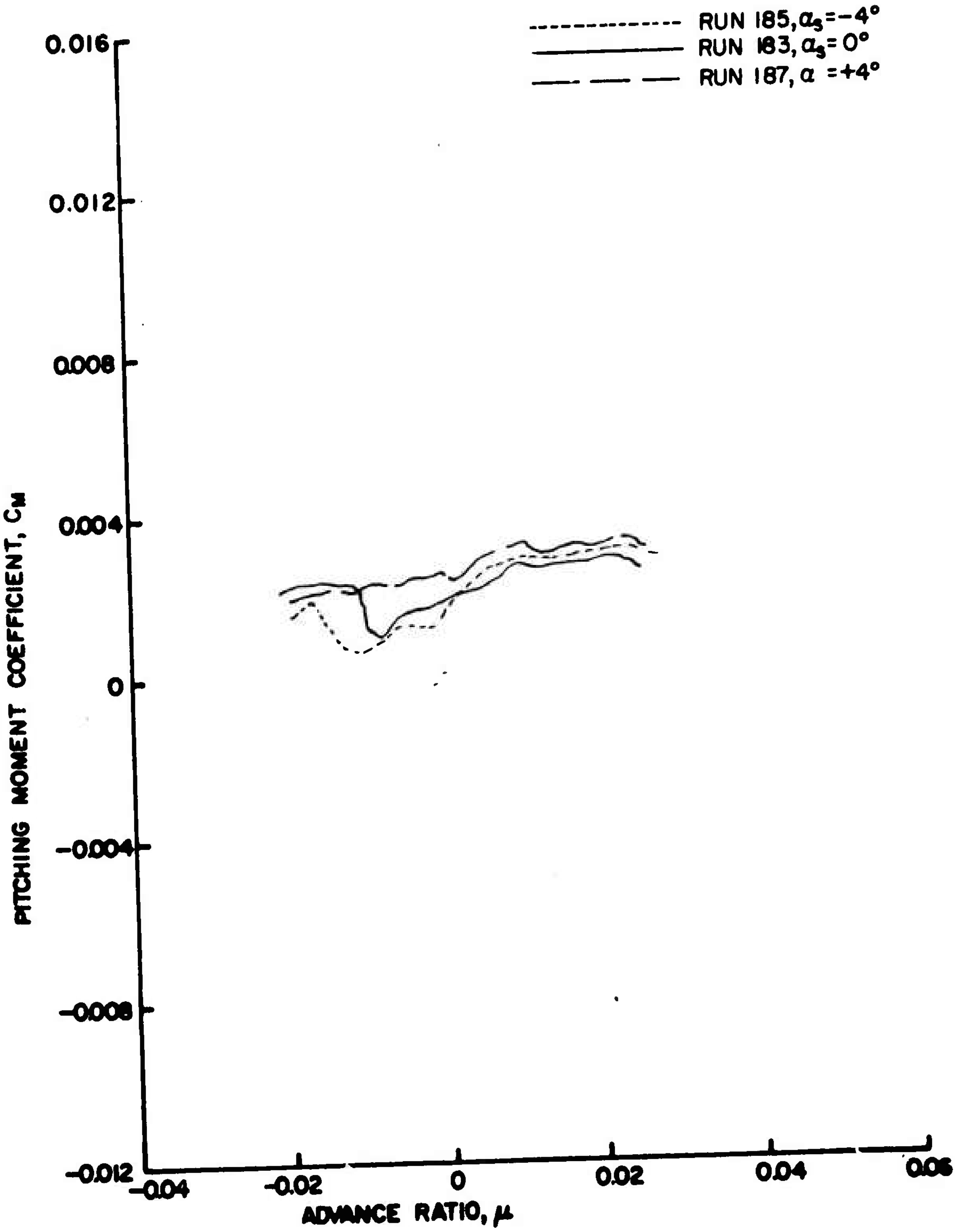

Figure 92d. Rotor Force and Moment Coefficients as Functions of Advance Ratio, $\theta_{.75R} = 10^\circ$, Wing Off, Fuselage On, $\frac{h}{D} = 0.30$.

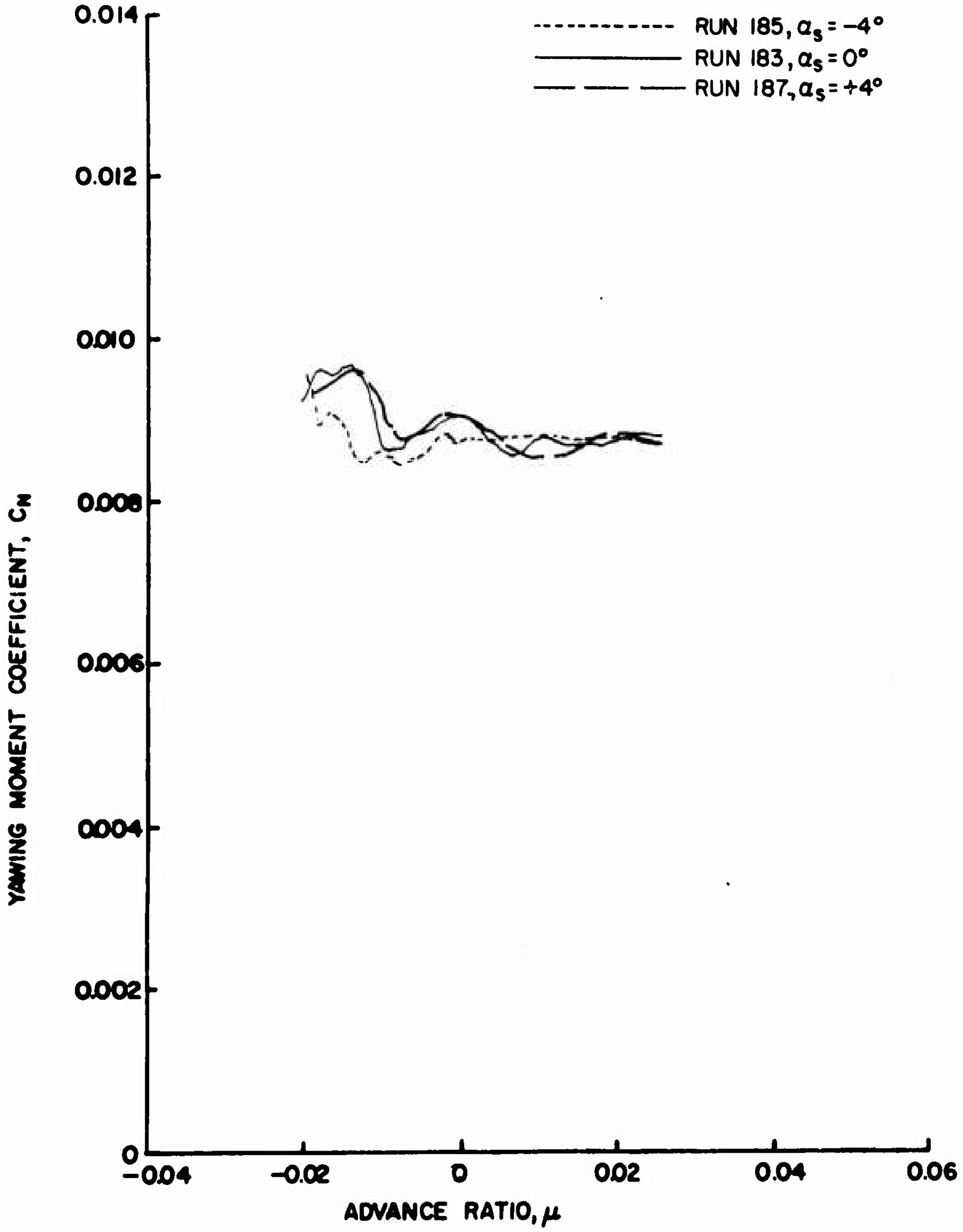

Figure 92e. Rotor Force and Moment Coefficients as Functions of Advance Ratio, $\theta_{.75R} = 10°$, Wing Off, Fuselage On, $\frac{h}{D} = 0.30$.

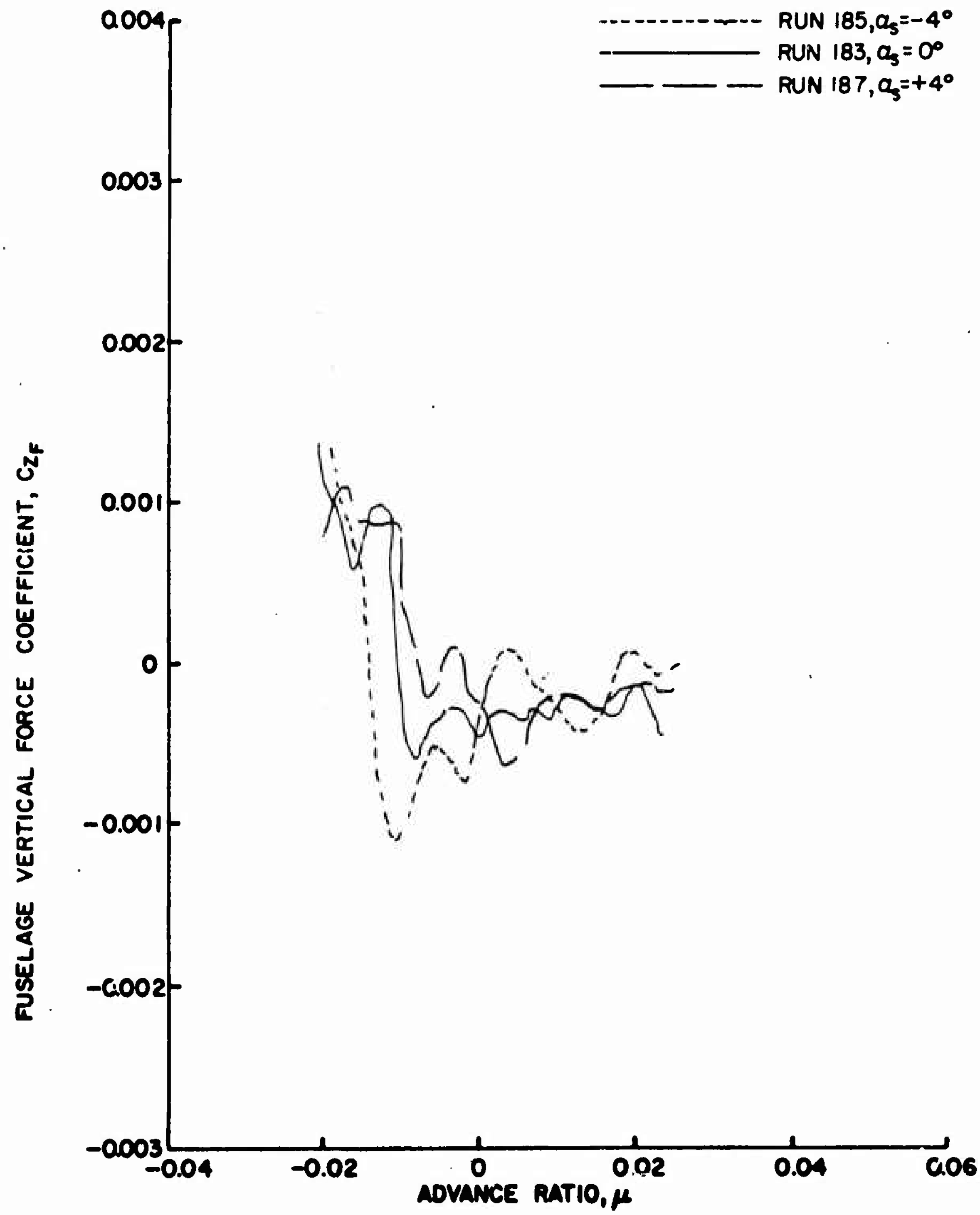

Figure 93a. Fuselage Vertical Force and Pitching Moment Coefficients as Functions of Advance Ratio, $\theta_{.75R} = 10^\circ$, Wing Off, Fuselage On, $\frac{h}{D} = 0.30$.

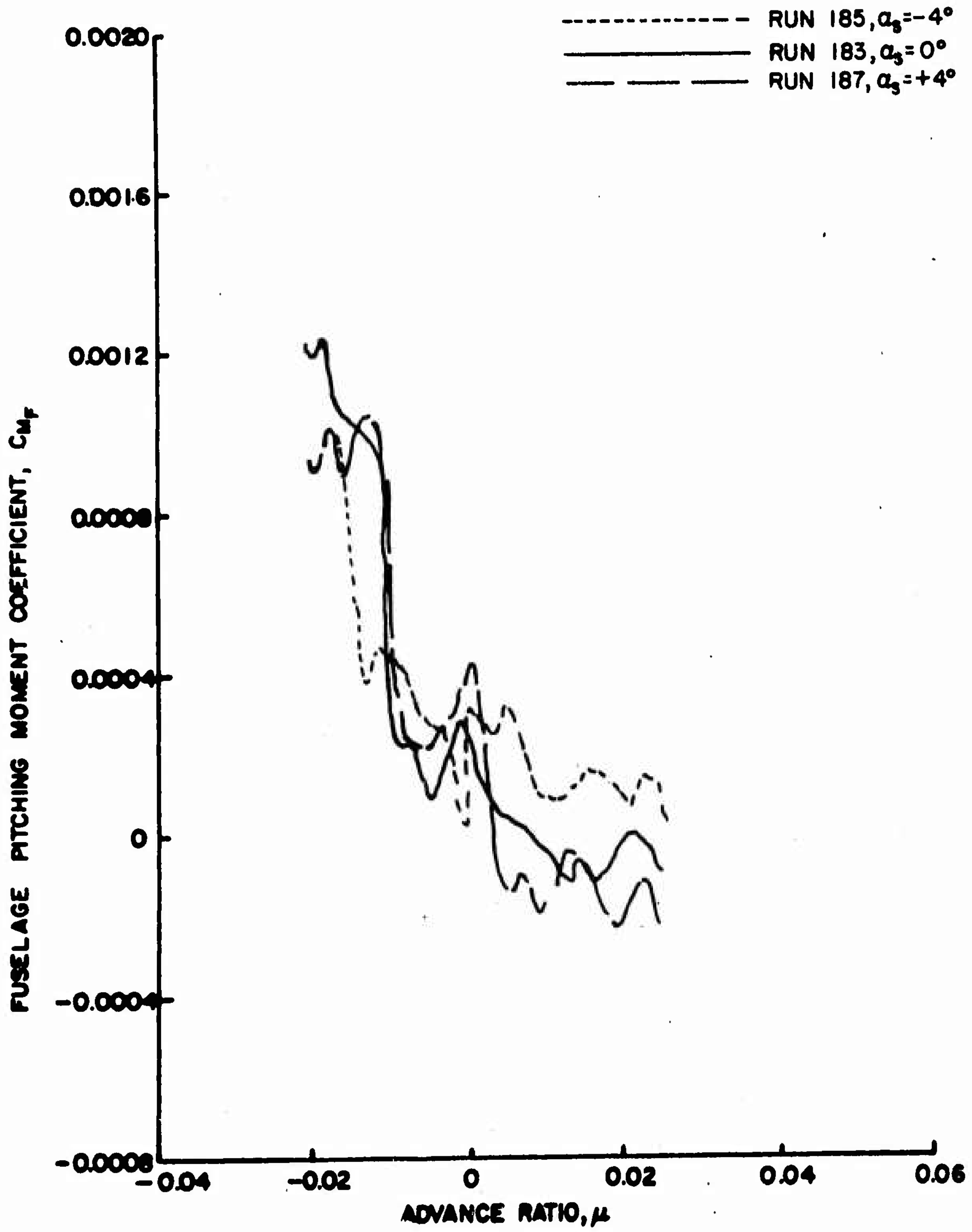

Figure 93b. Fuselage Vertical Force and Pitching Moment Coefficients as Functions of Advance Ratio, $\theta_{.75R} = 10^\circ$, Wing Off, Fuselage On, $\frac{h}{D} = 0.30$.

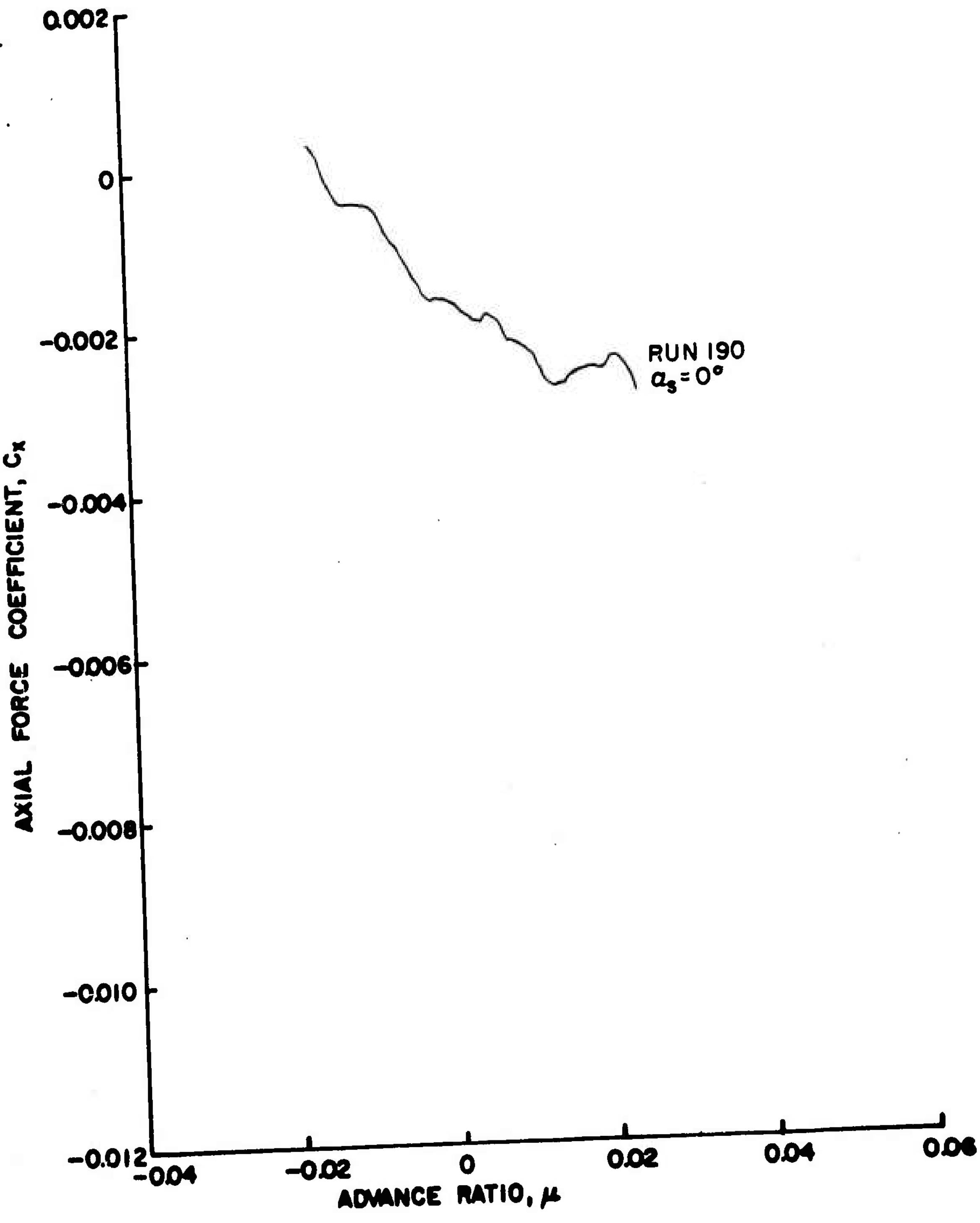

Figure 94a. Rotor Force and Moment Coefficients as Functions of Advance Ratio, $\theta_{.75R} = 12°$, Wing Off, Fuselage On, $\frac{h}{D} = 0.30$.

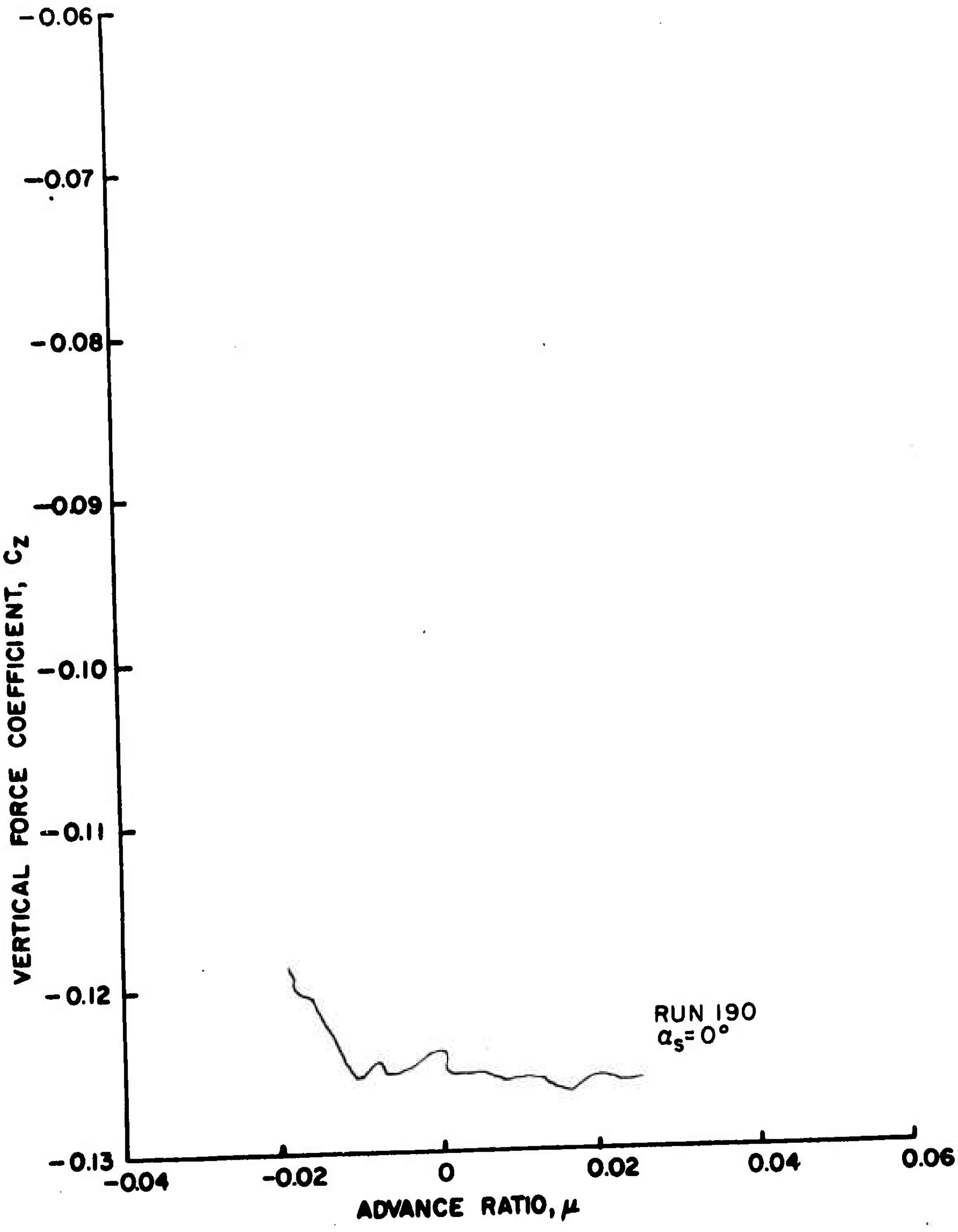

Figure 94b. Rotor Force and Moment Coefficients as Functions of Advance Ratio, $\theta_{.75R} = 12°$, Wing Off, Fuselage On, $\frac{h}{D} = 0.30$.

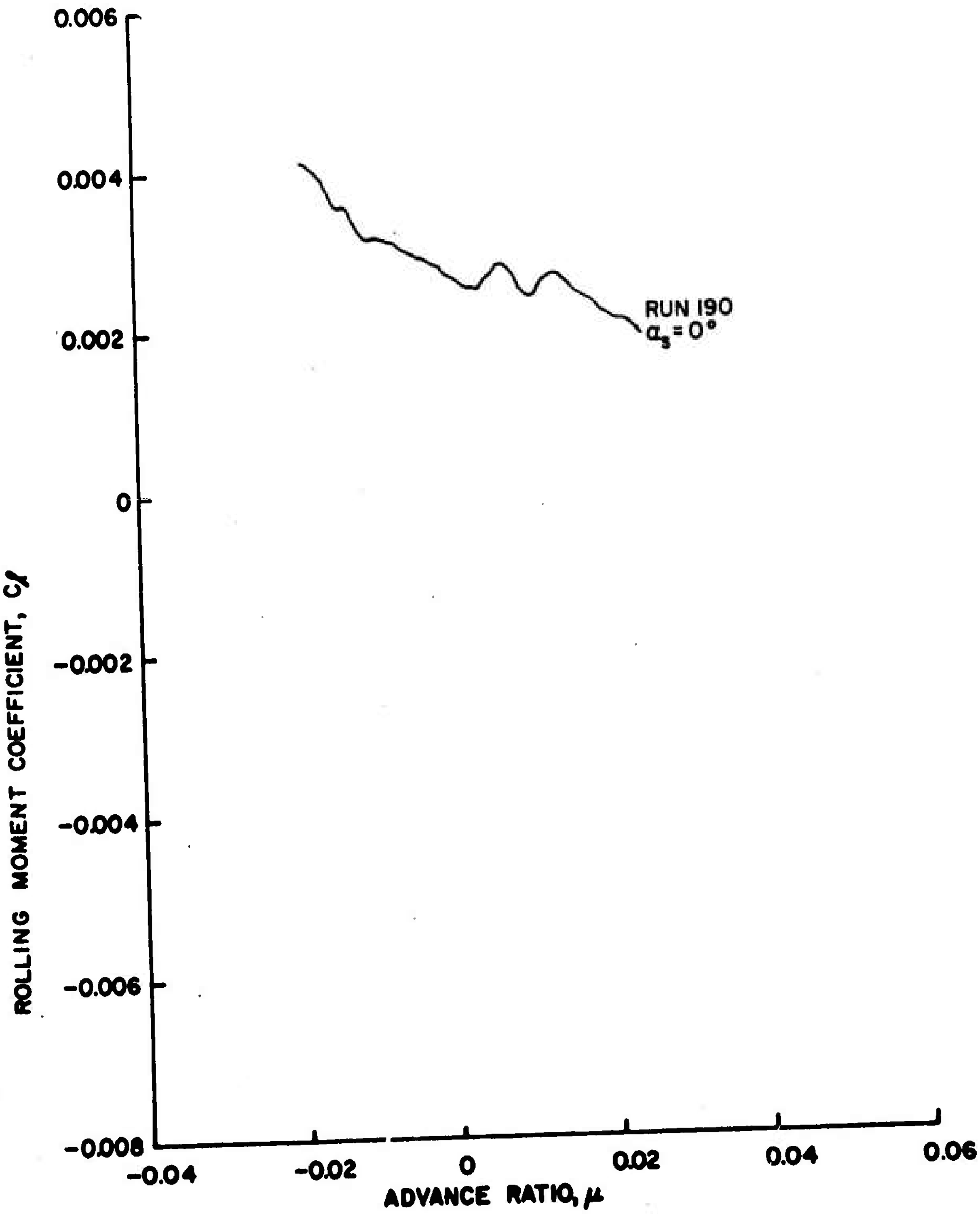

Figure 94c. Rotor Force and Moment Coefficients as Functions of Advance Ratio, $\theta_{.75R} = 12°$, Wing Off, Fuselage On, $\frac{h}{D} = 0.30$.

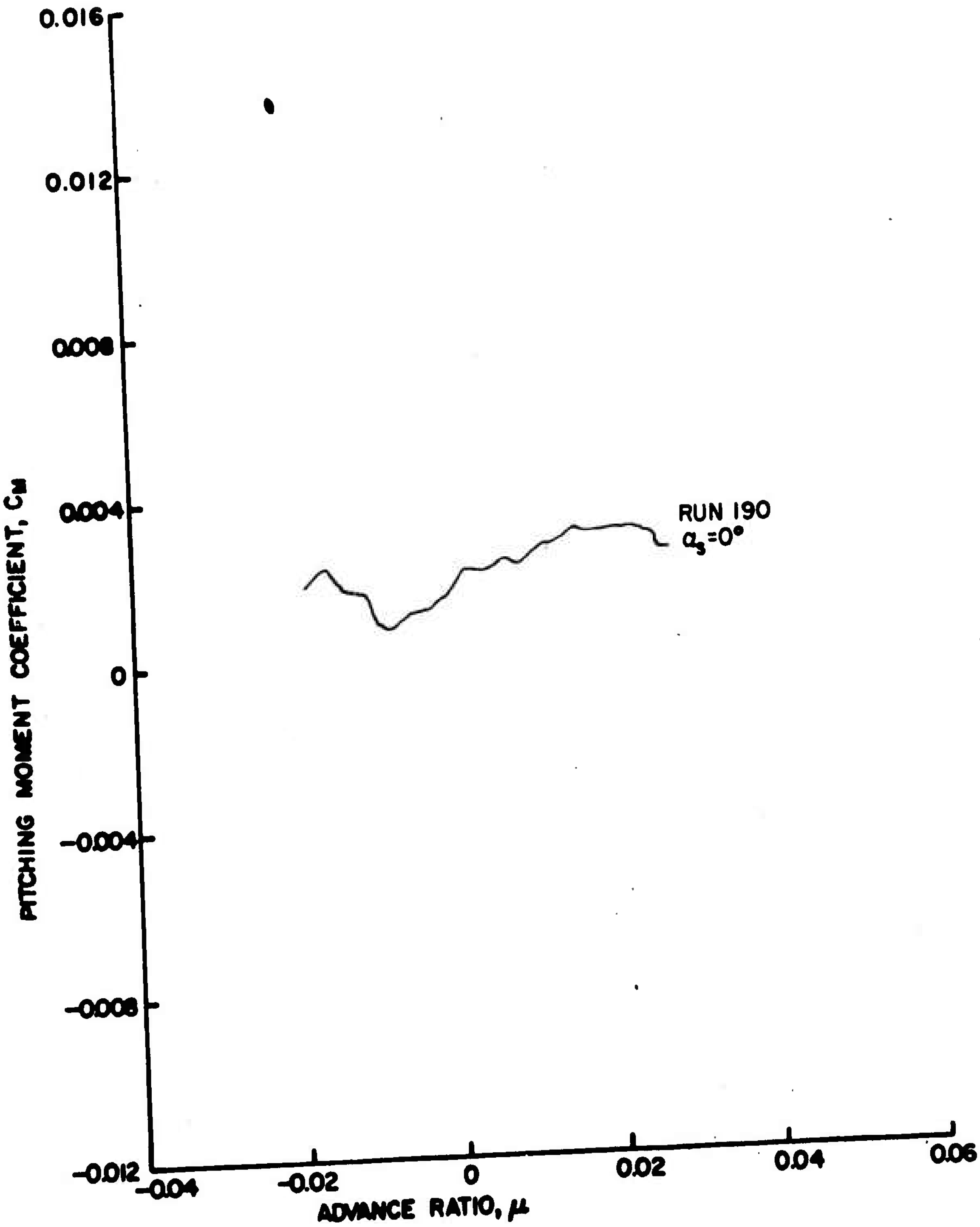

Figure 94d. Rotor Force and Moment Coefficients as Functions of Advance Ratio, $\theta_{.75R} = 12°$, Wing Off, Fuselage On, $\frac{h}{D} = 0.30$.

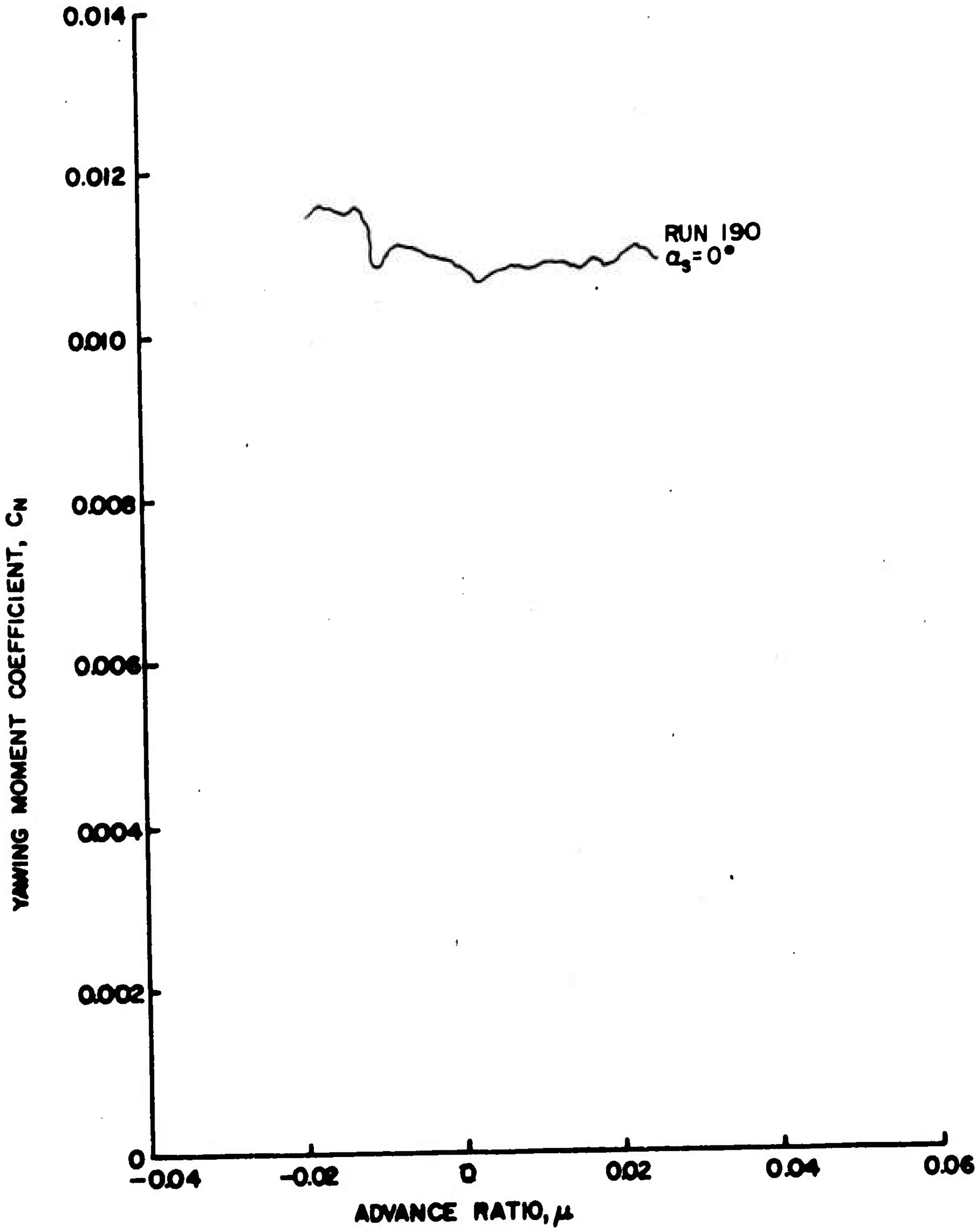

Figure 94e. Rotor Force and Moment Coefficients as Functions of Advance Ratio, $\theta_{.75R} = 12°$, Wing Off, Fuselage On, $\frac{h}{D} = 0.30$.

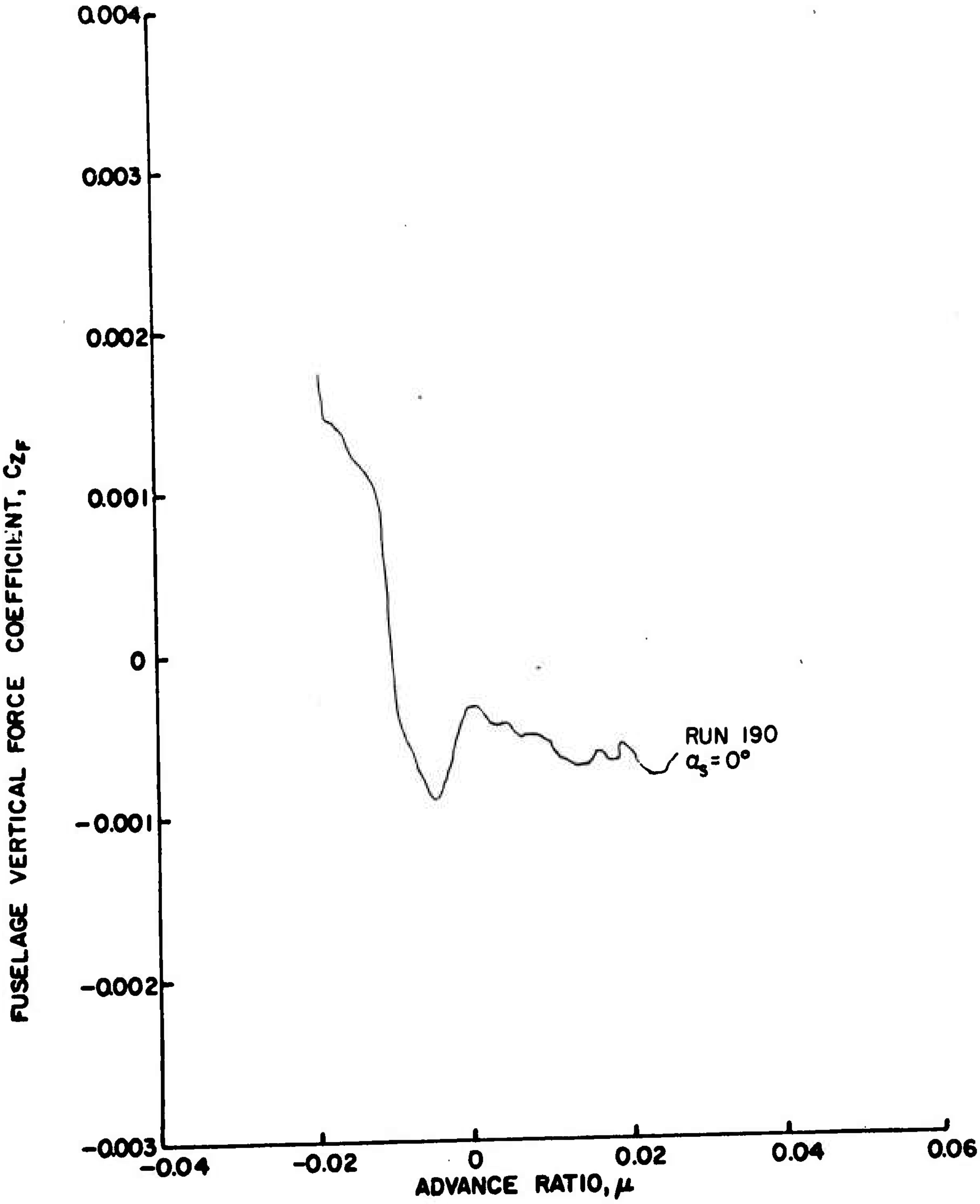

Figure 95a. Fuselage Vertical Force and Pitching Moment Coefficients as Functions of Advance Ratio, $\theta_{.75R} = 12°$, Wing Off, Fuselage On, $\frac{h}{D} = 0.30$.

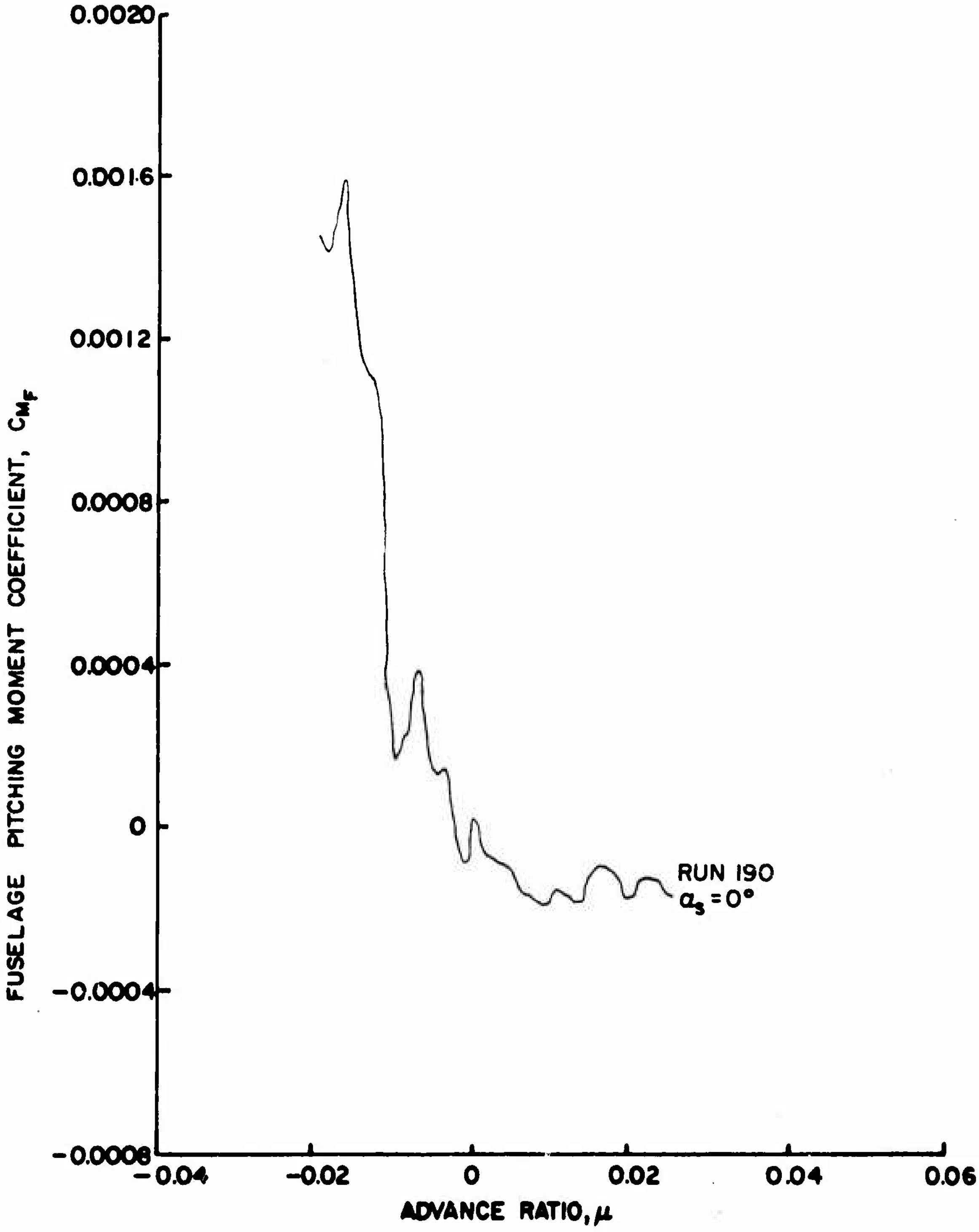

Figure 95b. Fuselage Vertical Force and Pitching Moment Coefficients as Functions of Advance Ratio, $\theta_{.75R} = 12°$, Wing Off, Fuselage On, $\frac{h}{D} = 0.30$.

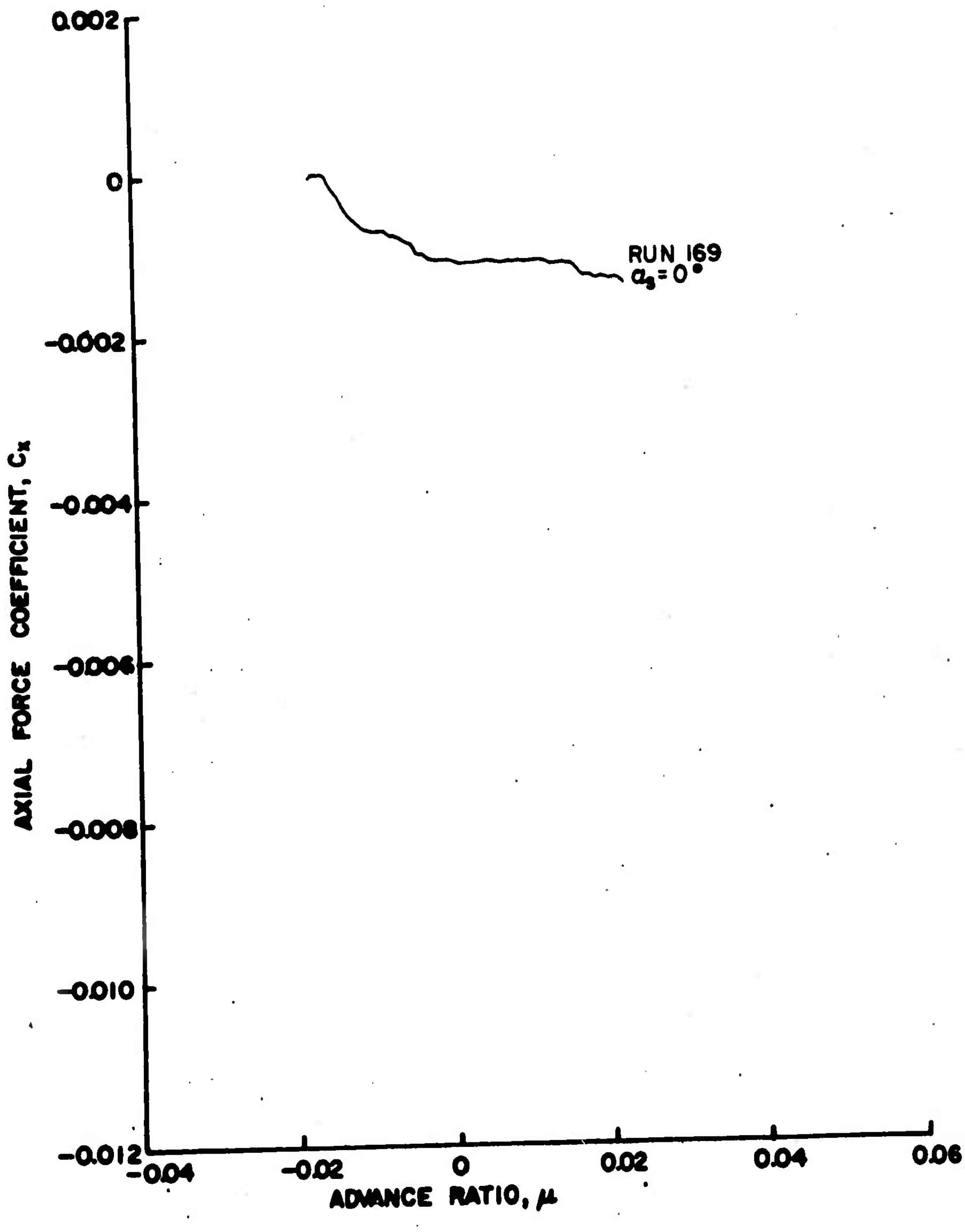

Figure 96a. Rotor Force and Moment Coefficients as Functions of Advance Ratio, $\theta_{.75R} = 8°$, Large Wing on High, $\frac{h}{D} = 0.30$.

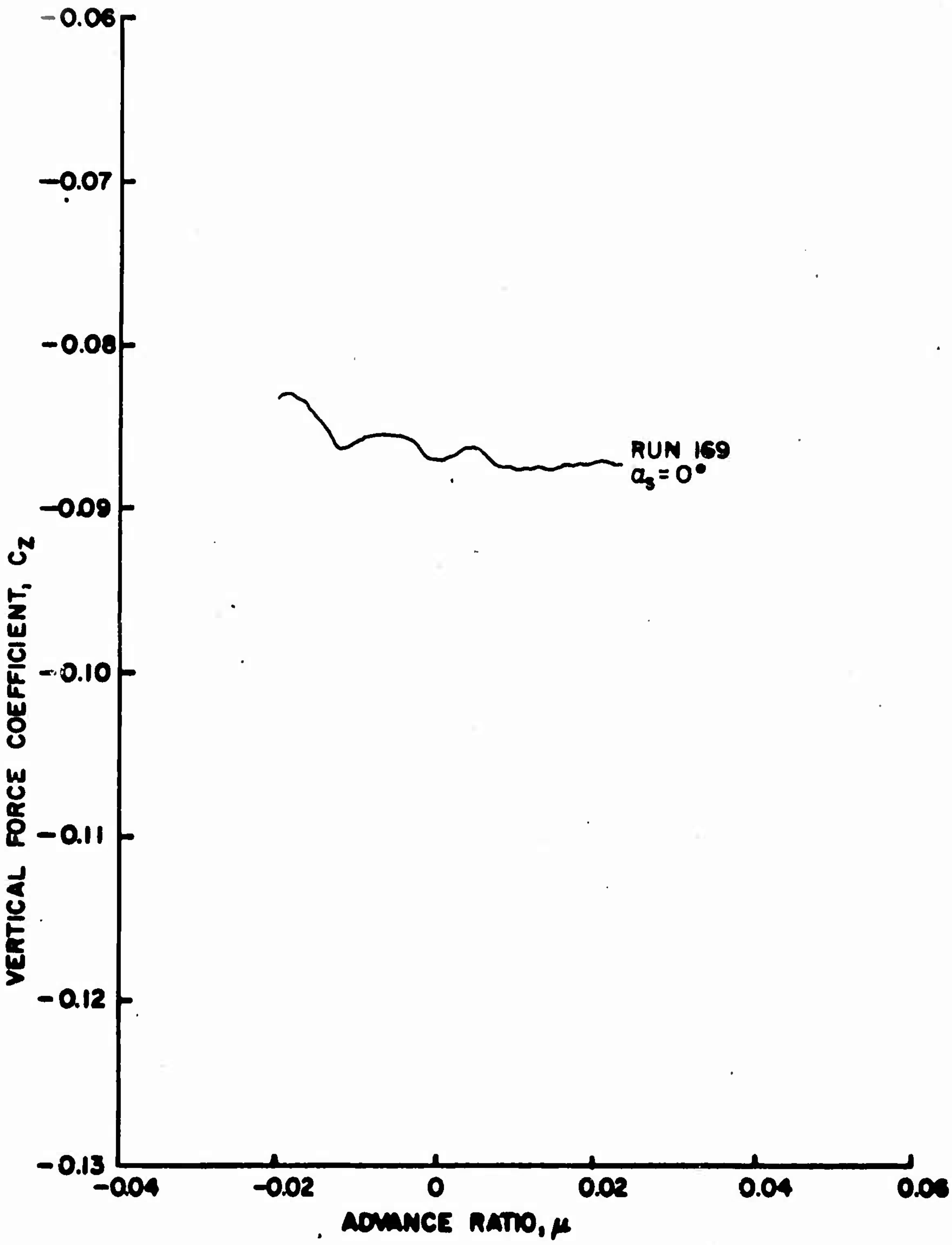

Figure 96b. Rotor Force and Moment Coefficients as Functions of Advance Ratio, $\theta_{.75R} = 8°$, Large Wing on High, $\frac{h}{D} = 0.30$.

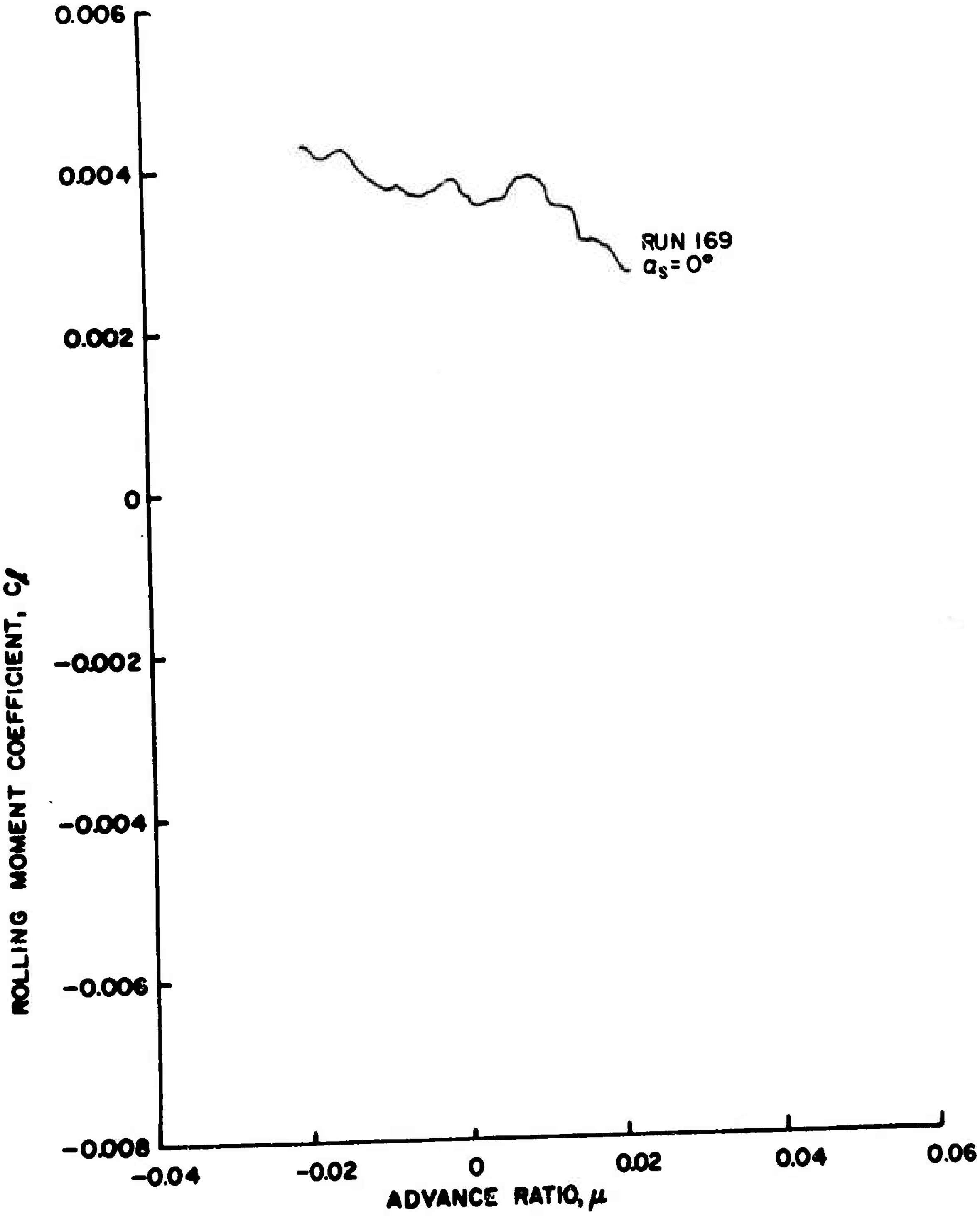

Figure 96c. Rotor Force and Moment Coefficients as Functions of Advance Ratio, $\theta_{.75R} = 8°$, Large Wing on High, $\frac{h}{D} = 0.30$.

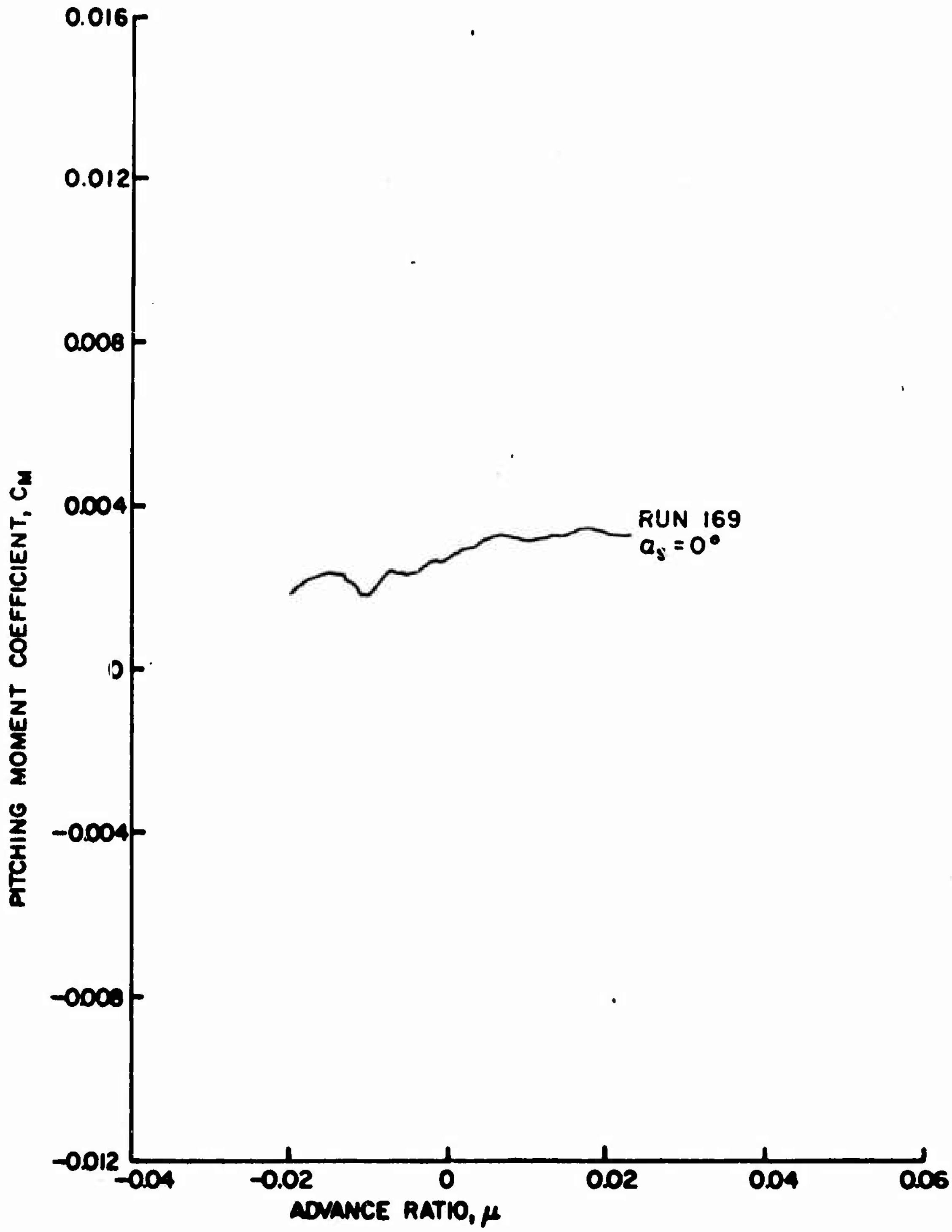

Figure 96d. Rotor Force and Moment Coefficients as Functions of Advance Ratio, $\theta_{.75R} = 8°$, Large Wing on High, $\frac{h}{D} = 0.30$.

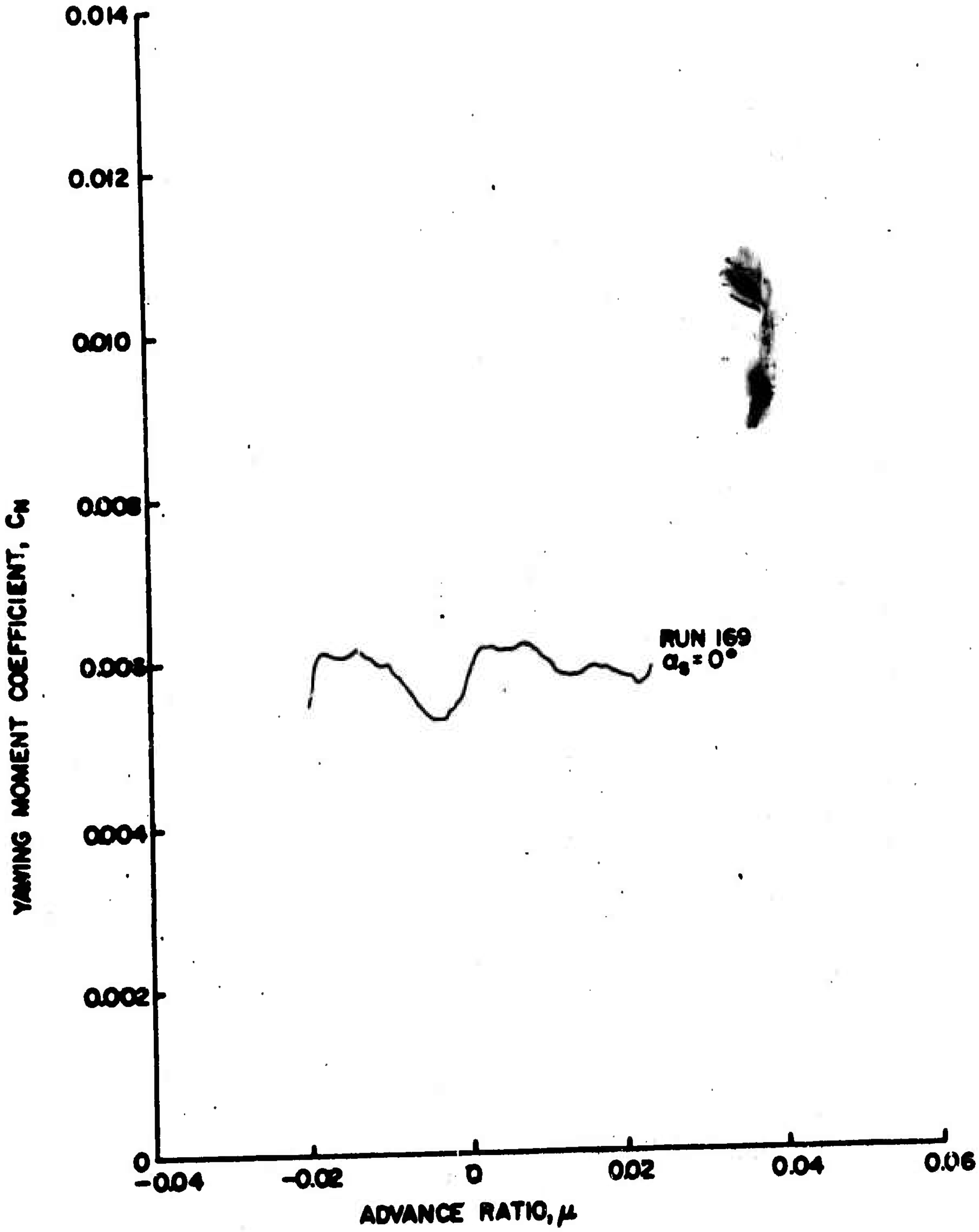

Figure 96e. Rotor Force and Moment Coefficients as Functions of Advance Ratio, $\theta_{.75R} = 8°$, Large Wing on High, $\frac{h}{D} = 0.30$.

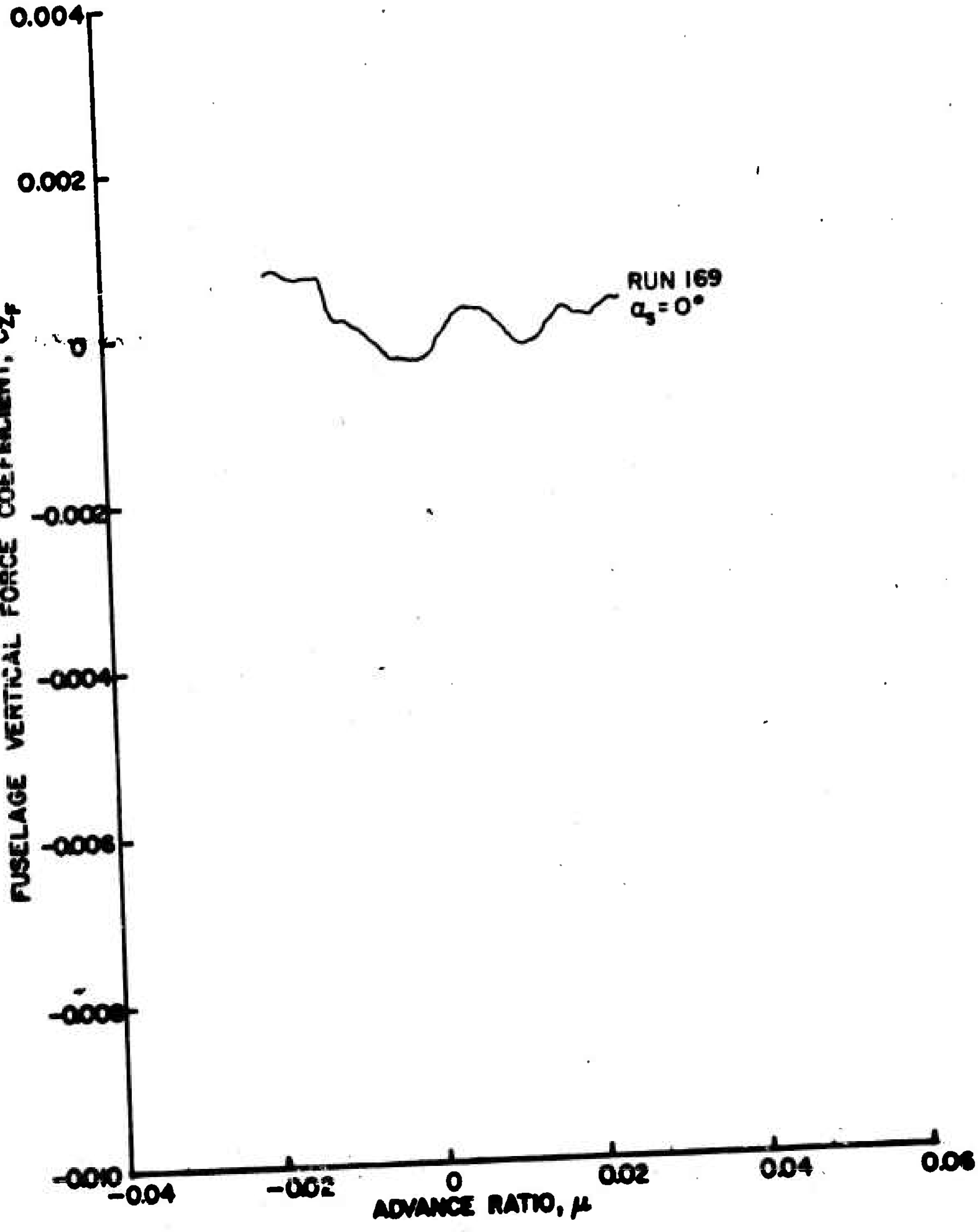

Figure 97a. Fuselage Vertical Force and Pitching Moment Coefficients as Functions of Advance Ratio, $\theta_{.75R} = 8°$, Large Wing on High, $\frac{h}{D} = 0.30$.

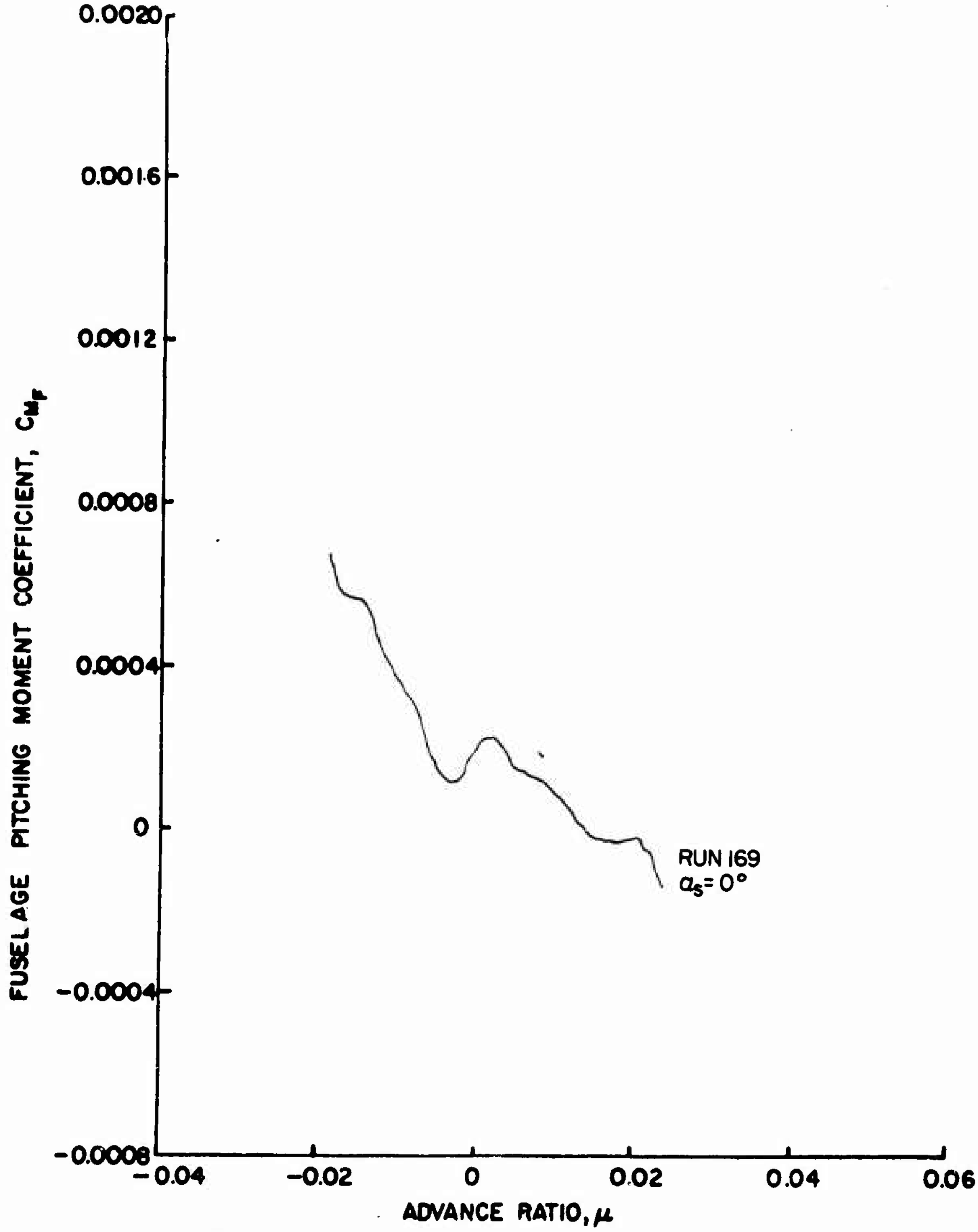

Figure 97b. Fuselage Vertical Force and Pitching Moment Coefficients as Functions of Advance Ratio, $\theta_{.75R} = 8°$, Large Wing on High, $\frac{h}{D} = 0.30$.

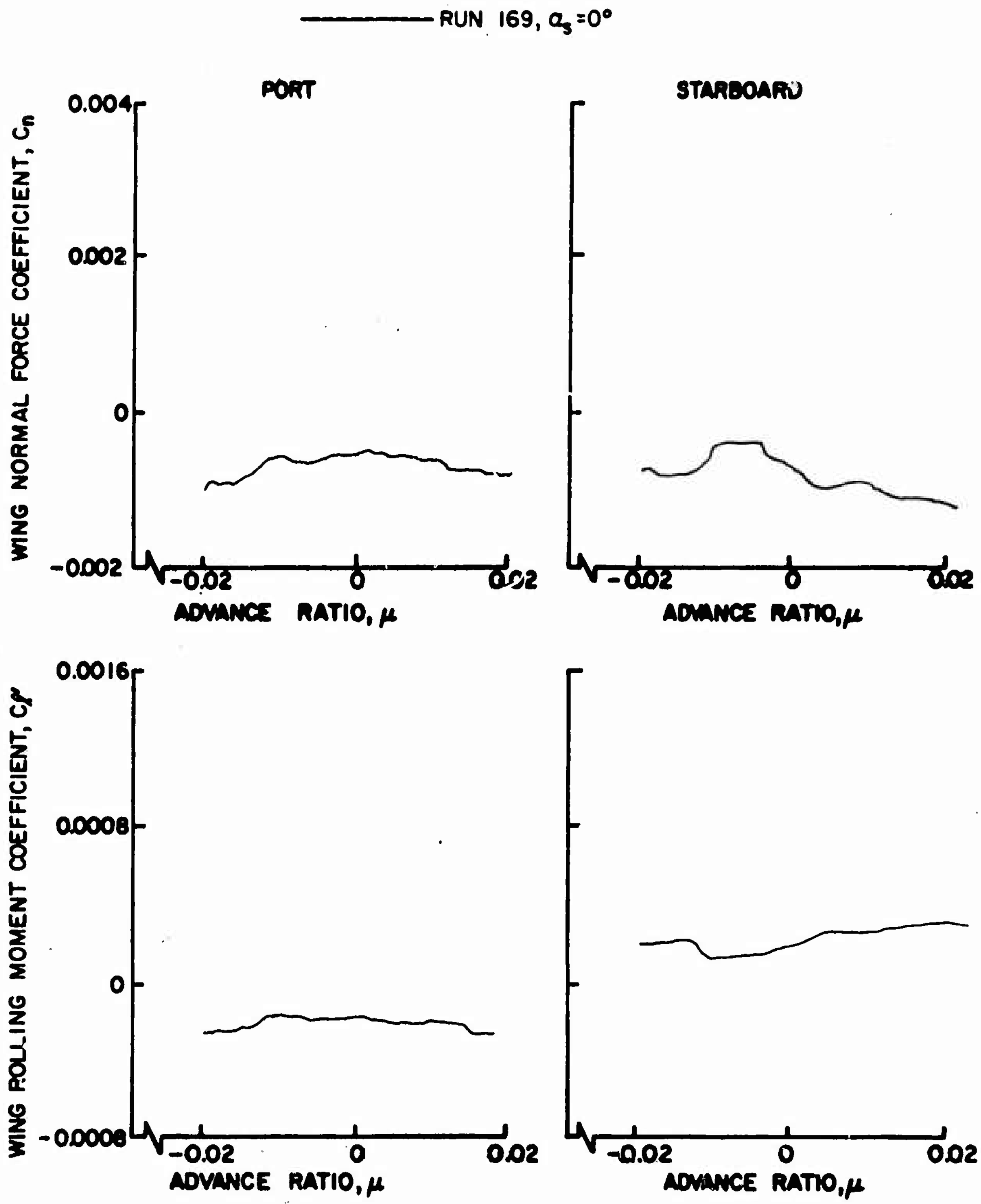

Figure 98. Wing Normal Force and Rolling Moment Coefficients as Functions of Advance Ratio, $\theta_{.75R} = 8^{\circ}$, Large Wing on High, $\frac{h}{D} = 0.30$.

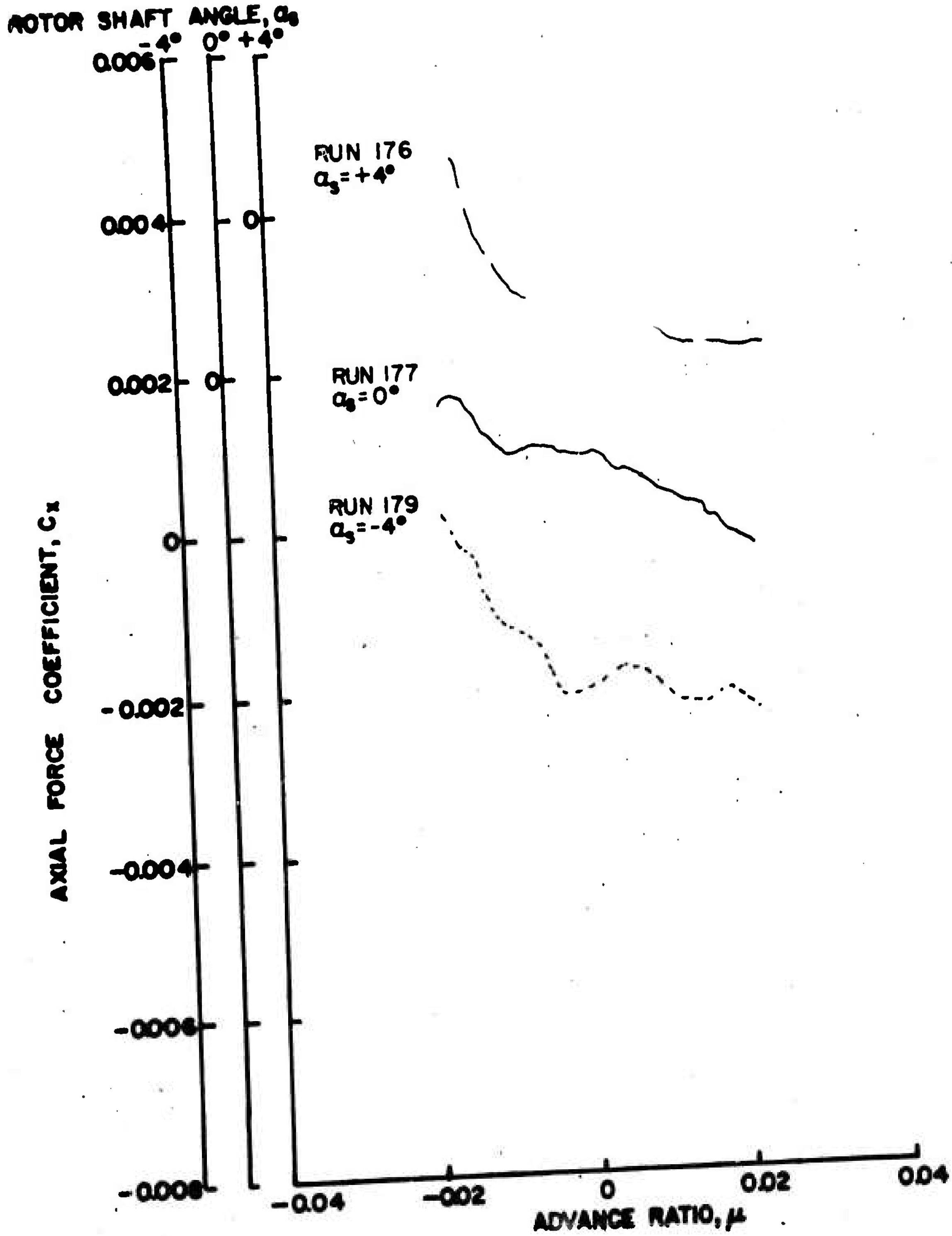

Figure 99a. Rotor Force and Moment Coefficients as Functions of Advance Ratio, $\theta_{.75R} = 8^\circ$, Large Wing on High, $\frac{h}{D} = 0.30$.

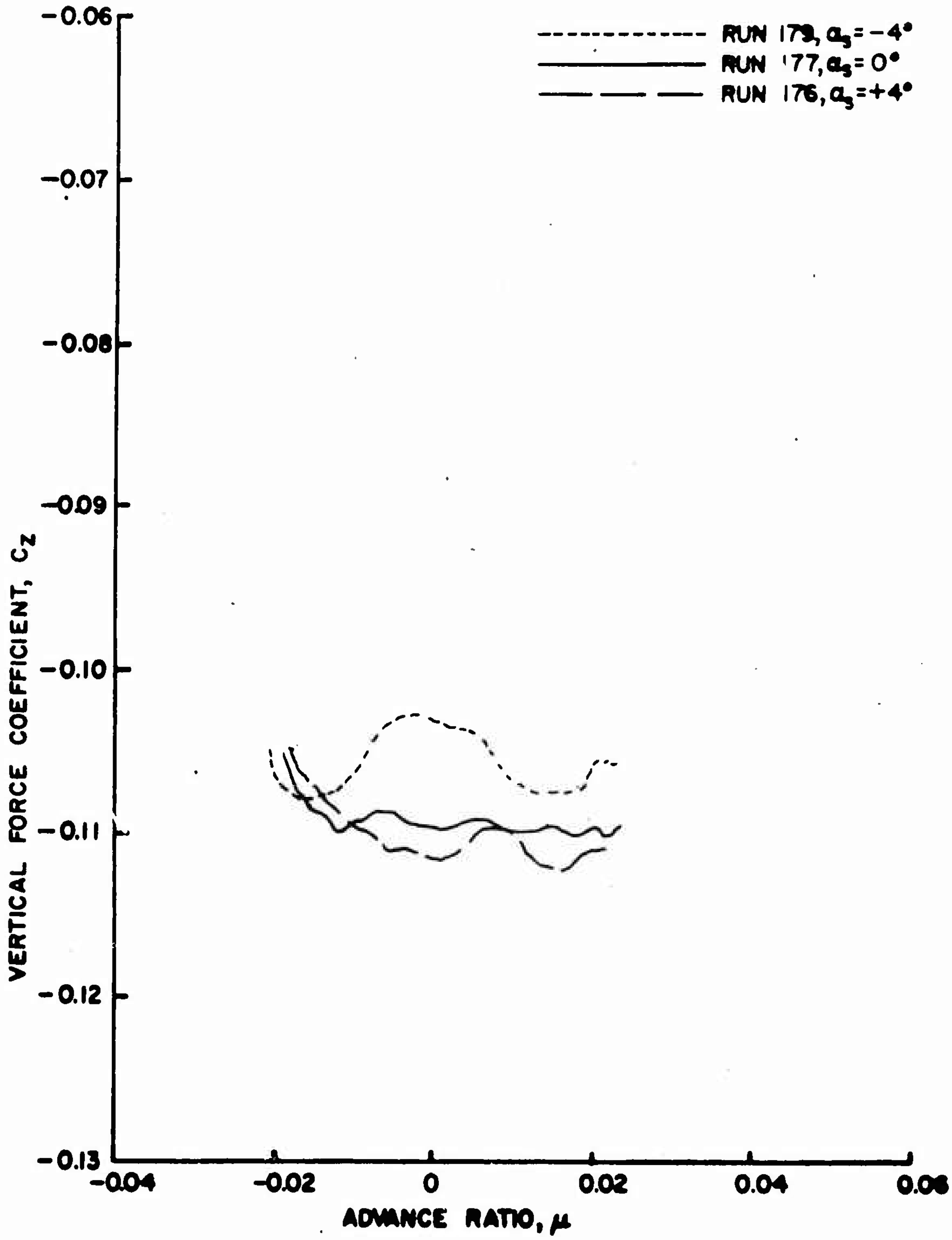

Figure 99b. Rotor Force and Moment Coefficients as Functions of Advance Ratio, $\theta_{.75R} = 8^{\circ}$, Large Wing on High, $\frac{h}{D} = 0.30$.

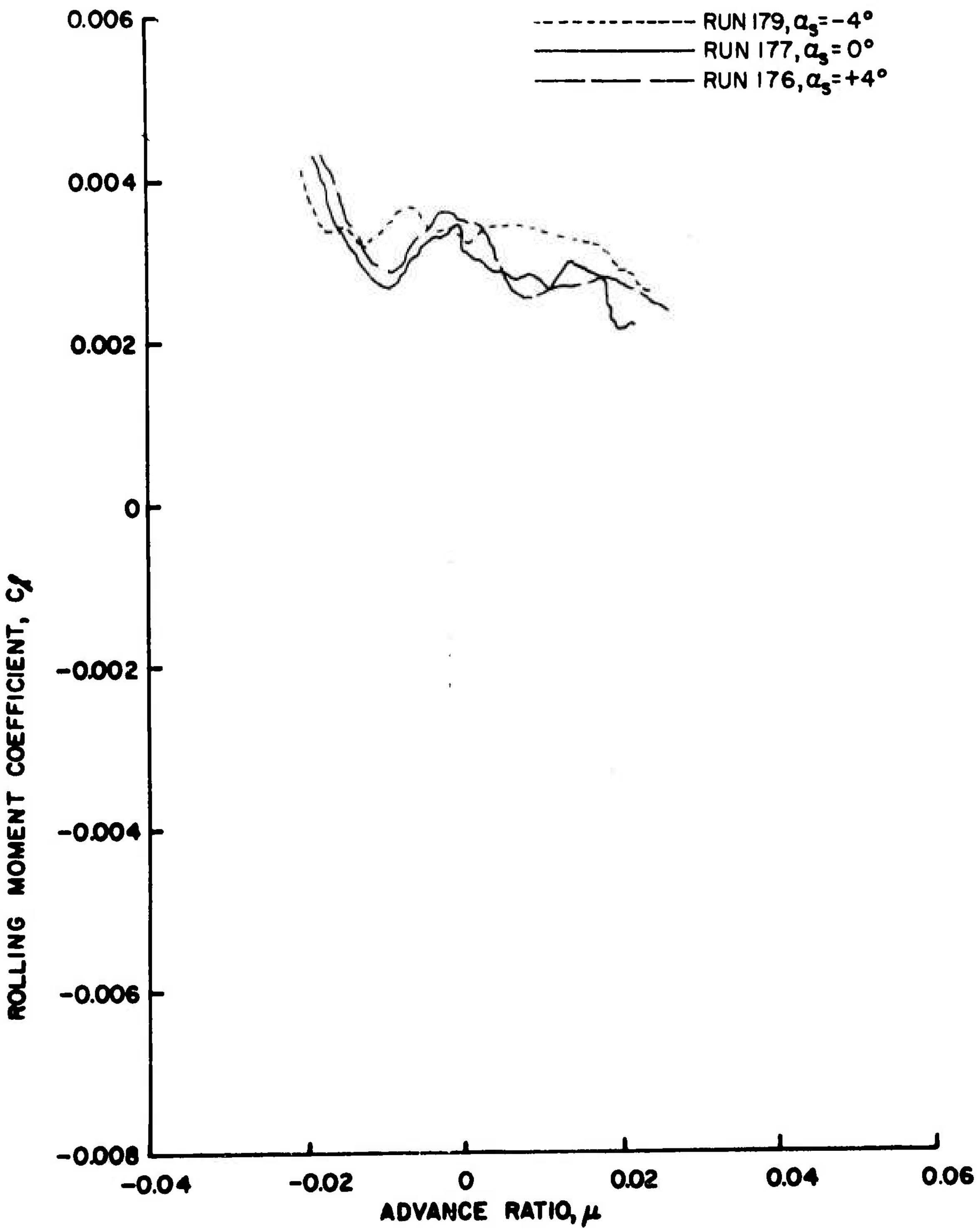

Figure 99c. Rotor Force and Moment Coefficients as Functions of Advance Ratio, $\theta_{.75R} = 8^\circ$, Large Wing on High, $\frac{h}{D} = 0.30$.

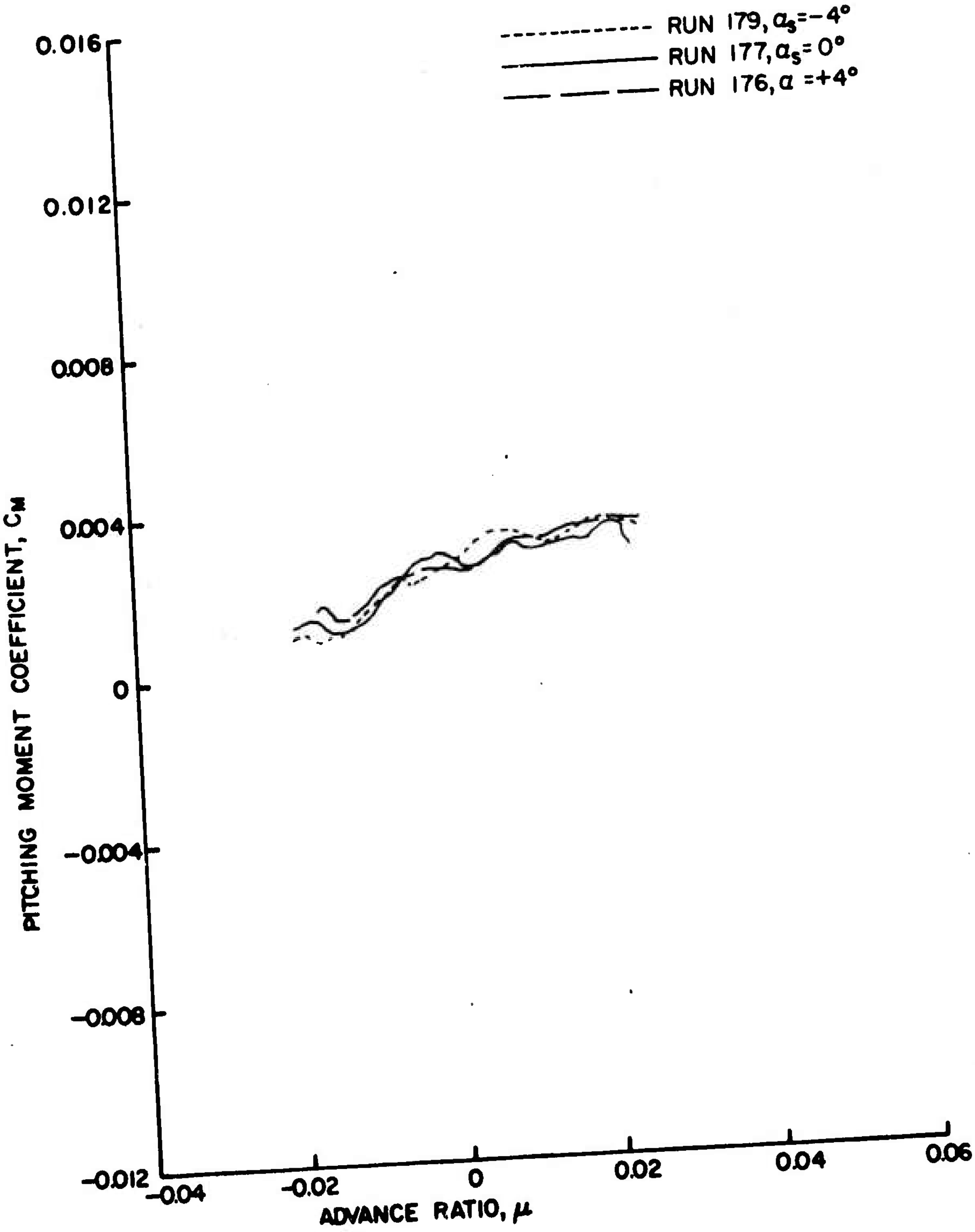

Figure 99d. Rotor Force and Moment Coefficients as Functions of Advance Ratio, $\theta_{.75R} = 8^\circ$, Large Wing on High, $\frac{h}{D} = 0.30$.

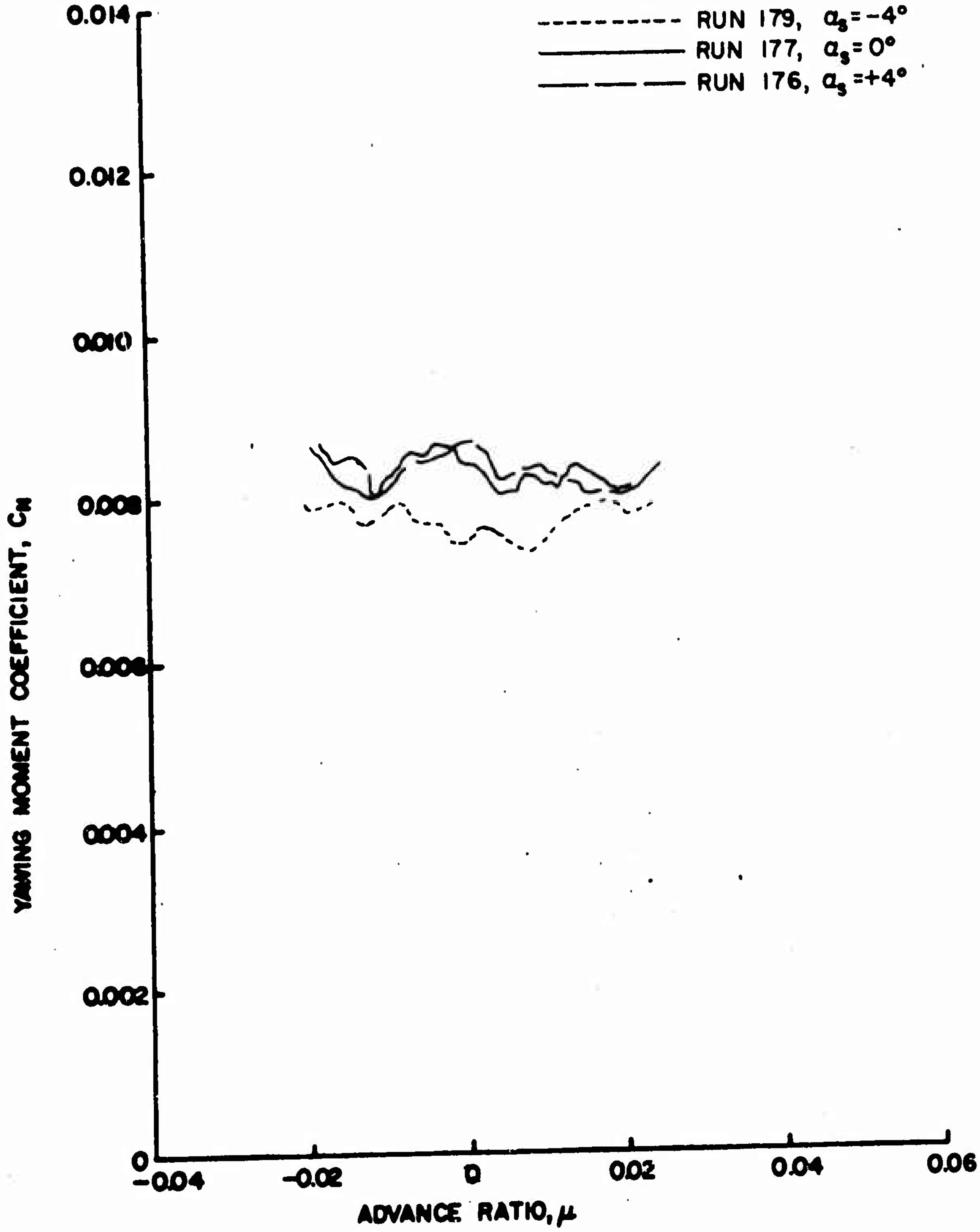

Figure 99e. Rotor Force and Moment Coefficients as Functions of Advance Ratio, $\theta_{.75R} = 8^{\circ}$, Large Wing on High, $\frac{h}{D} = 0.30$.

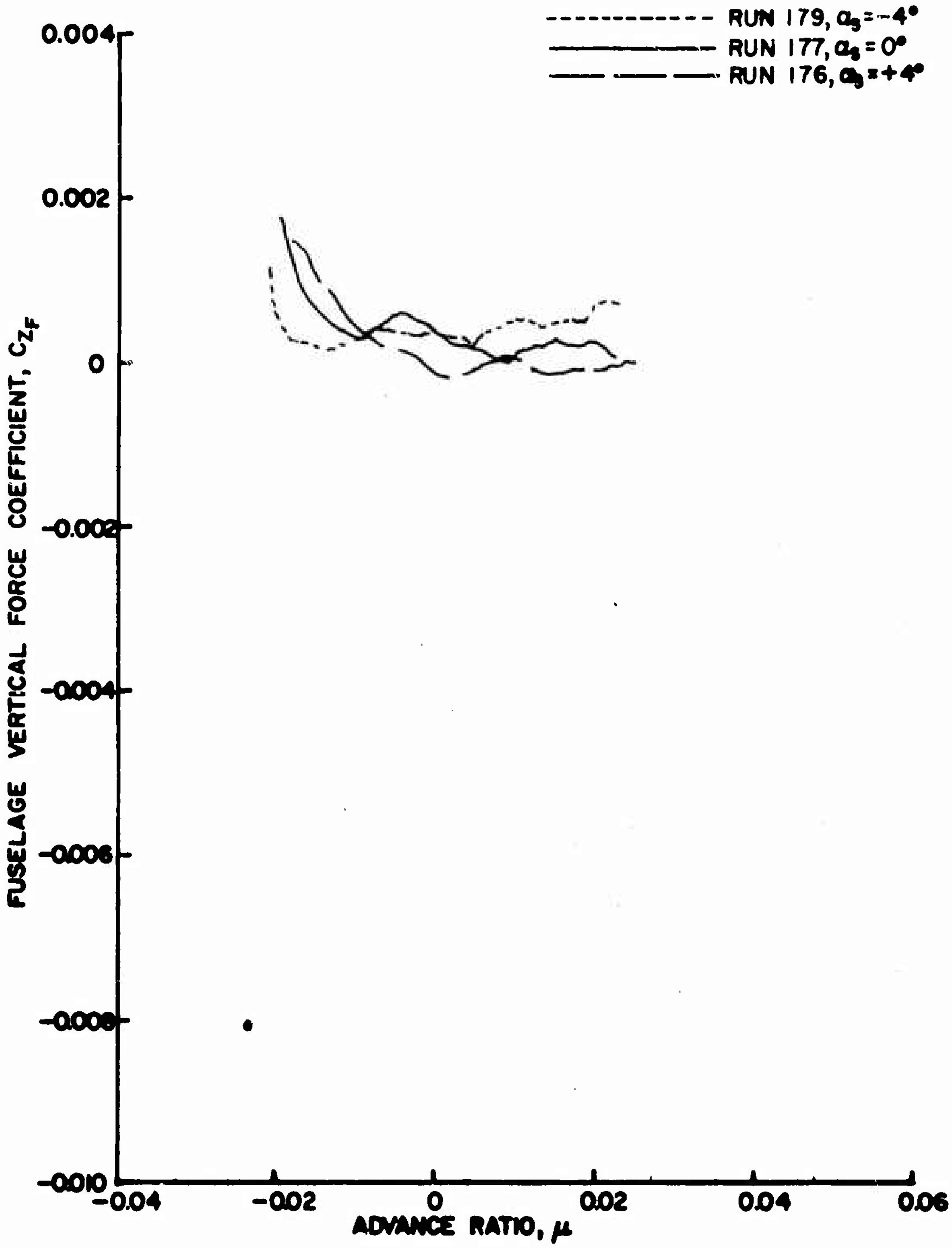

Figure 100a. Fuselage Vertical Force and Pitching Moment Coefficients as Functions of Advance Ratio, $\theta_{.75R} = 10°$, Large Wing on High, $\frac{h}{D} = 0.30$.

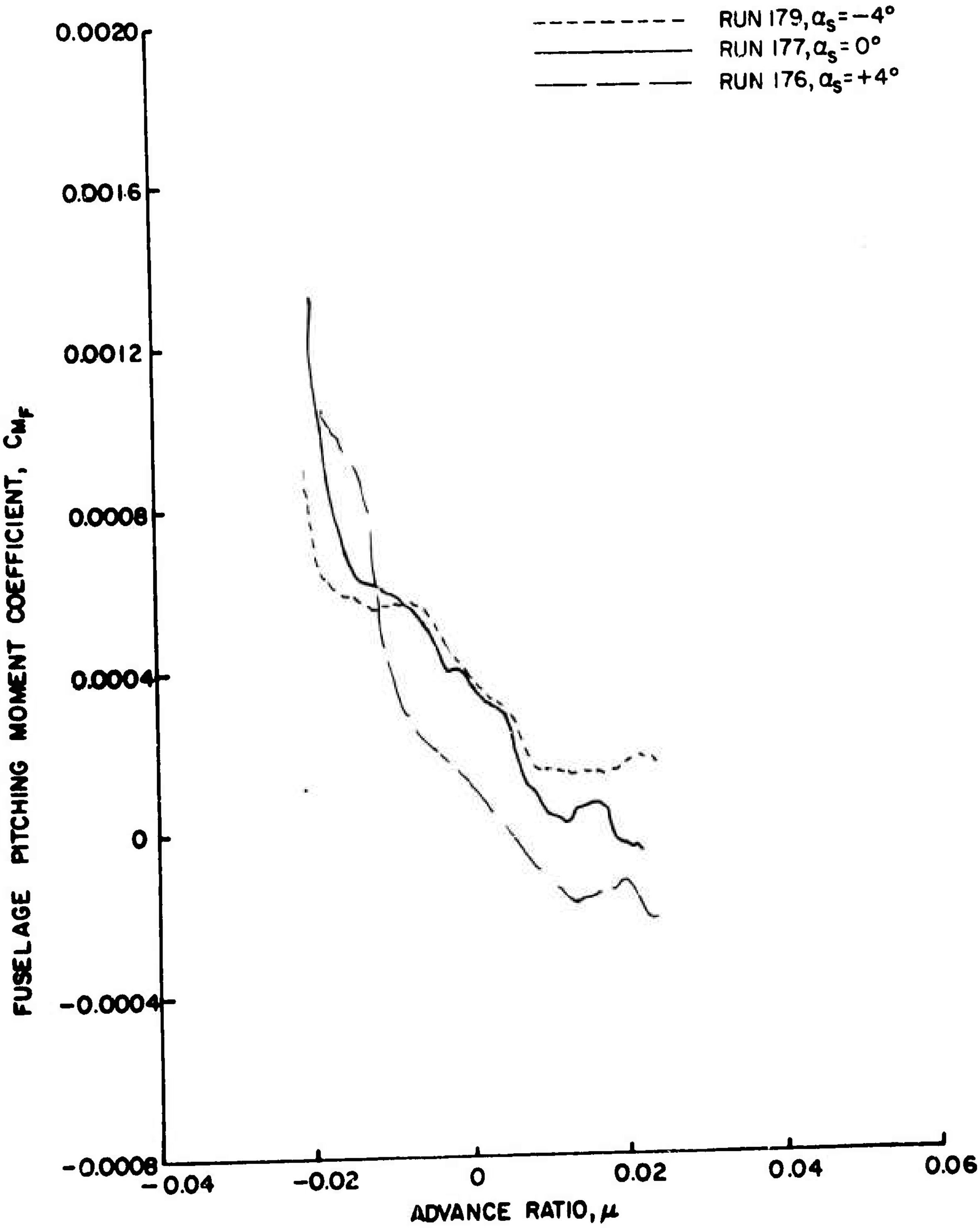

Figure 100b. Fuselage Vertical Force and Pitching Moment Coefficients as Functions of Advance Ratio, $\theta_{.75R} = 10°$, Large Wing on High, $\frac{h}{D} = 0.30$.

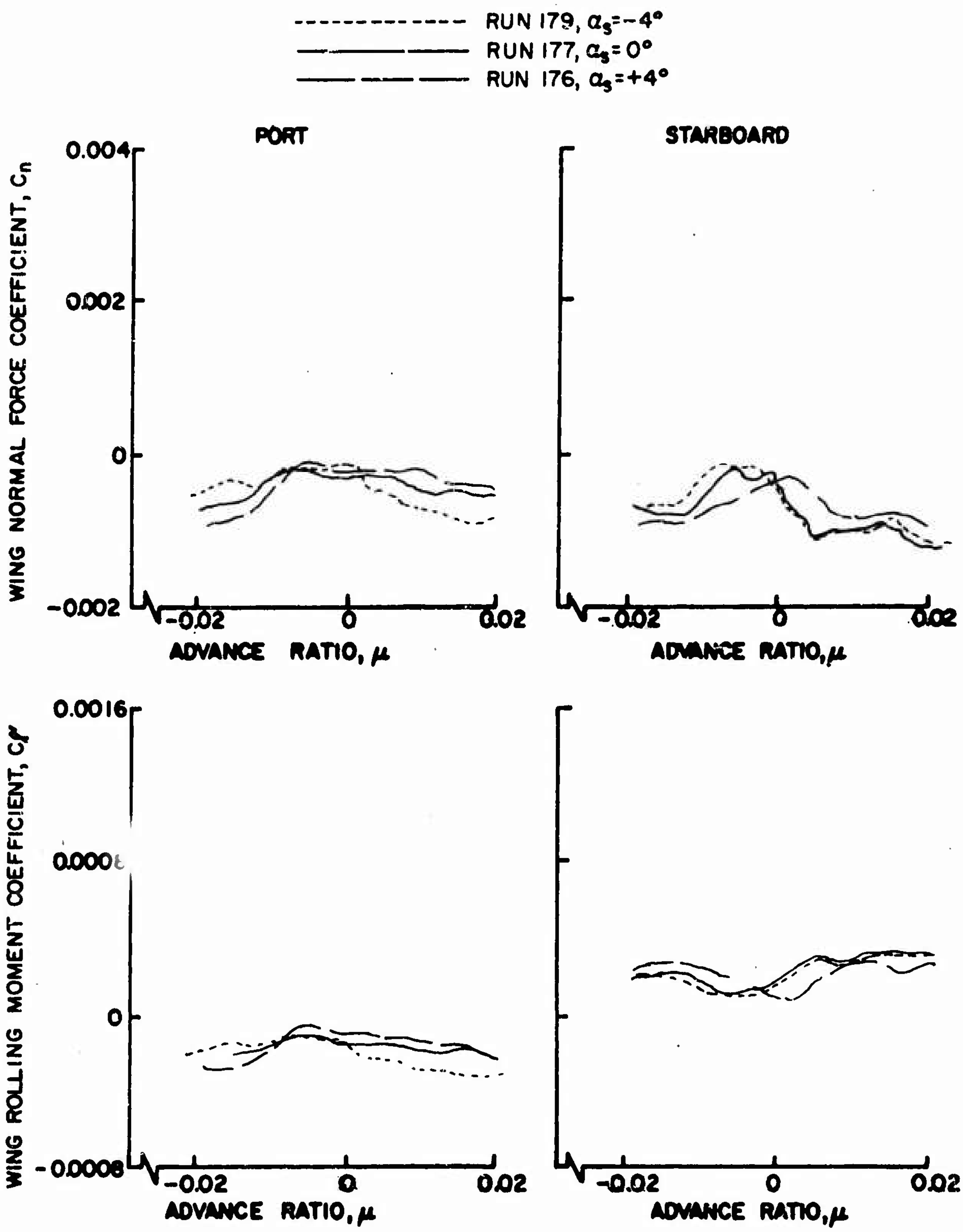

Figure 101. Wing Normal Force and Rolling Moment Coefficients as Functions of Advance Ratio, $\theta_{.75R} = 10^{\circ}$, Large Wing on High, $\frac{h}{D} = 0.30$.

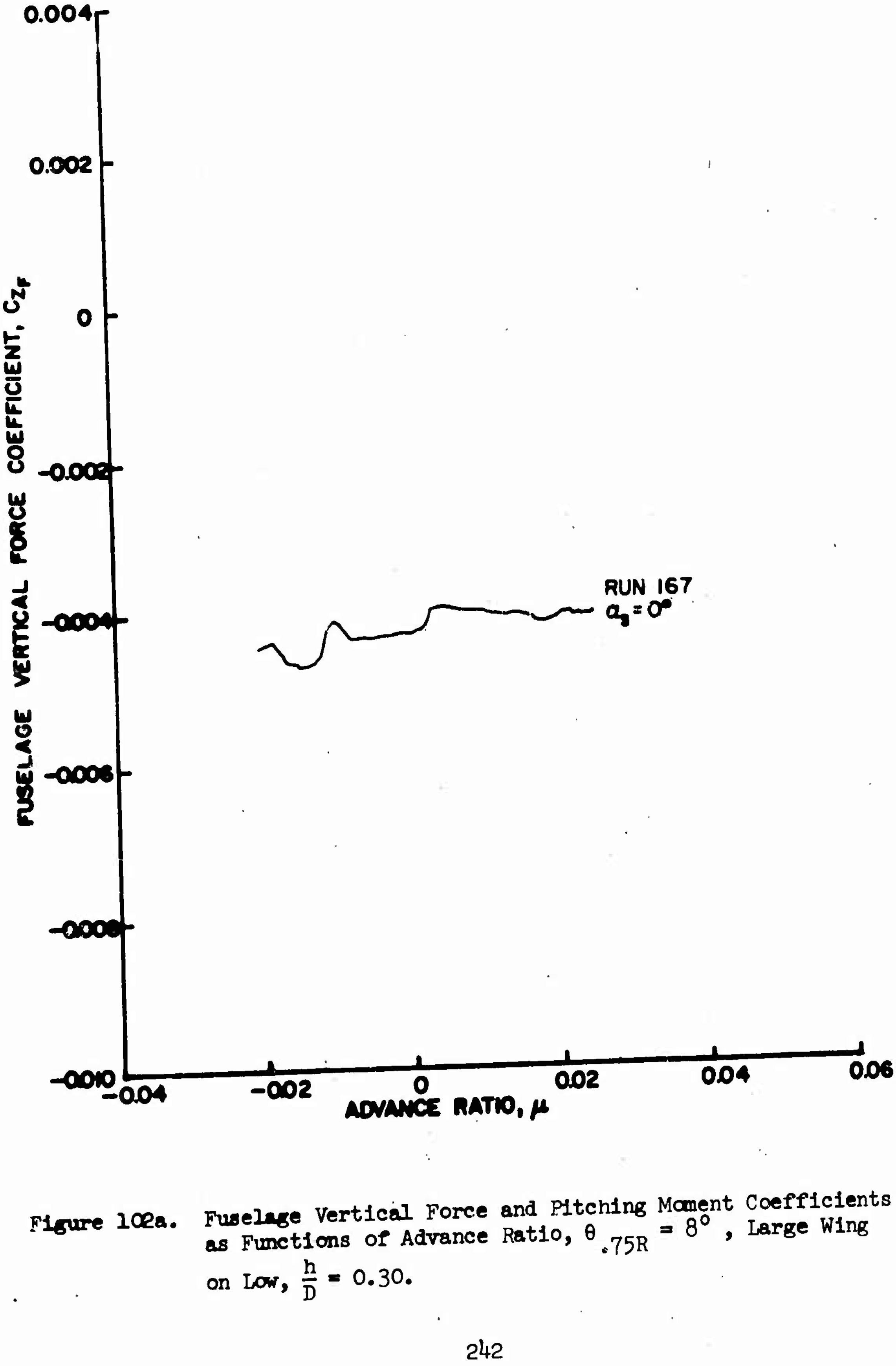

Figure 102a. Fuselage Vertical Force and Pitching Moment Coefficients as Functions of Advance Ratio, $\theta_{.75R} = 8°$, Large Wing on Low, $\frac{h}{D} = 0.30$.

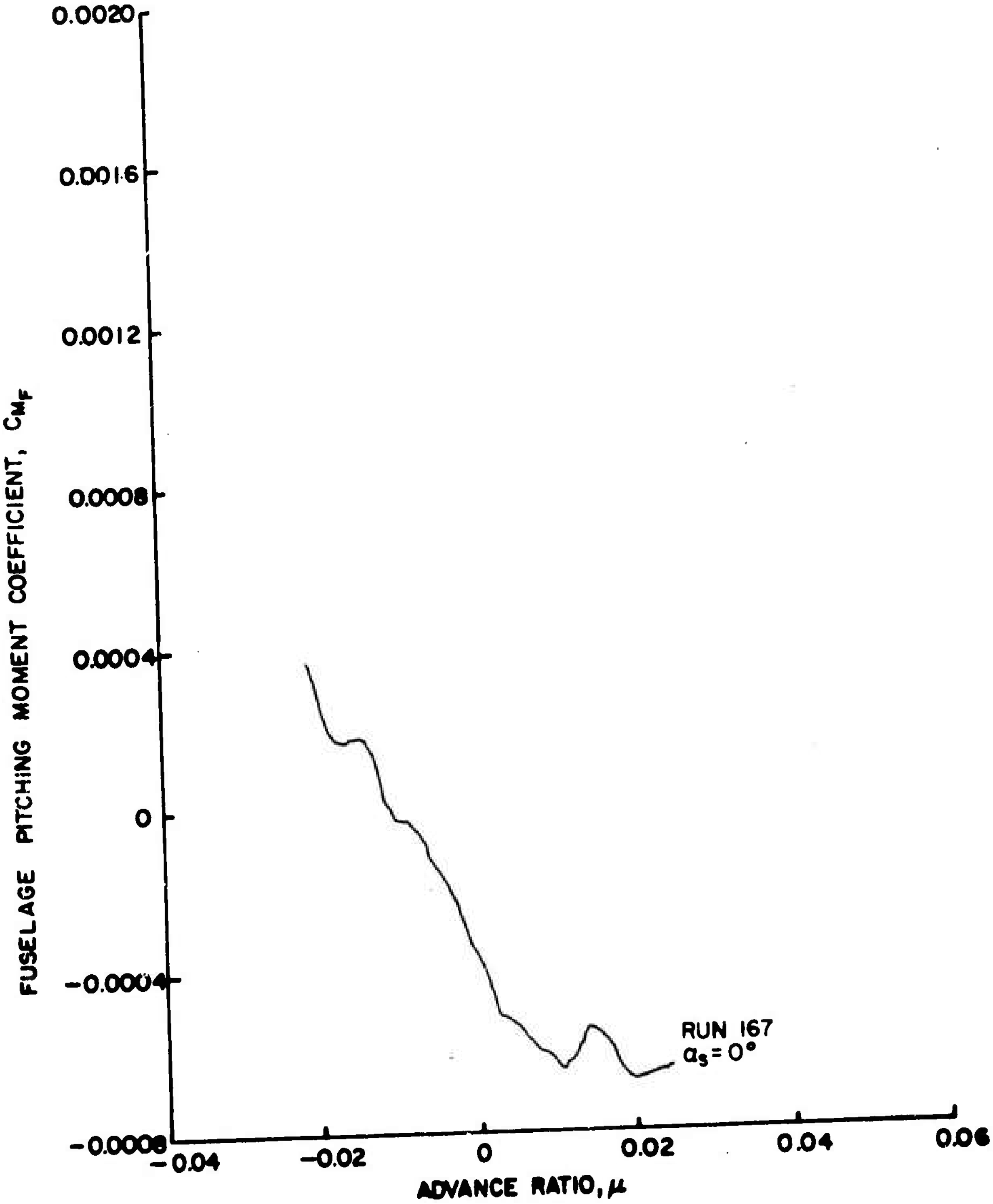

Figure 102b. Fuselage Vertical Force and Pitching Moment Coefficients as Functions of Advance Ratio, $\theta_{.75R} = 8°$, Large Wing on Low, $\frac{h}{D} = 0.30$.

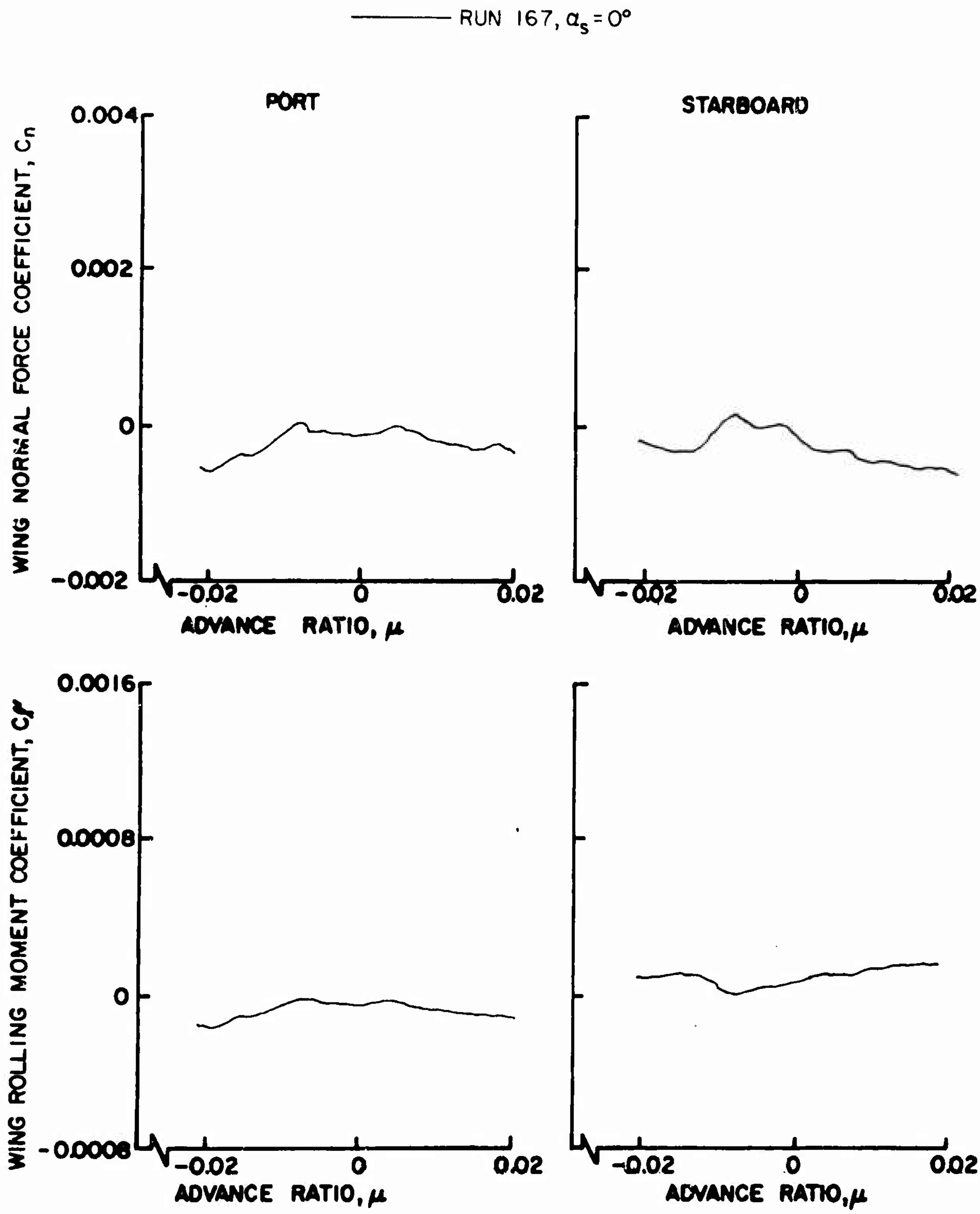

Figure 103. Wing Normal Force and Rolling Moment Coefficients as Functions of Advance Ratio, $\theta_{.75R} = 8°$, Large Wing on Low, $\frac{h}{D} = 0.30$.

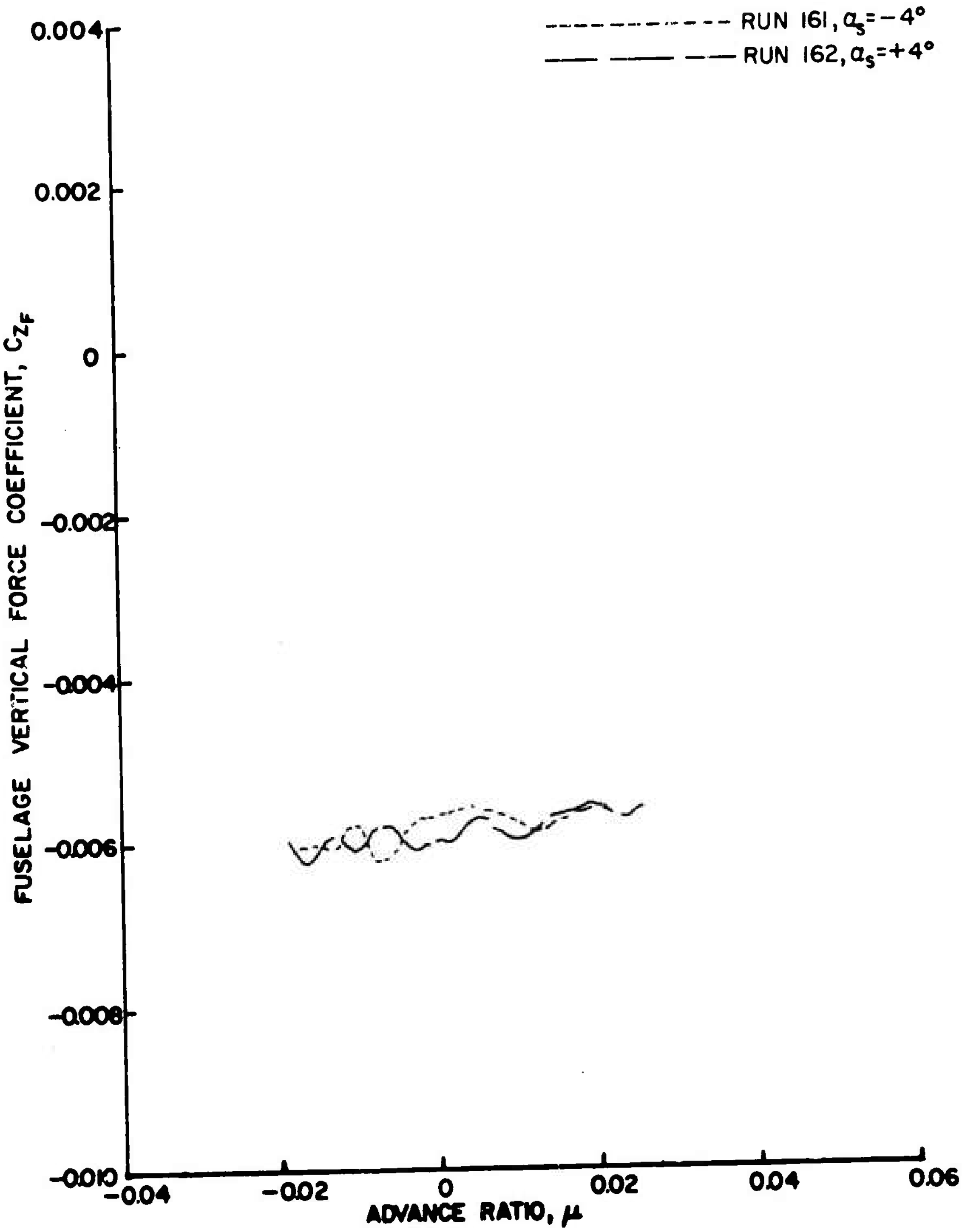

Figure 104a. Fuselage Vertical Force and Pitching Moment Coefficients as Functions of Advance Ratio, $\theta_{.75R} = 10°$, Large Wing on Low, $\frac{h}{D} = 0.30$.

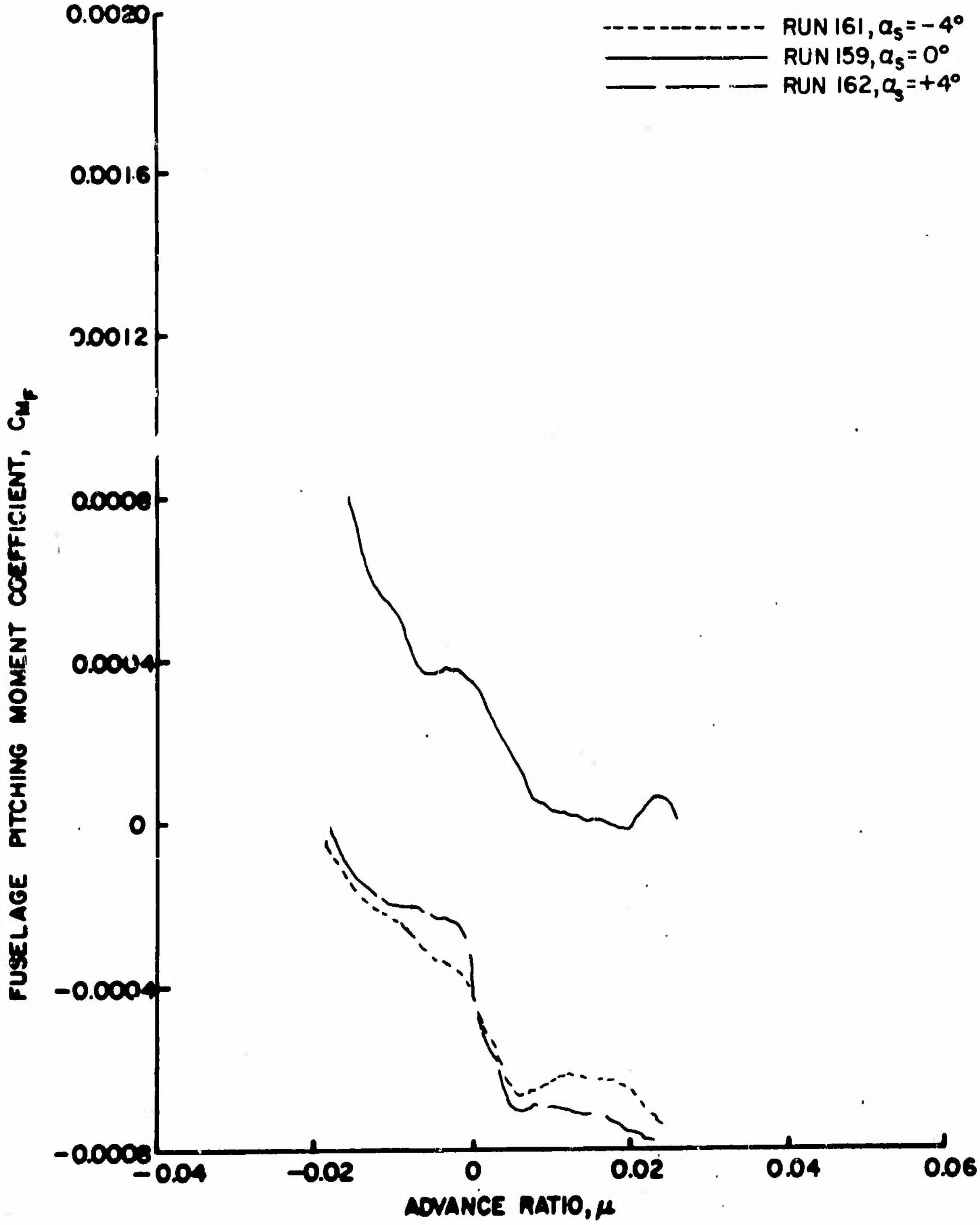

Figure 104b. Fuselage Vertical Force and Pitching Moment Coefficients as Functions of Advance Ratio, $\theta_{.75R} = 10°$, Large Wing on Low, $\frac{h}{D} = 0.30$.

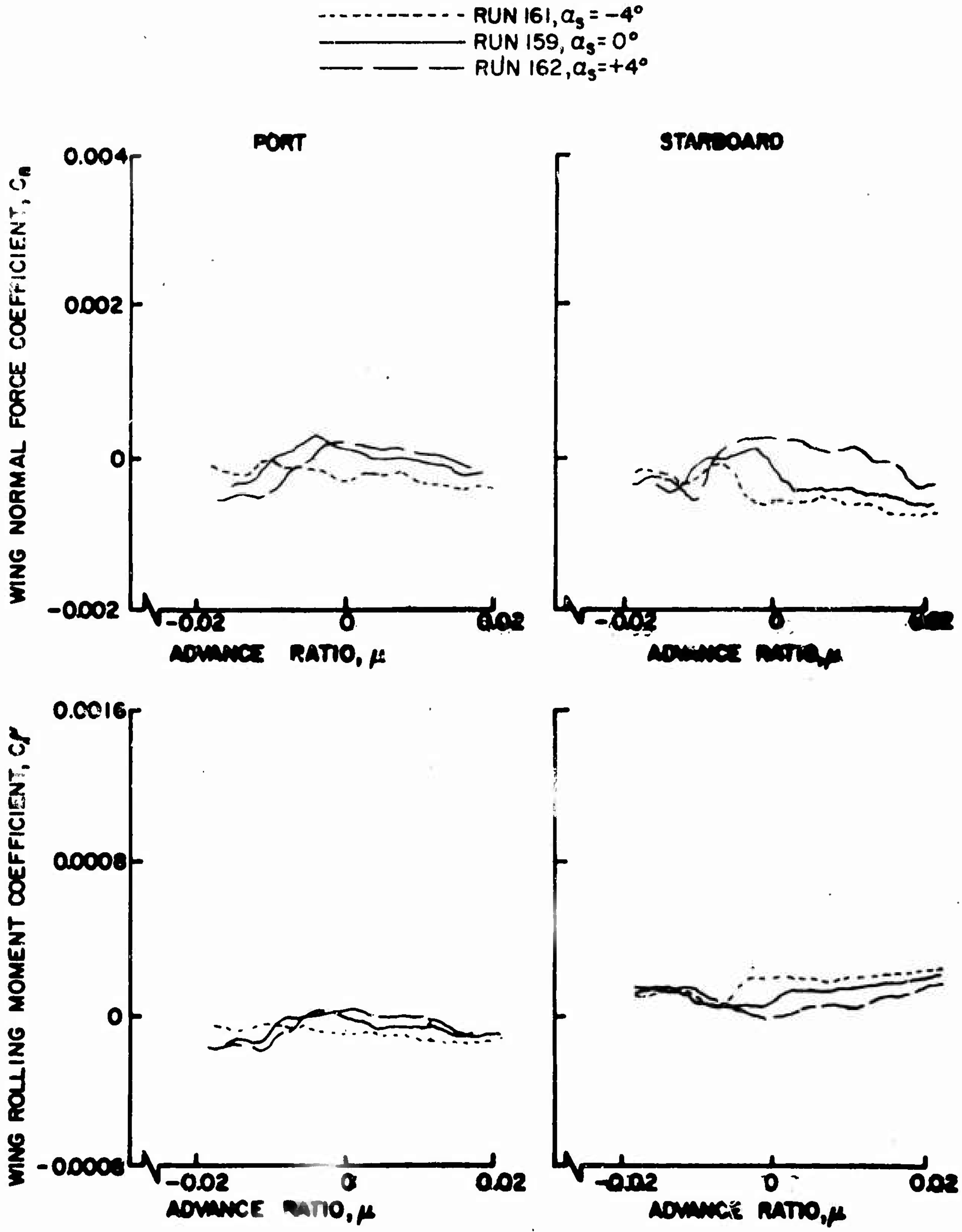

Figure 105. Wing Normal Force and Rolling Moment Coefficients as Functions of Advance Ratio, $\theta_{.75R} = 10^\circ$, Large Wing on ..., $\frac{h}{D} = 0.30$.

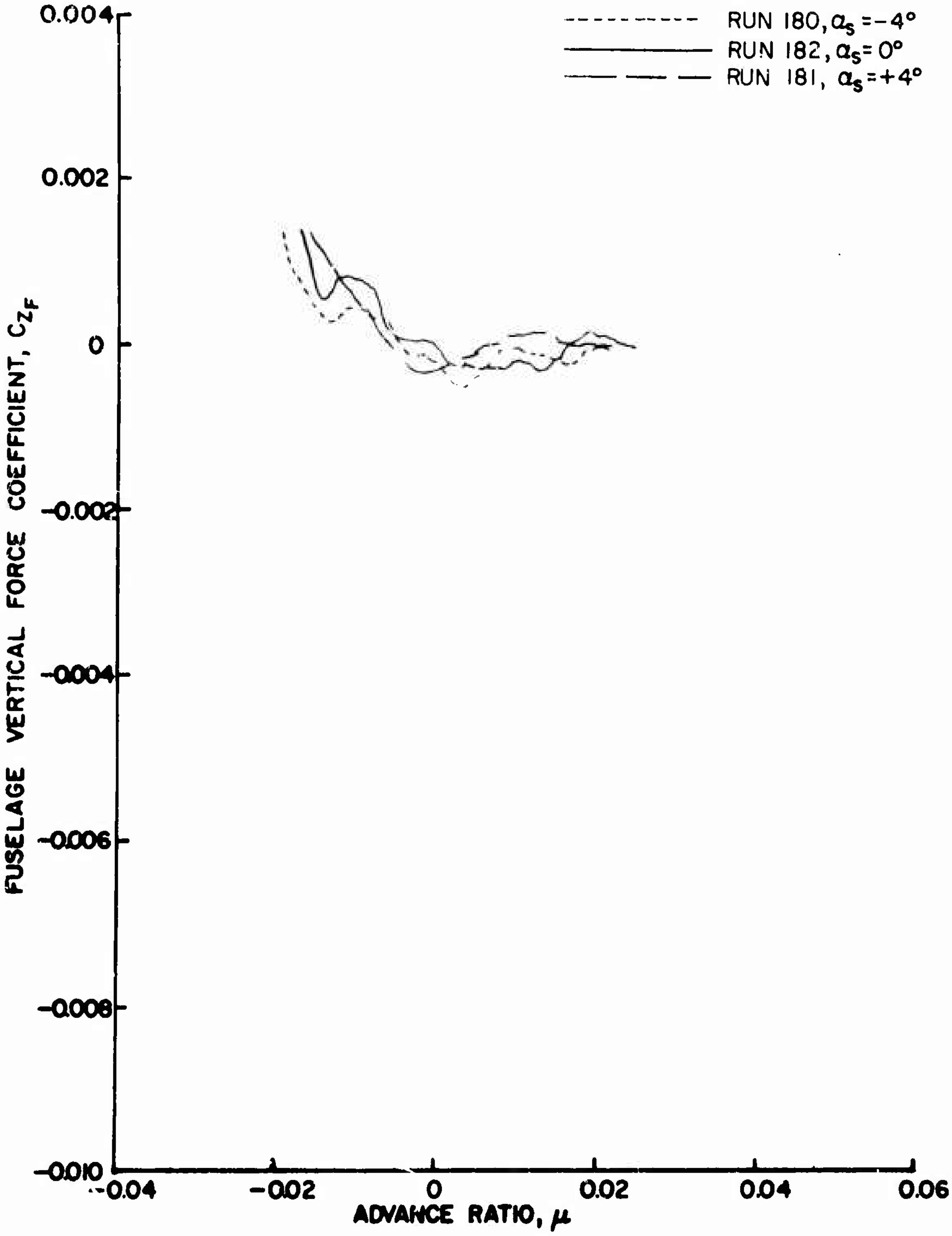

Figure 106a. Fuselage and Vertical Force and Pitching Moment Coefficients as Functions of Advance Ratio, $\theta_{.75R} = 10^{\circ}$, Small Wing on High, $\frac{h}{D} = 0.30$.

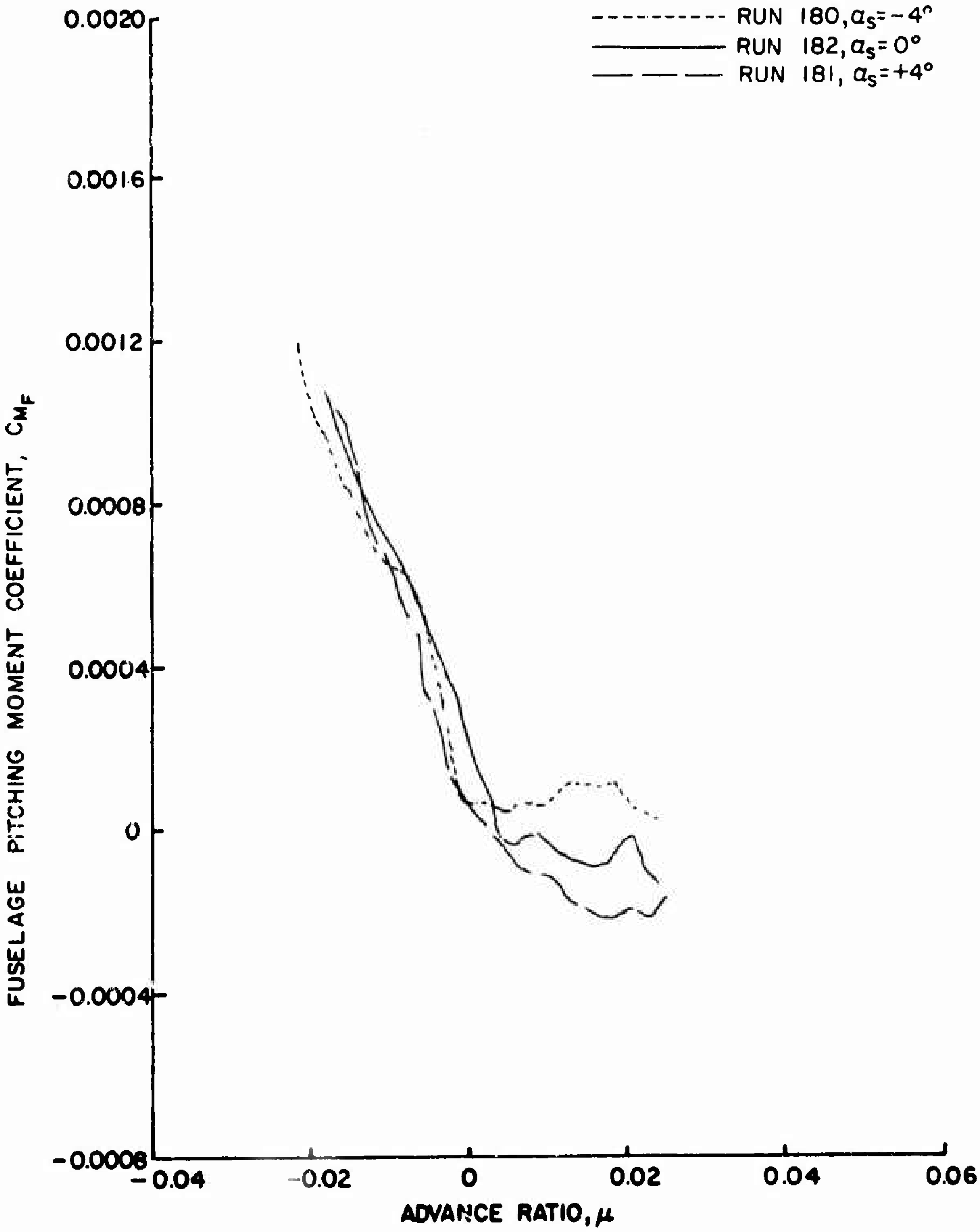

Figure 106b. Fuselage and Vertical Force and Pitching Moment Coefficients as Functions of Advance Ratio, $\theta_{.75R} = 10°$, Small Wing on High, $\frac{h}{D} = 0.30$.

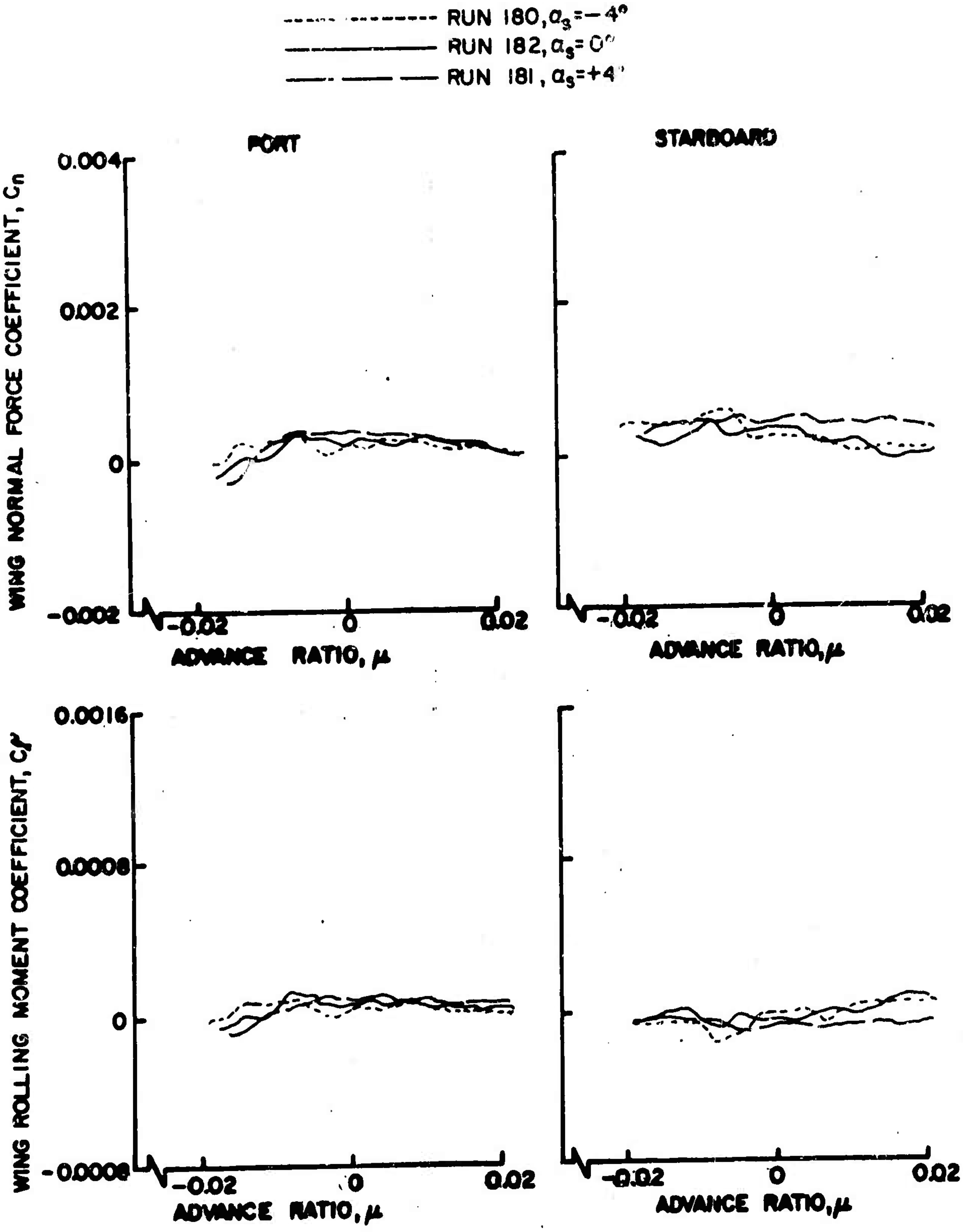

Figure 107. Wing Normal Force and Rolling Moment Coefficients as Functions of Advance Ratio, $\theta_{.75R} = 10^\circ$, Small Wing on High, $\frac{h}{D} = 0.30$.

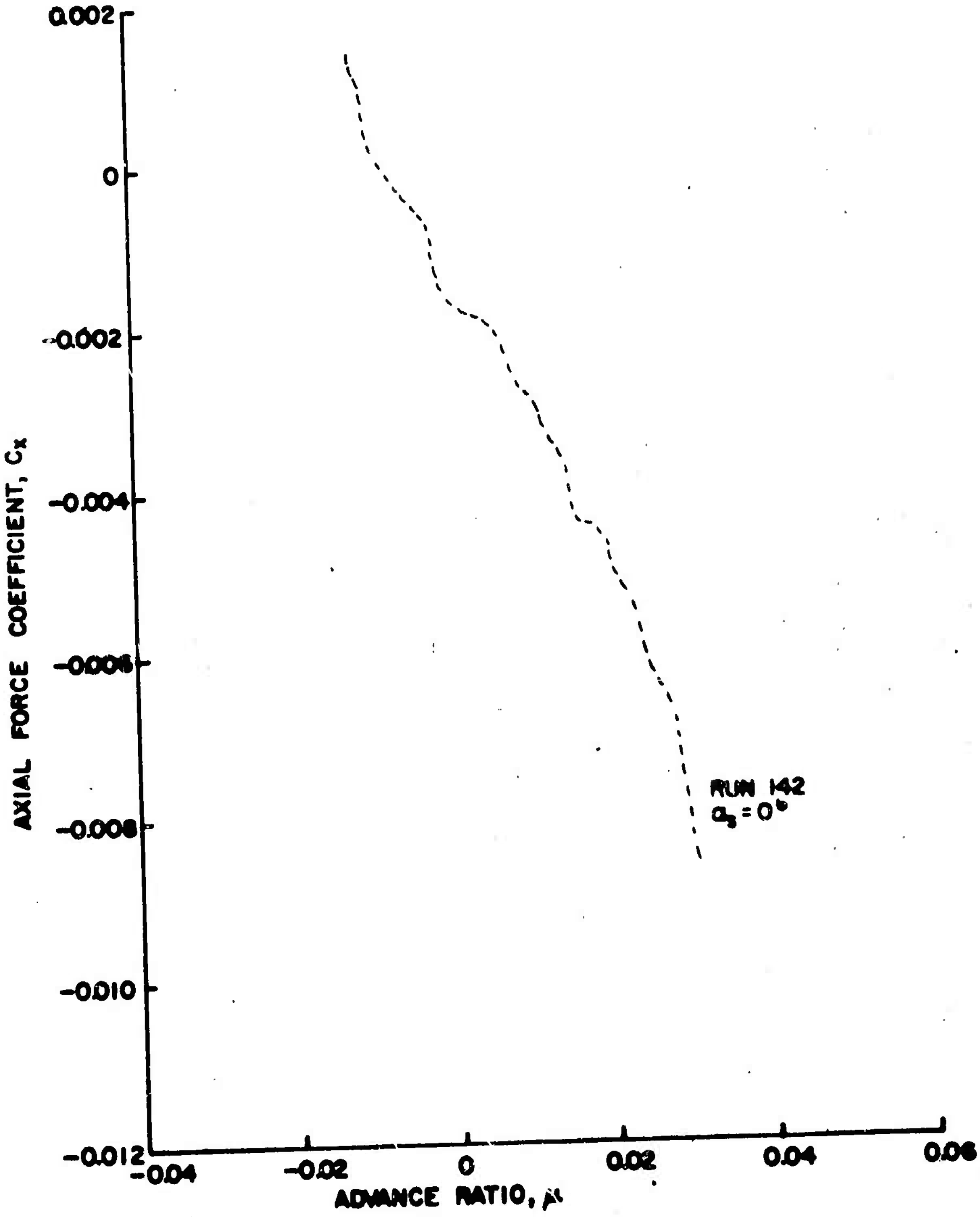

Figure 108a. Rotor Force and Moment Coefficients as Functions of Sideslip Ratio, $\theta_{.75R} = 8°$, Large Wing on High, $\frac{h}{D} = 0.75$.

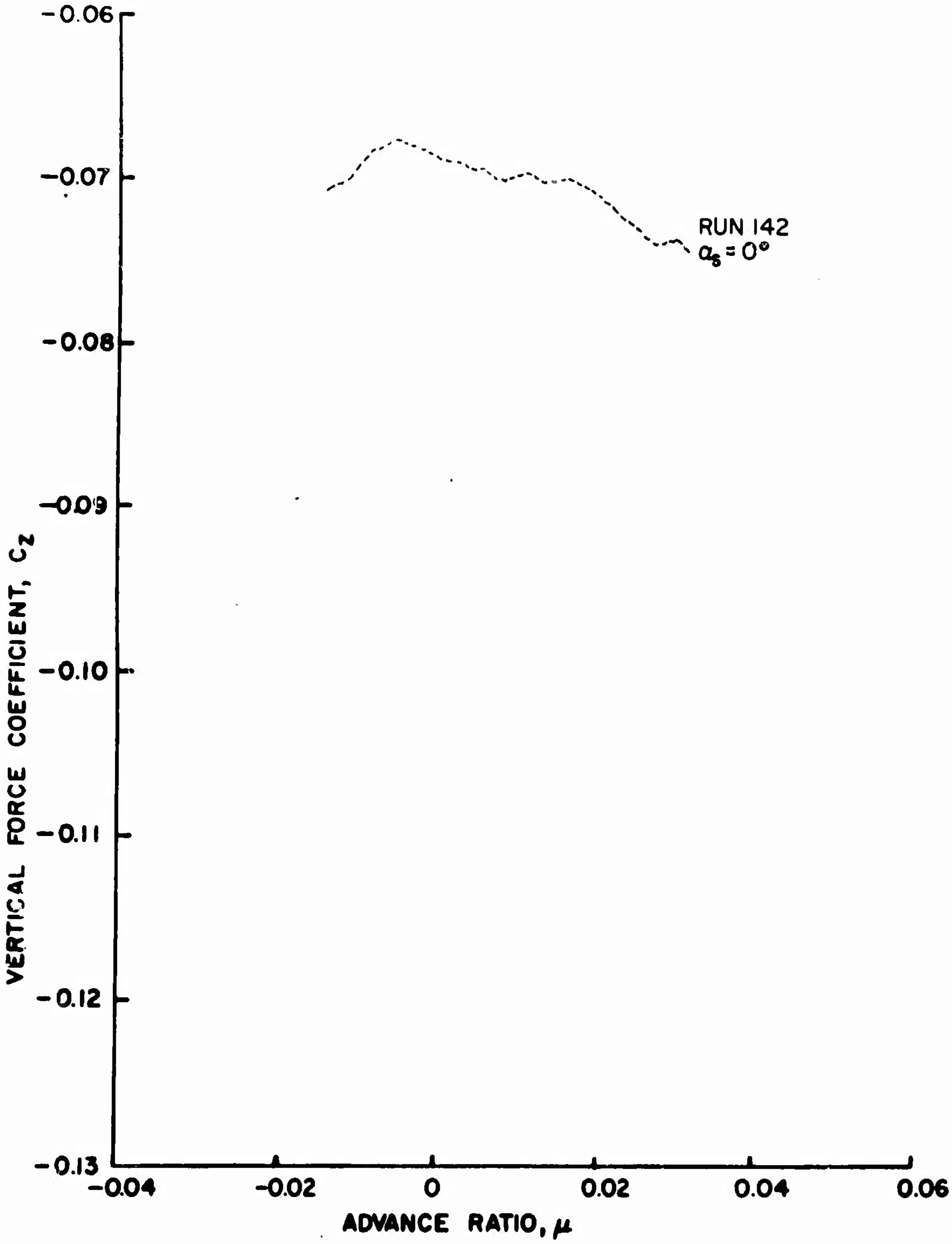

Figure 108b. Rotor Force and Moment Coefficients as Functions of Sideslip Ratio, $\theta_{.75R} = 8°$, Large Wing on High, $\frac{h}{D} = 0.75$.

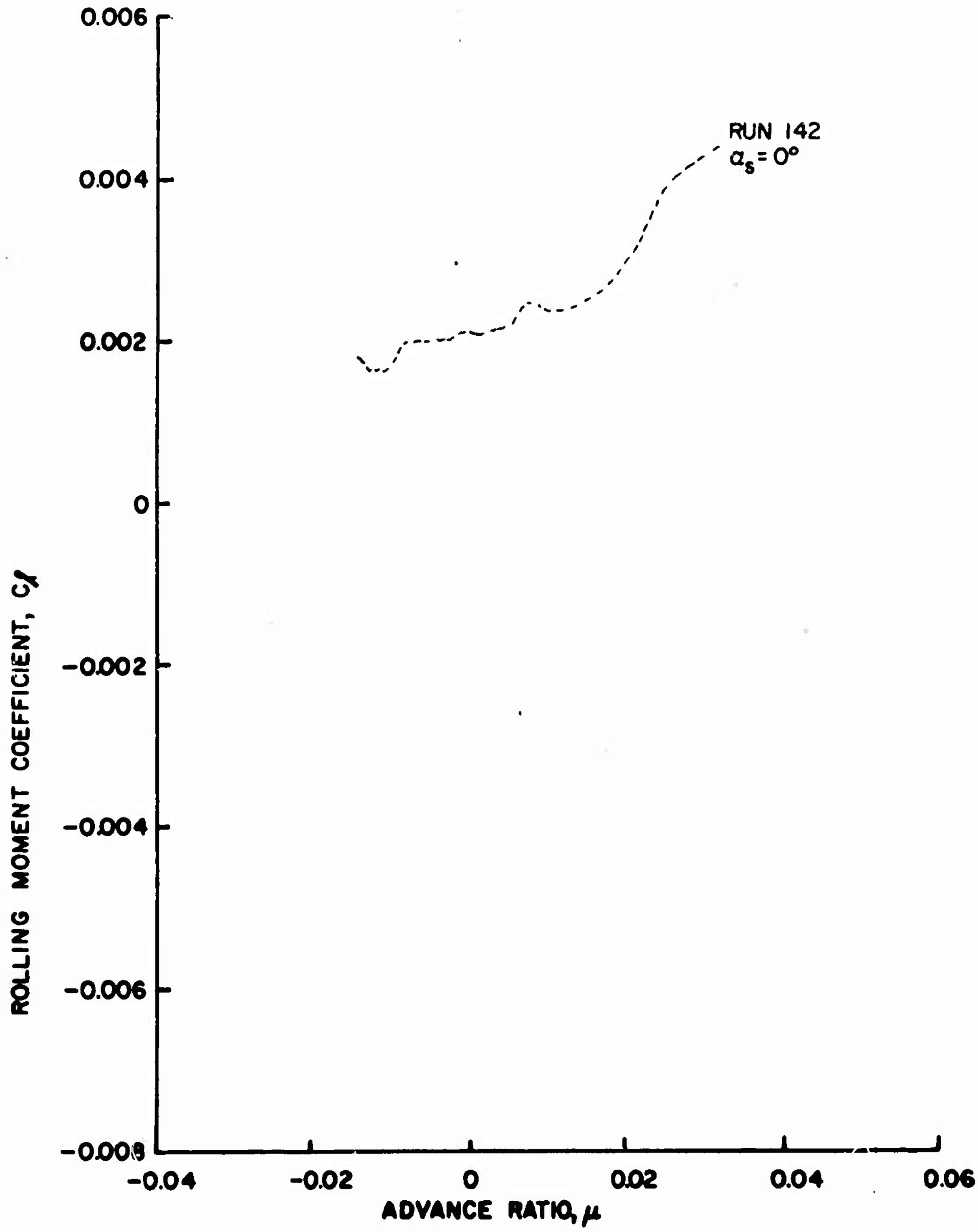

Figure 108c. Rotor Force and Moment Coefficients as Functions of Sideslip Ratio, $\theta_{.75R} = 8°$, Large Wing on High, $\frac{h}{D} = 0.75$.

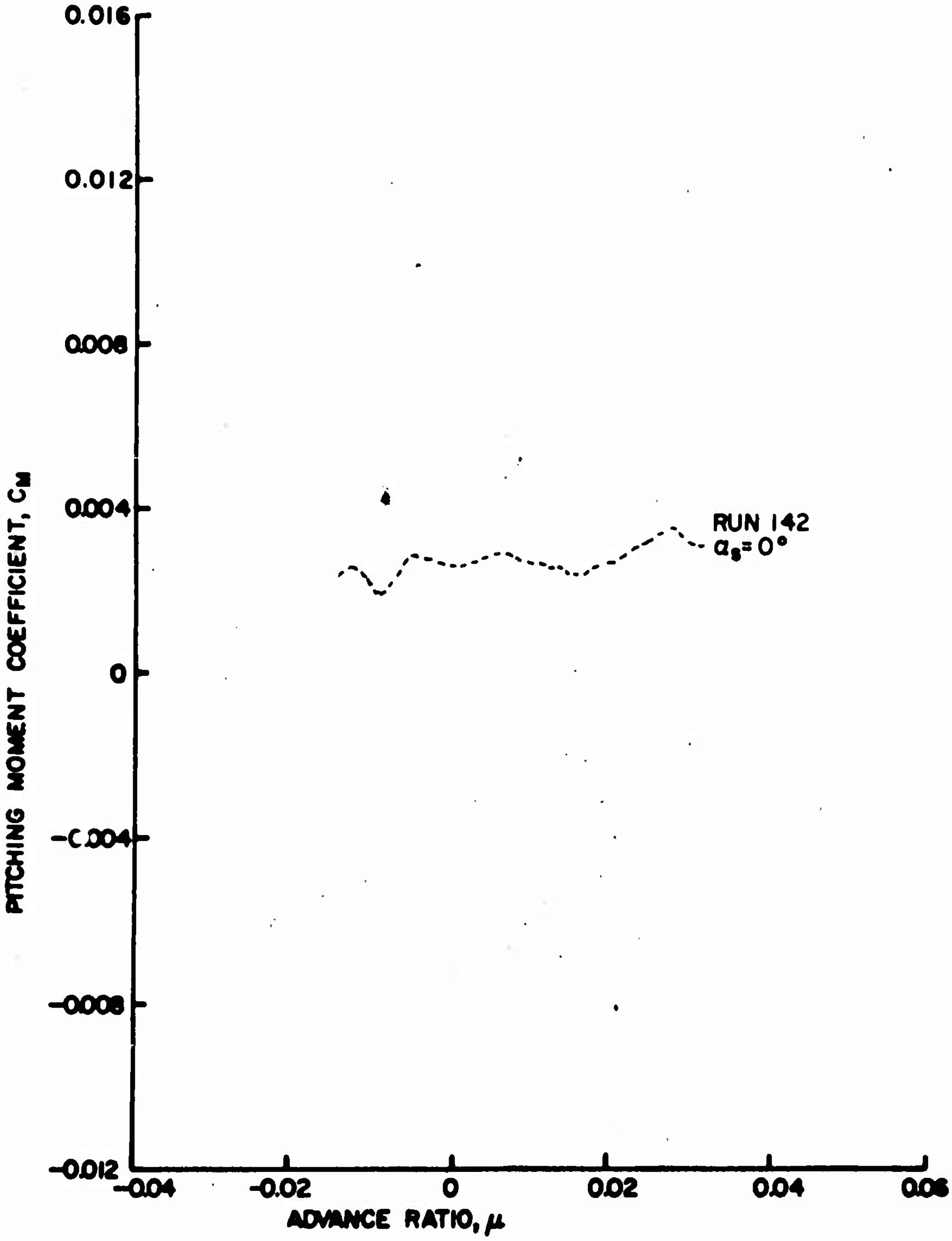

Figure 108d. Rotor Force and Moment Coefficients as Functions of Sideslip Ratio, $\theta_{.75R} = 8°$, Large Wing on High, $\frac{h}{D} = 0.75$.

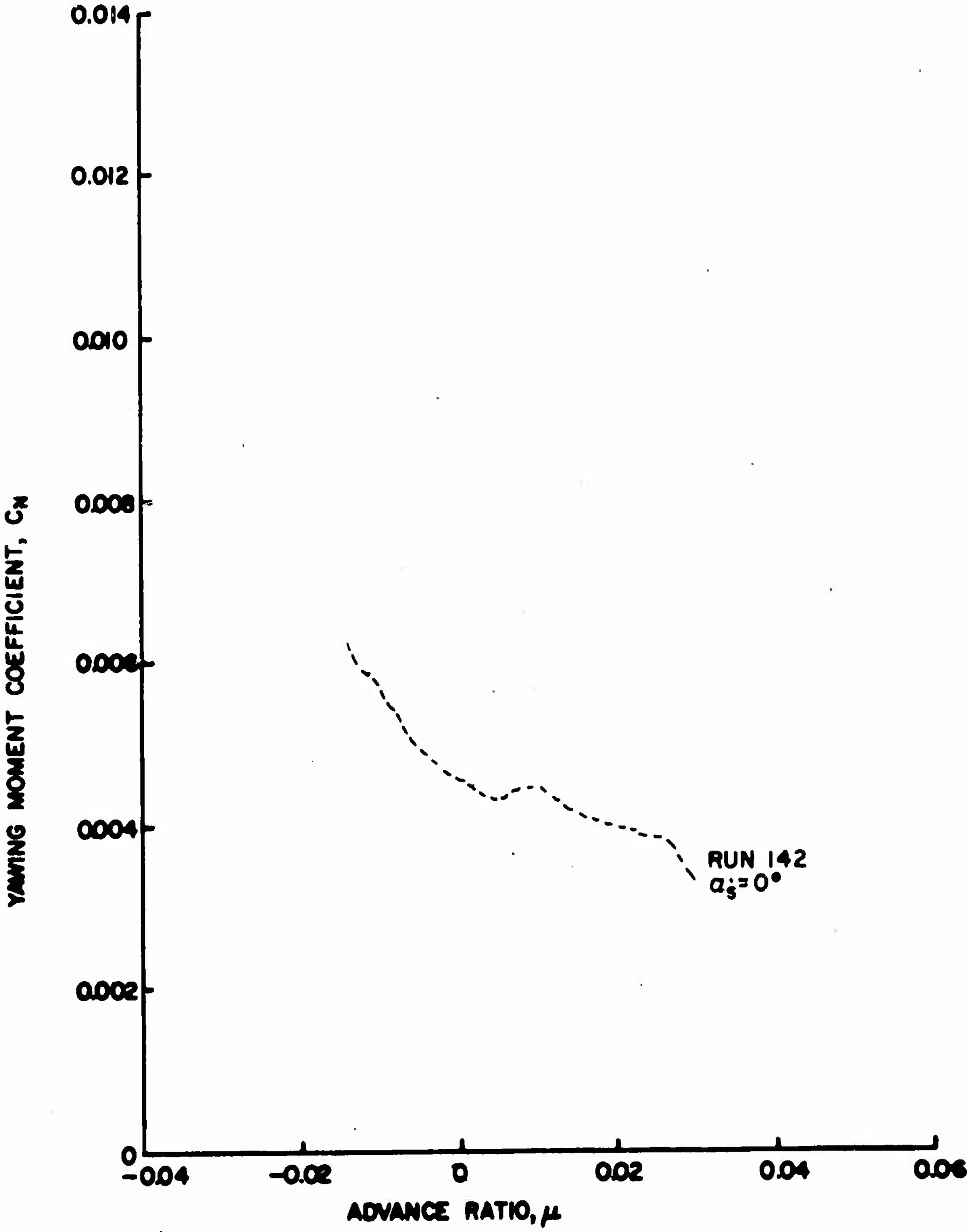

Figure 108e. Rotor Force and Moment Coefficients as Functions of Sideslip Ratio, $\theta_{.75R} = 8^{\circ}$, Large Wing on High, $\frac{h}{D} = 0.75$.

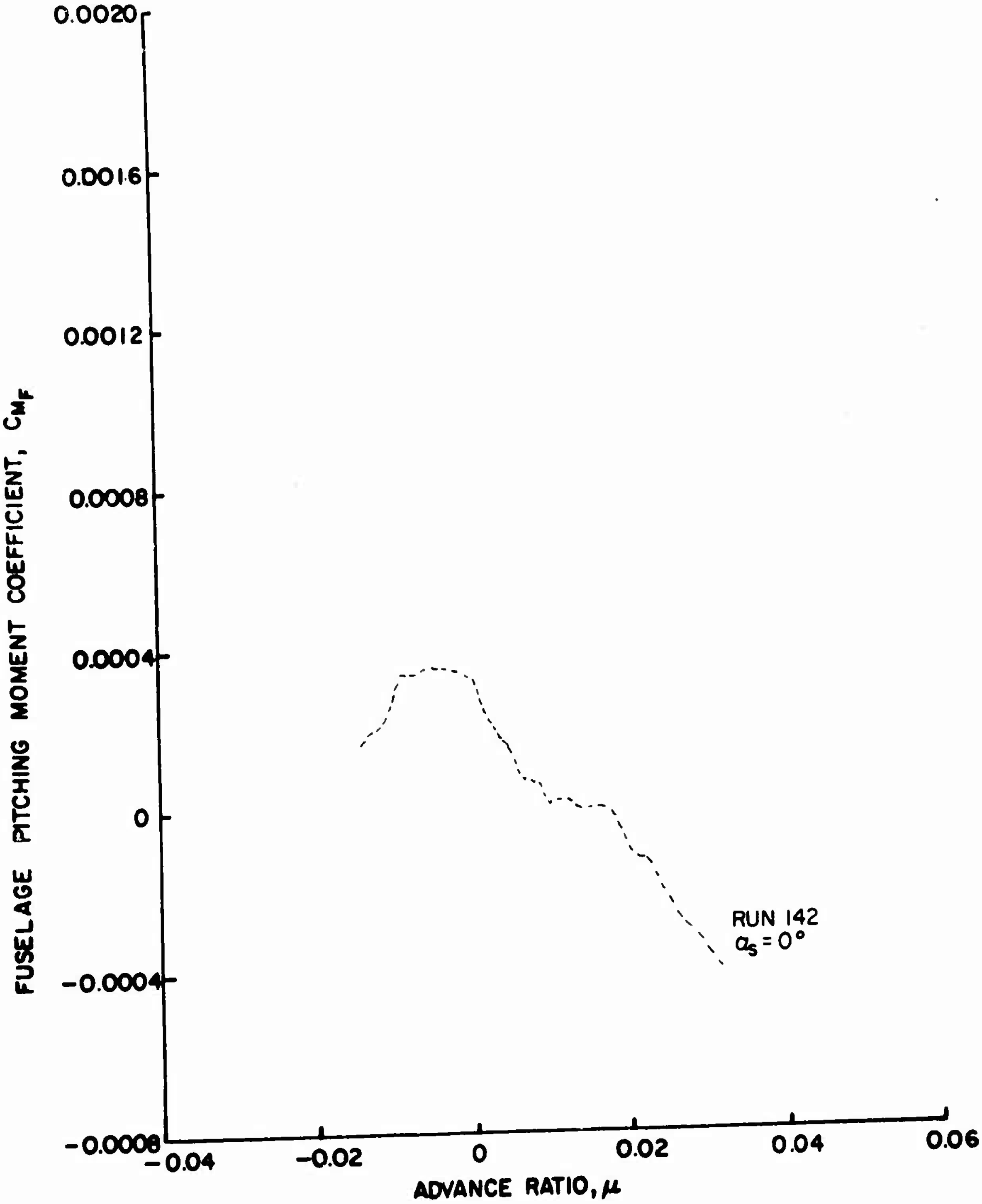

Figure 109. Fuselage Vertical Force and Pitching Moment Coefficients as Functions of Sideslip Ratio, $\theta_{.75R} = 8°$, Large Wing on High, $\frac{h}{D} = 0.75$.

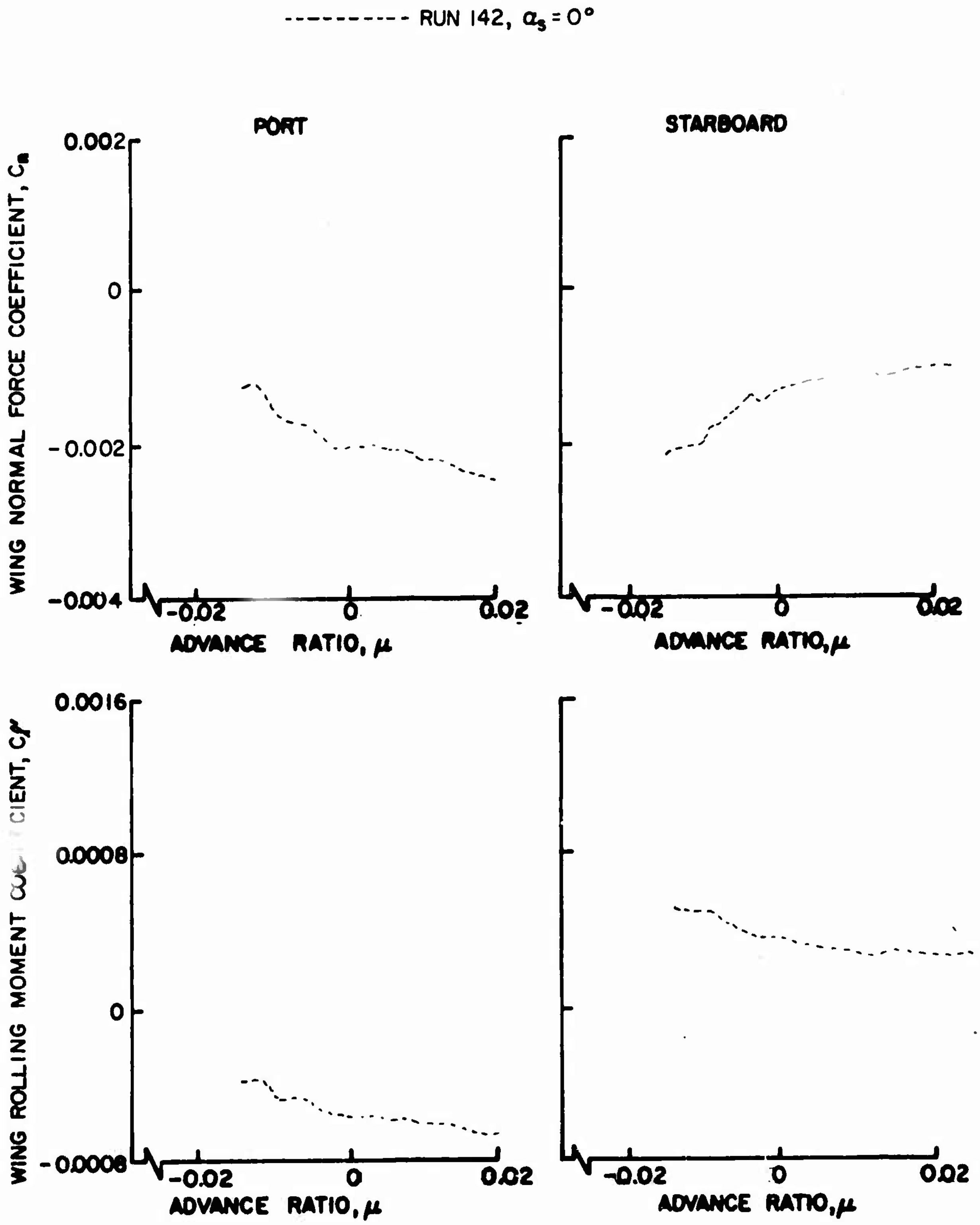

Figure 110. Wing Normal Force and Rolling Moment Coefficients as Functions of Sideslip Ratio, $\theta_{.75R} = 8°$, Large Wing on High, $\frac{h}{D} = 0.75$.

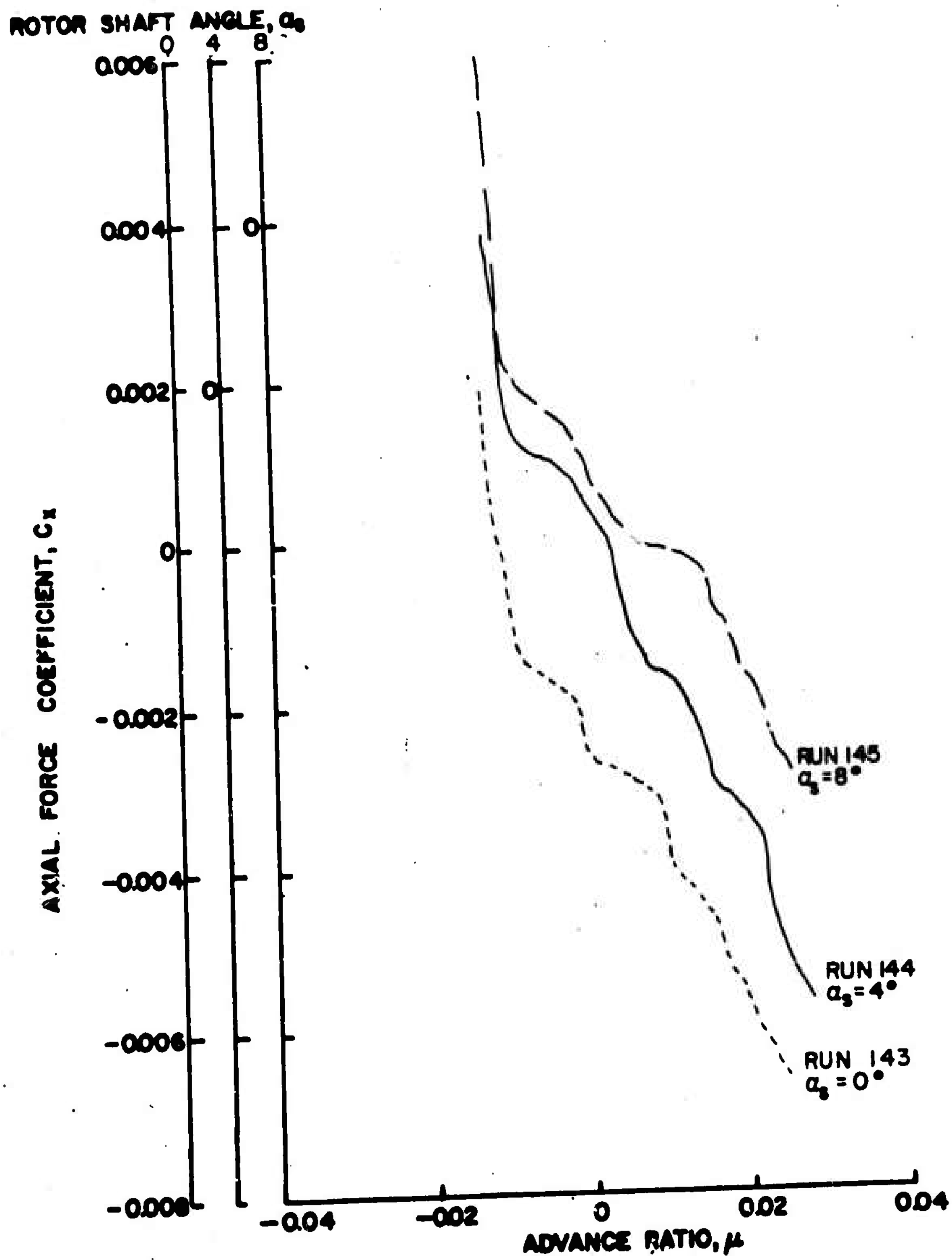

Figure 111a. Rotor Force and Moment Coefficients as Functions of Sideslip Ratio, $\theta_{.75R} = 10^\circ$, Large Wing on High, $\frac{h}{D} = 0.75$.

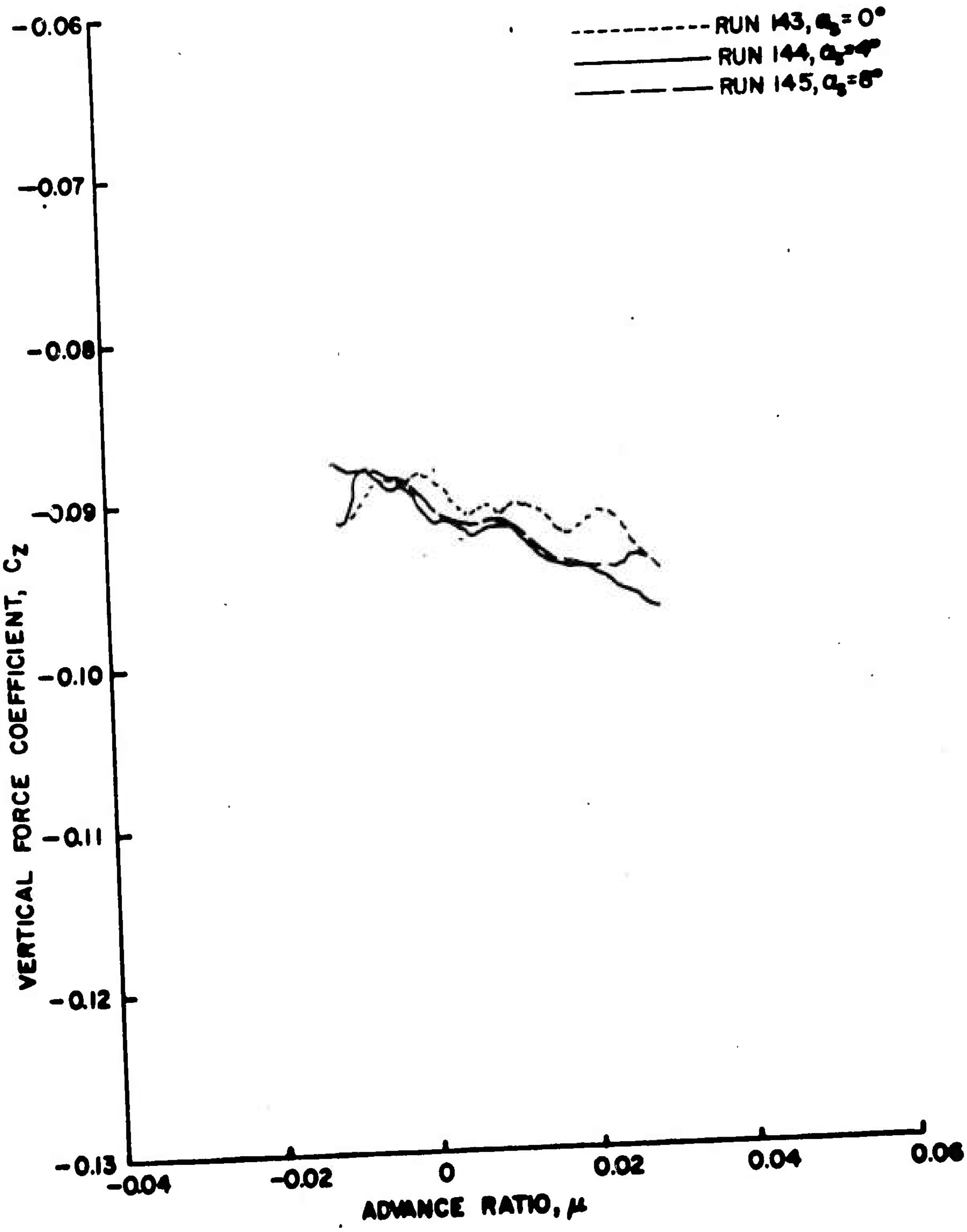

Figure 111b. Rotor Force and Moment Coefficients as Functions of Sideslip Ratio, $\theta_{.75R} = 10^\circ$, Large Wing on High, $\frac{h}{D} = 0.75$.

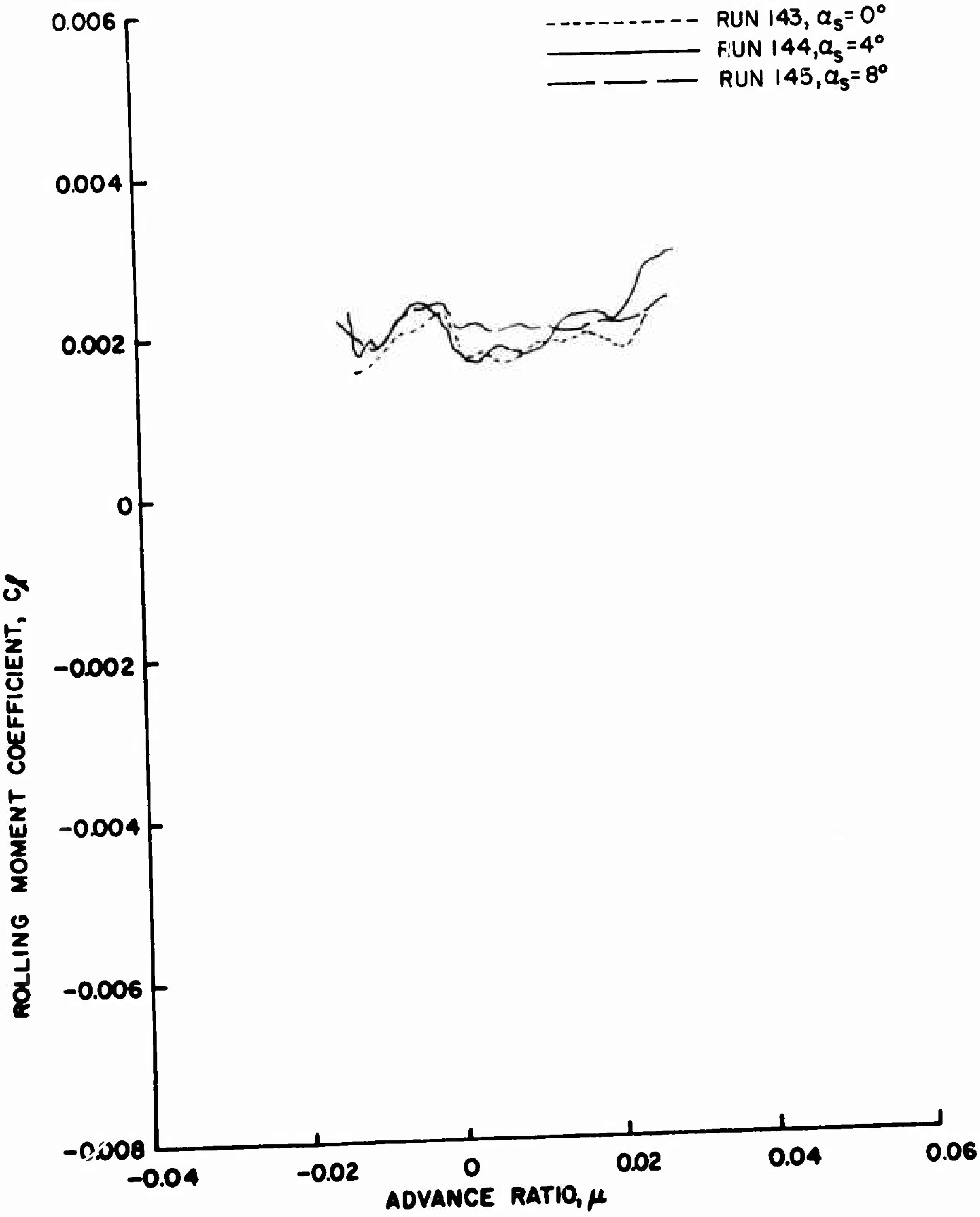

Figure 111c. Rotor Force and Moment Coefficients as Functions of Sideslip Ratio, $\theta_{.75R} = 10^\circ$, Large Wing on High, $\frac{h}{D} = 0.75$.

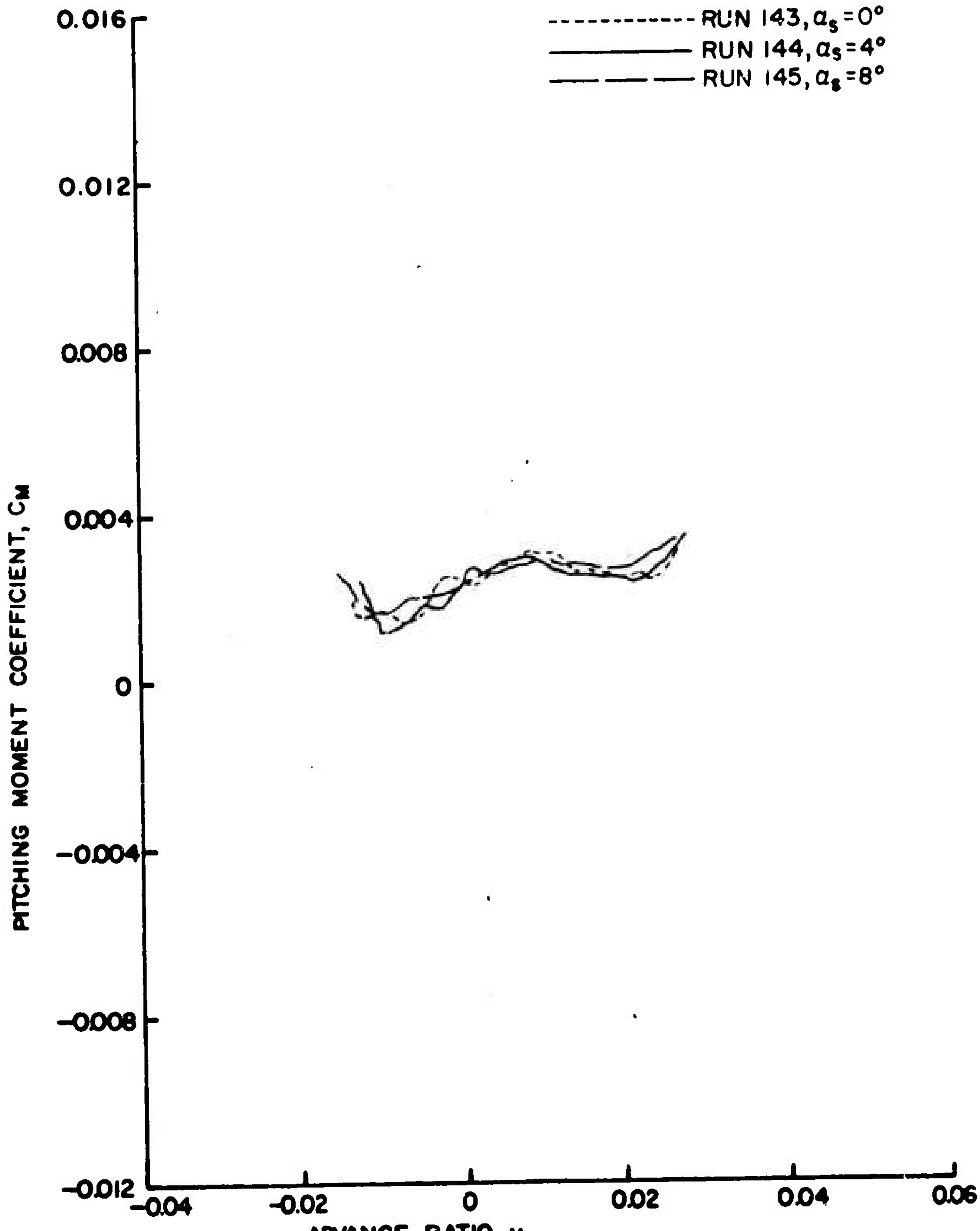

Figure 111d. Rotor Force and Moment Coefficients as Functions of Sideslip Ratio, $\theta_{.75R} = 10°$, Large Wing on High, $\frac{h}{D} = 0.75$.

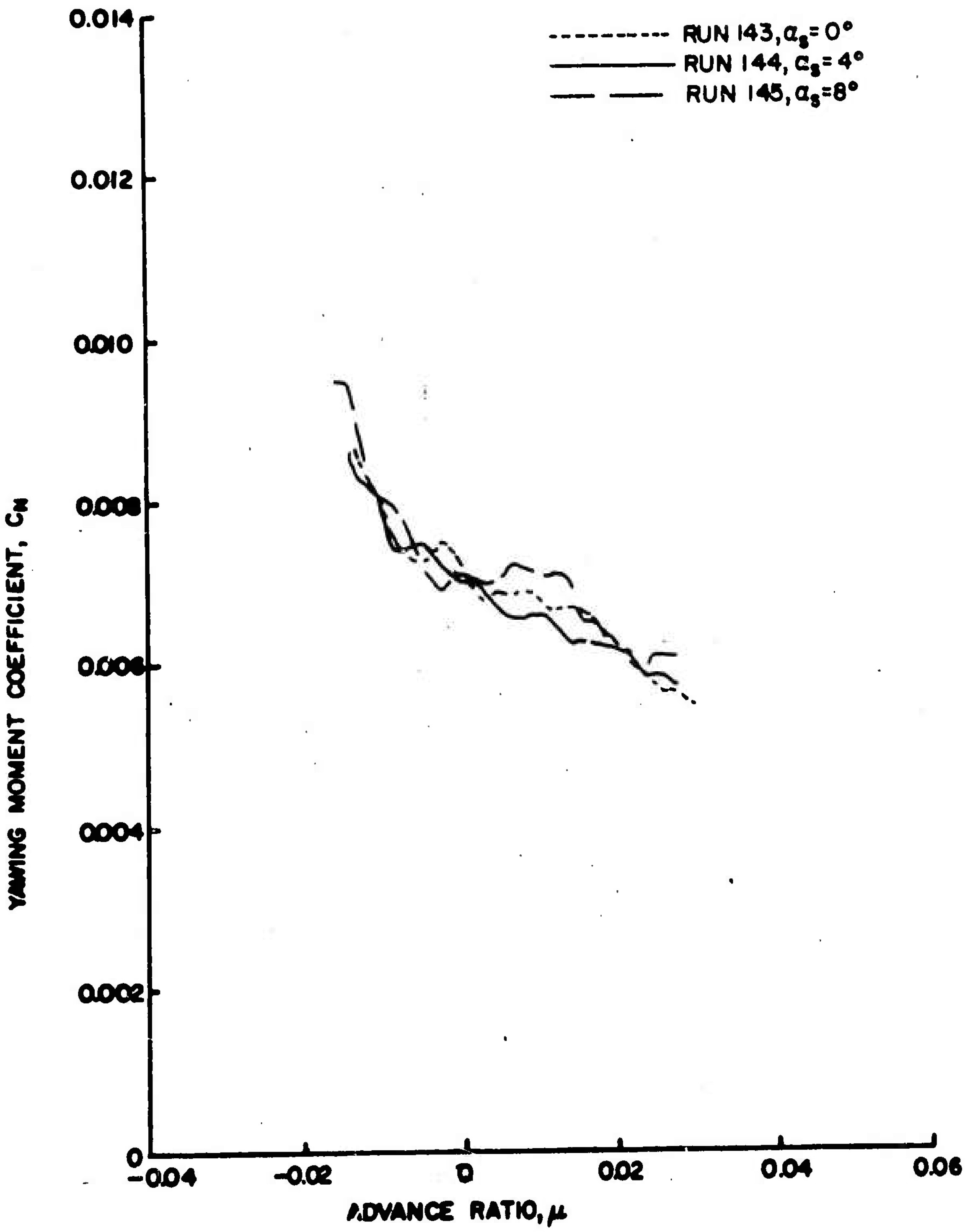

Figure 111e. Rotor Force and Moment Coefficients as Functions of Sideslip Ratio, $\theta_{.75R} = 10^\circ$, Large Wing on High, $\frac{h}{D} = 0.75$.

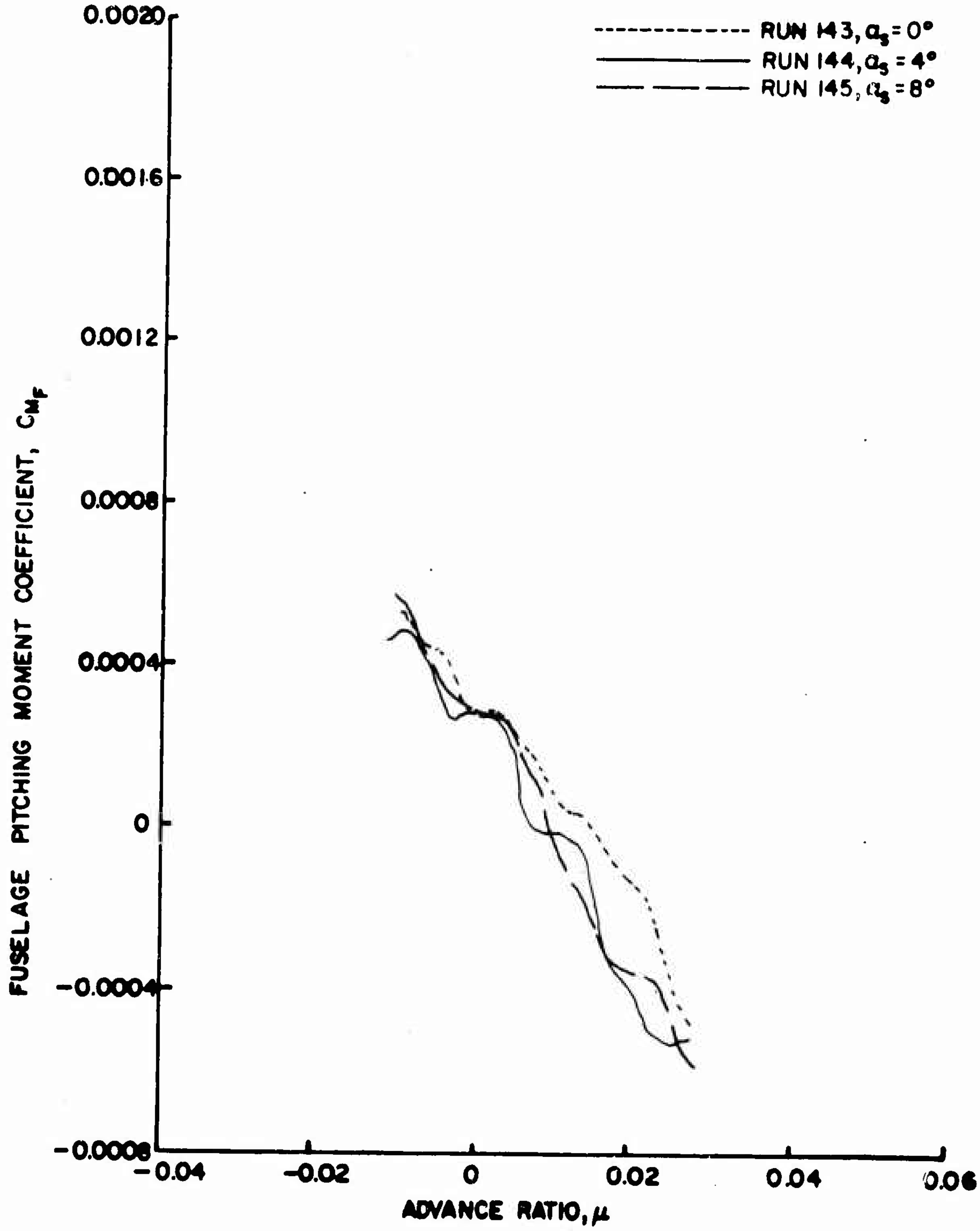

Figure 112. Fuselage Vertical Force and Pitching Moment Coefficients as Functions of Sideslip Ratio, $\theta_{.75R} = 10°$, Large Wing on High, $\frac{h}{D} = 0.75$.

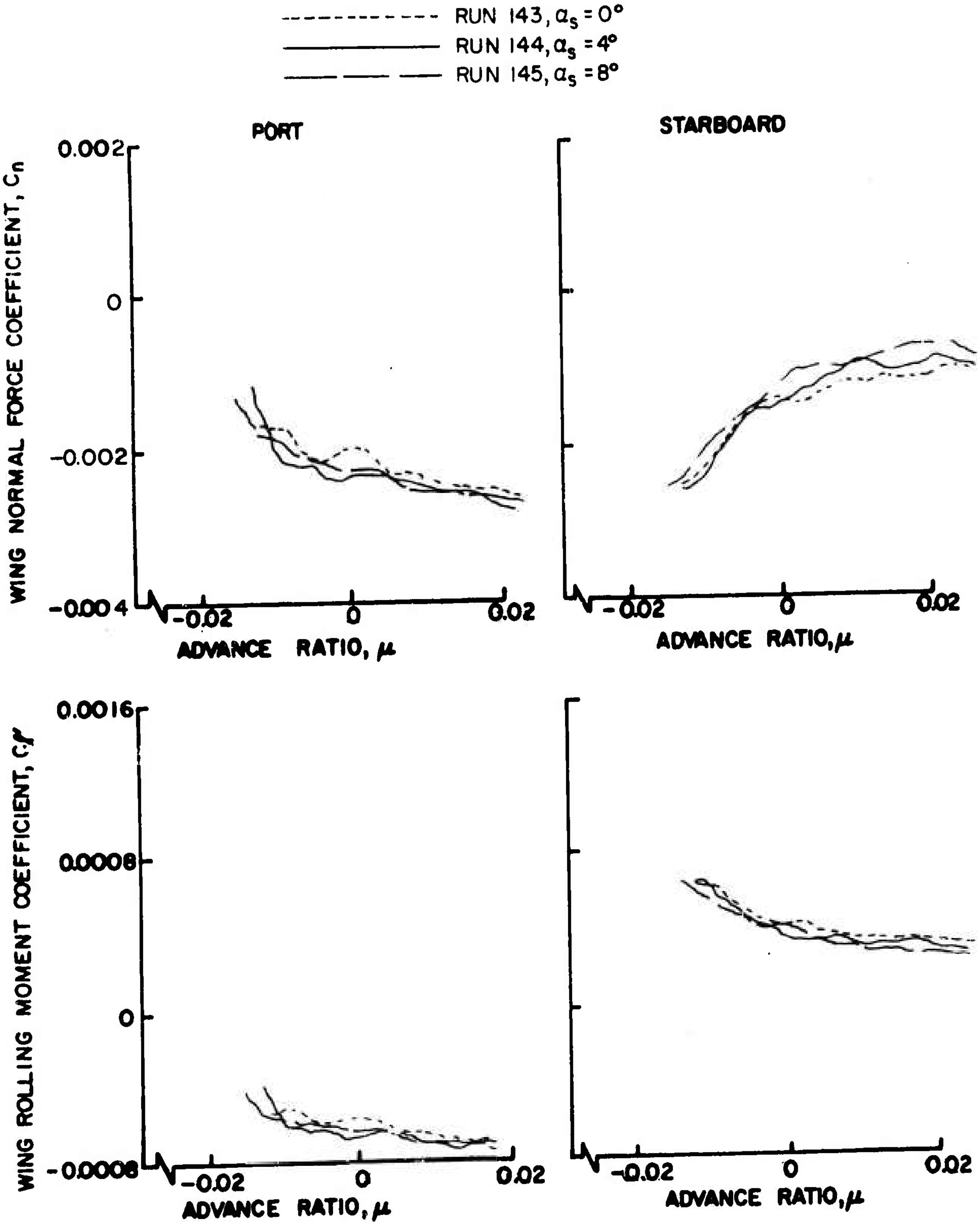

Figure 113. Wing Normal Force and Rolling Moment Coefficients as Functions of Sideslip Ratio, $\theta_{.75R} = 10^\circ$, Large Wing on High, $\frac{h}{D} = 0.75$.

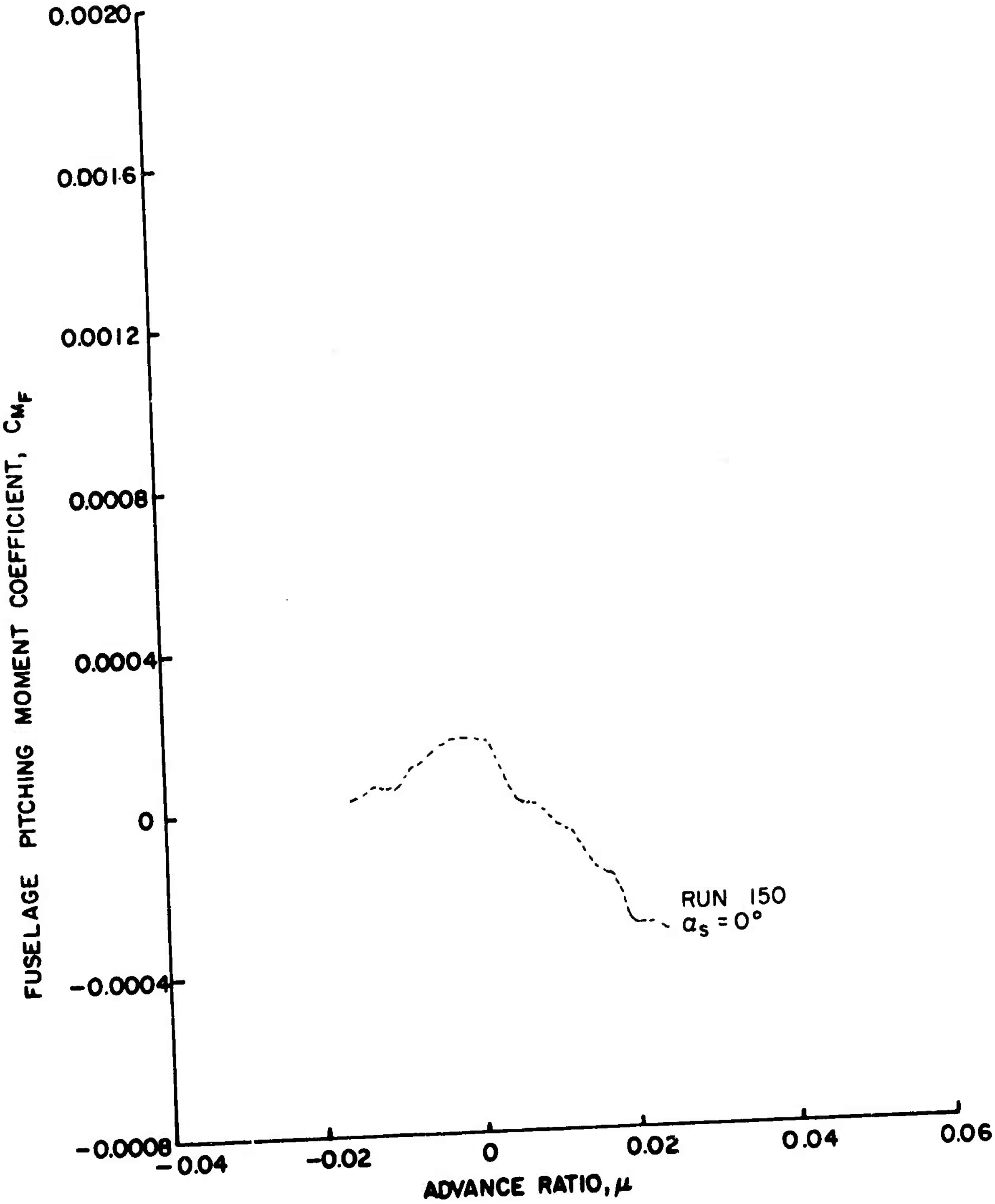

Figure 114. Fuselage Vertical Force and Pitching Moment Coefficients as Functions of Sideslip Ratio, $\theta_{.75R} = 8°$, Large Wing on Low, $\frac{h}{D} = 0.75$.

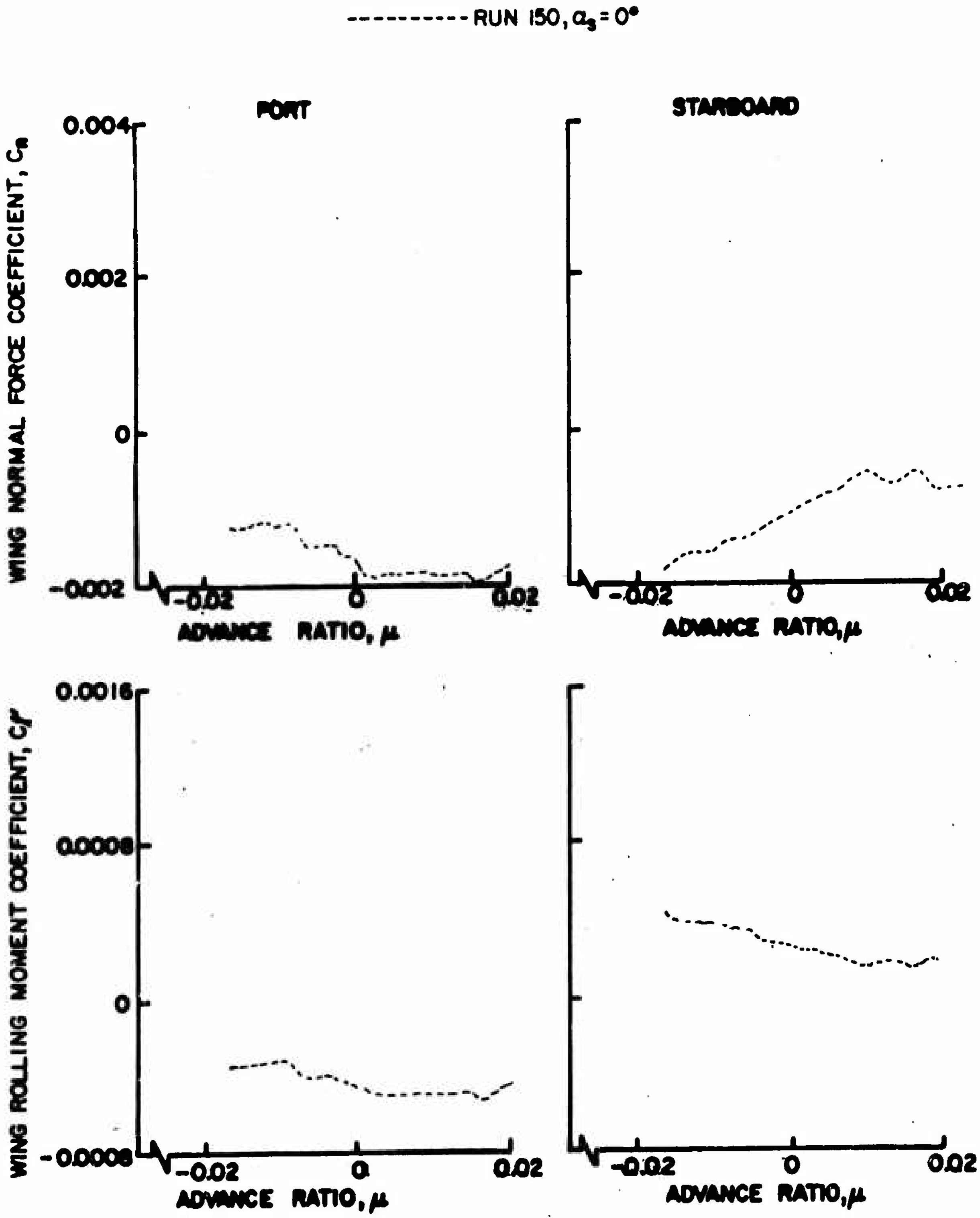

Figure 115. Wing Normal Force and Rolling Moment Coefficients as Functions of Sideslip Ratio, $\theta_{.75R} = 8^{\circ}$, Large Wing on Low, $\frac{h}{D} = 0.75$.

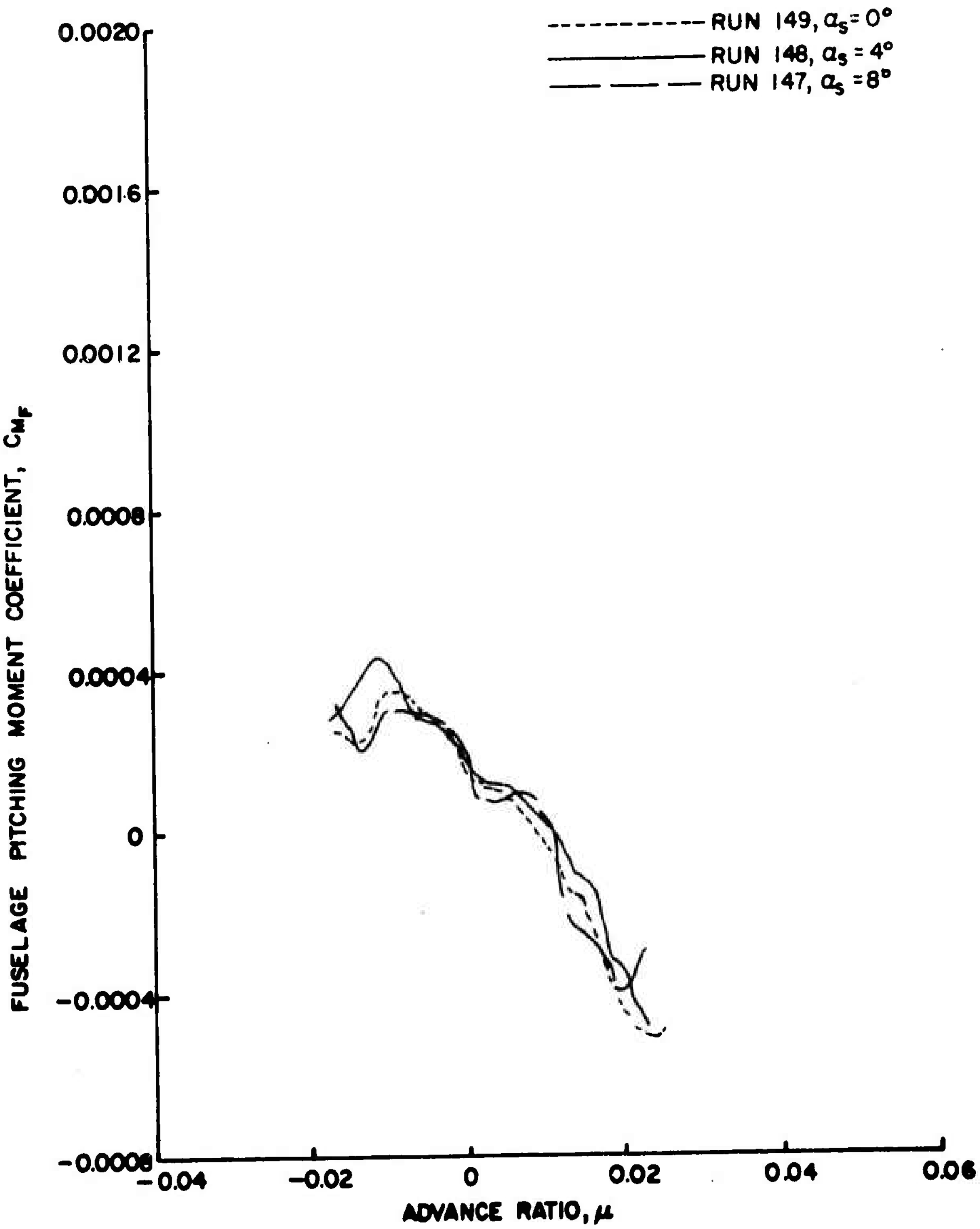

Figure 116. Fuselage Vertical Force and Pitching Moment Coefficients as Functions of Sideslip Ratio, $\theta_{.75R} = 10°$, Large Wing on Low, $\frac{h}{D} = 0.75$.

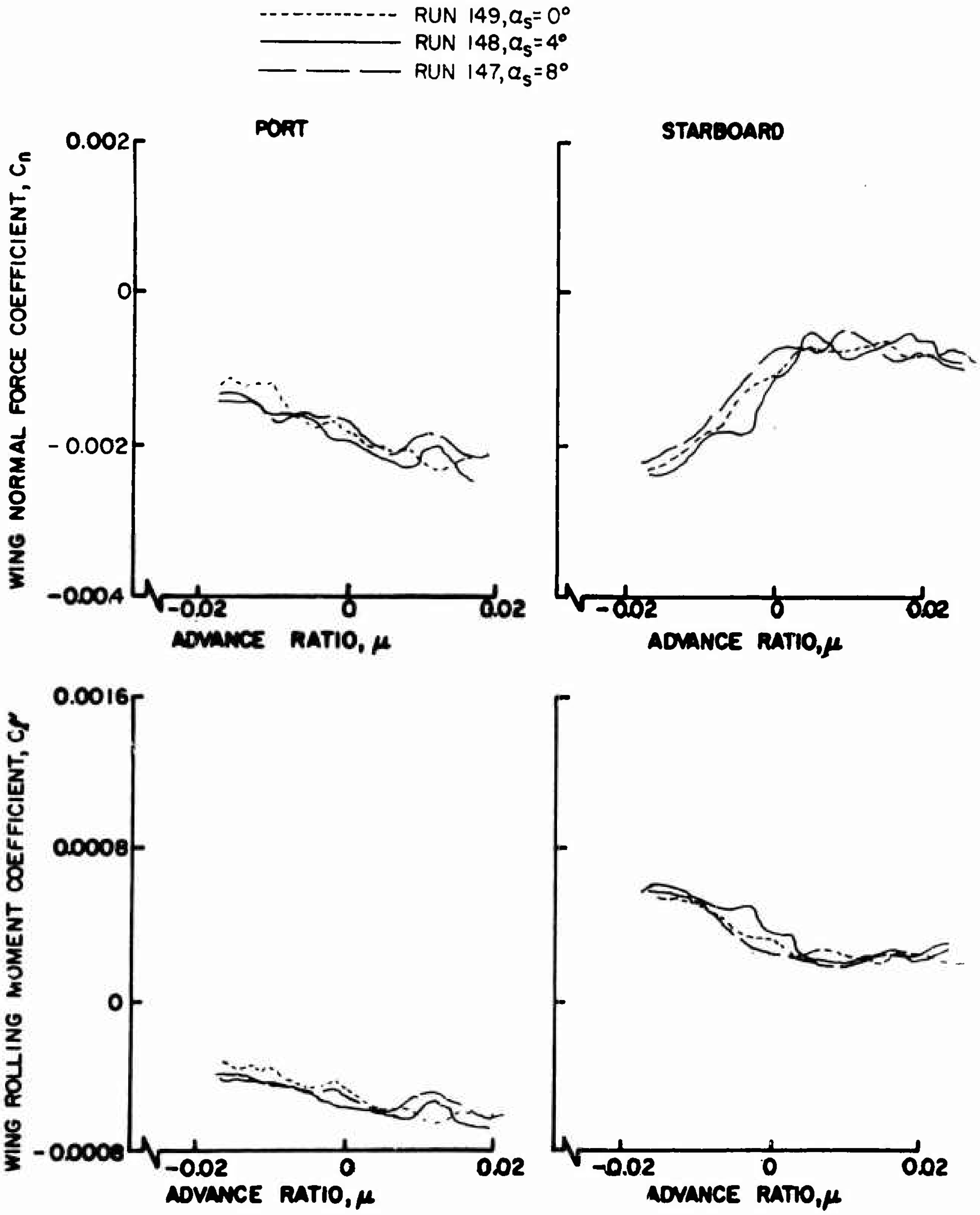

Figure 117. Wing Normal Force and Rolling Moment Coefficients as Functions of Sideslip Ratio, $\theta_{.75R} = 10°$, Large Wing on Low, $\frac{h}{D} = 0.75$.

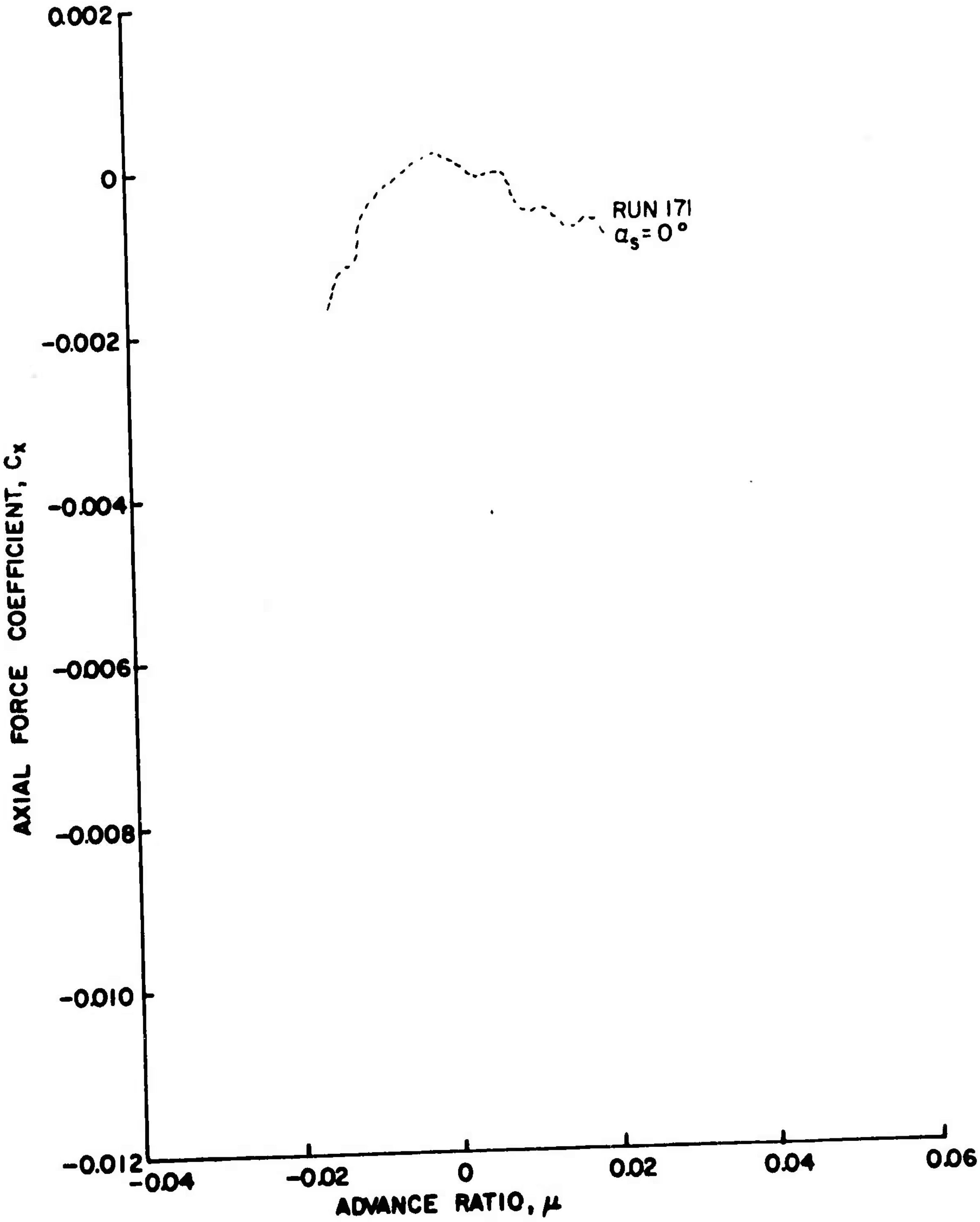

Figure 118a. Rotor Force and Moment Coefficients as Functions of Sideslip Ratio, $\theta_{.75R} = 8°$, Large Wing on High, $\frac{h}{D} = 0.30$.

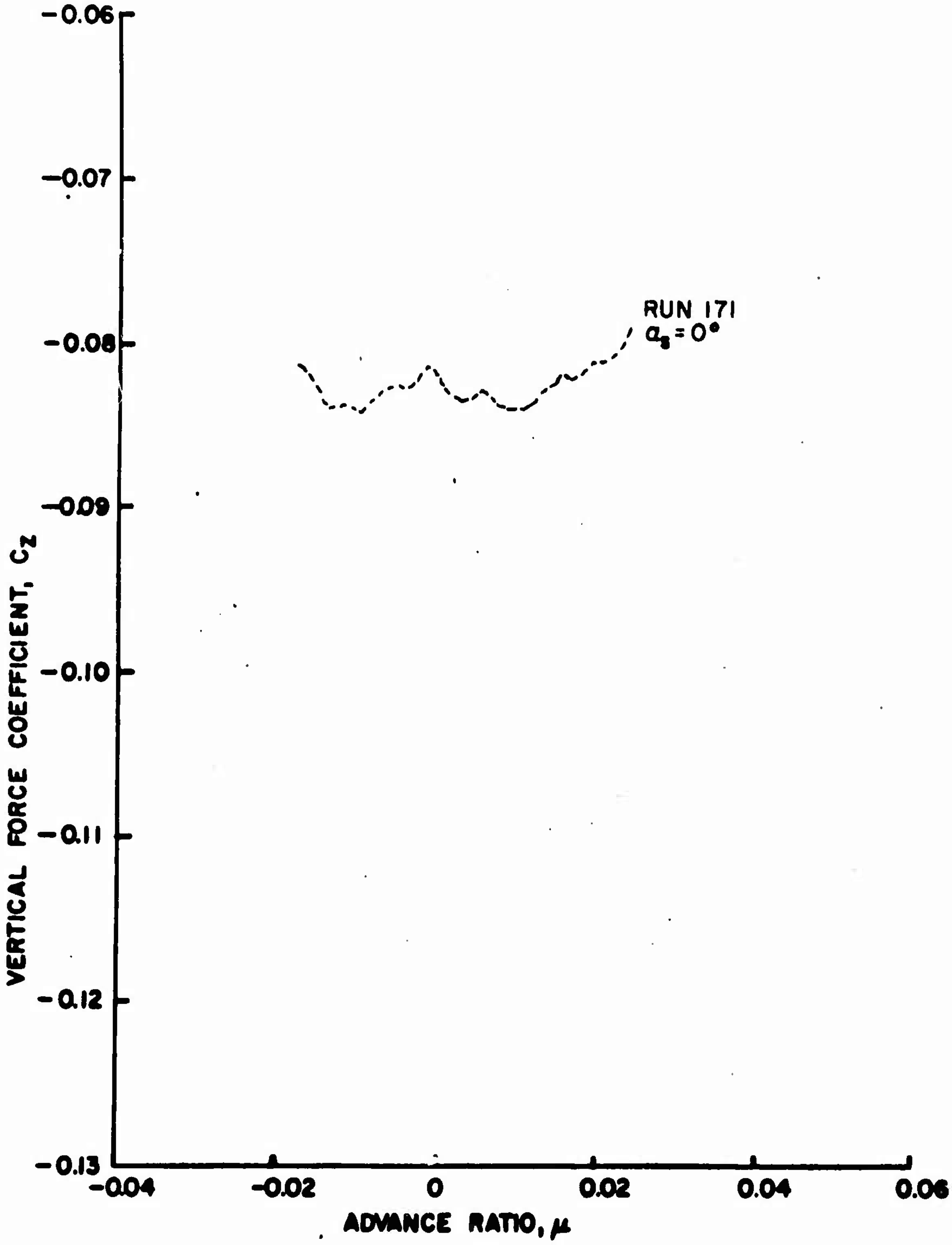

Figure 118b. Rotor Force and Moment Coefficients as Functions of Sideslip Ratio, $\theta_{.75R} = 8°$, Large Wing on High, $\frac{h}{D} = 0.30$.

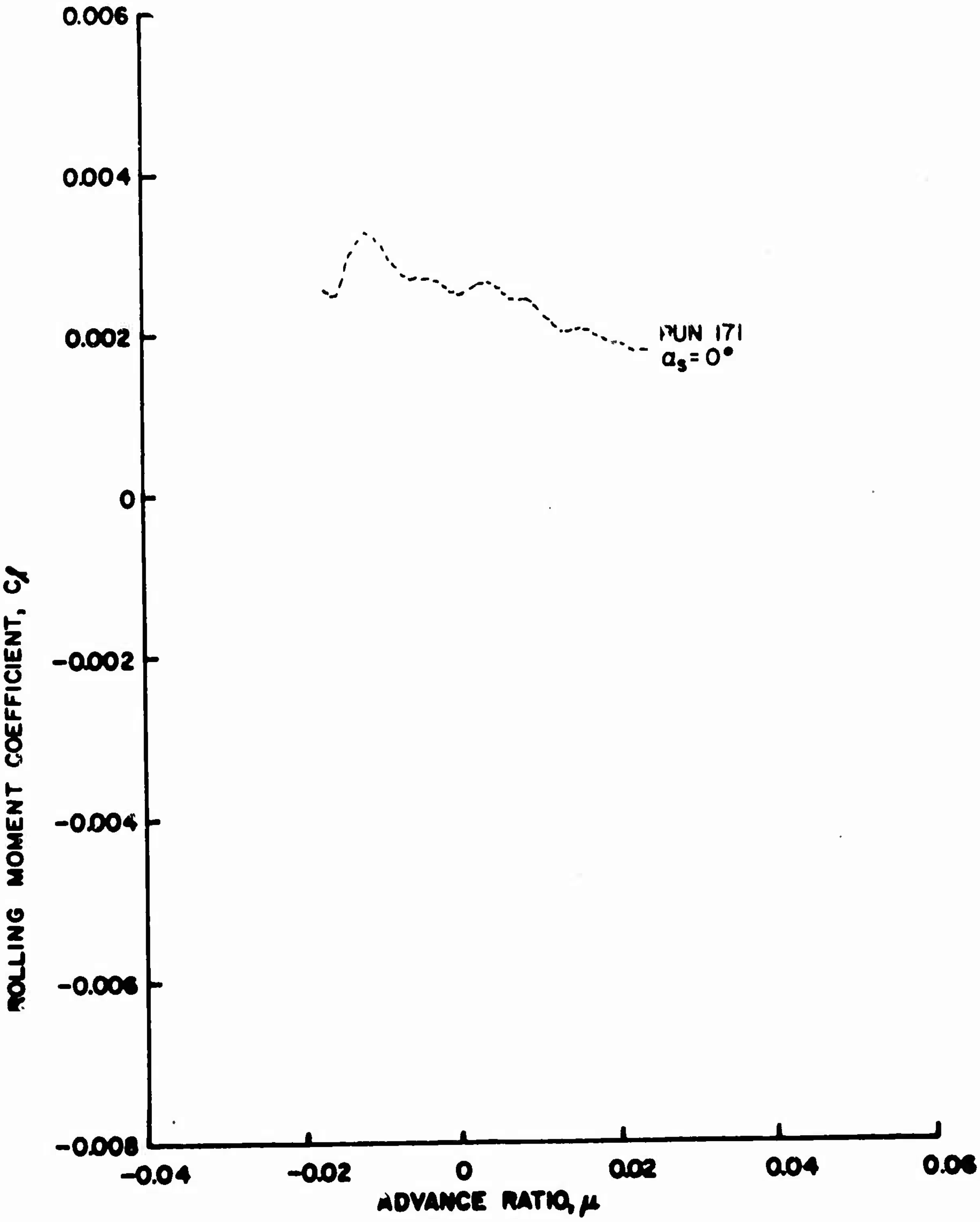

Figure 118c. Rotor Force and Moment Coefficients as Functions of Sideslip Ratio, $\theta_{.75R} = 8°$, Large Wing on High, $\frac{h}{D} = 0.30$.

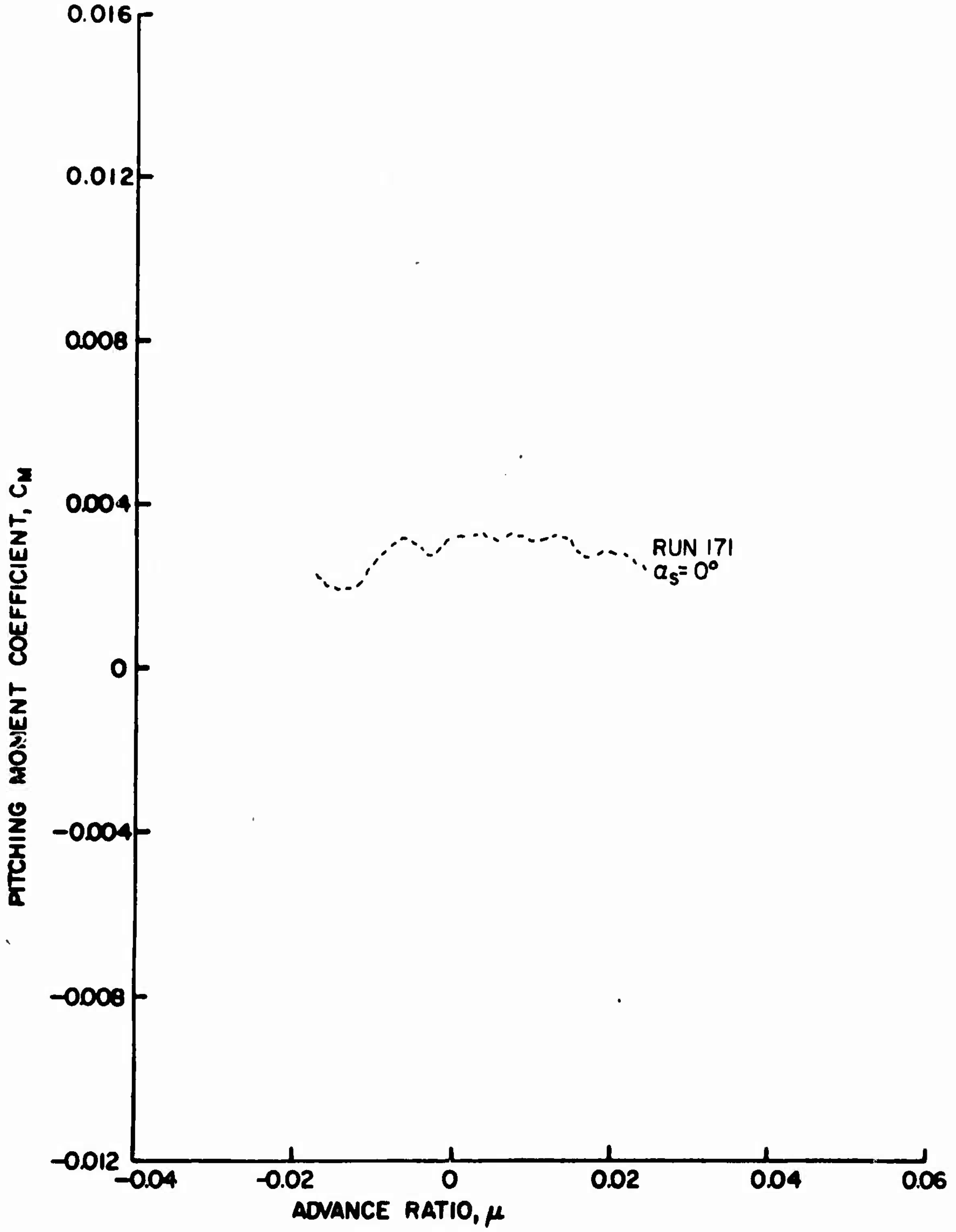

Figure 118d. Rotor Force and Moment Coefficients as Functions of Sideslip Ratio, $\theta_{.75R} = 8°$, Large Wing on High, $\frac{h}{D} = 0.30$.

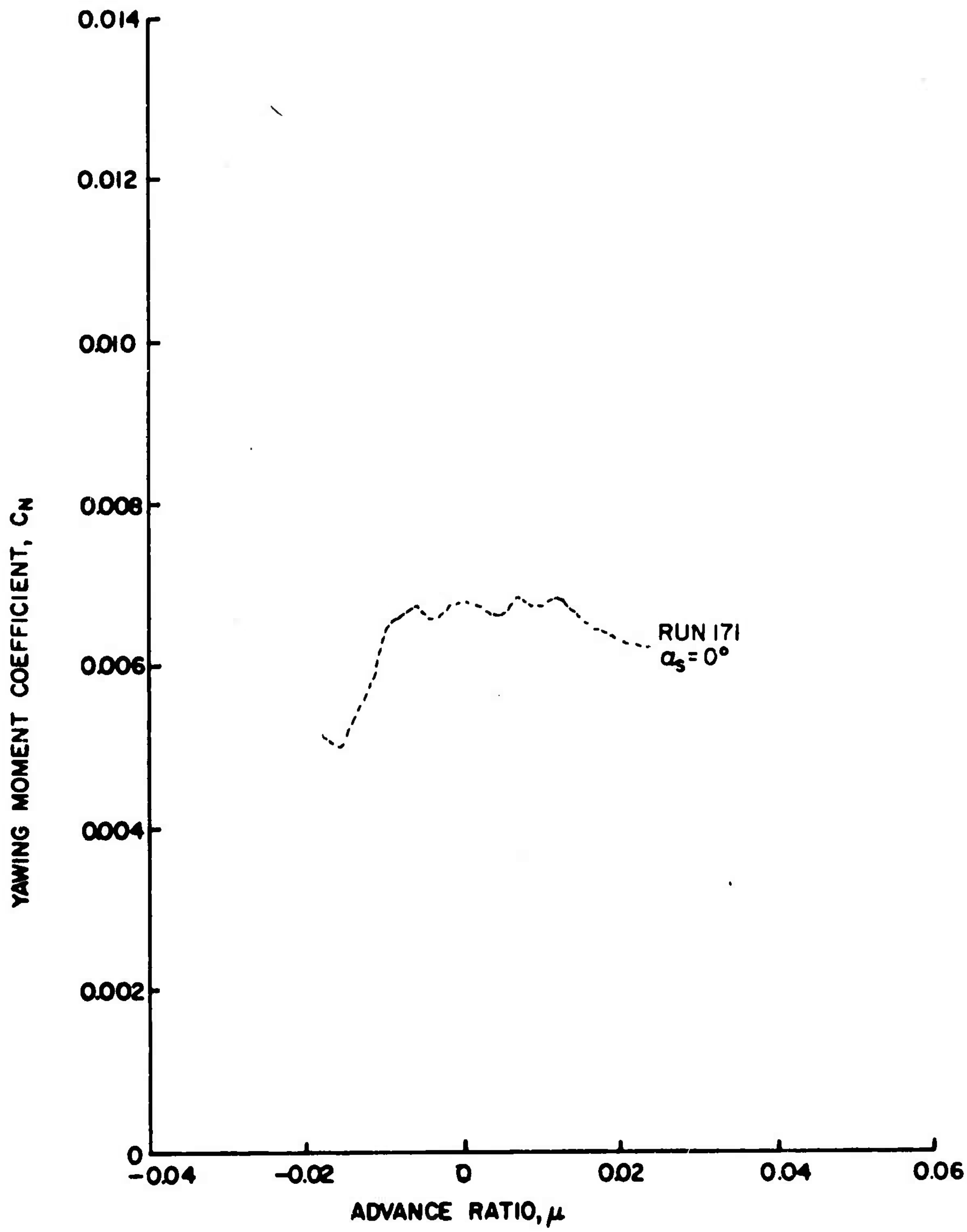

Figure 118e. Rotor Force and Moment Coefficients as Functions of Sideslip Ratio, $\theta_{.75R} = 8°$, Large Wing on High, $\frac{h}{D} = 0.30$.

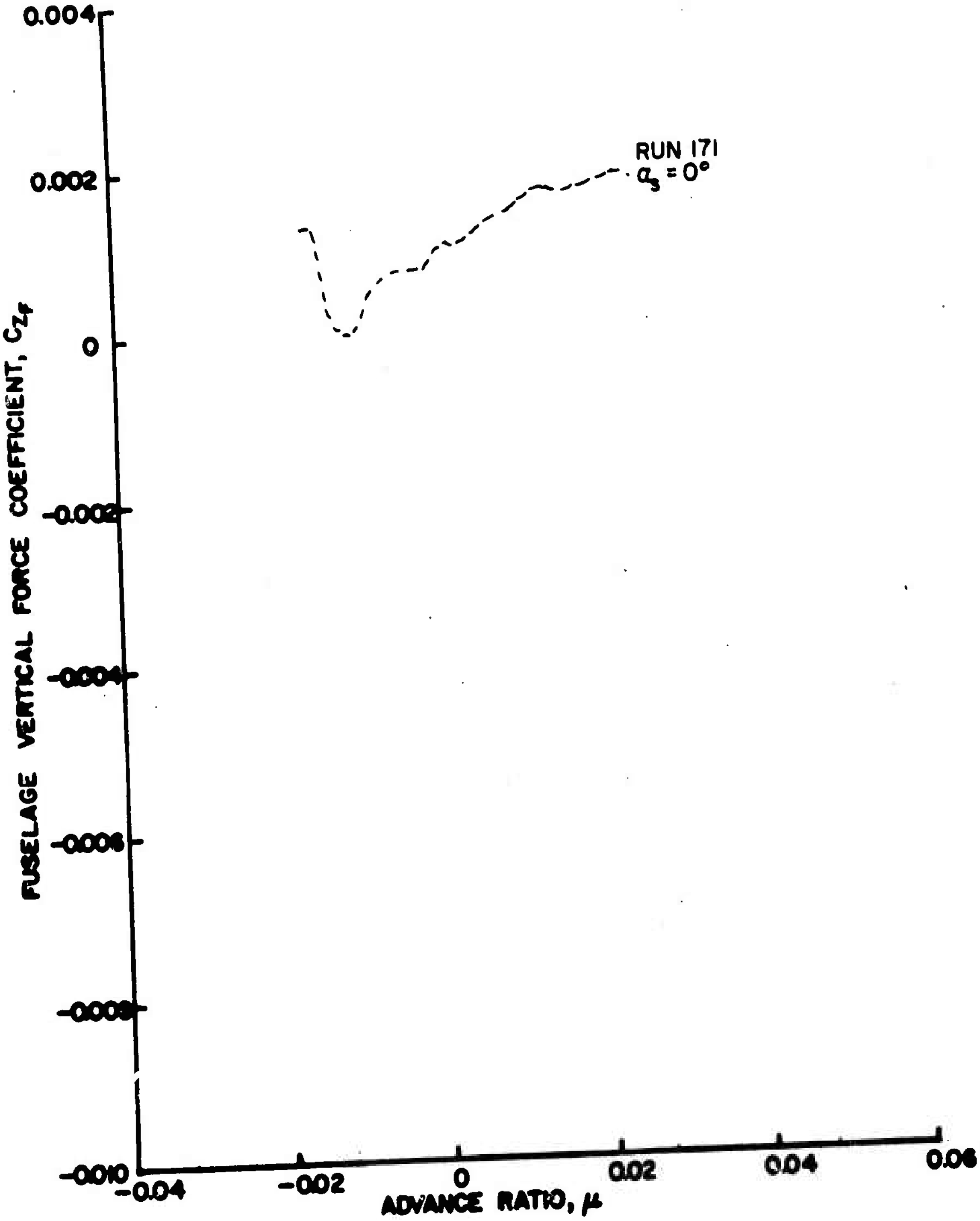

Figure 119a. Fuselage Vertical Force and Pitching Moment Coefficients as Functions of Sideslip Ratio, $\theta_{.75R} = 8°$, Large Wing on High, $\frac{h}{D} = 0.30$.

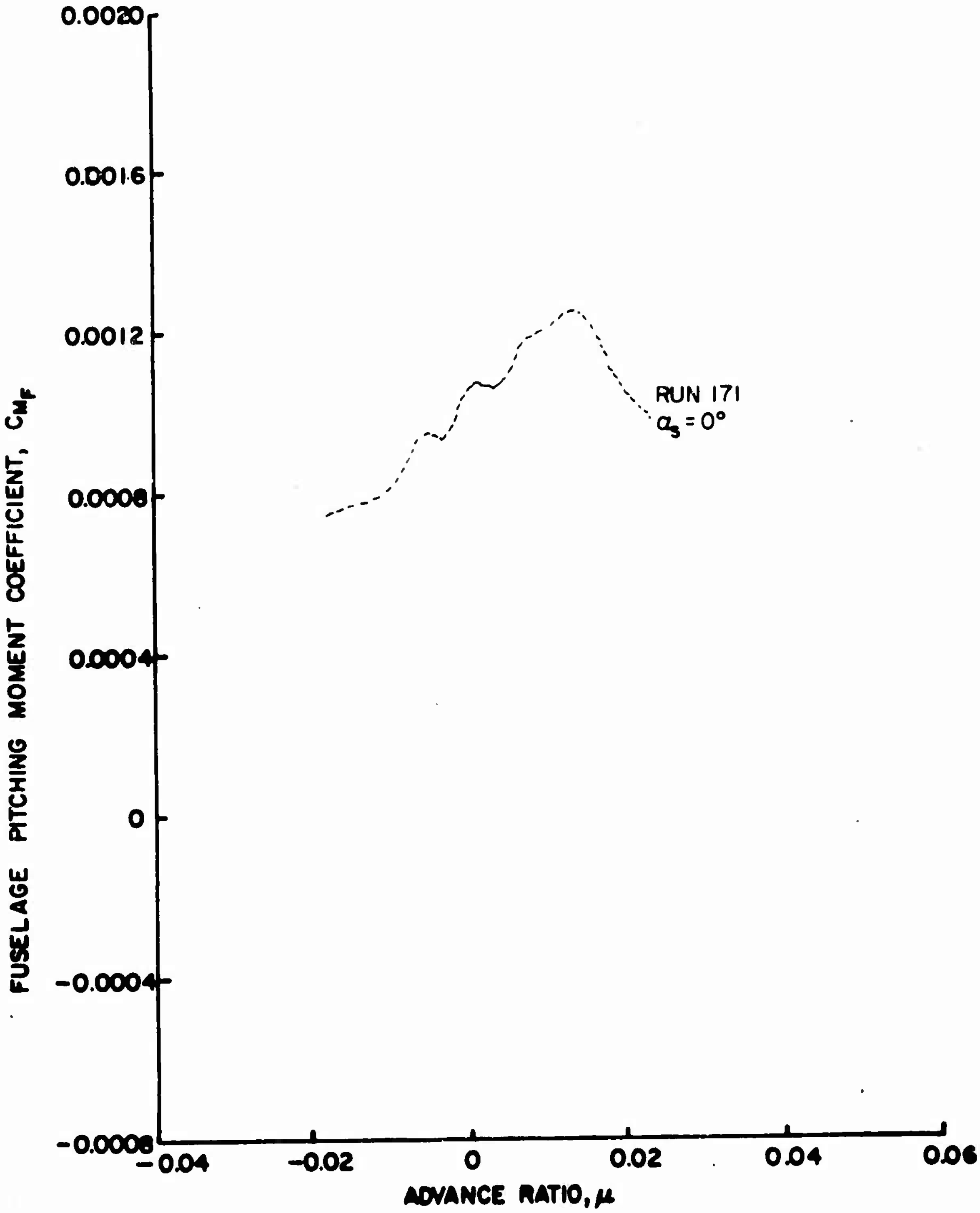

Figure 119b. Fuselage Vertical Force and Pitching Moment Coefficients as Functions of Sideslip Ratio, $\theta_{.75R} = 8°$, Large Wing on High, $\frac{h}{D} = 0.30$.

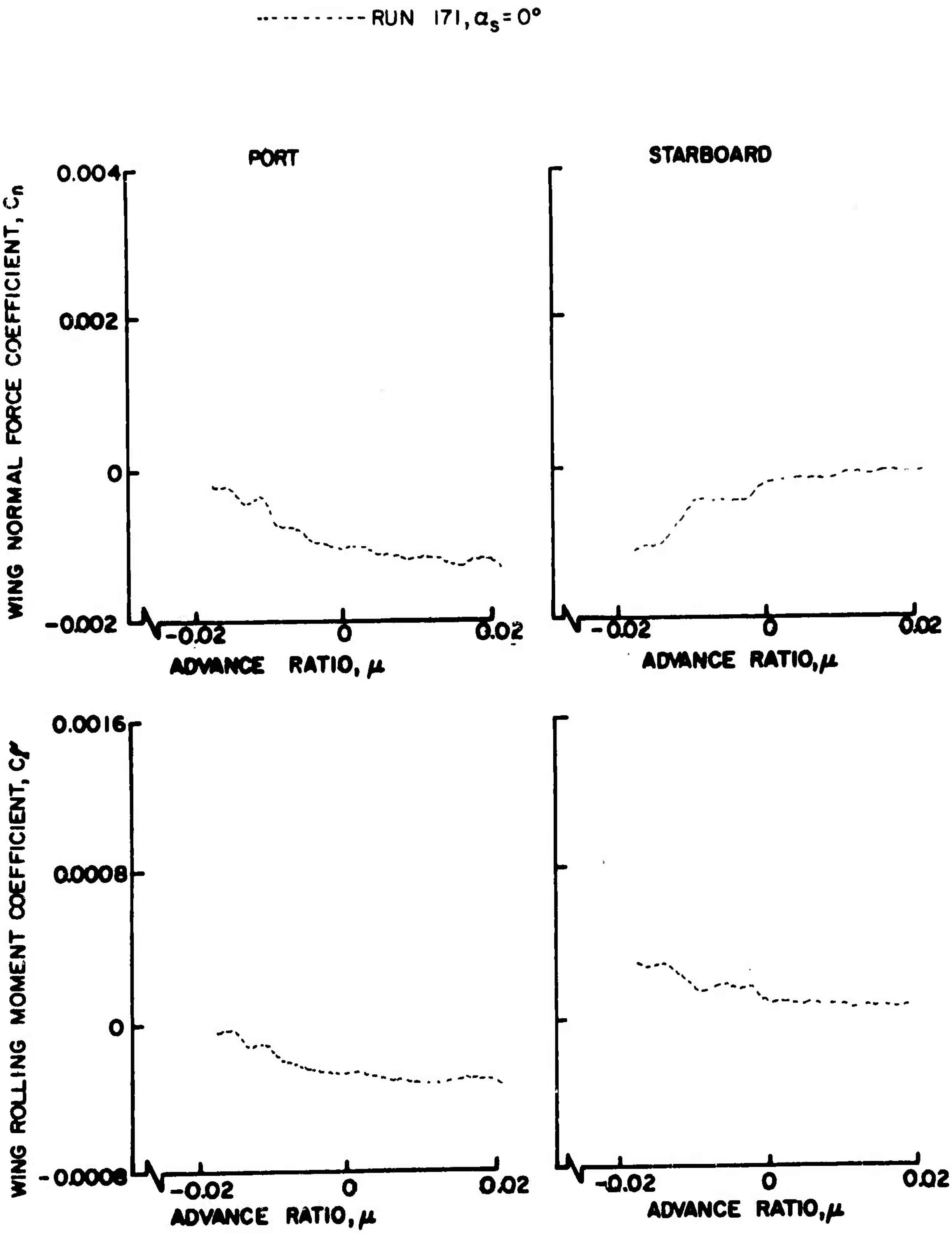

Figure 120. Wing Normal Force and Rolling Moment Coefficients as Functions of Sideslip Ratio, $\theta_{.75R} = 8^\circ$, Large Wing on High, $\frac{h}{D} = 0.30$.

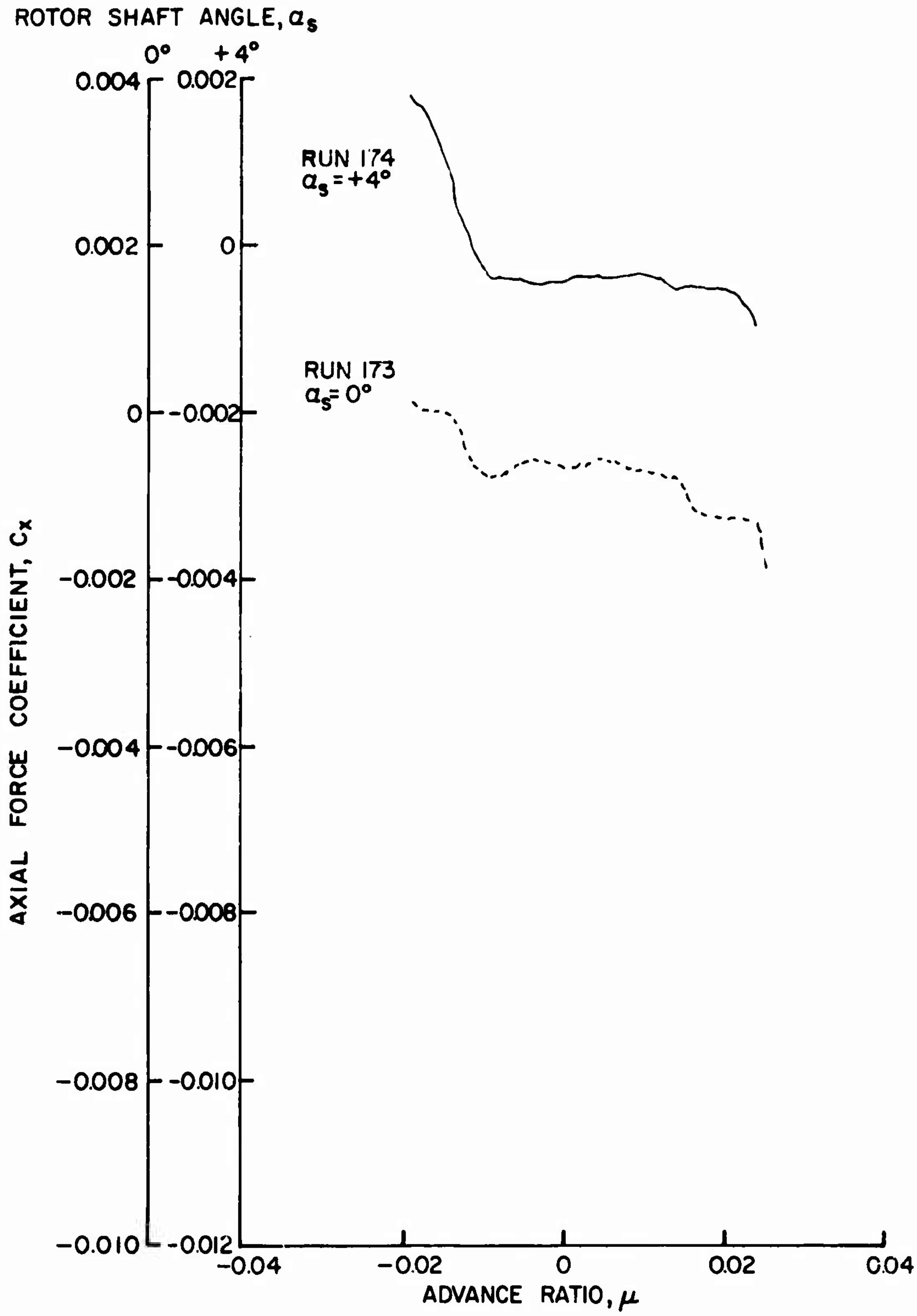

Figure 121a. Rotor Force and Moment Coefficients as Functions of Sideslip Ratio, $\theta_{.75R} = 10^\circ$, Large Wing on High, $\frac{h}{D} = 0.30$.

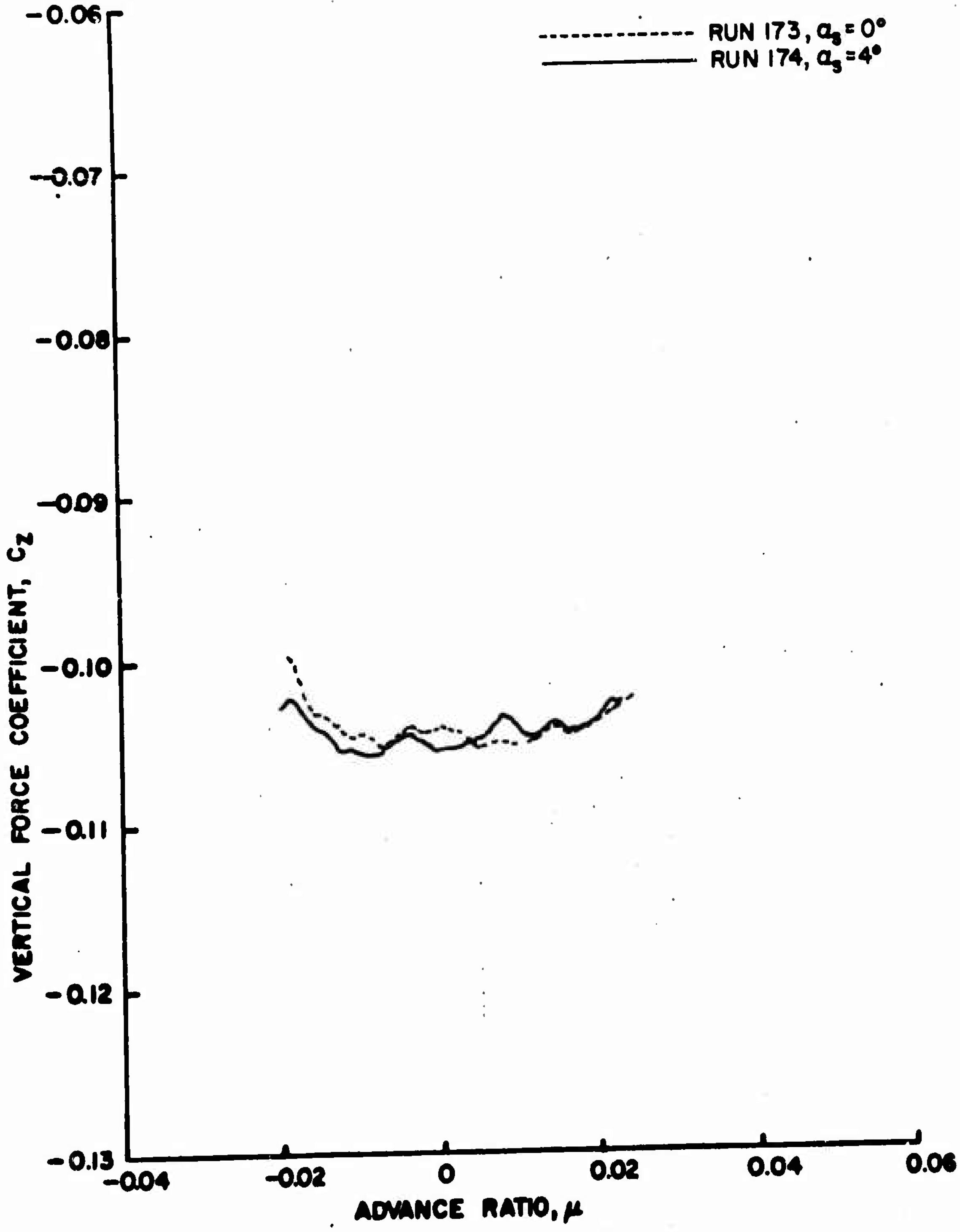

Figure 121b. Rotor Force and Moment Coefficients as Functions of Sideslip Ratio, $\theta_{.75R} = 10°$, Large Wing on High, $\frac{h}{D} = 0.30$.

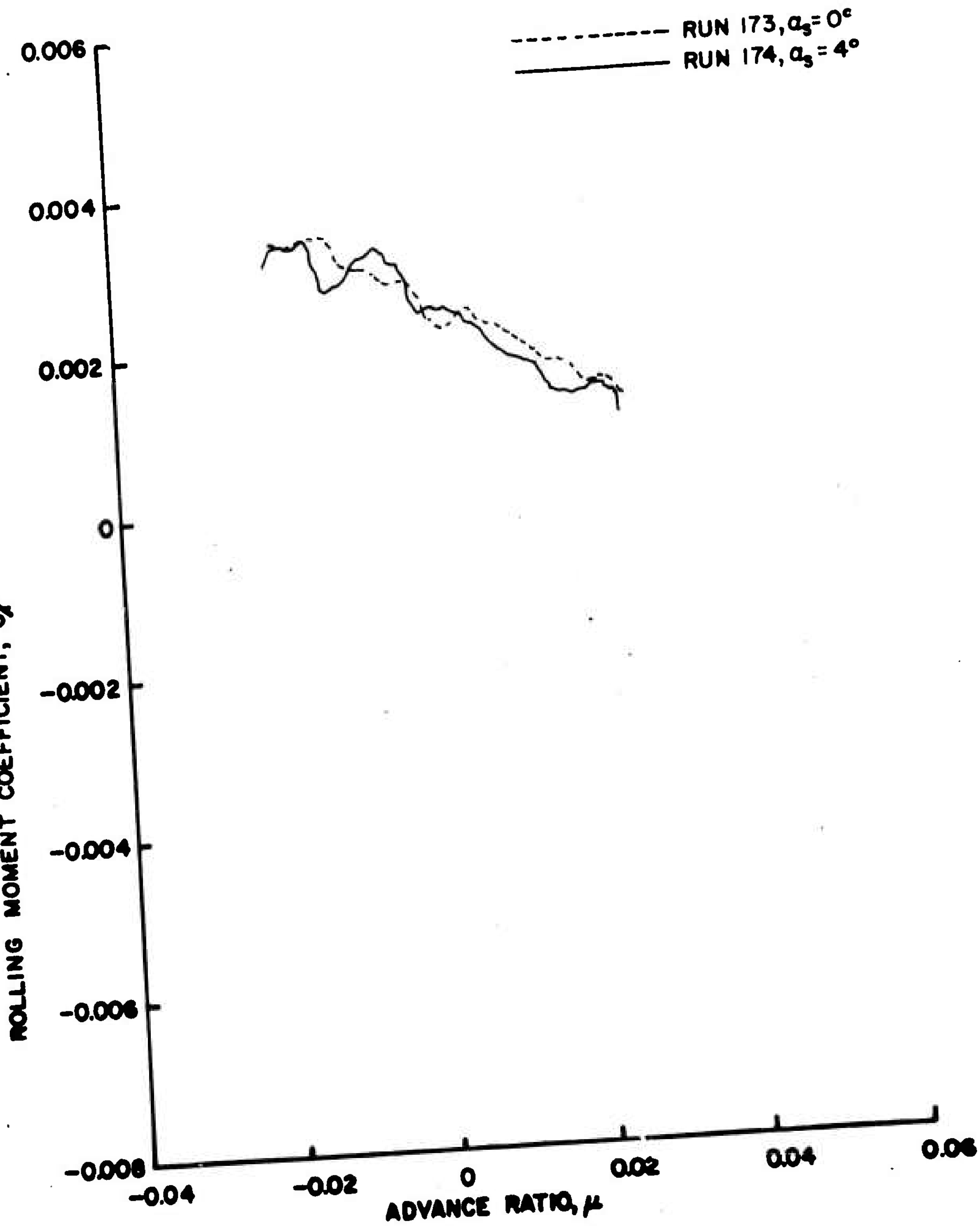

Figure 121c. Rotor Force and Moment Coefficients as Functions of Sideslip Ratio, $\theta_{.75R} = 10^\circ$, Large Wing on High, $\frac{h}{D} = 0.30$.

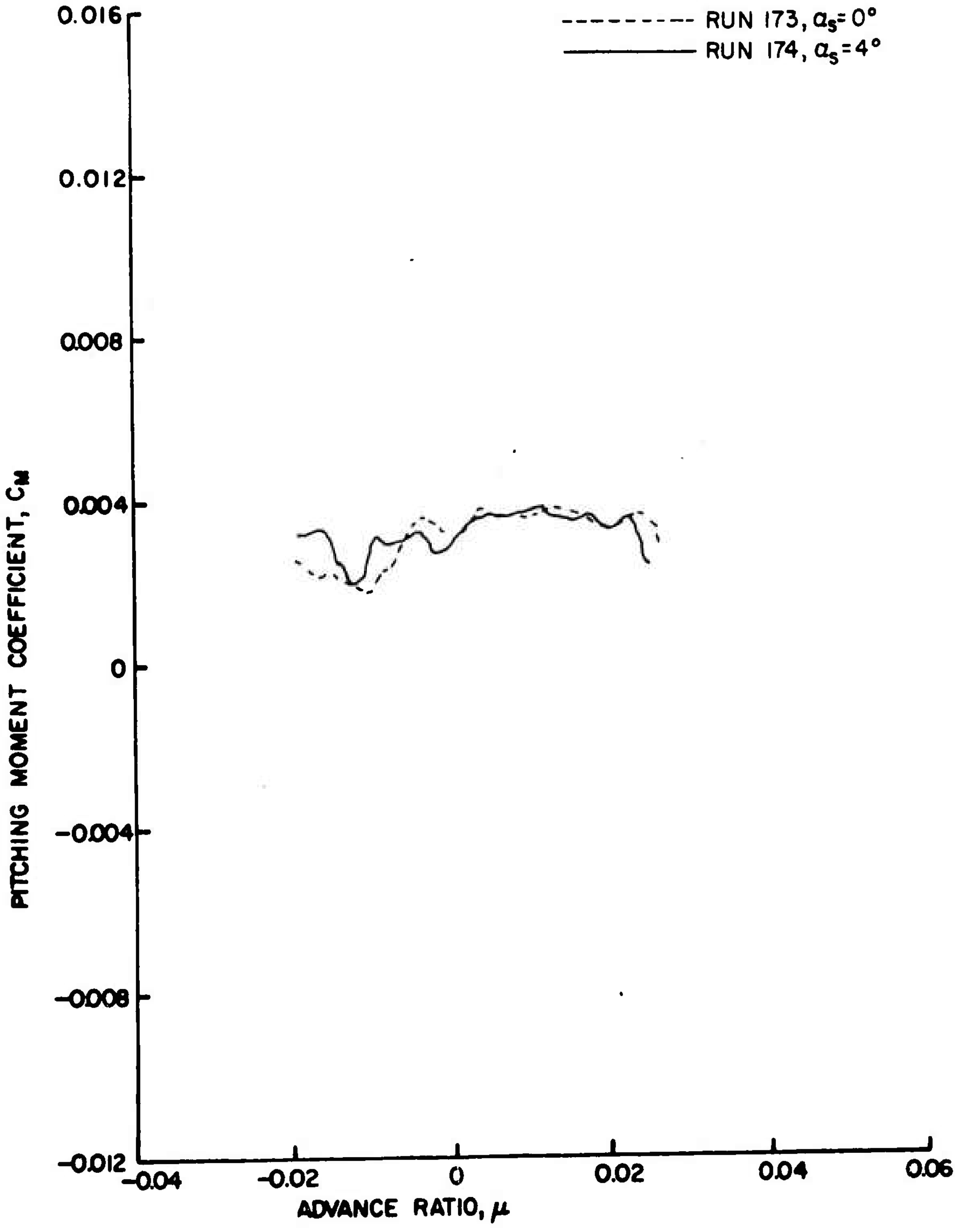

Figure 121d. Rotor Force and Moment Coefficients as Functions of Sideslip Ratio, $\theta_{.75R} = 10°$, Large Wing on High, $\frac{h}{D} = 0.30$.

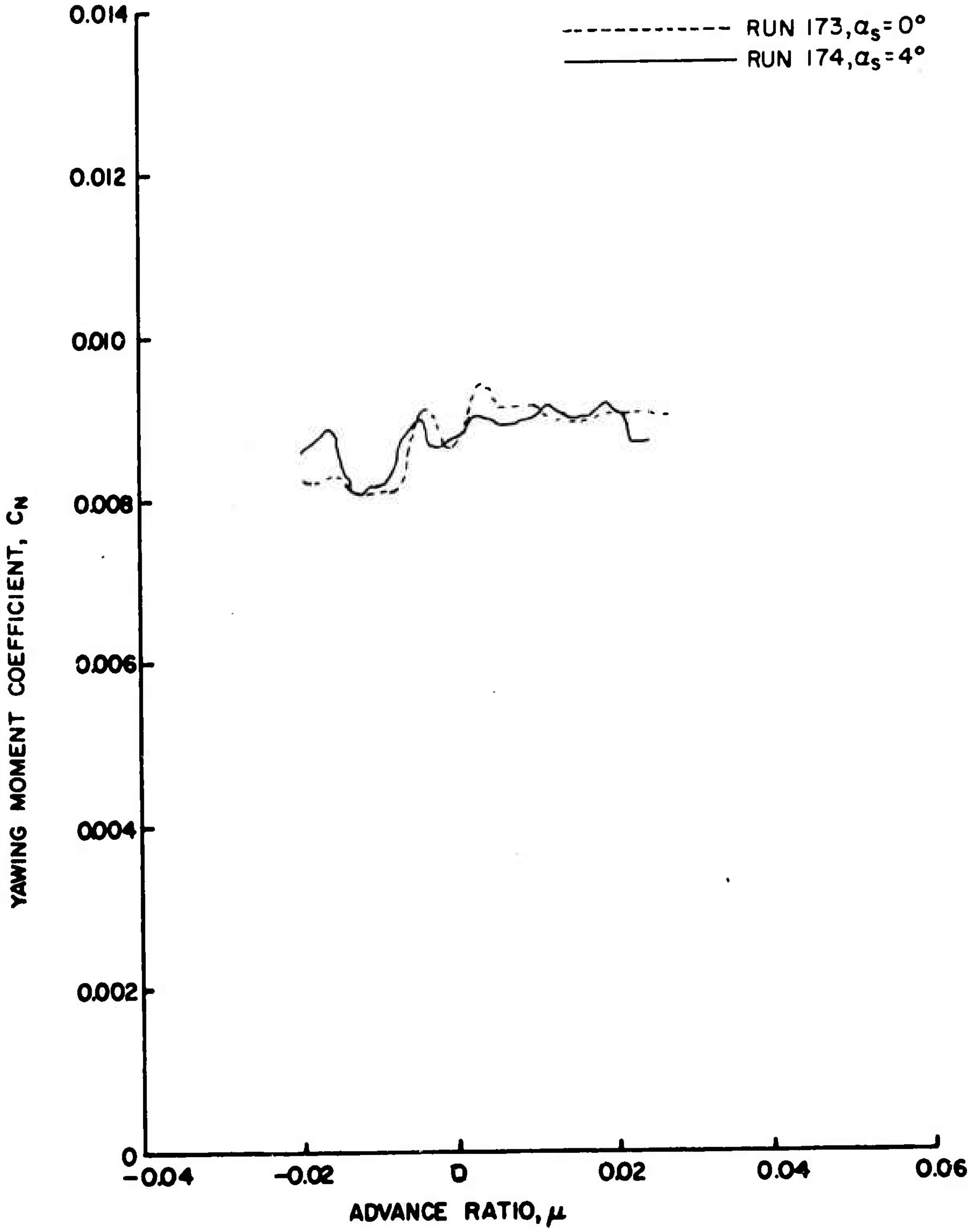

Figure 121e. Rotor Force and Moment Coefficients as Functions of Sideslip Ratio, $\theta_{.75R} = 10^{\circ}$, Large Wing on High, $\frac{h}{D} = 0.30$.

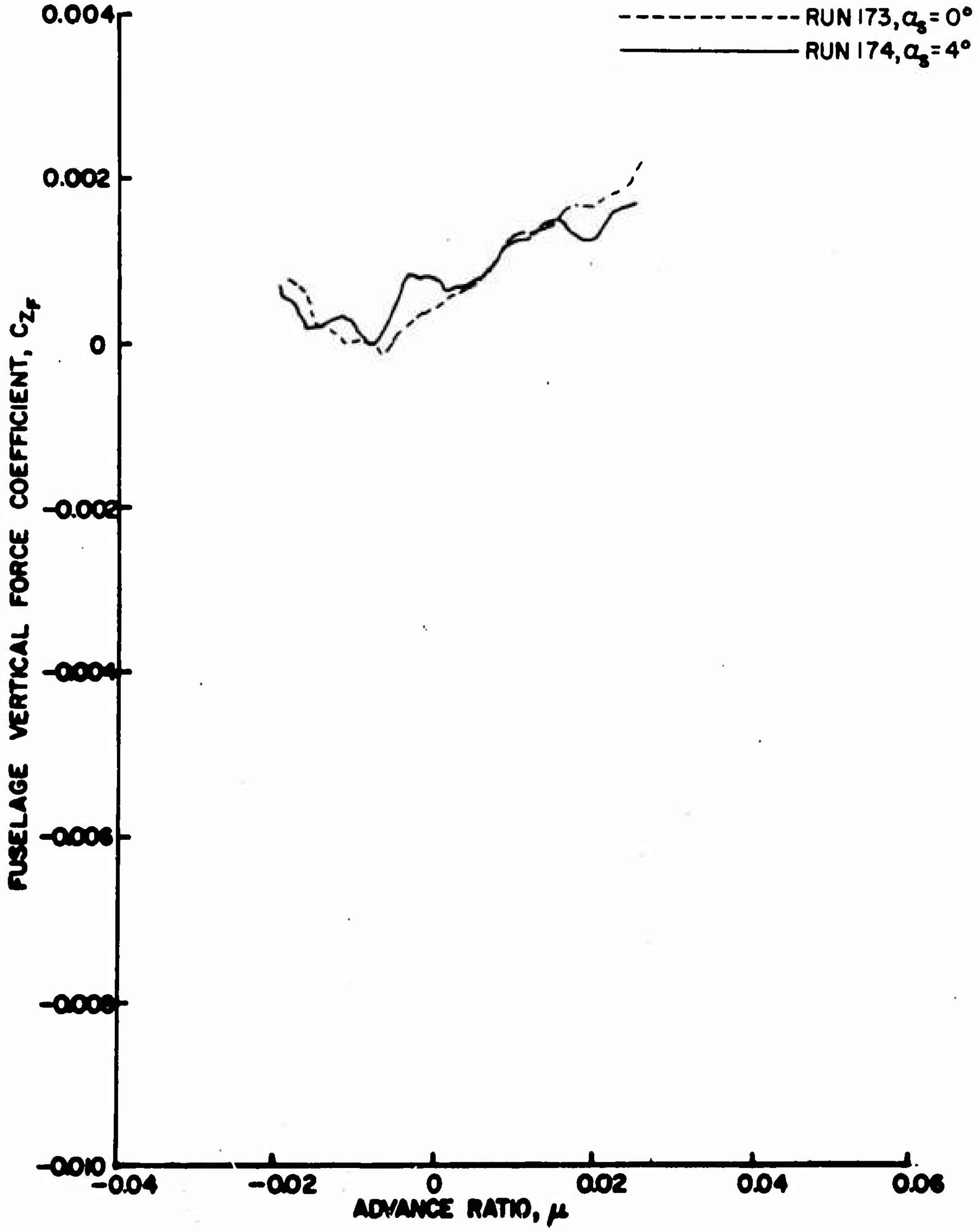

Figure 122a. Fuselage Vertical Force and Pitching Moment Coefficients as Functions of Sideslip Ratio, $\theta_{.75R} = 10°$, Large Wing on High, $\frac{h}{D} = 0.30$.

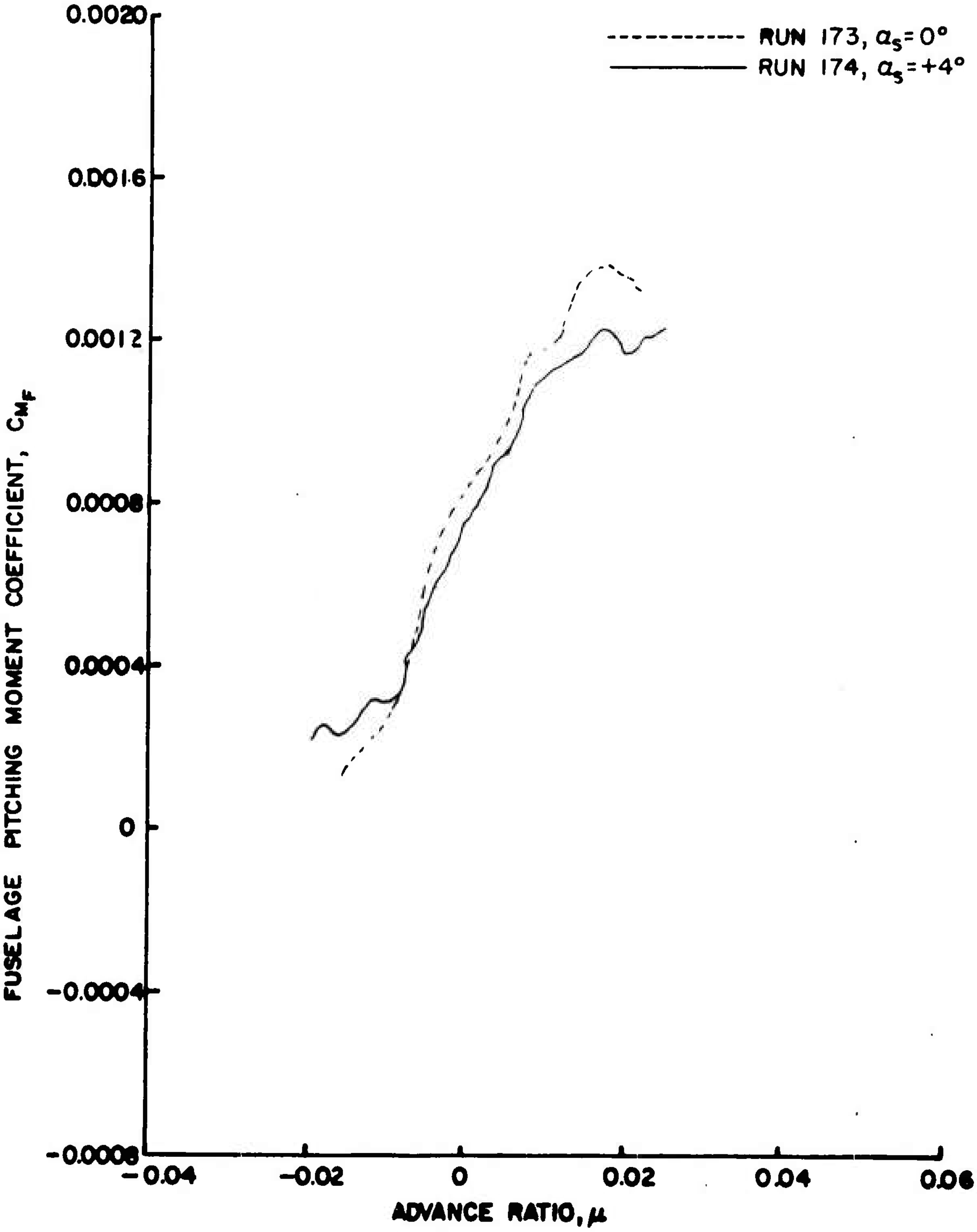

Figure 122b. Fuselage Vertical Force and Pitching Moment Coefficients as Functions of Sideslip Ratio, $\theta_{.75R} = 10°$, Large Wing on High, $\frac{h}{D} = 0.30$.

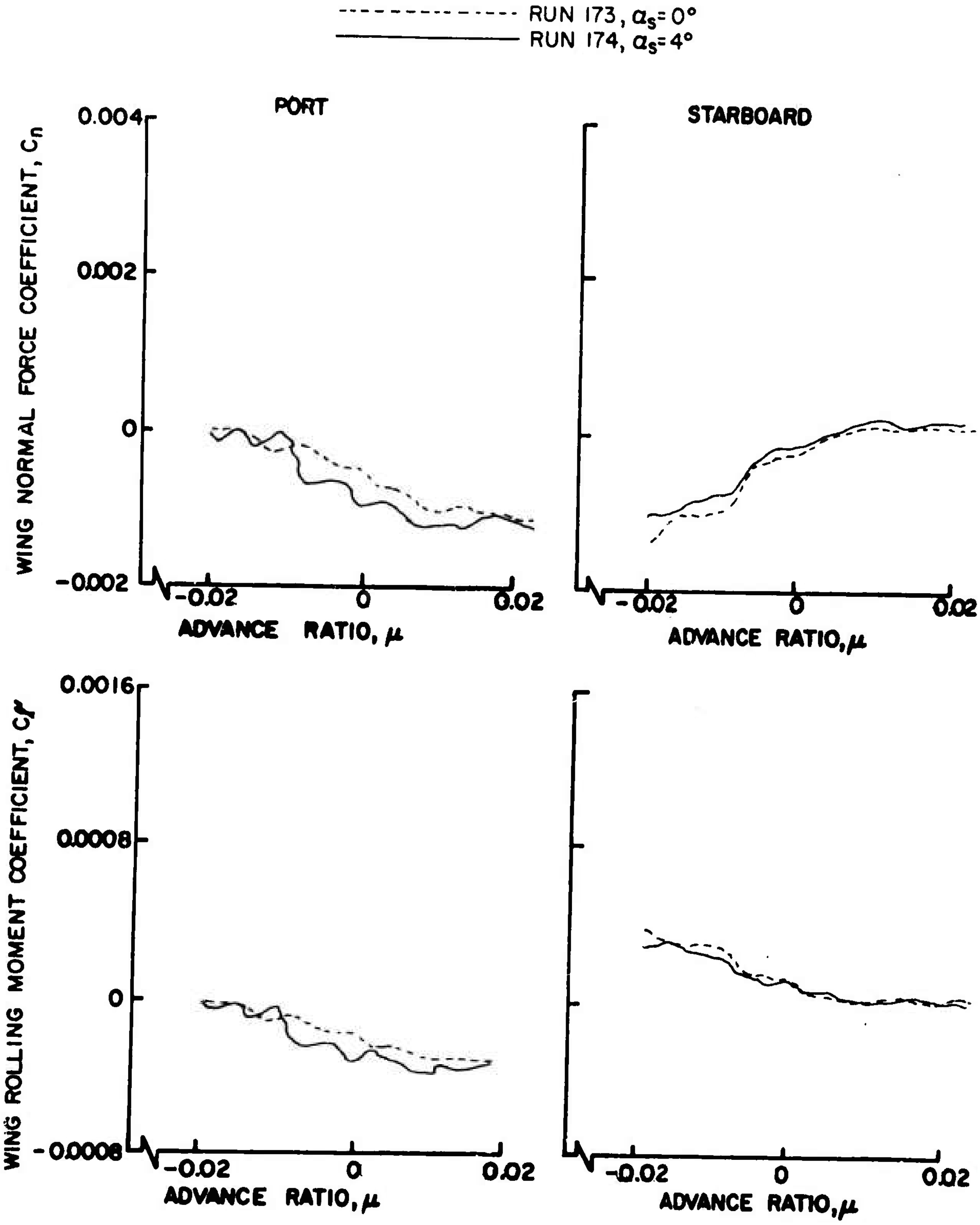

Figure 123. Wing Normal Force and Rolling Moment Coefficients as Functions of Sideslip Ratio, $\theta_{.75R} = 10°$, Large Wing on High, $\frac{h}{D} = 0.30$.

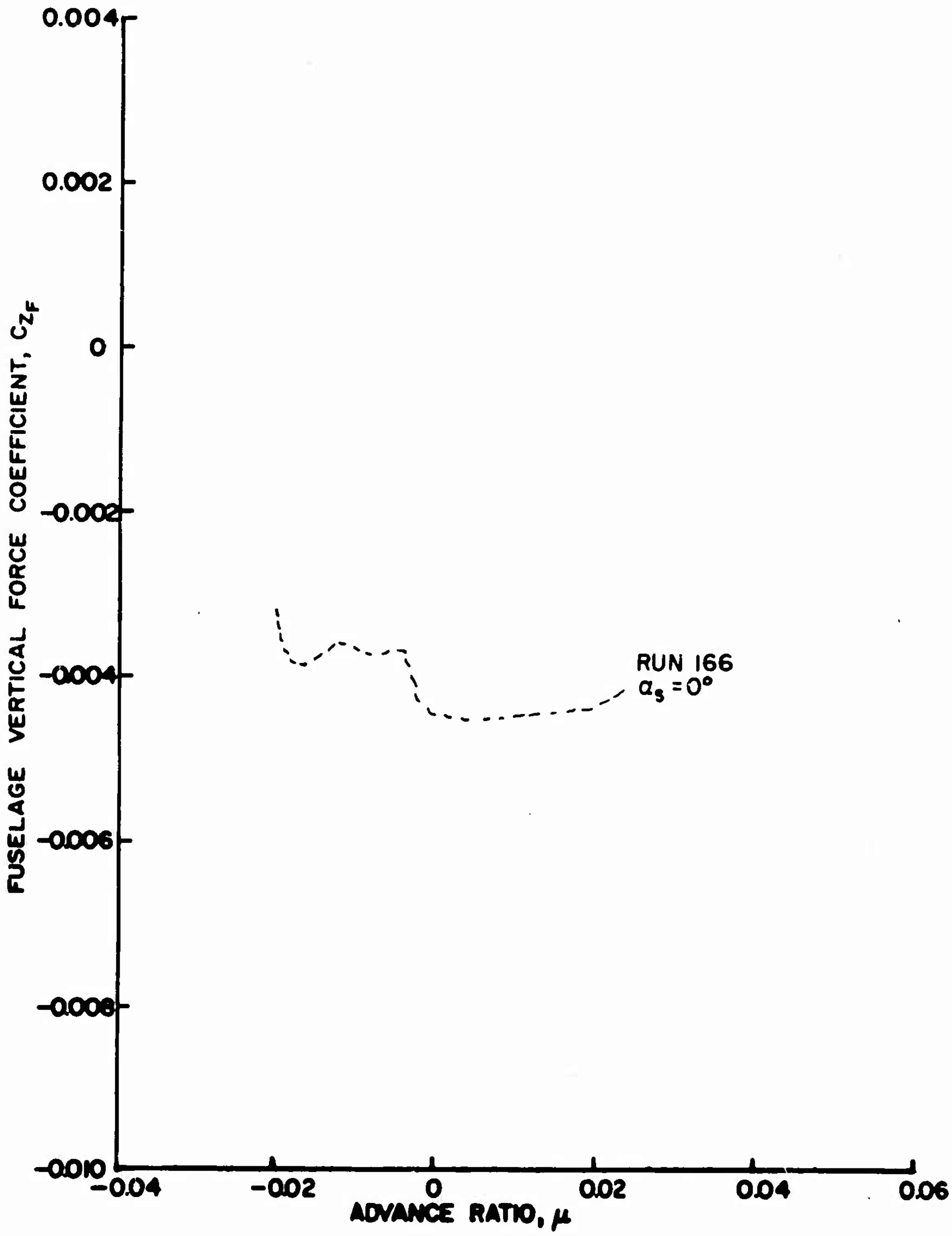

Figure 124a. Fuselage Vertical Force and Pitching Moment Coefficients as Functions of Sideslip Ratio, $\theta_{.75R} = 8°$, Large Wing on Low, $\frac{h}{D} = 0.30$.

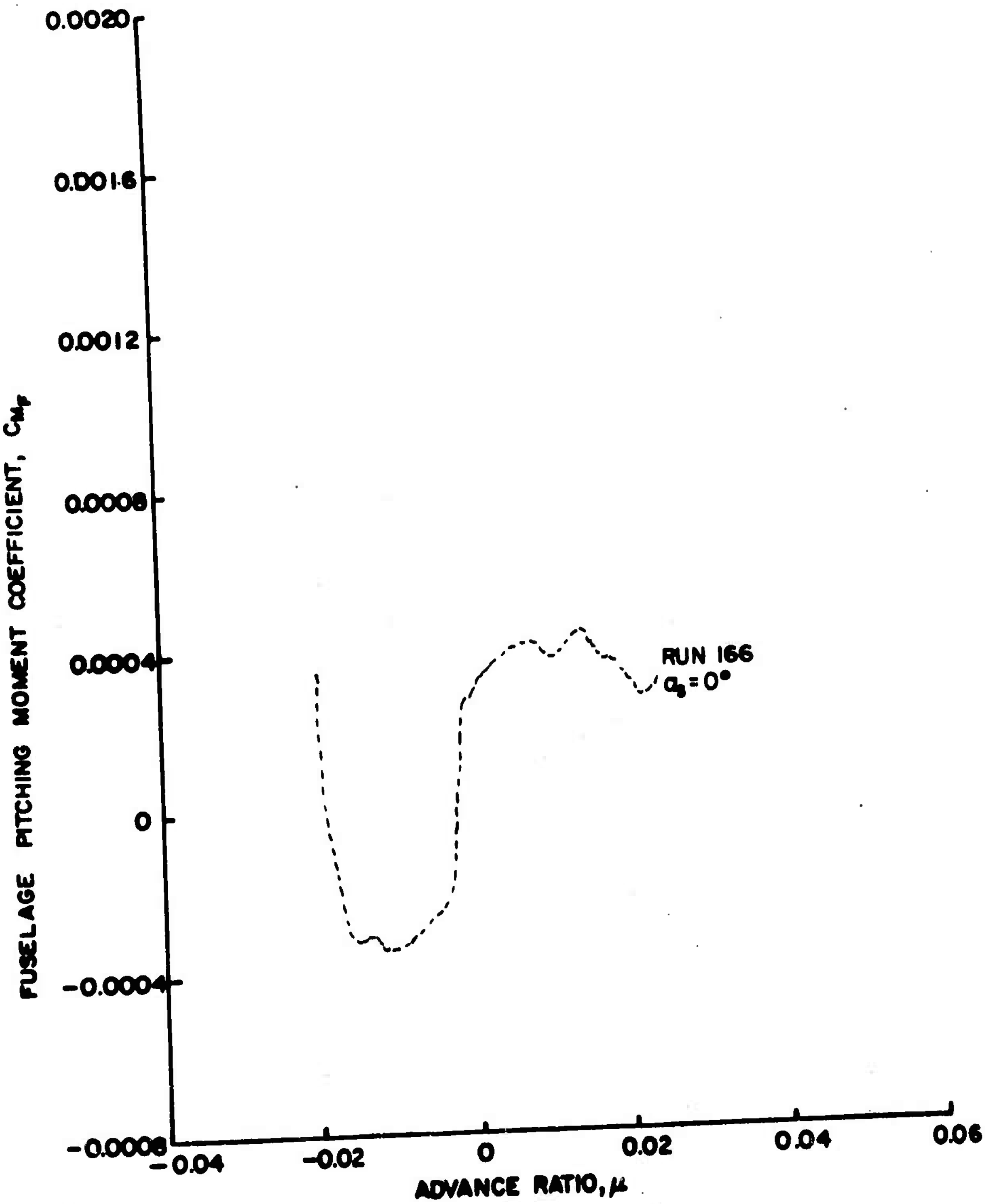

Figure 124b. Fuselage Vertical Force and Pitching Moment Coefficients as Functions of Sideslip Ratio, $\theta_{.75R} = 8°$, Large Wing on Low, $\frac{h}{D} = 0.30$.

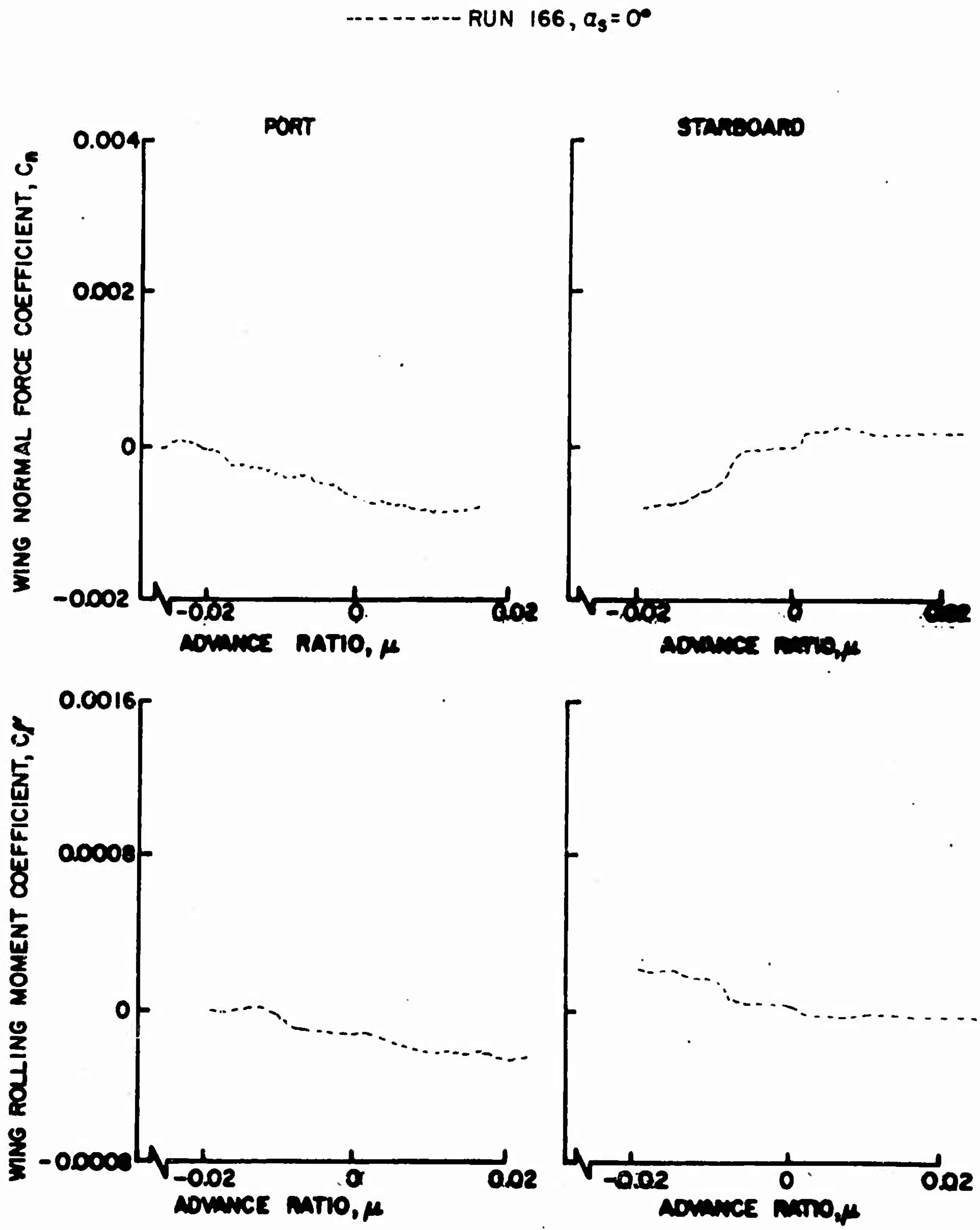

Figure 125. Wing Normal Force and Rolling Moment Coefficients as Functions of Sideslip Ratio, $\theta_{.75R} = 8°$, Large Wing on Low, $\frac{h}{D} = 0.30$.

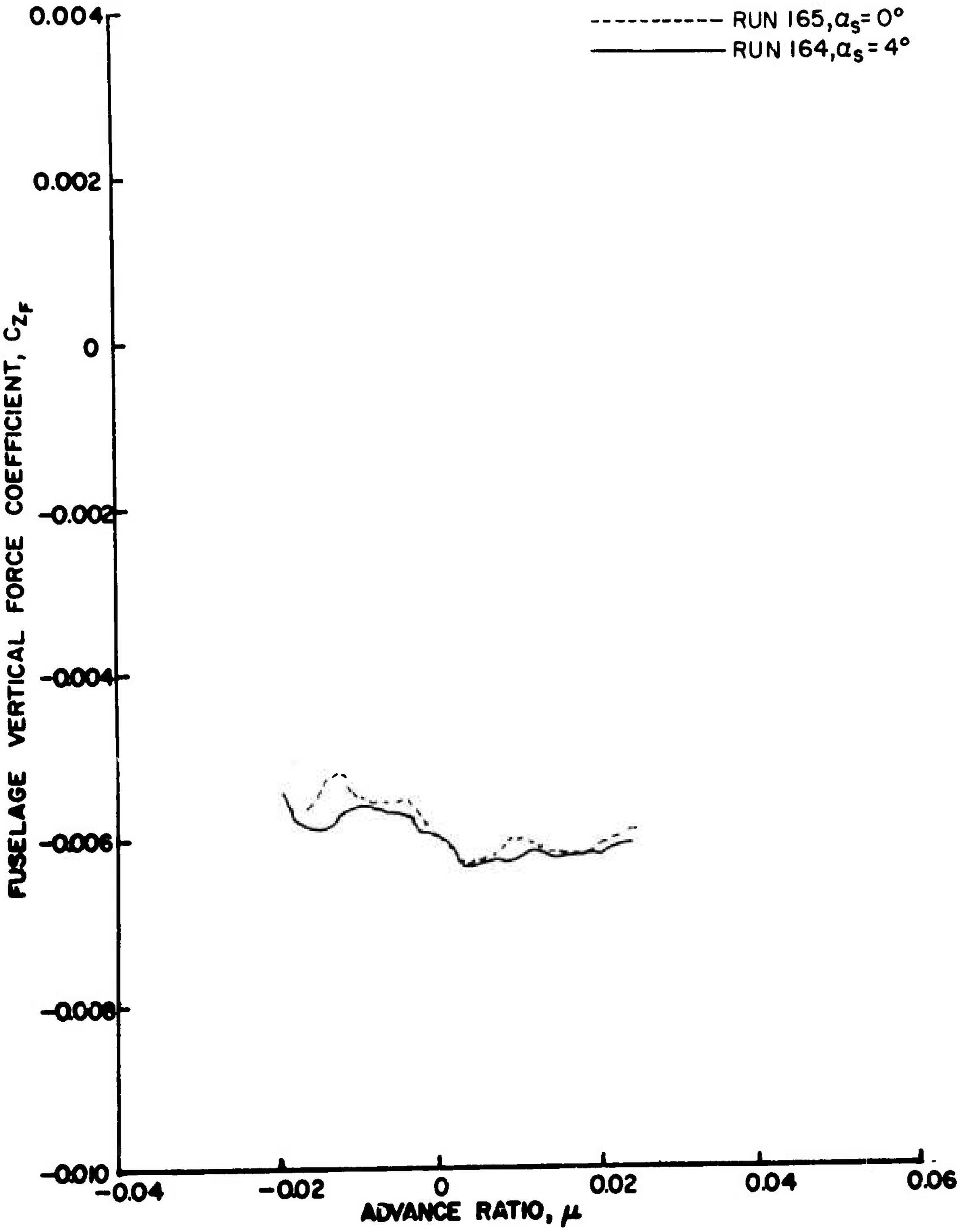

Figure 126a. Fuselage Vertical Force and Pitching Moment Coefficients as Functions of Sideslip Ratio, $\theta_{.75R} = 10^\circ$, Large Wing on Low, $\frac{h}{D} = 0.30$.

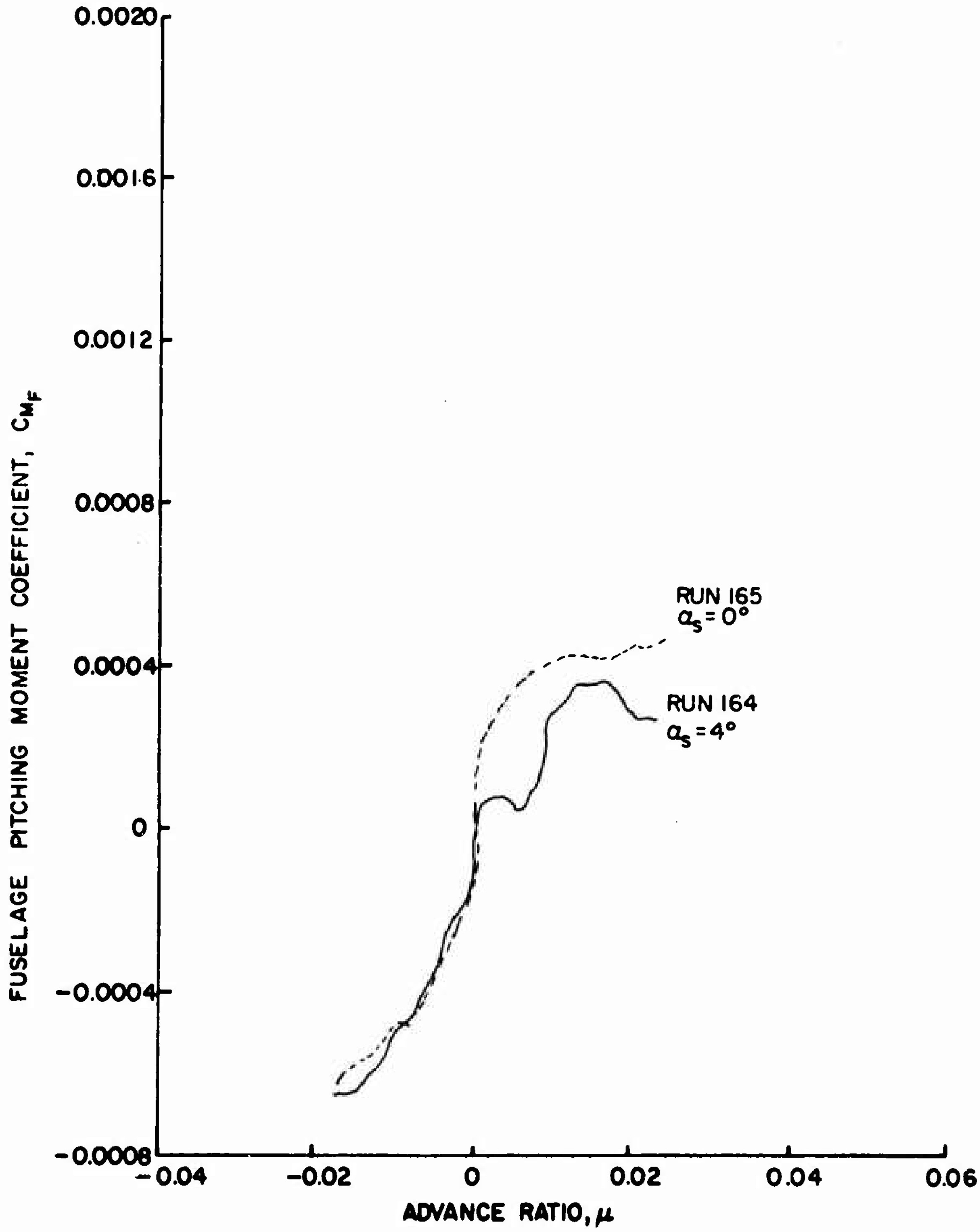

Figure 126b. Fuselage Vertical Force and Pitching Moment Coefficients as Functions of Sideslip Ratio, $\theta_{.75R} = 10°$, Large Wing on Low, $\frac{h}{D} = 0.30$.

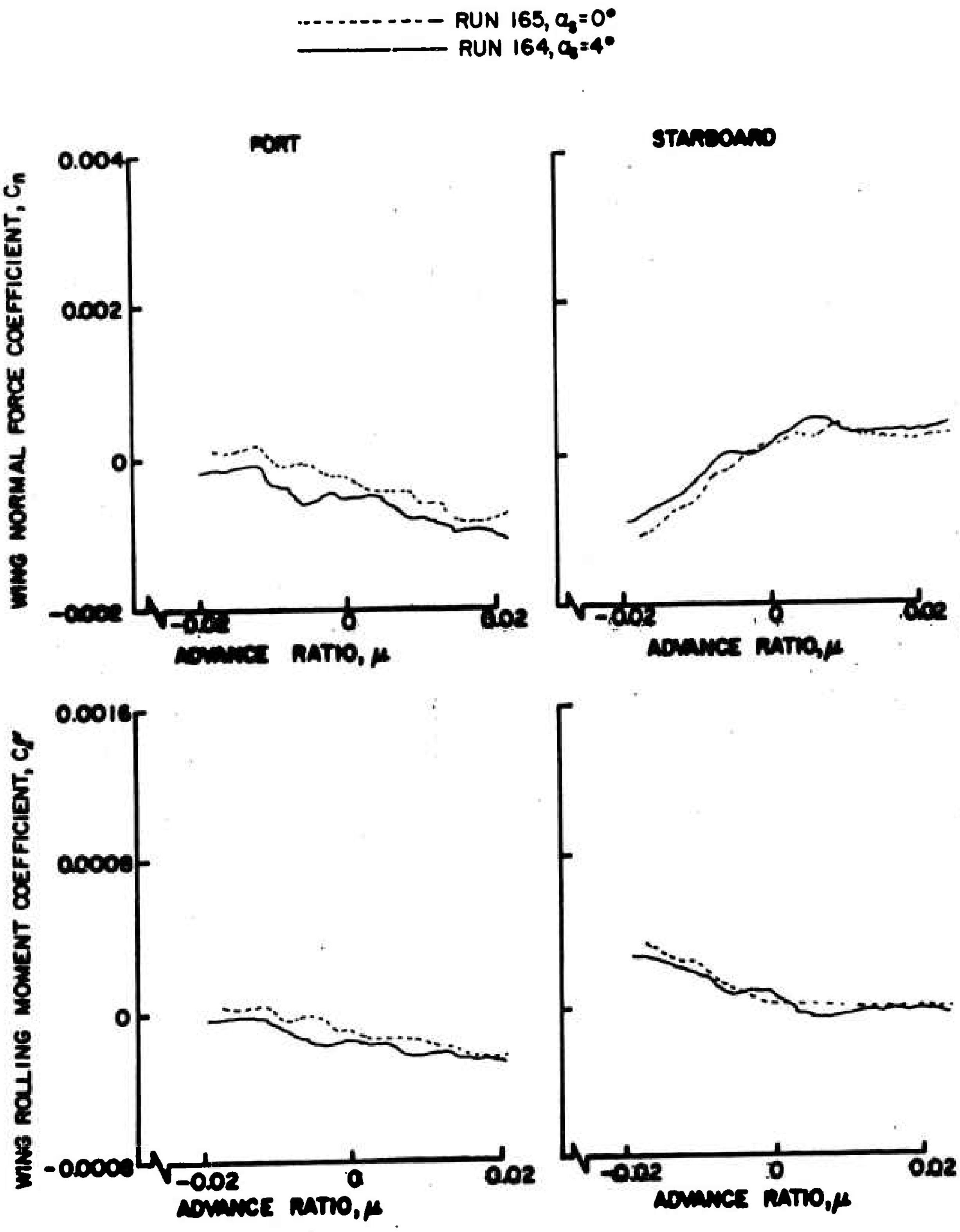

Figure 127. Wing Normal Force and Rolling Moment Coefficients as Functions of Sideslip Ratio, $\theta_{.75R} = 10^\circ$, Large Wing on Low, $\frac{h}{D} = 0.30$.

LITERATURE CITED

1. Bain, Lawrence J., and Landgrebe, Anton J., INVESTIGATION OF COMPOUND HELICOPTER AERODYNAMIC INTERFERENCE EFFECTS, United Aircraft Corporation; USAAVLABS Technical Report 67-44, U. S. Army Aviation Materiel Laboratories, Fort Eustis, Virginia, November 1967, AD 665 427.

2. Lynn, Robert R., WING-ROTOR INTERACTIONS, Journal of Aircraft, Vol. 3, No. 4, July-August 1966, pp. 326-332.

3. HIGH-PERFORMANCE HELICOPTER PROGRAM, Bell Helicopter Company; TRECOM Technical Report 64-61, U. S. Army Transportation Research Command, Fort Eustis, Virginia, October 1964.

4. Curtiss, H. C., Jr., Putman, W. F., and Traybar, J. J., GENERAL DESCRIPTION OF THE PRINCETON DYNAMIC MODEL TRACK; USAAVLABS Technical Report 66-73, U. S. Army Aviation Materiel Laboratories, Fort Eustis, Virginia, November 1966, AD 645 883.

5. Putman, William F., AN EXPERIMENTAL INVESTIGATION OF COMPOUND HELICOPTER AERODYNAMICS IN AND NEAR HOVERING FLIGHT, Aerospace Sciences Report 918, Princeton University, Princeton, New Jersey. (Unpublished)